Activation of MAIT cells, and their role in *Mycobacterium tuberculosis* infection



Matthew Bilton

Wolfson College

University of Oxford

A thesis submitted for the degree of

Doctor of Philosophy

Trinity 2016

This thesis is dedicated
to Mum and Roy.

Acknowledgements

First and foremost, I would like to express my sincere thanks to my DPhil supervisors Paul Klenerman and Ajit Lalvani for their guidance, direction, supervision and continued support over the past four years. Doing research is a huge privilege, and I am incredibly grateful for the numerous opportunities given to me.

I will always be thankful to Chris Willberg and James Ussher for such a great introduction to research; in particular, thank you Chris for all the help, advice, insight, and ideas for the past four years. I am hugely thankful to Nazneen Siddiqui, David Connell and Ann-Kathrin Reuschl for all of their support, advice, cell-splitting and Cat3 buddying. And thank you to Chris, Ayako, Leo and AK for all of your comments and critical reading of sections of this thesis.

I am indebted to all of the clinical team in London—to Onn-Min Kon, Hannah Jarvis, Sam Bremang, Hiromi Uzu and Helen Piotrowski for all the help collecting samples. In particular, Sam who worked tirelessly to enable the clinical research during my project. Thank you to Hila Novak at the Kennedy Institute in Oxford, and to all others at Imperial College who contributed to making my research possible—including the patients for their selfless donations. Thank you to the Jefferiss Research Trust, who awarded me funding to pursue this DPhil.

I am fortunate to have been able to work with such a fantastic group of people: AK 'the peacekeeper', Naz, Dave, Long, Alice, Luis, Umar, Paul, Amarjit, Mel, Hilary, Bianca, Ishita, Darren, Heather, Saranya, Shaima, Elihu, and last—but, by no means least, Rob, for the corner desk camaraderie. In Oxford: thanks Ayako, Jo and Alba for putting up with all the questions; Prabh, for allowing me choice of hood (sometimes); Chris, Tianqi, Bonnie, Andy, Genevieve, Matt J, Jacqui, Manu, Matt P, Flick, Tony, Tamsin, Emily, Narayan, Madda, Ruth and Madaleine for making the PMB the place it is; and Leo, for your taste in music (if not football team).

Outside the lab, thank you Mum and Roy for doing everything to support my education over the years, that has brought me to this point. Shout outs to my bro Dr. Sam, Emma, Shaun, June, Nana, Alan, David, Michelle, Loretta, Andrew, Alex, Louis, Nick and Leanne; and family #2 Phil, Paul, Katy and Mark. To Gido, Mateusz, Gio and all the other Wolfson & St. Cross footballers; to the CC—Jase, Alex and Dave; to Paul (thanks re: microscope stage) and to my 62/Magdalen/home friends. Thinking of my father and grandfather who are no longer here, to whom I would have loved to show this. And Éva, for sharing the ups and downs; for being so patient, kind, fun and positive; and for always being there for me—thank you.

Abstract

Mucosal associated invariant T (MAIT) cells are a population of innate-like lymphocytes, with an emerging role in tuberculosis (TB). They are characterised by the expression of high levels of CD161 and IL-18Rα, possession of a Vα7.2^{+} T cell receptor (TCR), and restriction by the MHC class I-related protein (MR1). MAIT cells can be activated by MR1 presenting microbe-derived riboflavin metabolites; or, by the cytokines IL-12 and IL-18 in a TCR-independent fashion. How human MAIT cells integrate these signals for their activation in response to *Mtb* is unclear. Lymphatic TB (LNTB) is a common extra-pulmonary manifestation of TB; however, little is known about the status of MAIT cells in LNTB — or in other granulomatous diseases, such as sarcoidosis.

In this study, an *in vitro* approach was used to probe MAIT cell activation by *Mtb*, and the roles of IL-12/-18, the TCR, cell–cell contact and the immunological synapse (IS). Following TCR ligation, TNFα expression was rapid and transient, and was enhanced following sustained IL-12/-18 exposure. IFNγ expression occurred following sustained exposure to ng/ml concentrations of IL-12/-18; however, alongside TCR stimulation, pg/ml concentrations were sufficient. Using an artificial bilayer system, CD161 was excluded from the central regions of the MAIT cell IS, whilst the distribution of IL-18Rα remained unaffected. In response to *Mtb* and BCG, MR1 was necessary for rapid activation and TNFα expression, IL-12/-18 were necessary for robust and sustained IFNy expression, whilst an anti-*Mtb* effect was indicated in an intracellular infection model. Assessment of patients with TB or sarcoid lymphadenopathy revealed a depletion of MAIT cells in the blood in sarcoidosis, but not LNTB. In both groups, MAIT cells could be detected within a proportion of sampled lymph nodes.

Overall, these findings indicate the importance of inflammatory cytokine signals in the induction of high-intensity and sustained MAIT cell effector function, including in response to *Mtb*. The observation of a numerical deficiency of MAIT cells in sarcoidosis requires further investigation.

Contributions

All work presented in this thesis is my own, except as follows:

Chapter 4

For the immunological synapse work, Chris Willberg and Jonathan Webber sorted the labelled MAIT cells by FACS. Hila Novak constructed the artificial bilayers, performed the TIRF microscopy and analysed the TIRFM images.

Chapter 5

James Ussher devised the E. coli antibody blockade experiment. Nazneen Siddiqui and Ann-Kathrin Reuschl provided help for the growth of Mycobacterium tuberculosis. Nazneen Siddiqui provided antibody titrations.

Chapter 6

Onn-Min Kon and Hannah Jarvis performed EBUS sampling. Hannah Jarvis, Sam Bremang, Hiromi Uzu and Helen Piotrowski took blood and sought patient consent. Sam Bremang collated patient demographic, diagnostic and other clinical information. Heather Lambie, Mica Tolosa-Wright and Aime Boakye processed blood. Chris Willberg and Alba Llibre provided the tonsillar tissue data.

Overview

List of Figures **xvii**

List of Tables **xxi**

List of Abbreviations **xxiii**

1 MAIT cells: Innate-like lymphocytes, responsive to microbes **1**
1.1 Introduction . . . 2
1.2 Innate, adaptive & unconventional immunity . . . 3
1.3 Interleukins-12 and -18 . . . 7
1.4 MHC class-I related molecule . . . 11
1.5 $CD161^{++}$/MAIT cells . . . 16
1.6 Tuberculosis . . . 28
1.7 Hypotheses . . . 37

2 Materials and Methods **39**
2.1 Reagents . . . 40
2.2 Cells . . . 43
2.3 Cytometric data acquisition and analysis . . . 46

3 IL-12, IL-18 and TCR stimulation of MAIT cells **49**
3.1 Introduction . . . 50
3.2 Chapter specific materials & methods . . . 54
3.3 Co-stimulation by IL-12, IL-18 & the TCR . . . 55
3.4 IL-12/-18 dose response & TCR stimulation . . . 62
3.5 Kinetics of the IL-12/18 and TCR responses . . . 76
3.6 Discussion . . . 90

4 Role of the immunological synapse in MAIT cell activation **101**
4.1 Introduction . . . 102
4.2 Chapter specific materials & methods . . . 106
4.3 Contact dependence of MAIT cell response . . . 109
4.4 Development of immunological synapse assay . . . 120
4.5 Discussion . . . 132

5 IL-12/-18 and MR1 in MAIT cell activation by bacteria 139
5.1 Introduction . . . 140
5.2 Chapter specific materials & methods . . . 144
5.3 Mechanisms of activation by bacteria . . . 147
5.4 Activation & response to live, virulent *Mtb* . . . 160
5.5 Discussion . . . 168

6 MAIT cells in sarcoid and tuberculous lymphadenopathy 177
6.1 Introduction . . . 178
6.2 Chapter specific materials & methods . . . 182
6.3 Flow cytometry analysis of PBMC and ITLN . . . 188
6.4 Imaging of MAIT cells by chip-cytometry . . . 198
6.5 Discussion . . . 210

7 Discussion 223
7.1 Activation of MAIT cells . . . 224
7.2 The role of MAIT cells in tuberculosis . . . 232
7.3 Summary . . . 247

Appendices

A BioLegend catalogue screen for PFA-stable epitopes 251

B Re-analysis of EBUS data with strict inclusion criteria 281

C Representative FACS gating and purity test 285

D Publications, presentations and awards 289

References 301

Contents

List of Figures **xvii**

List of Tables **xxi**

List of Abbreviations **xxiii**

1 MAIT cells: Innate-like lymphocytes, responsive to microbes **1**
1.1 Introduction . . . 2
1.2 Innate, adaptive & unconventional immunity . . . 3
1.2.1 MHC molecules display peptides, lipids and vitamins . . . 5
1.3 Interleukins-12 and -18 . . . 7
1.3.1 IL-12 + IL-18 synergise for IFNγ induction . . . 8
1.4 MHC class-I related molecule . . . 11
1.4.1 MR1 presents antigens from vitamin B_2 biosynthesis . . . 12
1.4.2 MR1 antigen processing and presentation pathway . . . 15
1.5 $CD161^{++}$/MAIT cells . . . 16
1.5.1 The development of MAIT cells begins in the thymus . . . 17
1.5.2 $CD161^{++}$ $CD8^{+}$ T cells include the MAIT cell subset . . . 19
1.5.3 Human MAIT cell phenotype and effector functions . . . 21
1.5.4 MAIT cells in infection, inflammation and disease . . . 25
1.6 Tuberculosis . . . 28
1.6.1 Immunopathological cycle during tuberculosis . . . 29
1.6.2 Induction of T cells, and their role in controlling *Mtb* . . . 31
1.6.3 The activation and role of MAIT cells in tuberculosis . . . 35
1.7 Hypotheses . . . 37

2 Materials and Methods **39**
2.1 Reagents . . . 40
2.1.1 Media and Buffers . . . 40
2.1.2 Antibodies . . . 41
2.2 Cells . . . 43
2.2.1 Bacterial cells . . . 43
2.2.2 Human cells and cell lines . . . 44

2.2.3 Isolation of human cells 44
2.3 Cytometric data acquisition and analysis 46
2.3.1 Flow cytometry 46
2.3.2 Chip cytometry 46
2.3.3 Statistical analysis 48

3 IL-12, IL-18 and TCR stimulation of MAIT cells 49
3.1 Introduction 50
3.1.1 *In vitro* investigations of MAIT cell activating signals 50
3.1.2 Chapter hypothesis and aims 52
3.2 Chapter specific materials & methods 54
3.2.1 Activation of CD8α^+ T cells 54
3.2.2 Statistical analyses 55
3.3 Co-stimulation by IL-12, IL-18 & the TCR 55
3.3.1 IL-12/-18 permits robust MAIT IFNγ expression 58
3.3.2 TCR signalling important for MAIT cell TNFα/CD69 60
3.4 IL-12/-18 dose response & TCR stimulation 62
3.4.1 Biphasic IFNγ-response to IL-12/-18 + TCR beads 63
3.4.2 CD161-expression & the dose-response to IL-12/-18 68
3.5 Kinetics of the IL-12/18 and TCR responses 76
3.5.1 Sustained TCR-stimulation increases IFNγ^+ (%) 76
3.5.2 TCR-stimulation leads to rapid TNFα-expression 78
3.5.3 Robust TCR responses require cytokine pre-exposure 85
3.5.4 TCR pre-stimulation enables cytokine-only response 87
3.6 Discussion 90
3.6.1 High & low thresholds for MAIT cell IFNγ-expression 90
3.6.2 MAIT cell expression of TNFα is rapid and transient 93
3.6.3 CD69 is a poor marker of rapid MAIT cell activation 94
3.6.4 MAIT vs. conventional CD8$^+$ T cell responses 96
3.6.5 Conclusions 98

4 Role of the immunological synapse in MAIT cell activation 101
4.1 Introduction 102
4.1.1 Structure and function of the immunological synapse 103
4.1.2 Chapter hypothesis and aims 105
4.2 Chapter specific materials & methods 106
4.2.1 Contact dependency of MAIT cell activation 106
4.2.2 Cytokine-mediated proliferation of MAIT cells 107
4.2.3 Assessment of the MAIT cell immunological synapse 108
4.3 Contact dependence of MAIT cell response 109

4.3.1 Cell-contact dependence for IFNγ/TNFα induction 111
4.3.2 Soluble mediators are sufficient for CD69 induction 113
4.3.3 TCR beads fail to reproduce APC–MAIT cell contact 115
4.4 Development of immunological synapse assay 120
4.4.1 MAIT cell FACS isolation and IL-15 expansion 123
4.4.2 TIRF microscopy of MAIT cell synapse formation 125
4.5 Discussion 132
4.5.1 Requirement for contact varies by MAIT function 132
4.5.2 IL-15 + β-Me enables MAIT cell expansion *in vitro* 134
4.5.3 Uniform surface distribution of MAIT cell IL-18Rα 135
4.5.4 Conclusions 136

5 IL-12/-18 and MR1 in MAIT cell activation by bacteria 139
5.1 Introduction 140
5.1.1 Summary and chapter aims 143
5.2 Chapter specific materials & methods 144
5.2.1 THP1 bacterial co-cultures with antibody blockade 144
5.2.2 Anti-mycobacterial assay and cytokine analysis 145
5.3 Mechanisms of activation by bacteria 147
5.3.1 Response to PFA fixed-*E. coli* and live *M. bovis* BCG 149
5.3.2 IL-12, IL-18 and MR1-dependent activation by BCG 153
5.4 Activation & response to live, virulent *Mtb* 160
5.4.1 Anti-mycobacterial effect of primary human MAITs 165
5.5 Discussion 168
5.5.1 MR1-signal is necessary for *Mtb*/BCG-induced TNFα 169
5.5.2 BCG/*Mtb* do not down-regulate the MAIT cell TCR 170
5.5.3 Anti-*Mtb* function of primary, human MAIT cells 172
5.5.4 Conclusions 173

6 MAIT cells in sarcoid and tuberculous lymphadenopathy 177
6.1 Introduction 178
6.1.1 Intrathoracic lymphadenopathy 178
6.1.2 Summary and chapter aims 181
6.2 Chapter specific materials & methods 182
6.2.1 Isolation of cells from TB and sarcoidosis patients 182
6.2.2 Case definitions and clinical characteristics 184
6.2.3 FACS screen for PFA-fixation compatible antibodies 186
6.3 Flow cytometry analysis of PBMC and ITLN 188
6.3.1 Activation status of MAIT cells in lymph node TB 190
6.3.2 Increased $CD4^+$ MAIT cells in sarcoidosis 192

6.3.3 Clinical features of high MAIT cell frequency in ITLN . . . 195
6.4 Imaging of MAIT cells by chip-cytometry . . . 198
6.4.1 Identification of chip-cytometry compatible mAbs . . . 198
6.4.2 Analysis of LNTB patient samples by chip-cytometry . . . 204
6.5 Discussion . . . 210
6.5.1 MAIT cells in lymphatic tuberculosis and sarcoidosis . . . 210
6.5.2 Chip cytometry for the assessment of EBUS-TBNA . . . 219
6.5.3 Conclusions . . . 221

7 Discussion **223**
7.1 Activation of MAIT cells . . . 224
7.1.1 MAIT activation signals vary by effector function . . . 225
7.1.2 MAIT cells exhibit several levels of activation . . . 226
7.1.3 MAIT cell 'bystander' activation? . . . 229
7.2 The role of MAIT cells in tuberculosis . . . 232
7.2.1 MAIT cells in TB may require IL-12/-18 and MR1 . . . 233
7.2.2 MAIT cells in tuberculous and sarcoid lymphadenitis . . . 235
7.2.3 Caveats . . . 238
7.2.4 Future perspectives . . . 241
7.3 Summary . . . 247

Appendices

A BioLegend catalogue screen for PFA-stable epitopes **251**

B Re-analysis of EBUS data with strict inclusion criteria **281**

C Representative FACS gating and purity test **285**

D Publications, presentations and awards **289**

References **301**

List of Figures

1.1 Conventional and unconventional T cell response times 4
1.2 MR1 antigens 13

2.1 Representative gating strategy for identification of CD161^{++}/MAIT cells 47

3.1 TCR beads + IL-12/-18 stimulation schematic 56
3.2 Activation-induced down-regulation of the Vα7.2^{+} TCR 57
3.3 IFNγ induction by IL-12 and IL-18 ± TCR stimulation 59
3.4 TNFα induction and CD69 up-regulation by IL-12 and IL-18 ± TCR stimulation 61
3.5 Two-fold dose titration of IL-12/-18 ± TCR beads 63
3.6 Four-fold dose titration of IL-12 and IL-12/-18 ± TCR beads 64
3.7 CD8α^{+} T cell IFNγ response to IL-12/-18 varies with dose according to CD161 expression 69
3.8 Biphasic IL-12/-18 induced down-regulation of Vα7.2 TCR 74
3.9 Sustained TCR stimulation enhances frequency of IFNγ-expressing CD161^{++}/MAIT cells 77
3.10 Sustained TCR stimulation of cytokine-activated MAIT cells reduces TNFα production 79
3.11 Sustained TCR stimulation of CD161^{++}/MAIT cells enhances CD69α production 81
3.12 MAIT cell Vα7.2 TCR downregulation requires sustained TCR signalling 84
3.13 Sustained IL-12/-18 exposure enhances rapid TCR driven TNFα-expression 86
3.14 TCR pre-stimulation licenses for a subsequent TCR-independent response 89

4.1 Model of the organisation of the immunological synapse 104
4.2 Preliminary transwell inhibition of CD161^{++}/MAIT cell activation by *E. coli* 110
4.3 Transwell inhibition of CD161^{++}/MAIT cell activation by *E. coli* . 111

4.4 Robust CD69-induction by soluble-mediators in response to bacteria 114
4.5 Partial recovery of contact-dependent CD161^{++}/MAIT activation using TCR beads 116
4.6 Only partial downregulation of CD161^{++}/MAIT cell TCR by transwell separated THP1 cells + *E. coli* 117
4.7 Test of cytokine mediated CD8α^{+} T cell proliferation 121
4.8 IL-15 and β-Me effectively induce MAIT cell expansion 124
4.9 MAIT cell immunological synapse formation 126
4.10 CD161 appears excluded from the pSMAC 127
4.11 IL-18Rα is present at the MAIT cell–bilayer synaptic interface . . . 128
4.12 MAIT cell IL-18Rα expression at the bilayer interface does not require TCR ligation 129

5.1 IL-12/-18 dependent activation of CD161^{++}/MAIT cells by *E. coli* 148
5.2 The CD161^{++}/MAIT cell responses to PFA-fixed *E. coli* and live BCG show qualitative differences 150
5.3 IL-12, IL-18 and MR1 are each important in the CD161^{++}/MAIT cell IFNγ response to live *M. bovis* BCG 154
5.4 Neither IL-12, IL-18, nor MR1 are necessary for CD161^{++}/MAIT cell CD69 response to live *M. bovis* BCG 155
5.5 MR1, but not IL-12/-18 is essential for the CD161^{++}/MAIT cell TNFα response to live *M. bovis* BCG 158
5.6 IL-12/-18 and MR1 are each important in the CD161^{++}/MAIT cell IFNγ response to live *M. tuberculosis* H37Rv 161
5.7 CD161^{++}/MAIT cell degranulation in response to live *Mtb* H37Rv is partially resistant to MR1-blockade 163
5.8 Most *M. tuberculosis* reactive CD161^{++}/MAIT cells are detected by TNFα production early, and CD107a capture late 164
5.9 MAIT cells reduce intracellular *M. tuberculosis* viability 166

6.1 Flow chart for intrathoracic lymphadenopathy patient recruitment . 184
6.2 MAIT cells are depleted in the blood of sarcoidosis, but not LNTB patients 189
6.3 MAIT cells express increased CD69 in blood and lymph nodes, in patients with intrathoracic lymphadenopathy 191
6.4 Increased usage of the CD4 co-receptor by MAIT cells in sarcoidosis patients with intrathoracic lymphadenpathy 193
6.5 High MAIT cell frequency in the ITLN is associated with high circulating frequency 195

6.6 Identification of PFA-stable activation markers expressed on MAIT cells . . . 199
6.7 CD25, CD69 and CD71 are expressed by MAIT cells in response to bacterial stimulation . . . 202
6.8 Imaging of MAIT cells by chip cytometry . . . 205
6.9 Identification of $CD8^+$ T cell activation markers by chip cytometry 207
6.10 Assessment by chip cytometry of MAIT cell activation in blood and the ITLNs of LNTB patients . . . 208

7.1 Modes of IL-12/-18 dependent IFNγ-expression by MAIT cells . . . 227
7.2 Modes of TCR and IL-12/-18 dependent TNFα-expression by MAIT cells . . . 228
7.3 TCR ligation may license MAIT cells for cytokine-only activation by viruses . . . 231
7.4 Future perspectives relating to MAIT cell activation by *Mtb* . . . 242

A.1 MAIT cell IL-18Rα expression at the bilayer interface does not require TCR ligation . . . 252

B.1 MAIT cell EBUS data reanalysed without one LTBI individual in the LNTB group . . . 282
B.2 MAIT cell EBUS data reanalysed without 5 *Mtb*-culture negative individuals in the LNTB group . . . 283

C.1 Representative gating strategy for sort purification of MAIT cells . 286
C.2 Representative purity assessment following MAIT cell sort . . . 287

List of Tables

1.1 Circulating frequency, co-receptor usage and restricting molecules of major unconventional T cells 5
1.2 MAIT cell depletion and enrichment as reported in various disease states 27

2.1 List of antibodies used 41

6.1 Demographic information for lymphadenopathy patients, and healthy controls 185
6.2 Features compared between low and high MAIT cell frequencies in the ITLN of patients with LNTB or sarcoidosis 196
6.3 Test of PFA-fixation compatible antibodies for detection of $CD8^+$ T cell activation markers 200

List of Abbreviations

AAV . . . . . ANCA associated vasculitis

ABCB1 . . . . . ATP-binding cassette sub-family B member 1

AC . . . . . Acute cholecystitis

Ac-6-FP . . . . . Acetyl-6-formyl pterin

AF . . . . . AlexaFluor

Ag . . . . . Antigen

AICL . . . . . Activation-induced C-type lectin

AIM2 . . . . . Absent in melanoma 2

ANCA . . . . . Associated with anti-neutrophil cytoplasmic autoantibodies

ANOVA . . . . . Analysis of variance

AP-1 . . . . . Activator protein 1

APC . . . . . Antigen presenting cell

AS . . . . . Ankylosing spondylitis

BAL . . . . . Bronchoalveolar lavage

BCR . . . . . B cell receptor

BEAS-2B . . . . . Human bronchial epithelial cell line

BFA . . . . . Brefeldin A

BSL3 . . . . . Biosafety Level 3

BpC . . . . . Bacteria per cell

Btn . . . . . Butyrophilin

β_2m β2-microglobulin

CBA . . . . . Cytometric Bead Array

CC . . . . . Chip cytometry

CF . . . . . Cystic fibrosis

CFU . . . . . Colony forming units

CLR . . . . . C-type lectin-like receptor

CMV . . . . . Cytomegalovirus

CNS . . . . . Central nervous system

COPD . . . . . Chronic obstructive pulmonary disease

cSMAC . . . . . Central SMAC

cTEC . . . . . Cortical thymic epithelial cell

CTL . . . . . Cytotoxic T lymphocyte

DAMP . . . . . Damage associated molecular pattern

DENV . . . . . Dengue virus

DH . . . . . Dermatitis herpetiformis

DIC . . . . . Differential interference contrast

DP . . . . . Double-positive

DN . . . . . Double-negative

DMSO . . . . . Dimethyl sulfoxide

DOPC 1,2 dioleoyl-sn-glycero-3-phosphatidylcholine

dSMAC . . . . . Distal SMAC

EBUS . . . . . Endobronchial ultrasound

EBUS-TBNA . . . EBUS-guided transbronchial needle aspiration

E. coli . . . . . *Escherichia coli*

EDTA . . . . . Ethylenediaminetetraacetic acid

ELISA . . . . . Enzyme-linked immunosorbent assay

Eomes . . . . . Eomesodermin

ER . . . . . Endoplasmic reticulum

FACS . . . . . Fluorescence-activated cell sorting

FC . . . . . Flow cytometry

FCS . . . . . Fetal calf serum

FM . . . . . Fibromyalgia

FSC . . . . . Forward scatter

Grz . . . . . Granzyme

GM-CSF . . . . . Granulocyte-macrophage colony-stimulating factor

GMFI . . . . . Geometric mean fluorescence intensity

HAART . . . . . Highly active antiretroviral therapy
HCV . . . . . Hepatitis C virus
HD . . . . . Haemodialysis
HIV . . . . . Human immunodeficiency virus
hMR1 . . . . . Human MR1
IBD . . . . . Inflammatory bowel disease
ICS . . . . . Intracellular cytokine staining
IFN . . . . . Interferon
Ii . . . . . Invariant chain
IL . . . . . Interleukin
ILL . . . . . Innate-like lymphocyte
iNKT cell . . . . . Invariant natural killer T cell
IQR . . . . . Interquartile range
IRAK . . . . . IL-1R associated kinase
IRM . . . . . Internal reflectance microscopy
ITLN . . . . . Intrathoracic lymph node
JAK . . . . . Janus kinase
LB . . . . . Luria-Bertani
LLT1 . . . . . Lectin-like transcript-1
LM . . . . . Listeria monocytogenes
LN . . . . . Lymph node
LNTB . . . . . Lymph node TB
LP . . . . . Lamina propria
LTBI . . . . . Latent tuberculosis infection
MAIT cell . . . . . Mucosal associated invariant T cell
MCMV . . . . . Murine cytomegalovirus
MDR-TB . . . . . Multi-drug resistant tuberculosis
MHC . . . . . Major histocompatability complex
MGIT . . . . . Mycobacterial Growth Indicator Tube
mMR1 . . . . . Murine MR1
MOI . . . . . Multiplicity of infection

MR1 . . . . . MHC class-I related molecule

MSMD . . . . . Mendelian susceptibility of mycobacterial disease

Mtb . . . . . *Mycobacterium tuberculosis*

MyD88 . . . . . Myeloid differentiation factor 88

NA . . . . . Numerical aperture

N.D. . . . . . No difference

NKC . . . . . NK gene complex

OADC . . . . . Oleic Acid Albumin Dextrose Catalase

OVA . . . . . Ovalbumin

PAMP . . . . . Pathogen associated molecular pattern

PBMC . . . . . Peripheral blood mononuclear cells

PBS . . . . . Phosphate buffered saline

PD-1 . . . . . Programmed cell death protein 1

PFA . . . . . Paraformaldehdye

PLC . . . . . Peptide loading complex

PLZF . . . . . Promyelocytic leukemia zinc finger

PMA . . . . . Phorbol myristate acetate

PRR . . . . . Pattern recognition receptor

pSMAC . . . . . Peripheral SMAC

RBC . . . . . Red blood cell

RD1 . . . . . Region of difference 1

RL-6-Me-7-OH . . 7-hydroxy-6-methyl-8-D-ribityllumazine

RL-6,7-diMe . . . 6,7-dimethyl-8-D-ribityllumazine

rRL-6-CH_2OH . . reduced 6-hydroxymethyl-8-D-ribityllumazine

RORC . . . . . Retinoic acid receptor-related orphan receptor-C

RORγt . . . . . Retinoic acid receptor-related orphan receptor-gamma

SA . . . . . Spondyloarthritis

SAP . . . . . SLAM-associated protein

SEM . . . . . Standard error of the mean

SI . . . . . Small intestine

SLAM . . . . . Signalling lymphocytic-activation molecule

SLE . . . . . Systemic lupus erythematosus

SMAC . . . . . Supramolecular activation complexes

SN . . . . . Supernatant

SSC . . . . . Side scatter

STAT . . . . . Signal transducer and activator of transcription

TAP . . . . . Transporter associated with antigen processing

TB . . . . . Tuberculosis

T_{CM} . . . . . T cell central memory

TCR . . . . . T cell receptor

T_{EM} . . . . . T cell effector-memory

T_{EMRA} . . . . . T cell terminally differentiated effector-memory

TGN . . . . . Trans-golgi network

T_H1 . . . . . T helper 1 cell

TIR . . . . . Toll-IL-1 receptor

TIRF . . . . . Total internal reflectance

TIRFM . . . . . TIRF microscopy

TLR . . . . . Toll-like receptor

TNF . . . . . Tumour necrosis factor

TRAIL . . . . . TNF- related apoptosis-inducing ligand

TRAF . . . . . TNF-associated factor

T2D . . . . . Type II diabetes

WHO . . . . . World Health Organisation

XDR-TB . . . . . Extensively drug-resistant tuberculosis

5-A-RU 5-amino-6-D-ribitylaminouracil

5-OE-RU . . . . . 5-(2-oxoethylideneamino)-6-D-ribitylaminouracil

5-OP-RU . . . . . 5-(2-oxopropylideneamino)-6-D-ribitylaminouracil

6-FP . . . . . 6 formylpterin

1

MAIT cells: Innate-like lymphocytes, responsive to microbes

Contents

1.1 Introduction 2
1.2 Innate, adaptive & unconventional immunity 3
1.2.1 MHC molecules display peptides, lipids and vitamins . . 5
1.3 Interleukins-12 and -18 7
1.3.1 IL-12 + IL-18 synergise for IFNγ induction 8
1.4 MHC class-I related molecule 11
1.4.1 MR1 presents antigens from vitamin B_2 biosynthesis . . 12
1.4.2 MR1 antigen processing and presentation pathway . . . 15
1.5 CD161^{++}/MAIT cells 16
1.5.1 The development of MAIT cells begins in the thymus . 17
1.5.2 CD161^{++} CD8^{+} T cells include the MAIT cell subset . 19
1.5.3 Human MAIT cell phenotype and effector functions . . 21
1.5.4 MAIT cells in infection, inflammation and disease . . . 25
1.6 Tuberculosis 28
1.6.1 Immunopathological cycle during tuberculosis 29
1.6.2 Induction of T cells, and their role in controlling *Mtb* . . 31
1.6.3 The activation and role of MAIT cells in tuberculosis . 35
1.7 Hypotheses 37

1.1 Introduction

A crucial role of the many cells that comprise the immune system is to protect us against pathogens. How they achieve this depends on their functional capacities, and pathogen detection capabilities. Innate cells such as macrophages, neutrophils and NK cells can participate in the immune response to infection without requiring prior exposure; whilst adaptive cells such as T and B lymphocytes develop with extraordinary diversity in their ability to detect pathogens, but which need to be selected for during infection. Characteristically, the small numbers of naïve T and B cells with specificity for a previously unseen pathogen can expand robustly during a primary infection, giving rise to a large number of effector cells as well as memory cells that can impart long-lasting protection.

The distinction between these types of immune cells however, has become increasingly blurred as a range of cells straddle the two [1, 2]. Mucosal associated invariant T (MAIT) cells are an 'innate-like lymphocyte', which are related closely to adaptive T cells in terms of their cell biology and early development, but demonstrate important features of innate cells — such as their abundance without the need for exposure to a specific pathogen.

This thesis will explore elements of the activation of MAIT cells by cytokine signals arising from innate detection of pathogens, the function of MAIT cells in response to pathogens and their role in disease. In particular, there is an emerging role for MAIT cells in tuberculosis (TB); a disease caused by *Mycobacterium tuberculosis* (*Mtb*) that is a significant burden to public health. The mechanisms of activation of MAIT cells will therefore be assessed, as will be the signals involved in their response to bacteria, including *Mtb* and their presence in TB patients at the site of disease. This introduction will focus on providing a suitable background, placing MAIT cells in the context of the wider immune system, what is known about their biology, their function *in vitro* and *in vivo*, and their emerging relevance to tuberculosis.

1.2 Innate, adaptive & unconventional immunity

The ability of certain cells to respond innately to pathogens frequently stems from pathogen detection capabilities that are hardwired into the germline, as in the case of pattern recognition receptors (PRRs). Pattern-recognition targets the most conserved pathogen and damage associated molecular patterns (PAMPs and DAMPs), providing a rapid basis for distinguishing the presence of self from non-self [3, 4]. In this way, cells of the innate immune system can act as sentinels

providing signals for the induction of adaptive immunity, and can attempt to eliminate pathogens early, prior to the formation of infectious focii. Targeting of highly conserved PAMPs renders adaptation costly — although PRRs are the subject of numerous examples of immune evasion and subversion strategies [5, 6]. Commensal microorganisms are sources of molecular patterns indistinguishable to those of pathogens, and therefore the response to PAMPs and DAMPs must be carefully regulated to avoid chronic inflammation [7].

By contrast, the ability of T and B cells to detect and response to pathogens stems from their somatically generated and specifically selected T and B cell receptors (TCRs and BCRs, respectively). TCRs and BCRs are formed by V(D)J recombination and selected on the basis of sensitivity and specificity for antigen (Ag). TCRs are heterodimers formed of either α and β, or γ and δ chains — with each a result of the V(D)J recombination events that occur during naïve T cell development within the thymus. While BCRs can bind directly to Ag [8, 9], TCRs of conventional $CD4^+$ or $CD8^+$ T cells recognise peptide antigens presented by major histocompatability complex (MHC) proteins, expressed on the surface of professional and non-professional antigen presenting cells (APCs) [10]. V(D)J recombination enables the generation of large number of unique receptors demonstrating extraordinary diversity [11]. However, prior to clonal expansion of T and B cells there must first be exposure to pathogen, which results in a lag period before adaptive immunity can be induced.

Unconventional (innate-like) lymphocytes express T or B cell receptors, but in contrast to conventional adaptive lymphocytes, are poised to respond to a range of pathogens through the detection of conserved molecules that resemble PAMPs. Invariant NKT (iNKT) and MAIT cells are αβ lineage T cells, which in humans express semi-invariant TCRα chains formed of Vα24-Jα18 and Vα7.2-Jα12/20/33, respectively, with limited TCRβ chains [12, 13]. Unlike conventional T cells which undergo selection mediated by cortical thymic epithelial cells (cTECs) presenting self-peptide MHC complexes [14], positive selection of iNKT and MAIT cells is mediated via their semi-invariant TCRs by $CD4^+CD8^+$ (double-positive; DP) thymocytes expressing CD1d or MHC class I-related protein (MR1), respectively [15, 16]. During T cell ontogeny, rearrangement of TCRγ and TCRδ chains also occurs in concert with TCRβ rearrangement. If functional TCRγδ expression occurs before the expression of a functional TCRβ–pre-TCRα pairing, the result is a γδ, rather than αβ lineage T cell [17, 18].

[1]Figure adapted from: *Godfrey DI, Uldrich AP, McCluskey J, Rossjohn J, Moody DB: The burgeoning family of unconventional T cells. Nat. Immunol. 2015, 16:1114–23* [19].

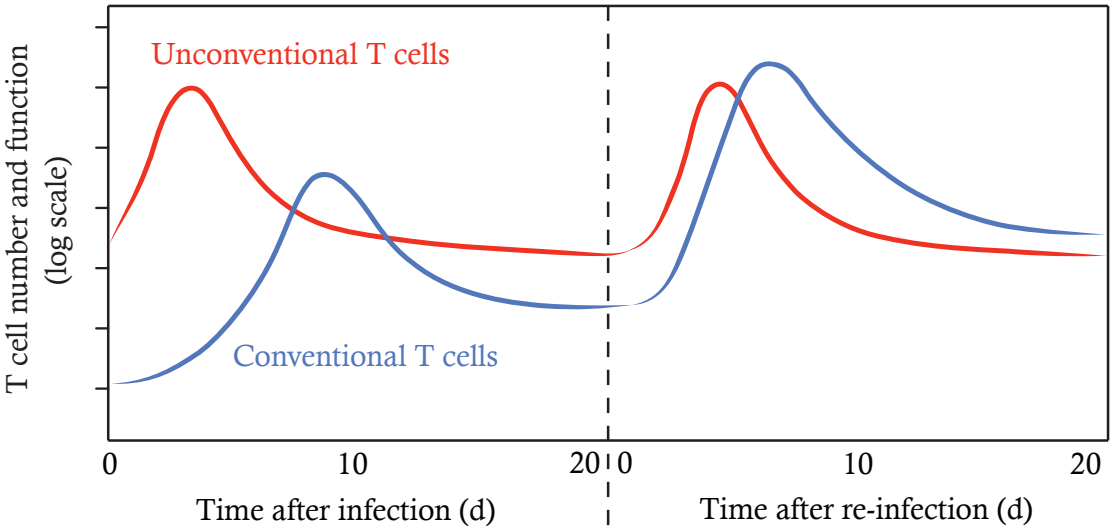


Figure 1.1: Conventional and unconventional T cell response times. Antigen-specific T cells are initially negligible in number, but expand robustly following T cell priming with a characteristic lag phase. Memory cells, however, remain following resolution of infection for a rapid recall in the event of a subsequent re-infection. Unconventional T cells are able to mount a rapid response to an infection without prior exposure in the absence of a lag period, as they already exist in relatively large numbers. These numbers remain approximately consistent in the event of future re-infection.[1]

As a result of their distinct developmental pathways and recognition of conserved non-peptide antigens, iNKT, MAIT and γδ T cells broadly share an innate-effector memory phenotype, with their abundance — particularly of MAIT and γδ T cells (see Table 1.1) — enabling them to bridge the kinetics and capacities of the innate and adaptive arms of the immune response. Thus they may play an important role at the first stages of infection, prior to induction of the adaptive immune response.

Table 1.1: Circulating frequency, co-receptor usage and restricting molecules of major unconventional T cells. Frequencies given as an approximate percentage of T cells in the peripheral blood, and vary considerably between mouse and man. Btn, butyrophilin. Table adapted from [19].

		iNKT cells	MAIT cells	γδ T cells
Frequency	Humans	0.1%	5%	5%
	Mice	1%	0.1%	1%
Co-receptor	Major	$CD4^+$	$CD8^+$	$CD4^-CD8^-$
	Minor	$CD4^-CD8^-$	$CD4^-CD8^-$	$CD8^+$
	Rare	$CD8^+$	$CD4^+$	$CD4^+$
Restricted by		CD1d	MR1	CD1c,d; Btn

1.2.1 MHC molecules display peptides, lipids and vitamins

Classical MHC molecules are highly polymorphic and of two classes [20, 21]. MHC class II is a heterodimer comprised by two transmembrane chains; each possessing membrane proximal, and distal domains [22]. The MHC class II peptide binding groove is formed by the membrane distal domains of each chain (α_1 and β_1), and largely presents peptide fragments to $CD4^+$ T cells derived following the lysosomal proteolysis of exogenous proteins internalised by endocytosis or phagocytosis [23], or cytosol and nuclear-derived material following autophagy [24].

By contrast, MHC class Ia molecules are heterodimers, with a three-domain transmembrane α chain, non-covalently bound to a membrane proximal β_2-microglobulin (β_2m) subunit [22]. The peptide-binding cleft is formed by anti-parallel α-helices (α_1 and α_2), which belong to the membrane distal α_1 and α_2 domains, respectively. Derived largely from intracellular degradation of cytosolic proteins by proteosomes, peptides are delivered into the endoplasmic reticulum (ER) by the transporter associated with antigen processing (TAP). Alternatively, retrotranslocation of exogenous antigens into the ER enables presentation of phagocytosis-derived antigen [23]. TAP is a constituent of the peptide loading complex (PLC) and facilitates peptide loading onto MHC class I for presentation to $CD8^+$ T cells that recognise this class of MHC. Additional components of the PLC include tapasin, calreticulin, ERp57, the MHC class I heavy chain and β_2m [23, 25].

1.2.1.1 MHC class Ib molecules can present a diverse range of antigens

In contrast to classical MHC class Ia, MHC class Ib molecules demonstrate limited polymorphism and together can present a diverse range of antigens to non-classical T cells. HLA-E, HLA-G and HFE are T cell interacting MHC-linked class Ib molecules, closely related to MHC class Ia. HLA-E and -G present peptides [26, 27], whilst HFE, with too narrow a groove, is considered to forego antigen binding for direct TCR ligation [28].

Other MHC class Ib molecules lie outside the MHC locus and can be considered more anciently diverged [25]. These include the CD1 family, able to present various lipids by virtue of hydrophobic pockets within the antigenic cleft, which can accommodate aliphatic hydrocarbons [29, 30]. CD1 molecules, like MHC class II, traffic through endocytic compartments, enabling access of endogenous and exogenous lipids. Lipid transfer proteins such as the saposins enable antigen loading onto CD1 molecules, and cell surface transit [31].

MR1, by contrast, possesses an antigen binding cleft composed of bulky and charged amino acids, occluding the binding of both peptide and lipid antigens. In

2012, MR1 was discovered to bind small molecules derived from the Vitamin B biosynthetic pathway of diverse microorganisms [30, 32]. The antigen processing pathway of MR1 is less well characterised relative to CD1, though MR1 resides largely intracellularly and traffics through endocytic compartments [33, 34]. Importantly, MR1 restricts the development and TCR dependent activation of MAIT cells, and will be introduced in greater detail in Section 1.4 (p. 11).

1.3 Interleukins-12 and -18

Following their exit from the thymus, naïve conventional T cells circulate between the blood stream and peripheral lymphoid organs in order to sample lymph nodes for signs of infection and the presence of cognate antigen [35]. Whilst TCR signalling and CD28 co-stimulation are sufficient for the activation of murine memory $CD8^+$ T cells, Curtsinger *et al.* established the resistance of naïve $CD8^+$ T cells to activation in the absence of a third-signal. This third-signal can be provided through exposure to IL-12 or type-I IFN — both signal transducer and activator of transcription (STAT) 4 inducers — enabling expansion and differentiation [36–38]. IL-12 mediated induction of Bcl-3 has been proposed to enhance $CD8^+$ T cell survival [39, 40], whilst induction of CD25 expression leads to pro-longed IL-2 sensitivity for sustained cell division [41–45].

IL-12 presence during initial antigen encounter is key for the avoidance of tolerance to subsequent re-stimulation [46] and for the generation of an effective $CD8^+$ T cell memory population [47]. During antigenic stimulation of naïve murine $CD8^+$ T cells *in vitro*, a large number of genes are up-regulated within 24 hours — however, the additional presence of IL-12 or IFNα is required to sustain expression over three days via histone-dependent chromatin remodelling [48].

The relative concentration of IL-12 during stimulation is also important for the dose-dependent induction of T-bet and repression of eomesodermin (Eomes) [49–51]. Whilst higher T-bet arising from increased IL-12 (and by extension, inflammation) can encourage the induction of short-lived effector cells, lower levels of IL-12 result in less T-bet — and cells exhibiting a greater propensity for long-lived memory [50].

Memory T cells can persist long-term following the initial expansion and subsequent contraction of the antigen-specific response to infection [52]. The response of memory $CD8^+$ T cells to TCR stimulation during re-infection includes rapid induction of effector functions such as cytolytic activity [36, 53, 54] and IFNγ production [55, 56]. However, phenotypic and functional heterogeneity exists within the $CD8^+$ memory T cell compartment. Cells exhibiting lymph-node homing

markers and with strong proliferative potential are designated central memory (T_{CM}), whilst those with the capacity to respond to chemokines and migrate to sites of tissue inflammation are designated effector memory (T_{EM}), or terminally-differentiated effector memory (T_{EMRA}). In human peripheral blood, $CD8^+$ T_{CM} cells are rarer than in lymph nodes, with the bulk of $CD8^+$ memory T cells composed of T_{EM} and T_{EMRA} [57]. $CD8^+$ T_{EM} cells are capable of rapid IFNγ-expression (within 5 hours) following stimulation with αCD3/CD28 beads, and can continue to express IFNγ following re-stimulation three or five days rest. By contrast, $T_{EMRA\ cells}$ are less responsive at 5 hours, and fail to express IFNγ following re-stimulation and are therefore functionally distinct [58].

1.3.1 IL-12 + IL-18 synergise for IFNγ induction

IL-12 can be expressed by phagocytic cells following PAMP detection, and through triggering T cell IFNγ can act as an important bridging molecule between innate and adaptive arms of the immune system [59]. IL-12 is a pro-inflammatory heterodimeric cytokine, detected by a heterodimeric receptor consisting of IL-12Rβ1 and IL-12Rβ2 chains. On binding IL-12p70, signalling proceeds through IL-12Rβ2 via the phosphorylation of associated janus kinases (JAKs). This results in phosphorylation of IL-12Rβ2, which in turn leads to the binding, activation and translocation to the nucleus of STAT4 [59].

IL-18 was initially described in 1989 as the IFNγ-inducing factor [60]. It is a pleiotropic cytokine, capable of enhancing Th1 and Th2 type responses [61, 62]. The IL-18R is heterodimeric, composed of IL-18Rα and IL-18Rβ chains. IL-18Rα can bind ligand independently — though with low affinity — whilst the recruitment of IL-18Rβ results in high-affinity binding. The association of both chains brings together Toll-IL-1 receptor (TIR) domains, allowing recruitment of myeloid differentiation factor 88 (MyD88). Signalling proceeds via the phosphorylation of four IL-1R-associated kinases (IRAKs) and oligomerisation of tumour necrosis factor–associated factor (TRAF) 6, leading to IκB degradation and activation of NF-κB [63]. IL-18 has also been shown to induce the serine-phosphorylation of c-Jun [64], a component of the transcription factor activator protein 1 (AP-1) that causes activation of the IFNγ-promoter [65].

Importantly, IL-18 synergises with IL-12 to induce IFNγ, shown first in anti-CD3 stimulated murine Th1 cells [66], and shortly after with enriched human T cells [67]. The mechanistic pathways underlying this synergy have not been fully determined, although there is evidence suggesting the importance of both IL-18 induced up-regulation of IL-12R [68] and IL-12 induced up-regulation of IL-18R

[69–71], with further reports noting increased expression of either or both IL-18R chains in a STAT4-dependent manner [72–75].

It is likely there is also physical cooperation between transcription factors. A model by Nakahira *et al.* proposed that IL-12 induced STAT4 is brought to the IFNγ-promoter following binding to IL-18-induced c-Jun, thereby faciliating IFNγ-expression [64]. Indeed, no response to IL-18 is observed in the absence of IL-12 by virus-specific murine $CD8^+$ T cells — despite the expression of IL-18Rα [76]. This suggests that expression or induction of IL-18Rα, is necessary but not sufficient for IFNγ expression — and given the resistance of IL-18Rα-expressing cells to respond to IL-18 alone [77, 78], unlikely to account in its entirety for the synergistic effects observed.

Responsiveness to IL-12 + IL-18 stimulation allows conventional — as well as innate — lymphoid cells to demonstrate innate-like behaviour [79]. Both NK cells and $CD8^+$ T cells responded in an IL-12 and IL-18 dependent manner to a murine *Burkholderia pseudomallei in vitro* infection model, and each can express IFNγ within 24 hours of exposure to recombinant IL-12 + IL-18 *ex vivo* [80].

Additionally, after initial exposure to Ovalbumin (OVA)-expressing Listeria monocytogenes (*Lm*), OVA-specific transgenic-TCR memory murine $CD8^+$ T cells expressed IFNγ within 8 hours of exposure to non-OVA expressing wild-type *Lm* [81]. Such antigen non-specific IFNγ expression had earlier been shown to protect $IFN\gamma^{-/-}$ mice from *Lm* infection, following adoptive transfer [82], demonstrating the ability of memory $CD8^+$ T cells to respond rapidly to infection via IL-12 and IL-18 in an innate-like manner — and identifying a protective role for non-antigen-specific IFNγ memory responses in mice [81, 82].

IFNγ-expression in response to IL-12 and IL-18 was shown in rested, but previously primed, murine Th1 cells [83]; and murine IL-12 + IL-18 responsive $CD8^+$ T cells (following overnight stimulation) were identified as $CD44^{hi}$ memory cells [84]. Similarly, purified human IL-18Rα$^+$ $CD45RO^+$ memory $CD4^+$ T cells could express IFNγ after 48 hours stimulation [85]. However, this contradicted some earlier reports whereby neither $CD4^+$ T cells from human bulk peripheral blood mononuclear cells (PBMC) [86, 87], nor human *in vitro* differentiated Th1 cell lines [88] responded to IL-12 and IL-18 alone, which had implied greater reliance on additional extra signals (TCR or cytokine) for IL-12 + IL-18 induction of IFNγ from human $CD4^+$ T cells.

Nonetheless, antigen-independent production of IFNγ by (relatively small subpopulations) of human $CD8^+$ T cells have also been observed [89–91]. In response to phorbol myristate acetate (PMA) and ionomycin stimulation, both

$CD4^+$ and $CD8^+$ human T cells from peripheral blood are capable of expressing type-I cytokines IFNγ, TNFα and the early activation marker CD69 [92], with antigen-specific IFNγ-production produced rapidly (within 6 hours) following re-stimulation [55]. However, the relative individual contributions of TCR, IL-12 and IL-18 signals to the induction of these effector-functions and their kinetics in effector-memory $CD8^+$ T cells remains unclear. Recently, we investigated the ability of bulk T cells from peripheral blood to respond to IL-12 + IL-18, and found that the main responding population are $CD8^+$ T cells expressing high levels of CD161 ($CD161^{++}$ $CD8^+$ T cells), which includes the MAIT cell population [93]. The influence of timing and TCR/IL-12/-18 signal integration on the threshold for activation of MAIT cells, MAIT cell effector functions induced, and strength and timing of the MAIT cell response will be assessed in this thesis.

1.4 MHC class-I related molecule

In 1995, Hashimoto *et al* reported their discovery of MR1 following a genomic screen attempting to identify MHC class I-related genes [94, 95]. *Mr1* gene fragments are present in marsupial (placental) but not monotreme (egg-laying) mammals, birds, reptiles, amphibia or teleost fish, indicating the likely emergence of MR1 in an evolutionary ancestor of placental mammals, approximately 160–220 million years ago [96].

In humans and mice, the MR1 sequence is highly conserved — α_1 and α_2 domains share 90% and 89% amino acid composition, respectively [97, 98]; whilst orangutan and chimpanzee *Mr1* genes exhibit 97.8% and 99.7% sequence homology with humans [99]. By comparison, human and bovine CD1b share 73% identity (85% for MR1), whilst human and mouse CD1d share 61% (90% for MR1) [100]. The predicted amino acid sequence of the α_1 and α_2 domains also revealed MR1 to be highly similar to classical MHC class I molecules in these putative ligand binding domains — more-so than other non-classical MHC divergent molecules, including the CD1 family [94]. However, unlike MHC class Ia, MR1 is non-polymorphic [101].

In 2003, the ability of murine MAIT cell hybridomas to respond directly to stimulation by murine MR1 (mMR1), and the requirement for MAIT cell expansion *in vivo* of MR1 and commensal gut flora, proved a link between the presence and activation of MAIT cells to the function of MR1 for the first time [102]. However, it remained unclear the extent to which MR1 functioned as an antigen presenting molecule. In characterising the rat *Mr1* gene, the deduced amino acid sequence appeared to contain the proper CD8 and β_2-microglobulin (β_2m) binding sites [103],

with further studies confirming stoichiometric association with β_2m [104, 105]. The generation of novel antibodies demonstrated the requirement for folded, ligand-bound MR1 for MAIT cell activation. Additionally, mutagenesis of MR1 within the MHC ligand binding region (A′ pocket) abrogated surface expression of folded MR1 and MAIT cell activation [106], consistent with the high degree of conservation of the MR1 ligand binding groove [96]. Together, these data argued strongly for an antigen presenting function of MR1, with the requirement for commensal bacteria for MAIT cell expansion suggesting a microbe-derived ligand for MR1.

1.4.1 MR1 presents antigens from vitamin B_2 biosynthesis

The nature of this ligand remained unknown, however. Co-immunoprecipitation experiments using human MR1 (hMR1) transfected HeLa cells, deduced a binding relationship with components of the PLC including TAP, hinting at a possible peptide ligand [105]. However, MAIT cells were present in TAP-deficient mice, arguing against a functional role for this association [102, 107], and MR1 surface expression and MAIT cell activation were not blocked by proteasome inhibitors [34, 108]. Following on from research identifying the ability of CD1d to present gylcosylceramides to iNKT cells [109], similar ligands — in particular α-mannosyl ceramide — were proposed to activate MAIT cells [110, 111].

In 2012, the Rossjohn and McCluskey groups attempted to refold MR1 in the presence of different candidate ligands — including lipid-based ligands such as had been suggested [111]. In doing so, they observed that RPMI-1640 media alone was, in fact, able to enhance MR1 refolding. By mass-spectrometry, they identified the RPMI-1640 derived ligand as 6-formylpterin (6-FP), a photodegradation product of folic acid (vitamin B_9) (Fig. 1.2 A). Subsequently, the crystal structure of MR1–6-FP was solved [32], identifying a novel category of antigen distinct from the peptides presented by MHC class I and II, and lipid/glycolipids by the CD1 family [32].

However, 6-FP was non-stimulatory for T cell lines transduced with the MAIT cell TCR (Jurkat.MAIT cells) [32]. MR1 refolding was therefore attepted in the presence of *Salmonella typhimurium* supernatant, which was able to activate Jurkat.MAIT cells. Mass spectrometry and additional functional assays revealed three ribityllumazines — riboflavin (vitamin B_2) derivatives that could activate MAIT cells: 7-hydroxy-6-methyl-8-D-ribityllumazine (RL-6-Me-7-OH), 6,7-dimethyl-8-D-ribityllumazine (RL-6,7-diMe), and reduced 6-hydroxymethyl-8-D-ribityllumazine (rRL-6-CH_2OH) [32] (Fig. 1.2 A).

[2]Figure adapted from: *McWilliam HE, Birkinshaw RW, Villadangos JA, McCluskey J, Rossjohn J: MR1 presentation of vitamin B-based metabolite ligands. Curr. Opin. Immunol. 2015* [112].

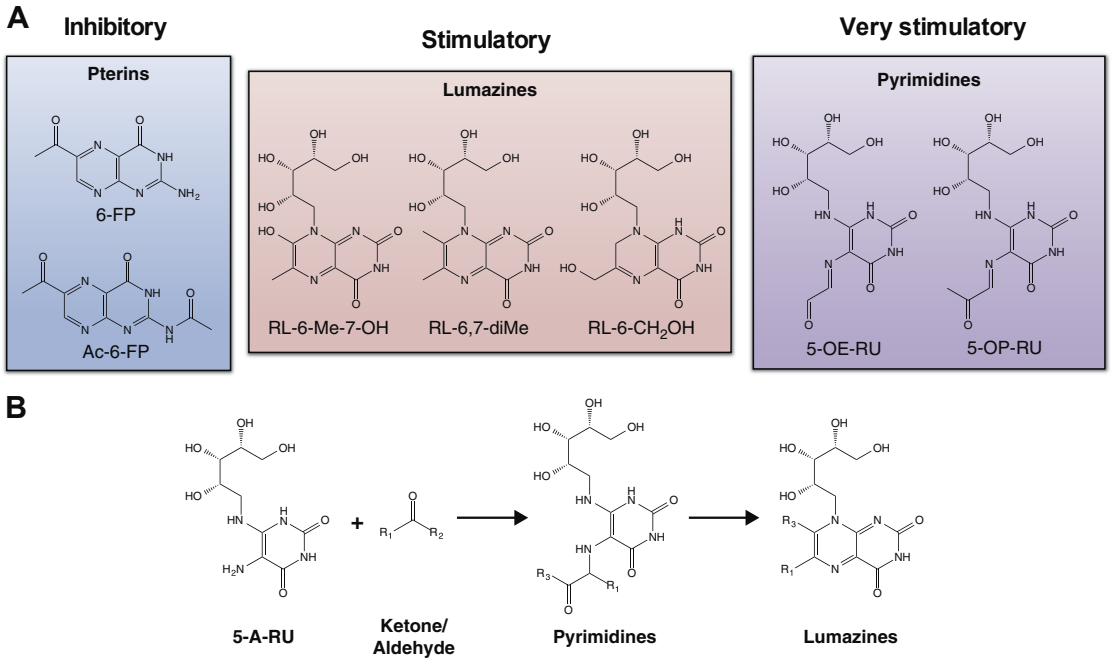


Figure 1.2: MR1 antigens. (A) Three classes of MR1 ligands have been identified thus far. The pterins are non-stimulatory, and therefore competitive inhibitors of MAIT cell activation. Ac-6-FP is a stronger inhibitor than 6-FP. The lumazines, and the pyrimidines shown are stimulatory — the pyrimidines exhibit stronger exogenous activation of MAIT cells. (B) 5-A-RU represents a key precursor to MAIT cell stimulatory MR1 ligands in the riboflavin biosynthesis pathway. Reaction with ketones or aldehydes derived from host or bacterial metabolic pathways leads to pyrimidine formation. The pyrimidines formed are unstable and condense to form lumazines in the absence of MR1 binding.[2]

Additional ligands have since been identified — acetyl-6-formylpterin (Ac-6-FP; Fig. 1.2 A) is non-stimulatory like 6-FP; but able to induce a greater and more sustained upregulation of MR1 expression with the additional acetyl moieity relative to 6-FP — and is a 100× more potent competitive inhibitor of MAIT cell activation [113]. Conversely, using a series of bacteria lacking riboflavin biosynthesis enzymes, 5-amino-6-D-ribitylaminouracil (5-A-RU) was identified as a key intermediate species that could give rise to more potent stimulatory ligands than the ribityllumazines identified so far. Whilst unable to active MAIT cells directly, 5-A-RU reacts with small glyoxal and methylglyoxal molecules (Fig. 1.2 B) that can be derived from ubiquitous host and microbial metabolic pathways, to form the chemically unstable pyrimidines 5-(2-oxopropylideneamino)-6-D-ribitylaminouracil (5-OP-RU) and 5-(2-oxoethylideneamino)-6-D-ribitylaminouracil (5-OE-RU) [112, 114].

Importantly, unlike 6-FP — the MR1 bound stimulatory antigens form direct contacts with the Tyr95 residue of the MAIT cell TCRα CDR3 region [115], whilst the pyrimidines are able to form additional contacts through the MAIT cell TCRβ

chain [114]. Under normal conditions pyrimidines condense quickly to form the less stimulatory ribityllumazine MR1 ligands (Fig. 1.2 B) — but interestingly MR1 binds and stabilises these 'transitory neo-antigen' pyrimidines derived from the combination of microbial and host metabolism, presenting them to MAIT cells for their activation [114].

1.4.2 MR1 antigen processing and presentation pathway

How the MR1 ligand is accessed by MR1, and the regulation of MR1 antigen presentation for MAIT cell activation is an active area of research. Despite the wide ranging expression of MR1 transcript [94, 98, 103], MR1 protein has been harder to observe. In particular, visualisation of MR1 at the cell surface has been rare, especially in non-transductant systems [34, 105, 116, 117]. However, culturing MR1-transfected cell lines at a reduced temperature enhanced detection of cell-surface MR1 (26°C) [108] — an experiment based on an earlier investigate of MHC class Ia [118] — and was proposed to indicate cell surface transit in the absence of antigen, but with low stability at body temperature [108]. This was consistent with the findings of Chua *et al.*, who were able to trap MR1 at the cell surface using antibodies that enhanced MAIT hybridoma activation [117].

MR1 resides largely within the ER [33, 34, 105, 119] under basal conditions in the absence of exogenous ligand [33]. Trafficking through endocytic compartments was indicated by early studies [34, 116], with the MHC class II chaperone the invariant chain (Ii) suggested to enhance MR1 surface expression and MAIT cell activation [34]. However, human bronchial epithelial cells (BEAS-2B) are able to activate MAIT cells, despite lacking Ii [119, 120].

More recently, it has been demonstrated that despite the ability of MR1 to access the cell surface at low levels in the absence of ligand, ER-resident MR1 can detect the presence of vitamin B antigens. This results in stabilisation and correct folding of the MR1-antigen complex, association with β_2m and egress from the ER for cell surface presentation [33]. Another study has argued for two modes of antigen processing and presentation, whereby exogenous ligand is loaded in the ER in a manner independent of VAMP4 and Rab6 — both of which are associated with the trans-golgi network (TGN)-endosome; whilst translocation of MR1 to the cell surface in response to *Mtb* derived ligands depended on both, indicating the importance of trafficking of MR1 through endocytic compartments for *Mtb* antigen presentation [119].

This is consistent with the observation that phagocytosis of intact paraformaldehyde (PFA)-fixed *E. coli* or *S. typhimurium* bacteria activated MAIT cells more efficiently than equivalent amounts of bacterial culture supernatant, or bacterial cell

lysates [121]. Furthermore, pre-activation of antigen presenting cells with TLR1, TLR2 or TLR6 agonists, with IFNα, or with IFNγ, enhanced the subsequent ability of THP1 antigen presenting cells to activate MAIT cells [121].

Together data from these reports suggest that MR1 resides largely intracellularly, within the endoplasmic reticulum and/or endocytic compartments [33, 119]. Sensing of exogenous ligand may occur primarily in the ER, allowing the correct folding and egress of MR1 to the cell surface — although some binding appears to take place on the cell surface [33, 119]. By contrast, intracellular infection with *Mtb* appears to require MR1 trafficking through the endosomes, suggesting alternative antigen processing pathways in response to exogenous antigen or intracellular infection [119]. Lastly, MR1 cell surface expression by cells expressing endogenous levels of MR1 appears to be tightly regulated — with intact bacteria and APC pre-activation able to enhance MR1 trafficking to the cell surface, leading to effective MAIT cell activation [121].

1.5 CD161^{++}/MAIT cells

Porcelli *et al.* first noticed an over-representation of two TCRα chains within CD4$^-$CD8$^-$ (double-negative; DN) T cells; Vα24-Jα18, used by iNKT cells, and Vα7.2-Jα33 [122]. Another study two years later found enhanced Vα7.2-Jα33 usage by CD8α$^+$ T cells as well [107, 123], with Vα7.2-Jα33 expressing cells identified in humans, mice and cattle. Their presence needed β_2-microglobulin — but not MHC class I or CD1, thereby indicating restriction by a distinct non-classical MHC class Ib molecule [107].

In 2003, Treiner *et al.* described Vα7.2-Jα33 TCR expressing cells in humans (and homologous Vα19-Jα33 in mice) as mucosal associated invariant T (MAIT) cells for the first time, on the basis of their preferential association with the gut lamina propria (LP) [102]. They were absent from germ free mice, as well as from mice or humans lacking B cells — indicating a requirement for B cells and commensal flora for their expansion [102]. Notably, MAIT cells were found to be restricted by a monomorphic major histocompatability complex class-I related molecule, MR1 [102].

In the following section, I will introduce the MAIT cell protein expression and tissue homing phenotype, discuss their development in the lymph nodes and periphery, and outline our current understanding of the role of MAIT cells in health and disease.

1.5.1 The development of MAIT cells begins in the thymus

MAIT cells are absent in nude mice [107] and present in the human thymus [124, 125] indicating passage through, and requirement for the thymus during ontogeny. Conventional T cells are selected on cTECs, presenting self-peptide MHC complexes [14]. MR1 is expressed by thymocytes in mice [117], and humans [126], and in contrast to conventional T cells, a murine transgenic study identified DP thymocytes as responsible for MAIT cell selection [16].

iNKT cells are similar to MAIT cells in many ways; they both express semi-invariant TCR repertoires restricted by MHC class Ib molecules, and are both dependent on the thymus and DP thymocytes for their development [15, 127]. Both iNKT and MAIT (but not γδ T) cells are absent from STAT3 [128] and RAR related orphan receptor C (RORC) [129] deficient individuals — and they both express the transcription factor promyelocytic leukemia zinc finger (PLZF) which drives the effector phenotype of iNKT cells [130, 131]. However, iNKT cells are dependent on signalling lymphocytic-activation molecule (SLAM) family member homotypic interactions between CD1d and Vα14^{+} DP cells, leading to recruitment of SLAM-associated protein (SAP), and signalling via Fyn and NF-κB [12, 132]. Patients lacking functional SAP completely lack iNKT [133], but not MAIT cells [124]. Indeed, unlike iNKT cells — which adopt a memory phenotype intrathymically [132] — MAIT cells exit the thymus as naïve cells [124]. Overall, these studies indicate divergent developmental pathways for iNKT and MAIT cells.

Despite their naïve phenotype and antigen-inexperience, MAIT cells in umbilical cord blood already express PLZF [125], high levels of CD161 and IL-18Rα [134] and demonstrate innate-effector functions in response to pathogens [126]. Maturation occurs within the secondary lymph nodes and peripheral mucosal sites, indicative of a step-wise developmental pathway [124, 125]. Data in support of this includes a phenotypic analysis of different second trimester human fetal tissues, in which CD161^{++} Vα7.2^{+} cells were identified as CD3$^{+/-}$ CD8αβ^{+} IL-18R^{-} PLZF^{lo} in the thymus, with PLZF expression initially occurring in the secondary lymphoid organs — and acquisition of a CD8αα^{+} CD45RO^{hi} IL-18Rα^{hi} PLZF^{hi} phenotype upon reaching the fetal small intestine, liver and lung [125]. These markers are also expressed by the wider cord blood CD161^{++} CD8^{+} T cell population [135] — however, the relative frequency of Vα7.2^{+} cells is low at this stage, suggesting that CD161 expression is developmentally pre-programmed, and occurs prior to the expansion of large numbers of clonotypic Vα7.2-Jα33 MAIT cells during infancy [136].

It was initially noted by Treiner *et al.* that MAIT cells are not present in germ free mice, or mice/human patients lacking B cells [102]. B cells have since been

shown to express MR1 in human intestinal mucosa [137] and to induce MAIT cell expansion in transgenic mice [124]. Reconstitution of germ-free mice with riboflavin producing bacteria also induces peripheral expansion of MAIT cells [138]. This indicates the expansion of MAIT cells in a manner dependent on both B cells and microbial colonisation. MAIT cells continue to increase in frequency during infancy and childhood, through to adulthood (30 years) — at which point numbers begin to decline over time [139].

Together, these findings indicate a developmental pathway for MAIT cells distinct from conventional and iNKT cells. Beginning in the thymus with MR1-dependent selection on DP thymocytes, MAIT cells subsequently mature within the peripheral lymphoid and mucosal sites, before microbial activation via MR1-expressing B cells in the periphery induces a population expansion — and with an eventual decline during middle and old age. Throughout much of life, this results in abundant MAIT cells that demonstrate broad specificity for microbes and an innate-effector/memory phenotype.

1.5.2 CD161^{++} CD8^{+} T cells include the MAIT cell subset

MAIT cells express high levels of CD161 [134], and as defined by MR1-tetramer staining, are mainly contained within the CD161^{++} CD8^{+} T cell subset [140], which conversely comprises approximately 90% Vα7.2 TCR-expressing cells [135]. CD161 is a homodimeric, type II transmembrane C-type (Ca^{2+}-dependent) lectin-like receptor (CLR) glycoprotein, initially cloned from an NK cell cDNA library [141]. The ligand for CD161 is lectin-like transcript-1 (LLT1) [142, 143], also a CLR, which shares structural homology with activation-induced C-type lectin (AICL) and CD69 [144]. Both CD161 and LLT1 are located in close proximity within the NK gene complex (NKC) [145].

Functionally, CD161 ligation on NK cells is considered inhibitory — both in terms of lytic activity [142, 143] and IFNγ-expression [142]. NK cell lysis of LLT1-expressing glioma cells was enhanced by siRNA interference of LLT1 [146], whilst degranulation/cytokine production was similarly enhanced by antibody blockade of LLT1 expression on Raji cells [147]. The function of CD161 on T cells is less clear; CD161 ligation on T cells has been suggested to permit transendothelial migration [148], to both enhance [136, 142] and diminish [147, 149] cytokine production, but not to affect degranulation/cytotoxicity [147, 149]. It is possible that using different antibody clones/methodologies has confounded these findings [150].

Despite limited expression by rodent cells, CD161 is expressed by approximately 90% of human NK cells and 25% of $\gamma\delta^{+}$ [151] and $\alpha\beta^{+}$ T cells [141]. CD161 was

found to identify developmentally distinct T cells — initially IL-17 producing CD4$^+$ T cells [152], later expanded to include IL-17 producing DN and CD8$^+$ T cells [153], all of which express retinoic acid receptor-related orphan receptor (ROR) C mRNA, which codes for the IL-17-driving transcription factor RORγt [153]. Indeed, transduction of CD4$^+$ T cells with RORC2 induced CD161, indicating a developmental link between the two [153]. CD161 expression is also linked to a population of IFNγ and IL-17 expressing FoxP3$^+$ CD4$^+$ Treg cells that can induce anergy in conventional T cells [154].

CD161 is expressed on CD8$^+$ T cells at both intermediate, and high levels [155]. It is the CD161^{++} CD8α$^+$ T cell subset that exhibits the strongest expression of markers associated with tissue homing and IL-17-expression, including RORγt, CCR2, CCR6, CXCR6 and IL-18Rα [156]. As well as CD161^{++} CD8$^+$ T cells [93], CD161$^{\text{int}}$ (but not CD161$^-$) CD8α+ T cells can also respond to IL-12 + IL-18, though less effectively [93, 136], reflecting a broad CD161-linked transcriptional profile, including expression of PLZF, RORγt, CCR6, CXCR6, MDR1, IL-12Rβ2 and IL-18Rα [136]. Importantly, both Vα7.2 expressing and non-expressing CD161^{++} CD8α$^+$ T cells express high levels of IL-18Rα and respond equivalently to IL-12/-18 stimulation [93]. Vα7.2$^-$ CD161^{++} CD8α$^+$ T cells were not activated in an MR1-dependent manner in response to fixed *E. coli* [136]; however another study has identified Vα7.2$^-$ MR1-restricted cells, which are capable of differentially recognising microbes [157].

1.5.3 Human MAIT cell phenotype and effector functions

MAIT cells can be identified by expression of their canonical semi-invariant Vα7.2 TCR [140], through which they're restricted by MR1 [102], and their expression high levels of CD161 [134]. They express mainly CD8αα or CD8αβ co-receptors, though DN and minor CD4$^+$ subpopulations have been identified [135, 140]. Additional markers expressed by circulating MAIT cells are consistent with an effector/memory differentiation phenotype (CD45RO$^+$ CD26$^{\text{hi}}$ CD27$^+$ CD28$^+$ CD95$^{\text{hi}}$). MAIT cells also express the multi-drug transporter ATP-binding cassette sub-family B member 1 (ABCB1), enabling the survival of chemotherapy [158], and implying xenobiotic efflux capacity [134, 159]. These, and a variety of additional cell surface proteins, effector proteins and transcription factors together define the MAIT cell phenotype.

1.5.3.1 MAIT cells express RORγt, PLZF, T-bet, Eomes and Helios

MAIT cells express RORγt [134, 135], a Th17 master transcription factor that induces CD161 expression [153], which they express at high-levels [134]. They also express PLZF (*ZBTB16*) [124, 125], which drives the effector phenotype of iNKT cells [130, 131], γδ T cells [160] as well as MAIT cells [130], and induces a memory phenotype in $CD4^+$ and $CD8^+$ T cells following ectopic expression [161]. PLZF is also essential for the development of MAIT cells, which are lacking in PLZF deficient mice [162]. Together, PLZF and RORγt co-expression can identify MAIT cells in peripheral blood [163].

Additionally, MAIT cells also express intermediate levels of T-bet [163] — a T-box transcription factor that controls IFNγ expression [164]; high levels of Eomesodermin (Eomes) [163] — a paralogue of T-bet required for $CD8^+$ T cell effector differentiation [165]; and intermediate levels of Helios [163] — a zinc-finger transcription factor that identifies T cell activation and proliferation [166]. Whilst T-bet is expressed at equivalent levels to conventional $CD8^+$ T cells; PLZF, RORγt, Eomes and Helios are each expressed more strongly by MAIT cells than either $CD4^+$ or $CD8^+$ conventional T cells [163]. On stimulation MAIT cells up-regulate T-bet [167], and express Blimp1 [168] — required for Granzyme (Grz) B expression, and the differentiation of $CD8^+$ T cells into cytotoxic effector cells [169].

1.5.3.2 MAIT cells display numerous cytokine receptors

Numerous cytokine receptors are expressed by MAIT cells, which can be detected as protein including IL-2Rβ^{int} [134], IL-7Rα [134, 170], IL-12Rβ1 [128], IL-18Rα [134, 135, 156], as well as IL-18Rβ and IL-23R that have been detected as transcripts [134, 135, 170] — and IL-2Rα [138], IL-2Rγ (common gamma chain) [171] and IL-15Rα [172] following activation.

The ability of MAIT cells to respond to stimulation via these receptors is an active area of investigation. In conjunction with TCR crosslinking, MAIT cells express increased IFNγ and IL-17A in response to IL-7 [170] and undergo enhanced proliferation in response to IL-12 [173] or IL-18 [167, 173], whilst the combination of IL-12 + IL-18 together with TCR crosslinking can induce MAIT cell expression of TNFα, CXCL10, CCL3 and CCL4 [173, 174]. Importantly, it has recently become clear that MAIT cells are capable of responding to certain cytokines independently of TCR crosslinking including IL-7 or IL-15, which can induce MAIT cell proliferation [173], increased perforin, GrzA, GrzB [170] and CD69 [175]; as well as IL-12 + IL-18, for which MAIT cells express IFNγ and are the main responding T cell subset [93]. How cytokine stimulation and TCR stimulation mutually regulate each other is not currently clear.

1.5.3.3 MAIT cells exhibit tropism for peripheral mucosal sites

Following the initial observation of MAIT TCR transcript enrichment within the gut LP [102], numerous studies have sought to characterise the blood, tissue and lymph node homing patterns of MAIT cells in health and disease. In peripheral blood, MAIT cells express a variety of chemokine receptors including CXCR4$^{+/-}$, CXCR6^{int}, CCR2^{+}, CCR5^{+}, CCR6^{+} and CCR9^{int} [124, 134, 176] as well as CD11a (part of LFA-1) [177] and α4β7 integrin [102, 178]. These markers are compatible with homing to numerous locations including peripheral tissues such as the lung, intestine and liver, and sites of inflammation [179].

Accordingly, in addition to their presence in blood where MAIT frequencies range between 1–10% of total T cells [138], they have been observed within numerous peripheral tissues and organs. MAIT cells are present throughout most of the length of the intestinal system [134], constituting approximately 60% of CD3^{+}CD4^{-} T cells in the jejunum [140], 1.5% of T cells in the ileum, 12% [180], 8.7% [181], and 0.1–16% [182] in the colon and 1.5% in the rectal mucosa [183]. The varying degrees of enrichment indicate preferential localisation to the early sections of the small intestine, though they may reflect methodological differences between studies [150]. MAIT cells also comprise up to 50% of T cells within the liver [134], 4–14% within adipose tissue [184], 0.4–10.5% in healthy skin dermis, 2.2–19.6% in epidermis [185], 1.6–5% within bronchial tissue [186], 1% in the endometrium and 1.8% in the cervix [187]. MAIT cells have been seen at similar frequencies in bone marrow and spleen to blood [173] and MAIT TCR transcripts have been observed in the kidney and ovaries [13]. The breadth of MAIT cell tissue homing patterns is suggestive of involvement in numerous infectious and inflammatory diseases at diverse anatomical locations.

1.5.3.4 MAIT cell cytolytic potential and cytokine-expression profile

On stimulation, MAIT cells can express surface markers of activation including IL-2Rα [138] and IL-2Rγ [171], which together with the basally expressed IL-2Rβ form the high-affinity IL-2R [188]. MAIT cells also express CD69 [138], which is considered to represent an immediate/early activation marker, undergoing up-regulation by T cells between 3–12 hours post-stimulation [189]. Functional roles of CD69 are still under investigation, but may include the inhibition of lymphocyte egress from secondary lymphoid organs [190] and immunoregulation [191, 192] with respect to intestinal inflammation [193] and/or the negative regulation of type-17 responses via galectin-1 — a recently identified CD69 ligand [194, 195].

MAIT cells can express interferon-γ (IFNγ), tumour necrosis factor-α (TNFα), IL-17A and IL-17F [93, 134, 170], each of which can exert numerous downstream

effects. For IFNγ, these include induction of anti-microbial effector functions, enhanced antigen processing and presentation, and the maturation/activation and differentiation of numerous cell subsets [196, 197]. In addition to cell death, TNFα is a robust inducer of NF-κB induction and can lead to the expression of pro-inflammatory cytokines and chemoattractants, as well as the induction of cell activation and differentiation [198]; whilst both IL-17A and IL-17F can similarly lead to expression of NF-κB, pro-inflammatory cytokines, numerous chemokines, acute phase response proteins, tissue remodelling proteins and anti-microbial peptides [199].

Granzymes are serine proteases, which on entering target cells can induce caspase-dependent/independent apoptosis. Entry of granzymes is largely dependent on the pore-forming capabilities of perforin [200], whilst a catalytic triad of serine, histidine and aspartic acid enable substrate cleavage. The target specificities are determined by differences in granzyme structures and only partially overlap, indicating divergent roles. GrzA and GrzK may exhibit more pro-inflammatory functions through triggering cytokine release and activation, whilst GrzB appears to correlate more closely to cytotoxicity [201, 202]. At rest, MAIT cells express GrzA, GrzK, but little GrzB or granulysin [163, 168]. Perforin may [163], or may not [168] be expressed by resting MAIT cells, with contradictory findings reported. Following MR1-mediated stimulation, however, MAIT cell GrzA and GrzK expression are diminished, whilst GrzB and perforin expression increased, indicating a switch to enhanced cytotoxic potential, consistent with an increase in Blimp1 expression [168]. The ability of MAIT cells to kill B cell lines exposed to fixed *E. coli* [168], and epithelial cell lines (HeLa) infected intracellularly with *Shigella flexneri* [149] has recently been demonstrated.

1.5.4 MAIT cells in infection, inflammation and disease

MAIT cells are capable of responding to TCR stimulation via MR1 [138], which presents antigens derived from riboflavin biosynthesis [32]. They can also respond to TCR-independent stimulation by cytokines such as IL-12 + IL-18 directly [93], or indirectly through TLR agonists such as LPS and ssRNA40 [93, 174, 203].

Phylogenetically diverse microorganisms possess the capacity to synthesise riboflavin, and therefore the capacity to activate MAIT cells via MR1. These include: Gram-negative bacteria — *Escherica coli*, *Pseudomonas aeroginosa*, *Klebsiella pneumoniae*, *Salmonella typhimurium*, *Shigella flexneri*; Gram positive bacteria — *Staphylococcus aureus* and *S. epidermis*; acid-fast mycobacteria — *Mycobacterium smegmatis*, *M. tuberculosis* and *M. abscessus*; and fungi — *Candida albicans*, *C.*

glabrata and *Saccharomyces cerevisiae* [32, 138, 149, 178, 204, 205]. As a result, MAIT cells are considered to be an important innate-like lymphocyte, widely responsive to microbes.

The capacity to respond to cytokines independently of TCR triggering, however, broadens the scope of MAIT cells to potentially contributing to the pathogenesis of chronic inflammatory and/or autoimmune disease. Additionally MAIT cells may contribute important functions during infection with bacteria lacking riboflavin biosynthetic pathways, or with viruses. Indeed, recently MAIT cells have been shown to be activated by dengue virus (DENV), hepatitis C (HCV) and influenza viruses in a TCR independent, IL-18 + IL-12/15/IFNα/β dependent manner — and supernatants from IL-12 + IL-18 stimulated MAIT cells were able to reduce HCV replication *in vitro*, potentially demonstrating a functional role for MAIT cells in viral infection [206].

1.5.4.1 MAIT cells are commonly depleted during pathogenesis

Whilst there are limitations for assessing the role of MAIT cells in human disease, peripheral blood represents an accessible and routinely accessed anatomical niche. As such, numerous studies have sought to characterise MAIT cell frequencies in the circulation during disease. Indeed, MAIT cells are depleted from the blood under a wide range of circumstances, including bacterial and viral infection [138, 175, 178, 183, 207–220], autoimmune diseases [156, 177, 180, 221–232], inflammatory diseases [184, 186, 233–237] and cancer [182, 238–241] (summarised in Table 1.2, p. 27).

In the context of autoimmunity, chronic inflammation and cancer, MAIT cells have also been found enriched at the site of disease/pathogenesis in numerous studies. Examples include multiple sclerosis, where MAIT cells accumulate within central nervous system lesions [221]; enrichment of MAIT cells within the synovial fluid in rheumatoid arthritis [226]; within the adipose tissue of obese adults and children [184] and an emerging role in the infiltration of tumours, such as colon cancer where they have been reported to express reduced IFNγ [182] (Table 1.2, p. 27).

In infectious disease, investigations identifying MAIT cell enrichment at the site of disease are currently lacking. Nonetheless, MAIT cells are depleted in the blood and enriched in the lungs and ascitic fluid of TB patients [178, 220, 244]. In addition, functional defects in circulating MAIT cells have been characterised, with increased exhaustion and decreased potential for cytokine production/cytotoxicity in TB [171, 207]; increased exhaustion, reduced CCR6 expression and reduced cytolytic potential in human immunodeficiency virus (HIV) infection [163, 209]; and reduced ability to respond to MR1 mediated stimulation in HCV infection [212].

Table 1.2: MAIT cell depletion and enrichment as reported in various disease states. Abbreviations: AAV—ANCA associated vasculitis; AC/SA/FM—Acute cholecystitis/Spondyloarthritis/Fibromyalgia; AS—Ankylosing spondylitis; CF—Cystic fibrosis; CNS—Central nervous system; COPD—Chronic obstructive pulmonary disease; DH—Dermatitis herpetiformis; HD—Haemodialysis; IBD—Inflammatory bowel disease; LN—Lymph node; N.D.—No difference; SI—Small intestine; SLE—Systemic lupus erythematosus; T2D—Type II diabetes. With reference to [242].

MAIT:	Depletion	Enrichment	Ref.
Infection			
TB	Blood	Lung/ascites	[138, 178, 207, 220]
Pneumopathy	Blood	—	[138]
HIV/AIDS	Blood/gut/LN	—	[175, 183, 208, 219]
HIV/TB	Blood	—	[209]
Chronic HCV	Blood	—	[210–212]
Acute HCV/HIV	Blood	—	[210]
Influenza (fatal)	Blood	—	[213]
Sepsis	Blood	—	[214]
CF + *P. aeruginosa*	Blood	—	[215]
Scrub typhus	Blood	—	[216]
Helicobacter pylori	Blood	N.D.	[217]
Cholera (children)	Blood	—	[218]
Autoimmunity			
Multiple sclerosis	Blood/N.D.	CNS/blood	[177, 221–225]
Psoriatic arthritis	—	Joints	[156]
Rheumatoid arthritis	Blood	Synovial fluid	[226, 227]
IBD	Blood/colon/SI	Inflamed mucosa	[180, 228, 229]
SLE	Blood	—	[226]
Coeliac disease	Blood, SI	—	[230]
AAV	Blood	—	[231]
Sjögren syndrome	Blood	Salivary gland	[232]
Inflammation			
DH	—	Lesional skin	[233]
Asthma	Blood/airways	—	[186]
T2D/obesity	Blood	Adipose tissue	[184]
AC/SA/FM	Blood	—	[234]
AS	Blood	Synovial fluid	[235, 236]
COPD	Blood	—	[237]
Transplant			
Kidney/HD	Blood	—	[243]
Cancer			
Kidney/brain	—	Tumours	[238]
Gastric/colon/lung	Blood	Colon cancer	[239]
Colorectal	Blood	Neoplasms	[182, 240, 241]

Evidence for the ability of MAIT cells to play a protective role has come from murine *in vivo* models of infection. Following infection with *K. pneumoniae*, $MR1^{-/-}$ mice exhibited lower temperatures, altered cytokine profiles and reduced survival compared to MR1-sufficient mice [245]. In a separate model of respiratory infection using the facultative intracellular pathogen *Francisella tularensis*, MAIT cells accumulated in the lungs of infected mice, expressed IFNγ, TNFα and IL-17 and reduced the burden of infection — relative to MR1-deficient mice [246]. In one murine model of mycobacterial infection, iVα19i-Tg MAIT cell deficient mice experienced increased bacterial burdens in the lungs early in infection, in contrast to those with normal numbers [247]. In another, iVα19iCα$^{-/-}$-Tg MAIT cells were similarly found with a lower burden of *M. tuberculosis* Erdman strain within the lungs, compared to control mice with normal TCR repertoires [248]. These studies indicate an important role for MAIT cells in infection — particularly pulmonary infection and in the context of mycobacteria. In light of this emerging role for MAIT cells in mycobacterial pulmonary disease, it is of increasing importance to better understand the role of MAIT cells in TB.

1.6 Tuberculosis

In 1882, Robert Koch first identified the 'tubercle bacillus' *Mycobacterium tuberculosis* as the causative agent of tuberculosis (TB) [249]. Between 1600–1800, TB is thought to have caused one fifth of all deaths in Europe and North America [250, 251], indeed *Mtb* is possibly responsible for more deaths throughout human history than any other single pathogen [252]. Without treatment the case fatality rate for patients with smear positive TB is thought to be approximately 70%, with death or cure typically occurring within three years of onset [253].

Following the isolation of antibiotics such as streptomycin in 1944, isoniazid in 1952 and rifamycins in 1957 [252] TB has become a curable disease. Nonetheless, in 2015 the World Health Organisation (WHO) estimated that globally 9.6 million people had developed active TB in the preceding year, with 1.5 million deaths, and therefore *Mtb* is a current leading cause of death by an infectious agent [254]. One key problem is the large reservoir of disease — approximately one third of the world's population is thought to be latently infected (LTBI) [255]. From latent infection, the risk of progression to active disease is thought to be approximately 5–10% — although we currently lack the tools to predict those most likely to progress to disease [256], thus precluding an effective strategy for widespread chemoprophylaxis of LTBI individuals.

With an estimated 480,000 cases of TB resistant to the two most powerful antibiotics (MDR-TB) in 2014 — and approximately 9.7% of these thought to exhibit extensive antibiotic resistance (XDR-TB) [254], novel immunotherapeutic strategies and vaccines may provide a better approach. Therefore, understanding the components of an effective immune response to TB in humans remains key.

1.6.1 Immunopathological cycle during tuberculosis

Following the expulsion of *Mtb* from an individual with TB [257], inhalation of infectious droplet nuclei introduces the bacilli into the airways and alveoli. Here, they can be engulfed by lung-resident phagocytic cells, with alveolar macrophages considered to be amongst the first encountered [258]. Through interactions with *Mtb* mediated by scavenger, mannose and complement receptors, *Mtb* can enter the macrophage [259], where it is sequestered before further host-cell–pathogen interactions determine whether *Mtb* is cleared, or infection is established [258]. Migration into the lung parenchyma, and the attraction of further inflammatory cells initiates granuloma formation — typically regarded as a host-attempt to segregate *Mtb*, although it is not clear which of host or *Mtb* benefit the most [260]. Primary TB can occur shortly following the initial infection — alternatively, a lengthy period of latency can follow, lasting indefinitely — or alternatively can eventually result in post-primary, reactivation tuberculosis [261].

Control of *Mtb*-bacilli during LTBI requires an adaptive immune response mediated by T cells [258, 262, 263]. Dendritic cell transport of *Mtb* to the lung draining lymph nodes is critical for the priming of adaptive T cells, but also plays an important role in the dissemination of bacilli to diverse anatomical locations, via the lymphatics [264, 265]. Following the priming of T cells in the lymph nodes, they eventually migrate to the site of infection where they can help control mycobacterial growth, and in the maintenance of the granuloma [266].

Disease state at the level of the organism is determined as an aggregate of gross pathology; this ranges from latent infection to sub-clinical or active disease. Individual granulomas and their control of *Mtb* can occur along a spectrum of states [267, 268]. Whilst solid granulomas may contain *Mtb* in a state of dormancy, necrotic and caseous granulomas are associated with active and replicating *Mtb* bacilli [268]. Loss of granuloma integrity precedes the dissemination of bacilli and the onset of tissue pathology in post-primary TB; resulting in the expulsion of bacilli and onwards spread of infection [253, 267].

1.6.1.1 Early events in the control of *M. tuberculosis*-infection

Once within in the alveoli, alveolar macrophages ingest *Mtb* bacilli, where they initially reside within the phagosome [269, 270]. The lysosome is a highly acidic intracellular compartment containing numerous and diversely acting soluble acid hydrolases — fusion of the lysosome with the *Mtb*-containing phagosome introduces *Mtb* to this harsh lysosomal environment, which can lead to its degradation [271–273]. However, *Mtb* bacilli possess numerous immune evasion strategies — including the ability to halt the phagolysosomal fusion process, enabling their survival within the phagosome [259, 271]. Failing this, virulent mycobacteria can translocate from the phagolysosome to the cytosol [274], or indeed establish infection within the lysosome, despite growth inhibiting conditions [275].

Autophagy (macroautophagy) is an important cell intrinsic homeostatic process, in which isolation membranes form at the ER-mitochondria contact site [276] enabling the engulfment of portions of the cytoplasm and/or damaged organelles by double-membraned autophagosomes [277]. Autophagic processes can also improve host control of *Mtb*, through enhanced maturation of *Mtb* containing phagosomes [278], capture of bacteria attempting to escape the phagosome [279] and the delivery of anti-bacterial peptides such as cathelicidin to the autophagosome, in a vitamin D_3-dependent manner [280, 281].

Important in the response to *Mtb* is the innate recognition of conserved mycobacterial PAMPs. This induces downstream signalling and gene transcription that can aid in the destruction of *Mtb*, as well as in instigating a larger inflammatory response [282–284]. Macrophage PRRs, of which the best studied are Toll-like receptors (TLRs), can recognise a variety of *Mtb* derived patterns; TLR2 homodimers, for example, can detect cell wall lipoproteins and glycolipids [285, 286]; whilst TLR2/1 or TLR2/6 heterodimers can recognise di- and triacylated lipoproteins, respectively [287, 288]. TLR4 and TLR9 can reside within the endosome, and can detect mycobacterial proteins/glycolipids, and DNA [287, 289].

Following entry of macrophages into the lung parenchyma and PRR ligation, secretion of cytokines — in particular TNFα [282] — and chemokines such as CCL2 and CXCL10, lead to a further influx of inflammatory cells [290]. These include additional macrophages as well as γδ T cells, NK cells, dendritic cells, neutrophils — and possibly MAIT cells. These cells provide early sources of additional cytokines, chemokines and anti-mycobacterial mediators [291, 292], as well as providing support for the nascently forming granuloma [290].

1.6.2 Induction of T cells, & their role in controlling *Mtb*

Following *Mtb*-uptake at the site of infection, dendritic cells can migrate to the lung-draining lymph nodes early in infection [293, 294]. This process is key for the induction of the adaptive immune response [264, 295] and precedes the appearance of *Mtb*-specific T cell mediated immunity in the lung [296]. However, there is a delay associated with priming of the adaptive immune system in TB — in murine cytomegalovirus (MCMV), for example, Ag-specific $CD4^+$ T cells begin to expand within 5–6 days [297], and are observed in PBMC within 7–14 days in human CMV [298]. By contrast, *Mtb*-specific $CD4^+$ T cells begin to expand 7–14 days post-infection in mice [264, 296], and are detected in the periphery approximately 4–7 weeks post-exposure/infection in macaques and humans [299–301]. This lag phase may allow for the multiplication of large numbers of bacilli, and is therefore considered to be detrimental for the host [302].

The onset of a T cell adaptive response is essential for containment of infection *in vivo*. MHC class $I^{-/-}$ and class $II^{-/-}$ mice, for example, experience increased bacterial burdens and succumb to infection earlier compared to wild type mice, with a particularly pronounced effect in the absence of $CD4^+$ T cells [303]. Notably, there is a 20-fold increase in risk associated for the progression from LTBI to active TB for HIV-infected individuals, illustrating the importance of CD4-mediated cellular immunity in human *Mtb* infection [304, 305].

1.6.2.1 Anti-mycobacterial roles of IFNγ and TNFα

$CD4^+$ and $CD8^+$ T cells exhibit a variety of anti-mycobacterial effector functions, notable of which is the expression of IFNγ and TNFα. These cytokines can activate macrophages resulting in the induction of autophagy, enhanced phagolysosomal fusion, and innate bactericidal functions such as the generation of reactive oxygen and nitrogen intermediates [281, 306–310].

Accordingly, in the absence of IFNγ mice exhibit deficiencies in their ability to produce reactive nitrogen species and control *Mtb* growth — with enhanced tissue necrosis, dissemination of bacilli and early death [311, 312]. In the murine model, $CD4^+$ T cells in particular are thought to be an important source of IFNγ [313]. In humans, evidence for the importance of IFNγ comes from multiple genetic defects related to the ability to express, or respond to IFNγ, which each lead to a mendelian susceptibility of mycobacterial disease (MSMD). So far, genetic defects identified include those related to the expression of IL-12Rβ1, IFNγR1 and 2, the IL-12p40 subunit and STAT1 as well as other mediators of the IFNγ-response [314].

IFNγ is also required for the control of *Mtb* by macrophages *in vitro* [308], whilst downregulation of IFNγR in $CD14^+$ cells infected with *Mtb*, but not the avirulent *M. smegmatis* is indicative of *Mtb* immune evasion [315]. Importantly, studies indicate the importance of balanced responses, with over-production of IFNγ leading to exacerbation of pathology and early death of *Mtb*-infected mice [316]. IFNγ is also reported to induce macrophage expression of the receptor for TNFα [317].

1.6.2.2 Importance of TNFα for granuloma initiation and structure

Much as MSMD highlights the importance of IFNγ in the response to *Mtb* in humans, anti-TNFα therapy has highlighted the importance of TNFα. Common in the treatment of inflammatory and autoimmune conditions such as rheumatoid arthritis; LTBI patients taking anti-TNFα therapy are at heightened risk of TB reactivation [318–320]. In latently *Mtb*-infected macaques, TNFα neutralisation results in reactivation that first occurs within the intrathoracic lymph nodes, whilst macaques infected prior to TNFα neutralisation experience more severe disease and widespread dissemination [321].

Mechanistically, murine experiments have found TNFα important for effective chemokine expression early in infection [322], with TNFα deficiency associated with delayed and defective granuloma formation — and an inability to control *Mtb* growth [323, 324]. In addition, TNFα may further modulate the expression of cytokines such as IFNγ and IL-12 — and cell-death mediators such as TNF-related apoptosis-inducing ligand (TRAIL), which are induced in the absence of TNFα [325, 326]. In the zebrafish model the absence of TNFα-signalling results in enhanced necrotic death [327], and necrotic granulomas can be seen in TB/HIV-1 co-infected individuals, who are deficient in TNFα [328]. Recent experiments have also differentiated between cellular sources of TNFα, finding that myeloid-derived TNFα, although important for the initial recruitment of cells, is dispensable for granuloma initiation, and maintenance of structure — indicating a specific importance of T cell derived TNFα [329].

1.6.2.3 $CD8^+$ T cells in tuberculosis

Whilst not as extensively studied in tuberculosis as $CD4^+$ T cells, there is increasing evidence to suggest a possible role for $CD8^+$ T cells in mediating protection and/or pathogenesis during *Mtb* infection [330]. In the murine model, deletion of the gene encoding β_2m resulted in increased *Mtb* bacterial loads and decreased survival, 6 weeks post intravenous (iv) infection [331]. Similar findings were also observed in mice deficient for TAP1, and not CD1d [332]. *In vivo* depletion of $CD4^+$ T cells (but

not $CD8^+$ T cells) has been observed to result in an increased *Mtb* burden during the acute stage of infection, with the converse seen during the latent stage, in which loss of $CD8^+$ (but not $CD4^+$) T cells resulted in a 10-fold increase in *Mtb* bacterial burden [262]. This finding led Van Pinxteren *et al* to propose non-redundant roles for $CD4^+$ and $CD8^+$ T cells, with $CD8^+$ T cells more important in the later stages of murine *Mtb* infection. Similarly, Mogues *et al* found that in the absence of $CD8^+$ T cells, mice demonstrated 10-fold greater bacterial burdens, although with similar histopathology and only slightly decreased survival compared to wild-type mice [303].

In comparison with the murine model, non-human primates such as the rhesus macaque can reproduce a broader range of tuberculosis disease as seen in humans, including latency, and as such are a useful model [333]. Depletion of $CD8^+$ T cells in either BCG vaccinated rhesus macaques, or those that were previously *Mtb*-infected but subsequently cured, each resulted in loss of immunity to subsequent *Mtb* infection, providing evidence of a protective role for memory $CD8^+$ T cells in this model [334]. Non-human primate studies have also shed some light on the role of cytokines within the tuberculosis granuloma, with a recent study by Gideon *et al* observing an inverse correlation between *Mtb* burden and T cell IL-17, TNFα and/or IFNγ/IL-2 expression within individual granulomas [335].

$CD8^+$ T cells are observed in human tuberculous lesions [336], with some evidence in support of a protective role in human *Mtb*-infection garnered from *in vitro* stimulation experiments and mycobacterial growth control assays. $CD8^+$ T cells can respond to *Mtb* derived peptides to express IFNγ [337, 338], which can enhance the ability of human macrophages to exhibit anti-*Mtb* activity [308]. $CD8^+$ T cells can express granulysin, which is able to mediate the direct killing of *Mtb*, or of intracellular *Mtb* in a perforin dependent manner [339]. Whilst $CD8^+$ T cells from purified protein derivative (PPD)-positive and negative subjects were found unable to mediate reduction of intracellular *Mtb* growth within infected human monocytes in one study [340], another found that $CD8^+$ T cells from healthy human TB contacts were able to control the growth of *Mtb in vitro*, and those from control subjects could not. In this second study IFNγ, TNFα and NO were identified as potential mediators of this effect [341].

$CD8^+$ T_{EMRA} cells expressing cell-surface TNFα have been identified as a binding target of anti-TNFα monoclonal antibody therapy, and as a result are susceptible to complement mediated lysis [342]. These $CD8^+$ T_{EMRA} cells express high levels of granulysin, and their loss may be an important factor in the enhanced susceptibility of patients undergoing TNFα-therapy to tuberculosis reactivation [342, 343]. Interestingly, work from the lab of D. Lewinsohn has emphasised the

important contribution of $CD8^+$ T cells not restricted by classical MHC class Ia molecules, to the pool of *Mtb*-reactive $CD8^+$ T cells [344]. Indeed, such non-classical $CD8^+$ T cells were found to predominate in *Mtb* uninfected individuals, and have since been identified as comprised largely of MAIT cells [178].

1.6.3 The activation and role of MAIT cells in tuberculosis

Despite prolonged exposure to *Mtb*-infected individuals, approximately 50% of close-contacts from middle and low-income countries show no signs of having developed an adaptive immune response, suggesting a lack of *Mtb* infection [345]. With an infectious dose thought to be as low as a single bacilli [346], this implies the ability of the immune system to mount sterilising responses prior to the induction of adaptive immunity, for which MAIT cells are ideally placed to contribute.

Interestingly, MAIT cells are depleted in the blood of HIV patients early in HIV-infection [183, 219]; before a substantial reduction in $CD4^+$ T cell numbers [347]. Furthermore, unlike $CD4^+$ T cells they fail to recover following highly active antiretroviral therapy (HAART) [219]. It is also noteworthy that HIV-positive individuals double their risk of progressing to active TB within their first year [348] and remain at a greater risk of developing TB compared to HIV-negative individuals despite restoration of $CD4^+$ T cell counts [349]. The loss of MAIT cells from peripheral blood therefore coincides with an early increase in risk of progressing to active tuberculosis. It is possible to speculate that this loss of MAIT cells contributes to the early increased risk of developing active TB in HIV-positive individuals.

MAIT cells express several chemokine receptors — including CCR5, which can detect CCL3 and CCL5 [179] (both of which can be expressed by *Mtb* infected alveolar macrophages [350, 351]), indicating the potential for MAIT cell accumulation at the site of infection. Accordingly, MAIT cells are depleted from the blood of TB patients and have been identified in the ascitic fluid of TB patients with tuberculous peritonitis [138, 178, 220]. MAIT cells are also reported to be enriched in the airways [178, 352], and have been visualised in *Mtb*-infected human lung tissue [138].

Ex vivo human MAIT cells respond to *Mtb*-infected lung epithelial cells in an MR1 dependent manner, and MAIT cells can express both IFNγ and TNFα in response to *Mtb* [178]. However, the ability of *Mtb* to trigger MAIT cell activation in response to IL-12 and IL-18, and the importance of this mechanism in bacterial infection is unclear. In a murine model of BCG infection, IL-12 but not MR1 was essential for MAIT cell effector function [247]. In contrast, Meierovics *et al.* found that for control of *F. tularensis* in murine cells, both MR1 and IL-12-p40 were equally important [246].

The importance of IL-12 in human mycobacterial infection is well documented [314]. IL-18 is secreted by *Mtb*-infected alveolar macrophages and is detected in TB pleurisy [353], and mice lacking IL-18 are more likely to succumb to *Mtb*-infection [354] indicating that IL-18 may also play an important role in TB immunity.

Together, these findings suggest an important role for MAIT cells in tuberculosis. Whether MAIT cells can be identified at additional sites of *Mtb*-infection will be assessed in Chapter 6 (p. 177). Likewise, MAIT cells are activated in response to IL-12 + IL-18 by bacteria, including *Mtb*, but the relative contributions of the IL-12/-18 and MR1 signals to the activation of MAIT cells by *Mtb* are not currently clear, and will form the basis of experiments in Chapter 5 (p. 139).

1.7 Hypotheses

MR1 and IL-12/-IL-18 signals are individually sufficient for MAIT cell activation, but the effect of the intersection of these signals, which is likely to occur during infection, is not clear. Similarly the context, requirement and sufficiency for these signals during MAIT cell activation by bacteria — and in particular *Mtb* — are not known. Lastly, despite an emerging role for MAIT cells in TB, site of disease assessments of MAIT cells are currently limited.

During the course of this thesis, I will therefore, broadly, seek to test the following hypotheses:

Hypothesis 1 TCR and IL-12/-18 signalling are able to converge and affect the threshold, timing and effects of MAIT cell activation.

Hypothesis 2 IL-12/-18 and MR1 signalling are each important for MAIT cell activation by bacteria including *Mtb*.

Hypothesis 3 MAIT cells are able to localise to additional sites of tuberculosis disease than those currently characterised — specifically, the mediastinal lymph nodes during lymphatic tuberculosis.

2
Materials and Methods

Contents

2.1 Reagents 40
2.1.1 Media and Buffers 40
2.1.2 Antibodies 41
2.2 Cells 43
2.2.1 Bacterial cells 43
2.2.2 Human cells and cell lines 44
2.2.3 Isolation of human cells 44
2.3 Cytometric data acquisition and analysis 46
2.3.1 Flow cytometry 46
2.3.2 Chip cytometry 46
2.3.3 Statistical analysis 48

2.1 Reagents

2.1.1 Media and Buffers

R10 500 ml RPMI-1640 (Sigma-Aldrich), 2 mM L-glutamine, 1× Penicillin-Streptomycin solution (Gibco) and 10% FCS (all Gibco).

Rh10 500 ml RPMI-1640, 10% Heat inactivated, filtered human serum (both Sigma-Aldrich), 2 mM L-glutamine and 1× Penicillin-Streptomycin solution (both Gibco).

THP1 media 500 ml RPMI-1640, 0.05 mM β-mercaptoethanol (both Sigma-Aldrich), 2 mM L-glutamine, 1× Penicillin-Streptomycin solution and 10% FCS (both Gibco).

Freezing mix 90% heat inactivated fetal calf serum (FCS; Gibco) and 10% dimethyl sulfoxide (DMSO; Sigma-Aldrich).

MACS Buffer PBS with 0.5% FCS (v/v; Gibco) and 2 mM Ethylenediaminetetraacetic acid (EDTA; Sigma-Aldrich); 0 22µm sterile filtered prior to use.

HBS/HSA 20mM HEPES, 140mM NaCl, 5mM KCl, 6mM glucose, 1mM CaCl, 2mM MgCl, 1% human serum albumin (HSA), pH 7.2.

7H9 broth 900 ml dH2O, 4.7g Middlebrook 7H9 broth base (Sigma), 10% Middlebrook Oleic Acid Albumin Dextrose Catalase (OADC) (BD), 0.5% glycerol (VWR) and 0.05% Tween80. 7H9 broth was 0 22µm sterile filtered through vacuum filtration units (Nalgene, ThermoFisher) and 10µg/ml amphotericin (Sigma) added.

7H10 agar 900 ml dH2O, 19.47g Middlebrook 7H10 agar base (Sigma), 0.5% glycerol and 0.05% Tween80. The agar base was autoclaved (121°C; 15 mins) and cooled before 10% OADC was added (50°C). Agar was poured into 90 mm petri dishes and allowed to solidify overnight. Sterility was confirmed for each batch. Plates were stored at 4°C.

Luria-Bertani (LB) agar 1000ml dH2O and 37g LB powder (Merck, Germany). LB agar was autoclaved (121°C; 15 mins), poured into petri dishes and allowed to solidify overnight. Sterility was confirmed for each batch. Plates were stored at 4°C.

Table 2.1: List of antibodies used. Key: CC—Chip cytometry; FC—Flow cytometry; Block—neutralisation or blocking antibody

Antibody	Colour	Clone	Company	Dilution	App.
CD3	Pe-Cy7	UCHT1	BioLegend	1:100	FC
	AF488	UCHT1	BioLegend	1:25	CC
	APC-Cy7	HIT3a	BioLegend	1:50	FC
	eFluor450	UCHT1	eBioscience	1:100	FC
	APC-AF750	7D6	ThermoFisher	1:20	FC
	POrange	UCHT1	Invitrogen	1:50	FC
CD4	QD605	S3.5	Invitrogen	1:200	FC
	VioGreen	VIT4	Miltenyi	1:50	FC
	BV421	SK3	BioLegend	1:25	CC
CD8	V450	RPA-T8	BD	1:10	FC
	VioGreen	BW135/80	Miltenyi	1:50	FC
	Pe-Cy7	SK1	BioLegend	1:50	FC
	PerCP-Cy5.5	RPA-T8	BD	1:20	FC
	PerCP-Cy5.5	RPA-T8	BioLegend	1:50	FC
	PerCP-Cy5.5	SK1	BioLegend	1:50	FC
	PE-Vio770	BW135/80	Miltenyi	1:50	FC
	AF700	RPA-T8	BD	1:10	FC
	BUV395	RPA-T8	BD	1:25	CC
CD25	PerCP-Cy5.5	M-A251	BioLegend	1:25	FC, CC
	PE	M-A251	BioLegend	1:25	FC, CC
CD26	PE	BA5b	BioLegend	1:25	CC
CD38	PerCP-Cy5.5	HIT2	BD	1:25	CC
CD45RO	BUV395	UCHL1	BD	1:25	CC

2.1.2 Antibodies

2.2 Cells

2.2.1 Bacterial cells

E. coli Single colonies of *E. coli* (DH5α) were picked, added to LB broth (5 ml) and cultured at 37°C overnight in a shaker incubator (225 rpm) alongside a sterility control (5ml LB with no *E. coli*). *E. coli* were pelleted by centrifugation (4,000 rpm; 5 mins) and washed ×2 in 13 ml PBS prior to fixation (2% v/v formaldehyde solution in PBS; 20 mins; 21°C). *E. coli* were washed ×2 in filter-sterilised PBS (4,000 rpm; 5 mins) prior to resuspension in 1ml filter sterilised PBS. The sterility control was processed identically. *E. coli* cell

Antibody	Colour	Clone	Company	Dilution	App.
CD69	PerCP-Cy5.5	FN50	BD	1:20	FC
	FITC	FN50	eBioscience	1:25	FC
	PE	FN50	BioLegend	1:25	FC, CC
CD71	PE	CY1G4	BioLegend	1:25	FC, CC
CD97	PE	VIM3b	BioLegend	1:25	CC
CD107a	Pe-Cy7	H4A3	BioLegend	1:1000	FC
CD131	PE	1C1	BioLegend	1:25	CC
CD137	PerCP-Cy5.5	4B4-1	BioLegend	1:25	CC
CD161	APC	191B8	Miltenyi	1:25	FC
	PE	191B8	Miltenyi	1:50	FC, CC
	AF488	702228	R&D Systems	1:25	ICC
CD279	BV421	EH12.2H7	BioLegend	1:25	CC
GrB	APC	GB11	Invitrogen	1:100	FC
IFNγ	PerCP-Cy5.5	4S.B3	eBioscience	1:25	FC
	V450	B27	BD Horizon	1:50	FC
	Pe-Cy7	4S.B3	eBioscience	1:25	FC
IL-18Rα	APC	H44	eBioscience	1:10	FC
	AF488	70625	R&D Systems	1:25	ICC
TNFα	FITC	MAb11	BioLegend	1:25	FC
	PE	MAb11	BioLegend	1:25	FC
	PerCP-Cy5.5	MAb11	BioLegend	1:25	FC
	V450	MAb11	BD	1:25	FC
Vα7.2	PE	3C10	BioLegend	1:50	FC, CC
	FITC	3C10	BioLegend	1:25	FC
	BV421	3C10	BioLegend	1:25	CC
	PerCP-Cy5.5	3C10	BioLegend	1:25	CC
mIgG2b	AF488	702228	R&D Systems	1:25	ICC
mIgG1	AF488	11711	R&D Systems	1:25	ICC
Live/dead	SYTOX blue		ThermoFisher	1:10000	FC
	Near IR		Invitrogen	1:1000	FC
	Violet		Invitrogen	1:1000	FC
IL-12p70		24190	R&D Systems	10µg/ml	Block
IL-18		125-2H	MBL Intl.	10µg/ml	Block
MR1		26.5	BioLegend	10µg/ml	Block
mIgG1		11711	R&D Systems	10µg/ml	Block
mIgG2a		MOPC-173	BioLegend	10µg/ml	Block

counts were estimated by flow cytometry (MACSQuant), standardising against pre-existing stocks. *E. coli* were added to experimental wells at 25 bacteria per cell (BpC) unless otherwise indicated.

***M. bovis* BCG** Lyophilised vials of approximately 5×10^6 *M. bovis* BCG (BCG vaccine Danish strain 1331; Statens Serum Institut) were resuspended in PBS and pelleted by microcentrifugation (8,000 rpm; 5 mins; 21°C). Supernatant was aspirated, and cells resuspended in the desired volume of R10 media (no antibiotics). Prior to use, BCG were passed through a fine-gauge insulin needle (BD) ×5 to disperse bacterial clumps.

***M. tuberculosis* H37Rv** *Mycobacterium tuberculosis* strain H37Rv was cultured in 7H9 broth to log phase, determined by optical density (OD) at 600nm of 1 (Ultrospec 10, GE Healthcare). Cultures were harvested and stored in 15% glycerol in 0.5ml aliquots (−80°C). Prior to use, bacteria were thawed (21°C) and the desired quantity added to Rh10 for a multiplicity of infection (MOI) of 10:1–2.5:1. Bacterial cell suspensions were sonicated (40 secs) in an ultrasonic waterbath (XUBA Analogue Ultrasonic Bath, Grant Instruments, UK) to disperse clumps. *Mtb* were then immediately added onto cells for infection. All work with *Mtb* was done under Biosafety Level 3 (BSL3) conditions in the Cat3 suite at the TB Research Unit (Dept. of Resp. Med., St. Mary's Campus, Imperial College London).

2.2.2 Human cells and cell lines

Peripheral Blood Mononuclear Cells Leukocyte cones (NHS Blood and Transport; NC24) or whole blood from healthy laboratory volunteers, or patients were obtained, and PBMC were separated by density gradient centrifugation over Lymphoprep (AXIS-SHIELD UK Limited). Cells were either used immediately, or counted and frozen in freezing mix at 2×10^7 cells/ml, prior to cryopreservation in liquid Nitrogen. Before each experiment using frozen PBMCs, vials were thawed rapidly in a water bath (37°C), washed with R10 ×2 (1,600 rpm; 5 mins) and resuspended at the desired concentration.

THP1 cells THP1 cells (ECACC, UK) were cultured at 37 °C, 5% CO_2 in THP1 media. Cells were maintained at between at 2×10^5 and 1×10^6.

2.2.3 Isolation of human cells

PBMC separation Whole blood was diluted with PBS and layered over Lymphoprep (Axis-Shield) prior to centrifugation (2,200 rpm; 22 mins; 21°C). PBMCs were aspirated using a pasteur pipette, and washed in R10 (1,800 rpm; 10 mins; 21°C) and again (1,600 rpm; 5 mins; 21°C). Cells were counted (Countess; Invitrogen) and either used immediately, or resuspended in freezer mix. 1 ml aliquots were added to cryovials, and frozen at a rate of approximately 1°C/min until reaching −80°C. Cryovials were transferred to liquid nitrogen for long term storage at −196°C.

Magnetic enrichment $CD8^+$ T cells and monocytes were positively enriched from PBMCs using Miltenyi MACS Separation MS/LS magnetic columns and CD8 or CD14 MicroBeads respectively, according to the manufacturer's protocol. Briefly, thawed or fresh PBMCs were washed in MACS buffer, counted and cooled to 4 °C. Cells were resuspended in 80 µl buffer + 20 µl of MicroBeads per 10^7 cells, and incubated at 4 °C for 15 minutes. Unbound MicroBeads were removed by washing in MACS buffer, and cells resuspended in 500 µl MACS for isolation of MicroBead-bound cells. After addition to an MS or LS column placed in a MACS separator magnetic field, unlabelled cells were removed by washing through with 500 µl (MS), or 3 ml (LS) MACS buffer, three times. The columns were removed, and enriched cells flushed out of the column with 1 ml (MS), or 5 ml (LS) MACS buffer. Sequential magnetic enrichments were performed by repeating the magnetic labelling step with MicroBeads of a different specificity, following the final wash step. Purity of enriched cells was consistently >90%.

Fluorescence-activated cell sorting $CD8\alpha^+$ T cells were magnetically enriched immediately prior to antibody/viability staining. $CD8\alpha^+$ T cells were counted (Countess; Invitrogen) and resuspended at up to 1×10^7 $CD8\alpha^+$ T cells per 100µl antibody cocktail. Cells were stained for CD3, CD8, CD161 and Vα7.2 (20 mins; 4°C), washed ×2 and resuspended in MACS buffer for sorting. A nucleic acid binding viability dye (SYTOX blue) was added and MAIT cells were FACS sorted by C. Willberg (Peter Medawar Building) on a Beckman Coulter MoFlo XDP cell sorter, or by J. Webber (Kennedy Institute of Rheumatology) or M. Paulsen (Imperial College London, St. Mary's campus) each using a BD FACSAria III sorter; each to consistently > 95% purity according to: electronic gating of live cells, lymphocytes (forward vs. side scatter properties) $CD3^+$, $V\alpha7.2^+$ and $CD161^{++}$. A representative sorting plot is included in Appendix C (p. 285).

2.3 Cytometric data acquisition and analysis

2.3.1 Flow cytometry

For immunofluorescent staining prior to flow cytometry, cells were washed ×2 in PBS (1,600 rpm; 5 mins; 4°C) and resuspended in antibody cocktail for surface staining according to dilutions listed in Table 2.1 (p. 41) (20 mins; 4°C). Cells were washed again ×2 (1,600 rpm; 5 mins; 4°C) before fixation (BD Cytofix/Cytoperm solution; 20 mins; 4°C) and permeabilisation through washing in permeabilisation buffer ×2 (BD Perm/Wash Buffer; 1,600 rpm, 5 mins; 4°C). Intracellular cytokine staining (ICS) was performed through resuspending cells in permeabilisation buffer (BD Perm/Wash Buffer) with the required antibodies to a final concentration as listed in Table 2.1 (20 mins; 4°C). Antibody solution was removed through washing ×2 (1,600 rpm; 5 mins; 4°C) and cells were resuspended in 100–200µl for analysis by flow cytometry. All flow cytometry in Oxford was performed on a MACSQuant Analyzer 10 (Miltenyi), whilst flow cytometry in London was performed on either a BD LSR II or BD LSRFortessa (Becton Dickinson). Data were analysed using FlowJo Version 10.1r5 for MacOS X. A representative plot of the electronic gating strategy used to identify $CD161^{++}$/MAIT cells, MAIT cells, $V\alpha7.2^{-}$ $CD161^{+}$ cells and $V\alpha7.2^{+}$ $CD161^{-}$ cells is presented in Fig. 2.1.

2.3.2 Chip cytometry

PBMCs, $CD8^{+}$ T cells or lymph node aspirates were processed as detailed above and as in Chapter 6.2 (p. 182). Cells were resuspended in PBS at up to 1×10^7 cells/ml, and cell solution was loaded onto ZellSafe chips (ZellKraftWerk) for cell attachment (5 mins; 21°C). Unattached cells were removed by washing with 200µl PBS ×3, prior to formaldehyde fixation (Fixation buffer; ZellKraftWerk) (20–60 minutes; 4°C). Fixation buffer was removed by washing with 200µl PBS ×3, and 200 µl of Storage Buffer was added for long term storage of chips at 4°C. For chip cytometry staining, storage buffer was removed and replaced with PBS prior to the initial bleach and background scan. A bleach step was performed prior to all antibody staining steps (ZellScanner ONE). 200µl antibody cocktails were made and added to the chips for staining (5 mins; 21°C), followed by 5× washes with 1ml PBS. Following a scan, cells were gated and fluorescence values calculated automatically. Manual corrections were made where necessary and data were exported and analysed using FlowJo Version 10.1r5 for MacOS X.

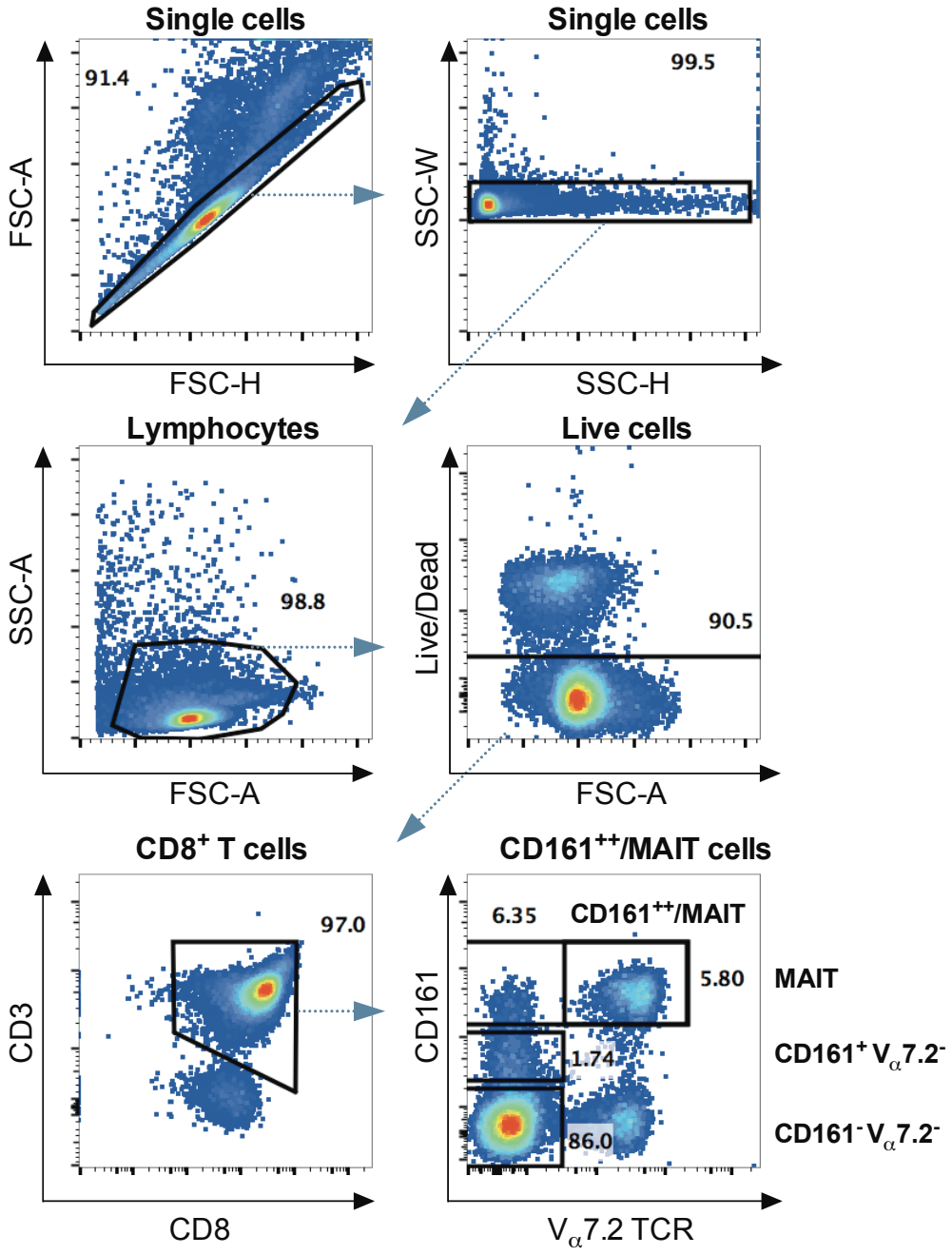


Figure 2.1: Representative gating strategy for identification of CD161^{++}/MAIT, MAIT, Vα7.2^{-} CD161^{+} and Vα7.2^{+} CD161^{-} cells. Single cells and lymphocytes were identified based on forward scatter (FSC) and side scatter (SSC) properties. CD8^{+} T cells were selected as CD3^{+} and CD8α^{+}, whilst CD161^{++}/MAIT, MAIT, Vα7.2^{-} CD161^{+} and Vα7.2^{+} CD161^{-} were identified through CD161 and Vα7.2 expression. Shown are representative plots following a magnetic CD8^{+} enrichment of PBMCs from a healthy donor.

2.3.3 Statistical analysis

All graphs were generated, and statistical tests performed using Prism 6 Version 6.0h for Mac OS X (GraphPad). Data were analysed by parametric or non-parametric statistical tests according to the observed spread of data, as indicated in the figure legends. Data following a log-normal distribution were plotted on a logarithmic scale, and where appropriate tests were performed on log-transformed values.

3

IL-12, IL-18 and TCR stimulation of MAIT cells

Contents

3.1 Introduction 50
3.1.1 *In vitro* investigations of MAIT cell activating signals . 50
3.1.2 Chapter hypothesis and aims 52
3.2 Chapter specific materials & methods 54
3.2.1 Activation of CD8α$^+$ T cells 54
3.2.2 Statistical analyses 55
3.3 Co-stimulation by IL-12, IL-18 & the TCR 55
3.3.1 IL-12/-18 permits robust MAIT IFNγ expression 58
3.3.2 TCR signalling important for MAIT cell TNFα/CD69 . 60
3.4 IL-12/-18 dose response & TCR stimulation 62
3.4.1 Biphasic IFNγ-response to IL-12/-18 + TCR beads . . . 63
3.4.2 CD161-expression & the dose-response to IL-12/-18 . . 68
3.5 Kinetics of the IL-12/18 and TCR responses 76
3.5.1 Sustained TCR-stimulation increases IFNγ$^+$ (%) 76
3.5.2 TCR-stimulation leads to rapid TNFα-expression 78
3.5.3 Robust TCR responses require cytokine pre-exposure . 85
3.5.4 TCR pre-stimulation enables cytokine-only response . . 87
3.6 Discussion 90
3.6.1 High & low thresholds for MAIT cell IFNγ-expression . 90
3.6.2 MAIT cell expression of TNFα is rapid and transient . . 93
3.6.3 CD69 is a poor marker of rapid MAIT cell activation . . 94
3.6.4 MAIT vs. conventional CD8$^+$ T cell responses 96
3.6.5 Conclusions 98

3.1 Introduction

3.1.1 *In vitro* investigations of MAIT cell activating signals

Antibody cross-linking of components of the T cell receptor (TCR) complex is a simple and comparable approach to understanding T cell activation through TCR signalling [355]. Despite being nearly uniformly T_{EM} (i.e. CD45RA$^-$ CD45RO$^+$ CD27$^+$) [124], Turtle *et al.* found that stimulation of CD161^{++} CD8α^+ T cells using αCD3 coated plates was insufficient to induce IFNγ-expression — although this could be augmented through co-stimulation by αCD28 [167]. Interestingly, various additional investigations using such stimuli have been performed on MAIT cells, generally finding increased resistance to TCR-induced IFNγ-expression, than in non-MAIT conventional memory T cells [138, 140, 356, 357]. In a congenic MAIT^{hi} mouse model [357], IFNγ could be detected from memory CD4$^+$ and memory CD8α^+ T cells by Cytometric Bead Array (CBA) after 42–45 hours stimulation with αCD3/CD28 beads, but interestingly not from MAIT cells [357]. Similarly, using a novel MR1 tetramer to isolate MAIT cells, Reantragoon *et al.* found that after 60 hours stimulation with αCD3/CD28 beads large amounts of IFNγ could be detected by CBA from conventional CD161$^-$ MR1-tetramer$^-$ T cells — but not from fluorescence-activated cell sorting (FACS) purified MAIT cells [140]. Together, these findings suggest that MAIT cells are relatively refractory to TCR ligation.

Several of these and other studies have argued for a role of cytokines in permitting MAIT cells to respond robustly to TCR stimulation. Turtle *et al.* found that IL-18 was able to replace αCD28 co-stimulation to boost CD161^{++} CD8α^+ T cell IFNγ production following αCD3 stimulation [167]. And after 24 hours stimulation by αCD3/CD28 coated beads in the presence of IL-12, Annibali *et al.* detected approximately 10× more IFNγ by enzyme-linked immunosorbent assay (ELISA) from CD161^{++} CD8α^+ T cells compared to stimulation without IL-12 [356]. Other cytokines have also been found to boost activation. Following 48 hours stimulation with αCD3/CD28 beads, the addition of IL-1β + IL-23, or more strikingly IL-7, enhanced the number of IFNγ$^+$ MAIT cells detected by flow cytometry. Additionally, IL-7 treatment boosted Vα7.2 TCR expression suggesting (but not proving) that IL-7 induces TCR up-regulation, permitting an enhanced response to TCR stimulation [170]. It is therefore possible that cytokine co-stimulation is necessary to licence MAIT cells to express IFNγ in response to TCR ligation.

MAIT cells can up-regulate CD69, and express TNFα — and both are commonly used as markers of T cell activation and effector function. However, the mechanisms of TNFα- and CD69-induction remain unclear, and some inconsistencies in the

literature exist. For example, Le Bourhis *et al.* reported that bacteria-fed monocytes can induce MAIT cell CD69-expression in an MR1-dependent manner [138] — whilst, a more recent study by Dias *et al* found that CD69 expression was minimally abrogated by MR1 blockade. In C57BL/6 mice, MAIT cells expressed CD69 in response to intranasal administration of the MAIT cell stimulatory MR1 ligand 5-OP-RU. However, in contrast with IFNγ-expression, no enhancement of CD69 expression on co-administration of the TLR2 agonist Pam2Cys was observed. This suggests that presentation of ligand is sufficient — and TLR induced cytokine co-stimulation not necessary — for CD69 expression *in vivo* [358]. Nonetheless, in a cohort of patients with ulcerative colitis, MAIT cell CD69 expression correlated with IL-18 serum levels [180]; and after 40 hours, CD69 is up-regulated on human MAIT cells stimulated with IL-12/-18 alone [182]. These findings are supportive of a relationship between CD69-expression on MAIT cells and the presence of cytokines.

3.1.1.1 MAIT cell TNFα-expression may occur with distinct dynamics

Both the kinetics of response and signals involved in the induction of MAIT cell TNFα-expression also remain to be resolved. In the congenic MAIT^{hi} mouse model; TNFα, unlike IFNγ, was detected from MAIT cells at a high level, after 42 – 45 hours stimulation with αCD3/CD28 beads, compared to conventional memory CD4$^+$ and CD8α$^+$ T cells [357]. Conversely — none was detected by Reantragoon *et al.* by CBA after 60 hours αCD3/CD28 bead stimulation of sort purified human MAIT cells (in contrast to conventional T cells) [140]. Interestingly, Gracey *et al.* found that following a 24 hour stimulation with THP1 cells infected with PFA-fixed *S. typhimurium*, about 20% of human MAIT cells expressed TNFα. However, approximately 70% of MAIT cells expressed TNFα following a shorter 12 hour exposure to αCD2/CD3/CD28 beads with Brefeldin A [236]. These findings suggest that either αCD2/CD3/CD28 beads are more potent for TNFα-induction than PFA-killed *S. typhimurium*, or the dynamics of activation are such that MAIT cells express TNFα preferentially at 12 hours and this is a transient effect. The longer Brefeldin A exposure in the 12 hour experiment may also have played a role, and so this will need to be clarified with further experiments.

Together, these findings suggest MAIT cells are more resistant to TCR stimulation for IFNγ-expression than would be expected for conventional T_{EM} CD8α$^+$ T cells. However this appears to depend on the presence or absence of co-stimulatory cytokines. MAIT cells appear capable of expressing TNFα in response to TCR cross-linking in the absence of cytokine co-stimulation, but this may occur with distinct kinetics compared to IFNγ-expression. Finally, CD69 expression is commonly used

as a broad and early activation marker for MAIT cells; however it is not clear what activating signals, or additional effector mechanisms CD69-expression is associated with. This chapter will attempt to address some of these outstanding questions.

3.1.2 Chapter hypothesis and aims

MAIT cells can respond to IL-12 and IL-18 independently of TCR stimulation to express IFNγ [93]; however in the context of infection, both cytokines and TCR signalling are likely to factor. Therefore it remains unclear what the relative contributions of each are in the activation of MAIT cells. It is possible that the kinetics and intensity of IFNγ-expression — as well as sensitivity to cytokine stimulation could be affected by TCR triggering, although this has not been shown. Similar questions surround TNFα, and CD69 expression. As these are distinct effector functions with different roles, it stands to reason that they may be induced in distinct ways. Therefore, how TCR and cytokine signals integrate for distinct outcomes, especially in terms of the kinetics and intensity of the MAIT cell effector response needs to be further examined.

Ultimately, the aim of performing experiments *in vitro* is to better understand and predict the behaviour of cells *in vivo*. MAIT cells are typically identified on the basis of their T cell receptor expression, and defined through their restriction by MR1. An appropriate response to dangerous, or alternatively, harmless bacteria will depend on the nature of the relationship between signals arising from TCR stimulation by microbial riboflavin biosynthetic intermediates — and stimulation by PAMP induced cytokines from the inflammatory milieu. Thus far, it is established that MAIT cells can respond to either, but how both cytokines and TCR signals together combine to affect the timing and extent of the MAIT cell response has not been determined. As IL-12 and IL-18 are sufficient to induce a cytokine-driven response from MAIT cells, whilst MAIT cells appear resistant to TCR crosslinking alone compared with conventional CD8α$^+$ T_{EM} — this chapter hypothesises a synergistic relationship between TCR stimulation and stimulation by IL-12/-18. Utilising an *in vitro* approach with recombinant cytokines and αCD2/CD3/CD28 coated beads, the aims of this chapter are as follows:

Aim 1 Evaluate the functional outcomes of MAIT cell activation following the integration of different combinations of TCR, IL-12 and IL-18 signals.

Aim 2 Investigate the sensitivity of MAIT cells to IL-12/-18 mediated activation in the presence and absence of TCR stimulus.

Aim 3 Assess the importance for MAIT cell activation of the timing and sequence of TCR and IL-12/-18 signals.

3.2 Chapter specific materials & methods

Chapter-specific materials and methods are detailed below. Please also refer to Chapter 2 for further information as required.

3.2.1 Activation of CD8α$^+$ T cells

CD8α$^+$ T cells were prepared as detailed in Chapter 2. Cells were seeded at 2×10^5 per well of a 96 well U-bottom plate in R10 media + 1× Penicillin-Streptomycin solution (Gibco). TCR beads (T cell activation/expansion kit; Miltenyi Biotech) were prepared through the addition of biotinylated αCD2, αCD3 and αCD28 antibodies to anti-Biotin MACSiBead particles, at 10 µg/ml according to manufacturers instructions. For CD8α$^+$ T cell activation, TCR beads were added at a bead per cell ratio of 1:2. IL-12 and IL-18 (both Miltenyi Biotech) were added at 50 ng/ml; except in the dose-response experiments, where they were added from 0–50 ng/ml in two, or four-fold increasing concentrations. In all cases Brefeldin A (BFA; eBioscience) was added at 1/1000 dilution (1×) for the final 4 hours. For the 24 hour IL-12, IL-18 and TCR bead co-stimulation and dose-response experiments, TCR beads, IL-12 and/or IL-18 were added for the duration of the experiment. For the timing of the TCR response experiments, IL-12 and IL-18 were added for 25 hours; with TCR beads added at the same time, or for the final 5 hours only. For the timing of the IL-12 and IL-18 response, IL-12 and IL-18 were added for either 25 hours or for the final 5 hours, with TCR beads added only for the final 5 hours.

3.2.1.1 TCR pre-stimulation with αCD3/CD28 coated plates

αCD3 and αCD28 were added to PBS (to a final concentration of 5µg/ml each); both Miltenyi Biotech). 100µl of antibody solution were added to each well of a 96-well flat bottom high-binding ELISA microplate (Greiner); alternatively PBS was added to control wells. The plate was then left overnight (4°C). The following day, each well was washed by aspirating solution and replacing with 120µl PBS ×5. After the final wash, PBS was replaced with R10, and incubated for 2 hours at 37°C. The R10 was removed, and CD8α$^+$ T cells added at 2×10^5 cells/well in fresh R10. The cells were briefly spun down for attachment to the plate (1,200 rpm; 30 seconds) and cultured for 18 hours. Cells were removed from the wells, pooled and washed ×2 (1,600rpm; 5 min). Rested and TCR pre-stimulated cells were re-seeded in a 96-well U-bottom plate at 2×10^5, for further stimulation.

3.2.2 Statistical analyses

Data were analysed in GraphPad Prism software Version 6.0h (La Jolla, CA, USA). Comparisons between groups were made by one or two way ANOVA, with Holm-Sidak's correction for repeated measures comparisons; or paired t-test for comparisons between two groups. Statistical significance was defined as $p < 0.05$. For the generation of IL-12/-18 dose response curves, non-linear regression analyses in Section 3.4 were performed in order to generate either 4-parameter dose-response curves, or a more complex biphasic model. For each dataset, 4-parameter and biphasic models were compared for best-fit using the extra sum-of-squares F test. Where indicated by a statistical significance of $p < 0.05$, the more complex model was fit. From the resulting curves, EC50 + 95% confidence intervals (95% CI) and HillSlopes were determined. Where appropriate, linear-regressions were instead performed to formally rule-out a dose-response. In all graphs, data are presented as mean ± standard error of the mean (SEM) unless otherwise indicated.

3.3 Co-stimulation by IL-12, IL-18 & the TCR



Figure 3.1: TCR beads + IL-12/-18 stimulation assay. Positively isolated CD8α$^+$ T cells were stimulated with 50 ng/ml IL-12, IL-18 and/or αCD2/3/28 coated beads (TCR beads) for 24h, before assessment for activation status by flow cytometry.

In response to IL-7 exposure, MAIT cells respond better to TCR stimulation, coincident with enhanced expression of Vα7.2 [170]. Conversely, expression of high levels of CD161 along with the canonical Vα7.2 TCR segment are routinely used for the identification of MAIT cells, within the CD8α$^+$ or DN, or more rarely the CD4$^+$ T cell compartment. More recently, the discovery of ligands for MR1 have allowed for the production of MR1 tetramers, which, in some cases have replaced the use of Vα7.2 antibodies for unequivocal MAIT cell identification [140, 359].

Both Vα7.2 and tetramer staining, however, rely on MAIT cell expression of their TCR in order to detect MAIT cells; yet it is well established that upon activation by p-MHC, T cells internalise and target their TCR complexes for degradation [360]. There are functional implications resulting from TCR down-regulation as well as potential difficulties in detecting activated MAIT cells by flow cytometry when Vα7.2 is decreased or absent. It is, therefore, of interest to understand what signals lead to TCR down-regulation upon activation of MAIT cells, and the extent to which this occurs.

The total (surface + internal) expression levels of Vα7.2 within the CD161^{++} CD8α^{+} T cell subset were therefore assessed following stimulation of enriched CD8α^{+}T cells with IL-12, IL-18 and TCR beads as shown in Fig. 3.1. Amongst unstimulated CD161^{++} CD8α^{+} T cells, the frequency expressing Vα7.2 TCR was $92.1 \pm 2.1\%$ (± SEM; Fig. 3.2A). Following IL-12 or IL-18 stimulation independently, no decrease in frequency was observed; whilst following IL-12/-18 stimulation this reduced to $90.0 \pm 3.2\%$ of unstimulated ($p < 0.05$; Fig. 3.2 B, C). Stimulation with TCR beads similarly led to little (p = ns) decrease in Vα7.2-expression. This was, however, augmented through the addition of IL-12 (but not IL-18), dropping to $71.5 \pm 2.6\%$ relative to unstimulated. TCR beads + IL-12/-18 led to the largest decrease in Vα7.2^{+} cells — to $37.7 \pm 3.5\%$ of unstimulated ($p < 0.0001$). Together, this indicates a synergistic effect of the combined stimuli and demonstrates the extent of TCR down-regulation upon activation by IL-12/-18 + TCR beads.

Most (> 90%) of resting CD161^{++} CD8α^{+} T cells typically express Vα7.2 (Fig. 3.2 A and [135]), and there is broad functional overlap described between Vα7.2 expressing and non-expressing CD161^{++} CD8α^{+} T cells [136]. Given this, and the robust Vα7.2 down-regulation observed; to avoid excluding the most activated MAIT cells, all further analyses in this chapter, unless otherwise specified, will be focussed on the total CD161^{++} CD8α^{+} T cell subset (CD161^{++}/MAIT cells).

3.3.1 IL-12/-18 permits robust MAIT IFNγ expression

Next, CD161^{++}/MAIT cell expression of IFNγ was assessed by ICS. After 24 hours stimulation with either IL-12 or IL-18, no production of IFNγ (p = ns) was detected, whilst in combination IFNγ was expressed by $42.4 \pm 6.5\%$ ($p < 0.0001$), with a range of 12.3–64.5% indicating substantial donor variability (Fig. 3.3 A). Co-culture with TCR beads alone led to few IFNγ^{+} cells. However, IFNγ expression was similar following TCR beads + IL-12 (mean $37.8 \pm 2.5\%$; $p < 0.0001$) and IL-12/-18 stimulation (p = ns). By contrast, the IFNγ response following TCR beads + IL-18 ($10.7 \pm 2.0\%$; $p < 0.0001$) was 27.1% lower than TCR beads + IL-12 ($p <$

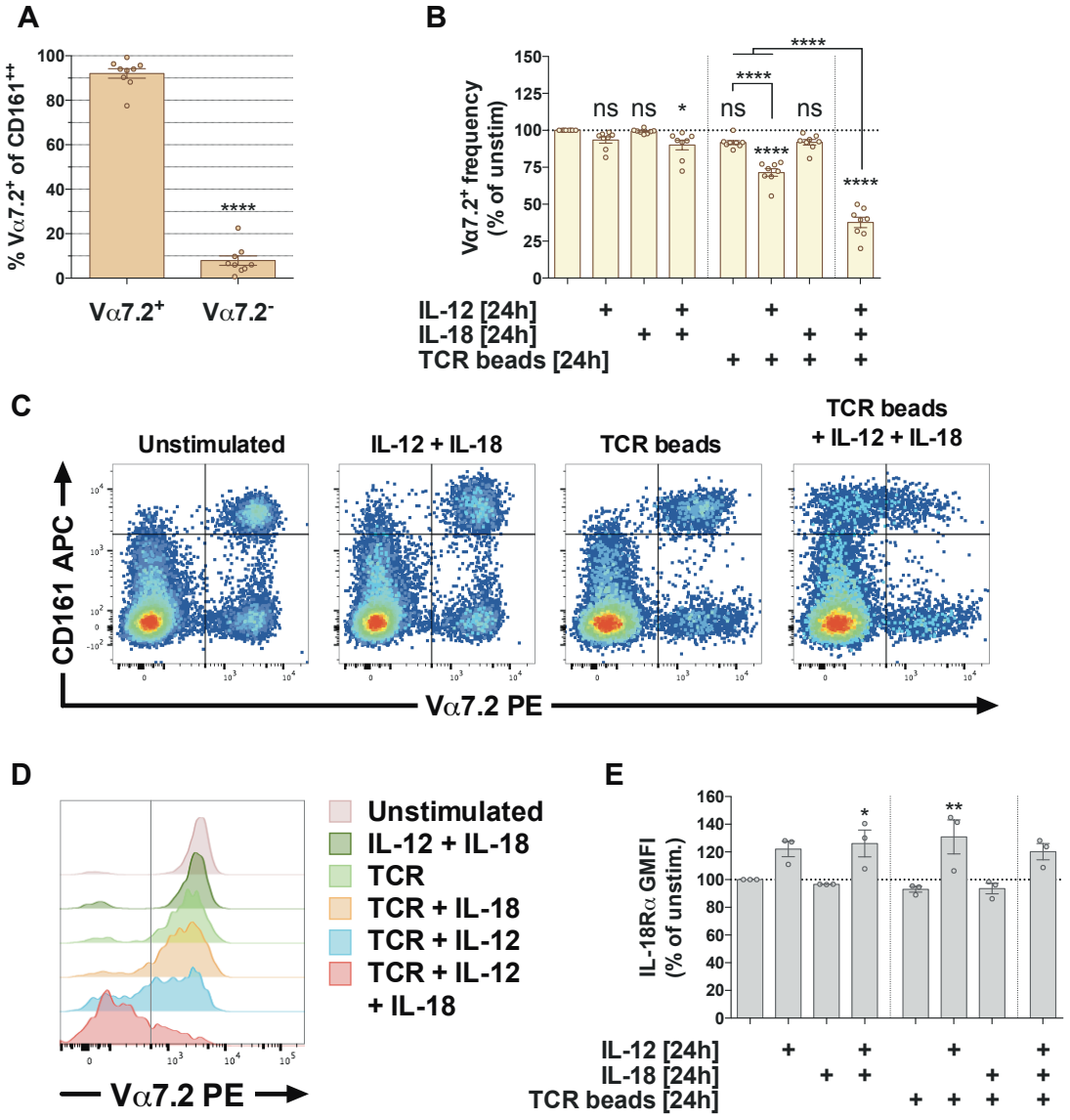


Figure 3.2: Activation-induced down-regulation of the Vα7.2$^+$ TCR. Positively isolated CD8α$^+$ T cells were stimulated with 50 ng/ml IL-12, IL-18 and/or αCD2/3/28 coated beads for 24h, before assessment of Vα7.2 (surface + internal) or IL-18Rα (surface only) expression by flow cytometry. (A) CD161^{++} CD8α$^+$ T cell Vα7.2 expression of unstimulated cells and (B) shown as a percentage of the unstimulated frequency per donor. (C, D) Representative FACS plots of (C) CD8α$^+$ T cells and (D) CD161^{++} CD8α$^+$ T cells, following different stimuli. (E) IL-18Rα GMFI of CD161^{++} CD8α$^+$ T cells. All graphs show mean ± SEM. Stagger-offset histogram shows modal y-axis scaling (% max. count per condition). Data analysed by one-way ANOVA with Holm-Sidak's multiple comparison test (B, E), or paired t-test (A). For all tests, ****$p < 0.0001$, **$p < 0.01$, *$p < 0.05$, ns = non-significant.

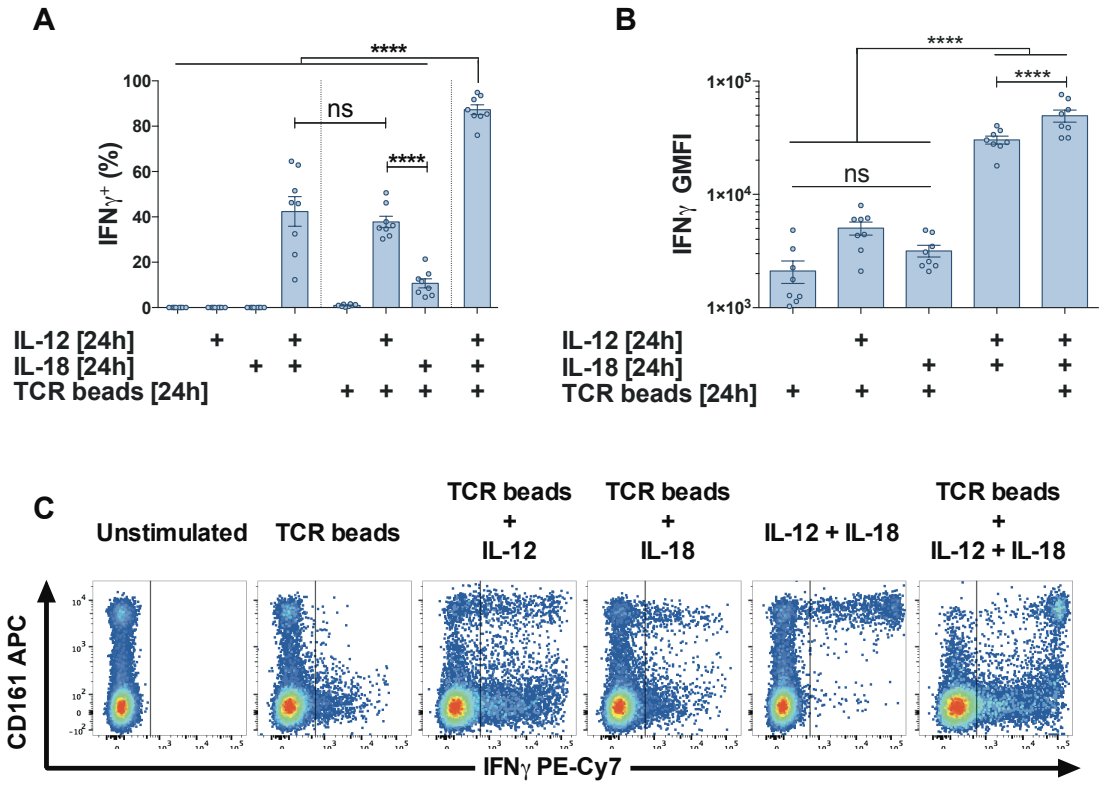


Figure 3.3: IFNγ induction by IL-12 and IL-18 ± TCR stimulation. Positively isolated CD8α$^+$ T cells were stimulated with 50 ng/ml IL-12, IL-18 and/or αCD2/3/28 coated beads for 24h before assessment of activation status by flow cytometry. (A) CD161^{++}/MAIT cell IFNγ production expressed as frequency (%) of population responding, or, (B) as the Geometric Mean Fluorescence (GMFI) of the IFNγ$^+$ cells. (C) Representative FACS plot of CD8α$^+$ T cells following different stimuli. All graphs show mean ± SEM. Data analysed by one-way ANOVA with Holm-Sidak's multiple comparison test. For all tests, ****$p < 0.0001$, ***$p < 0.001$, **$p < 0.01$, *$p < 0.05$, ns = non-significant.

0.0001), whereas in the presence of TCR beads + IL-12/-18, the vast majority of CD161^{++}/MAIT cells were IFNγ$^+$ (mean 87.3 ± 2.2%; $p < 0.0001$).

3.3.1.1 IFNγ GMFI as a proxy for *per cell* expression of IFNγ

Whilst the relative frequency of IFNγ$^+$ cells can reveal, broadly, the ability of CD161^{++}/MAIT cells to respond at a population level, the IFNγ GMFI can give an approximation of the strength of activation of individual cells. Therefore, through inspection of the IFNγ GMFI of CD161^{++}/MAIT cells above the threshold of activation (Fig. 3.3 B, C), the relative *per cell* expression of IFNγ can be estimated for each stimulation. Strikingly, culture with TCR beads + IL-12/-18, resulted in a very bright mean GMFI ($4.9 \pm 0.6 \times 10^4$) — higher than each other condition

($p < 0.0001$). Interestingly, despite a similar proportion of CD161^{++}/MAIT cells expressing IFNγ following stimulation with IL-12/-18 vs. IL-12 + TCR beads, the cells activated by IL-12/-18 demonstrated an approximately 6× higher IFNγ GMFI ($3.0 \pm 0.2 \times 10^4$ vs. $0.50 \pm 0.07 \times 10^4$) — at 65% of the relative intensity of IL-12/-18 + TCR beads. By contrast, TCR beads + IL-12 could induce IFNγ at 10.6%, and TCR beads + IL-18 only 6.6% of the intensity of IL-12/-18 + TCR beads respectively.

These data suggest that whilst IFNγ production by CD161^{++}/MAIT cells can occur following stimulation by the TCR in combination with IL-12, the presence of IL-18 is required for robust IFNγ production by individual CD161^{++}/MAIT cells. Interestingly, CD161^{++}/MAIT cells activated by IL-12/-18 (and lacking TCR stimulation) are able to also produce robust amounts of IFNγ whilst cells lacking IL-12 or IL-18, even if undergoing TCR stimulation, are not.

3.3.2 TCR signalling important for MAIT cell TNFα/CD69

In contrast to the release of IFNγ, few CD161^{++}/MAIT cells were able to produce TNFα in response to IL-12/-18 (mean $5.1 \pm 1.0\%$; p = ns vs. unstim.; Fig. 3.4 A). Similarly, few CD161^{++}/MAIT cells expressed TNFα in response to TCR beads alone (mean $3.8 \pm 0.6\%$; p = ns vs. unstim.). However, in response to the combination of TCR beads with either IL-12 or IL-18, the mean frequencies were $14.7 \pm 1.8\%$ and $12.0 \pm 2.0\%$ respectively (both $p < 0.0001$ vs. unstim.). When cultured with IL-12/-18 + TCR beads, TNFα-expression increased to $37.7 \pm 3.2\%$ ($p < 0.0001$). The GMFI of TNFα$^+$ MAIT cells (Fig. 3.4 B) was in general lower than that of IFNγ (Fig. 3.3 B, p. 59), but whilst there were no significant differences in TNFα GMFI between any of the stimulations involving TCR beads, a marginally lower signal was detected following stimulation with IL-12/-18 vs. IL-12/-18 + TCR beads ($p < 0.05$).

These data suggest that, in contrast to IFNγ expression, TCR-crosslinking is largely necessary but not sufficient for expression of TNFα at 24h, with a synergistic effect following the combination of TCR beads and either IL-12 or IL-18 — with the greatest synergistic effect and highest frequency of responding cells following stimulation by TCR beads + IL-12/-18.

3.3.2.1 TCR cross-linking is sufficient for robust expression of CD69

Unlike IFNγ and TNFα, which are not expressed by CD161^{++}/MAIT cells under resting conditions, CD69 was expressed on the cell surface by mean $19.2 \pm 2.9\%$ of unstimulated CD161^{++}/MAIT cells (Fig. 3.4 C). Whilst no increase was seen following IL-12 stimulation (p = ns), CD69 was up-regulated following IL-18

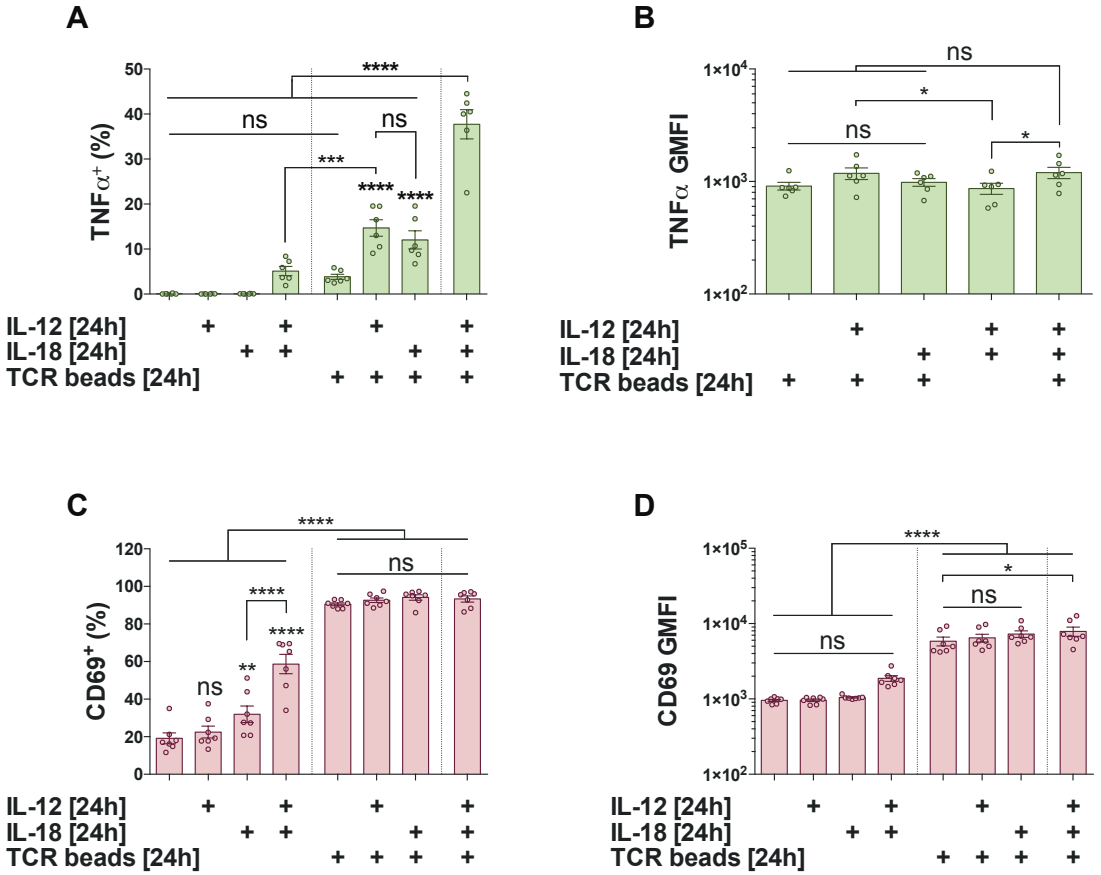


Figure 3.4: TNFα induction and CD69 up-regulation by IL-12 and IL-18 ± TCR stimulation. Positively isolated CD8α$^+$ T cells were stimulated with 50 ng/ml IL-12, IL-18 and/or αCD2/3/28 coated beads for 24h, before assessment of activation status by flow cytometry. Graphs show CD161^{++}/MAIT cell TNFα expression (A, B) or CD69 upregulation (C, D) as a frequency (%) of population responding (A, C) or GMFI of responding cells (i.e. above the threshold of activation) (B, D). All graphs presented as mean ± SEM. Data analysed by one-way ANOVA with Holm-Sidak's multiple comparison test. For all tests, ****$p < 0.0001$, ***$p < 0.001$, **$p < 0.01$, *$p < 0.05$, ns = non-significant.

stimulation alone (mean +12.8%; $p < 0.01$) and IL-12/-18 stimulation (mean +39.5%; $p < 0.0001$). Following any stimulation with TCR beads, either in the presence or absence of additional cytokines, > 90% of MAIT cells were CD69$^+$ ($p < 0.0001$). As with TNFα expression, despite the increased proportion of CD161^{++}/MAIT cells expressing CD69 following IL-12/-18 stimulation, the GMFI of CD69 amongst activated (CD69$^+$) CD161^{++}/MAIT cells was higher for all stimulations involving TCR beads relative to IL-12/-18 ($p < 0.0001$; Fig. 3.4 D).

These results indicate that although CD69 expression can be induced by IL-12/-18, neither IL-12, nor IL-18 are necessary for robust CD69 expression, whereas TCR-crosslinking (with CD2/28 co-stimulation) is sufficient.

3.4 IL-12/-18 dose response & TCR stimulation

TCR signalling can synergise with IL-12/-18 stimulation to robustly increase the frequency of IFNγ$^+$ CD161^{++}/MAIT cells, although interestingly the increase in IFNγ GMFI on additional stimulation via the TCR compared to IL-12/-18 is relatively less pronounced (see Section 3.3.1, p. 58). However, these data were generated using relatively high concentrations of cytokine (50 ng/ml). Whether TCR signalling results in a greater sensitivity to IL-12/-18 at lower concentrations, or simply enables more cells to respond above a cytokine concentration threshold (i.e. closer to 50 ng/ml) is unclear. To initially assess the effect of TCR signalling on CD161^{++}/MAIT cell sensitivity to IL-12/-18, a two-fold serial dilution dose titration of IL-12/-18 (0.81 – 50 ng/ml) was performed for 24h in the presence and absence of TCR beads, before cells were stained internally for IFNγ and TNFα by ICS.

In broad agreement with the earlier data (see Section 3.3.1), stimulation of MAIT cells with IL-12/-18 in the presence of TCR beads led to a greater frequency of IFNγ$^+$ CD161^{++}/MAIT cells than did stimulation with IL-12/-18 alone (Fig. 3.5 A). Interestingly, whilst there was no production of IFNγ with TCR beads alone (mean 0.9 ± 0.6%), 22.4 ± 2.2% were IFNγ$^+$ on culture with TCR beads and the lowest concentrations of IL-12/-18 tested (0.81 ng/ml). Similar sensitivity to IL-12/-18 after TCR-crosslinking was also seen for TNFα expression, albeit with fewer cells responding (Fig. 3.5 B). In the absence of TCR-crosslinking, both the frequency of responding cells, and the IL-12/-18 sensitivity for IFNγ and TNFα expression were lower.

3.4.1 Biphasic IFNγ-response to IL-12/-18 + TCR beads

To better capture the dynamic range of the TCR-triggered CD161^{++}/MAIT cell response to IL-12 and IL-18 at low-doses, CD8α$^+$ T cells were next cultured with four-fold increasing concentrations of IL-12/-18 (0.012 – 50 ng/ml) ± TCR beads. As a similar proportion of CD161^{++}/MAIT cells responded to IL-12 + TCR beads vs. IL-12/-18 (but not IL-18 + TCR beads), the dose-response of TCR-stimulated CD161^{++}/MAIT cells to IL-12 was also assessed. 24 hours post-stimulation, cells were surface stained for CD69, stained on the surface + internally for Vα7.2 TCR, and stained internally for IFNγ and TNFα. Data were additionally analysed by non-linear regression analysis (see Section 3.2.2), which permits EC50 and IC50 values to be generated, as well as the top plateau and HillSlopes. Each describe the data in different, but complementary ways. EC50/IC50 values indicate the concentration required for half the maximal effect, whilst the top plateau indicates

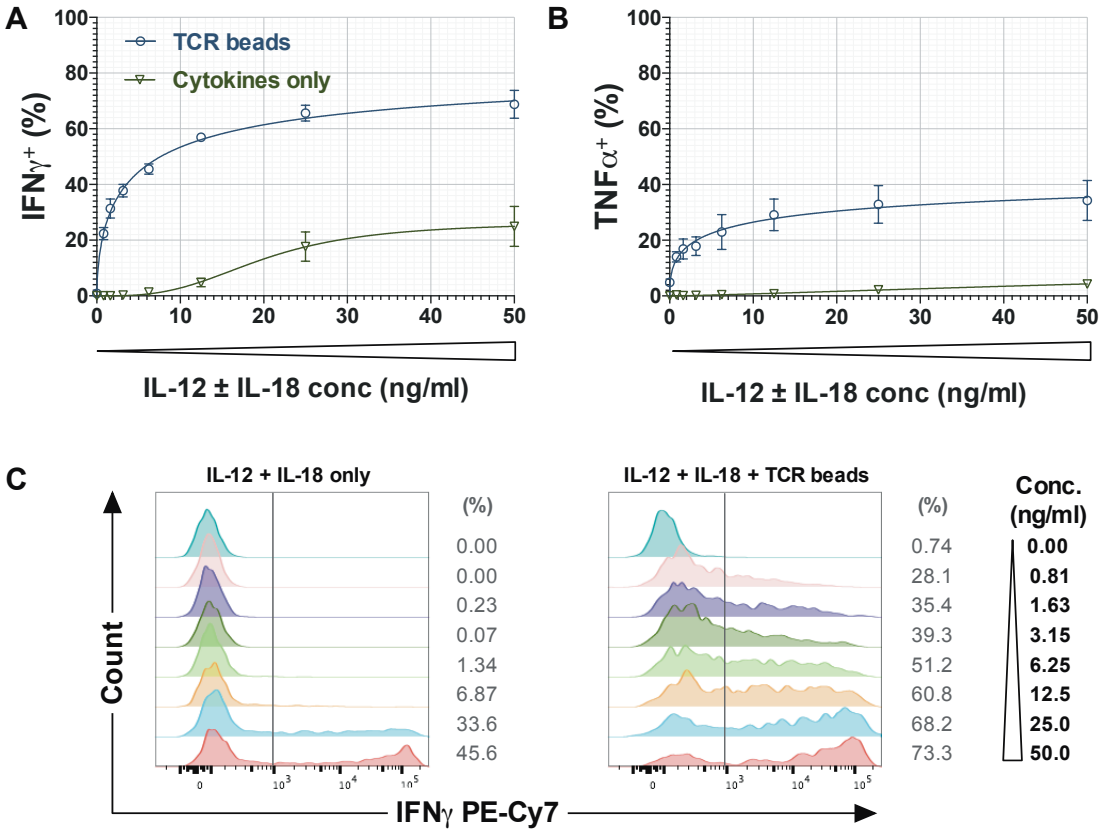


Figure 3.5: Two-fold dose titration of IL-12/-18 ± TCR beads shows TCR signalling enhancement of CD161^{++}/MAIT cell response to IL-12/-18. CD8α^{+} T cells were stimulated with two-fold increasing concentrations of IL-12/-18 (0 – 50 ng/ml each), in the presence or absence of αCD2/3/28 coated beads for 24h. Graphs show (A) frequency of IFNγ^{+} MAIT cells and (B) frequency of TNFα^{+} MAIT cells. (C) Representative FACS plot of IFNγ expression by MAIT cells. Graphs show mean ± SEM. Half-offset histogram shows modal *y*-axis scaling (% max. count per condition).

the maximum predicted response, and the HillSlope indicates the steepness of the curve. HillSlopes of < 1 are shallow, of 1 are standard, and > 1 are considered steep. Where a biphasic model is predicted, each parameter can be used to describe the two phases individually.

As in Fig. 3.5, no IFNγ was detected following stimulation with TCR beads alone (Fig. 3.6 A). However, at the lowest concentration tested (0.012 ng/ml), there was already a detectable response to TCR beads + IL-12 (mean $7.3 \pm 1.6\%$) and TCR beads + IL-12/-18 (mean $7.0 \pm 1.8\%$). By contrast, in the absence of TCR beads, CD161^{++}/MAIT cells needed IL-12/-18 concentrations of $\geqslant 3.13$ ng/ml — approximately 250-fold higher — before IFNγ^{+} CD161^{++}/MAIT cells were observed (mean $4.8 \pm 0.8\%$ IFNγ^{+}). The estimated plateau for CD161^{++}/MAIT cells responding to IL-12/-18 only was $36.6 \pm 2.6\%$, for IL-12 + TCR beads it was

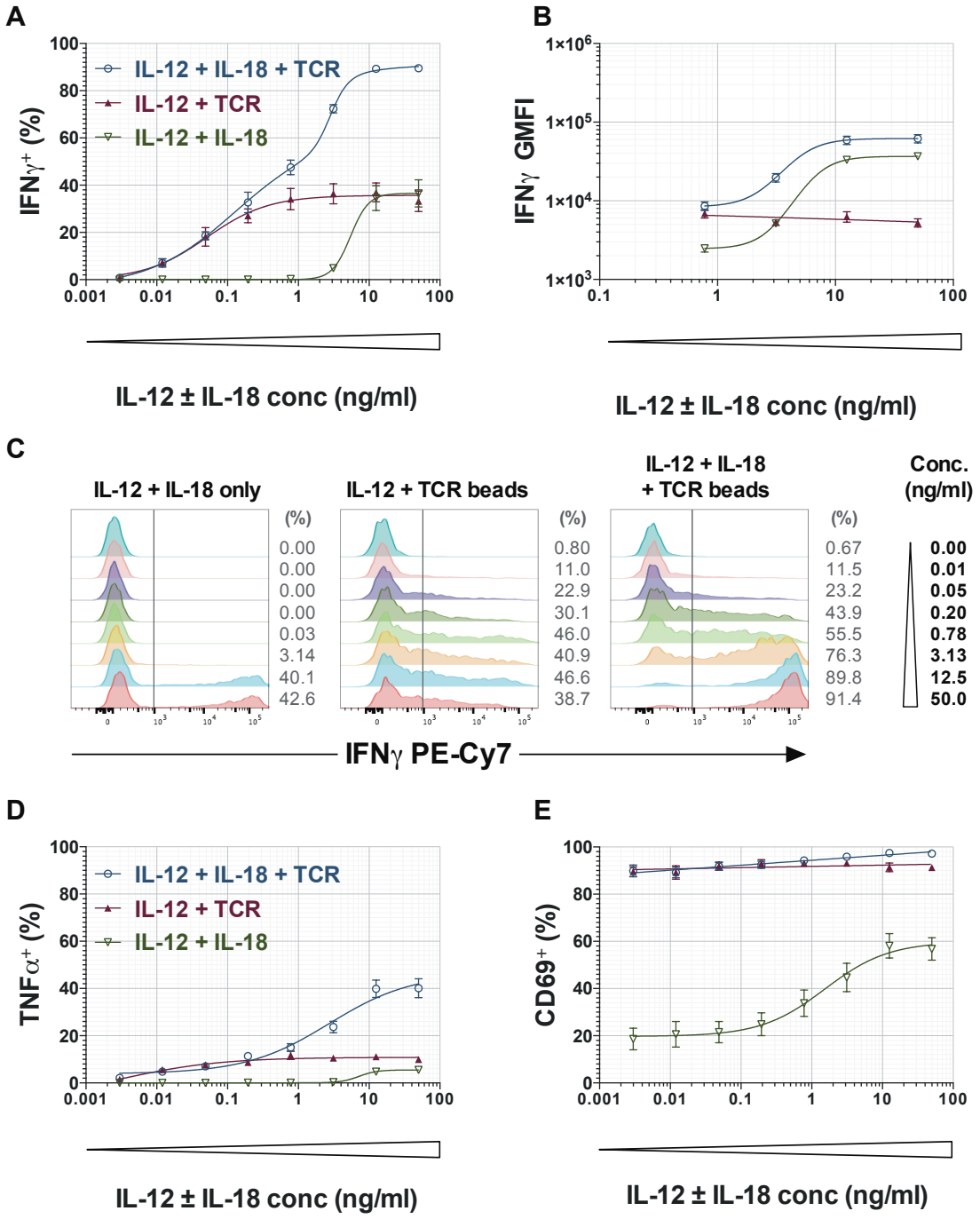


Figure 3.6: Four-fold dose titration of IL-12 and IL-12/-18 ± TCR beads, showing a biphasic IFNγ$^+$ (%) response to IL-12/-18 + TCR beads and the importance of IL-12/-18 for IFNγ GMFI. CD8α$^+$ T cells were stimulated with four-fold increasing concentrations of IL-12/-18 (0 – 50 ng/ml respectively), in the presence or absence of αCD2/3/28 coated beads. (A) Frequency of IFNγ$^+$ CD161^{++}/MAIT cells. (B) IFNγ GMFI of IFNγ$^+$ CD161^{++}/MAIT cells. (C) Representative FACS plot of IFNγ expression by CD161^{++}/MAIT cells. Graphs show mean ± SEM. Half-offset histogram shows modal *y*-axis scaling (% max. count per condition). (D) Frequency of TNFα$^+$ CD161^{++}/MAIT cells. (E) TNFα GMFI of TNFα$^+$ CD161^{++}/MAIT cells.

35.7 ± 2.0%, whilst for IL-12/-18 + TCR beads it was 90.6 ± 2.1%. $CD161^{++}$/MAIT cells responded to TCR beads + IL-12 with an EC50 of 0.051 ng/ml (95% CI, 0.027–0.097), and a HillSlope of 0.99 (Fig. 3.6 A). By contrast, $CD161^{++}$/MAIT cells responded to IL-12/-18 alone with an EC50 of 5.5 ng/ml (95% CI, 3.3–9.0), approximately 110-fold higher. In addition, the HillSlope (3.4) was far steeper.

Interestingly, the IFNγ response to TCR beads + IL-12/-18 followed a biphasic model ($p = 0.038$), with an $EC50_1$ of 0.085 ng/ml (95% CI, 0.012 – 0.62), approximately similar to that of TCR beads + IL-12, and an $EC50_2$ of 2.5 ng/ml (95% CI, 1.1 – 5.3) — approximately similar to that of IL-12/-18 in the absence of TCR beads. The first and second-phase HillSlopes were 0.93 and 1.9, again each reflecting the IL-12 + TCR beads, and IL-12/-18 curves, respectively.

For the GMFI of $IFN\gamma^{+}$ $CD161^{++}$/MAIT cells, curves were fitted using data from IL-12/-18 threshold concentrations above 0.78 ng/ml (Fig. 3.6 B). These indicated an EC50 for IL-12/-18 of 6.5 ng/ml, and a HillSlope of 3.3, whilst indicating an EC50 for IL-12/-18 + TCR of 4.8 ng/ml and a HillSlope of 3.0. In the absence of a clear dose-response, a linear regression was instead performed for IFNγ GMFI following stimulation with IL-12 + TCR beads, finding $r^2 = 0.089$ and a slope deviating non-significantly from zero.

Thus, TCR stimulation increased the sensitivity to IL-12/-18 (decreasing the EC50) for cells expressing IFNγ. Interestingly, for IFNγ-expression on a *per cell* basis, the EC50 remained relatively high for IL-12/-18 — independently of whether or not there was also concurrent TCR stimulation. Similarly, in the presence of TCR beads, MAIT cells responded to IL-12 with high sensitivity high (low EC50), even in the absence of IL-18. However, no dose response for *per cell* IFNγ expression increase was seen in the absence of IL-18, suggesting TCR + IL-12 stimulation is sufficient to permit IFNγ-expression, but IL-18 is additionally required for high IFNγ-expression.

3.4.1.1 TNFα-response to IL-12/-18 + TCR beads shows higher EC50

In agreement with earlier data the TNFα response was lower than for IFNγ — reaching a $TNF\alpha^{+}$ plateau at 46.4% for IL-12/-18 + TCR, 10.9% for IL-12 + TCR, and 5.5% for IL-12/-18 (Fig. 3.6 C). Following stimulation by IL-12/-18 + TCR beads, at 2.7 ng/ml (95% CI, 0.97 – 7.7) the EC50 was similar to the IFNγ response for IL-12/-18 and for the second-phase of the IL-12/-18 + TCR bead response, although with broad confidence intervals and a relatively shallow HillSlope (0.74). For IL-12/-18 only, the EC50 was even higher at 7.2 ng/ml (95% CI, 4.1 – 12.7) and with a steeper HillSlope (3.5), again reflecting the cytokine-only mediated dose-response of the IFNγ response, albeit with fewer responsive cells — and again

with broad confidence intervals. In contrast to IL-12/-18 ± TCR beads, the EC50 for the response to IL-12 + TCR beads was very low, at 0.0031 ng/ml, although with extremely broad 95% confidence intervals (95% CI, 1.9×10^{-7} – 49.8), reflecting both the low plateau of max. TNFα (%) under these conditions, and ability of max. TNFα (%) to be reached with low IL-12 concentrations.

These data indicate that CD161^{++}/MAIT cells are less responsive to cytokines alone for TNFα-expression — although they also express TNFα in a dose-dependent manner following stimulation with TCR beads and IL-12/-18, but not IL-12 alone. In the presence of TCR beads, CD161^{++}/MAIT cells also appear to exhibit a higher IL-12/-18 concentration threshold for TNFα-expression compared to IFNγ-expression at this time point.

3.4.1.2 CD69 is up-regulated in an IL-12/-18 dose-dependent manner

Unlike the IFNγ and TNFα responses, CD161^{++}/MAIT cells expressed CD69 robustly to TCR beads in the absence of cytokines. However, some further up-regulation of CD69 on TCR-triggered CD161^{++}/MAIT cells was observed on addition of IL-12/-18. Fitting a 4-parameter dose-response curve to the data generated with IL-12/-18 + TCR beads indicated a bottom-plateau of 89.1 ± 2.5%, rising to a top-plateau 98 ± 2.5% (a span of 8.95%). By contrast, in the absence of TCR beads a bottom-plateau of 19.7 ± 3.4%, and a top-plateau of 60.0 ± 6.4% were indicated (a span of 40.2 %). In the presence and absence of TCR beads, CD161^{++}/MAIT cells responded to IL-12/-18 with EC50 values of 0.39 ng/ml (95% CI, 0.025 – 6.23) and 1.5 ng/ml (95% CI, 0.46 – 5.1) for CD69 expression, respectively. The curve fitted to the IL-12 + TCR bead stimulation data was ambiguous, and a linear regression found $r^2 = 0.05$ with the slope deviating non-significantly from zero, in agreement with the CD161^{++}/MAIT cell TNFα response to 24h stimulation with IL-12 + TCR beads.

These data indicate that in the absence of TCR stimulation, CD161^{++}/MAIT cells express CD69 in response to IL-12/-18 stimulation in a dose dependent manner — interestingly with a lower EC50 (and therefore higher sensitivity) than the IL-12/-18 IFNγ response, indicating a lower threshold for IL-12/-18 induced CD69- versus IFNγ- response. However, not all CD161^{++}/MAIT cells are capable of expressing CD69 in response to IL-12/-18 only, whilst in response to TCR stimulation CD161^{++}/MAIT cells express CD69 uniformly and robustly.

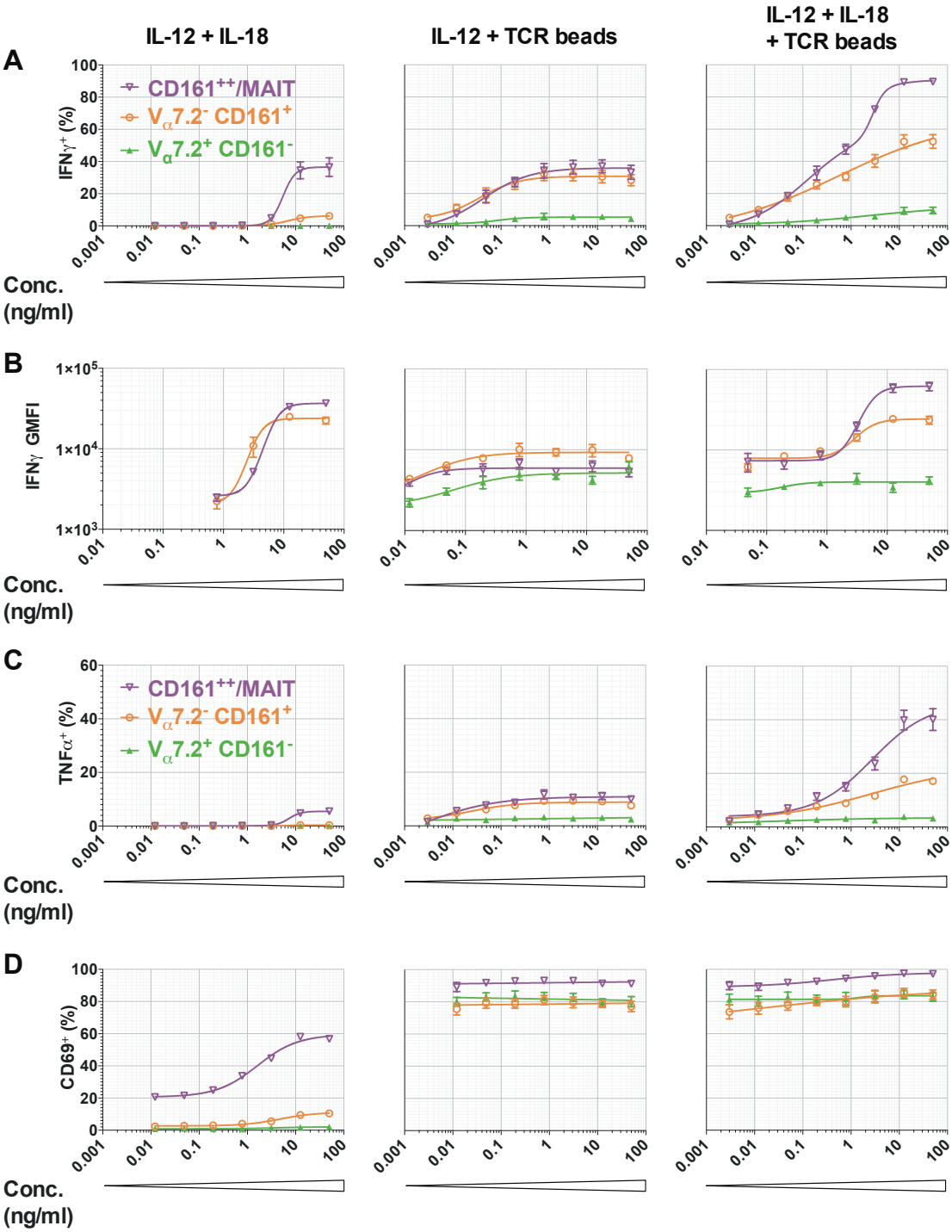


Figure 3.7: Response to IL-12/-18 varies with dose according to CD161 expression. CD8α$^+$ T cells were stimulated with four-fold increasing concentrations of IL-12/-18 (0 - 50 ng/ml each), in the presence or absence of αCD2/3/28 coated beads for 24h, and the activation status of CD161^{++}/MAIT, Vα7.2$^-$ CD161$^+$ and Vα7.2$^+$ CD161$^-$ CD8α$^+$ T cell subsets was assessed. (A) Frequency of IFNγ$^+$ cells. (B) IFNγ GMFI of IFNγ$^+$ cells. (C) Frequency of TNFα$^+$ cells. (D) Frequency of CD69$^+$ cells. Graphs show mean ± SEM.

3.4.2 CD161-expression & the dose-response to IL-12/-18

Whilst CD161^{++} CD8α^{+} T cells respond most strongly to IL-12/-18 [93], CD161^{+} CD8α^{+} T cells are also capable of responding to IL-12/-18, albeit to a reduced extent. This is reflected in their limited expression of certain phenotypic traits (such as expression of IL-18Rα, and the transcription factors RORγt, and PLZF) characteristic of CD161^{++}/MAIT cells [136]. Unlike MAIT cells, CD161^{+} CD8α^{+} cells are MHC class I-restricted, although they are both effector-memory T cells [361]. Whether the CD161^{++}/MAIT cell sensitivity to IL-12/-18 at lower concentrations in the context of TCR stimulation is unique to CD161^{++}/MAIT cells, however, or shared with CD161^{+}, or CD161^{-} CD8α^{+} T cells, is unclear. Therefore, the response to IL-12/-18 ± TCR stimulation was compared between, CD161^{++}/MAIT, CD161^{+} and CD161^{-} CD8α^{+} T cells. Cells were gated as Vα7.2^{-} CD161^{+} to ensure exclusion of any MAIT cells overlapping with the CD161 mid-expressing population, and as Vα7.2^{+} CD161^{-} CD8α^{+} T cells to control for TCR expression.

3.4.2.1 CD161^{+} cells are less responsive to IL-18 for IFNγ-expression

In comparison with the robust IFNγ response by CD161^{++}/MAIT cells following stimulation with 50 ng/ml IL-12/-18 (mean 36.6 ± 5.7%) the maximum IFNγ response by the Vα7.2^{-} CD161^{+} cells was much lower (mean 6.1 ± 1.1%), whilst the Vα7.2^{+} CD161^{-} cells remained IFNγ^{-} (mean 0.15 ± 0.09%; Fig. 3.7 A). Both the CD161^{++}/MAIT and Vα7.2^{-} CD161^{+} cells had a relatively high EC50 for IL-12/-18 (5.5 and 7.0 ng/ml) respectively. In addition, despite the relatively large gap in IFNγ^{+} (%) frequency between the two, the IFNγ GMFI of responding cells was of a similar order of magnitude at 50 ng/ml ($3.7 \pm 0.1 \times 10^4$ vs. $2.2 \pm 0.2 \times 10^4$; Fig. 3.7 B), indicating that once activated by IL-12/-18, CD161^{++}/MAIT and Vα7.2^{-} CD161^{+} cells are capable of expressing similar amounts of IFNγ.

On stimulation with TCR beads and 50 ng/ml IL-12, however, CD161^{++}/MAIT, and Vα7.2^{-} CD161^{+} cells reached similar IFNγ^{+} frequencies (mean 33.2 ± 4.4% and 28.3 ± 6.9% respectively). Again, Vα7.2^{+} CD161^{-} cells remained largely IFNγ^{-} (mean 4.3 ± 1.4%). For all three subpopulations, the EC50 was similarly low (0.04 – 0.08 ng/ml), reflecting low threshold IL-12 concentrations needed to broadly activate cells.

The IFNγ GMFI of activated cells were also equivalently low following 50 ng/ml IL-12 + TCR stimulation ($5.3 \pm 0.6 \times 10^3$ vs. $7.9 \pm 0.8 \times 10^3$ vs. $6.2 \pm 0.9 \times 10^3$ for CD161^{++}/MAIT, Vα7.2^{-} CD161^{+} and Vα7.2^{+} CD161^{-} cells, respectively), indicating a reduced capacity for activated cells in each subpopulation to express higher IFNγ levels in response to this stimulus.

Following the addition of IL-18 to the IL-12 + TCR bead stimulation, the maximum frequency of IFNγ$^+$ Vα7.2$^+$ CD161$^-$ cells increased to $9.4 \pm 2.1\%$, whilst the frequency of IFNγ$^+$ Vα7.2$^-$ CD161$^+$ cells increased to $52.4 \pm 4.3\%$ and the frequency of IFNγ$^+$ CD161^{++}/MAIT cells rose to $90.0 \pm 1.2\%$. The Vα7.2$^-$ CD161$^+$ cells responded with an EC50 value of 0.54 ng/ml, whilst Vα7.2$^+$ CD161$^-$ cells demonstrated a higher EC50 of 2.4 ng/ml. The CD161^{++}/MAIT cells response followed a biphasic model as mentioned previously, with an $EC50_1$ of 0.085 ng/ml, and an $EC50_2$ of 2.5 ng/ml.

As with stimulation by IL-12/-18 in the absence of TCR beads, the responding CD161^{++}/MAIT and Vα7.2$^-$ CD161$^+$ cells both exhibited relatively high maximum IFNγ GMFIs ($6.2 \pm 0.8 \times 10^4$ vs. $2.4 \pm 0.3 \times 10^4$ respectively) compared to the Vα7.2$^+$ CD161$^-$ cells ($0.42 \pm 0.04 \times 10^4$) — approximately 16-fold and 6-fold lower than the CD161^{++}/MAIT and Vα7.2$^-$ CD161$^+$ cells respectively. However, the maximum GMFI for CD161^{++}/MAIT cells was approximately 3-fold higher than the Vα7.2$^-$ CD161$^+$ cells, indicating that CD161^{++}/MAIT cells, in addition to responding most uniformly, are able to express IFNγ most robustly on activation.

3.4.2.2 EC50 for TNFα-response similar for CD161^{++} & CD161$^+$ cells

Following 24h stimulation, the frequency of TNFα$^+$ cells in each subset was reduced, relative to those expressing IFNγ (Fig. 3.7 C, p. 69). However, the dose-response curves broadly reflected those of IFNγ expression (Fig. 3.7 A). Following maximal (50 ng/ml) IL-12/-18 stimulation, the CD161^{++}/MAIT cell response was $5.5 \pm 1.1\%$, whilst the Vα7.2$^-$ CD161$^+$ and Vα7.2$^+$ CD161$^-$ cells expressed negligible TNFα ($0.38 \pm 0.09\%$ and $0.04 \pm 0.02\%$ respectively). After stimulation with IL-12 + TCR, the maximum CD161^{++}/MAIT cell response rose to $10.0 \pm 0.5\%$, whilst the Vα7.2$^-$ CD161$^+$ cells to increased to $7.6 \pm 0.40\%$ and the Vα7.2$^+$ CD161$^-$ cells to $2.5 \pm 0.7\%$.

Similarly to the IFNγ response, IL-12/-18 + TCR beads induced the greatest TNFα response across the three sub-populations, with maximal TNFα (%) frequencies of $40.1 \pm 4.1\%$, $17.2 \pm 1.0\%$ and $3.2 \pm 0.5\%$ for the CD161^{++}/MAIT, Vα7.2$^-$ CD161$^+$ and Vα7.2$^+$ CD161$^-$ cells respectively. Interestingly, the EC50 values of the TCR-triggered CD161^{++}/MAIT and Vα7.2$^-$ CD161$^+$ cells differed relative to their IFNγ response — both 2.7 ng/ml — indicating an approximately 4–5-fold higher IL-12/-18 concentration requirement for an equivalent increase in TNFα vs. IFNγ production after 24h stimulation.

Nonetheless, despite the differences in TNFα$^+$ (%) frequency, the similar EC50 of the CD161^{++}/MAIT and Vα7.2$^-$ CD161$^+$ cells indicates an overarching similarity in the intrinsic response to IL-12/-18 + TCR stimulation between responding cells from each of the CD161-expressing subsets.

3.4.2.3 Few CD161$^+$ cells express CD69 in response to IL-12/-18 alone

Whilst a proportion of CD161^{++}/MAIT cells basally express CD69 (mean 18.6 ± 4.6%), neither Vα7.2$^-$ CD161$^+$, nor Vα7.2$^+$ CD161$^-$ cells expressed any CD69 at baseline (mean 2.6 ± 0.5 and 1.1 ± 0.1% CD69$^+$ respectively; Fig. 3.7 D, p. 69). Stimulating with IL-12/-18 increased CD69-expression of CD161^{++}/MAIT cells to a maximum of 56.8 ± 4.8%, with an EC50 of 1.6 ng/ml, whilst Vα7.2$^-$ CD161$^+$ and Vα7.2$^+$ CD161$^-$ cells were max. 10.5 ± 1.8% and 2.0 ± 0.2% CD69$^+$, with increased EC50 values of 4.7 and 4.2 ng/ml respectively. These data indicate a greater resistance to CD69-expression in response to IL-12/-18 alone, for the Vα7.2$^-$ CD161$^+$ and Vα7.2$^+$ CD161$^-$ CD8α$^+$ T cells, relative to CD161^{++}/MAIT cells.

Following stimulation with TCR beads + IL-12, each subpopulation robustly up-regulated their expression of CD69 (to mean 89.9±2.7%, 73.6±4.4% and 81.3±3.3% for CD161^{++}/MAIT, Vα7.2$^-$ CD161$^+$ and Vα7.2$^+$ CD161$^-$ cells respectively), demonstrating a shared capacity to detect the TCR stimulus. Nonetheless, with the addition of increasing concentration of IL-12, the 4 parameter dose-response curves generated were ambiguous. Therefore, linear regressions were generated with values of $r^2 = 0.014$, 0.0044 and 0.013 for for CD161^{++}/MAIT, Vα7.2$^-$ CD161$^+$ and Vα7.2$^+$ CD161$^-$ cells respectively, with each slope differing non-significantly from zero ($p > 0.5$). This indicates that with TCR-stimulation, no IL-12-dependent dose response for CD69-expression was observed across the three sub-populations.

With the addition of increasing IL-12/-18 doses to the TCR bead stimulus, the maximum CD69-expression for CD161^{++}/MAIT cells increased from 89.9 ± 2.5% to 97.2 ± 0.72% (EC50 = 0.39 ng/ml), whilst for Vα7.2$^-$ CD161$^+$ cells CD69 expression increased from 73.6 ± 4.4% to 84.4 ± 2.9% (EC50 = 0.39 ng/ml). By contrast, the Vα7.2$^+$ CD161$^-$ cells showed little further up-regulation of CD69 (81.3 ± 3.3% to 82.9 ± 2.7%); with linear regression finding $r^2 = 0.0074$ and the slope deviating non-significantly from zero ($p > 0.5$).

These data indicate that the Vα7.2$^-$ CD161$^+$ cells that are capable of responding to IL-12/-18 for CD69-expression do so with a similar sensitivity to IL-12/-18 compared to CD161^{++}/MAIT cells. However, far fewer Vα7.2$^-$ CD161$^+$ cells are capable of responding to IL-12/-18 in the absence of TCR stimulation. By contrast, Vα7.2$^+$ CD161$^-$ cells show little sign of a dose-dependent response to IL-12/-18; either in the presence, or absence of TCR beads.

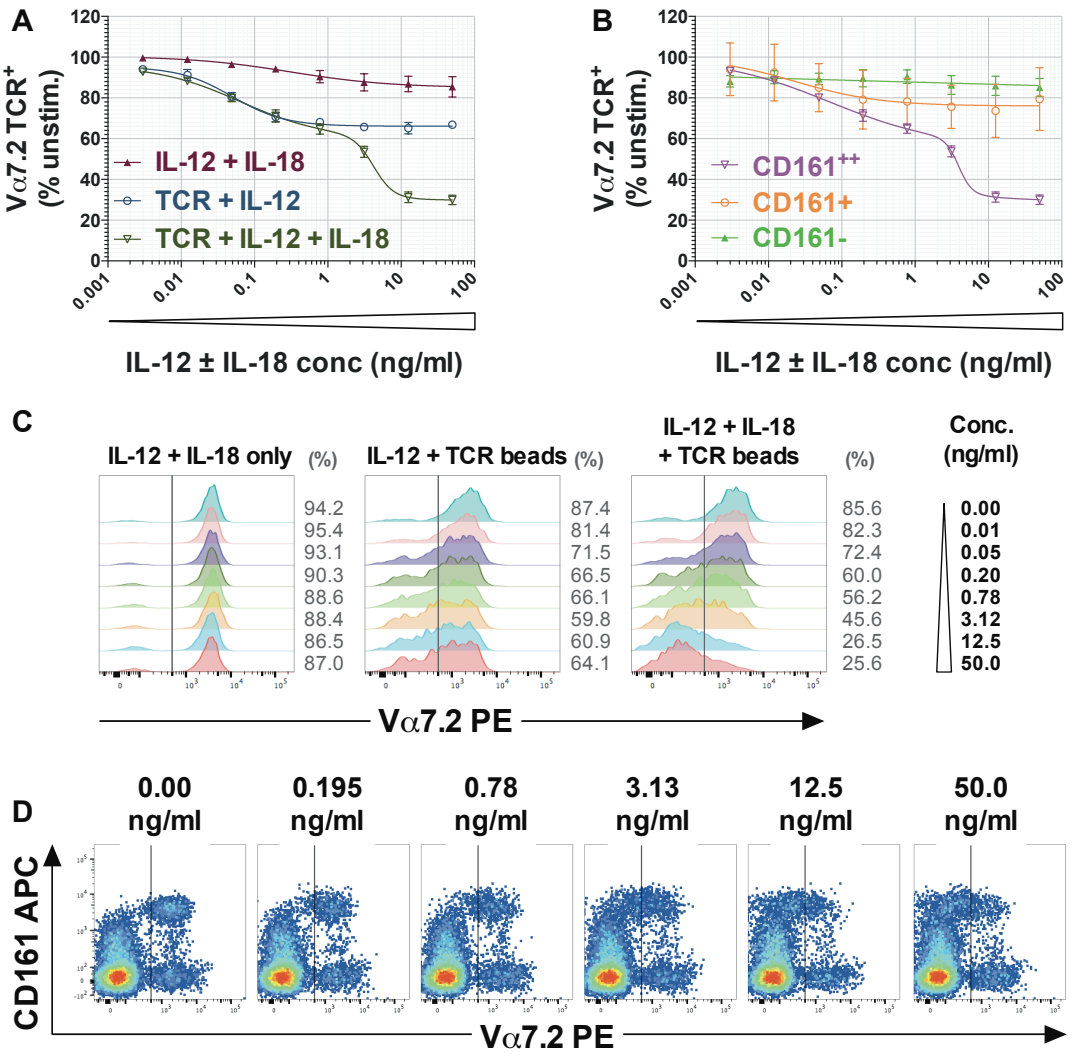


Figure 3.8: Biphasic IL-12/-18 induced down-regulation of Vα7.2 TCR. CD8α$^+$ T cells were stimulated with four-fold increasing concentrations of IL-12/-18 (0 – 50 ng/ml) ± TCR beads for 24h. (A) Expression of Vα7.2 TCR on CD161^{++}/MAIT cells, and (B) on CD161^{++}, CD161$^+$ and CD161$^-$ CD8α$^+$ T cells following different treatments, relative to donor max. (C) Representative FACS plot of Vα7.2 TCR expression on CD161^{++}/MAIT cells, and (D) CD8α$^+$ T cells. Graphs show mean ± SEM. Half-offset histogram shows modal y-axis scaling (% max. count per condition).

3.4.2.4 Down-regulation of the MAIT cell TCR follows biphasic model

Following 24h stimulation with 50 ng/ml of both IL-12 and IL-18 + TCR beads, CD161^{++}/MAIT cells substantially down-regulated their Vα7.2^{+} TCR (Section 3.3). Whether this also occurs at lower concentrations, however, remains unclear. To analyse Vα7.2 expression following stimulation with increasing doses of IL-12 ± IL-18 ± TCR beads, Vα7.2^{+} TCR expression for CD161^{++} cells (Fig. 3.8 A–D), CD161^{+} cells and CD161 cells (Fig. 3.8 B, D) was assessed and normalised per donor vs. unstimulated.

After culture with 50 ng/ml each of IL-12/-18, the mean Vα7.2^{+} TCR expression of CD161^{++}/MAIT cells was 85.4 ± 5.0% of unstimulated, a reduction of approximately 15% (IC50 = 0.31 ng/ml, 95% CI, 0.02 to 1.6). By contrast, following stimulation with TCR beads + max. IL-12, expression was reduced approximately 33% to 66.8±1.6% (IC50 = 0.05 ng/ml, 95% CI, 0.03 to 0.09). Vα7.2 TCR expression was reduced most strongly by culture with 50 ng/ml IL-12/-18 to 29.9 ± 2.3% of maximum — a reduction of approximately 70%. Furthermore, the dose-dependency of the decrease in Vα7.2 TCR expression amongst CD161^{++} cells was biphasic ($p = 0.006$), with an $IC50_1$ of 0.07 ng/ml (95% CI, 0.02 to 0.27), and an $IC50_2$ of 4.2 ng/ml (95% CI, 2.4 to 7.4). Of note, the percentage of the total Vα7.2 TCR reduction due to each phase was split about 50% (i.e. 54.1% due to the more potent phase). In contrast to the reduction of Vα7.2^{+} TCR expression within the CD161^{++} CD8α^{+} T cell subset, the Vα7.2^{+} TCR expression level following IL-12/-18 + TCR bead stimulation amongst CD161^{+} cells was more variable at 79.5±15.4% of unstimulated with an IC50 of 0.024 ng/ml (95% CI, 3.4×10^{4} to 1.6). For the CD161^{-} cells; whilst the Vα7.2^{+} TCR expression was 85.1 ± 4.4% of unstimulated, neither dose-response curve could be fit. Therefore, a linear-regression was performed finding the slope non-significantly deviating from zero ($p = 0.28$, $r^2 = 0.04$).

These data indicate that, at lower concentrations and with co-incident stimulation with TCR beads, the MAIT cell TCR expression is reduced with similar sensitivity and to a similar extent by either IL-12 or IL-12/-18. Conversely, TCR stimulation + IL-12 alone failed to further reduce Vα7.2 expression by the TCR-triggered CD161^{++} cells, with exposure to relatively higher levels of IL-12/-18 required for this secondary drop of Vα7.2 TCR expression. Despite some reduction in the Vα7.2 expression amongst CD161^{+} CD8α^{+} T cells, this occurred to a smaller extent than with the first-phase reduction amongst the CD161^{++} CD8α^{+} T cell population. The CD161^{++}/MAIT cells, but not the Vα7.2^{-} CD161^{+} cells were able to respond further at higher cytokine concentrations.

Overall, these data show that CD161^{++}/MAIT cells weakly down-regulate their TCR following exposure to IL-12/-18 alone. TCR beads and IL-12 stimulation induce a modest down-regulation; whilst Vα7.2 is robustly down-regulated following stimulation by TCR beads + IL-12/-18. Importantly, during TCR stimulation modest TCR down-regulation occurs at low concentrations of IL-12/-18, whilst robust down-regulation occurs at high concentrations of IL-12/-18, reflecting a heightened activation state. Vα7.2 CD161^{+} and CD161^{-} cells, conversely, show little down-regulation of their TCR, in line with a reduced activation state induced by TCR beads + IL-12/-18 in combination.

3.5 Kinetics of the IL-12/18 and TCR responses

3.5.1 Sustained TCR-stimulation increases IFNγ^{+} (%)

Antigen-specific rapid effector function in CD8α^{+} T cells is possible in under 6 hours post-stimulation [55], however, in order to robustly activate MAIT cells by IL-12/-18 in a TCR independent manner, > 16h cytokine exposure is necessary. The presence of some cytokine is necessary for CD161^{++}/MAIT cell activation by TCR beads, and so far experiments in this chapter have been performed to permit sufficient time for a robust cytokine-dependent response to occur (25h). Nonetheless, in the context of an optimal cytokine exposure (25h) — whether MAIT cells can respond more robustly to a rapid (5h), or sustained (25h) TCR stimulation has not been tested. Therefore, in order to assess how TCR stimulation length could affect activation of CD161^{++}/MAIT cells within the context of an IL-12 and/or IL-18 cytokine milieu, CD8α^{+} T cells were enriched from PBMCs and stimulated with IL-12 ± IL-18 for 20 hours. Subsequently, cells were additionally stimulated by the addition of TCR beads for the final 5 hours of culture — alternatively, TCR beads were included for the whole 25 hours, or not at all. Brefeldin A was added for the final 4 hours of culture (either 1h, or 21h post addition of TCR beads, as appropriate), and cells were stained and analysed by flow cytometry for surface-expression of CD69 as well as internal IFNγ + TNFα, and total Vα7.2 expression (Fig. 3.9).

As shown in Fig. 3.9 A, in the absence of IL-12/-18 stimulation, no IFNγ was detected from CD161^{++}/MAIT cells cultured with TCR beads for 5h (mean $1.9 \pm 0.7\%$) or for 25h (mean $0.92 \pm 0.2\%$). By contrast, in the presence of IL-12 and 5h TCR beads, IFNγ-expression could be detected in $6.8 \pm 1.6\%$ of CD161^{++}/MAIT cells ($p < 0.05$). This was, however, increased ($p < 0.0001$) by stimulation with IL-12 and TCR beads for 25h, following which $36.8 \pm 2.6\%$ CD161^{++}/MAIT cells were IFNγ^{+} ($p < 0.0001$). IL-18 exposed CD161^{++}/MAIT cells responded less well

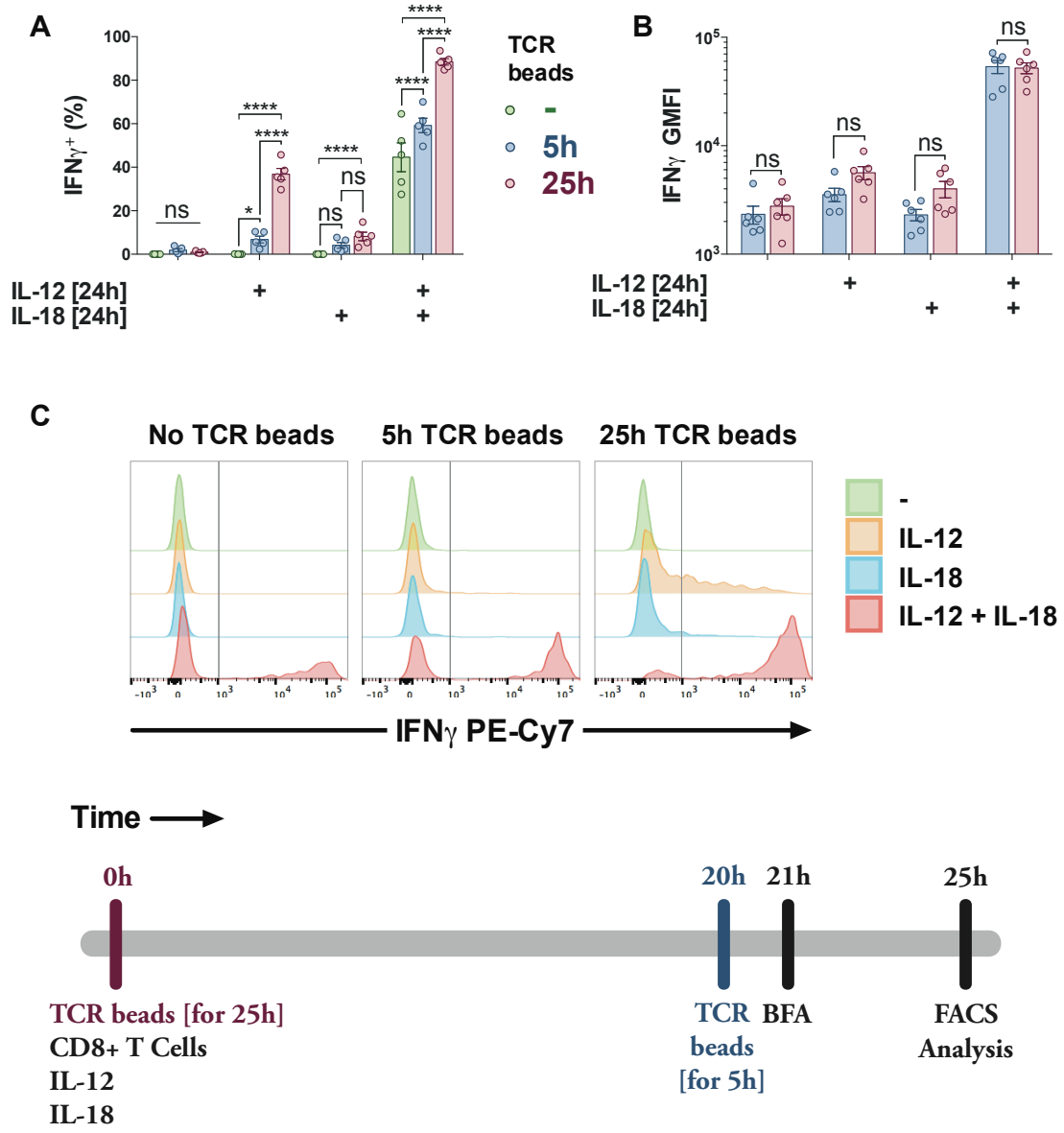


Figure 3.9: Sustained TCR stimulation of cytokine activated MAIT cells enhances frequency, but not GMFI of IFNγ$^+$ expression. CD8α+ T cells were stimulated with IL-12 and/or IL-18 for 25h at 50 ng/ml respectively, in the presence or absence of αCD2/3/28 coated beads for the final 5h, or the whole 25h, before assessment for activation markers by flow cytometry. (A) Frequency of IFNγ$^+$ MAIT cells. (B) GMFI of IFNγ$^+$ MAIT cells. (C) Representative FACS plot of IFNγ expression on CD161^{++}/MAIT cells. Half-offset histogram shows modal y-axis scaling (% max. count per condition). Data analysed by two-way ANOVA with Holm-Sidak's multiple comparison test. Graphs show mean ± SEM. For all tests, ****$p < 0.0001$, ***$p < 0.001$, **$p < 0.01$, *$p < 0.05$, ns = non-significant.

to TCR stimulation, both in the presence of TCR beads for 5h (mean $4.1 \pm 1.3\%$; p = ns), and 25h (mean $8.2 \pm 2.0\%$; $p < 0.0001$). After 25h stimulation with IL-12/-18, $44.6 \pm 6.6\%$ of CD161^{++}/MAIT cells were IFNγ^{+}, in agreement with previous results. Additional stimulation with TCR beads for 5h increased the frequency of IFNγ^{+} cells to $59.2 \pm 3.3\%$ — an increase of +14.6% vs. IL-12/-18 only ($p < 0.0001$), whilst 25h concurrent TCR stimulation resulted in $88.4 \pm 1.5\%$ IFNγ^{+} CD161^{++}/MAIT cells — an increase of +29.2% vs. 5h TCR stimulation ($p < 0.0001$), and +43.8% vs. IL-12/-18 only ($p < 0.0001$).

Interestingly — on inspection of the IFNγ GMFI of activated cells, there was little difference in GMFI following stimulation by TCR beads for either 5h or 25h, irrespective of IL-12 ± IL-18 exposure (p = ns; Fig. 3.9 B). This suggests cytokine stimulation — but not TCR stimulation — affects the IFNγ GMFI of activated cells. In particular, there was a notable absence of cells expressing an intermediate level of IFNγ following the shorter TCR stimulation, despite the increase in the frequency of IFNγ^{+} cells. This indicates that the additional cells expressing IFNγ following TCR stimulation (vs. IL-12/-18 stimulation only) were able to individually express a higher level of IFNγ-expression (GMFI) very rapidly. Each cell was exposed to IL-12/-18 for the entire 25 hours, so this supports the notion that for IFNγ-expression, more sustained TCR signalling results in a greater frequency of responding cells. However, as illustrated by the responding cell GMFIs — for the relative amount of IFNγ-expressed *per cell*, it is the presence of IL-12/-18, and not TCR stimulation length which is key.

3.5.2 TCR-stimulation leads to rapid TNFα-expression

In Section 3.3.2, TCR stimulation alone was unable to induce TNFα-expression from CD161^{++}/MAIT cells (approx. 4% TNFα^{+}), although with IL-12/-18 co-stimulation, this increased to approx. 40%. In agreement with those data, no TNFα-expression was apparent in the absence of cytokine co-stimulation following culture with TCR beads for 25h ($2.8 \pm 0.2\%$; p = ns; Fig. 3.10 A). However, after 25h stimulation with TCR beads + either IL-12 or IL-18, some TNFα-expression was evident ($12.3 \pm 1.2\%$; $p < 0.001$; and $8.6 \pm 0.6\%$; $p < 0.01$ respectively). In response to stimulation with 25h TCR beads and IL-12/-18, this rose to $35.0 \pm 3.0\%$ — a mean difference of +29.7% vs. IL-12/-18 stimulation only ($p < 0.0001$). Interestingly, even in the absence of cytokines, 5h TCR bead stimulation resulted in detectable TNFα-expression by $25.0 \pm 2.8\%$ CD161^{++} /MAIT cells; a mean increase of +22.2% vs. the more sustained 25h TCR bead stimulation ($p < 0.0001$). Increased frequencies of TNFα-expressing CD161^{++}/MAIT cells were also seen for 5h vs. 25h TCR

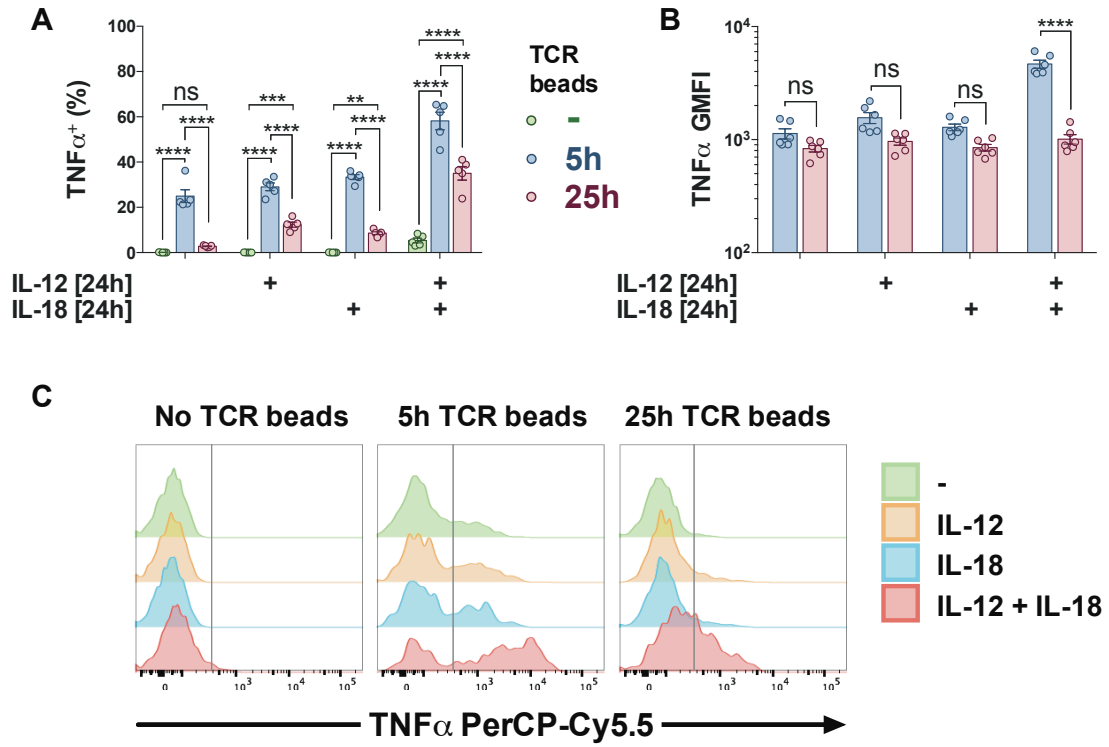


Figure 3.10: Sustained TCR stimulation of cytokine-activated MAIT cells reduces frequency and GMFI of TNFα-expressing CD161^{++}/MAIT cells. CD8α+ T cells were stimulated with IL-12 and/or IL-18 for 25h at 50 ng/ml respectively, in the presence or absence of αCD2/3/28 coated beads for the final 5h, or the whole 25h. (A) Frequency of TNFα^{+} MAIT cells. (B) GMFI of TNFα^{+} MAIT cells. (C) Representative FACS plot of TNFα expression on CD161^{++}/MAIT cells. Half-offset histogram shows modal y-axis scaling (% max. count per condition). Data analysed by two-way ANOVA with Holm-Sidak's multiple comparison test. Graphs show mean ± SEM. For all tests, ****$p < 0.0001$, ***$p < 0.001$, **$p < 0.01$, *$p < 0.05$, ns = non-significant.

stimulation with IL-12 (+16.7%; $p < 0.0001$), IL-18 (+24.8%; $p < 0.0001$) and IL-12/-18 exposure (+23.1%; $p < 0.0001$).

Notably, whilst there were relatively minor differences in the GMFIs of 5h vs. 25h TCR-stimulated TNFα^{+} CD161^{++}/MAIT cells following exposure to IL-12, IL-18 or no cytokine; there was an approximately 4.6-fold increase in GMFI of TNFα detected in the 5h TCR stimulated cells pre-exposed to IL-12/-18 ($p < 0.0001$; Fig. 3.10 B). The increased frequency of TNFα-expressing cells following exposure to 5h TCR beads alone indicates that TNFα-expression by CD161^{++}/MAIT cells is a rapid TCR-driven response, for which cytokine co-stimulation is not necessary. Conversely, the increased level of fluorescence intensity following pre-exposure to IL-12/-18, suggests that for *enhanced* TNFα-expression on a *per cell* basis, both a recent TCR stimulation — together with exposure to cytokine co-stimulation — are necessary.

3.5.2.1 Sustained TCR signalling necessary for robust CD69-expression

CD69 is commonly described as an immediate-early marker of T cell activation, being detectable as early as 2–4 hours post activation [362–364]. On CD161^{++}/MAIT cells, CD69 is up-regulated by IL-12/-18 alone in a dose-dependent manner (Section 3.4); although TCR bead stimulation in the absence of cytokine is sufficient to induce CD69-expression uniformly and robustly amongst CD161^{++}/MAIT cells. Whether 5h stimulation with TCR beads is sufficient for robust CD69 up-regulation by CD161^{++}/MAIT cells — or indeed, whether CD69 is the best marker of their immediate-early activation during *in vitro* experiments — is not clear.

In the absence of any stimulation — and in contrast to both IFNγ and TNFα — 18.9 ± 3.8% of CD161^{++}/MAIT cells were basally CD69^{+}. Following a more sustained 25h TCR bead stimulation (in the absence of cytokines), 88.4 ± 2.0% expressed CD69^{+}, an increase of +69.5% (Fig. 3.11 A; $p < 0.0001$). After a shorter 5h TCR bead stimulation, by contrast, 28.7 ± 6.0% of CD161^{++}/MAIT cells were CD69^{+}, an increase of only +9.8% vs. unstimulated ($p < 0.01$). Concurrent to this, TNFα-expression increased by +24.9% (Fig. 3.10) — resulting in an approximately equivalent level of TNFα and CD69 expression amongst CD161^{++}/MAIT cells (25.0 ± 2.8% vs. 28.7 ± 6.0% respectively.

Following exposure to IL-12/-18 only, 60.5 ± 4.6% of CD161^{++}/MAIT cells were CD69^{+} — an increase of +41.6% vs. unstimulated. This increased to 68.8 ± 2.8% with additional 5h TCR bead stimulation — a modest increase of only +8.34% ($p < 0.01$), and of a similar size to that following the 5h TCR bead-only stimulation vs. basal expression levels. With a more sustained 25h TCR bead stimulation in the presence of IL-12/-18, 97.1 ± 0.6% CD161^{++}/MAIT cells expressed CD69^{+} — an increase of +36.6% vs. IL-12/-18 only. Examining the CD69 GMFI of the CD69^{+} CD161^{++}MAIT cells similarly indicates increased *per cell* CD69-expression following sustained 25h TCR bead stimulation (irrespective of cytokine presence) vs. the rapid 5h response (all $p < 0.0001$ vs. 5h TCR beads; Fig. 3.11 B). Contrasting with the CD69-response to IL-12/-18, very few CD161^{++}/MAIT cells expressing TNFα could be detected (5.3 ± 1.0%). However, in the presence of TCR beads (5h) TNFα-expression increased approximately 11-fold to 58.2 ± 3.9%. This demonstrates that the majority of CD161^{++}/MAIT cells had been activated within 5 hours, but did not upregulate CD69 at the surface.

Together, these data indicate that whilst 5h TCR stimulation is sufficient to see an increase in CD69-expression, TNFα-expression is a more sensitive marker of early activation. CD69, by contrast, is up-regulated robustly and broadly by more sustained 25h TCR-triggering of CD161^{++}/MAIT cells, remaining detectable (unlike

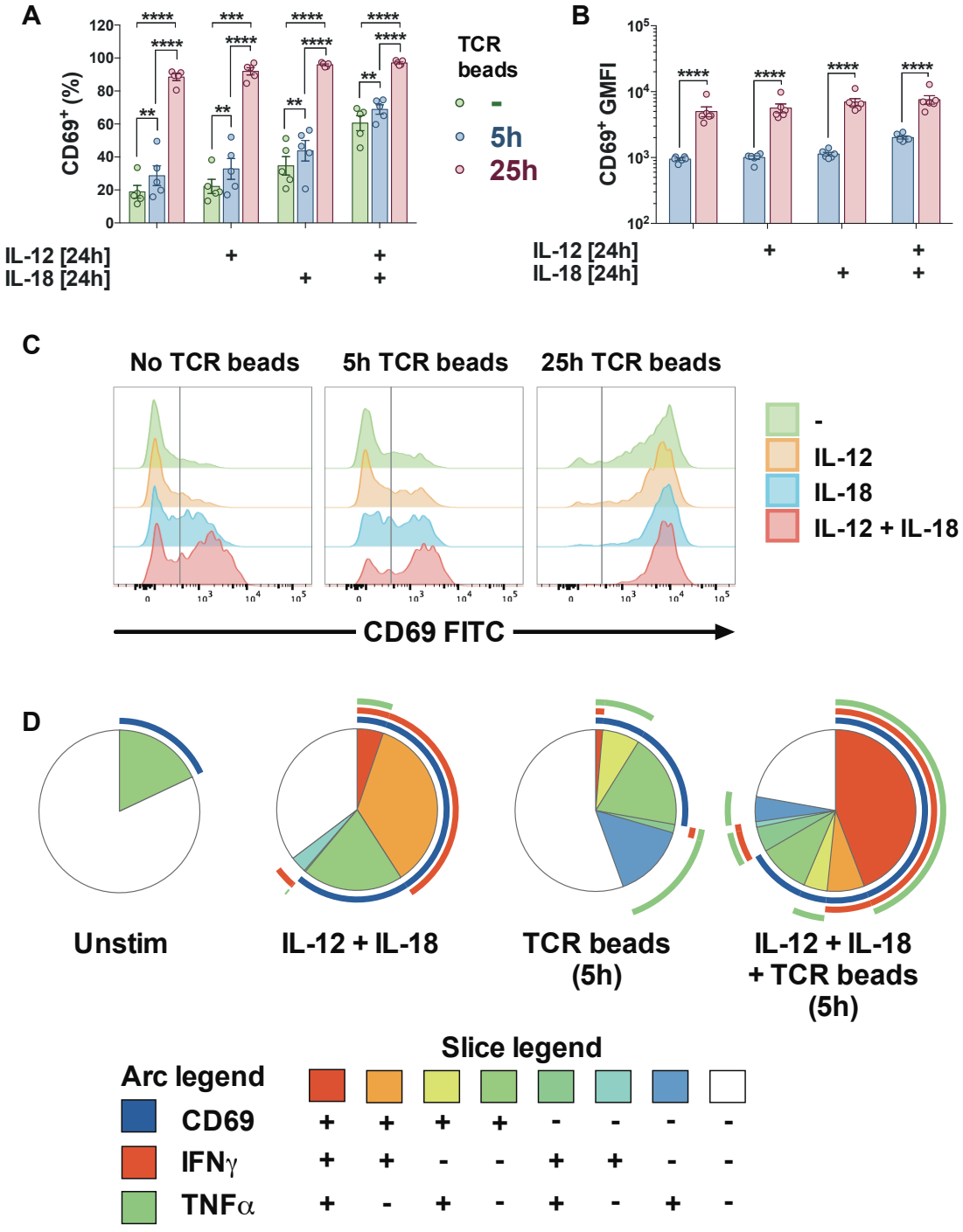


Figure 3.11: Sustained TCR stimulation of cytokine-activated CD161^{++}/MAIT cells enhances CD69α production. CD8α+ T cells were stimulated with IL-12 and/or IL-18 for 25h at 50 ng/ml respectively, in the presence or absence of αCD2/3/28 coated beads for the final 5h, or the whole 25h. (A) Frequency of CD69^{+} CD161^{++}/MAIT cells. (B) GMFI of CD69^{+} CD161^{++}/MAIT cells. (C) Representative FACS plot of CD69 expression on CD161^{++}/MAIT cells. (D) Pie-charts illustrating overlap of poly-functional CD161^{++}/MAIT cell responses. Half-offset histogram shows modal y-axis scaling (% max. count per condition). Data analysed by two-way ANOVA with Holm-Sidak's multiple comparison test. Graphs show mean ± SEM. ****$p < 0.0001$, **$p < 0.01$.

TNFα-expression), such that after 25h approximately 90% of CD161^{++}/MAIT cells were CD69^{+} (vs. 3% TNFα^{+}).

3.5.2.2 Analysis of the CD161^{++}/MAIT cell poly-functional response

Interestingly, analysis of the poly-functional response amongst the CD161^{++}/MAIT cells indicated that in response to IL-12/-18, there were CD69^{+} cells that remained IFNγ^{-}, whilst the vast majority of IFNγ^{+} cells were CD69^{+} (Fig. 3.11 D) — suggesting IFNγ-expression as secondary to CD69-up-regulation following cytokine stimulation. However; the frequency of CD69-*only* expressing CD161^{++}/MAIT cells (i.e. CD69^{+}, yet IFNγ^{-} and TNFα^{-}) following IL-12/-18 exposure was $20.3 \pm 1.9\%$ — approximately equivalent to unstimulated ($18.9 \pm 3.8\%$), or 5h TCR only stimulation ($18.8 \pm 5.0\%$).

This hints that many of the CD161^{++}/MAIT cells expressing CD69 following IL-12/-18 or 5h TCR bead stimulation, may in fact have been expressing CD69 prior to stimulation. In support of this, a majority of the TNFα^{+} cells following 5h TCR only stimulation also remained CD69^{-} ($9.0 \pm 1.6\%$ TNFα^{+} CD69^{+} vs. $16.7 \pm 3.8\%$ TNFα^{+} CD69^{-}; Fig. 3.11 D). If so, the initial CD69-expressing cells may in fact be more resistant to both IL-12/-18 and TCR stimulation. Further experiments will be needed to verify this.

3.5.2.3 Vα7.2 TCR down-regulation requires sustained TCR signalling

Given the extent of Vα7.2^{+} TCR down-regulation seen earlier, the sensitivity of TCR-stimulated CD161^{++}/MAIT cells to low concentrations of IL-12/-18 for Vα7.2^{+} TCR down-regulation, and the ability of IL-12/-18 exposed CD161^{++}/MAIT cells to respond functionally to 5h TCR stimulation by rapidly expressing TNFα; it was of interest to determine whether short 5h TCR stimulation would be sufficient for IL-12/-18 activated CD161^{++}/MAIT cells to down-regulate their TCR — or whether a more sustained TCR stimulation was necessary.

In agreement with previous experiments, little Vα7.2 TCR down-regulation was observed in cells not exposed to any cytokine, whether stimulated with TCR beads for 5, or 25h (p = ns; Fig. 3.12 A). Following exposure to IL-12, there was no further decrease after 5h TCR stimulation (p = ns), whilst following 25h TCR beads + IL-12 there was a decrease of -19.5% vs. IL-12 only ($p < 0.0001$), and a decrease of -12.6% vs. IL-12 + 5h TCR beads ($p < 0.01$). No further decrease in Vα7.2 TCR expression was seen following IL-18 stimulation with either 5h or 25h TCR stimulation vs. cytokine only. By contrast, whilst IL-12/-18 stimulation was able to reduce Vα7.2 TCR expression to 85.6% of unstimulated, there was no further decrease following

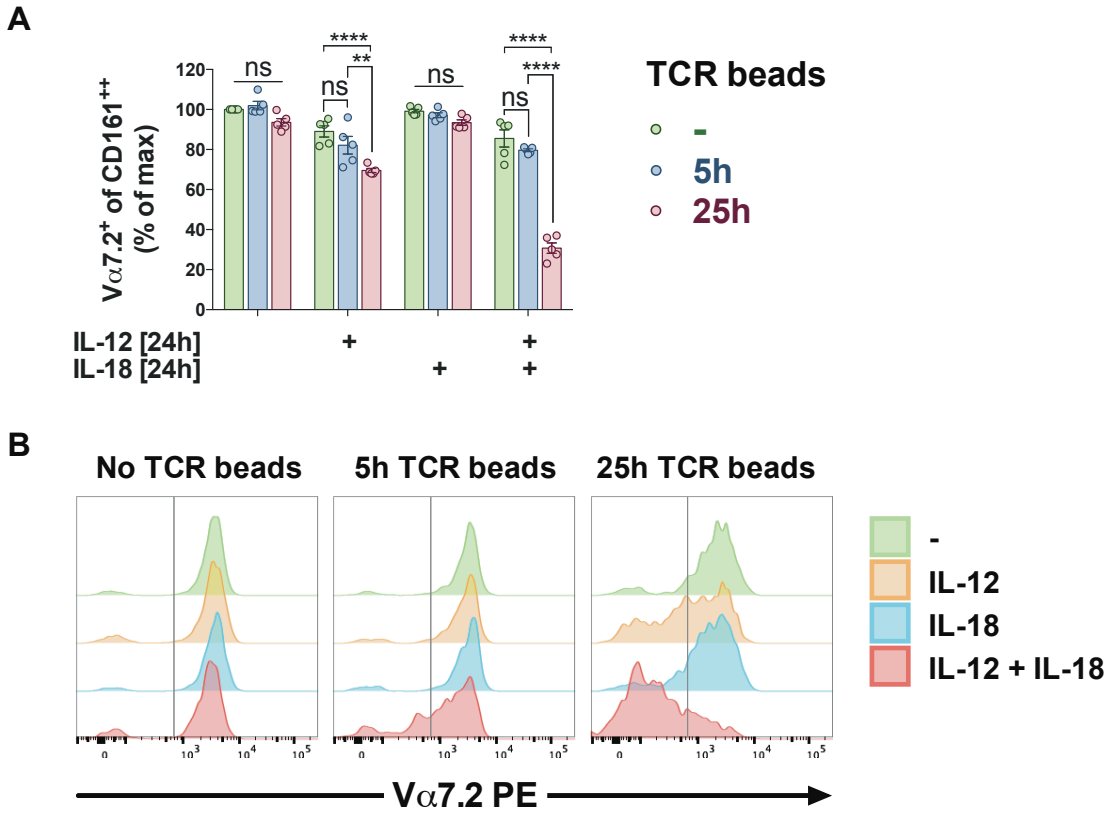


Figure 3.12: MAIT cell Vα7.2 TCR downregulation requires sustained TCR signalling and occurs most robustly following IL-12/-18 stimulation. CD8α+ T cells were stimulated with IL-12 and/or IL-18 for 25h at 50 ng/ml respectively, in the presence or absence of αCD2/3/28 coated beads for the final 5h, or the whole 25h. (A) Frequency of CD161^{++} cells expressing Vα7.2^{+} TCR relative to donor maximum. (B) Representative FACS plots of Vα7.2^{+} TCR expression on CD161^{++} cells. Half-offset histogram shows modal y-axis scaling (% max. count per condition). Data analysed by two-way ANOVA with Holm-Sidak's multiple comparison test. Graphs show mean ± SEM. For all tests, ****$p < 0.0001$, ***$p < 0.001$, **$p < 0.01$, *$p < 0.05$, ns = non-significant.

stimulation with IL-12/-18 + 5h TCR beads — however, the Vα7.2 reduction following co-stimulation with IL-12/-18 + 25h TCR beads was demonstrated broadly, with only 30.8 ± 2.6% of CD161^{++}/MAIT cells remaining Vα7.2^{+}.

These data indicate that in the presence of adequate IL-12, or IL-18; sustained TCR signalling is necessary for the down-regulation of the Vα7.2^{+} MAIT cell TCR.

3.5.3 Robust TCR responses require cytokine pre-exposure

Whilst the TCR-independent CD161^{++}/MAIT cell IFNγ-response to IL-12/-18 occurs robustly following sustained cytokine stimulation, the TNFα-response to TCR stimulation alone occurs far more rapidly (Sections 3.5.1 and 3.5.2). However, it is

not clear whether > 16h cytokine exposure is necessary in the context of enhancing the rapid (5h) TCR response, or whether concurrent cytokine co-stimulation is sufficient. In particular, the TNFα response to 5h TCR stimulation was robust, yet required IL-12/-18 for the highest TNFα GMFI levels detected. To determine this, IL-12/-18 exposure occured prior to the rapid 5h TCR stimulation, and was sustained for the duration of the experiment. Whether cells can demonstrate high TNFα fluorescence-intensity in the presence of IL-12/-18 for a 5h TCR stimulation only — or whether a more sustained cytokine pre-exposure is required — is unclear.

In order to investigate this, the 5h versus 25h assay was modified by exposing magnetically enriched CD8α$^+$ T cells to IL-12/-18 (each 50ng/ml) overnight, introducing the TCR beads only for the final 5h (or not at all) — or, instead, by exposing the CD8α$^+$ T cells to both IL-12/-18 and TCR beads for 5h only (Fig. 3.13). In the absence of TCR beads, no IFNγ was expressed by CD161^{++}/MAIT cells in response to the short 5h IL-12/-18 stimulation ($0.28 \pm 0.08\%$; p = ns); whilst in conjunction with TCR stimulation $11.7 \pm 2.2\%$ of CD161^{++}/MAIT cells were IFNγ$^+$ ($p < 0.05$). Overnight pre-exposure to IL-12/-18, prior to 5h TCR stimulation resulted in a +47.5% increase in IFNγ$^+$ CD161^{++}/MAIT cells ($59.2 \pm 3.3\%$; $p < 0.0001$; Fig. 3.13 A). In terms of *per cell* IFNγ-expression, there was little increase in IFNγ GMFI of TCR bead activated cells, following additional exposure to 5h IL-12/-18 ($+2.9 \times 10^3$ vs. 5h TCR beads only; p = ns), whilst by contrast, overnight pre-exposure to IL-12/-18 before TCR stimulation substantially enhanced IFNγ GMFI ($+5.3 \times 10^4$ vs. 5h IL-12/-18 + TCR beads; $p < 0.0001$; Fig. 3.13 D).

In similarity to the IFNγ response, there was no TNFα-expression observed following IL-12/-18 exposure for 5h only ($0.07 \pm 0.03\%$; p = ns). However, in contrast — TNFα was expressed in response to 5h TCR stimulation only ($25.1 \pm 2.8\%$), but with reduced additional effect of exposing the cells to concurrent IL-12/-18 (+4.9%; p = ns; Fig. 3.13 B). Likewise, there was minimal increase of TNFα GMFI vs. 5h TCR stimulation only ($+4.3 \times 10^2$; p = ns) in contrast with the more sustained 25h cytokine exposure ($+3.4 \times 10^3$; $p < 0.0001$; Fig. 3.13 D).

The effects of short IL-12/-18 exposure on CD69-expression, were broadly in line with the TNFα-response — there were minimal increases in the frequencies of CD69-expressing CD161^{++}/MAIT cells following 5h IL-12/-18 exposure, in comparison to stimulation either in the presence and absence of TCR beads (both p = ns; Fig. 3.13 C). There was also no enhancement of CD69 GMFI following 5h IL-12/-18 co-stimulation (+73.8; p = ns), whilst the GMFI following overnight pre-exposure to IL-12/-18 was slightly increased vs. concurrent IL-12/-18 exposure (9.0×10^2; $p < 0.0001$; Fig. 3.13 D).

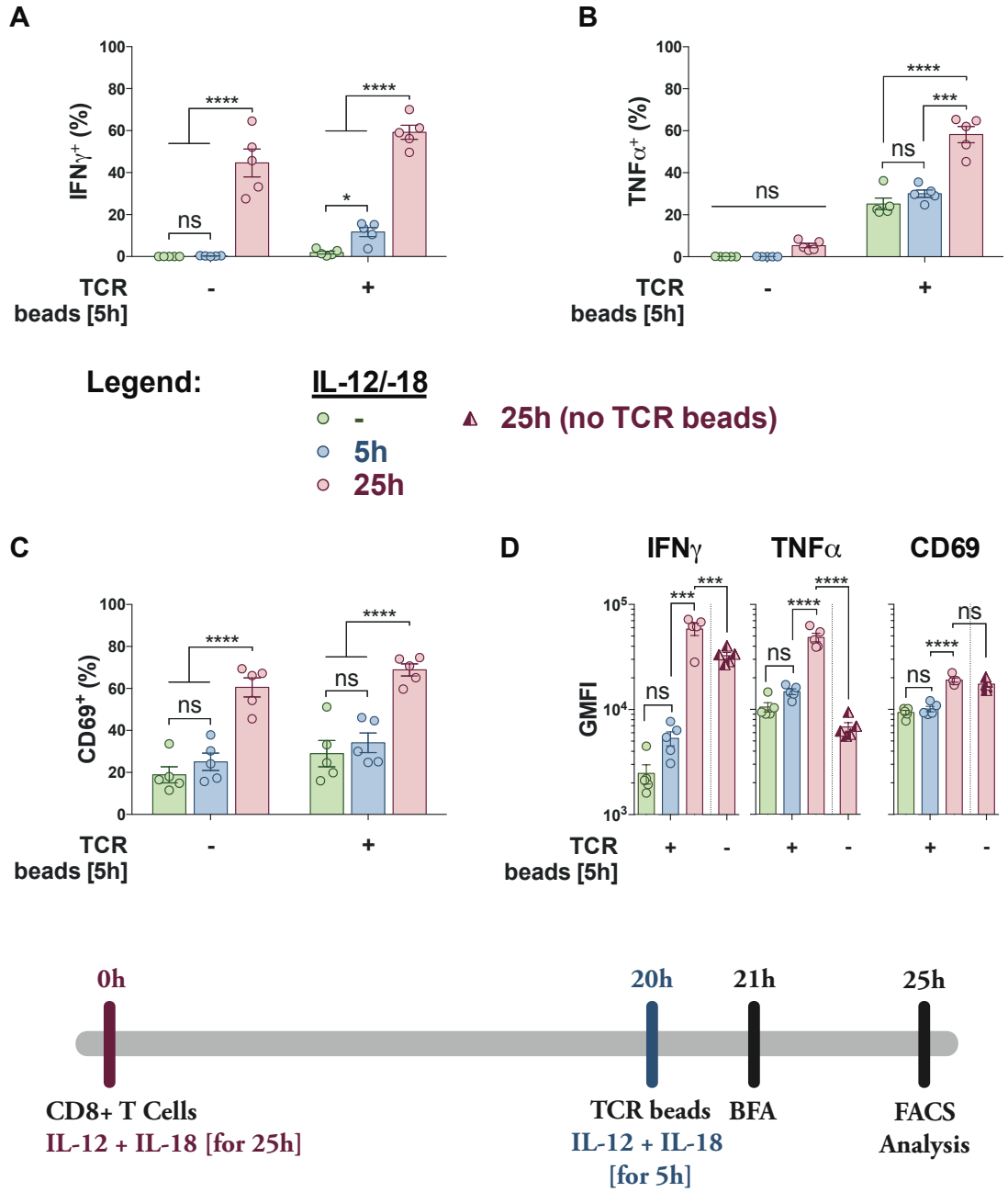


Figure 3.13: Sustained exposure to IL-12/-18 enhances the frequency and GMFI of the rapid CD161^{++}/MAIT cell TCR driven TNFα response. CD8α+ T cells were stimulated with IL-12 and/or IL-18 for 5 or 25h at 50 ng/ml each, in the presence or absence of αCD2/3/28 coated beads for the final 5h, before assessment for activation markers by flow cytometry. (A) Frequency of IFNγ$^+$CD161^{++}/MAIT cells. (B) Frequency of TNFα$^+$ CD161^{++}/MAIT cells. (C) Frequency of CD69$^+$ CD161^{++}/MAIT cells. (D) GMFI of IFNγ TNFα and CD69 of activated CD161^{++}/MAIT cells. Data analysed by one-way ANOVA with Holm-Sidak's multiple comparison test. Graphs show mean ± SEM. For all tests, ****$p < 0.0001$, ***$p < 0.001$, **$p < 0.01$, *$p < 0.05$, ns = non-significant.

These data show that 5h exposure to IL-12/-18 is insufficient to induce IFNγ, TNFα, or CD69 in the absence of TCR stimulation. In conjunction with TCR stimulation, 5h IL-12/-18 exposure was sufficient to slightly increase the frequency of IFNγ$^+$ — but not TNFα$^+$, nor CD69$^+$ CD161^{++}/MAIT cells. And no enhancement was observed on a *per cell* basis for TCR stimulated cells, on additional exposure to 5h IL-12/-18 irrespective of IFNγ, TNFα, or CD69 read-out.

3.5.4 TCR pre-stimulation enables cytokine-only response

Despite the link between CD161-expression and ability to respond to IL-12/-18 without TCR stimulation, the response within an individual to IL-12/-18 is not uniform amongst CD161^{++}/MAIT cells. Between individuals there is typically also large variability in terms of the magnitude of the IFNγ-response (10 – 70%), even when saturating concentrations (50 ng/ml) of the cytokines are used. The cause for this is not yet explained, although it could be due to recent activation history in recirculating CD161^{++}/MAIT cells. Certainly, in the presence of a prolonged TCR stimulus, there is a broad and robust dose-dependent response to IL-12/-18, demonstrating the effect of TCR stimulation in licensing cells to respond to IL-12/-18.

In order to test the hypothesis that TCR-stimulated CD161^{++}/MAIT cells are more capable of subsequently responding to IL-12/-18-only stimulation — but in a TCR-independent manner — CD8α$^+$ T cells were either rested overnight, or pre-stimulated with αCD3/28 coated plates. Cells were then recovered, washed, and re-plated for stimulation with IL-12/-18 and/or TCR beads, before staining for IFNγ, TNFα and CD69 (Fig. 3.14).

Comparing the response between 24h rested cells, or those pre-stimulated with αCD3/28 coated plates, no difference in CD161^{++}/MAIT cell IFNγ-expression was observed following subsequent rest (+1.4%; p = ns), or a subsequent TCR bead stimulation (+4.87%; p = ns). However, $34.3 \pm 5.2\%$ of rested CD161^{++}/MAIT cells responded to IL-12/-18 exposure — in line with previous results — whilst strikingly $84.6 \pm 6.2\%$ of TCR pre-stimulated cells expressed IFNγ in response to subsequent IL-12/-18, with no TCR beads present (+50.2%; $p < 0.0001$).

The IFNγ-responses of rested and pre-stimulated CD161^{++}/MAIT cells were of a similar magnitude following subsequent TCR bead + IL-12/-18 stimulation with $81.3 \pm 1.6\%$ and $88.2 \pm 3.7\%$ IFNγ$^+$ respectively (+6.3%; p = ns).

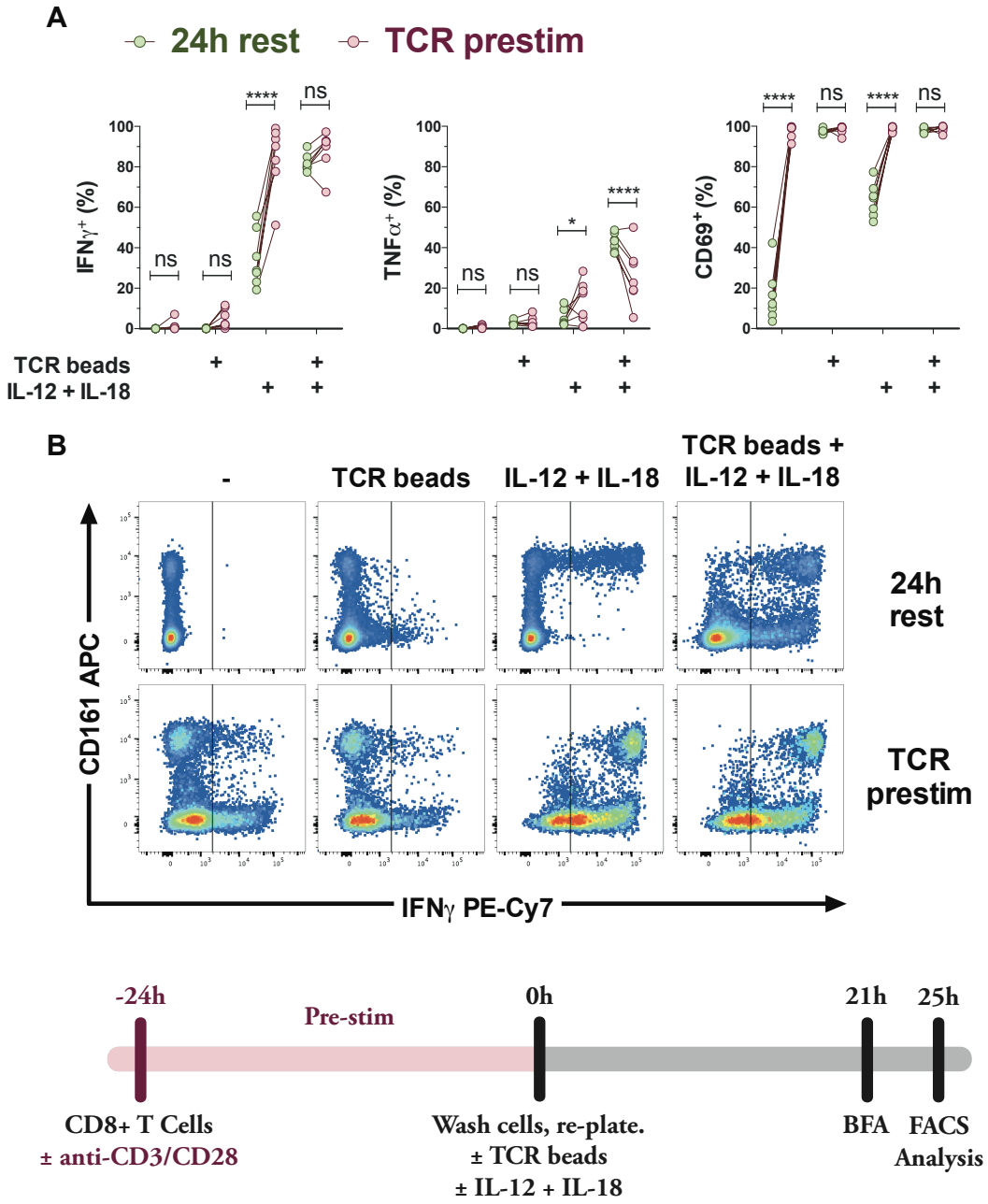


Figure 3.14: TCR pre-stimulation licences for a subsequent TCR-independent IL-12/-18 dependent response. CD8α+ T cells were rested, or stimulated with plate-bound αCD3/28 for 24h. Cells were then washed, resuspended in fresh plates and cultured ± IL-12/-18 (50 ng/ml each) ± αCD2/3/28 coated beads for 25h, before assessment for activation markers by flow cytometry. (A) Frequency of IFNγ$^+$, TNFα$^+$ and CD69$^+$ MAIT cells. (B) Representative FACS plot of IFNγ expression on different CD161-expressing CD8α$^+$ T cell subsets. Data analysed by one-way ANOVA with Holm-Sidak's multiple comparison test. Graphs show mean ± SEM. For all tests, ****$p < 0.0001$, ***$p < 0.001$, **$p < 0.01$, *$p < 0.05$, ns = non-significant.

3.5.4.1 TNFα-expression is reduced following prior TCR stimulation

No differences in TNFα-expression were observed between rested, or TCR pre-stimulated cells after further rest (+0.84%; p = ns), or TCR bead stimulation (+0.57%; p = ns). There was a small increase in ability to express TNFα following IL-12/-18 stimulation in the TCR pre-treated group ($14.1 \pm 3.7\%$) compared to the 24h rest group ($5.19 \pm 1.6\%$); an increase of +8.9% ($p < 0.05$), in similarity with the IFNγ-response, although of a smaller magnitude. Interestingly, the frequency of TNFα$^+$ CD161^{++}/MAIT cells subjected to TCR bead + IL-12/-18 stimulation was lower within the TCR pre-stimulation group ($25.9 \pm 5.3\%$) compared to the 24h rest group ($42.7 \pm 1.7\%$); a decrease of −16.8% ($p < 0.0001$). This indicates that following TCR stimulation, CD161^{++}/MAIT cells are less able to express TNFα in response to subsequent TCR stimulation.

In contrast to the IFNγ and TNFα responses, CD69 was up-regulated robustly following TCR pre-stimulation; although it is worth noting that there was no obvious loss of CD69-expression following a 24h rest period after transfer from the αCD3/CD28 coated plate ($97.6 \pm 1.2\%$ CD69$^+$).

Overall, these data indicate that — at least in the short-term — TCR stimulation (even in the absence of co-stimulatory signals) alters the functional phenotype of CD161^{++}/MAIT cells in the following ways: (1) they are uniformly capable of responding to IL-12/-18 in a TCR independent manner to express IFNγ, (2) they are slightly more capable of expressing TNFα in response to IL-12/-18 only, (3) they are less capable of responding to a subsequent TCR stimulus for TNFα-expression — whilst CD69 expression persists at high levels.

3.6 Discussion

3.6.1 High & low thresholds for MAIT cell IFNγ-expression

This chapter began with the aim of investigating how TCR signalling would interact with IL-12 and IL-18 stimulation, individually, for MAIT cell activation. Following systematic assessment, TCR, IL-12 and IL-18 signals were each able to cooperate in a synergistic manner — but with the nature and extent of the outcome depending on the effector function, concentration of cytokines, and the order/timing of exposure to activating signals.

Previous investigations using αCD3/CD28 beads to assess the sufficiency of TCR stimulation for MAIT cell activation have focussed on IFNγ as the functional read-out — in general MAIT cells have been found able to express relatively

little in response to TCR stimulation alone [138, 140, 356, 357]. In this study, flow cytometry was used to determine IFNγ-expression on a *per cell* basis, and stimulation with αCD2/CD3/CD28 (TCR) beads alone was unable to induce IFNγ from $CD161^{++}$/MAIT cells whether following 5 hours stimulation, or a longer 24 hours stimulation. This suggests that TCR stimulation alone is not sufficient to induce IFNγ from MAIT cells at these time points.

On stimulation with TCR beads in the presence of IL-12, the signals acted synergistically to activate a proportion of $CD161^{++}$/MAIT cells to express IFNγ. TCR beads + IL-18 combined less efficiently — although that there was any IFNγ-expression indicates that other cytokines may also synergise independently with TCR stimulation to activate MAIT cells for IFNγ production. Nonetheless, only in the presence of both IL-12 and IL-18 together were $CD161^{++}$/MAIT cells capable of expressing IFNγ at a high-intensity — this was independent of concurrent TCR stimulation, and required longer than 5 hours exposure to IL-12/-18 (data not shown).

Whilst stimulation with the TCR beads was not necessary for an increase in IFNγ-expression intensity, it did consistently boost the frequency of $CD161^{++}$/MAIT cells expressing IFNγ in response to IL-12/-18. As IL-12/-18 stimulation resulted in high intensity IFNγ-expression, by extension, TCR stimulation increased the frequency of $CD161^{++}$/MAIT cells expressing IFNγ at a high-intensity. Furthermore, this effect did not require the TCR signal and IL-12/-18 to occur at the same time; pre-stimulation of the $CD161^{++}$/MAIT cells with αCD3/CD28 coated plates enabled uniform expression of high-intensity IFNγ by $CD161^{++}$/MAIT cells to IL-12/-18 in an otherwise TCR-independent manner. This may be of particular relevance for the involvement of MAIT cells in viral infection. Viruses do not activate MAIT cells via MR1, however TCR ligation following MR1 presentation of commensal bacteria-derived antigen may license additional MAIT cells to contribute to the TCR-independent response.

Assessment of the dose-response to IL-12 and IL-18, revealed that $CD161^{++}$/MAIT cell IFNγ-production followed a biphasic model. Interestingly, whilst no IFNγ-expression was observed in the absence of cytokine stimulation, extremely low concentrations of IL-12 — 12 pg/ml — were sufficient for the appearance of some $IFN\gamma^{+}$ $CD161^{++}$/MAIT cells. By contrast, IL-12/-18 were required at relatively high concentrations ($>$ 3 ng/ml) for high-intensity IFNγ-expression. Despite the innate-like ability of MAIT cells to respond to cytokine stimulation independently of TCR ligation, this indicates that control nonetheless exists in order to prevent aberrant responses. Either TCR ligation is required for low concentrations of

cytokine, in which case control is provided via TCR-MR1 interactions — or proximity to sources of IL-12/-18 may ensure a sufficiently high concentration to lead to MAIT cell IFNγ-expression. Alternatively, very high concentrations of IL-12/-18 in the tissues may activate MAIT cells in a manner that leads to further amplification of inflammation, and a detrimental outcome.

It is of interest to note that, in the presence of TCR beads, the two phases of the IL-12/-18 biphasic dose response curve appear to correspond with the dose-response curves of IL-12 with TCR beads (high sensitivity), and IL-12/-18 without TCR beads (low sensitivity), respectively. For robust MAIT cell IFNγ-expression both cytokines IL-12/-18 were required, and at a high concentration — irrespective of the presence of a TCR stimulus. This further supports a role for TCR stimulation in enhancing sensitivity to, and reducing the threshold for IL-12 stimulation for weaker IFNγ-expression — whilst for robust MAIT cell IFNγ-expression TCR stimulation does not effect the high-threshold of IL-12 and IL-18 stimulation for more intense IFNγ-expression.

3.6.2 MAIT cell expression of TNFα is rapid and transient

TNFα-expression is often also used as a read-out of MAIT cell activation; however the kinetics of the MAIT cell TNFα response, and the role of the TCR signal + IL-12/-18 are poorly defined. Following 24 hours stimulation with TCR beads, very little TNFα-expression was observed — yet approximately 20% of cells expressed TNFα following a shorter 5 hour stimulation with TCR beads only. This demonstrates that a $CD161^{++}$/MAIT cell functional response to TCR stimulation is possible in the absence of cytokines, but with kinetics that are rapid and transient.

With a short 5 hour TCR stimulation, concurrent IL-12/-18 co-stimulation led to no enhancement in the frequency of $TNF\alpha^{+}$ $CD161^{++}$/MAIT cells. This contrasted with the IFNγ-response, where enhancement was seen — although this was still minimal. The frequencies of $TNF\alpha^{+}$ cells after both 5, and 25 hours TCR stimulation were, however, enhanced by 24 hours (pre-)stimulation with IL-12/-18, with a notable increase in the intensity of TNFα-expression following 5 hours TCR stimulation with 25 hours IL-12/-18 (pre-)exposure. Therefore, whilst IL-12/-18 (pre-)stimulation is necessary for high-intensity TNFα-expression (as for IFNγ) — this argues that (in contrast to the IFNγ response) TNFα-expression remains rapid, and transient, even with pro-longed cytokine co-stimulation.

Despite being a sub-optimal time point for assessing TNFα-expression, assessment of 24h stimulation with TCR beads nonetheless revealed a $CD161^{++}$/MAIT cell dose dependency for TNFα-expression in response to IL-12/-18. At this time

point, TNFα-expression occurred with a similar sensitivity to IL-12/-18 to that of high-intensity IFNγ-expression — i.e. despite the transient nature of TNFα-expression in response to TCR stimulation, more sustained TNFα-expression (albeit at a low intensity) can occur when MAIT cells are maximally activated, as is likely within an inflammatory milieu.

Pre-stimulation of $CD161^{++}$/MAIT cells with αCD3/CD28 coated plates enabled only slightly more cells to express TNFα in response to IL-12/-18 only, in contrast to the more striking increase for IFNγ-expression. Interestingly, there was a consistent decrease in the frequency of $TNF\alpha^{+}$ cells in response to IL-12/-18 + TCR stimulation amongst those that had been pre-stimulated with αCD3/CD28. This suggests that not only is $CD161^{++}$/MAIT cell TNFα-expression rapid onset and transient in nature, but also that $CD161^{++}$/MAIT cells become anergic to further TCR stimulation for TNFα-expression.

Together these data indicate that IFNγ- and TNFα-expression by MAIT cells are differentially regulated, with a reduced requirement for cytokine co-stimulation for rapid TNFα-expression; and an anergy for TNFα-expression which subsequently follows. In the presence of high concentrations of IL-12/-18, IFNγ-expression can occur with a high intensity. This is also true for TNFα, although high intensity expression occurs only rapidly following TCR ligation. High concentrations of IL-12/-18 however, can prolong TNFα-expression at a lower intensity, reflecting the high level of MAIT cell activation.

3.6.3 CD69 is a poor marker of rapid MAIT cell activation

CD69 has been described as an immediate-early marker of T cell activation, although its regulation by IL-12/-18 in combination with TCR signalling, and the kinetics of up-regulation by MAIT cells is not clear. In this study, 24 hour stimulation with TCR beads alone lead to a uniform and robust up-regulation of CD69 amongst $CD161^{++}$/MAIT cells. There was, however, a dose-dependent expression of CD69 in response to IL-12/-18, indicating that both cytokine and TCR signalling are each independently sufficient to induce CD69-expression on $CD161^{++}$/MAIT cells. This suggests that $CD161^{++}$/MAIT cell expression of CD69 reflects activation, but is non-specific to the mode of activation.

Notably, whereas TNFα-expression occurred within 5 hours of TCR stimulation, this was enough time only to see extremely modest CD69-up-regulation on $CD161^{++}$/MAIT cells. Indeed, analysis of the poly-functional response to 5 hour TCR stimulation and 24 hour IL-12/-18 (pre-)stimulation revealed that nearly all IFNγ-expressing cells induced by IL-12/-18 were $CD69^{+}$, whereas nearly all

TNFα-expressing cells induced by TCR stimulation alone were $CD69^{-}$ — despite the uniform capacity of $CD161^{++}$/MAIT cells to express CD69 in response to TCR stimulation. This suggests that for *in vitro* experiments, TNFα is expressed prior to CD69 up-regulation and is therefore a better marker for immediate-early activation for *in vitro* stimulation assays.

Expression of CD69 by MAIT cells is also often used as a biomarker to gauge the activation status of MAIT cells *in vivo* in disease [180, 231]. It is worth noting that, typically, a proportion of MAIT cells from PBMC express CD69 basally in healthy donors. It is not yet clear whether steady-state CD69-expression signifies that MAIT cells are poised to respond to TCR and/or cytokine stimulation, or if they are more likely to resist further activation. Interestingly, analysis of the poly-functional response to 5 hour TCR stimulation ± 24 hour IL-12/-18 (pre-)stimulation revealed that similar proportions of $CD161^{++}$/MAIT cells remained CD69 only mono-functional cells in response to IL-12/-18, or TCR beads, or indeed in the absence of any stimulation.

From these data, it is tempting to speculate that MAIT cells expressing basal-levels of CD69 are less responsive to IL-12/-18 or TCR stimulation than those not initially expressing CD69. Certainly, following αCD3/CD28 pre-stimulation of $CD161^{++}$/MAIT cells with a subsequent 24 hour rest period, $CD161^{++}$/MAIT cells were still found to be expressing CD69 — and these cells were less capable of expressing TNFα in response to further TCR stimulation. Whether CD69-expression by circulating MAIT cells is indicative of a functional exhaustion will need to be investigated further.

3.6.3.1 Vα7.2 down-regulation requires sustained activation

Despite the importance for identification of MAIT cells, and the functional implications, little is known about the role of IL-12 and IL-18 in the down-regulation of the MAIT cell TCR. After 24 hours stimulation with TCR beads + IL-12/-18, Vα7.2 expression was substantially decreased, whereas 5 hours TCR + IL-12/-18 stimulation was insufficient — even with 21 hours pre-stimulation with IL-12/-18.

Interestingly, the dose-response of the Vα7.2 TCR down-regulation in response to IL-12/-18 + TCR beads followed a biphasic model that mirrored the induction of IFNγ. After an initial decrease in Vα7.2 expression corresponding to the effect of TCR beads + IL-12 only, a second phase of TCR down-regulation reflected the greater activation of MAIT cells at higher concentrations of IL-12/-18.

These data suggest that MAIT cell TCR down-regulation occurs in response to sustained activation in the presence of inflammatory cytokines, offering a mechanism

to restrict prolonged TCR dependent activation. However, this does not appear to negate the ability of MAIT cells to produce IFNγ, which continues to be expressed at high-intensity in response to IL-12/-18, even as the TCR is entirely absent.

3.6.4 MAIT vs. conventional CD8$^+$ T cell responses

A number of markers can be used to differentiate CD161^{++}/MAIT cells from conventional CD8$^+$ T cells [134, 136, 156]. Nonetheless given overlap in effector functions, and other markers such as CD8α, the extent to which MAIT cell activation reflects that of conventional MHC class I-restricted CD8$^+$ T cells is of interest. In Section 3.7 (p. 69), the concentration dependency of CD161^{++}/MAIT cell activation by IL-12 ± IL-18 was compared with that of two different conventional CD8$^+$ T cell subsets — CD161$^+$ CD8$^+$ T cells, which are nearly uniformly effector-memory, and CD161$^-$ CD8$^+$ T cells, of which approximately 25% demonstrate a naïve phenotype [361]. In the present study, only a small proportion of CD161$^-$ CD8$^+$ T cells were able to to express IFNγ following overnight stimulation with TCR beads + IL-12 in comparison with CD161^{++} and CD161$^+$ expressing populations — and only CD161^{++}/MAIT cells were able to respond robustly to the highest concentrations of IL-12 + IL-18. This is consistent with previous findings that expression of CD161 defines a transcriptional and functional phenotype [136]. However, in contrast to the other CD8$^+$ T cell populations, the CD161^{++}/MAIT cells demonstrated the capacity to respond uniformly and at the highest intensity to IL-12/-18 in the presence of TCR beads, or to IL-12/-18 alone when at high concentration.

Conventional memory CD8$^+$ T cells are considered capable of rapid TCR-driven activation, expressing cytokines within hours of antigen exposure [55]. Whilst few CD161^{++}/MAIT cells were observed expressing IFNγ within 5 hours of TCR stimulation alone in Fig. 3.9 (p. 77) they were able to express TNFα, demonstrating rapid induction of CD161^{++}/MAIT cell effector function via TCR stimulation. Indeed, this TCR driven TNFα expression was similar to that observed for CD161$^+$ — but not CD161$^-$ CD8$^+$ T cells (data not shown) indicating further overlap of functional capacities between CD161^{++}, CD161$^+$, and not the naïve cell-containing CD161$^-$ CD8$^+$ T cell population.

Recently, a study by Slichter *et al* directly compared MAIT cells against CD45RO$^+$ memory CD8$^+$ T cells in their ability to respond to TCR stimulation — irrespective of their CD161 expression status — finding equivalent responses after 6 hours [174]. However, consistent with results in Section 3.5.2 (p. 78), TNFα expression by MAIT cells was not detectable following more extended (24 hour) TCR stimulation. This was in direct contrast to conventional memory CD8$^+$ T cells,

which continued to express TNFα at this later time point [174]. In Section 3.5.2, IL-12/-18 co-stimulation was found to prolong MAIT cell TNFα expression at these later time points, as well as leading to induction of IFNγ. Together, therefore, these findings indicate that MAIT and non-MAIT memory $CD8^+$ T cells demonstrate similar rapid responses to TCR stimulation in the absence of additional signals. However, CD161 expressing $CD8^+$ T cells to an extent, and CD161 highly-expressing MAIT cells in particular, possess the ability to combine TCR signalling with IL-12 + IL-18 for augmentation of the TCR driven response.

3.6.5 Conclusions

Whilst further mechanistic investigations will be required to tease apart the interactions between signals at the transcriptional level, the two phases of the TCR + IL-12/-18 dose response, together with the rapid and transient higher-intensity expression of TNFα and the slower-onset high-intensity IFNγ-expression at high IL-12/-18 concentrations appear to reflect several modes of activation.

In the absence of cytokines, $CD161^{++}$/MAIT cells are capable of expressing low-levels of TNFα, but not IFNγ, in response to TCR stimulation. In the presence of low levels of IL-12 acting as a third signal, $CD161^{++}$/MAIT cells are sensitised to respond to TCR stimulation for low-levels of IFNγ-expression. Conversely, following pre-exposure to high concentrations of IL-12/-18 for extended periods ($>$ 16 hours), $CD161^{++}$/MAIT cells can express high-levels of TNFα in a rapid and transient fashion following TCR ligation.

A proportion of $CD161^{++}$/MAIT cells are individually capable of expressing high levels of IFNγ in a TCR-independent manner following extended IL-12/-18 exposure. Following a TCR-signal event, this function appears to extend to the vast majority of MAIT cells, which no longer require TCR signalling to express IFNγ in response to IL-12/-18. However, the MAIT cell TCR is subsequently down-regulated, possibly preventing further expression of TNFα. CD69 is up-regulated after 24 hours, independently of the nature of the activation signal.

3.6.5.1 Summary of findings

- $CD161^{++}$/MAIT cells can express IFNγ and TNFα with low or high-intensities on a *per cell* basis, reflecting different levels of activation.
- $CD161^{++}$/MAIT cells do not express IFNγ in response to TCR stimulation in the absence of cytokine signals.

- Picograms per ml concentrations of IL-12 are sufficient to enable lower intensity TCR driven IFNγ-expression.
- High intensity CD161^{++}/MAIT cell IFNγ-expression requires higher bioavailability (nanograms per ml) of, and sustained exposure to IL-12/-18.
- TCR signalling licences otherwise non-responsive MAIT cells to respond to IL-12/-18 in a TCR independent manner.
- High intensity CD161^{++}/MAIT TNFα-expression requires sustained pre-exposure to IL-12/-18 — but is rapid and transient following TCR signalling.
- CD69 expression occurs later than TNFα-expression, but encompasses the majority of activated cells — and some which are not cytokine producers.
- TCR down-regulation occurs after sustained TCR + IL-12/-18 stimulation, reflecting a higher state of activation, and coinciding with reduced ability to express TNFα.

4

Role of the immunological synapse in MAIT cell activation

Contents

4.1 Introduction 102
4.1.1 Structure and function of the immunological synapse . . 103
4.1.2 Chapter hypothesis and aims 105
4.2 Chapter specific materials & methods 106
4.2.1 Contact dependency of MAIT cell activation 106
4.2.2 Cytokine-mediated proliferation of MAIT cells 107
4.2.3 Assessment of the MAIT cell immunological synapse . . 108
4.3 Contact dependence of MAIT cell response 109
4.3.1 Cell-contact dependence for IFNγ/TNFα induction . . . 111
4.3.2 Soluble mediators are sufficient for CD69 induction . . . 113
4.3.3 TCR beads fail to reproduce APC–MAIT cell contact . 115
4.4 Development of immunological synapse assay 120
4.4.1 MAIT cell FACS isolation and IL-15 expansion 123
4.4.2 TIRF microscopy of MAIT cell synapse formation . . . 125
4.5 Discussion 132
4.5.1 Requirement for contact varies by MAIT function . . . 132
4.5.2 IL-15 + β-Me enables MAIT cell expansion *in vitro* . . . 134
4.5.3 Uniform surface distribution of MAIT cell IL-18Rα . . . 135
4.5.4 Conclusions 136

4.1 Introduction

In Chapter 3, the effect of cytokine concentration on CD161^{++}/MAIT cell activation was investigated. Whilst TCR-independent activation occurred following exposure to concentrations in the nanomolar range, concomitant TCR stimulation enabled the CD161^{++}/MAIT cells to detect cytokines at extremely dilute picomolar concentrations. Nonetheless, despite the lower threshold of activation, the same relatively higher nanomolar concentrations were required for more robust IFNγ responses, irrespective of TCR stimulation.

These results were determined through culture with exogenously added recombinant cytokine, uniformly distributed throughout the cell culture media. *In vivo*, cytokines originate from cellular sources, inevitably forming concentration gradients as they diffuse away from the activated cells. Different possibilities therefore exist for the concept of cytokine mediated, antigen-independent activation of MAIT cells. On the one hand, very high cytokine levels may activate MAIT cells efficiently from a distance; whilst on the other, minimal amounts may be sufficiently potent at close proximity. Different combinations of cytokines may further modify this balance. Therefore, it is not clear how a high threshold to TCR-independent activation translates to the regulation of MAIT cell activation for the *in vivo* response to infection.

A recent study investigating the ability of MAIT cells to respond to bacterially infected cells in a contact-independent manner, found that B cells infected with *E. coli* were unable to induce IFNγ, TNFα, or CD69 from MAIT cells when separated by a transwell [365]. Given the ability of MAIT cells to respond to cytokine-only stimulation [93], this is surprising. It was not clear, however, whether the concentration of soluble-mediators was high enough to overcome the TCR-independent threshold of activation, or whether the correct combinations of cytokines were produced by B cells infected with *E. coli*. Stimulatory contact with between T cells and APCs typically results in the formation of a structure termed the 'immunological synapse' [366] (Fig. 4.1). If the presence of MAIT cell activating cytokines are present and at high enough concentrations to be detected, yet no activation is seen, this could indicate the requirement for the formation of such a structure.

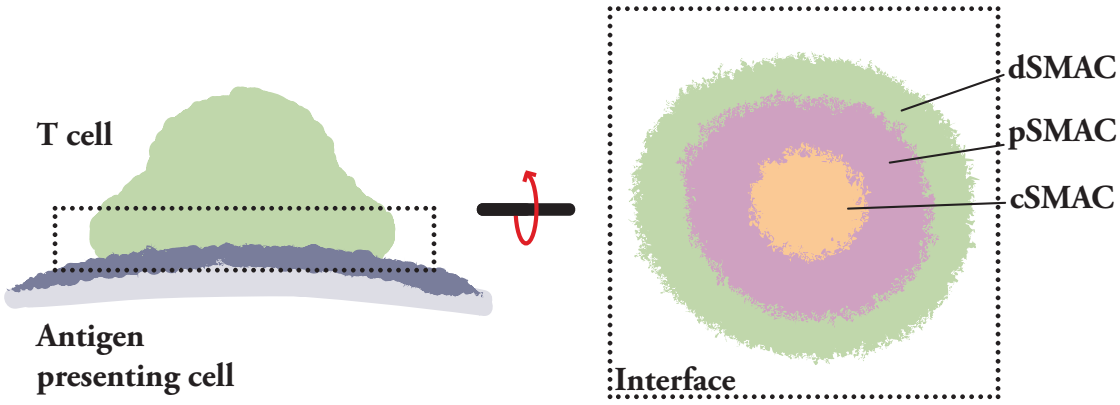


Figure 4.1: Model of the organisation of the immunological synapse. Left: T cell binding to antigen presenting cell. Right: Rotated view to illustrate the T cell surface at the interface. From outside to inside: the dSMAC contains proteins with large ectodomains, such as CD45, whilst the pSMAC comprises integrins. TCR microclusters originate from distal regions where the signals are generated — before traversing the pSMAC, terminating within the cSMAC.[1]

4.1.1 Structure and function of the immunological synapse

Antigen-dependent activation via TCR ligation is a hallmark of T cells and occurs following response to pMHC, adhesion and co-stimulatory interactions between cells that occur at the nanometer scale [367]. These events typically manifest through the formation of an immunological synapse — an arrangement of three zones, or, supramolecular activation complexes (SMACs), of different structural and functional characteristics, arranged in a bull's eye structure. Active TCR–MHC interactions begin as signalling microclusters in the most distal SMAC (dSMAC), before traversing the peripheral SMAC (pSMAC), eventually arriving at the central SMAC (cSMAC). The pSMAC is physically delineated by adhesion interactions between integrins such as LFA-1–ICAM-1; whilst the dSMAC on the outer edge contains proteins with large ectodomains such as CD45 [367, 368]. These are excluded from the central regions, yet are nonetheless important for T cell activation [369]. In addition, multifocal immunological synapses are also possible in which neither CD45, nor ICAM-1 are excluded from the site of accumulation of TCR [368, 370] (Fig. 4.1).

Conventional cytotoxic CD8α^+ T lymphocytes (CTLs) are capable of forming immunological synapses with defined SMACs [371]; the characteristics of MAIT cell immunological synapse formation, however, have not yet been assessed. Immunological synapses confer several functions which may be of importance to the TCR-dependent and -independent activation of MAIT cells. Accumulation

of receptors and signalling adapters at the cell–cell interface increases their relative concentrations, in turn enhancing the likelihood of positive interactions and leading to stability and prolonged signalling [372]. By contrast, phagocytosis and degradation of proteins (such as the TCR) occurs at the cSMAC, leading to termination of membrane proximal signalling [368, 372]. Recently, T cells were also observed to shed TCR microvesicles at the immunological synapse with B cells, indicating a novel mechanism of TCR down-regulation [373]. Interestingly, B cell exposure to such cognate TCR microvesicles led to their uptake and B cell Ca^{2+} signalling, demonstrating bi-directional intercellular communication facilitated by immunological synapse formation [373].

The targeted delivery of soluble mediators such as cytotoxic molecules can also be facilitated by immunological synapses [367]. The formation of a defined pSMAC ring through LFA-1–ICAM-1 interactions between $CD8\alpha^+$ T cells and target cells *in vitro*, has been shown to confine lytic molecules to the synaptic cleft, increasing the effectiveness of cytotoxicity [374]. In addition, despite lacking TCRs, and therefore TCR–pMHC interactions, an imaging study of NK cells revealed the capacity for LFA-1–ICAM-1 interactions to prevent the diffusion of LAMP-1 across the surface of degranulating cells, indicating a focussed area of degranulation [375]. The same concept can be applied to targeted delivery of cytokines. Indeed, activated helper T cells (T_H cells) can express cytokines in two modes; either away from the APC in a multidirectional manner, or polarised directly towards the activating APC [376]. Together, these studies suggest that polarised delivery of cytokines could have an important effect in both TCR-dependent, as well as -independent activation of T cells; especially in subsets such as MAIT cells which are capable of both.

4.1.2 Chapter hypothesis and aims

MAIT cells can respond to cytokines independently of TCR stimulation, but so far evidence is lacking that this can occur in response to infection, in an entirely contact-independent manner. One study which investigated the contact-dependence of MAIT cell activation found that transwell separation of MAIT cells from *E. coli* infected B cells inhibited the MAIT cell response [365]. However, the B cells used may not have expressed the necessary cytokines, and the number of APCs may have been insufficient to account for the dilution of soluble signal with transwell separation. Performing the experiment whilst accounting for these variables may enable detection of a contact-independent response.

[1]Figure adapted from: *Dustin ML: The immunological synapse. Cancer Immunol. Res. 2014, 2:1024.* [367].

Importantly, TCR stimulation fails to induce IFNγ expression from MAIT cells, without adequate co-stimulation. One mechanism through which the two could synergise would be the accumulation of co-stimulatory receptors at the point of interaction between MAIT and antigen presenting cells. In particular, IL-12 and IL-18 co-operate with the TCR to induce IFNγ expression, and delivery of soluble mediators directly across the synaptic cleft would ensure exposure to sufficient levels to mediate activation.

With this in mind, two hypotheses were generated. 1) Monocytic cells or a monocytic cell line known to activate MAIT cells in an IL-12/-18 dependent manner ([93] and see Section 5) as opposed to B cells, would indeed lead to the activation of MAIT cells in a contact-independent manner, as predicted by their ability to respond to cytokines independently of TCR stimulation; and, 2) receptors important for the activation of MAIT cells could be visualised at the immunological synapse. Utilising an approach of physically separating MAIT cells and APCs across a transwell support; and through the use of an artificial bilayer system [373], this chapter has the following three aims:

Aim 1 Design an assay to investigate the ability of monocytic APCs to express soluble mediators capable of inducing MAIT cell activation; either directly, or through providing co-stimulation in the absence of an immunological synapse.

Aim 2 Develop a protocol for the expansion of a pure population of MAIT cells in order to test the ability of MAIT cells to form an immunological synapse on an artificial bilayer.

Aim 3 Using total internal reflectance fluorescence (TIRF) and confocal microscopy, investigate the presence and location of CD161 and IL-18Rα at the immunological synapse.

4.2 Chapter specific materials & methods

Chapter-specific materials and methods are detailed below. Please also refer to Chapter 2 for further information as required.

4.2.1 Contact dependency of MAIT cell activation

CD8α$^+$ T cells and PFA-fixed *E. coli* were prepared, and THP1 cells maintained as detailed in Chapter 2. Experiments were performed in 24-well tissue culture flat-bottomed plates (Corning). THP1 cells were seeded at 8×10^4, or 3×10^5 in 500µl R10 and *E. coli* added at 25 bacteria per cell (BpC) as indicated in the figure legends. Alternatively, human recombinant IL-12 (Miltenyi) and IL-18 (MBL) were added in 500µl R10 (each at 50ng/ml). For transwell separation of CD8α$^+$ T cells, CD8α$^+$ T cells were seeded at 2×10^5 directly onto a 0.4µm pore polyester membrane transwell support (Corning), or alternatively added in the absence of transwell support. Blocking antibody against MR1 (26.5; BioLegend) or mIgG2A isotype control (BioLegend) were added at 10µg/ml as indicated. BFA (eBioscience) was added at 1× (1/1000) for the final 4 hours. For analysis, cells were aspirated and pelleted by microcentrifuge (3,500rpm; 5 mins) before transfer to a 96-well U-bottom plate. Cells were washed ×2 (1,600rpm; 5 mins; 4°C) before surface staining, ICS (detailed in Chapter 2) and assessment by flow cytometry (MACSQuant 10; Miltenyi).

4.2.2 Cytokine-mediated proliferation of MAIT cells

For the cytokine-mediated proliferation of MAIT cells, CD8α$^+$ T cells were prepared by magnetic enrichment as in Chapter 2. Alternatively, following CD8α$^+$ T cell enrichment, MAIT cells were FACS sorted by C. Willberg (Peter Medawar Building) or by J. Webber (Kennedy Institute of Rheumatology) to consistently $> 95\%$ purity according to: electronic gating of live cells, lymphocytes (forward vs. side scatter properties) CD3$^+$, Vα7.2$^+$ and CD161^{++}. Cells were then cultured with IL-2 (20 U/ml; Roche), IL-7 (20ng/ml; PeproTech), IL-12 (50ng/ml; Miltenyi), IL-15 (50ng/ml; Miltenyi) and/or β-Mercaptoethanol (at 2.85×10^{-5} dilution; Sigma) as indicated for 6 days.

For initial assessment of proliferation and phenotype, CD8α$^+$ T cells were washed in PBS ×2 (1,600 rpm; 5 mins; 4°C) prior to surface staining, ICS and counting by flow cytometry (MACSQuant 10). Alternatively, sorted MAIT cells were washed in R10 ×2 (1,600 rpm; 5 mins; 4°C) prior to assessment of immunological synapse formation.

4.2.3 Assessment of the MAIT cell immunological synapse

Following proliferation of FACS sorted MAIT cells, cells were transported to the Kennedy Institute of Rheumatology, Oxford, in 200 µl R10 by M. Bilton, prior to resuspension in supplemented HEPES buffered saline (20mM HEPES, 140mM NaCl, 5mM KCl, 6mM glucose, 1mM CaCl, 2mM MgCl,1% human serum albumin (HSA), pH 7.2) referred to subsequently as HBS/HSA [373].

Lipid bilayers were created by H. Novak and comprised 1,2 dioleoyl-sn-glycero-3-phosphatidylcholine (DOPC) containing 12.5 mol%1,2-dioleoyl-*sn*-glycero-3-[(*N*-(5-amino-1-carboxypentyl)iminodiacetic acid)succinyl] (nickel salt) (DGS-NTA-Ni) deposited on coverslips that were cleaned with peroxidated sulphuric acid and rinsed with pure water [373]. Bilayers were also embedded with αCD3-AlexaFluor (AF) 568 Fab (UCHT-1) at 30 molecules per µm^2 for conditions as indicated, and ICAM-1-AF405 at 250 molecules per µm^2.

For formation of immunological synapses, MAIT cells were added to the bilayers by M. Bilton/H. Novak in HBS/HSA and imaged live for MAIT cell immunological synapse formation, or incubated (15 mins; 37°C) prior to fixation in 2% paraformaldehyde (PFA) (10 mins; 21°C) for immunostaining. Cells were then blocked with 5 % casein (> 30 mins; 21°C), prior to surface staining by directly conjugated αCD161-AF488 (702228), αIL-18Rα-AF488 (70625) or mIgG2b-AF488 (702228) and mIgG1-AF488 (11711) isotype controls, respectively (all R&D) (1 hour; 21°C). Each step was followed by 3× washes with 150 µl HBS/HSA.

Following the final washes, total internal reflectance microscopy (TIRFM) imaging was performed by H. Novak using a Nikon Ti microscope, controlled by Nikon Elements software. The instrument was fitted with a 100× TIRF objective, 1.49 numerical aperture (NA). Alternatively, bilayers were transported to the Dunn School of Pathology and imaged by confocal microscopy performed by M. Bilton using an Olympus Fluoview FV1000 inverted IX81 motorised microscope, fitted with a 60× 1.35 NA Oil UPlanSApo objective. Image analysis was performed in Volocity 6.3 (Perkin Elmer).

4.3 Contact dependence of MAIT cell response

CD161^{++}/MAIT cells can respond to cytokines in a TCR independent manner; yet a report evaluating the contact dependence of MAIT cell activation in the context of bacterial infection found that loss of contact inhibited MAIT cell activation [365].

To independently assess whether microbe-induced soluble mediators are sufficient for CD161^{++}/MAIT activation; an assay using solute-permeable, cell-impermeable

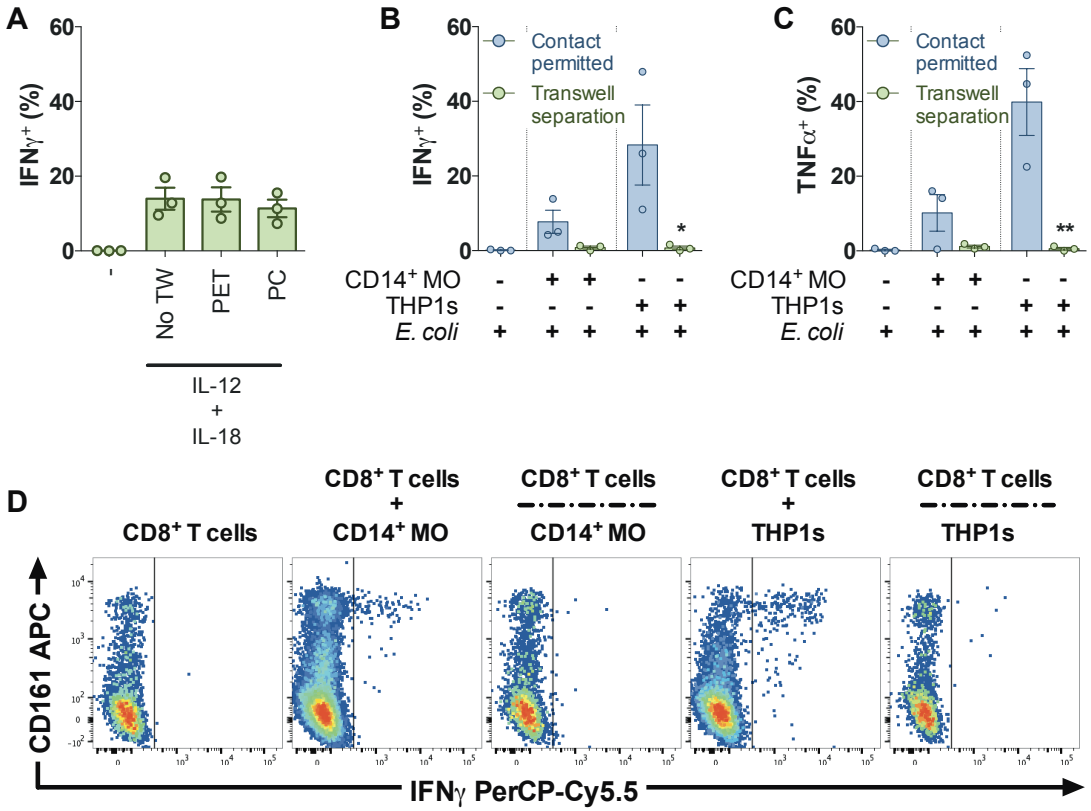


Figure 4.2: Preliminary transwell inhibition of CD161^{++}/MAIT cell activation by *E. coli*. (A) CD8α$^+$ T cells were enriched from PBMCs with magnetic beads and stimulated overnight with IL-12/-18 (50 ng/ml each) either directly (No TW), or across 0.4 µm polyester (PET)/polycarbonate (PC) transwell supports, before assessment for CD161^{++}/MAIT cell IFNγ-expression. (B) Magnetically enriched CD8α$^+$ T cells were cultured with 8×10^4 THP1 cells or autologous CD14$^+$ monocytes in the presence of PFA-fixed *E. coli* at a BpC ratio of 25:1 for 24 hours, or they were separated from the bacteria-fed monocytes by a transwell membrane support. Frequency of (B) IFNγ$^+$ and (C) TNFα$^+$ CD161^{++}/MAIT cells were then assessed by ICS. (D) Representative FACS plot of CD161^{++}/MAIT cell IFNγ expression. Graphs show mean ± SEM. Data analysed by one-way ANOVA with Holm-Sidak's multiple comparison test. $^{**}p < 0.01$, $^{*}p < 0.05$.

transwell membranes was optimised. To test different transwell membranes, CD8α$^+$ T cells were magnetically enriched from PBMCs, and stimulated with 50 ng/ml recombinant IL-12/-18 separated across a polyester or polycarbonate membrane (0.4 µm pore size), for 24 hours. No difference in CD161^{++}/MAIT cell IFNγ-expression was observed following separation with the polyester membrane indicating little impediment to the free diffusion of cytokine (Fig. 4.2 A).

Subsequently, CD8α$^+$ T cells were cultured with 8×10^4 THP1 cells, or magnetically enriched CD14$^+$ autologous monocytes, each fed with PFA-fixed *E. coli* at a bacteria per cell (BpC) ratio ratio of 25:1, for 24 hours. CD8α$^+$ T cells were either left in contact with the APCs, or separated by a polyester transwell support,

before assessment for CD161^{++}/MAIT cell IFNγ- and TNFα-expression. Without transwell separation, IFNγ was expressed by $7.7 \pm 5.4\%$, and $28.3 \pm 10.7\%$ of CD161^{++}/MAIT cells following co-culture with autologous monocytes, or THP1 cells, respectively. In this initial test, physical separation of autologous monocytes from CD161^{++}/MAIT cells did appear to completely abrogate IFNγ-expression, as did separation from THP1 cells ($p < 0.05$; Fig. 4.2 B, D). Similarly, $10.2 \pm 4.9\%$ and $39.9 \pm 9.0\%$ of CD161^{++}/MAIT cells expressed TNFα in response to contact with *E. coli*-fed autologous monocytes and THP1 cells, respectively; and no TNFα-expression was observed following transwell separation of the CD161^{++}/MAIT cells from the monocytes, or THP1 cells ($p < 0.01$; Fig. 4.2 C).

4.3.1 Cell-contact dependence for IFNγ/TNFα induction

As THP1 cells were more efficient at activating CD161^{++}/MAIT cells in a contact-dependent manner, and were known to be capable of activating MAIT cells in a TCR independent manner ([93] and see Chapter 5), they were used in subsequent experiments in an effort to maximise the effect size of the response. The EC50 for IL-12/-18 stimulation is relatively high in the absence of TCR stimulation at approximately 5 ng/ml, with a lower threshold of activation at approximately 3 ng/ml (see Section 3.4.1). One potential explanation for the lack of contact-independent response is that the combined expression of soluble mediators by THP1 cells was low relative to the volume of the culture well, and thus below this threshold concentration for contact-independent activation of MAIT cells. The numbers of THP1 cells seeded were therefore increased 3.75-fold from 8×10^4 to 3×10^5 per well, and the frequency of contact-dependent IFNγ-expression by CD161^{++}/MAIT cells subsequently increased from approx. 30% to $51.4 \pm 6.1\%$ ($p < 0.0001$ vs. unstimulated; Fig. 4.3 A, B). TNFα-expression, however, remained at $35.9 \pm 4.9\%$ ($p < 0.0001$ vs. unstimulated; Fig. 4.3 C, D) indicating that unlike IFNγ, cell number was not limiting for TNFα-expression.

However, despite the increase in THP1 cells seeded, the frequency of activated CD161^{++}/MAIT cells nonetheless dropped with physical separation from approx. 50% to $5.8 \pm 3.3\%$ for IFNγ-expression ($p < 0.0001$); and approx. 36% to $6.9 \pm 1.5\%$ for TNFα-expression ($p < 0.0001$; Fig. 4.3 C, D). Nonetheless, it is worth noting the minor proportion of cells that did appear to exhibit capacity to respond in a contact-independent manner following the increase in THP1 cell number ($p =$ ns). One explanation for the transwell-mediated abrogation of IFNγ- or TNFα-expression is a loss of TCR stimulation via MR1. In order to provide a comparison for loss of the TCR signal whilst permitting cell-cell contact, isotype control or

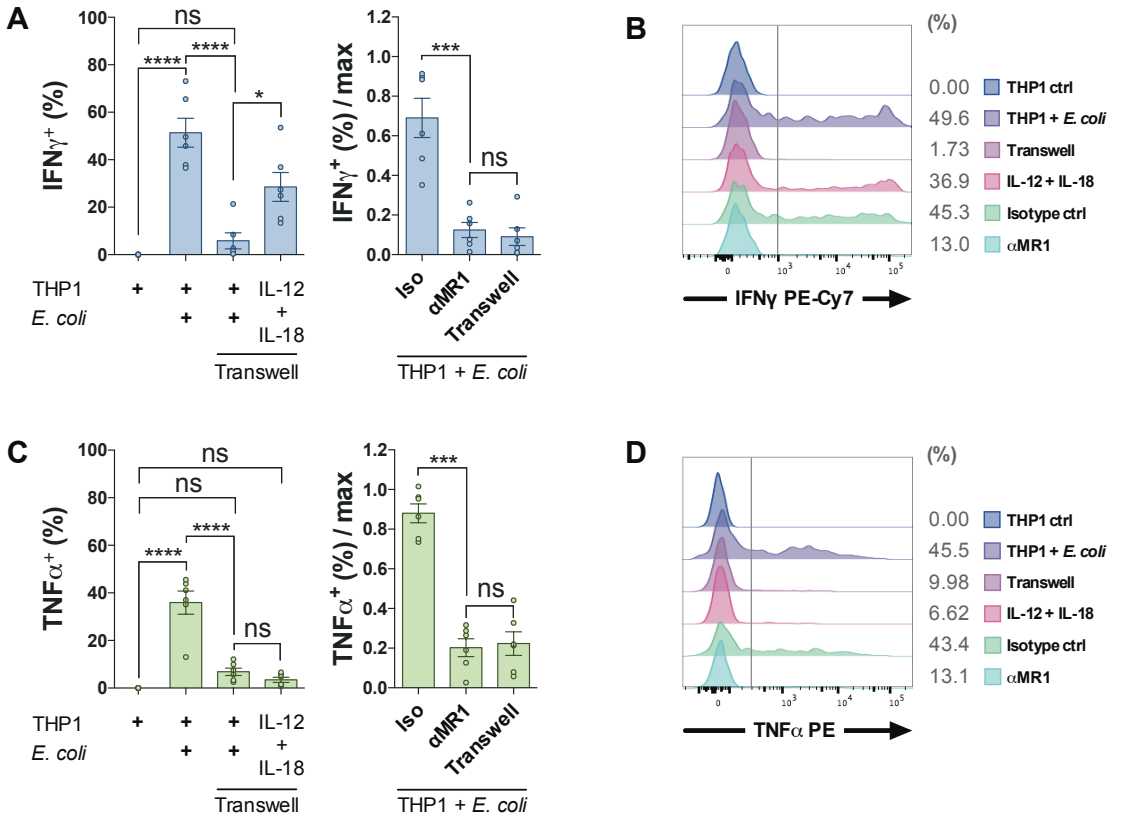


Figure 4.3: Transwell inhibition of CD161^{++}/MAIT cell activation by *E. coli*. CD8α$^+$ T cells were cultured with 3×10^5 THP1 cells in the presence of PFA-fixed *E. coli* (25:1 BpC), or separated by a transwell membrane support. Alternatively, CD8α$^+$ T cells were stimulated with IL-12/-18 (50 ng/ml each) added across a transwell membrane. αMR1 blocking antibody (clone 26.5) or isotype control were added to the THP1 + *E. coli* co-culture (each at 10 µg/ml) as indicated. After 24h, CD8α$^+$ T cells were assessed for cytokine production by flow cytometry and ICS. (A, B) IFNγ$^+$ and (C, D) TNFα$^+$ cells as a frequency of CD161^{++}/MAIT cells (left), or relative to response in the absence of blocking antibody (right). (B, D) Representative FACS plots of CD161^{++}/MAIT cell (B) IFNγ or (D) TNFα expression. Data analysed by one-way ANOVA with Holm-Sidak's multiple comparison test. Graphs show mean ± SEM. For all tests, ****$p < 0.0001$, ***$p < 0.001$, **$p < 0.01$, *$p < 0.05$, ns = non-significant.

αMR1 (clone 26.5) mAbs were also added to the co-culture for the duration of the experiment. Indeed, both MR1-blockade ($p < 0.001$ vs. isotype control) and transwell inhibition resulted in a similar abrogation of the IFNγ-response to *E. coli* fed THP1 cells (12.5 ± 3.8% and 9.1 ± 4.4% of maximal contact-permitted activation, respectively; p = ns; Fig. 4.3 A, B), with equivalent decreases of the TNFα-response (20.2 ± 4.5% and 22.3 ± 6.0% of maximal, respectively; p = ns; Fig. 4.3 C, D), indicating no difference between transwell separation of cells vs. blockade of MR1. It is worth noting, however, that despite permitting MAIT cell–THP1 contact, αMR1 treatment may affect the nature of this contact. There

was a small response by CD161^{+} and CD161^{-} CD8α^{+} T cells expressing IFNγ in response to direct co-culture with *E. coli*-fed THP1s (approx. 6%, and 1%, respectively), which was abrogated following transwell separation (data not shown). Very few non-MAIT CD8α^{+} T cells were found to express IFNγ in response to PFA-fixed *E. coli*-fed autologous monocytes in Fig. 4.2 (p. 110), however the use of THP1s instead of autologous monocytes, the unknown HLA-type of donor cells used, the use of fixed bacteria (and possible damage to protein-derived antigen presentation to HLA-restricted T cells [377]) makes assessment and interpretation of the contact-dependent activation of non-MAIT CD8^{+} T cells difficult.

4.3.2 Soluble mediators are sufficient for CD69 induction

Following direct co-culture with *E. coli* fed THP1s, the majority of CD161^{++}/MAIT cells up-regulated CD69 ($92.7 \pm 0.9\%$; $p < 0.0001$; Fig: 4.4 A, B). Interestingly, in contrast to the strong abrogation of IFNγ- and TNFα-expression, transwell separation could only modestly reduce the CD69 up-regulation to $80.6 \pm 6.2\%$ ($p < 0.05$); 87.1% of the maximal CD69 expression, whilst MR1-blockade could only reduce CD69 expression to 75.3% of the maximal expression observed ($p < 0.05$). In contrast to this sizeable proportion (approx. 80%) of MAIT cells expressing CD69 following transwell separation, the frequency of CD69 expressing non-MAIT CD8α^{+} T cells (CD161^{+} and CD161^{-} CD8α^{+} T cells) remained low at approximately 7% and 3% of each sub-population, respectively (data not shown). This is consistent with CD161^{++}/MAIT cells possessing a capability to detect soluble mediators expressed by *E. coli*- fed THP-1s with a sensitivity not demonstrated by bulk non-MAIT CD8α^{+} T cells. Overall, however, these data indicate that the CD161^{++}/MAIT CD69 response to bacteria is dependent on neither MR1 activation, nor cell-cell contact — and therefore soluble mediators are largely sufficient at the concentrations detected following diffusion across the transwell support.

4.3.2.1 Soluble mediators are insufficient for Vα7.2 down-regulation

In Chapter 3, the effect of TCR and cytokine stimulation on CD161^{++}/MAIT cell Vα7.2 TCR expression was investigated, finding that sustained activation by the combination of TCR beads, IL-12 and IL-18 synergistically induced a large proportion of CD161^{++}/MAIT cells to down-regulate their TCR. In this set of experiments, culture with *E. coli*-fed THP1 cells induced CD161^{++}/MAIT cells to similarly down-regulate their TCR expression to $44.5 \pm 6.0\%$ of max. (Fig: 4.4 C, D), which was abrogated by both transwell separation ($97.2 \pm 0.7\%$; $p < 0.0001$) and MR1-blockade ($97.4 \pm 1.1\%$; $p < 0.0001$) to a similar extent ($p =$ ns).

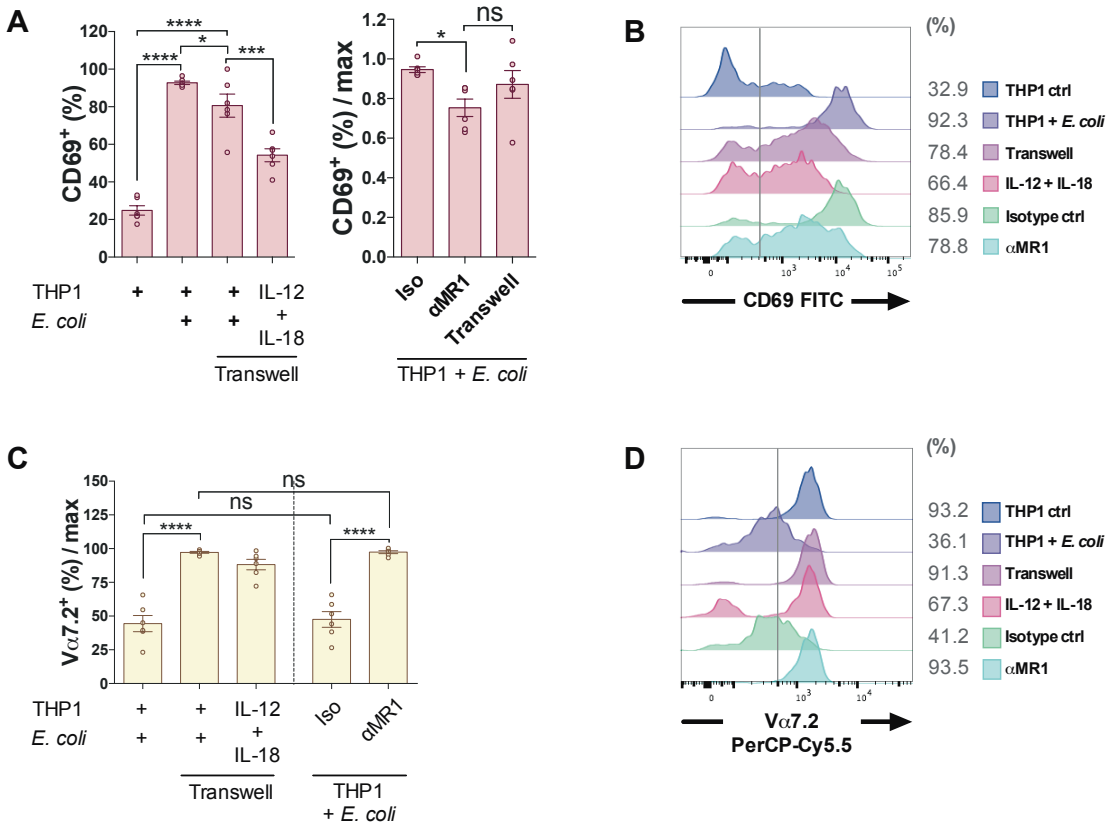


Figure 4.4: Robust CD69-induction by soluble-mediators in response to bacteria. CD8α$^+$ T cells were cultured with 3×10^5 THP1 cells in the presence of PFA-fixed *E. coli* (25:1 BpC), or separated by a transwell membrane support. Or CD8α$^+$ T cells were stimulated with IL-12/-18 (50 ng/ml each) added across a transwell membrane. Alternatively αMR1 blocking antibody (clone 26.5) or isotype control were added to the THP1 + *E. coli* co-culture (each at 10 µg/ml). After 24h, CD8α$^+$ T cells were assessed for cytokine production by flow cytometry and ICS. (A) CD69$^+$ TNFα$^+$ cells as a frequency of CD161^{++}/MAIT cells (left), or relative to response in the absence of blocking antibody (right). (C) Vα7.2$^+$ CD161^{++}/MAIT cells relative to unstimulated per donor, following conditions as shown. (B, D) Representative FACS plots of CD161^{++}/MAIT cell (B) CD69- or (D) Vα7.2-expression. Graphs show mean ± SEM. Data analysed by one-way ANOVA with Holm-Sidak's multiple comparison test. ****$p < 0.0001$, ***$p < 0.001$, *$p < 0.05$, ns = non-significant.

Together, these results indicate that under the experimental conditions tested, the soluble mediators released by *E. coli*-fed THP1s were insufficient to induce CD161^{++}/MAIT cell IFNγ- or TNFα-expression, or Vα7.2 TCR down-regulation — although this appears to largely be accounted for through the absence of the MR1 signal. By contrast, CD69 expression was unaffected by transwell separation, indicating that soluble mediators were sufficient for bacteria-induced CD69 expression. Interestingly, the expression of CD69 following transwell separation was greater than that induced by the recombinant IL-12/-18 control (each at 50 ng/ml), indicating that even saturating concentrations of IL-12/-18 failed to recapitulate the extent of CD69 up-regulation, suggesting therefore that further cytokines released from the *E. coli*-fed THP1s are likely involved.

4.3.3 TCR beads fail to reproduce APC–MAIT cell contact

In the absence of co-stimulatory cytokine signals, CD161^{++}/MAIT cells do not respond well to TCR stimulation; in particular with regards to IFNγ-expression (see Section 3.3.1). However, even if insufficient for TCR-independent activation at the levels present in these experiments, low-levels of soluble mediators produced by bacterially infected APCs may play an essential role in the co-stimulation of CD161^{++}/MAIT cells. To test this, CD8α^{+} T cells were physically separated from the *E. coli*-fed THP1 cells as described, and cultured in the presence or absence of αCD2/CD3/CD28 coated beads in order to recapitulate the MR1-signal but without cell-cell contact.

As expected, little induction of IFNγ or TNFα was observed following culture with TCR beads alone vs. unstimulated ($0.7 \pm 0.1\%$ and $4.3 \pm 0.6\%$; both $p =$ ns); similar to the response to soluble-mediators alone ($5.8 \pm 3.3\%$ and $6.9 \pm 1.5\%$ for IFNγ and TNFα, respectively). The TNFα response to soluble mediators was increased minimally on addition of TCR beads (+3.7%; $p =$ ns), whilst IFNγ-expression increased to $18.1 \pm 4.6\%$ (+12.3% vs. no TCR beads; $p < 0.01$; Fig. 4.5 A, C) suggesting that TCR stimulation sensitised CD161^{++}/MAIT cells to respond to bacteria-induced soluble-mediators for IFNγ-expression. Negligible increases in the expression of IFNγ and TNFα by CD161^{+} and CD161^{-} CD8^{+} T cells were observed (Fig. 4.5 C; data not shown) consistent with a different ability of non-MAIT CD8α^{+} T cells to respond to the same soluble mediators during otherwise equivalent TCR stimulation.

Of note, and by comparison, the effect size of TCR bead exposure on CD161^{++}/MAIT cell cytokine-expression was far larger following exposure to 50 ng/ml rIL-12

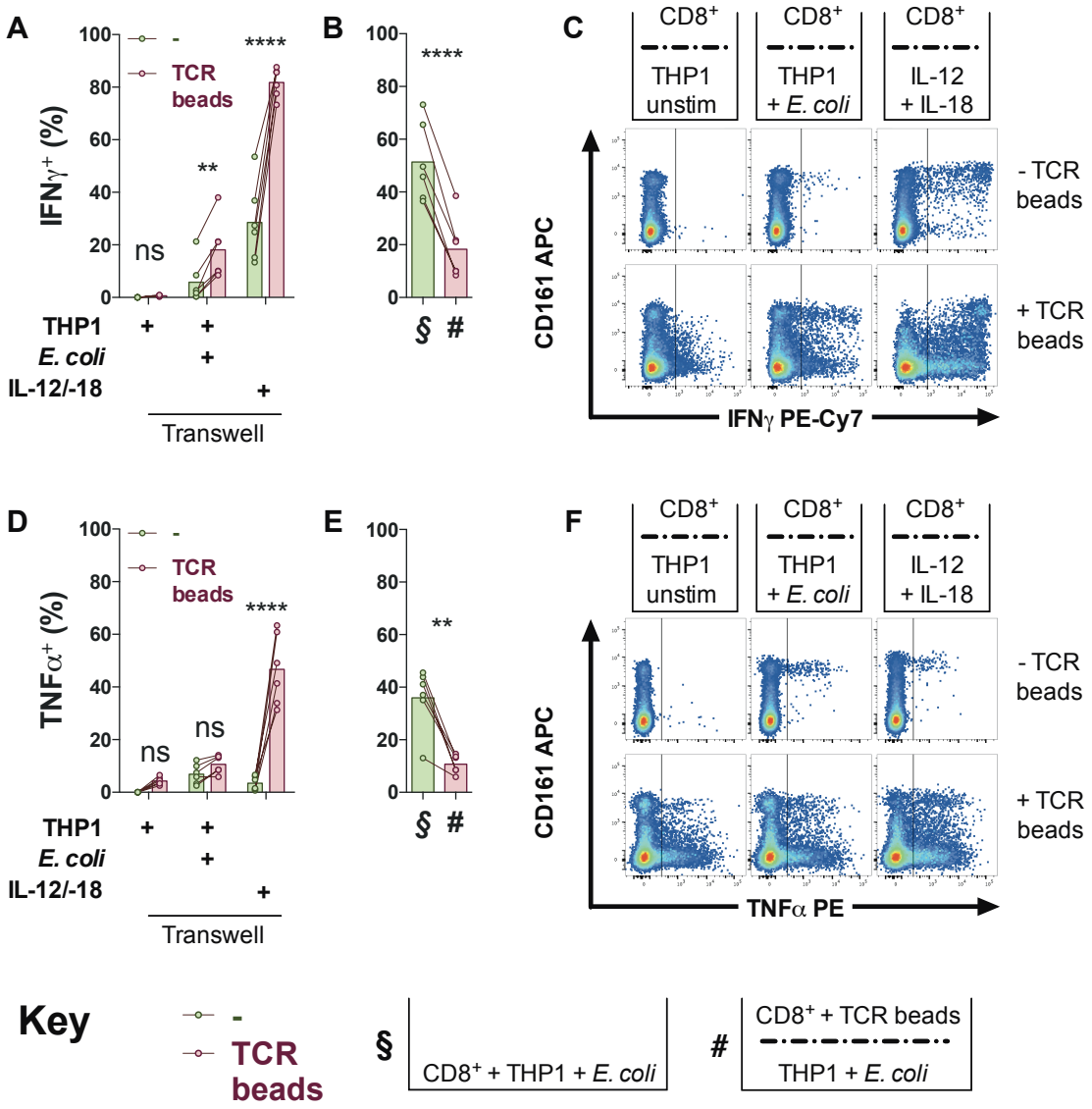


Figure 4.5: TCR beads only partially recover contact-dependent CD161^{++}/MAIT activation by *E. coli*. CD8α$^+$ T cells were cultured in a transwell membrane support above either THP1 cells ± PFA-fixed *E. coli* (25:1 BpC), or IL-12/-18 (50 ng/ml each) in the absence of THP1 cells. αCD2/3/28 beads were added to CD8α$^+$ T cells as indicated. (B, E) CD8α$^+$ T cells were cultured with THP1 cells + *E. coli*, or they were separated by a transwell membrane support and αCD2/3/28 beads added. After 24h, CD8α$^+$ T cells were assessed for cytokine production by flow cytometry and ICS. (A, B) Frequency of IFNγ$^+$ CD161^{++}/MAIT cells. (D, E) Frequency of TNFα$^+$ CD161^{++}/MAIT cells. (C) Representative FACS plot of IFNγ and (F) TNFα expression on CD8α$^+$ T cells. Key: § CD8α$^+$ T cells + THP1 cells + *E. coli*, no transwell separation. # CD8α$^+$ T cells + TCR beads (transwell support), THP1 cells + *E. coli* (beneath). Graphs show mean ± SEM. Data analysed by (A, D) one-way ANOVA with Holm-Sidak's multiple comparison test and (B, E) paired t-test. For all tests, ****$p < 0.0001$, ***$p < 0.001$, **$p < 0.01$, *$p < 0.05$, ns = non-significant.

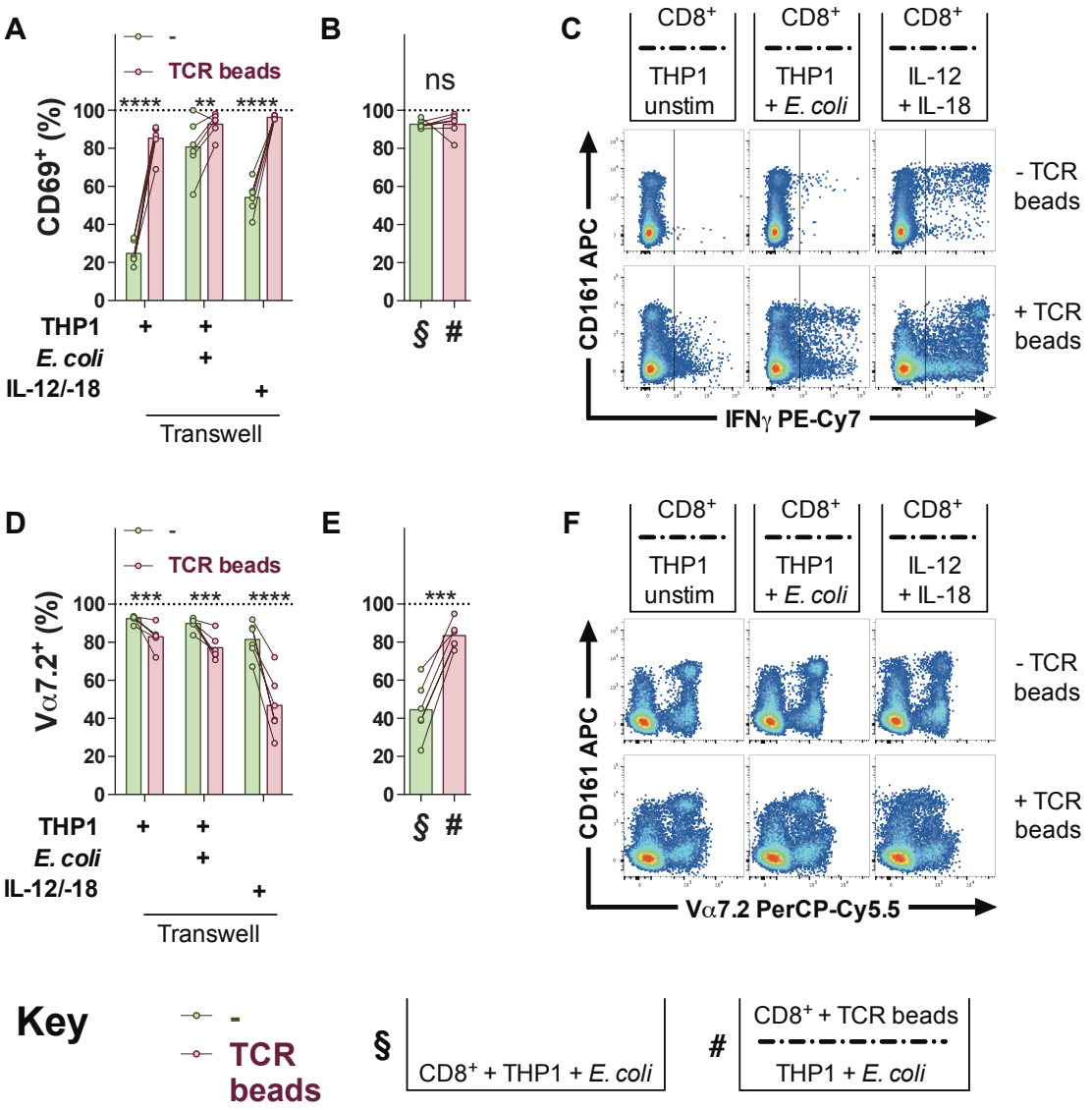


Figure 4.6: TCR bead stimulation induces only partial CD161^{++}/MAIT cell TCR-downregulation by transwell separated THP1 cells + *E. coli*. CD8α$^+$ T cells were cultured in a transwell membrane support above either THP1 cells ± PFA-fixed *E. coli* (25:1 BpC), or IL-12/-18 (50 ng/ml each) in the absence of THP1 cells. αCD2/3/28 beads were added to CD8α$^+$ T cells as indicated. (B, E) CD8α$^+$ T cells were cultured with THP1 cells + *E. coli* (25:1 BpC), or they were separated by a transwell membrane support and αCD2/3/28 beads added. After 24h, CD8α$^+$ T cells were assessed for cytokine production by flow cytometry and ICS. (A, B) Frequency of CD69$^+$ CD161^{++}/MAIT cells. (D, E) Frequency of Vα7.2$^+$ expression amongst CD161^{++}/MAIT cells. (C) Representative FACS plot of CD69 and (F) Vα7.2 expression on CD8α$^+$ T cells. # CD8α$^+$ T cells + TCR beads (transwell support), THP1 cells + *E. coli* (beneath). Graphs show mean ± SEM. Data analysed by (A, D) one-way ANOVA with Holm-Sidak's multiple comparison test and (B, E) paired t-test. For all tests, ****$p < 0.0001$, ***$p < 0.001$, **$p < 0.01$, *$p < 0.05$, ns = non-significant.

+ rIL-18 + TCR beads (+53.2% for IFNγ-expression and +43.2% for TNFα-expression vs. no TCR beads), suggesting CD161^{++}/MAIT cell exposure to less than saturating levels of soluble-mediators in the culture media. Furthermore, despite the large effect-size when TCR beads were combined with rIL-12 + rIL-18; culture of CD161^{++}/MAIT cells with TCR beads and exposure to, but physical separation from, APCs was unable to recapitulate the full extent of activation of THP1–MAIT cell contact-permissive co-culture (Fig. 4.5 B). Indeed the frequency of IFNγ^{+} CD161^{++}/MAIT cells separated by a transwell support and exposed to TCR beads remained substantially lower than the frequency following cell–cell contact ($-33.1 \pm 2.8\%$; $p < 0.0001$), with a similar reduction in the level of TNFα-expression also observed (-25.2%; $p < 0.01$). There could be several reasons for this — TCR beads were added to mimic MR1-mediated stimulation, but the TCR stimulation they provide may be qualitatively inferior to the authentic MR1 signal provided by THP1 cells. Alternatively, the absence of immunological synapse formation, and targeted delivery of cytokine, may account for the reduction in response.

4.3.3.1 Soluble-mediators + TCR beads minimally reduce Vα7.2 TCR

Unlike IFNγ- and TNFα-expression, CD69 was up-regulated robustly following exposure to TCR beads alone (+60.5% vs. unstimulated; Fig. 4.6 A). Exposure to soluble-mediators alone was also able to induce CD69 up-regulation (+55.8%), although this was further enhanced with the addition of TCR beads (+12.1% vs. transwell separation; $p < 0.01$). Notably, no drop in expression of CD69 was observed following stimulation by soluble mediators + TCR beads vs. contact-permissive co-culture ($\pm 0.0\%$; $p =$ ns; Fig. 4.6 B), indicating the sufficiency of TCR beads + THP1-expressed soluble mediators to replicate the signals provided by APC–MAIT cell contact for CD69-induction.

Conversely, little Vα7.2 TCR down-regulation was observed with TCR beads alone vs. unstimulated (-9.6%; $p < 0.001$; Fig. 4.6 D); or with TCR beads and soluble mediators vs. exposure to soluble mediators only (-12.7%); $p < 0.001$). Likewise, whilst contact-permitted co-culture with THP1 cells induced a robust TCR down-regulation, this was not replicated following transwell separation with additional TCR bead exposure (+39% vs. direct co-culture; $p < 0.001$; Fig. 4.6 E).

In summary therefore, the soluble mediators produced by THP1 cells in response to PFA-fixed *E. coli* were capable of inducing CD69 expression and providing co-stimulation for the activation of TCR bead stimulated CD161^{++}/MAIT cells to express IFNγ. However, the effect-size of the IFNγ response remained far smaller than that following direct co-culture with the THP1 cells — despite sharing the

same culture media, and being provided with exogenous TCR stimulation. By contrast, the soluble mediators present were unable to induce TNFα-expression by CD161^{++}/MAIT cells in the presence or absence of TCR beads; with the Vα7.2 TCR being only modestly down-regulated relative to direct co-culture.

One caveat is the timing of the experiment; it is possible that further interrogation of the TNFα response following a shorter stimulation with TCR beads would reveal a larger co-stimulatory effect of the soluble mediators for this effector function, as the CD161^{++}/MAIT TNFα response is rapid and transient — especially in the absence of saturating cytokine concentrations (see Section 3.5.2).

4.4 Development of immunological synapse assay

The results in Section 4.3 argue for the importance of cell–cell contact for the activation of CD161^{++}/MAIT cells by bacteria, which is not completely recapitulated through stimulation via αCD2/CD3/CD28 TCR beads. Both MR1 blockade and transwell separation demonstrated similar inhibitory effects; and of note, both interventions should inhibit immunological synapse formation.

There are several relevant features of the immunological synapse that might explain the weakness of the contact independent, and/or TCR independent response. The high cytokine threshold of activation of MAIT cells in a TCR-dependent manner could be overcome more readily with targeted delivery of IL-12/-18 directly into the synaptic cleft. Following this, it is interesting to hypothesise that the relevant cytokine receptors may preferentially re-locate to the immunological synapse to facilitate this.

In order to assess this using an artificial bilayer platform (developed by the M. Dustin group), a protocol for the efficient isolation of sufficient numbers of pure MAIT cells was required. MAIT cells can comprise a large number (10–15%) of circulating CD8α^{+} or DN T cells; however the number can vary substantially between individuals ($< 1\% - 30\%$). This provides experimental challenges where large numbers of functional MAIT cells are required. Using the artificial bilayer system required such numbers; and therefore an expansion protocol was needed to guarantee their generation on demand. However, as the biological response to TCR stimulation was to be subsequently tested, such a protocol would require a TCR-independent approach to the induction of MAIT cell expansion. Initially, therefore the capacity of different cytokines to induce the TCR-independent proliferation of MAIT cells was assessed.

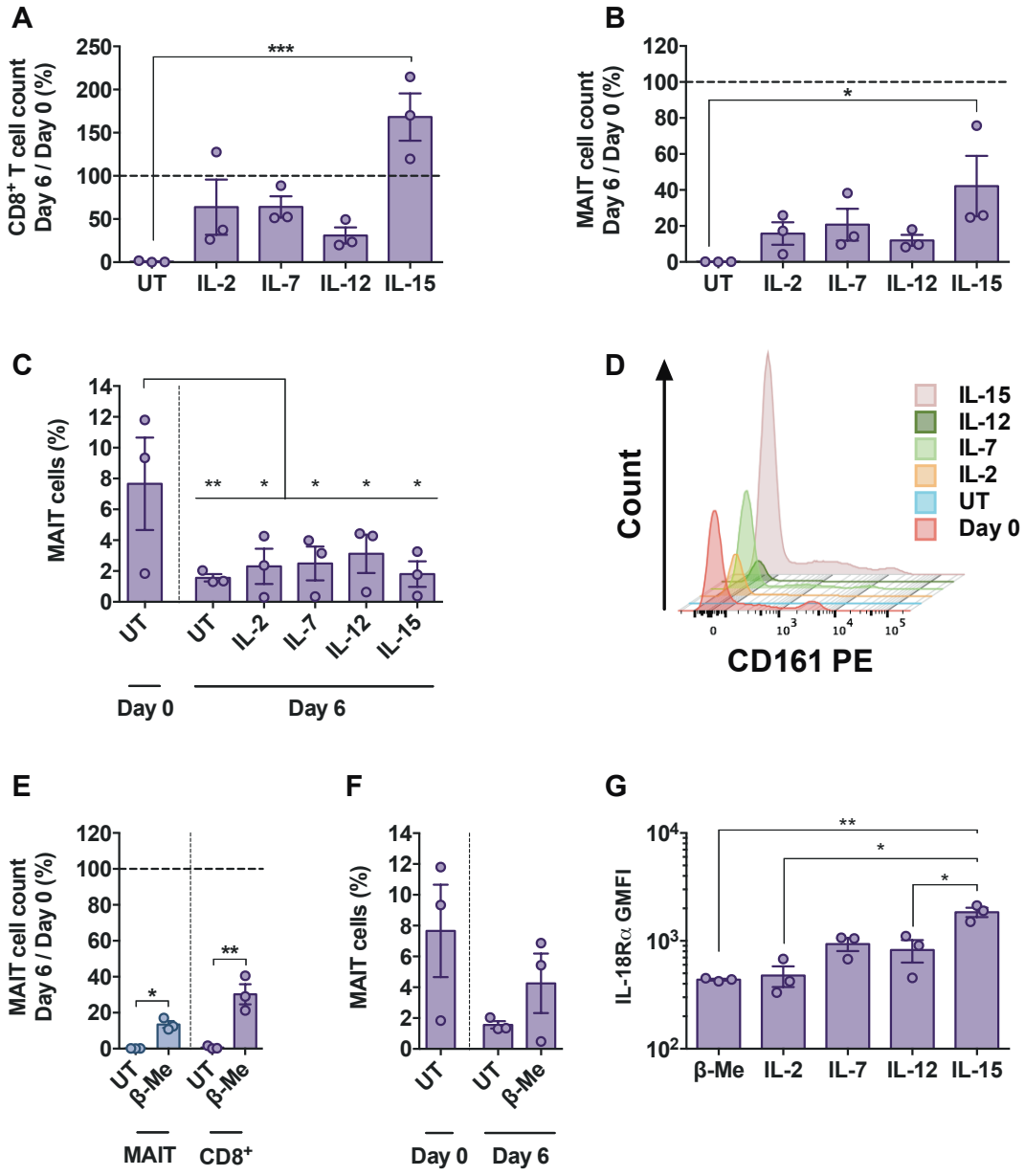


Figure 4.7: Test of cytokine mediated CD8α$^+$ T cell proliferation. (A – D, G) CD8α$^+$ T cells were enriched from PBMCs before culture in R10 media with IL-2 (20 U/ml), IL-7 (20 ng/ml), IL-12 (50 ng/ml) or IL-15 (50 ng/ml) for 6 days; and/or, (E – G) cells were cultured for 6 days in R10 media supplemented or not with β-mercaptoethanol (β-Me). (A, E) Total CD8α$^+$ T cell and (B, E) MAIT cell live events recorded at day 6 relative to numbers seeded at day 0. (C, F) MAIT cell relative frequency as % of total CD8α$^+$ T cells. (D) Representative histogram of CD8α$^+$ T cells at day 0 and day 6 post-stimulation, *y*-axis represents number of events recorded. (G) IL-18Rα GMFI of MAIT cells after 6 days culture in R10 + IL-15 (50 ng/ml). Graphs show mean ± SEM. Data analysed by (A – C, G, F) one-way ANOVA with Holm-Sidak's multiple comparison test and (E) paired t-test. For all tests, $^{***}p < 0.001$, $^{**}p < 0.01$, $^{*}p < 0.05$.

CD8α$^+$ T cells were magnetically enriched from PBMCs before being seeded at 2×10^5 cells/well in a 96 U-bottom format, in R10 culture medium containing IL-2 (20 U/ml), IL-7 (20 ng/ml), IL-12 (50 ng/ml), IL-15 (50 ng/ml), or with no additional cytokines. The CD8α$^+$ T cells were cultured for 6 days, before counting by flow cytometry.

Following the 6 days culture, very few cells were recovered in the absence of any cytokine stimulation ($0.7 \pm 0.5\%$ of cells seeded), whilst IL-2, IL-7 and IL-12 stimulation each resulted in detectable CD8α$^+$ T cells remaining at day 6 ($63.8 \pm 32.0\%$, $64.1 \pm 12.2\%$ and $31.0 \pm 9.3\%$ of cells seeded, respectively). Only stimulation with IL-15, however, was able to induce a consistent increase in CD8α$^+$ T cells recovered at day 6, relative to those seeded at day 0 ($168.2 \pm 27.5\%$; Fig: 4.7). In comparison with bulk CD8α$^+$ T cells, fewer MAIT cells were recoverable on day 6 than were seeded, irrespective of cytokine stimulation type (Fig: 4.7 B) — with a selective proliferation of non-MAIT CD8α$^+$ T cells as shown by the decrease in MAIT cell frequency as a proportion of CD8α$^+$ T cells (Fig: 4.7 C).

As a reducing agent widely used in the cell-culture media of THP1 cells, the effect of including β-mercaptoethanol (β-Me) in the 6 day CD8α$^+$ T cell culture media was also assessed. Whilst fewer than seeded, viable MAIT cells ($13.4 \pm 1.9\%$; $p < 0.05$) and bulk CD8α$^+$ T cells ($30.3 \pm 5.6\%$; $p < 0.01$) were recovered following culture in media containing β-Me, despite the lack of any additional stimuli, indicating the ability of β-Me to enhance CD8α$^+$ T cell and MAIT cell survival.

Finally, with the intention of investigating relevant cell-surface receptors at the MAIT cell immunological synapse, the effect of each cytokine on IL-18Rα-expression on day 6 was assessed, finding that IL-15 led to the strongest induction of IL-18Rα-expression vs. no cytokine/β-Me ($p < 0.01$).

4.4.1 MAIT cell FACS isolation and IL-15 expansion

Given these data, both IL-15 and β-Me were taken forward for further tests. CD8α$^+$ T cells were magnetically enriched as before, seeded at 2×10^5 per well, and cultured for 6 days in the presence of IL-15 + β-Me, or β-Me only. After 6 days culture in the presence of β-Me only, 3.6×10^3 viable CD8α$^+$ T cells were recovered, whilst 1.3×10^5 viable CD8α$^+$ T cells were recovered following the addition of IL-15 ($p < 0.01$). In contrast to the earlier experiment, the number of viable MAIT cells recovered was also increased from 2.3×10^2 with β-Me only, to 1.3×10^4 with β-Me + IL-15 ($p < 0.001$); comparable to the numbers of MAIT cells seeded (1.2×10^4 on day 0; Fig: 4.8 A).

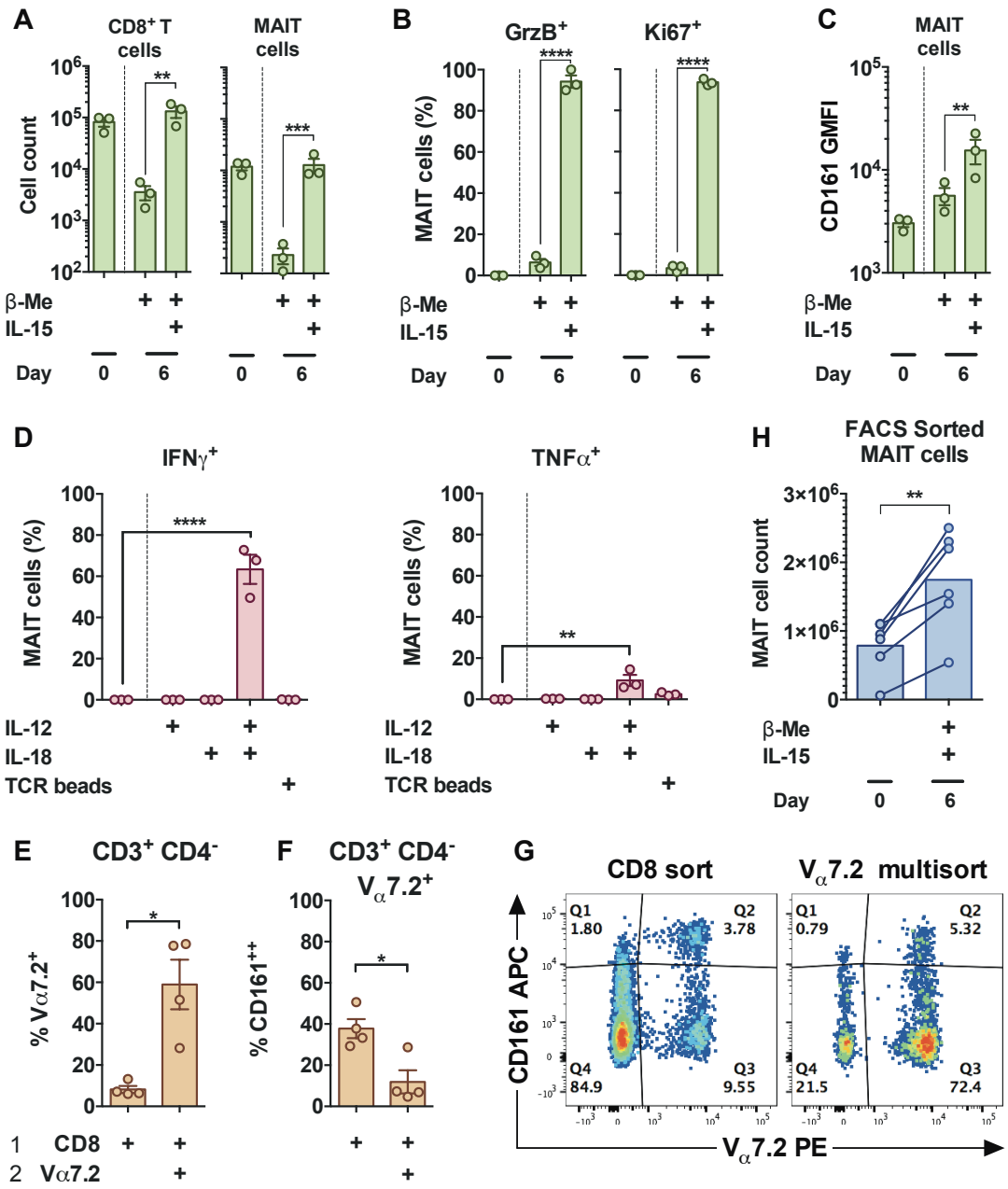


Figure 4.8: IL-15 and β-Mercaptoethanol effectively induce MAIT cell expansion. (A – D) CD8α$^+$ T cells were enriched from PBMCs and cultured with β-Me ± IL-15 (50 ng/ml). (A – C) Live total CD8α$^+$ T or MAIT cells were then (A) counted, or (B) assessed for Granzyme B (GrzB), Ki67, or (C) CD161 expression by flow cytometry. (D) IL-15 expanded CD8α$^+$ T cells were stimulated with IL-12 ± IL-18 (50 ng/ml), or αCD2/3/28 beads for 24h, before ICS for IFNγ and TNFα. (E – G) PBMC were stained with αVα7.2-PE and selected with αCD8 only, or αCD8 then αPE magnetic beads. (E) Proportion Vα7.2$^+$ of CD4$^-$ T cells, and (F) proportion CD161^{++} of Vα7.2$^+$ CD4$^-$ T cells. (G) Representative enrichment FACS plots. (H) Post-CD8α magnetic enrichment, CD161^{++} Vα7.2$^+$ cells were isolated by FACS. MAIT cells were cultured with IL-15 + β-Me for 6 days, and viable cells enumerated by automated cell counter. Graphs show (A–D, E, F) mean ± SEM or (H) mean. Data analysed by (A – D) one-way ANOVA with Holm-Sidak's multiple comparison test and (H – F) paired t-test. For all tests, ****$p <$ 0.0001, ***$p < 0.001$, **$p < 0.01$.

On assessing the phenotype of the 6 day cultured MAIT cells, $94.2 \pm 3.0\%$ of MAIT cells expressed Granzyme B (GrzB) following IL-15 stimulation, indicating an activated phenotype, vs. $6.3 \pm 1.7\%$ of cells treated with β-Me ($p < 0.0001$). Likewise, 93.7±0.9% of MAIT cells expressed Ki67 following 6 days IL-15 stimulation, indicating recent proliferation, in comparison with $3.4 \pm 1.0\%$ of β-Me treated MAIT cells ($p < 0.0001$; Fig: 4.8 B). Interestingly CD161-expression was also increased following IL-15 stimulation ($p < 0.01$; Fig: 4.8 C). Next, the IL-15 stimulated MAIT cells were assessed to ensure they remained functional; and were therefore washed and re-stimulated with IL-12 and IL-18 alone or in combination, or TCR beads alone, prior to ICS. Similarly to stimulation directly *ex vivo*, IL-15 stimulated MAIT cells did not respond to IL-12, IL-18, nor TCR beads alone, but expressed IFNγ (63.4±7.1%; $p < 0.0001$) and TNFα (9.2±2.7%) in response to IL-12/-18 (Fig: 4.8 D).

In order to isolate a pure population of cells, fluorescence-assisted cell sorting (FACS) is the gold standard approach — however, a multi-step magnetic enrichment was initially tested for MAIT cell enrichment, due to potential benefits including speed and lower cost. PBMCs were stained with αCD8 coated MultiSort magnetic beads and αVα7.2-PE, before positive selection of magnetically labelled cells. The magnetic MultiSort beads were then cleaved enzymatically and split into two fractions, with one undergoing a second round of enrichment with αPE magnetic beads. Magnetic enrichment of $CD8\alpha^+$ T cells routinely results in purities > 90%, however analysis of cells following two-sequential sorts revealed a Vα7.2 purity of $59.0 \pm 12.0\%$ (Fig: 4.8 E); whilst the proportion of $CD161^{++}$ cells within the Vα7.2 subset decreased from $37.8 \pm 4.6\%$ to $11.9 \pm 5.6\%$ ($p < 0.05$), indicating a selective enrichment of the more populous $CD161^-$ $V\alpha7.2^+$ T cell subset (Fig: 4.8 F).

FACS was therefore used to isolate an extremely pure population of MAIT cells; initially from two donors. Despite the induction of MAIT cell proliferation through 6 days of IL-15 stimulation, there was little increase observed so far in absolute numbers of viable MAIT cells recovered. Hypothesising that this was due to competition with more rapidly expanding naïve $CD8\alpha^+$ T cells, expansion was tested post-MAIT cell isolation. FACS purified MAIT cells from two donors were seeded at 2×10^5 cells per well, and cultured with IL-15 in β-Me supplemented R10 media for 6 days. Viable cells were enumerated, and were observed to increased in absolute numbers by a factor of approximately 2. In all subsequent experiments in this chapter, this protocol was followed with the resulting expansion of viable MAIT cells shown in Fig. 4.8 H (mean fold increase of viable MAIT cells vs. MAIT cells seeded: 3.3 ± 1.1; $p < 0.01$).

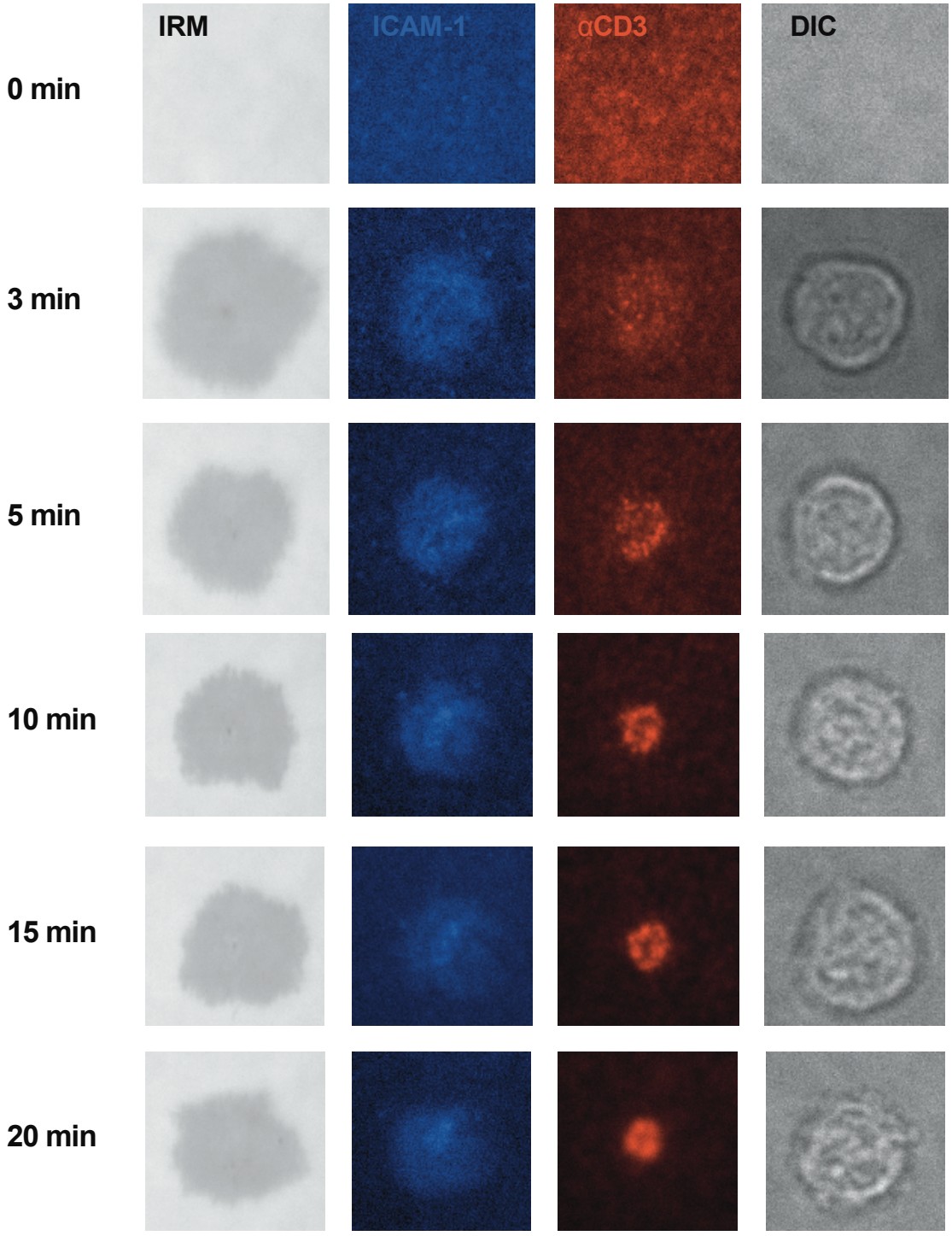


Figure 4.9: Live cell imaging of MAIT cell immunological synapse formation. MAIT cells were prepared following the optimised CD8α-enrichment, FACS sort and IL-15-expansion protocol. The expanded cells were then added to ICAM-1-AF405/αCD3-AF568 embedded artificial lipid bilayers and imaged live by TIRF microscopy at intervals as indicated. IRM – internal reflectance microscopy, DIC – differential interference contrast.

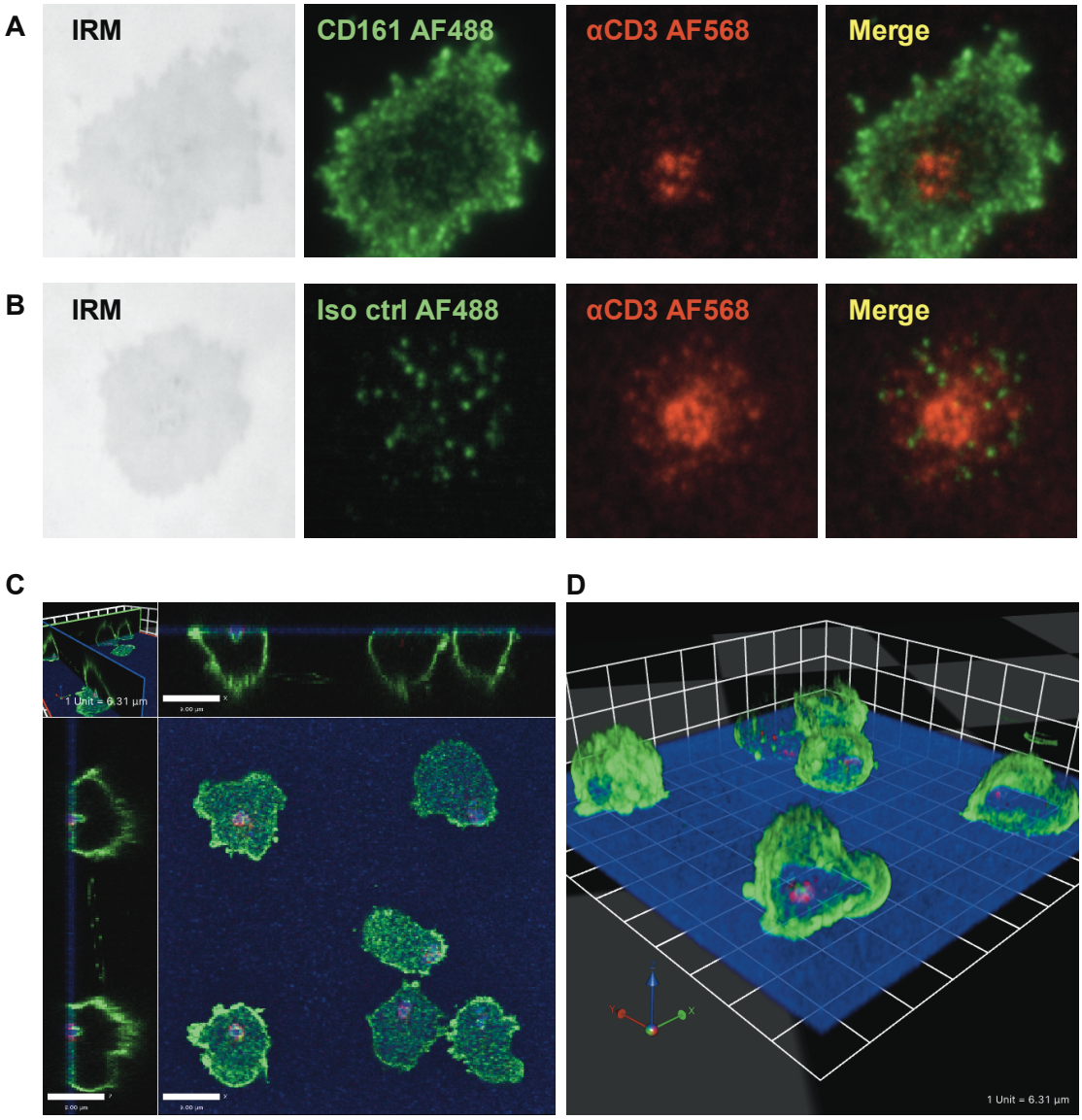


Figure 4.10: CD161 appears excluded from the pSMAC. IL-15 expanded MAIT cells were added to ICAM-1-AF405/αCD3-AF568 embedded artificial lipid bilayers for 5 minutes, before fixation and staining. (A) TIRFM images of CD161 expression and αCD3 binding at the MAIT cell-bilayer interface, or (B) isotype control staining. (C) Orthogonal and (D) 3D opacity views of ICAM-AF405 (blue), CD161-AF488 (green) and αCD3-AF568 (red).

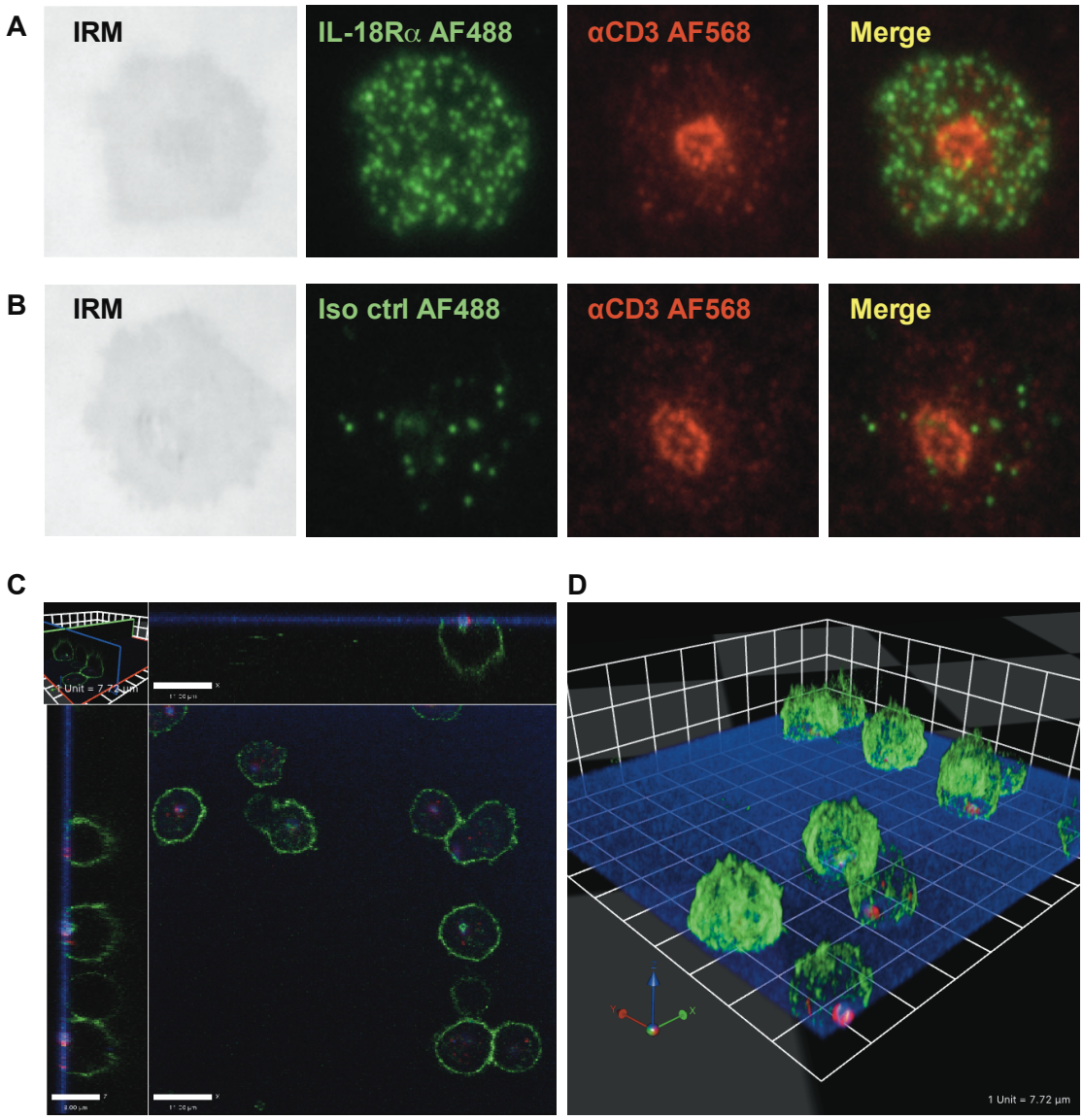


Figure 4.11: IL-18Rα is present at the MAIT cell–bilayer synaptic interface. IL-15 expanded MAIT cells were added to ICAM-1-AF405/αCD3-AF568 embedded artificial lipid bilayers for 5 minutes, before fixation and staining. (A) TIRFM images of IL-18Rα expression and αCD3 binding at the MAIT cell-bilayer interface, or (B) isotype control staining. (C) Orthogonal and (D) 3D opacity views of ICAM-AF405 (blue), IL-18Rα-AF488 (green) and αCD3-AF568 (red).

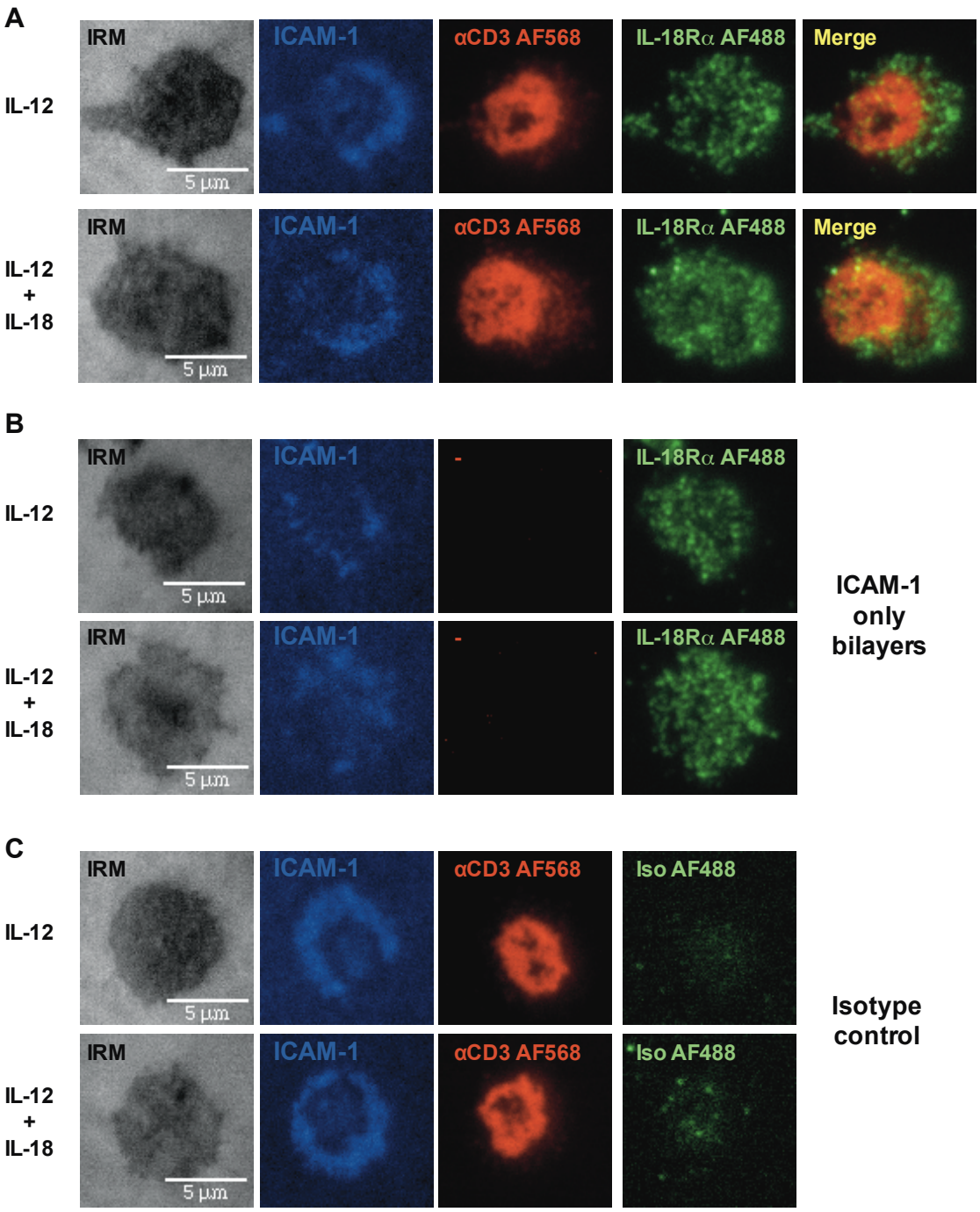


Figure 4.12: MAIT cell IL-18Rα expression at the bilayer interface does not require TCR ligation. IL-15 expanded MAIT cells were re-stimulated with IL-12, or IL-12/-18 overnight, before addition to ICAM-1-AF405 embedded artificial lipid bilayers, ± αCD3-AF568, for 5 minutes, followed by fixation and staining. (A) TIRFM images of IL-18Rα expression, αCD3 and ICAM-1 binding at the MAIT cell-bilayer interface, or (B) IL-18Rα expression, and ICAM-1 binding in the absence of αCD3, or (C) isotype control staining.

4.4.2 TIRF microscopy of MAIT cell synapse formation

To test the capacity of MAIT cells to form a canonical immunological synapse using an artificial bilayer platform, MAIT cells were sorted from fresh human PBMCs by FACS and cultured with IL-15 for 6 days as described. MAIT cells were then harvested, washed, and transferred to artificial bilayers embedded with AF405 labelled ICAM-1 and AF546 labelled αCD3, for imaging by total internal reflectance fluorescence (TIRF) microscopy. TIRFM was performed in real-time (by H. Novak), and single cell images captured at regular intervals (Fig. 4.9) illustrating the association of an individual MAIT cell with the artificial bilayer (internal reflectance microscopy; IRM), formation of the peripheral supramolecular activation complex (pSMAC) through ICAM-1 accumulation, and the formation of the central supramolecular activation complex (cSMAC) — identified through αCD3 accumulation.

CD161 is highly expressed on MAIT cells and there is some evidence to suggest a co-stimulatory role in MAIT cell activation [136]. However, no role has yet been described for CD161 at the immunological synapse. Therefore, the MAIT cell immunological synapse assay was first used to investigate the presence of CD161 at the interface between the MAIT cell and the artificial bilayer. As shown in Fig. 4.10 A, CD161 staining was visible at the periphery of the cell, within the dSMAC — and interestingly appeared to be absent from the cSMAC. Confocal microscopy confirmed that CD161 staining was visible uniformly on the outer surface of the MAIT cells (Fig. 4.10 C, D).

Next, the localisation of IL-18Rα was assessed. In contrast to CD161, TIRFM images indicate that following synapse formation, IL-18Rα was detectable across the interface of the cell (Fig. 4.11 A). However, subsequent confocal microscopy revealed that, like CD161 staining, IL-18Rα could be detected throughout the cell surface (Fig. 4.11 C), indicating that the staining observed at the bilayer interface was not a specific redistribution to the immunological synapse, but most likely part of uniform distribution of IL-18Rα across the cell surface.

From previous experiments, it is clear that TCR signalling in the absence of further co-stimulation does not lead to certain effector functions such as IFNγ production. Therefore, it was hypothesised that exposure to IL-12/-18 would provide the necessary co-stimulatory signals required for a redistribution of receptor to the synaptic cleft.

MAIT cells were expanded as before for 6 days with IL-15, before being washed and re-stimulated with IL-12, or IL-12/-18 for 24 hours. MAIT cells were then

added to the artificial bilayers embedded with either fluorescently labelled ICAM-1 and αCD3, or ICAM-1 only for 5 minutes, after which they were fixed and stained for IL-18Rα.

TIRF microscopy was then performed on MAIT cells, with the images shown in Fig. 4.12. Following stimulation with either IL-12, or IL-12/-18, no differences in IL-18Rα staining were observed, with equivalent IL-18Rα staining visible at the MAIT cell – bilayer interface, irrespective of cytokine stimulation (Fig. 4.12 A). Interestingly, the same was true with ICAM-1 only (i.e. no αCD3) bilayers, indicating that IL-18Rα is not excluded from the interface of non-canonical immunological synapses (Fig. 4.12 B). This suggests that integrin-only cell–cell interactions may be sufficient for localisation of IL-18Rα proximal to the surface of cytokine secreting antigen presenting cells, where IL-18 concentration is likely to be highest — independently of TCR ligation. This may be of particularly relevance to MAIT cell activation in situations where cytokines are produced but MR1 antigen is not present, such as in viral infection.

In summary, a protocol was developed for the TCR-independent expansion of purified MAIT cells, following which they were increased in number and functional. An artificial bilayer system was then used to investigate the localisation of CD161 and IL-18Rα at the immunological synapse, finding that IL-18Rα is present and distributed uniformly across the bilayer interface, whilst CD161 — a surface receptor expressed at characteristically high levels by MAIT cells — appeared to be excluded. In the absence of αCD3 from the bilayer, IL-18Rα was still observed at the bilayer interface, indicating that TCR triggering is not a pre-requisite for IL-18Rα presence at the site of cell-cell contact.

4.5 Discussion

4.5.1 Requirement for contact varies by MAIT function

This chapter began by hypothesising that MAIT cells could be activated by monocytic cells exposed to bacteria through exposure to soluble mediators alone in a contact independent manner. Initially, relatively low levels of MAIT cell activation were observed, even with contact permitted between MAIT cells and PFA-fixed *E. coli*-fed autologous monocytes or THP1 cells — and no activation was observed following physical separation. Through using the THP1 cell line as opposed to autologous monocytes, and by increasing the number of APCs seeded per well, the extent of contact-dependent activation was enhanced for IFNγ-, but not TNFα-expression; though it is worth noting that TNFα-expression by MAIT

cells is favoured at earlier time points than tested. Whilst not reaching statistical significance, with the increased number of THP1 cells a small proportion of cells did appear to express IFNγ following transwell separation, suggesting the capacity of certain MAIT cells to respond to soluble mediators in this way. However, the vast majority of MAIT cells did not express IFNγ following physical separation. Of note, the effect was the same following MR1-blockade, suggesting this was largely due to loss of MR1–TCR interactions.

Interestingly, whilst neither IFNγ nor TNFα were able to be induced through soluble mediators alone, CD69 expression was induced robustly. This effect was greater than that following stimulation with 50 ng/ml each of IL-12/-18, indicating that cytokines other than IL-12/-18 were likely to be present and at sufficient potency to induce MAIT cell CD69-expression. In addition to its role as a marker of MAIT cell activation by either TCR or cytokine stimulation, there may also be functional implications of MAIT cell CD69 expression that have not yet been defined. CD69 expression has been linked to the prevention of T cell exit from secondary lymphoid organs [193], as well as potentially playing an immumoregulatory role during inflammation [191–193]. The function of CD69 expression on MAIT cells, and the identity of the bacteria-induced cytokines responsible will require further investigation.

4.5.1.1 TCR beads incompletely recapitulate MAIT cell–APC contact

TCR beads were then included, in order to add-back the TCR signal without the possibility of polarised delivery of cytokine across an immunological synapse. IFNγ-expression was increased in response, demonstrating that TCR stimulation increases the sensitivity of MAIT cells to detect cytokines, without the delivery of cytokine directly into the synaptic cleft. Furthermore, this demonstrates the ability for soluble mediators to co-stimulate MAIT cell activation driven by TCR stimulation.

A useful feature of using TCR beads in this experiment is that, in contrast to APC dependent stimulation, all T cells present should be subject to equivalent strength non-specific TCR-crosslinking signals. Murine experiments have demonstrated that $CD8^+$ T cells are able to undergo bystander activation by microbes, independent of cognate antigen detection [81], whilst antigenic and inflammatory signals can function in synergy to induce the activation of murine memory $CD8^+$ T cells [378]. Despite inhibition of $CD161^{++}$/MAIT cell activation following transwell separation, small numbers of activated $CD161^{++}$/MAIT cells were nonetheless observed in some donors. By contrast, negligible activation of non-MAIT $CD161^+$ and $CD161^-$ $CD8\alpha^+$ T cells was observed following culture with PFA-fixed *E. coli*

across a transwell insert in Fig. 4.5 C (p. 116), consistent with observations that CD161^{++}/MAIT cells are more capable than bulk CD8$^+$ T cells of responding to TLR-derived cytokine signals independently of TCR ligation [93, 203]. Furthermore, unlike MAIT cells, non-MAIT CD8α^+ T cells (including effector-memory CD161$^+$ CD8α^+ T cells) did not appear to show enhanced sensitivity to soluble-mediators following TCR-ligation. It is possible that optimisation of the transwell experiment for the activation of non-MAIT effector-memory CD8$^+$ T cells may support such a role for bacteria-induced soluble mediators in synergising with TCR signals for contact-independent activation of these cells too, as supported by a number of murine studies [76, 82, 379, 380]. Nonetheless, these data suggest a greater role for soluble mediators in supporting TCR dependent activation of CD161^{++}/MAIT cells than non-MAIT CD8$^+$ T cells in human bacterial infection, which further experiments will be required to confirm.

Recently, another study investigating the contact independent activation of MAIT cells found that IFNγ and Granzyme B expression could be induced from a small proportion of MAIT cells through culture in the supernatant of TLR8 agonist-stimulated monocytes, and this could be enhanced with the addition of TCR beads [174]. These results are consistent with the data presented here. Additionally, data presented here show that exposure to TCR beads in the presence of soluble mediators, cannot activate MAIT cells to the same extent as following contact-dependent activation directly by THP1 cells. Whether this is due to a qualitatively inferior stimulation by TCR beads, or through the absence of directed delivery of soluble mediators across an immunological synapse is not clear.

4.5.2 IL-15 + β-Me enables MAIT cell expansion *in vitro*

In order to utilise an artificial bilayer platform (developed by M. Dustin), it was necessary to expand a pure population of MAIT cells *ex vivo*, whilst avoiding stimulation and potential down-regulation of the MAIT cell TCR, or functional exhaustion, so that they could be subsequently utilised experimentally. MAIT cells have been reported to proliferate in response to TCR stimulation, TCR stimulation plus cytokines, *E. coli* stimulation and PHA-crosslinking plus cytokines [125, 134, 167, 168], but an approach using a single cytokine has not been reported. IL-2, IL-7 and IL-15 are each cytokines that can stimulate T cell proliferation *in vitro*, and all bind to multi-subunit receptors sharing the common γ-chain [381], whilst IL-12 is established in helping to drive T cell proliferation. Additionally, MAIT cells express transcription factors T-bet and Eomes [163], responsible for inducing IL-15 responsiveness [382]. Testing each of these cytokines identified IL-15 as

inducing more robust expansion of MAIT cells relative to the others. FACS sorted MAIT cells subsequently proliferated with IL-15 stimulation in media containing β-Me, with an approximately 3-fold expansion of viable MAIT cells relative to those seeded. IL-15 stimulation led to additional signs of activation, including expression of Granzyme B, as well as induction of CD161 and IL-18Rα expression, but responded to IL-12/-18 stimulation in combination without responding to IL-12, IL-18 or TCR stimulation individually. This protocol will be useful for future experiments requiring large numbers of functional MAIT cells.

4.5.3 Uniform surface distribution of MAIT cell IL-18Rα

Following addition of MAIT cells to the artificial bilayers, they formed canonical immunological synapses with identifiable cSMAC, pSMAC and dSMAC zones, as exhibited by conventional $CD8^+$ T cells [374]. CD161 delineated the dSMAC, which is consistent with a co-stimulatory role, whereas IL-18Rα was found distributed throughout the entire interface, and indeed, surface. Addition of cytokine co-stimulatory signals did not lead to any detectable increase in IL-18Rα accumulation at the interface, but there was similarly no loss of IL-18Rα at the interface in the absence of αCD3, without cSMAC formation. This shows that even in the absence of TCR stimulation, LFA-1–ICAM-1 interactions are sufficient to bring IL-18Rα into close-proximity with potential cellular sources of cytokine.

Whilst IL-18Rα can bind IL-18 with low-affinity, IL-18Rβ is required for high-affinity binding and signalling. Despite homogenous staining of IL-18Rα across the MAIT cell surface, including at the interface, it is possible that IL-18Rβ localisation, and not IL-18Rα is a limiting factor. Attempts were made to visualise MyD88 — a key membrane proximal molecule for IL-18 signalling — to identify the location and distribution of IL-18 signalling events following synapse formation. Although unsuccessful at the time of writing, this will be an interesting future avenue of investigation.

4.5.4 Conclusions

The similar effect of transwell separation and MR1-blockade on MAIT cell activation would argue for a necessary role for TCR stimulation in response to activated APC. However, TCR bead stimulation couldn't compensate for MR1-mediated activation. Presumably, MAIT cells were still capable of forming integrin mediated interactions with the *E. coli*-fed THP1s following MR1-blockade; yet were unable to express IFNγ better than the transwell separated cells. This would also argue against weaker,

transient interactions providing the necessary signals for activation, either through absence of polarised delivery, or the absence of more complex positive-feedback loops between the MAIT cell and the APC.

A recent computational study examining the spatiotemporal dynamics of cytokine signalling, focussed on the short (nm) scale of the immunological synapse, and the long (µm) scale of cells interacting with each other in a contact-independent manner. Their results predicted that cytokine signaling is enhanced by immunological synapse formation — with a liming effect of three-dimensional diffusion of cytokine away from the expressing cell [383]. Large volume, flat-bottom tissue-culture wells as used in the transwell experiments are likely to exaggerate the effect of cytokine diffusion away from producing cells, inhibiting MAIT cell activation in the absence of MR1-mediated immunological synapses. How this translates to infection *in vivo* isn't clear. Nonetheless, a higher-threshold for activation by soluble mediators in the absence of contact would restrict the opportunity for aberrant responses during infection. On the other hand, it remains consistent with a bystander role for MAIT cells during exposure to abnormally high levels of cytokines, perhaps such as those in densely populated sites of disease in mucosal tissues, or during virus-induced cytokine-storms.

4.5.4.1 Summary of findings

- Contact was necessary for the MAIT cell IFNγ response to bacterial infection of THP1 cells, whilst soluble mediators were sufficient for robust CD69-expression.
- Soluble mediators could provide adequate co-stimulation for TCR bead stimulated MAIT cells.
- TCR beads were insufficient to compensate for loss of THP1–MAIT cell contact; likely through loss of a physiological immunological synapse.
- A simple 6-day technique for trebling purified MAIT cells was developed, using IL-15 and β-Me supplementation of R10 media.
- MAIT cells form immunological synapses on TCR cross-linking plus LFA-1–ICAM-1 interactions on an artificial bilayer.
- CD161 is localised to the dSMAC, whilst IL-18Rα can be visualised over the entire MAIT cell, including the pSMAC and cSMAC.
- IL-18Rα can be visualised at the interface in the absence of TCR stimulation.

5

IL-12/-18 and MR1 in MAIT cell activation by bacteria

Contents

5.1 Introduction 140
5.1.1 Summary and chapter aims 143
5.2 Chapter specific materials & methods 144
5.2.1 THP1 bacterial co-cultures with antibody blockade . . . 144
5.2.2 Anti-mycobacterial assay and cytokine analysis 145
5.3 Mechanisms of activation by bacteria 147
5.3.1 Response to PFA fixed-*E. coli* and live *M. bovis* BCG . 149
5.3.2 IL-12, IL-18 and MR1-dependent activation by BCG . . 153
5.4 Activation & response to live, virulent *Mtb* 160
5.4.1 Anti-mycobacterial effect of primary human MAITs . . 165
5.5 Discussion 168
5.5.1 MR1-signal is necessary for *Mtb*/BCG-induced TNFα . 169
5.5.2 BCG/*Mtb* do not down-regulate the MAIT cell TCR . . 170
5.5.3 Anti-*Mtb* function of primary, human MAIT cells 172
5.5.4 Conclusions 173

5.1 Introduction

MAIT cells possess the ability to respond to bacteria through the detection of riboflavin-synthetic intermediates presented on MR1 [32, 114, 115, 205]. Numerous species of bacteria possess the necessary metabolic pathway for MR1 ligand production, including *Mycobacterium tuberculosis* (*Mtb*), which can activate MAIT cells in an MR1-dependent manner [178]. *Mtb* is a bacterial pathogen of huge burden to global health — in 2014, an estimated 1.4 million people died from tuberculosis, more than from any other single infectious agent [254]. Given the urgent need to better understand tuberculosis disease, *Mtb* serves as a valuable model pathogen — especially in novel areas of immunology such as investigations of MAIT cell activation and effector function.

Mtb infection spreads mainly by the aerosol route [346]. Following inhalation of bacilli, alveolar macrophages are amongst the first cells encountered in the airways and serve as a natural host for *Mtb* infection. After the uptake of bacilli, they can be transported into the lung parenchyma, where subsequent recruitment of additional phagocytic cells, as well as the eventual influx of adaptive lymphocytes, leads to establishment of the tuberculous granuloma [258, 260]. *Mtb* are capable of numerous immune evasion strategies, including several that enable the delay and avoidance of adaptive T cell immunity. Examples include the secretion of immunodominant 'decoy' antigens such as Ag85B, delayed migration of DCs to the lymph nodes, induction of regulatory T cell subsets, subversion of MHC class II antigen-processing and presentation, and the inhibition of phagosome-lysosome fusion [384, 385].

Despite these capacities for immune evasion, *Mtb* infection does not necessarily mean progression to active disease. Close household-contacts of patients with active TB disease are amongst those most likely to be exposed to infectious bacteria, yet approximately 50–70% show no signs of developing a latent TB infection (LTBI) [345, 386]. This could be due to avoidance of exposure, despite the close-contact — or alternatively, through mounting successful, sterilising innate-immune responses. For exposed individuals who do become latently infected, the risk of progressing to active disease also varies, with approximately 90–95% of LTBI individuals avoiding progression to active TB disease over the course of their lifetime [258]. In the absence of accurate predictive tools to identify those most likely to reactivate and spread the infection, and with an estimated third or the world's population latently infected, this represents a substantial reservoir of disease.

At each stage of *Mtb* infection — prior to the induction of adaptive immunity; following the establishment of latent infection; or during active disease — MAIT

cells could play an important role in TB immunology and/or pathology. In response to *Mtb*, MAIT cells are capable of expressing IFNγ and TNFα [138, 178] — both essential in the induction of antimicrobial macrophage functions and for the maintenance of granuloma structure and integrity [258].

$CD8^+$ T cells can suppress intracellular *Mtb* through contact-dependent mechanisms [387], as well as being able to directly kill *Mtb* [339]. Adaptive $CD8^+$ T cells from healthy household contacts, but not community controls, were able to control intracellular mycobacterial growth [341], and iNKT cells — an innate-like lymphocyte with similarities to MAIT cells — are capable of suppressing intracellular *Mtb* [388]. MAIT cells have been shown to kill bacterially infected cells [149, 168]; indeed MAIT cell clones, and murine MAIT cells have been reported to kill intracellular *Mycobacterium bovis* BCG [13, 247]; a strain of mycobacteria closely related to *Mtb*, but lacking the virulence locus region of difference 1 (RD1) [389]. The ability of primary, human MAIT cells to suppress virulent intracellular *Mtb* has not yet been tested.

Despite the ability of MAIT cells to respond to exogenous IL-12/-18, the extent of involvement of IL-12 and/or IL-18 for MAIT cell activation in mycobacterial infection is not clear. Using a murine model of BCG infection, Chua *et al.* found that MR1 was essential only for the generation of MAIT cells — whilst IL-12, and not MR1, was necessary for the activation of MAIT cells to express IFNγ, and for mycobacterial control [247]. Other reports examining the activation of MAIT cells by mycobacteria have all indicated an important role for MR1, although without examining the role of cytokine signals, such as IL-12 and IL-18 [178, 220, 390]. This apparent discrepancy remains to be resolved.

E. coli also possess the necessary riboflavin biosynthetic pathways for expression of activatory MR1 ligands [391] and as a model organism have been widely used in studies of the response of MAIT cells to bacteria in a variety of contexts (eg. [121, 187, 212, 392, 393]). In order to avoid overgrowth of cell culture in overnight *in vitro* experiments, numerous studies have also elected to use bacteria fixed with paraformaldehyde (PFA) solution in order to assess MAIT cell activation (e.g. [121, 187, 212, 392, 393]. Upon fixation, bacteria are likely to lose the ability to undergo active metabolism and therefore will cease production of MR1 stimulatory ligands, however several investigations have also observed that despite such fixation, bacteria retain their ability to stimulate MAIT cells efficiently and in an MR1 dependent manner (e.g. [121, 212, 213, 392, 393]). Indeed, Dias *et al.* recently published a protocol for the use of *E. coli* in MAIT cell studies, demonstrating the retention of MAIT cell stimulatory activity by *E. coli* following PFA-fixation for 1—10 minutes

[394]. Loss of ability to actively synthesise MR1-ligands, and differences in the nature of the MR1 antigen processing and presentation pathway between fixed and unfixed bacteria may nonetheless influence the nature of the MAIT cell response, and this an important caveat to bear in mind. However, these studies indicate that PFA-fixed *E. coli* remain a suitable model for assessment of the mechanisms of MAIT cell activation by riboflavin-synthesising bacteria, in particular in light of their broad relevance to the MAIT cell literature in which they commonly feature.

5.1.1 Summary and chapter aims

A key characteristic of MAIT cells are their ability to recognise bacterial metabolites presented on MR1. Tuberculosis is a disease of bacterial aetiology and global significance, and worthy of focus. MAIT cells are activated by mycobacteria in an MR1-dependent manner, yet an important study of MAIT cell function *in vivo* using a murine model of BCG infection, found that the MR1 signal was not important for induction of anti-mycobacterial MAIT cell effector functions, including IFNγ-expression — instead finding a key-role for the innate cytokine IL-12.

As IL-12 synergises with IL-18 for human MAIT cell activation, and MAIT cells are activated by mycobacteria in an MR1-dependent fashion; this chapter hypothesises that both MR1 and IL-12/-18 cytokine signals are important for the activation of human MAIT cells by bacteria. Given the ability of IL-12/-18 and TCR signals to induce different MAIT cell effector functions more robustly at 5 hours (TNFα) and 24 hours (IFNγ) post-stimulation, this chapter also hypothesises that MR1 and IL-12/-18 signals play distinct roles in the induction of these MAIT cell effector functions by bacteria at early, and later time points.

Lastly, murine MAIT cells, and human MAIT cells clones have been reported to suppress intracellular BCG although the ability of primary human MAIT cells to exert a similar effect on live, virulent *Mtb* has not been tested. This chapter therefore hypothesises that MAIT cells can demonstrate anti-mycobacterial effector function against live *Mtb* H37Rv in an intracellular-infection model.

Aim 1 Using a THP1 and PFA-fixed *E. coli* model assay, make an initial assessment of the contribution of MR1- and IL-12/-18 signals for the activation of $CD161^{++}$/MAIT cells by bacteria over time.

Aim 2 Assess the requirement for MR1, IL-12 and IL-18 signals combined and individually in the $CD161^{++}$/MAIT cell response to mycobacteria (BCG and *Mtb*); and with regards to different effector functions over time.

Aim 3 Assess the ability of primary human MAIT cells to exert anti-mycobacterial effector functions against virulent *Mtb* in an intracellular-infection assay.

5.2 Chapter specific materials & methods

Chapter-specific materials and methods are detailed below. Please also refer to Chapter 2 for further information as required.

5.2.1 THP1 bacterial co-cultures with antibody blockade

CD8α$^+$ T cells, PFA-fixed *E. coli* were prepared, and THP1 cells maintained as detailed in Chapter 2. THP1 cells were seeded at 8×10^4 per well of a 96 well U-bottom plate (*E. coli* and BCG) or 2×10^5 per well of a 48-well flat bottom plate (*Mtb*). For *E. coli* experiments, bacteria were added at a ratio of 25 bacteria per cell (BpC); for BCG experiments, bacteria were added at a BpC of approximately 5:1 and for *Mtb* experiments, at a BpC ratio of 10:1. Alternatively, an equivalent volume of sterility control (*E. coli* and BCG) or glycerol vehicle control (*Mtb* were added). Blocking antibodies against IL-12p70 (clone 24190; R&D Systems Europe), IL-18 (clone 125-2H; MBL International, USA), MR1 (clone 26.5, BioLegend), or isotype control mIgG1 (clone 11711; R&D) or mIgG2a (clone MOPC-173; BioLegend) antibodies were added to the THP1 cells at 10µg/ml). CD8α$^+$ T cells were added at an effector:target (E:T) ratio of 2.5 CD8α$^+$ T cells per THP1 cell either concurrently to addition to THP1 cells, bacteria and antibodies, or the following morning for 5 hour experiments. Fluorescently labelled αCD107a antibody was added with CD8α$^+$ T cells where indicated. Brefeldin A (BFA; eBioscience) was added at 1× (1/1000) for the final 4 hours; 1 hour post-addition of CD8α$^+$ T cells for the 5 hour experiments, and either 16 hours (*E. coli* and *Mtb*) or 20 hours (BCG) post-addition of CD8α$^+$ T cells for 20–24 hour experiments.

For the *Mtb* experiments, cells were transferred to eppendorf tubes for surface staining (20 mins; 4°C) before transfer to 96 well V-bottom plates for the remainder of the experiment. Cells were resuspended in 4% paraformaldehyde (PFA) (BD Cytofix/Cytoperm) (1 hour; 4°C) for fixation prior to transfer out of BSL3 and intracellular cytokine staining (ICS), performed in permeabilisation buffer (BD Permeabilisation solution). Cells were washed by centrifugation (2,000 rpm microcentrifuge or 1,600rpm centrifuge; 5 mins; 4°C) ×2 between each step. Cells were analysed by flow cytometry (LSRII; BD). For the *E. coli* and BCG experiments, the above protocol was followed, with the exceptions that cells were surface stained *in situ* in 96 well U-bottom plates, fixed for 20 minutes and analysed by MACSQuant 10 (Miltenyi).

5.2.1.1 THP1 co-culture with dose-titration of BCG and *E. coli*

For assessment of the bacterial dose response of CD161^{++}/MAIT cells, THP1 cells were seeded at 8×10^4 per well of a 96 well U-bottom plate, with PFA-fixed *E. coli* at BpC ratios of 25:1–1.6:1; or alternatively BCG at BpC ratios of 12.5:1–1.6:1. CD8α$^+$ T cells were added at 2×10^5 per well (E:T of 2.5:1) and sterility control was added to the negative wells. Fluorescently labelled αCD107a antibody was added for the duration of the experiment, where indicated. After 20 hours co-culture, BFA (eBioscience) was added at 1× (1/1000) for the final 4 hours. Cells were then processed for surface staining and ICS as for *E. coli* and BCG experiments above, prior to analysis by flow cytometry (MACSQuant 10).

5.2.2 Anti-mycobacterial assay and cytokine analysis

THP1 cells were activated to a macrophage-like phenotype with 50 ng/ml phorbol 12-myristate 13-acetate (PMA; Sigma) for 72 hours. THP1 cells were detached from the culture flask through incubating with pre-warmed PBS + EDTA solution (10mM; Sigma) (10 mins; 37°C), followed by sharp tapping of the flask to dislodge cells. Use of cell scrapers was avoided due to an empirically observed decrease in the viability of THP1 cells (viability assessed through trypan blue exclusion; data not shown). Activated THP1 cells were seeded at $0.8 - 1.0 \times 10^5$ per well of a flat-bottom 48 well-plate in R10 (no antibiotics), and rested overnight, prior to transfer to BSL3 the following morning. For intracellular infection, *Mtb* were sonicated to disperse clumps, and added to THP1 cells at a BpC of 10:1 in fresh RPMI media + 10% heat-inactivated human serum (Rh10) for 2–4 hours. Free bacteria were removed by gentle washing ×2 followed by addition of Rh10 + gentamycin (50µg/ml; Sigma) for a further 2 hours to kill extracellular bacilli. Due to decreasing viability of THP1 cells beyond 24 hours, experiments were not followed up beyond this time point.

For the sorting of MAIT cells, blood was taken from healthy volunteers and PBMCs were separated, and rested overnight (37°C). CD8α$^+$ T cells were enriched and MAIT cells were FACS sorted by M. Paulsen (Imperial College London, St. Mary's campus) to consistently > 99% purity according to: electronic gating of live cells, lymphocytes (forward vs. side scatter properties) CD3$^+$, Vα7.2$^+$ and CD161^{++}. After two hours, gentamycin was removed by gentle washing ×2 with R10, and MAIT cells added at E:T ratios of 1:1, 0.4:1 and 0.16:1. After 24 hours, cell supernatant (SN) was removed and filtered by microcentrifugation through 0.22µm membranes (5,000 rpm; 5 mis; 4°C) ×2 to remove any Mtb, followed by storage at −80°C for subsequent analysis. 0.1% Triton-X aqueous solution was

used to disrupt THP1 cell membranes and release *Mtb* bacilli. Cell lysates were serially diluted, and plated with a 4-log fold dynamic range. Plates were sealed, and incubated for 4 weeks (37°C) prior to colony counting by eye. SN cytokine analysis was performed using a custom V-PLEX Human Cytokine Kit (Meso Scale Discovery), according to manufacturers instructions. Samples were plated in duplicate. Plates were read using the MESO QuickPlex SQ 120 imager (Meso Scale Diagnostics), and analyte concentrations were calculated using Discovery Workbench 4.0.12 (Meso Scale Diagnostics).

5.3 Mechanisms of activation by bacteria

To assess the contribution of IL-12/-18 signals and MR1 to the activation of CD161^{++}/MAIT cells, THP1 cells were seeded with PFA-fixed *E. coli*, and cultured for 20 hours. CD8α^+ T cells were added at an E:T ratio of 2.5:1 for all 20 hours; or for the final 5 hours only. Blocking antibodies against IL-12 and IL-18, or against MR1 were added with THP1 cells. Brefeldin A (BFA) was included for the final 4 hours, before ICS and assessment of IFNγ-expression by flow cytometry.

After the 5 hour co-culture, $25.8 \pm 3.7\%$ CD161^{++}/MAIT cells expressed IFNγ (Fig. 5.1 A, D). IL-12/-18-blockade had little inhibitory effect (p = ns), whilst conversely, IFNγ-expression was completely inhibited by αMR1 (-23.5%; $p < 0.0001$). Following the 20 hour co-culture, IFNγ-expression increased to $70.6 \pm 5.2\%$ (Fig. 5.1 B, D), with both MR1-blockade and IL-12/-18-blockade reducing IFNγ-expression approximately equally (to $27.8 \pm 4.7\%$ and $26.5 \pm 3.3\%$ IFNγ^+ respectively; both $p < 0.0001$ vs. isotype control; Fig. 5.1 B). Culture in the presence of antibodies against IL-12, IL-18 and MR1 totally abrogated IFNγ-expression (-68.1% vs. isotype control; $p < 0.0001$; Fig. 5.1 B).

Normalisation of the data against the maximum IFNγ-response following no-blockade, revealed a reduced ability of MR1-blockade to inhibit IFNγ-expression by 26.5% of the relative-maximum over the course of the longer experiment ($p < 0.001$). Conversely IL-12/-18-blockade was 32.7% more effective in reducing IFNγ-expression over the longer experiment ($p < 0.0001$; Fig. 5.1 C). These data illustrate a switch in the relative dominance of the IL-12/-18 and MR1 signals for CD161^{++}/MAIT cell activation by PFA-fixed *E. coli* over time.

As strong and sustained activation of MAIT cells can result in TCR down-regulation, expression of the MAIT cell TCR was assessed as a percentage of CD161^{++} CD8α^+ cells expressing Vα7.2$^+$, relative to unstimulated. Following 5

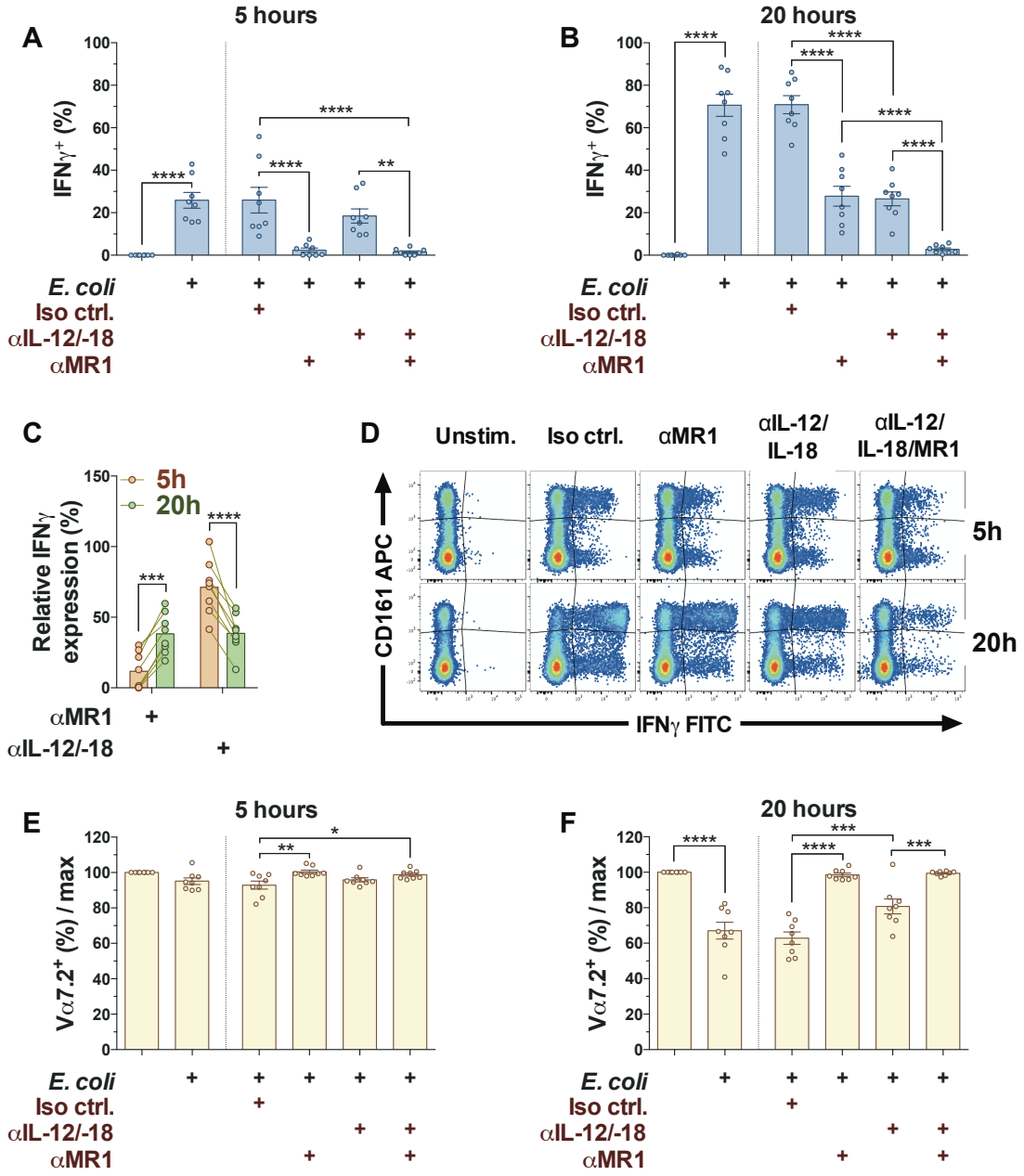


Figure 5.1: *E. coli* stimulation leads to IL-12/-18 dependent activation of CD161^{++}/MAIT cells. CD8α$^+$ T cells were cultured with THP1 cells fed with PFA-fixed *E. coli* (BpC 25:1) in the presence or absence of αIL-12/-18 and/or αMR1 (clone 26.5) blocking antibodies (each at 10 µg/ml) for 20h, or CD8α$^+$ T cells were added to THP1 cells + *E. coli* ± blocking antibodies for the final 5h of culture. (A, B) Frequency of IFNγ$^+$ and (E, F) Vα7.2$^+$ CD161^{++}/MAIT cells following (A, E) 5h and (B, F) 20h co-culture; Vα7.2 expression shown relative to unstimulated per donor. (C) IFNγ expression relative to no blocking antibody, following addition of blocking antibodies, as indicated. (D) Representative FACS plot of IFNγ by CD8α$^+$ T cells. Data analysed by one-way ANOVA with Holm-Sidak's multiple comparison test. For all tests, ****$p < 0.0001$, ***$p < 0.001$, **$p < 0.01$, *$p < 0.05$.

hours stimulation, there was little decrease in Vα7.2$^+$ CD161^{++}/MAIT cells (-4.9%; p = ns), although this was inhibited by MR1-blockade ($p < 0.01$; Fig. 5.1 E).

After 20 hours stimulation there was a much more substantial TCR down-regulation, with $67.1 \pm 4.8\%$ Vα7.2$^+$ (-32.9%; $p < 0.0001$ vs. unstimulated; Fig. 5.1 F). This was abrogated partially through IL-12/-18 blockade ($+17.9\%$ vs. isotype control; $p < 0.001$) and entirely by MR1-blockade ($+35.7\%$; $p < 0.0001$ vs. isotype control; Fig. 5.1 F). In contrast to IFNγ-expression, no decrease in the effect of MR1-blockade was observed with increasing time — indeed as TCR down-regulation occurred after 20 hours stimulation, MR1-blockade only had an effect at this later time point.

These data show that a proportion of CD161^{++}/MAIT cells can respond rapidly PFA-fixed *E. coli* (i.e. within 5 hours), and this is dependent on MR1 but largely independent of IL-12/IL-18. By contrast, the majority of CD161^{++}/MAIT cells can respond to *E. coli* stimulation after 20 hours; with an increased role of IL-12/IL-18, and decreased role of MR1 contributing to activation at this time point. TCR down-regulation also occurs after 20 hours (but not by 5 hours), and this can be partially abrogated through IL-12/-18-blockade; and completely stopped by blocking MR1. The partial, but incomplete, rescue of TCR expression through IL-12/-18- versus MR1-blockade suggests other signals in addition to IL-12/-18 may be expressed by THP1 cells in response to PFA-fixed *E. coli* that could synergise with MR1 to induce TCR down-regulation.

5.3.1 Response to PFA fixed-*E. coli* and live *M. bovis* BCG

In order to investigate the activation of CD161^{++}/MAIT cells by live *Mycobacterium bovis* (*M. bovis*) BCG, to determine an appropriate BpC ratio, and to investigate some of the effector mechanisms of CD161^{++}/MAIT cells induced, a dose-titration of bacteria per cell (BpC) for BCG was performed side-by-side with fixed *E. coli*. CD8α^+ T cells were enriched from PBMCs, and cultured with THP1 cells for 24 hours with bacteria added at BpC of 25:1–1.6:1 (*E. coli*) or 12.5:1–1.6:1 (BCG). Linear trends for IFNγ-, CD69-, TNFα- and Granzyme B expression, as well as Vα7.2 down-regulation and degranulation (measured through CD107a capture) were assessed.

Following stimulation with PFA-fixed *E. coli* at 25:1 BpC, CD161^{++}/MAIT cells robustly expressed IFNγ ($67.9 \pm 5.3\%$; $p < 0.001$; Fig. 5.2 A), CD69 ($92.1 \pm 2.3\%$; $p < 0.001$; Fig. 5.2 B), down-regulated their TCR ($31.9 \pm 4.4\%$; $p < 0.001$; Fig. 5.2 C), expressed TNFα ($16.0 \pm 2.0\%$; $p < 0.01$; Fig. 5.2 D), degranulated ($84.2 \pm 2.7\%$; $p < 0.0001$; Fig. 5.2 E), and expressed Granzyme B ($82.5 \pm 3.9\%$; $p < 0.001$; Fig. 5.2 F).

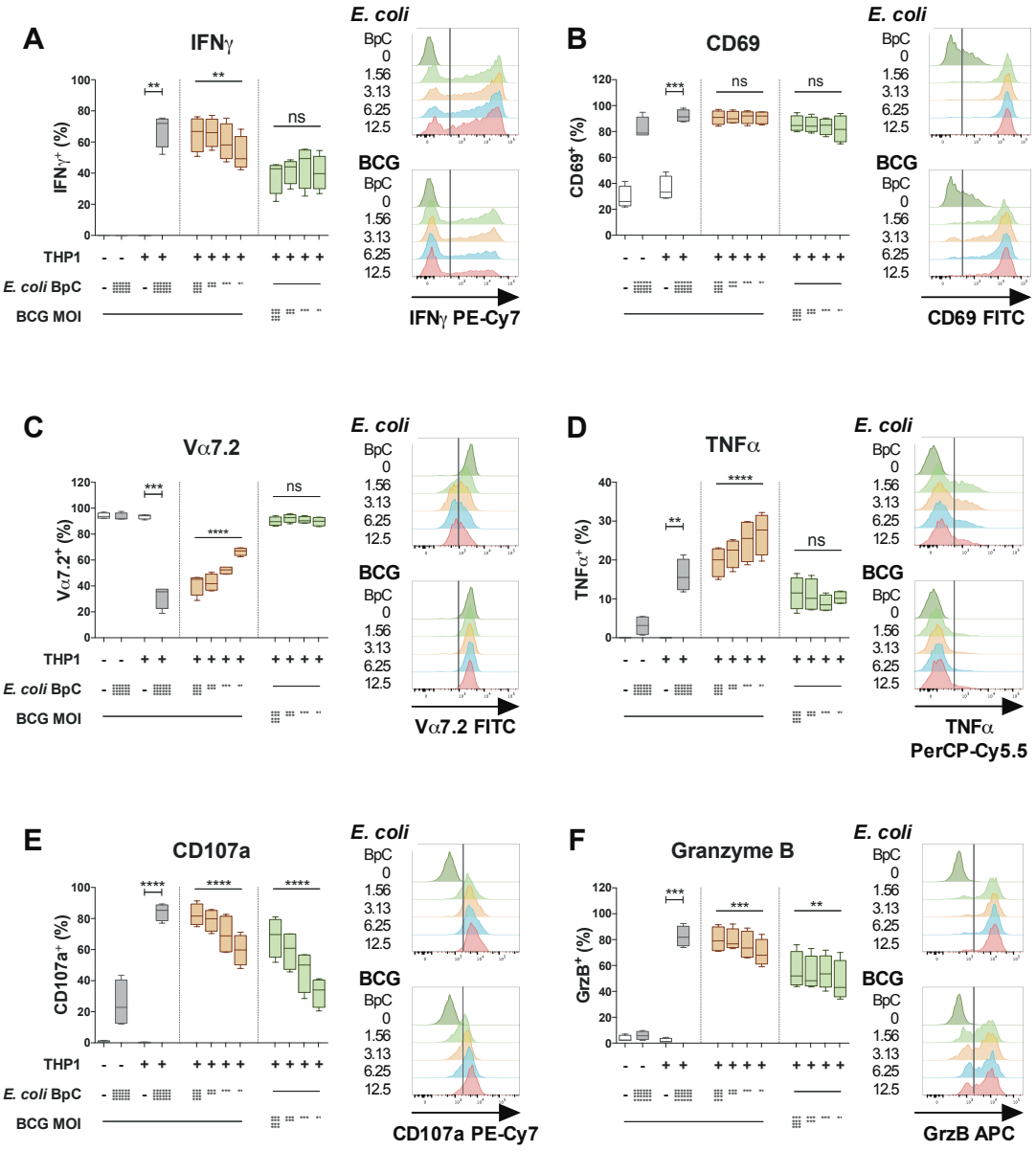


Figure 5.2: The CD161^{++}/MAIT cell responses to PFA-fixed *E. coli* and live BCG show qualitative differences. CD8α^+ T cells were cultured in the presence or absence of THP1 cells along with PFA-fixed *E. coli* (25:1–1.6:1 BpC) or live BCG (12.5:1–1.6:1 BpC). After 24 hours, CD8α^+ T cells were assessed for cytokine production by flow cytometry and ICS. (A) Frequency of IFNγ^+, (B) CD69$^+$, (C) Vα7.2$^+$, (D) TNFα^+, (E) CD107a$^+$ and (F) Granzyme B$^+$ CD161^{++}/MAIT cells. Data analysed by one-way ANOVA with post-test for linear trend, or by t-test. For all tests, ****$p <$ 0.0001, ***$p < 0.001$, **$p < 0.01$, *$p < 0.05$, ns = non-significant.

In response to decreasing BpC ratios for PFA-fixed *E. coli*, linear trends were observed with decreasing expression of IFNγ ($p < 0.01$), decreasing degranulation ($p < 0.0001$), decreasing expression of Granzyme B ($p < 0.001$), and a decreasing level of TCR down-regulation ($p < 0.0001$). Interestingly, a linear trend in the reverse direction was observed with TNFα-expression, which increased, despite decreasing BpC ratios ($p < 0.0001$; Fig. 5.2 D). CD69-expression, by contrast, was unchanged with decreasing BpC ratios, indicating that even at the lowest BpC ratio tested (1.6:1), there were sufficient signals to robustly induce CD69 up-regulation.

In contrast with the response to PFA-fixed *E. coli*, only degranulation (Fig. 5.2 E) and Granzyme B expression (Fig. 5.2 F) decreased in response to culture with reduced numbers of live *M. bovis* BCG ($p < 0.0001$; and $p < 0.01$ respectively), whilst interestingly, there was no change in expression of IFNγ (Fig. 5.2 A), CD69 (Fig. 5.2 B), Vα7.2$^+$ TCR (Fig. 5.2 C), or TNFα (Fig. 5.2 D; all p = ns).

There are several caveats to note which make direct comparisons difficult, including differences between live and fixed bacilli which may impact the supply of ligand for MR1, or affect the stimulation of pattern-recognition receptors. Whilst serial dilutions were performed in an identical manner, the initial numbers are to be taken as approximations only (see Chapter 5.2). Therefore, with the exception of CD107a and Granzyme B, the effector mechanisms induced by live BCG did not vary with dose. Whether this would remain true with even more BCG than those tested is unclear. Experiments were performed using extremely limited stocks of lyophilised BCG, and this precluded testing higher BpC ratios. Furthermore, assessment of TNFα-expression occurred after 24 hours stimulation. Data presented earlier (see Chapter 3.5.2) revealed that CD161^{++}/MAIT cell TNFα expression occurs rapidly following TCR stimulation, and in a transient manner, with cells subsequently exhibiting a degree of anergy to further TNFα-expression. It is possible that assessment of TNFα-in response to BCG exposure at 5 hours would reveal a stronger dose-dependence. Whilst counter-intuitive, this is also consistent with the decrease in TNFα-expression in response to more *E. coli* resulting from an increased, early, burden of activation of CD161^{++}/MAIT cells due to increased abundance of bacteria. Broader, more rapid activation of CD161^{++}/MAIT cells, at high BpC ratios, can therefore reduced the pool of CD161^{++}/MAIT cells capable of expressing TNFα$^+$ cells after 24 hours. It is also worth noting that this decreased TNFα-expression at high BpC corresponds well with decreasing expression of the TCR. Interestingly, this indicates a series of events beginning with a down-regulation of the TCR due to activation of CD161^{++}/MAIT cells in response to bacteria, and leading to a reduction of cells capable of expressing TNFα.

In summary, PFA-fixed *E. coli* and live *M. bovis* BCG are two distinct sources of, and inducers of CD161^{++}/MAIT cell activating stimuli. In a side-by-side test, the killed bacteria acted as potent stimuli, inducing robust levels of IFNγ, and high levels of degranulation. TNFα was also induced robustly; but perhaps due to the timing of the response, lower BpC ratios identified more TNFα^{+} cells at the later time point. By contrast, the live mycobacteria were able to activate CD161^{++}/MAIT cells to express IFNγ, CD69, TNFα and Granzyme B — interestingly, with no down-regulation of TCR. Degranulation was induced robustly, and was the only effector mechanism induced by BCG that showed a strong relationship to the BpC ratio. That there was a linear trend for degranulation suggests that the availability of the degranulation-inducing signal, possibly MR1-ligand alone, was limiting — and increased in step with BCG BpC ratios. Alternatively, microbe-specific differences, or active metabolism may have limited the expression by THP1 cells of co-stimulatory mediators with BCG, reducing the dose-dependency and extent of various effector responses.

5.3.2 IL-12, IL-18 and MR1-dependent activation by BCG

The THP1 antibody-blockade experiment was next modified in order to assess the timing and nature of activating signals for the response of CD161^{++}/MAIT cells to live *M. bovis* BCG. As little difference was observed between BpC ratios tested and availability of BCG was limited, THP1 cells were infected with BCG at an estimated MOI of 5:1 and cultured for 24 hours. CD8α^{+} T cells were enriched from PBMCs and added for either the final 5 hours, or for the entire 24 hours. Blocking antibodies were added for the duration of the THP1 infection (24 hours).

After 5 hours, a relatively small population of CD161^{++}/MAIT cells were activated to express IFNγ ($8.7 \pm 1.4\%$; $p < 0.0001$; Fig. 5.3 A, D). Blocking IL-12 led to little change vs. isotype control (-1.63%; $p =$ ns), whilst αIL-18 interestingly led to a reproducible increase in IFNγ detected ($+7\%$; $p < 0.0001$). Conversely, MR1-blockade totally inhibited IFNγ-expression after 5 hours (-8.3%; $p < 0.0001$), in the presence or absence of additional blocking antibodies. After 24 hours, the expression of IFNγ increased, with $41.6 \pm 3.1\%$ IFNγ^{+} CD161^{++}/MAIT cells ($p < 0.0001$ vs. 5 hours; Fig. 5.3 C). Single blockade of IL-12 or IL-18 reduced this to $18.1 \pm 1.7\%$ ($p < 0.0001$) and $11.2 \pm 1.0\%$ ($p < 0.0001$), respectively; whilst blocking both reduced IFNγ expression to $3.8 \pm 0.5\%$ ($p < 0.0001$). By contrast, MR1-blockade failed to reduce IFNγ-expression at this time point ($35.7 \pm 4.1\%$; $p =$ ns). The addition of αMR1 to αIL-12, or αIL-18 had little further impact (both $p =$ ns vs. αIL-12 or αIL-18 alone, respectively), whilst blocking IL-12 and

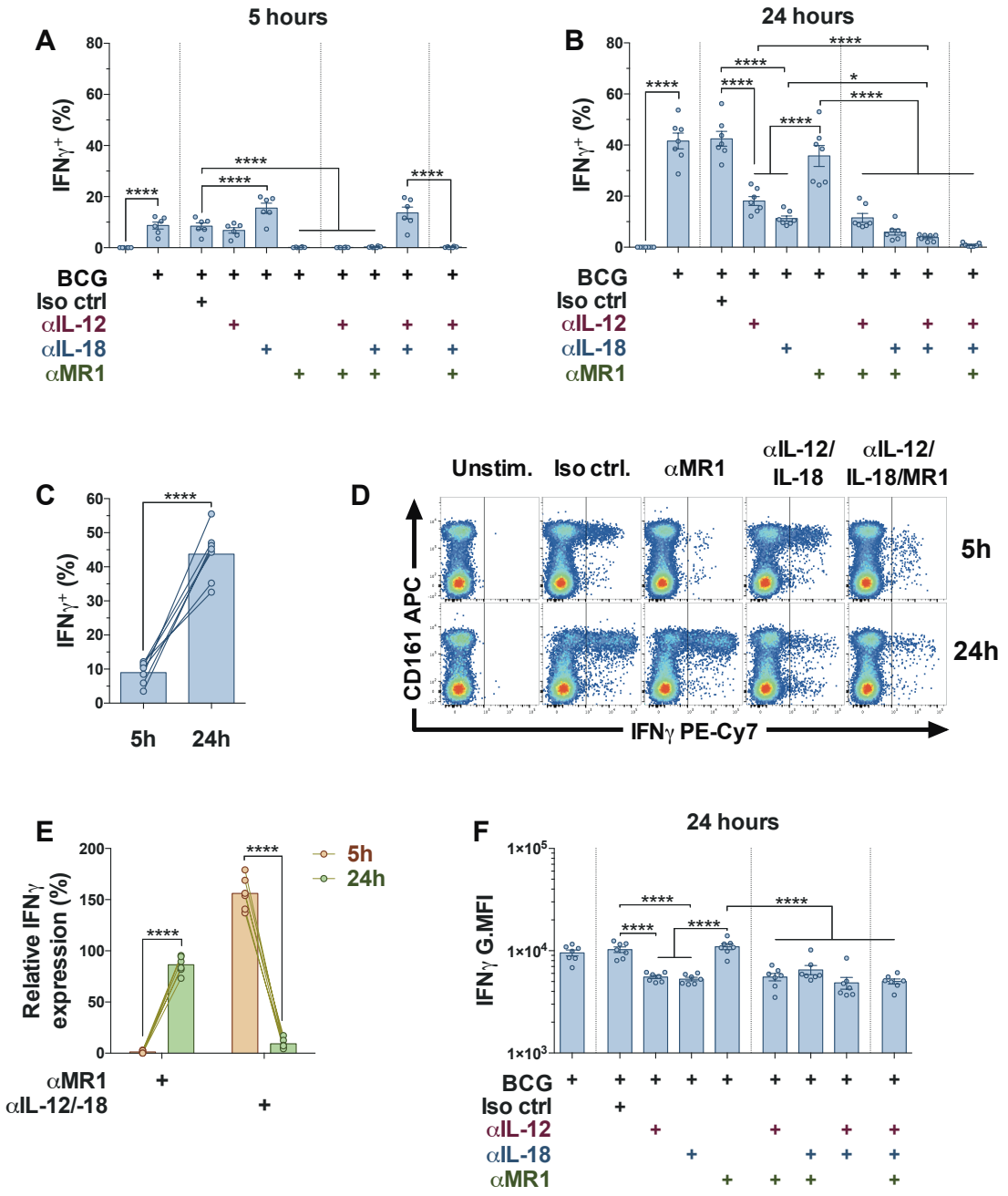


Figure 5.3: IL-12, IL-18 and MR1 are each important in the CD161^{++}/MAIT cell IFNγ response to live *M. bovis* BCG. CD8α^{+} T cells were cultured with THP1 cells infected with live *M. bovis* BCG (BpC approx. 5:1) ± αIL-12, αIL-18 and/or αMR1 blocking antibodies (each 10 µg/ml) for 24h. Alternatively, CD8α^{+} T cells were added for the final 5h of culture only. (A, B) Frequency of IFNγ^{+} CD161^{++}/MAIT cells following (A, C) 5h and (B, C) 24h co-culture. (D) Representative FACS plot of IFNγ expression on CD8α^{+} T cells. (E) Frequency of IFNγ^{+} CD161^{++}/MAIT cells after 5 vs. 24h stimulation relative to the IFNγ response at each time point in the absence of antibodies. (F) Geo. MFI of IFNγ on IFNγ^{+} CD161^{++}/MAIT cells. Data analysed by (A, B, F) one-way or (E) two-way ANOVA, each with Holm-Sidak's multiple comparison test, or (C) paired t-test. For all tests, ****$p < 0.0001$, ***$p < 0.001$, **$p < 0.01$, *$p < 0.05$, ns = non-significant.

IL-18 together further reduced IFNγ-expression relative to IL-12 only (−14.3%; $p < 0.0001$) and IL-18 only (−7.5%; $p < 0.05$; Fig. 5.3 B, D).

The inability of IL-12/-18-blockade to reduce IFNγ-expression after 5 hours; and inability of MR1-blockade to reduce IFNγ-expression after 24 hours reflects a switch in the dominance of the MR1 vs. IL-12/-18 signal from the 5- to the 24-hour co-culture, in similarity to the response to *E. coli* (Fig. 5.3 E).

As a proxy for *per cell* IFNγ-expression, geometric mean fluorescence intensity (GMFI) was also assessed (Fig. 5.3 F). After 24 (but not 5) hours, differences in the GMFI of IFNγ-expression were apparent, with lower IFNγ GMFI of activated cells following blockade of either IL-12, or IL-18 (both $p < 0.0001$) — but no reduction following MR1-blockade (p = ns).

These data indicate that in response to live BCG, early production of IFNγ is driven by the MR1 signal — but relatively few cells are able to respond at this time point. By contrast, a greater proportion of CD161^{++}/MAIT cells express IFNγ after a longer co-culture, which appears to be largely independent of TCR signalling. Interestingly, blocking IL-12 and IL-18 together led to a greater inhibition than either alone, whilst blocking MR1 and either IL-12 or IL-18 had little effect (over blocking just the cytokine), suggesting that both IL-12 and IL-18 may synergise with additional signals not blocked in this experiment. Nonetheless, the extent of abrogation following IL-12, and in particular IL-18 blockade, demonstrates the importance of both for the CD161^{++}/MAIT cell IFNγ response to live mycobacteria *in vitro*.

5.3.2.1 IL-12, IL-18 and MR1 in the CD69 response to BCG

In similarity to the IFNγ response, CD69 was up-regulated by a small proportion of cells following the 5 hour co-culture (+15.9%; $p < 0.0001$), with no effect of blocking IL-12/-18 (+1.0%; p = ns; Fig. 5.4 A). MR1-blockade was able to abrogate CD69-expression slightly (−4.6%; $p < 0.01$), with a stronger abrogation following blockade of IL-12/-18/MR1 (−7.8%; $p < 0.0001$), although this remained greater than unstimulated (+6.1%; $p < 0.001$). After 24 hours, CD69 was up-regulated robustly, with expression by 94.3 ± 1.0% of CD161^{++}/MAIT cells (+65.6%); $p < 0.0001$; Fig. 5.4 A) — an increase of 52.6% vs. 5 hours co-culture ($p < 0.0001$; Fig. 5.4 B). Blocking MR1 had little impact on CD69 expression after 24 hours co-culture (−3.0%; p = ns), as did blocking IL-12/-18 (−0.1%; p = ns), although co-culture in the presence of αIL-12, αIL-18 and αMR1 blocking antibodies reduced CD69 expression by 10.6% ($p < 0.05$; Fig. 5.4 A).

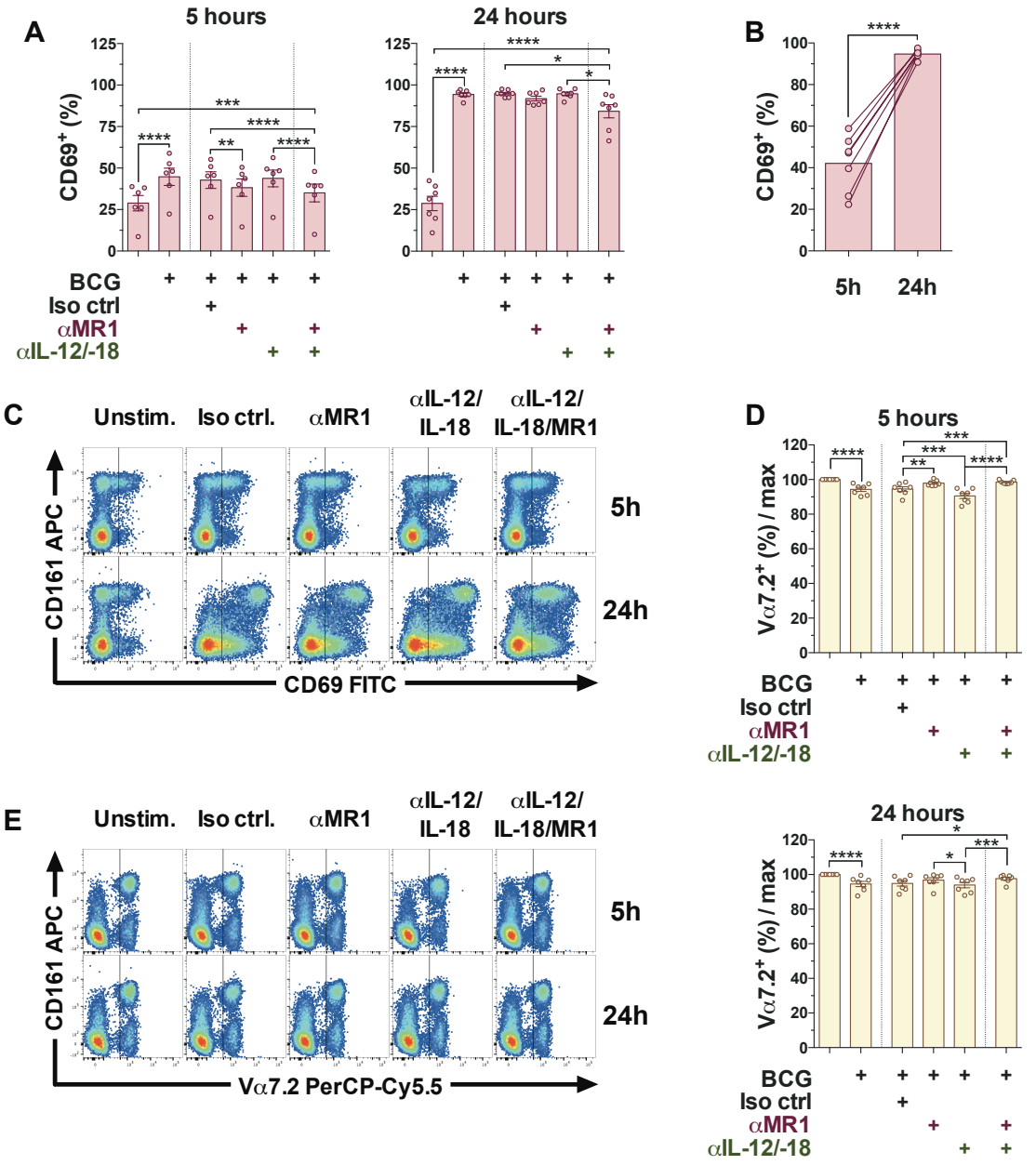


Figure 5.4: Neither IL-12, IL-18, nor MR1 are necessary for CD161^{++}/MAIT cell CD69 response to live *M. bovis* BCG. CD8α$^+$ T cells were cultured with THP1 cells infected with live *M. bovis* BCG (BpC approx. 5:1) ± αIL-12 + αIL-18 and/or αMR1 blocking antibodies (each 10 µg/ml) for 24h. Alternatively, CD8α$^+$ T cells were added for the final 5h of culture only. (A, B) Frequency of CD69$^+$ CD161^{++}/MAIT cells following 5 and 24 hours co-culture. (C) Representative FACS plot of CD69 expression on CD8α$^+$ T cells. (D) Frequency of Vα7.2$^+$ CD161^{++}/MAIT cells (relative to unstimulated per donor) following 5 and 24 hours co-culture. (E) Representative FACS plot of Vα7.2 expression on CD8α$^+$ T cells. Data analysed by (A, D) one-way ANOVA, each with Holm-Sidak's multiple comparison test, or (B) paired t-test. For all tests, ****$p < 0.0001$, ***$p < 0.001$, **$p < 0.01$, *$p < 0.05$.

Vα7.2$^+$ TCR expression was minimally down-regulated at each time point by CD161^{++}/MAIT cells, with a relative reduction of expression of 5.6% ($p < 0.0001$) and 5.5% ($p < 0.0001$) after 5 and 24 hours co-culture, respectively (Fig. 5.4 D, E). This was inhibited by MR1-blockade at 5 hours ($p < 0.01$) and through the combination of αIL-12/-18/MR1 blocking antibodies at 24 hours ($p < 0.001$).

Together, these data indicate that CD69 is robustly induced by BCG after 24, but not yet by 5 hours co-culture; and neither IL-12, IL-18 nor MR1 are necessary for this — and that exposure to BCG-infected THP1s is unable to induce a robust TCR down-regulation.

5.3.2.2 IL-12, IL-18 and MR1 in the TNFα response to BCG

TNFα was expressed strongly in response to BCG infected THP1s after 5 hours co-culture (37.3±2.3%; $p < 0.0001$; Fig. 5.5 A). Whilst inhibition was observed following addition of αIL-12, αIL-18 surprisingly increased TNFα-expression (+11.4%; $p < 0.0001$) — although this reflected the IFNγ response at this time point. The same increase in TNFα-expression was seen with αIL-12 and αIL-18 in combination (+9.3% vs. isotype control; $p < 0.001$), although not with αIL-12 alone indicating that IL-12 was not involved in this unexpected response. Strikingly, MR1-blockade entirely inhibited TNFα-expression at 5 hours (−38.1%; $p < 0.0001$ vs. isotype control). The same was true in the presence of αIL-18 indicating that the stimulatory effect seen with this blocking antibody was dependent on TCR-mediated stimulation.

After 24 hours co-culture, 14.1 ± 1.8% of CD161^{++}/MAIT cells were TNFα$^+$ ($p < 0.0001$; Fig. 5.5 B) — a decrease of 22.9% vs. 5 hours ($p < 0.001$; Fig. 5.5 C). In contrast to the IFNγ-response, blocking either IL-12, or IL-18 individually had little impact on TNFα-expression (−2.0% and −2.4% respectively; both $p =$ ns), whilst blocking both together led to slightly more inhibition (−5.0%; $p < 0.01$). As with the TNFα-response at 5 hours, MR1-blockade led to near total inhibition (−11.0%; $p < 0.0001$).

Analysis of the poly-functional response after 5 hours co-culture revealed a proportion of cells expressing TNFα alone (Fig. 5.5 E). Interestingly, the few IFNγ$^+$ cells present after 5 hours co-culture were either IFNγ$^+$ CD69$^+$ TNFα$^+$ triple-expressing cells, or IFNγ$^+$ TNFα$^+$ double-expressing cells; but none were IFNγ only expressing cells. This suggests that during early activation by BCG, IFNγ- and TNFα-expression are co-regulated. Additionally, a proportion of cells were identified as expressing CD69 alone.

As approximately 20% of circulating MAIT cells express CD69 under basal conditions, and given the rapid kinetics of the TNFα-response indicated in Chapter

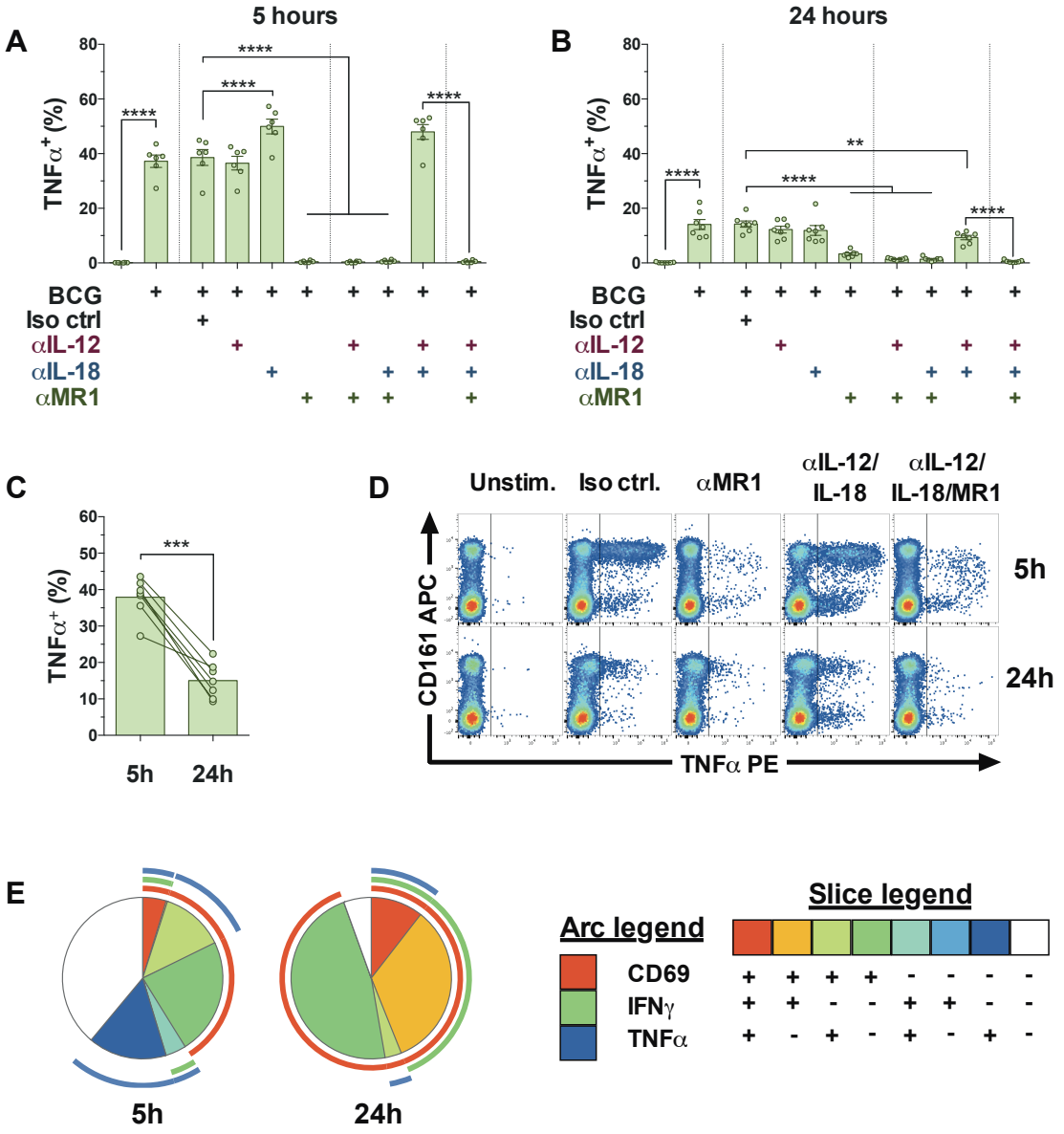


Figure 5.5: MR1, but not IL-12/-18 is essential for the CD161^{++}/MAIT cell TNFα response to live *M. bovis* BCG. CD8α$^+$ T cells were cultured with THP1 cells infected with live *M. bovis* BCG (BpC approx. 5:1) ± αIL-12, αIL-18 and/or αMR1 blocking antibodies (each 10 µg/ml) for 24h. Alternatively, CD8α$^+$ T cells were added for the final 5h only. (A, B) Frequency of TNFα$^+$ CD161^{++}/MAIT cells following (A, C) 5h and (B, C) 24h co-culture. (D) Representative FACS plot of TNFα expression on CD8α$^+$ T cells. (E) Overlapping IFNγ, TNFα and CD69 expression profile after 5 and 24h. Data analysed by (A, B) one-way ANOVA with Holm-Sidak's multiple comparison test, or (C) paired t-test. For all tests, ****$p < 0.0001$, ***$p < 0.001$, **$p < 0.01$.

3, it is possible that these CD69-only expressing cells are not responding to the BCG. After 24 hours co-culture, the vast majority of cells express CD69, encompassing the IFNγ producing cells. The proportion of TNFα$^+$ cells is far lower at this time point, but the majority of these are encompassed by IFNγ-expressing cells; and thus are CD69$^+$ IFNγ$^+$ TNFα$^+$ triple-producing cells (Fig. 5.5 E). These data demonstrate that CD69 is the most sensitive marker for identifying BCG-responsive CD161^{++}/MAIT cells — although basal expression of CD69 renders the specificity less clear.

In summary, the TNFα-response is more evident at the 5 hour time point, and is strikingly inhibited by blocking MR1 indicating the necessity for MR1-signal. Unlike IFNγ-expression, there was minimal effect of blocking IL-12/-18 at 24 hours; which was in contrast to blocking MR1, even at this later time point. There was an increase in TNFα-expression at this time point with inclusion of the αIL-18 blocking antibody — as with IFNγ-expression, although this was not evident by 24 hours, with either IFNγ or TNFα. The antibody was included for the duration of the experiment (i.e. before addition of CD8α$^+$ T cells), and therefore could have affected autocrine IL-18 signalling. Alternatively, other non-specific antibody mediated effects may have been involved. Further experiments may shed some light on the reason for this effect.

5.4 Activation & response to live, virulent *Mtb*

As BCG exhibits important differences from *Mtb*, such as the absence of the virulence locus RD1 [389], the role of MR1 and IL-12/-18 in the CD161^{++}/MAIT cell response to *Mtb* was next assessed. THP1 cells were seeded and infected with *Mtb* H37Rv at a MOI of 10. Blood was taken from healthy donors, CD8α$^+$ T cells were magnetically enriched, and cultured with THP1 cells for the duration of the experiment (20 hours), or the morning following the infection for 5 hours. Fluorescent-antibody against CD107a (CD107a–Pe-Cy7) was included with the CD8α$^+$ T cells in order to identify degranulating cells. Brefeldin A was added for the final 4 hours, and cells were assessed for expression of IFNγ and TNFα and for down-regulation of the MAIT cell TCR.

After 5 hours co-culture, $12.4 \pm 5.3\%$ of CD161^{++}/MAIT cells expressed IFNγ; as with the response to BCG this was inhibited totally through MR1-blockade (-11.6%; $p < 0.05$) with a partial, although statistically non-significant effect observed following IL-12/-18-blockade (-4.5%; $p =$ ns; Fig. 5.6 A). After the longer 20 hour co-culture, IFNγ-expression increased to $31.5 \pm 2.2\%$ ($+18.7 \pm 5.8\%$; $p < 0.05$). This was abrogated partially by MR1-blockade (-11.6%; $p < 0.0001$ vs. iso.

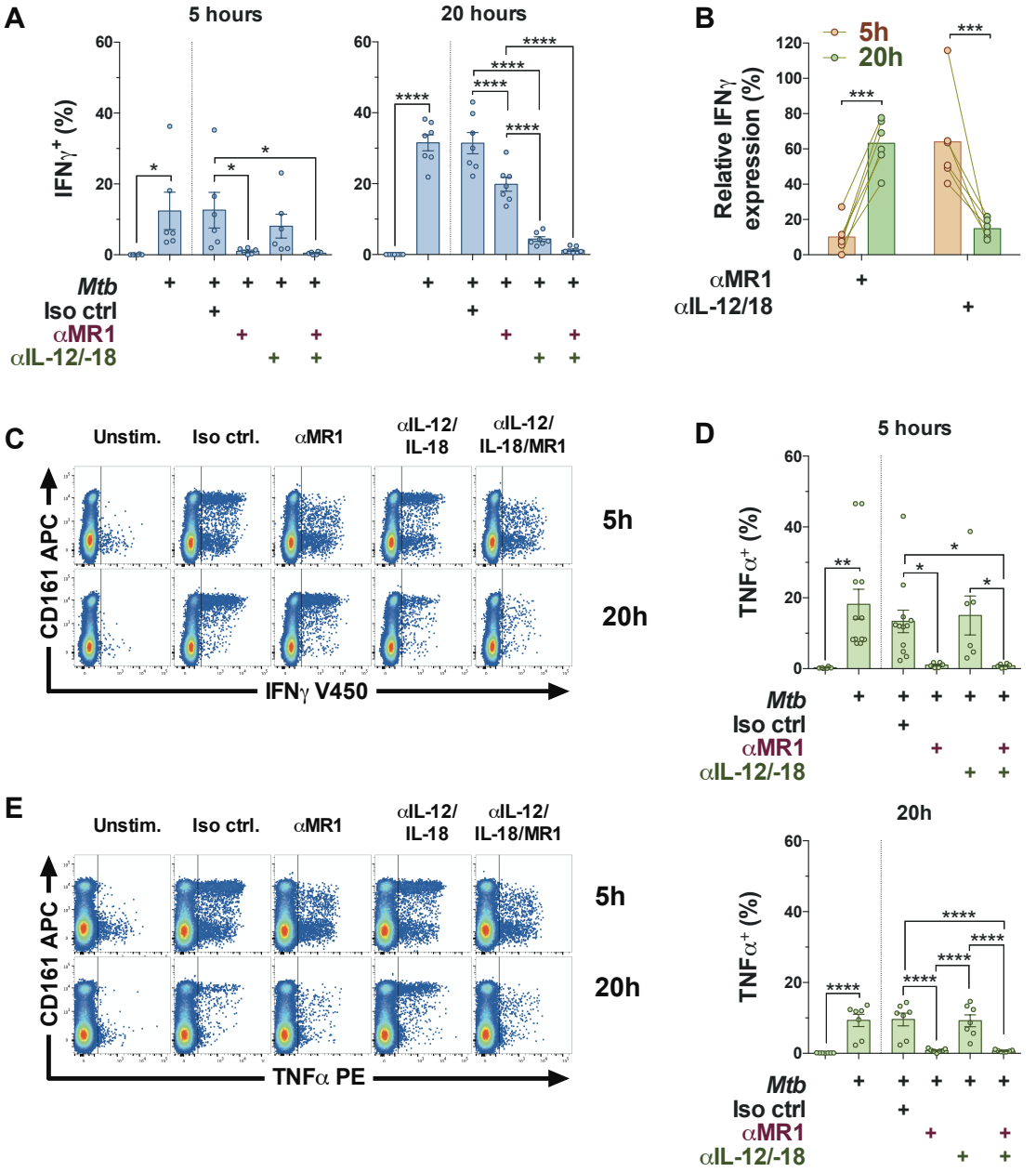


Figure 5.6: IL-12/-18 and MR1 are each important in the CD161^{++}/MAIT cell IFNγ response to live *M. tuberculosis* H37Rv. CD8α^{+} T cells were cultured with THP1 cells + live *Mtb* H37Rv (BpC approx. 10:1) ± αIL-12/-18 and/or αMR1 blocking antibodies (each 10 µg/ml) for 20h, or CD8α^{+} T cells were added for the final 5h. (A) Frequency of IFNγ^{+} CD161^{++}/MAIT cells after 5h or 20h co-culture. (B) CD161^{++}/MAIT cell IFNγ response after 5 vs. 20h relative to donor max. per time point. (C) Representative plot of IFNγ expression on CD8α^{+} T cells. (D) Frequency of IFNγ^{+} CD161^{++}/MAIT cells after 5h or 20h co-culture. Data analysed by (A, D) one-way or (B) two-way ANOVA, with Holm-Sidak's multiple comparison test. For all tests, ****$p <$ 0.0001, ***$p < 0.001$, **$p < 0.01$, *$p < 0.05$, ns = non-significant.

control), and nearly entirely through IL-12/-18-blockade (−27.1%; $p < 0.0001$) or the combination of IL-12/-18/MR1-blockade (−30.2%; $p < 0.0001$; Fig. 5.6 A).

Comparing the frequency of IFNγ^+ CD161^{++}/MAIT cells as a proportion of donor maximum (i.e. following THP1 co-culture with no blocking antibodies), the relative effect of MR1-blockade was markedly decreased by 20 hours (+53.2% IFNγ^+; $p < 0.001$) whilst the relative effect of IL-12/-18 blockade was increased by a similar magnitude (−49.2% IFNγ^+; $p < 0.001$; Fig. 5.6 B), indicating a similar switch in the dominance of IL-12/-18 and MR1 signals over time in the activation of CD161^{++}/MAIT cells by *Mtb*, compared to *E. coli* and BCG.

The TNFα-response followed the same pattern at the earlier 5 hour time point, with $18.2 \pm 6.3\%$ TNFα^+ CD161^{++}/MAIT cells ($p < 0.01$ vs. unstimulated); a response which was inhibited through MR1-blockade (−16.5% ;$p < 0.05$), or in the additional presence of αIL-12/-18 (−16.7%; $p < 0.05$). IL-12/-18 blockade in the absence of αMR1 had little effect (−2.5%; p = ns; Fig. 5.6 D). Following 20 hours co-culture, $9.3 \pm 1.7\%$ of CD161^{++}/MAIT cells expressed TNFα — in contrast to the IFNγ-response, this was wholly abrogated by MR1-blockade (−8.8%; $p < 0.0001$); with no effect of IL-12/-18 blockade (−0.4%; p = ns; Fig. 5.6 D).

In order to detect degranulating cells, αCD107a–Pe-Cy7 was added together with the CD8α$^+$ T cells. Following the short, 5 hour co-culture, $14.9 \pm 5.0\%$ of CD161^{++}/MAIT cells stained positive for CD107a — and this was inhibited through MR1- (−12.7%; $p < 0.05$), but not IL-12/-18-blockade (−1.2%; p = ns; Fig. 5.7 A). After 20 hours co-culture, the proportion of αCD107a-labelled cells increased to $47.3 \pm 5.8\%$. IL-12/-18-blockade did not reduce this (+1.2%; p = ns), whilst MR1-blockade did (−25.7%; $p < 0.0001$). Notably, unlike TNFα-expression, this was not a total inhibition. Blockade with αIL-12/-18 and αMR1 antibodies in combination failed to further inhibit degranulation (−5.0%; p = ns), indicating that this was not being driven by IL-12 and/or IL-18.

There was very little down-regulation of the CD161^{++}/MAIT cell TCR in response to *Mtb* — after 5 hours co-culture, expression remained at $98.6 \pm 1.1\%$ of unstimulated — whilst after the longer 20 hour co-culture, expression was $92.8 \pm 2.2\%$ of unstimulated; a decrease of approximately 7% ($p < 0.01$; Fig. 5.7 C).

Assessment of the poly-functionality of the response to *Mtb* revealed that at 5 hours, most of the responding cells were encompassed within the TNFα-expressing subset; with a small number of IFNγ^- cells staining positive for CD107a; and vice versa (Fig. 5.8 A). However, after 20 hours stimulation, the vast majority of *Mtb*-responsive CD161^{++}/MAIT cells were CD107a$^+$; whilst only a minor subpopulation

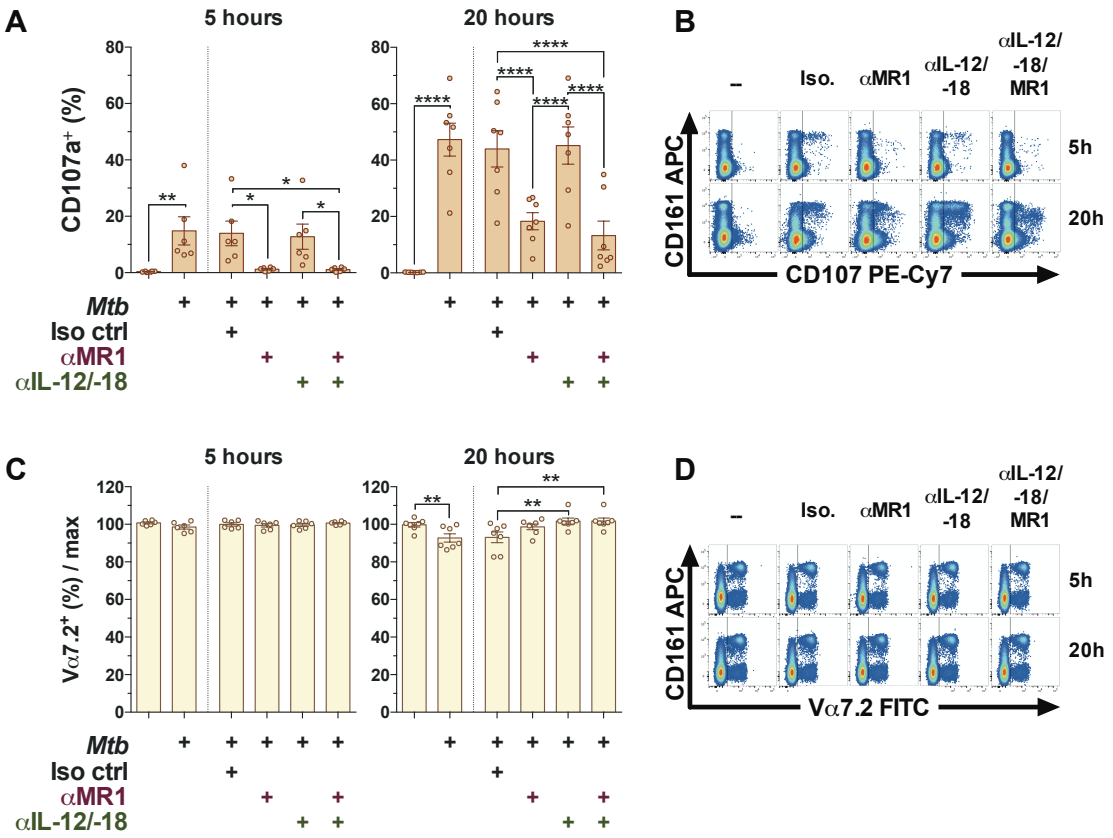


Figure 5.7: CD161^{++}/MAIT cell degranulation in response to live *Mtb* H37Rv is partially resistant to MR1-blockade. CD8α^{+} T cells were cultured with THP1 cells + live *Mtb* H37Rv (BpC approx. 10:1) ± αIL-12/-18 and/or αMR1 blocking antibodies (each 10 µg/ml) for 20h, or CD8α^{+} T cells were added for the final 5h. (A) Frequency of CD107a^{+} CD161^{++}/MAIT cells after 5h or 20h co-culture. (B) Representative plot of CD107a expression on CD8α^{+} T cells. (C) Frequency of Vα7.2^{+} CD161^{++} CD8α^{+} T cells after 5h or 20h co-culture, relative to maximum. (D) Representative plot of Vα7.2 expression on CD8α^{+} T cells. Data analysed by one-way ANOVA, with Holm-Sidak's multiple comparison test. For all tests, ****$p < 0.0001$, ***$p < 0.001$, **$p < 0.01$, *$p < 0.05$.

expressed TNFα. The majority of the IFNγ-expressing, and TNFα-expressing cells were contained within the CD107a^{+} population (Fig. 5.8 A).

After the shorter co-culture, MR1-blockade led to near total inhibition; by contrast IL-12/-18-blockade had only minimal effect on CD161^{++}/MAIT cell activation, including in the proportion of cells exhibiting mono-, bi-, or tri-functionality (Fig. 5.8 B). Following the longer co-culture, MR1-blockade led to a slight increase in the proportion of CD107a^{-} IFNγ^{+} cells; whilst a proportion of cells continued to express both IFNγand CD107a. By contrast, IL-12/-18-blockade resulted in a large increase in CD107a^{+} cells expressing neither IFNγ, nor TNFα; with a minor sub-population of CD107a^{+} cells expressing TNFα. IL-12/-18/MR1-blockade

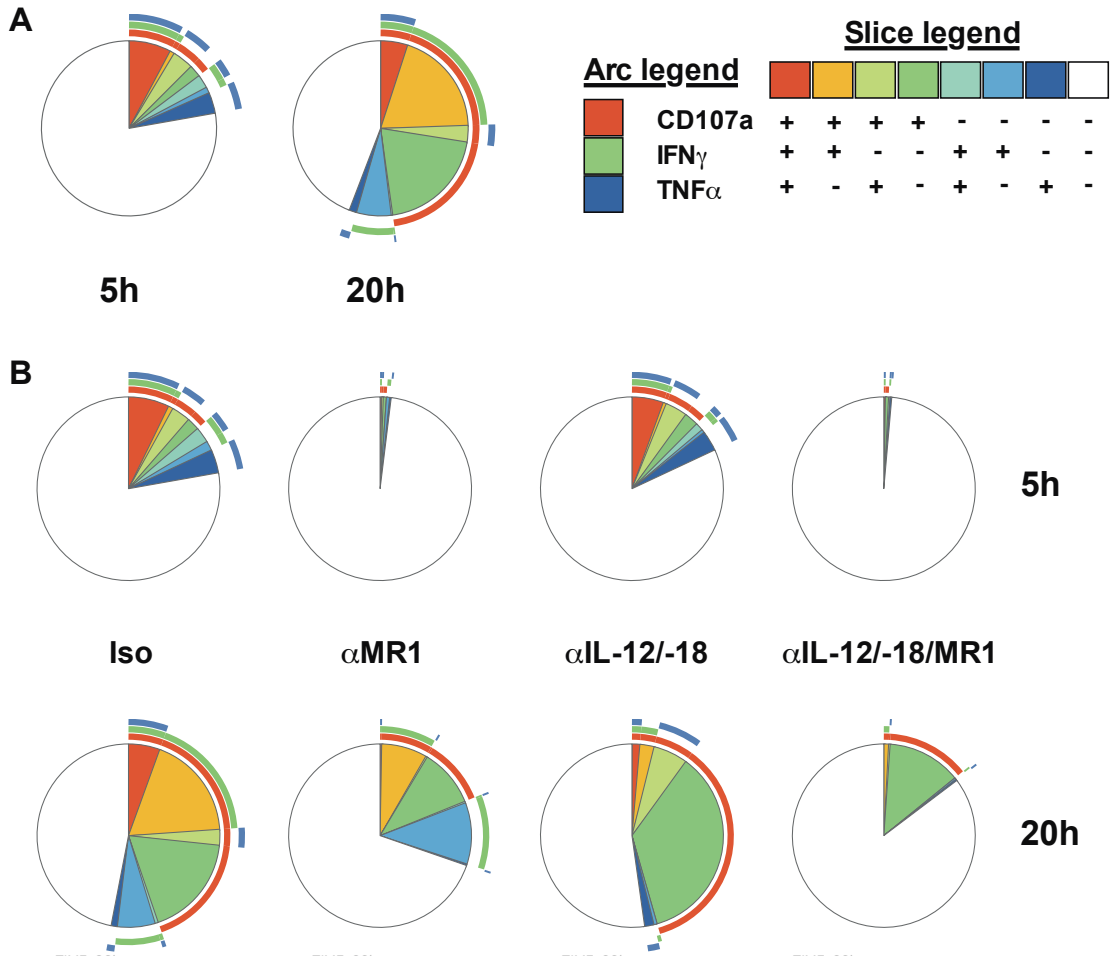


Figure 5.8: Most *M. tuberculosis* reactive CD161^{++}/MAIT cells are detected by TNFα production early, and CD107a capture late. CD8α^{+} T cells were cultured with THP1 cells + live *Mtb* H37Rv (BpC approx. 10:1) ± αIL-12/-18 and/or αMR1 blocking antibodies (each 10 µg/ml) for 20h, or CD8α^{+} T cells were added for the final 5h. (A) Polyfunctional response after 5h or 20h co-culture. (B) Polyfunctional response following antibody blockade.

resulted in a minor proportion of activated CD161^{++}/MAIT cells — all of which were positive for CD107a only.

Together, these data suggest that, as with *E. coli* and BCG, MR1 drives the rapid activation of CD161^{++}/MAIT cells to express IFNγ and TNFα and degranulate in response to *Mtb*; in a manner independent of both IL-12 and IL-18. However, whilst TNFα-expression remained MR1-dependent even after the lengthier 20 hour co-culture, degranulation occurred to a limited extent in the absence of MR1-signal. Unlike both the cytotoxic (CD107a) and TNFα-responses; sustained IFNγ-expression was entirely dependent on IL-12 and/or IL-18, with a redundancy of MR1 at this later time point. Thus MR1 presentation of ligand, but neither IL-12

nor IL-18, are essential for induction of the CD161^{++}/MAIT cell TNFα-response to *Mtb*; whilst loss of the MR1 signal can inhibit the rapid expression of IFNγ within 5 hours, and partially reduce the IFNγ-response whilst in the presence of all other bacteria-induced signals. In the absence of IL-12 and IL-18, however, no CD161^{++}/MAIT cell IFNγ response to *Mtb* occurs, which are therefore necessary for a sustained MAIT cell IFNγ-response to *Mtb*.

5.4.1 Anti-mycobacterial effect of primary human MAITs

In order to assess the anti-mycobacterial effector functions of MAIT cells against virulent *Mtb*, an *Mtb* intracellular infection and MAIT cell co-culture assay was developed. As they can activate CD161^{++}/MAIT cells through both MR1- and IL-12/-18-dependent mechanisms (see earlier), the THP1 cell line was used in order to reduce inter-experimental variability. For the induction of a macrophage-like phenotype, THP1 cells are commonly activated with phorbol 12-myristate 13-acetate (PMA) for 48–72 hours, with concentrations ranging from 5–200 ng/ml [395–402]. THP1 cells were therefore activated with 50 ng/ml PMA for 72 hours, and rested overnight prior to infection with *Mtb* at a MOI of 10:1. Initial tests indicated good infection of THP1 cells under these conditions, although with residual extracellular bacilli (Fig. 5.9 A). Therefore, cells were cultured in Rh10 supplemented with gentamycin for a further 2 hours to kill extracellular bacilli, whilst permitting intracellular infection. FACS sorted MAIT cells were added to the intracellularly infected THP1 cells for 24h. Following the co-culture, THP1 cells were lysed and lysates plated for 4 weeks for *Mtb* CFU enumeration.

Between experiments there was a log-fold level of variability in the number of viable *Mtb* recovered in the absence of MAIT cells (range: 3.6×10^4 to 3.6×10^5; Fig. 5.9 B). However, the addition of MAIT cells reproducibly reduced the number of *Mtb* CFUs recovered (geometric mean of ratios 0.67 ± 0.051; $p < 0.001$ vs. no MAIT cells; Fig. 5.9 B), whilst analysis of viable CFUs following dose-titration of MAIT cells revealed a linear-trend ($p < 0.05$; Fig. 5.9 C). Together, these data indicate that primary human MAIT cells are able to limit the number of viable *Mtb* following the intracellular infection of THP1 cells.

Analysis of supernatants revealed expression of pro-inflammatory cytokines, with detectable MAIT cell expression of (as geometric mean values): IFNγ (20.0 pg/ml; $p < 0.05$), IL-2 (9.6 pg/ml; $p < 0.01$) and IL-17 (26.6 pg/ml; $p < 0.05$; Fig. 5.9 D). THP1 cells expressed cytokines in response to *Mtb*, including TNFα (140.5 pg/ml; $p < 0.0001$), IL-6 (10.3 pg/ml; $p < 0.0001$), GM-CSF (9.1 pg/ml; $p < 0.01$), IL-1β (99.5 pg/ml; $p < 0.01$) and IL-12p40 (19.4 pg/ml; $p < 0.001$),

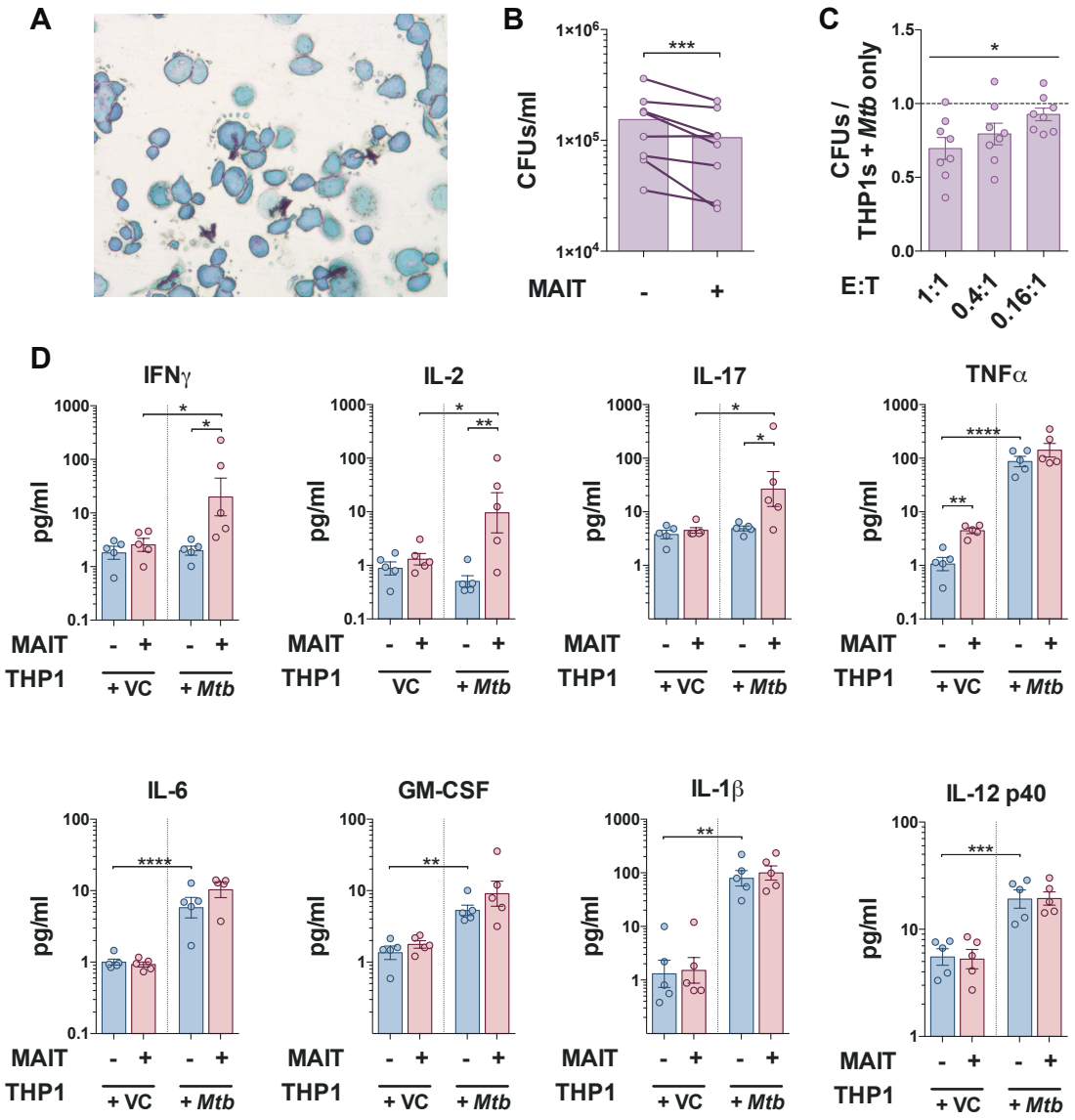


Figure 5.9: MAIT cells reduce intracellular *M. tuberculosis* viability. Activated THP1 macrophages were infected with *M. tuberculosis* H37Rv for 2–4h. FACS-sorted MAIT cells were added following removal of extracellular bacilli. After 24h co-culture, THP1 cells were lysed and serial dilutions plated on 7H10 for enumeration of *Mtb* CFUs. Supernatants were assessed for secreted cytokines by MSD multiplex analysis. (A) Ziehl-Neelsen acid-fast stain of *Mtb* following *Mtb* infection of THP1 cells at MOI 10:1 for 2 hours. (B) CFUs recovered following addition of MAIT cells vs. THP1 cells only. (C) Relative CFUs recovered following addition of MAIT cells at E:T ratios as indicated. (D) Supernatant cytokines detected by MSD multiplex cytokine-detection assay. Data analysed by (B, D) converting values to Log(values) and/or performing (B) paired t-test, (C–D) one-way ANOVA with (C) post-test for linear-trend and (D) Holm-Sidak's multiple comparison test. For all tests, $^{****}p < 0.0001$, $^{***}p < 0.001$, $^{**}p < 0.01$, $^{*}p < 0.05$.

however this precluded assessment of these cytokines for subtle MAIT cell expression. Additionally, supernatants were assessed for IL-7, IL-10, IL-12p70 and IL-15 with no detection observed (data not shown).

These data suggest that primary, human MAIT cells are able to exert an anti-mycobacterial effect on intracellular *Mtb*, which occurs with concomitant release of IFNγ IL-2 and IL-17 from MAIT cells — and TNFα IL-6, GM-CSF, IL-1β and IL-12p40 from THP1 cells infected with *Mtb*.

5.5 Discussion

The initial aims of this chapter were to assess the contributions of IL-12/-18, and MR1 signals in the activation of CD161^{++}/MAIT cells by different bacteria. Therefore, co-culture assays of CD8α^{+} T cells with THP1 cells fed *PFA*-fixed *E. coli*, live *M. bovis* BCG and finally live *Mtb* H37Rv, were performed. Overall, both signals were shown to be important, depending on the kinetics and effector functions assessed. In response to *E. coli*, IFNγ was expressed by CD161^{++}/MAIT cells rapidly, although with an increase in responding cells after 20 hours. MR1-blockade largely inhibited IFNγ-expression at the earlier time point, whilst at the later time point cytokine and MR1 signalling were each found to reduce the frequency of IFNγ^{+} cells by approximately half. IL-12/-18 and MR1 blockade together completely abrogated IFNγ-expression.

In response to live *M. bovis* BCG, fewer CD161^{++}/MAIT cells expressed IFNγ at both 5 and 24 hours compared to the fixed *E. coli* at comparable time points. The same was true with live *Mtb* at 5 and 20 hours. This could reflect differences in the respective BpC ratio, differences in APC activation by fixed vs. live cells — or differences between *E. coli* and mycobacteria (or indeed, all three). As with the fixed *E. coli*, MR1-blockade resulted in a complete inhibition of IFNγ-expression in response to BCG and *Mtb* at 5 hours, whilst IL-12/-18 blockade had no effect at this early time point. Of note, this indicates that neither IL-12, nor IL-18 are necessary for the rapid MR1-driven activation of CD161^{++}/MAIT cells in response to the bacteria tested.

Following 20–24 hours co-culture, IL-12/-18 blockade had a substantial inhibitory effect on activation by BCG and *Mtb* — greater than was observed in the co-culture with *E. coli*. Interestingly, in contrast to the *E. coli* co-culture, MR1-blockade alone had no effect on IFNγ-expression in response to BCG at the later time point. Whilst not compared directly, it is possible that the extra four hours co-culture in the BCG experiment (24 vs. 20 hours) enabled a greater proportion of cells to

respond to cytokine-mediated activation, whilst the extra time perhaps reduced further the proportion of cells activated due to MR1. In support of this, co-culture with live *Mtb*, which was also for 20 hours, resulted in a slightly enhanced effect of αMR1-only blockade at the later time point relative to BCG. Nonetheless, in the case of each assay, the data indicate a strong switch in the dominance of MR1 signal at 5 hours, to a cytokine-signal dominance at later time points.

In the BCG co-culture, IL-12- and IL-18-only blockade were additionally performed. Substantial (but incomplete) inhibitory effects of blocking either individually were seen. Of note, blocking both MR1 + IL-12 together also failed to lead to a complete inhibition of IFNγ-expression — suggesting the presence of additional signals that could synergise with IL-18 for IFNγ-induction. Conversely, blockade of IL-18 alone led to a stronger inhibition of the IFNγ-response than blocking IL-12 or MR1, indicating an important role of IL-18 in the activation of MAIT cells by mycobacteria. Furthermore, assessment of the *per cell* IFNγ-expression of activated cells found that after 24 hours only IL-12 and IL-18 blockade — either individually, or combined — had inhibitory effects on the ability of activated CD161^{++}/MAIT cells to express higher-levels of IFNγ; whilst MR1-blockade had no effect. This emphasises the fact that, whilst able to drive early activation in a proportion of cells, other cells are able express IFNγ independently of MR1, with no detrimental effect on the amount of IFNγ expressed.

5.5.1 MR1-signal is necessary for *Mtb*/BCG-induced TNFα

Whilst IFNγ expression became dependent on IL-12 and IL-18 increasingly with time, TNFα-expression in response to BCG or *Mtb* remained dependent on MR1 signal at both early, and later time points. In further contrast to IFNγ-expression, the TNFα-response was far greater at the early 5 hour time point, vs. the later, 20–24 hour time point. This is consistent with the induction of CD161^{++}/MAIT cell expression of TNFα by TCR beads indicating that transient expression of TNFα-expression is a CD161^{++}/MAIT cell intrinsic feature — and that neither BCG, nor *Mtb*-infected APC provide signals to induce a more sustained TNFα-response.

Analysis of CD69-expression by CD161^{++}/MAIT cells during the BCG-infection model similarly reflected TCR bead activation, with only minimal up-regulation apparent by 5 hours; and with robust up-regulation by 24 hours. Whilst there was a slight inhibitory effect of blocking MR1 on the early up-regulation of CD69, and of MR1/IL-12/-18 on the up-regulation of CD69 by 24 hours — this was of a negligible effect-size and points to MR1, IL-12 and IL-18 each being dispensable for the induction of CD69 by mycobacteria. Therefore, additional signals are likely

able to induce CD69-expression as well. However, given the ability of recombinant IL-12/-18 and/or TCR beads in inducing CD69 expression, it is likely that there is substantial redundancy in signals with CD69-inducing capacity.

5.5.2 BCG/*Mtb* do not down-regulate the MAIT cell TCR

In order to optimise the BCG THP1-infection assay and assess the effector functions induced by live mycobacteria, a titration of MOI was performed and compared against PFA-fixed *E. coli*. Neither IFNγ, nor TNFα, were expressed to the same extent in response to the highest doses of BCG vs. *E. coli*; nor demonstrated a significant linear trend with increasing MOI. The reasons for this are not clear, however IFNγ-expression at 24 hours is reliant on IL-12/-18, and it is possible that live mycobacteria take proportionately longer to trigger the relevant pattern recognition receptors (PRRs) for expression of these cytokines than do fixed *E. coli*. Similarly, fixed *E. coli* may provide a more readily-available source of MR1-ligand than live mycobacteria, limiting the extent of TCR-mediated activation.

Notably, a reduced ratio of *E. coli* led to a higher observed frequency of TNFα$^+$ CD161^{++}/MAIT cells at 24 hours. Whilst counter-intuitive, higher BpC ratios also led to decreased expression of the MAIT cell Vα7.2 TCR — it therefore seems plausible that higher BpC led to broader TNFα-expression by CD161^{++}/MAIT cells more rapidly, with an increase in the extent of TCR down-regulation. In turn, fewer TNFα$^+$ cells were observed at the 24 hour time point investigated. Thus TCR down-regulation may serve to limit the expression of TNFα within 24 hours of the initial MR1-exposure; past an initial transient burst.

However, it is interesting that no TCR down-regulation occurred in response to the BCG dose-titration, even at the highest BpC tested (approximately 12.5:1). Similarly, in the antibody-blockade experiments using BCG at an MOI of approximately 5:1, and *Mtb* at 10:1, little TCR down-regulation was also seen. Whether this is due to differences in the nature of the MR1 or co-stimulatory signals induced by *E. coli* vs. mycobacteria — or fixed vs. live cells, is not clear.

Interestingly, CD107a-capture occurred robustly in response to higher BCG BpC ratios; and whilst a large proportion of CD161^{++}/MAIT cells degranulated in response to *Mtb* — it was not possible to inhibit this entirely through MR1-blockade. In these experiments, CD107a expression was observed through incubation with αCD107a antibodies for the duration of the co-culture. Degranulation at any point within the course of the experiment (and not just a 4 hour window, as with BFA inhibition of cytokine exocytosis) should result in binding of antibody. Therefore, CD107a-capture occurs cumulatively, and with high sensitivity.

The inability of IL-12/-18/MR1-blockade to completely inhibit CD107a-capture in response to *Mtb* may indicate additional signals capable of inducing $CD161^{++}$/MAIT cell degranulation in response to *Mtb*. Furthermore, analysis of the poly-functional response to *Mtb* at 20 hours in the presence or absence of αMR1, revealed populations of $IFN\gamma^{+}$ $CD107a^{-}$ and $IFN\gamma^{-}$ $CD107a^{+}$ cells. As well as suggesting the ability of degranulation to occur in a minor proportion of cells in an MR1-independent manner, these data also indicate that the signals are distinct from IL-12/-18, which are required for the IFNγ response following MR1-blockade.

5.5.3 Anti-*Mtb* function of primary, human MAIT cells

Whilst MAIT cells have been reported capable of killing bacterially infected cells, the ability of MAIT cell to demonstrate an anti-*Mtb* effect has not been demonstrated. In order to address this question, an intracellular infection assay using the virulent lab strain H37Rv was developed. There are many technical challenges associated with the use of slow growing, and highly virulent *Mtb* for *in vitro* growth control experiments. The slow growing nature means a lag-time of 3–4 weeks for feedback on experimental changes, limiting the ability to optimise experiments. Simultaneously, there are balances to be struck between the stress of infected cells exposed to a high-burden of bacterial infection, vs. the requirement to detect large effect sizes.

Following infection with *Mtb*, THP1 cell viability was found to decrease beyond 24 hours (data not shown) — therefore, the ability of MAIT cells to exhibit an anti-*Mtb* effect at the 24 hour time point was assessed. A pure population of primary, human MAIT cells were found able to reproducibly abrogate the recovery of viable *Mtb*, consistent with their ability to lyse epithelial cells infected with *E. coli* and *S. flexneri* [149], and kill B cells exposed to PFA-fixed *E. coli* [168]. However, there are several important caveats to note. Despite controlling for the relative degree of THP1 cell death in the presence and absence of MAIT cells, data were not generated for the absolute number of viable THP1 cells remaining at the end of the experiment. In the absence of this data, it is difficult to assess the contribution of THP1 cell death to the detection of viable *Mtb* colonies remaining. Similarly, despite identifying a reduction of viable *Mtb* remaining within adherent THP1 cells, data were not generated for the number and/or viability of *Mtb* released into the cell culture solution. For this, the nature of death of *Mtb*-infected THP1 cells is likely to be important in determining the local outcome of infection. Controlled apoptosis of *Mtb*-infected macrophages may lead to better control of bacilli through bactericidal mechanisms such as efferocytosis [403], whilst *Mtb*-induced macrophage cell death is associated with accelerated intracellular *Mtb* growth [404]. It is possible

that bacteria not recovered from adherent THP1s following MAIT cell exposure, nonetheless persist free in solution in a virulent state. Quantifying the extent of release of viable and non-viable mycobacteria following MAIT cell exposure will help better understand the nature of the MAIT cell–*Mtb*-infected macrophage interaction, and future experiments should seek to address this.

5.5.4 Conclusions

In the murine model of *in vivo* BCG infection performed by Chua *et al.*, IL-12 was found to be necessary for IFNγ expression and the induction of macrophage effector functions, whilst MR1 was not. Data presented here are consistent with MR1 being unnecessary for certain $CD161^{++}$/MAIT cell functions in response to *Mtb* infection, including sustained IFNγ expression. Degranulation however was partially dependent on MR1, whilst rapid IFNγ- and TNFα-expression were entirely dependent on MR1. Therefore, either degranulation, rapid IFNγ- and TNFα-expression play only a minimal role *in vivo* in humans — or there is indeed a role for MR1 in the induction of anti-mycobacterial MAIT cell effector functions, in contrast to the murine BCG study. Additional human studies using *in vitro* intracellular infection assays, or *in vivo* studies using other mouse strains (e.g. the novel congenic mouse strain expressing high levels of MAIT cells [357]) will be required to better understand this. Interestingly, there were no major differences between MAIT cell activation by *Mtb* or BGC. This suggests that despite the difference in virulence between the two strains, MAIT cell activation is not impacted. This further suggests that BCG remains a good model for assessing mycobacteria induction of MAIT cell effector functions.

So far, no role for IL-18 in the MAIT cell response to *Mtb* has been demonstrated. Experiments with live BCG and *Mtb* both support the conclusion that IL-18 is necessary for sustained IFNγ-expression, as blockade of this cytokine alone in the BCG assay led to a near total abrogation of IFNγ-expression — with a similar effect seen following IL-12/-18 blockade in the *Mtb* assay. IL-18 is synthesised as pro-IL-18, which requires post-translational processing by caspase-1 via inflammasomes into the bioactive form [405]. IL-18 can be expressed in response to detection of *Mtb* through cytosolic pattern recognition receptors (PRRs) such as absent in melanoma 2 (AIM2) [406], or NLRP3 [407] and has been implicated in playing a critical role in protecting mice from *Mtb* infection [354]. Conversely, IL-18 may contribute to TB pathogenesis — indeed inflammasome activation has been proposed to play a key role in causing excess inflammation in patients with tuberculosis-associated immune reconstitution inflammatory syndrome [408]. Given the ability of $CD161^{++}$/MAIT

cells to respond to IL-18 expressed in response to mycobacterial infection, MAIT cells may be an important effector of IL-18 mediated protection or pathology.

Interestingly, a recent study by Rothchild *et al.*, investigated the capacity of invariant natural killer T cells — another subset of innate-like lymphocytes — to limit mycobacterial growth. They found that iNKT cell IFNγ-expression was driven by IL-12/-18, but conversely CD1d-driven effector function was necessary for the control of *Mtb* growth in a manner independent of TNFα and cytotoxicity, but dependent on GM-CSF [388]. It is not yet clear how this may relate to MAIT cell function — GM-CSF expression was assessed in this chapter, but not observed at levels significantly above that expressed by THP1 cells alone in response to *Mtb*-infection. Additional MAIT cell *Mtb* growth-control experiments will therefore be needed to ascertain both the effect of MAIT cells on the viability of *Mtb*-released from dead and dying macrophages, and the mechanisms involved in this and in reducing viable *Mtb* recovered from adherent macrophages.

5.5.4.1 Summary of findings

- MR1 is necessary for rapid CD161^{++}/MAIT cell expression of IFNγ and TNFα in response to *E. coli*, BCG and *Mtb*.
- BCG and *Mtb* can induce robust TNFα-responses, but do not provide signals for sustained TNFα-expression by CD161^{++}/MAIT cells.
- IL-12/-18 are essential for sustained CD161^{++}/MAIT cell cell IFNγ-expression in response to BCG and *Mtb*, with a key role for IL-18; MR1 is dispensable.
- TCR down-regulation in response to robust activation by *E. coli*-fed THP1 cells coincided with a reduction in CD161^{++}/MAIT cell TNFα-expression.
- No down-regulation of the MAIT cell TCR was observed following co-culture with BCG or *Mtb*-infected THP1 cells.
- CD161^{++}/MAIT cells degranulated robustly in response to BCG and *Mtb*; this was not entirely MR1-dependent.
- Primary, human MAIT cells could reduce the recovery of viable intracellular *Mtb* in a THP1 infection model.

6

MAIT cells in sarcoid and tuberculous lymphadenopathy

Contents

6.1 Introduction 178
6.1.1 Intrathoracic lymphadenopathy 178
6.1.2 Summary and chapter aims 181
6.2 Chapter specific materials & methods 182
6.2.1 Isolation of cells from TB and sarcoidosis patients . . . 182
6.2.2 Case definitions and clinical characteristics 184
6.2.3 FACS screen for PFA-fixation compatible antibodies . . 186
6.3 Flow cytometry analysis of PBMC and ITLN 188
6.3.1 Activation status of MAIT cells in lymph node TB . . . 190
6.3.2 Increased $CD4^+$ MAIT cells in sarcoidosis 192
6.3.3 Clinical features of high MAIT cell frequency in ITLN . 195
6.4 Imaging of MAIT cells by chip-cytometry 198
6.4.1 Identification of chip-cytometry compatible mAbs . . . 198
6.4.2 Analysis of LNTB patient samples by chip-cytometry . 204
6.5 Discussion 210
6.5.1 MAIT cells in lymphatic tuberculosis and sarcoidosis . . 210
6.5.2 Chip cytometry for the assessment of EBUS-TBNA . . 219
6.5.3 Conclusions 221

6.1 Introduction

6.1.1 Intrathoracic lymphadenopathy

Following inhalation of bacilli and initial events in the lung parenchyma, dendritic cell transportation of *Mtb* to the lung-draining lymph nodes is an important event leading to the induction of adaptive immunity [294, 302]. Immunologically, the role of lymph nodes in TB has classically been viewed within this context, of being the major site for the priming of T cells. Radiologically, enlarged lymph nodes are a characteristic feature of primary TB — in comparison to cavitation of lung tissue and spread of disease, which are hallmarks of post-primary TB [261].

Conventionally, tuberculosis is viewed as a pulmonary disease, with the major immunological events and pathology occurring in the lung [258]. Recently, a more lymphocentric model of tuberculosis has been proposed, in which transport of *Mtb* to the lymph nodes is not just part of the host attempt to induce adaptive immunity, but an integral part of the immunopathologic cycle [265]. Establishing a chronic infection of the lymph nodes may be an important prelude to subsequent spread of bacteria — both haematogenous for extra-pulmonary disease, and via the lymphatics for spread to distinct sites within the lung [265]. In support of this, the development of extra-pulmonary disease does not require active pulmonary disease [409]. Furthermore, reactivation of disease sites are often distinct from the initial (Ghon) focus of infection, frequently occurring in the lower-perfusion apical and posterior segments of the upper lobes — locations typically associated with onwards transmission [261].

As with lesions occurring within the lung parenchyma, granulomas are a characteristic feature of intrathoracic lymph node tuberculosis [410]. Granulomas represent an active attempt by the host immune system to constrain the bacteria, although they may also be beneficial for *Mtb* [260]. Local immune responses within the lymph node, especially those able to maintain the structure and integrity of the granuloma, may be crucial for establishing *Mtb* containment. Failure of containment may alternatively lead to the dissemination of viable bacilli through the lymphatics to diverse anatomical sites [265]. Therefore anti-mycobacterial effector functions within the lymph node could play a crucial early role in determining the outcome of infection.

Murine models have shown that MAIT cells can play a role in protective immunity against bacterial pulmonary infection [246] and mycobacterial infection *in vivo* [247]. In humans, several studies have also reported MAIT cells to be depleted [138, 178, 207, 220] and functionally modulated/deficient in the peripheral blood

of TB infected patients — expressing increased programmed cell death protein 1 (PD-1), and expressing decreased IFNγ following *ex vivo* stimulation [207, 220]. Conversely, MAIT cells have been observed in transplant unsuitable donor lungs [178] and *Mtb*-infected lung tissue [138]; present in ascitic fluids from patients with tuberculous peritonitis [220], and enriched in the bronchoalveolar lavage (BAL) of TB patients (unpublished [244]) indicating their presence at sites of disease.

Within lymphoid tissue, studies in humans have so far reported a general paucity of MAIT cells [13, 134, 173, 175], consistent with their lack of expression of lymph node homing markers CCR7 and CD62L [134, 156]. However, MAIT cells do express the chemokine receptors CCR2, CCR5 and CCR6 [134, 156]; each of which are associated with the recruitment of T cell in tuberculosis [291]. Whether MAIT cells can be recruited to the intrathoracic lymph nodes during active *Mtb*-infection of the lymph node — therefore suggesting an important role in lymphatic tuberculosis — is not clear.

Sarcoidosis is also a granulomatous disease, that similarly to tuberculosis can lead to intrathoracic lymphadenopathy. However, in contrast to tuberculosis, sarcoidosis is of unknown aetiology [411]. Sarcoid — unlike TB — granulomas are characteristically discrete and non-caseating [412]. Nonetheless, with both pathological and clinical features in common, the two can be hard to distinguish [413]. Whilst TB can be diagnosed through the detection of *Mtb* at the site of infection, sarcoidosis relies on ruling out differential diagnoses; most notably, tuberculosis [412] — although immunological signs may also be informative. For example; despite lacking sensitivity, a $CD4^+/CD8^+$ T cell ratio of > 3.5 is highly specific for sarcoidosis (53–59% sensitivity; 93–96% specificity) [414].

There are also differences evident at the level of gene expression. In a recent transcriptional profiling study of endobronchial ultrasound-guided transbronchial needle aspiration (EBUS-TBNA) samples, computational machine learning allowed successful discrimination between tuberculous and sarcoid causes of granulomatous mediastinal lymphadenitis. Nonetheless, a broad degree of overlap was also evident, highlighting similarities in the underlying granulomatous response within EBUS-TBNA samples of TB and sarcoidosis patients [415]. This is broadly in line with what has been observed in the peripheral blood [416].

Given these similarities, sarcoidosis offers an interesting comparison with tuberculosis. The absence of mycobacteria in sarcoidosis may result in the failure of MAIT cell trafficking to the affected lymph nodes. Conversely the presence of otherwise similar inflammatory processes may induce MAIT cells to exhibit signs

of activation, or other phenotypic differences/abnormalities. Neither have yet to be assessed for MAIT cells in the context of sarcoidosis.

EBUS-TBNA is a minimally-invasive clinical technique, increasingly used to diagnose and differentiate intrathoracic tuberculous and/or sarcoid lymphadenitis [415, 417–420]. For immunological research, however, there are limited tools available suited to investigating low yield, biosafety level 3 (BSL3) EBUS-TBNA samples from tuberculosis patients — in particular, those that can reveal information at the single cell level. Flow cytometry is one such technique, however a key limitation is that samples can be analysed only once, and the number of parameters is limited by the number of fluorescence detectors of the flow cytometer, the availability of fluorochromes, and the properties of light. Single cell gene-expression studies are possible, although usually requiring physical separation of single cells by FACS or similar; which can be difficult following treatments (e.g. paraformaldehyde fixation) required to make possibly *Mtb*-contaminated BSL3 samples safe. Fluorescence microscopy is compatible with fixation, and samples can be stored for further imaging — however microscopy is normally limited to 3–5 fluorescent labels, and analysis is typically limited to relatively small numbers of cells.

Chip cytometry is a novel imaging based technology that allows cell-suspensions to be fixed and stored indefinitely, after being immobilised on a microfluidic chip [421]. Through using photo-bleachable fluorochromes directly conjugated to primary antibodies; multiple rounds of staining, imaging and bleaching are theoretically possible. Chip cytometry could therefore prove a valuable tool in assessing clinical samples — including EBUS-TBNA samples from patients with lymphatic tuberculosis.

6.1.2 Summary and chapter aims

The studies above indicate that in many TB patients the lymph node is a site of active disease, and of importance in relation to subsequent spread of infection. As with pulmonary disease, it is likely that immunological mechanisms with access to the site of disease are engaged in order to attempt to eliminate the infection. MAIT cells are a bacterially-responsive innate-like lymphocyte with an emerging role in tuberculosis immunology, including the ability to express IFNγ, TNFα and to reduce the recovery of viable *Mtb* bacilli *in vitro*. However, MAIT cells are typically rare in the lymph nodes [13, 134, 173, 175]. Whether they are recruited to *Mtb*-infected lymph nodes, is unclear.

Sarcoidosis is a granulomatous disease of unknown aetiology. There is currently little evidence surrounding the involvement, or not, of MAIT cells within the lymph

nodes during sarcoid lymphadenitis. However, the presumed absence of bacteria and the typical aversion to lymph node homing may suggest that MAIT cells are not typically present. Nonetheless broad similarities in the underlying granulomatous response make sarcoidosis an interesting point of comparison with TB.

Lastly, chip cytometry is a novel imaging based technique that promises the ability to store clinical samples long term, for subsequent and theoretically limitless analysis. Whether this approach is suitable in the context of investigating MAIT cells in EBUS-TBNA samples from patients with lymphatic tuberculosis is not clear.

This chapter therefore hypothesises that MAIT cells are recruited to, and activated at the site of disease in intrathoracic lymph node tuberculosis; whilst absent from the intrathoracic lymph nodes during sarcoidosis. Secondly; that MAIT cells are depleted in the blood of TB patients with lymphadenopathy — but not of sarcoidosis patients. Thirdly; that chip cytometry is a useful tool for the assessment of MAIT cells within PBMC and EBUS-TBNA clinical samples from patients. In addressing these hypotheses, this chapter has two main aims:

Aim 1 Assess the frequency, and activation state of MAIT cells within the peripheral blood and intrathoracic lymph nodes of patients with tuberculosis and sarcoidosis.

Aim 2 Optimise and assess a novel imaging technique useful for the storage and investigation of MAIT cells within clinical patient samples.

6.2 Chapter specific materials & methods

Chapter-specific materials and methods are detailed below. Please also refer to Chapter 2 for further information as required.

6.2.1 Isolation of cells from TB and sarcoidosis patients

Human intrathoracic lymph node (ITLN) biopsies were obtained (OM Konn, H Jarvis) from adult patients with lymphadenitis undergoing endobronchial ultrasound transbronchial needle aspiration (EBUS-TBNA) at the Dept. of Respiratory Medicine, St. Mary's Hospital, London. Two or three separate passes were made, and samples obtained were ejected directly into 5ml saline. Samples were then double contained and placed on ice for approximately 1–3 hours, after which they were transferred into the Cat3 laboratory. In order to isolate single cells, the heterogenous suspension was passed through a 70 µm MACS SmartStrainer (Miltenyi) directly into a 15 ml falcon tube. The solid material was agitated against the 70 µm mesh

using the rubber tipped plunger of a 1 ml syringe, and washed through with PBS to a total of 13 ml. Cells were pelleted by centrifugation (1,600 rpm; 4°C; 5 min), and resuspended in 1× red blood cell (RBC) lysis buffer (4°C; 10 min; BioLegend). The cell suspension was washed ×2 in 13 ml PBS (1,600 rpm; 4°C; 5 min), before the pellet was transferred to a 96 well V-bottom plate for initiation of flow cytometric analysis (LSR-II) — or added to a ZellSafe cell chip (ZellKraftwerk) for chip cytometric analysis (ZellScannerONE). In either case, cells were fixed (4% PFA; 4°C; 60 min) before removal from the Cat3 in adherence with local safety protocols.

Tonsillar tissue was obtained (A Llibre, C Willberg) from the ENT Department, John Radcliffe Hospital, Oxford. Single cell suspensions were prepared by mechanical disruption of tonsil samples, prior to analysis by flow cytometry (MACSQuant 10; A Libre, C Willberg).

6.2.1.1 Processing of PBMCs

Blood was taken by venipuncture by the attending research nurses (S Bremang, H Uzu, H Piotrowski), and PBMCs isolated (H Lambie, M Tolosa-Wright, Aime Boakye) by layering on Ficoll-Paque PREMIUM (GE Healthcare) and separating by density gradient centrifugation (2,200 rpm; 22 mins; 21° C). The PBMC layer was washed by centrifugation in 50 ml R10 media (1,800 rpm; 10 mins) and again (1,600 rpm; 5 mins), before incubation with 1× RBC lysis buffer (4°C; 10 min; BioLegend). Further processing and analysis was performed as per EBUS-TBNA.

6.2.2 Case definitions and clinical characteristics

Suspected tuberculosis and sarcoidosis patients were undergoing planned bronchoscopies due to radiologically abnormal lymph nodes, and were recruited opportunistically (Fig. 6.1). For this study patients subsequently diagnosed with tuberculosis or sarcoidosis were therefore classified as having lymph node involvement. Further definitions for tuberculosis or sarcoidosis and patient clinical characteristics are provided below. The demographic information of patients enrolled are detailed in Table 6.1.

Lymph node tuberculosis Clinical diagnosis of active lymph node tuberculosis was confirmed by microbiological culture or PCR where possible (10/15 patients). In the absence of either, diagnosis was based on radiological features by CT-Scan and/or chest X-ray consistent with intrathoracic lymphadenopathy, a positive tuberculin skin test and/or *Mtb*-specific IFNγ release assay, response to treatment, the presence of symptoms, and/or demographic risk factors. 1/15 patients was diagnosed as LTBI with lymphadenitis, and was included

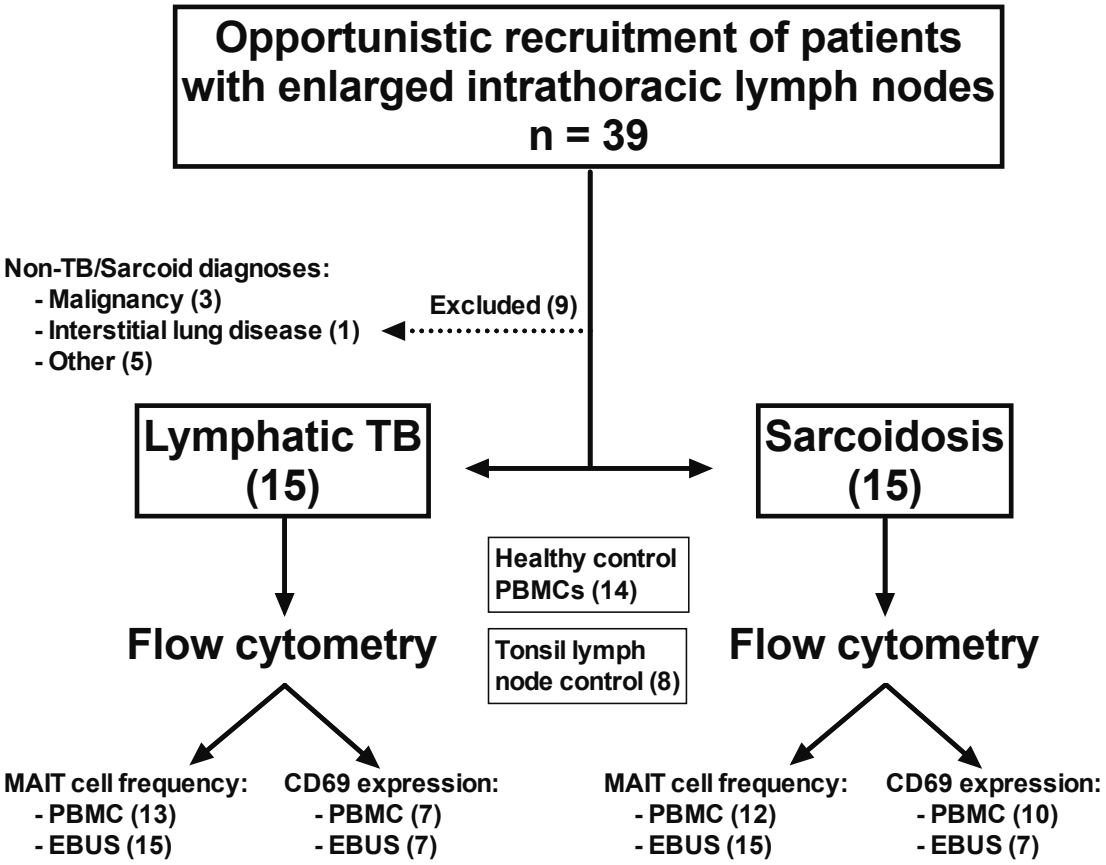


Figure 6.1: Flow chart for intrathoracic lymphadenopathy patient recruitment. Flow chart to illustrate opportunistic recruitment of patients at St. Mary's Hospital, London, and use of patient samples collected.

in the study. To account for the lack of culture confirmation for five patients including the LTBI patient, repeat analyses excluding these patients were performed. These did not, however, affect the results (see Appendix B, p. 281).

Sarcoidosis Clinical diagnosis of sarcoidosis was determined by assessment of clinical and radiological features, no evidence of malignancy, negative TB-specific IFNγ release assay, negative microbiological culture and no development of tuberculosis within 6 months of diagnosis. 14/15 patients were not undergoing therapy, whilst one patient was undergoing steroid treatment. One patient yielded a non-diagnostic lymph node sample and was diagnosed as probable sarcoidosis.

6.2.2.1 Clinical characteristics

Lymph node tuberculosis At the time of sampling, no patients were undergoing anti-*Mtb* therapy. Further treatment comprised one patient on antibiotics and

Table 6.1: Demographic information for lymphadenopathy patients, and healthy controls.

	All	LNTB	Sarcoid	Healthy
N	44	15	15	14
Age — yr				
Median	40	38	52	34
IQR	31–52	31–49	46–65	27–40
Gender				
Male	22	10	8	4
Female	22	5	7	10
Ethnicity				
White (UK)	15	2	5	8
White (Other)	3	0	1	2
Asia (India/Pakistan)	11	7	4	0
Asia (Other)	6	2	2	2
Black (Caribbean)	4	2	2	0
Black (Other)	3	1	1	1
Middle East (Iran)	2	1	0	1

one patient undergoing anti-TNFα therapy. Of the 15 patients included in the study, 4 had additional pulmonary involvement, of which one also had central nervous system involvement and one also had pleural involvement. One further patient had spinal involvement (no pulmonary involvement).

6.2.3 FACS screen for PFA-fixation compatible antibodies

Approximately 2.5×10^8 PBMCs were thawed, and washed in pre-warmed R10 media × 2 (1,600 rpm; 5 mins). 1.5×10^8 cells were resuspended in 20 ml R10 and stimulated with 50 ng/ml PMA and 250 ng/ml ionomycin for 16 hours. 1×10^8 cells were resuspended in 20 ml R10 and left unstimulated overnight.

The following morning, stimulated and unstimulated cells were washed ×2 in 50 ml R10 (1,600 rpm; 5 mins). Unstimulated cells were stained with CTV as follows. PBMCs were pelleted (1,600 rpm; 5 mins), resuspended in PBS (1,600 rpm; 5 mins), and washed one further time in PBS (1,600 rpm; 5 mins). Cells were resuspended in 1 ml PBS, and CTV (Invitrogen) added to a final dilution of $1/2 \times 10^5$ of stock concentration. Cells were vortexed to mix, and left in the dark to stain (10 mins, 21°C). 10 ml ice cold R10 was added to quench the CTV, cells were spun down (1,600 rpm; 5 mins), resuspended in 1 ml R10 and transferred to a fresh

tube. 13 mls R10 were added, and the process repeated twice more. Cells were then incubated (37°C; 5 min) to allow excess dye to diffuse away, before centrifugation (1,600 rpm; 5 mins) and resuspension in R10. Stimulated and unstained PBMCs, and unstimulated CTV stained PBMCs were pooled for further staining.

PBMCs were then washed (1,600 rpm; 5 mins) and resuspended in 1 ml PBS for antibody staining. Briefly, L/D NIR (Invitrogen), CD3 Pe-Cy7 (eBioscience), CD8-VioGreen (Miltenyi), Vα7.2 PerCP-Cy5.5 (BioLegend) and CD161-APC (Miltenyi) antibodies were added and cells were incubated in the dark (15 mins; 4°C). Cells were then washed ×2 (1,600 rpm; 5 mins) and split into two. Half the cells were then stained with CFSE as follows.

Cells to be CFSE stained were resuspended in 25 ml PBS, and pre-diluted CFSE (Invitrogen) was added to a final concentration of $1/5 \times 10^6$. Cells were vortexed to mix, and incubated (10 mins; 37°C). 25 mls ice cold PBS was added to stop the stain, and cells were incubated in the dark (5 mins; 4°C) before washing ×3 (1,600 rpm; 5 mins). Cells were transferred to a fresh 15 ml falcon tube between each wash. After the final wash, cells were resuspended in 5 mls 4% PFA (Zellkraftwerk) and incubated in the dark to fix (15 mins; 4°C). Cells were resuspended in PBS, washed ×2 (1,600 rpm; 5 mins) and recombined with the unfixed PBMCs.

Antibody screening was performed using a 'LegendScreen' kit (BioLegend), consisting of four 96-well plates with lyophilised, pre-titrated, PE-conjugated antibodies. Before seeding cells in the 96-well plates for antibody screening, antibodies were reconstituted according to the manufacturers instructions. PBMCs were then resuspended into 35 ml PBS containing 1/20 FcX TruStain Fc receptor block (BioLegend), incubated (5 mins; 21°C) and 100 µl of cell suspension was added per well. PBMCs were incubated in the dark to stain (20 min; 4°C), before being washed in PBS ×2 (1,600 rpm; 5 mins) and resuspended in 4 % PFA (BioLegend) for fixation. Cells were washed ×2, and resuspended in 100 µl PBS for analysis by flow cytometry (MACSQuant).

6.3 Flow cytometry analysis of PBMC and ITLN

Intrathoracic lymph node (ITLN) aspirates were obtained from patients through endobronchial ultrasound-guided transbronchial needle aspiration (EBUS-TBNA). Samples were subsequently transferred to the BSL3 lab for surface antibody staining, with secondary intracellular antibody staining following an extended fixation period. In all cases where possible, paired blood samples were taken. PBMCs were isolated and subsequently processed in parallel with EBUS-TBNA samples. PBMC and ITLN samples were each assessed for MAIT cell[1] frequency within the T cell

[1]Defined as $CD3^+$ $CD161^{++}$ $V\alpha7.2^+$ T cells.

compartment; and in a proportion of patients, for CD69 expression. Patient diagnoses were confirmed retrospectively, and demographic information is detailed in Table 6.1 (p. 185).

Following flow cytometric analysis of PBMC from each group, MAIT cells in the healthy control group were found to comprise a median of 3.6% of T cells (IQR, 2.3–4.8%; Fig. 6.2 A). Interestingly, in sarcoidosis patients this dropped to 0.4% of T cells (IQR, 0.1–1.8%; $p < 0.01$), whilst in LNTB patients, MAIT cell frequencies were comparable to the healthy control group (2.6%; IQR, 1.1–4.4%; $p =$ ns; Fig. 6.2 A). It is interesting to note this, as MAIT cells are reported to be depleted in the peripheral blood of patients with TB [138, 178].

In lieu of EBUS-TBNA samples from healthy control patients, MAIT cell frequencies within the tonsils of tonsillectomy patients were assessed, and compared with EBUS-TBNA samples from LNTB and sarcoidosis patients. In the tonsillar tissues, MAIT cells comprised 0.10% (IQR, 0.049–0.16%), whilst in sarcoidosis and LNTB patients MAIT cell frequencies were 0.17% (IQR, 0.063–0.90%) and 0.55% (IQR, 0.20–4.1%), respectively (Fig. 6.2 B).

In each case, the median MAIT cell frequency was low, reflecting a paucity of MAIT cells within lymph nodes; however an increase was observed in LNTB EBUS-TBNA samples vs. tonsillar tissue LN control ($p < 0.01$; Fig. 6.2 B). Of note, in both LNTB and sarcoidosis patient groups, there were patients with unusually high MAIT cell frequencies (max. 14.4% and 6.3%, respectively), indicating substantial heterogeneity between patients (Fig. 6.2 B).

In order to test the hypothesis that MAIT cells would be found enriched within the inflamed lymph nodes in LNTB and/or sarcoidosis; matched samples — where possible — were assessed for MAIT cell frequencies in peripheral blood and ITLN. Broadly, there were a lower number of MAIT cells within the ITLN compared to the peripheral blood in LNTB patients, reflected in the difference in respective median frequencies in PBMC (2.6%, IQR 1.1–4.4%) vs. ITLN (0.55%, IQR 0.25–3.7%). However, there was no statistically significant difference between compartments within individuals ($p =$ ns; Fig. 6.2 C). Indeed, whilst frequencies in the ITLN dropped in some patients, they were raised in others. The same was also broadly evident in sarcoidosis patients — (0.42%, IQR 0.09–1.8% in PBMC vs. 0.17%, IQR 0.06–0.90% in ITLN; $p =$ ns; Fig. 6.2 C).

These data indicate that MAIT cells are depleted from the peripheral blood of patients with sarcoidosis; but interestingly, not those with LNTB. As a group, MAIT cells appear to be present at higher numbers in the ITLNs of LNTB patients, compared to the tonsillar tissue used as a lymph node control. However, matched PBMC and ITLN samples from the same patients indicate substantial heterogeneity between individuals, with regards to enrichment of MAIT cells within the ITLN.

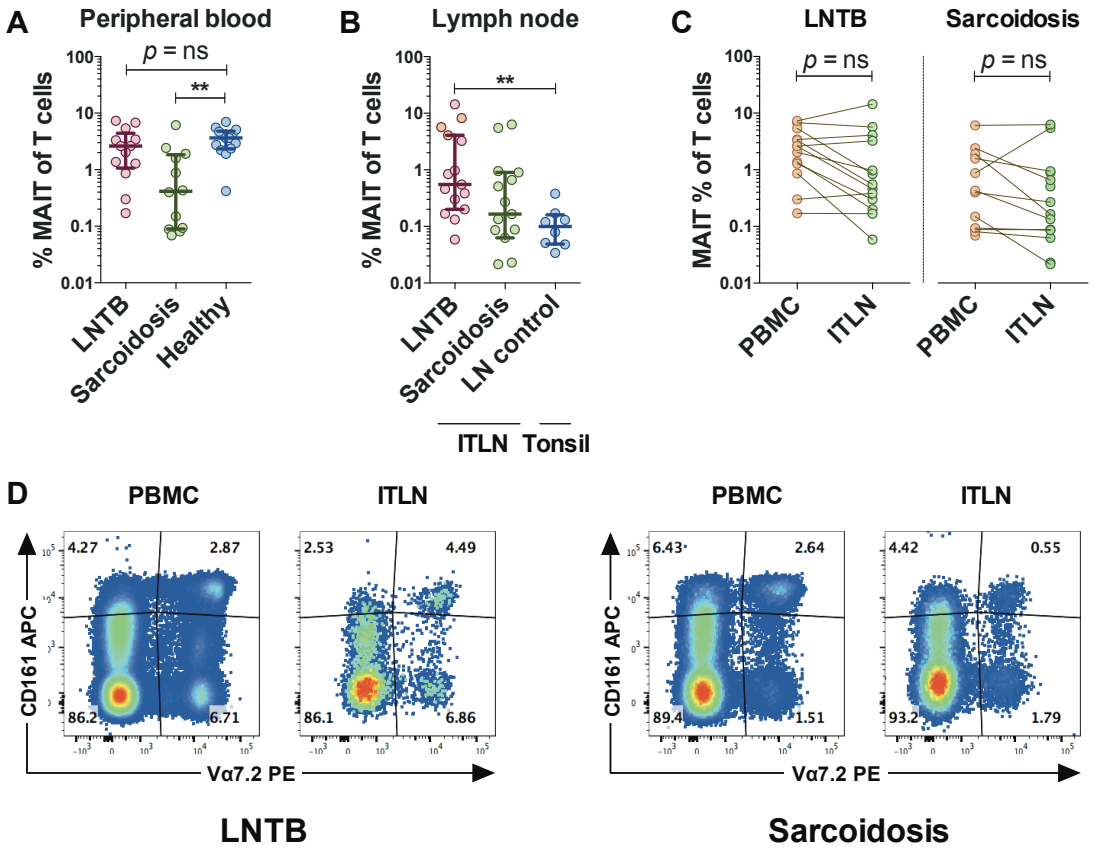


Figure 6.2: MAIT cells are depleted in the blood of sarcoidosis, but not LNTB patients. PBMCs and EBUS-TBNA, or tonsillar tissue were assessed for MAIT cell frequencies, as a proportion of total T cells. (A) MAIT cell frequency in PBMCs from lymph node TB (LNTB) and sarcoidosis patient groups, or healthy controls. (B) MAIT cell frequency in EBUS-TBNA samples from LNTB or sarcoidosis patient groups, or in tonsillar tissue homogenates from tonsillectomy patients. (C) Paired PBMC and intrathoracic lymph node (ITLN) MAIT cell frequencies in LNTB and sarcoidosis patients. (D) Representative paired plots of MAIT cells in the T cell compartment of LNTB and sarcoidosis patients. Data shown as median ± IQR; analysed by (A, B) Kruskal-Wallis test with Dunn's multiple comparison post-test, and (C) Wilcoxon matched-pairs signed rank test. For all tests, $^{**}p < 0.01$, ns = non-significant.

6.3.1 Activation status of MAIT cells in lymph node TB

In order to assess the activation state of cells in both PBMCs and the ITLN in LNTB and sarcoidosis patients, MAIT cell CD69 expression was examined and comparisons made between compartments, disease state, and with bulk T cells.

In LNTB patients, there was a wide range of CD69-expression in both PBMCs and in the ITLN. However, a median of 41.2% (IQR, 13.9–56.9%) of MAIT cells expressed CD69 in PBMCs, rising to 60.7% (IQR, 28.6–82.7) in the ITLN (p = ns; Fig. 6.3 A). This trend was more apparent, and statistically significant within

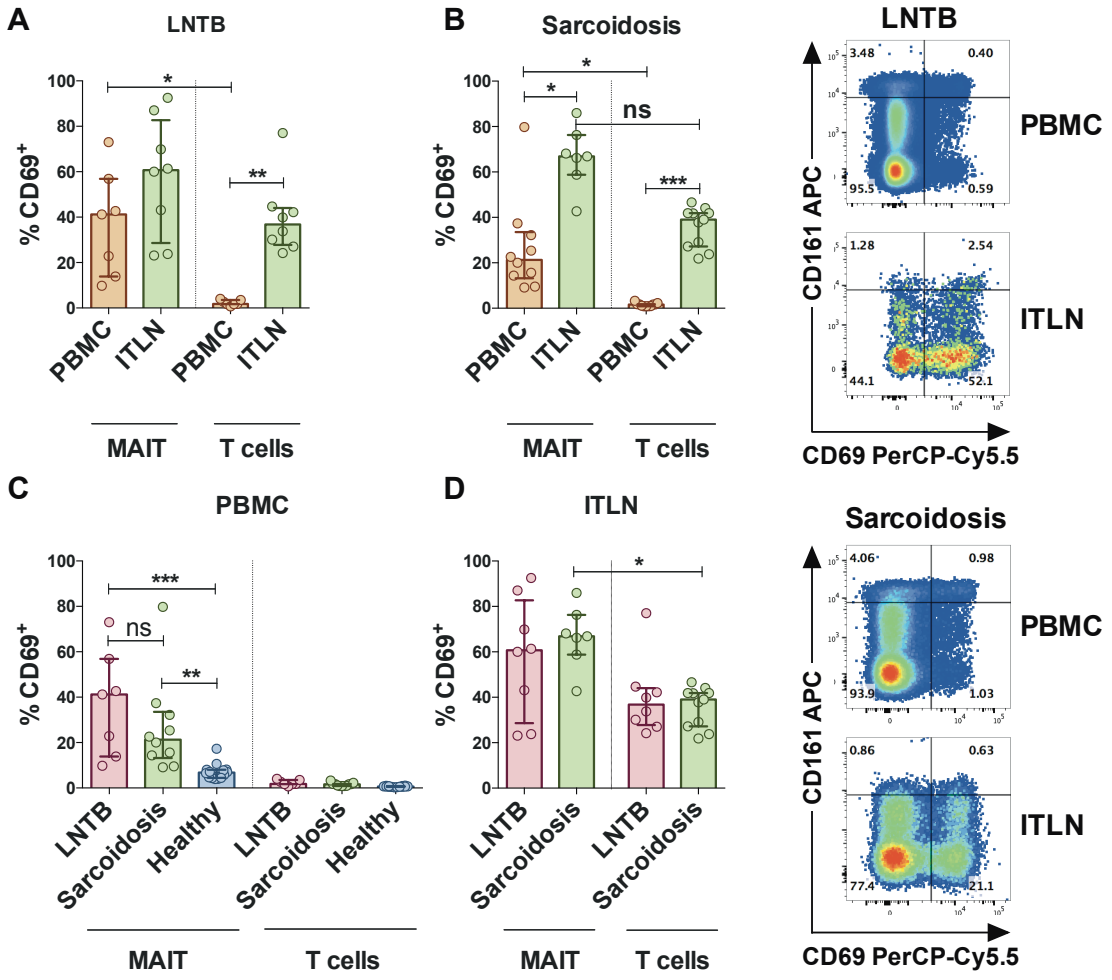


Figure 6.3: MAIT cells express increased CD69 in blood and lymph nodes, in patients with intrathoracic lymphadenopathy. PBMC and EBUS-FNA samples were assessed for MAIT, and bulk T cell CD69-expression. (A) CD69-expression in LNTB and (B) sarcoidosis patients, in PBMC and ITLN. (C) CD69-expression in LNTB, sarcoidosis and healthy controls, in PBMC. (D) CD69-expression in LNTB and sarcoidosis patients, in ITLN. Data shown as median ± IQR; analysed by Kruskal-Wallis test with Dunn's multiple comparison post-test. $***p < 0.001$, $**p < 0.01$, $*p < 0.05$, ns = non-significant.

the bulk T cells, of which a median 1.8% (IQR, 1.7–3.5%) expressed CD69 within PBMCs vs. 36.8% (IQR, 27.8–44.1%) in the ITLN ($p < 0.01$; Fig. 6.3 A). In sarcoidosis patients a median of 21.3% (IQR, 13.2–33.5%) of MAIT cells expressed CD69 in PBMCs, compared to 66.9% (IQR, 58.8–76.3%) within the ITLN ($p < 0.05$; Fig. 6.3 B). As in LNTB patients, few bulk T cells in PBMC expressed CD69 (1.6%; IQR 0.9–1.8%), with a similar increase in the ITLN (39.1%; IQR, 27.2–41.9%; $p < 0.001$; Fig. 6.3 B). These data indicate broad T cell activation (as defined by CD69 expression) in the ITLN relative to PBMC.

Directly comparing LNTB patients, sarcoidosis patients and healthy control donors revealed a reduction in the median frequency of circulating MAIT cells expressing CD69 in sarcoidosis patients relative to LNTB patients; although this was not statistically significant (−19.9%; p = ns; Fig. 6.3 C). However, both were found to express CD69 to a greater extent relative to the healthy control group. Whilst apparent with the sarcoidosis patients (21.3% vs. 6.8%; $p < 0.01$) this was more pronounced with the LNTB patients (41.2% vs. 6.8%; $p < 0.001$). Little CD69 expression was observed from bulk T cells from each of the three groups (Fig. 6.3 C). Within ITLN aspirates, no difference was seen between LNTB and sarcoidosis, either with respect to MAIT or bulk T cell expression of CD69. CD69 expression by cells within tonsillar tissue control group was not assessed.

To summarise, peripheral blood MAIT cells in both LNTB and sarcoidosis patients expressed increased CD69 relative to a healthy control group. Blood MAIT cells of LNTB patients showed the most pronounced increase, indicating a heightened state of activation of circulating MAIT cells in these patients. Notably, CD69 expression was not seen in bulk circulating T cells in the same patients. However, within the ITLN; bulk T cells were found to express CD69 in both LNTB and sarcoidosis, although with no difference between these groups. MAIT cells in both groups similarly expressed CD69, with some patients demonstrating robust CD69-expression (> 60%). Together, these data indicate that MAIT cells present within inflamed lymph nodes express increased CD69, as do MAIT cells circulating in the peripheral blood of patients with sarcoidosis, or more noticeably, tuberculosis with intrathoracic lymphadenopathy.

6.3.2 Increased CD4$^+$ MAIT cells in sarcoidosis

MAIT cells are typically either CD8α^+, or double-negative in the use of their co-receptor. However, the development of an MR1-tetramer confirmed that MAIT cells can also express CD4; although these typically comprise a small fraction of the total MAIT cell population [140]. In order to assess whether MAIT cell co-receptor usage was skewed in sarcoidosis patients as has been reported for bulk T cells [414], circulating MAIT cells within each patient group were assessed for their expression of CD4 and/or CD8 co-receptors.

Little difference was observed between patient groups with respect to single positive (SP) CD4$^-$ CD8$^+$, CD4$^+$ CD8$^+$ double-positive (DP), or CD4$^-$ CD8$^-$ double negative (DN) MAIT cells. However, interestingly there were significant increases in the frequency of CD4$^+$ SP MAIT cells in sarcoidosis (median 4.3%, IQR 1.8–12.5%) relative to both LNTB patients (0.8%, IQR, 0.7–2.4%; $p < 0.05$)

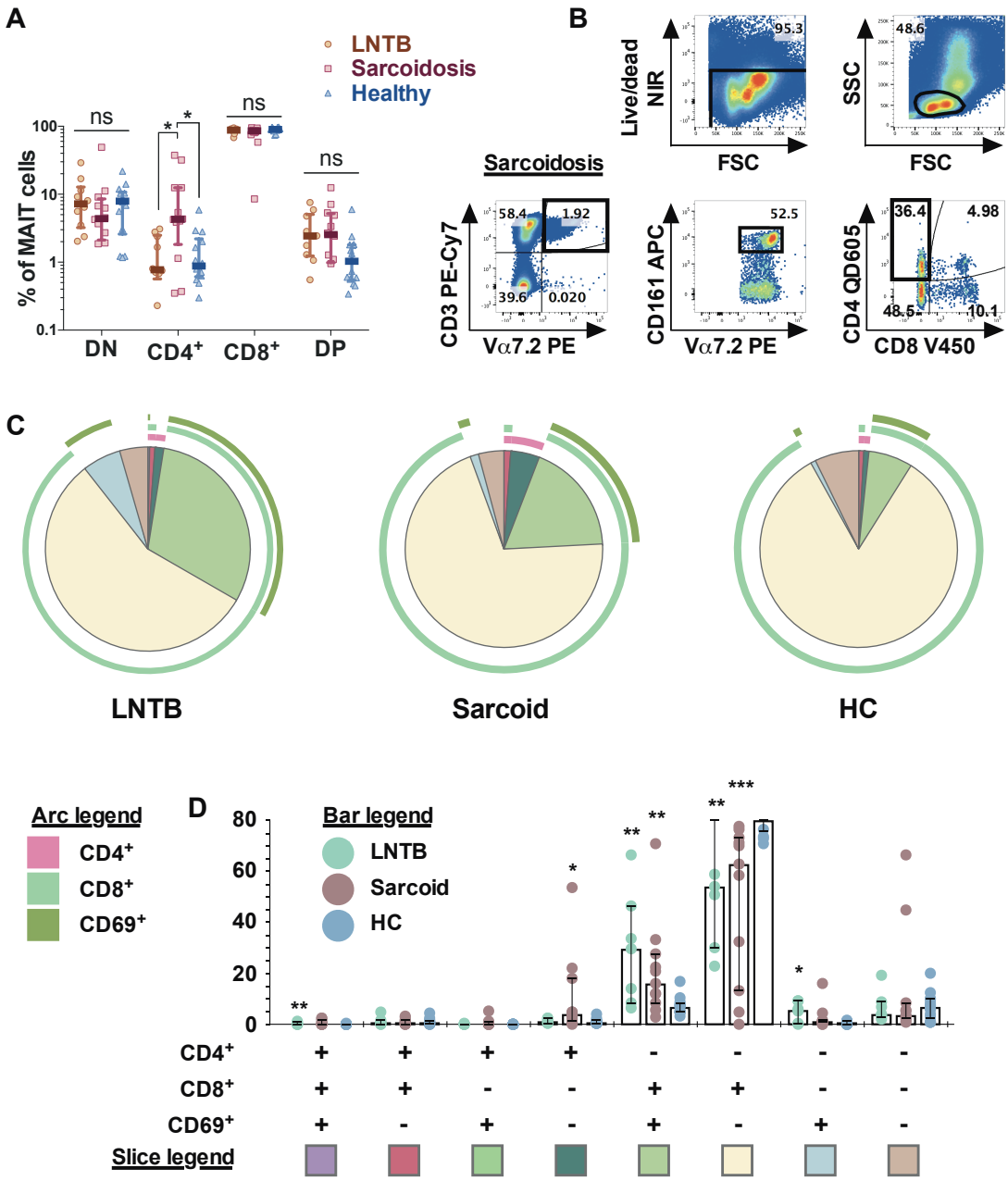


Figure 6.4: Increased usage of the CD4 co-receptor by MAIT cells in sarcoidosis patients with intrathoracic lymphadenopathy. MAIT cells in the peripheral blood of LNTB, sarcoidosis patients and healthy controls were assessed for co-receptor usage. (A) MAIT cells gated according to $CD4^+$, $CD8^+$, $CD4^+$ $CD8^+$ (DP), or $CD4^-$ $CD8^-$ (DN). (B) FACS plot of high $CD4^+$ MAIT cell sarcoidosis patient. (C, D) MAIT cell combined co-receptor usage and CD69-expression were expressed as (C) pie charts, and (D) a bar chart for each patient group assessed. Pie chart shows median values. Data analysed by (A) Kruskal-Wallis test with Dunn's multiple comparison post-test, (D) Wilcoxon signed rank test. $***p < 0.001$, $**p < 0.01$, $*p < 0.05$, ns = non-significant.

and to the healthy control group (0.9%, IQR, 0.6–2.2%; $p < 0.05$; Fig. 6.4). While the median differences were relatively small, in some patients CD4-expressing MAIT cells comprised a large proportion of the population (max. 36.4% of MAIT cells; Fig. 6.4 B).

In order to assess whether MAIT cell co-receptor expression was linked to altered activation status in these patients, CD69 expression and co-receptor usage was also examined. In all three groups, CD69-expression largely occurred within the $CD8^+$ T MAIT cell subpopulation; although there was a larger proportion of DN MAIT ($p < 0.05$), and $CD8^+$ MAIT cells ($p < 0.01$) expressing CD69 in LNTB patients than in the healthy controls (Fig. 6.4 C, D). The $CD4^+$ MAIT cells in sarcoidosis patients, however, did not express CD69.

Together, these data indicate that there is an enrichment of circulating MAIT cells expressing the CD4 co-receptor in sarcoidosis patients, although these do not appear to exhibit an activated phenotype by CD69-expression. By contrast, approximately half of the MAIT cells lacking either CD4, or CD8 co-receptor were found to express CD69 in LNTB patients. Further experiments will be needed to identify the functional significance of CD4 or CD8 co-receptor expression in MAIT cells, and their relevance to MAIT cell function in sarcoidosis and tuberculosis.

6.3.3 Clinical features of high MAIT cell frequency in ITLN

As highlighted through analyses of gene-expression in tuberculosis and sarcoidosis [415, 416]; there is a great deal of similarity underlying the immune activation evident in both. As individual patients exhibiting relatively high numbers of MAIT cells within the ITLN were found in both LNTB and sarcoidosis patient groups, it was unclear whether there were common histopathological features that might explain this, irrespective of the diagnosis. All data for sarcoidosis and tuberculosis patients with lymphadenopathy were therefore pooled, and the cohort was split according to high (above median) and low (below median) MAIT cell frequency within the ITLN sample (designated 'High MAIT (%)' and 'Low MAIT (%)'). Samples in each group were then further stratified according to age, diagnosis, circulating MAIT cell frequency and CD69 expression, lymph node histology and self-reported symptoms.

Several differences between the high and low MAIT cell groups were observed. The median age of the high MAIT cell (%) group was 37 (IQR, 31–47), whilst that of the low MAIT cell (%) group was 52 (IQR, 46–69), a difference between medians of 15 years ($p < 0.01$; Table 6.2; Fig. 6.5 A). Similarly, the median frequency of circulating PBMC MAIT cells, within the high MAIT (%) group was 3.0% of T cells (IQR, 2.1–6.0%), compared to 0.30% (IQR, 0.09–1.1%) within the low MAIT

Table 6.2: Features compared between low (< median) and high (> median) MAIT cell frequencies in the ITLN of patients with LNTB or sarcoidosis. ITLN sample data from 30 patients were pooled, and tabulated according to less than, or greater than median ITLN MAIT cell frequencies (i.e. 0.42% of ITLN T cells). Median age — less than 46 years (cohort median); high MAIT (%) (blood) — above cohort median (1.37% of T cells); symptom score $\geqslant 2$ — for two of: breathlessness, fever or night sweats, cough, weight loss, and malaise.

ITLN samples:	**All**	**Low MAIT (%)**	**High MAIT (%)**
N	30	15	15
Below median age	15 (30)	4	11
Circulating MAIT cells			
High MAIT (%)	13 (26)	2	11
High CD69 (%)	8 (16)	4	4
Diagnosis			
LNTB	15 (30)	6	9
Sarcoidosis	15 (30)	9	6
ITLN histological features			
Non-diagnostic	5 (30)	2	3
Reactive lymph node	4 (25)	1	3
Any necrosis	6 (25)	2	4
Granulomas	17 (25)	8	9
Non-necrotising	15 (17)	8	7
Caseating/necrotic	2 (17)	0	2
Symptom score $\geqslant$ 2	9 (30)	3	6

(%) group ($p < 0.0001$; Table 6.2; Fig. 6.5 B). There was, however, no significant difference between the median CD69-expression levels of circulating MAIT cells, in patients with high (24.2%, IQR 15.4–39.0%) or low (30%, IQR 14.7–69.0%) MAIT cell frequency within the ITLN (p = ns; Table 6.2; Fig. 6.5 C).

Examination of some the histopathological features of the patient lymph-node aspirates revealed no further clear differences between patients with low and high MAIT cell ITLN frequencies (Table 6.2). Of the 25 samples of sufficient (diagnostic) quality, four indicated no granulomas/necrosis (reactive) — three in the high MAIT (%) group; one in the low MAIT (%) group. Six samples indicated necrosis (two without identifiable granulomas) — with two in the low MAIT (%) group, and four in the high MAIT (%) group. 15 samples yielded identifiable non-necrotic granulomas — split evenly between low and high (%) MAIT groups. Only two samples identified necrotic granulomas — both within the high MAIT (%) group. Patients were also scored according to self-reported symptoms — breathlessness,

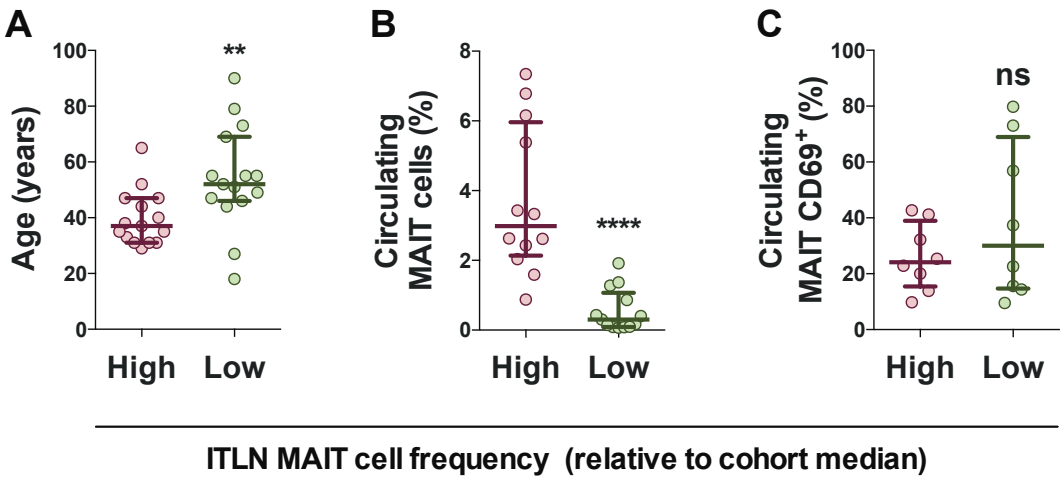


Figure 6.5: High MAIT cell frequency in the ITLN is associated with high circulating frequency. LNTB and sarcoidosis patient data were pooled, and split into high ($> 0.42\%$) and low ($< 0.42\%$) MAIT cell frequency within the ITLN. Comparisons of (A) age, (B) circulating MAIT cell frequency as proportion of T cells, and (C) proportion of CD69-expressing circulating MAIT cells, were then made. Data shown as median ± IQR; analysed by Mann-Whitney U test, $^{****}p < 0.0001$, $^{**}p < 0.01$, ns = non-significant..

fever or night sweats, cough, weight loss and malaise. There were nine patients in total reporting two, or more of these symptoms — three in the low MAIT (%) group and six in the high MAIT (%) group (Table 6.2).

In summary, no clear differences between patients with higher and lower ITLN MAIT cell frequencies were identified through assessing their diagnosis, histological features or clinical signs — although bigger sample sizes could help given likely substantial heterogeneity between individuals. By contrast, high ITLN MAIT cell frequencies coincided with lower age, and higher frequencies of circulating MAIT cells. Overall, despite heterogeneity between individuals, MAIT cells present at the site of lymphadenopathy in both LNTB and sarcoidosis, express CD69 — indicative of a heightened activation state. Within the peripheral blood, MAIT cells in these patients also appear activated in both LNTB and sarcoidosis relative to healthy control donors, in contrast to the behaviour of the bulk circulating T cells. However, those with higher MAIT cell frequencies in the ITLN appeared to be younger, with increased peripheral blood MAIT cells, in comparison with those with fewer ITLN MAIT cells — and with no consistent histopathological or clinical differences to further differentiate between them.

6.4 Imaging of MAIT cells by chip-cytometry

6.4.1 Identification of chip-cytometry compatible mAbs

Initially developed in 2009 [421], chip-cytometry is a novel imaging-based technology that enables the long-term storage and re-imaging of samples. To investigate clinical samples from LNTB patients using this technique, it was necessary first to identify primary antibodies compatible with 4% PFA fixation; a pre-requisite for decontaminating BSL3 samples for further analysis, and for long-term storage.

Chip-cytometry utilises rounds of antibody staining, fluorescent imaging, and fluorophore bleaching. In contrast to standard microscopy techniques, where the use of a fluorescently labelled secondary antibody is often used to provide signal amplification; directly conjugated antibodies are necessary to avoid re-binding targets labelled with antibodies of the same isotype as in previous imaging cycles.

Many antibodies used in flow cytometry bind antigen optimally prior to fixation; in particular those commonly used to identify surface-expressed markers of activation. Therefore, to identify candidate antibodies for use in chip-cytometry imaging, a commercial antibody screening kit was used to identify antibodies (by flow-cytometry) amenable to labelling PFA-fixed epitopes. The kit was additionally used to differentiate expression of markers by cell-type, including MAIT cells.

The antibody-screening kit consists of multiple 96-well plates; each well seeded with lyophilised and pre-titrated PE-bound antibodies. Reconstitution of the antibodies, addition of cells, and the use of an automated multi-sample flow cytometer capable of handling 96-well plates, enables screening of cells for 332 different surface markers. Further addition of suitably labelled additional antibodies is also possible for multi-parametric flow-cytometry.

The intention was to test the ability of each PE-labelled antibody in the kit to bind PFA-fixed cells, and to compare against unfixed cells; whilst assessing the ability of antibodies to identify stimulated and resting cells, and to distinguish different cell populations. In order to achieve this within a single well, an antibody panel accommodating the PE-labelled antibody, together with antibodies against CD3, CD8, CD161, Vα7.2 TCR, and CTV, CFSE and live/dead (amine reactive) labelling dyes was designed.

The emission spectra of both CTV and CFSE can overlap with commonly used fluorescent antibodies, especially at the high concentrations typically used — in particular, CFSE signal can bleed into the PE channel. Therefore, a titration was performed to identify a lower-level concentration for each dye (Fig. 6.6 A, p.

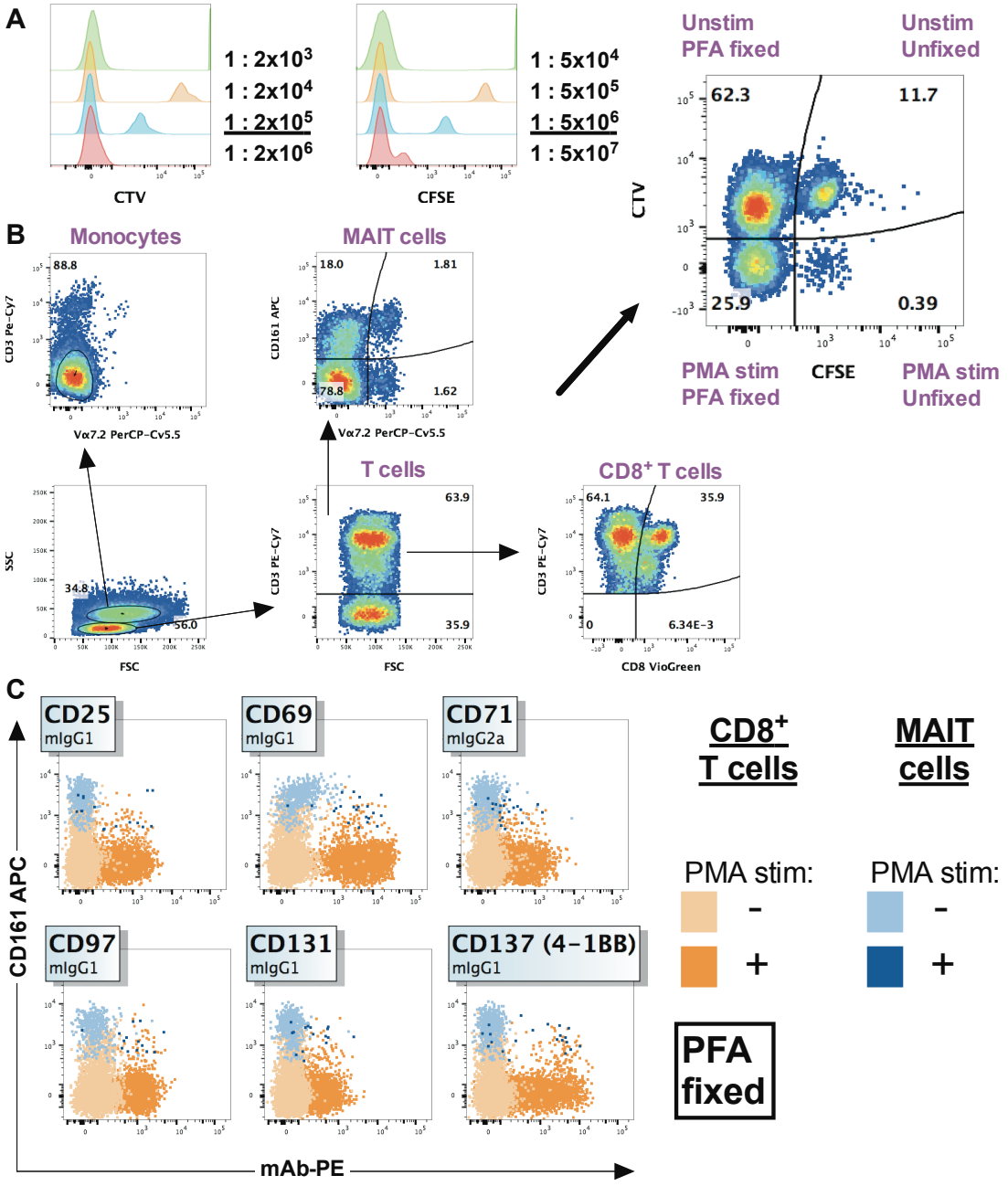


Figure 6.6: Identification of PFA-stable activation markers expressed on MAIT cells. (A) A dose titration was performed of CTV and CFSE staining on PBMCs. (B–C) PBMCs were either stimulated with PMA, or left unstimulated — and either fixed with PFA, or left unfixed. Fixed cells were labelled with CTV, and stimulated cells were labelled with CFSE. All cells were labelled with antibodies against CD3, CD8, CD161, Vα7.2 and a live/dead marker was used — all pre-fixation, to identify live CD8$^+$ T cells and MAIT cells. Stained PBMCs were added to a well containing the PE-conjugated antibody clone to be tested. All cells were fixed and analysed by flow cytometry.

Table 6.3: Test of PFA-fixation compatible antibodies for detection of CD8$^+$ T cell activation markers.

	Unstimulated	PMA stimulated	
Target	**CD8$^+$ T cells**	**CD8$^+$ T cells**	**MAIT cells**
CD69	-	++	++
CD137 (4-1BB)	-	++	++
HLA-A2	+	++	++
HLA-DQ	+	++	++
CD25	-	+	+
CD71	-	+	+
CD97	-	+	+
CD131	-	+	+
CD55	+	++	-/+
CD87	-	+	-/+
CD108	-	+	-/+
CD134	-	+	-/+
CD274 (B7-H1)	-/+	+	-/+
CD278 (ICOS)	-	+	-/+
CD319 (CRACC)	-/+	+	-/+
CLEC12A	-/+	+	-/+
CD54	-	-/+	-/+
CD96	-	-/+	-/+
CD132	-	-/+	-/+
NPC (57D2)	-	+	-
CD51	-	-/+	-
CD355 (CRTAM)	-	-/+	-

199), and tested with a full antibody panel to ensure adequate compensation of spectral overlap between channels (data not shown).

Subsequently, the panel was used in conjunction with the antibody screening kit. PBMCs were stimulated with PMA and ionomcyin, or rested overnight. The following day, rested cells were stained with CTV, before all cells were pooled together and stained with the live/dead marker and antibodies against CD3, CD8, CD161 and Vα7.2 TCR. The cells were then re-divided; half were stained with CFSE, whilst the remainder were fixed with 4% PFA for 20 minutes. All cells were pooled, and added to each well of the 'LegendScreen' kit, as per manufacturers instructions, for binding of PE labelled antibody. Post-staining, all cells were subsequently fixed, and analysed by flow cytometry.

Live cells were gated as monocytes or lymphocytes according to forward, and side-scatter properties. Lymphocytes were subsequently identified as CD8$^+$ T cells

through CD3- and CD8-expression, whilst MAIT cells were gated as $CD3^+$ $CD161^{++}$ $V\alpha7.2^+$ cells (Fig. 6.6 B). Each antibody was then compared against its isotype control to identify those capable of binding both unfixed, and PFA-fixed epitopes; and those following PMA stimulation, or rest (see Appendix A, p. 251).

Additionally, data were analysed to identify antibodies specifically capable of binding activation markers expressed by PFA-fixed $CD8^+$ T and MAIT cells, following PMA stimulation or rest. These data are summarised qualitatively in Table 6.3. In particular, 6 markers were observed expressed on activated, fixed $CD8^+$ T and MAIT cells — and not expressed on resting cells; CD25, CD69, CD71, CD97, CD131 and CD137 (Fig. 6.6 C).

CD25 (IL-2Rα) and CD69 have both been established to indicate MAIT cell activation by bacteria [149, 394], although MAIT cell expression of CD25 has not yet been assessed following activation by IL-12/-18 alone. Furthermore, CD71 — the transferrin receptor — has not yet been described as a marker of MAIT cell activation. Therefore, experiments were performed in order to validate this observation of CD71 as a MAIT cell activation marker, and to assess the respective abilities of CD25 and CD71 to indicate responsiveness to TCR, cytokine and bacterial stimulation. CD69-expression was also assessed for comparison, although investigated more thoroughly earlier in this thesis.

Magnetically enriched $CD8^+$ T cells were cultured with TCR beads and/or IL-12/-18 overnight, before antibody staining and assessment of $CD161^{++}$/MAIT cell activation by flow cytometry (Fig. 6.7 A–C). As seen previously, a proportion of $CD161^{++}$/MAIT cells expressed CD69 without stimulation (mean $12.9 \pm 3.8\%$), which was not the case with either CD25 or CD71.

Following stimulation with IL-12/-18 only, $CD161^{++}$/MAIT cells were capable of expressing CD25 (+18.0%; $p < 0.05$), CD69 (+34.8%; $p < 0.0001$) and CD71 (+21.8%; $p < 0.01$; Fig. 6.7 A). Following TCR stimulation in the absence of cytokine co-stimulation, the increased expression of each vs. unstimulated was +55.5%, +79.2% and +42.2%, respectively (all $p < 0.0001$); whilst stimulation by IL-12/-18 + TCR beads enabled expression by +81.7%, +79.9% and +83.5% respectively, vs. unstimulated (all $p < 0.0001$; Fig. 6.7 A).

Assessment of the polyfunctional response indicated that in response to each stimulation, CD69 expression encompassed all activated MAIT cells (Fig. 6.7 B). In response to IL-12/-18 stimulation, all CD25-expressing cells co-expressed CD69 and CD71; whilst a small minority of CD71-expressing cells co-expressed CD69, but not CD25.

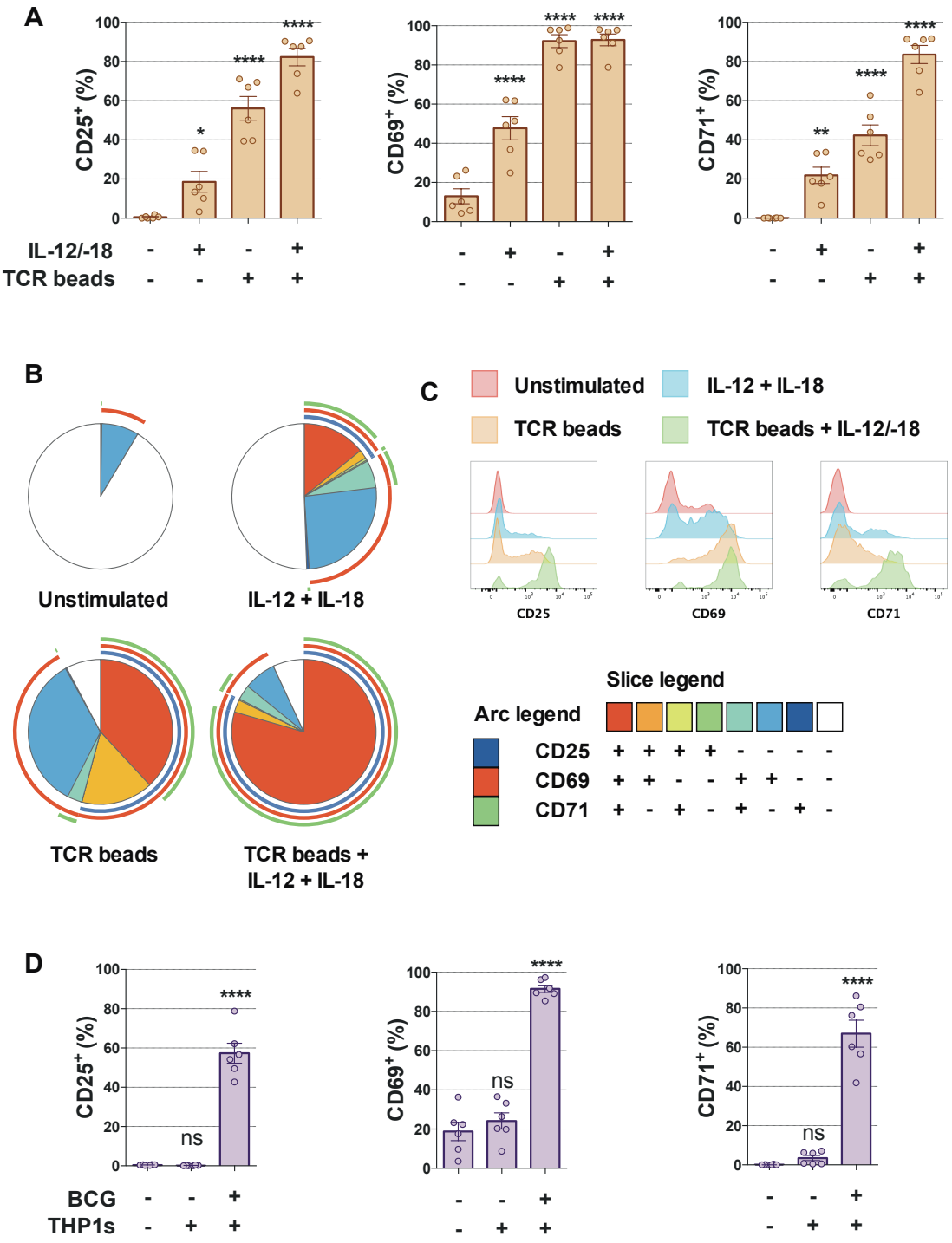


Figure 6.7: CD25, CD69 and CD71 are expressed by MAIT cells in response to bacterial stimulation. CD8$^+$ T cells were magnetically enriched from PBMCs, and (A–C) stimulated for 24 hours with IL-12 + IL-18 (50 ng/ml each) and/or TCR beads, or (D) CD8$^+$ T cells were cultured with THP1 cells infected with BCG (MOI 5) for 24 hours. Cells were surface stained for CD25, CD69 and CD71 without fixation. Data analysed by one-way ANOVA with Holm-Sidak's multiple comparison test. ****$p < 0.0001$, ***$p < 0.001$, **$p < 0.01$, *$p < 0.05$, ns = non-significant.

Following TCR bead stimulation alone, the majority of MAIT cells were $CD69^+$; and over half of these co-expressed CD25; with a smaller proportion of CD25, CD69 and CD71 co-expressing MAIT cells (Fig. 6.7 B). Nearly all CD71-expressing cells co-expressed CD25 in response to TCR beads, with a proportion of $CD25^+$ cells that co-expressed CD69, but not CD71.

In response to stimulation by TCR beads + IL-12/-18, the level of expression of CD25 and CD71 was similarly high, with nearly all CD71 expressing cells co-expressing CD25; and vice versa. Only a small minority of additional cells expressed CD69 without co-expression of either CD25 or CD71 (Fig. 6.7 B).

Next, BCG infected THP1 cells (Fig. 6.7 D) were co-cultured with magnetically enriched $CD8^+$ T cells overnight, before antibody staining and assessment of $CD161^{++}$/MAIT cell activation by flow cytometry. No expression of CD25, or CD71 was seen in the absence of bacterial stimulation; whilst a proportion of MAIT cells expressed CD69 ($18.8 \pm 4.7\%$). In response to BCG infected THP1s, increased expression of CD25 (+57.0%; $p < 0.0001$), CD69 (+72.7%; $p < 0.0001$) and CD71 (+66.9%; $p < 0.0001$) were all observed.

Together, these data confirm expression of CD25 and CD71 in response to BCG; whilst illustrating the respective responses to IL-12/-18 and/or TCR stimulation. Indeed, CD69 appeared to demonstrate a greater sensitivity to TCR stimulation, although with slightly less specificity given the basal expression levels. Neither CD25, nor CD71 are expressed by resting MAIT cells, however; and whilst these were expressed weakly in response to IL-12/-18 alone, they were up-regulated more strongly in response to TCR beads. Both were expressed robustly in response to stimulation by IL-12/-18 and TCR beads, and in response to *in vitro* stimulation with BCG. CD25, CD69 and CD71 should therefore be appropriate markers for assessment of MAIT cell activation with EBUS-TBNA samples from LNTB patients.

6.4.2 Analysis of LNTB patient samples by chip-cytometry

Prior to assessment of activation markers, antibodies against CD3, CD4, CD8, CD161 and Vα7.2 were tested to establish a five-colour anchor panel for current and future investigations requiring identification of MAIT cells by this technique.

The Zellscanner-ONE has five fluorescent detection channels corresponding to BUV395, BV421, AF488, PE and PerCP-Cy5.5. Common fluorophores in each of those channels can be bleached for re-staining with different antibodies conjugated to the same fluorophores, with the exception of AF488 which is quite photostable. However, background subtraction enables the AF488 channel to be used twice — if each use is restricted to identifying lineage-distinct cells to ensure mutual exclusivity

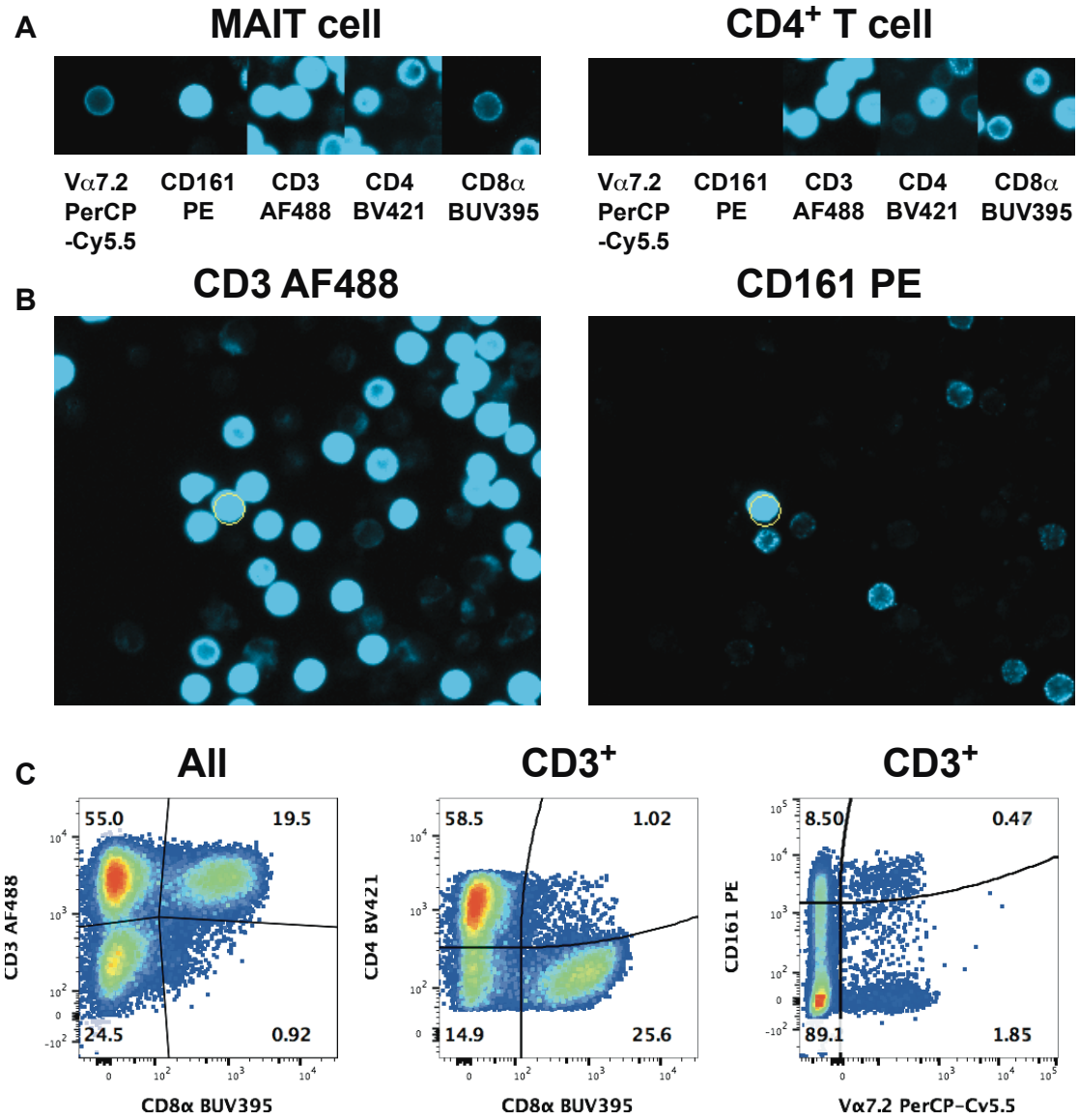


Figure 6.8: Imaging of MAIT cells by chip cytometry. PBMCs from a LNTB patient were immobilised on a Zellsafe chip, and fixed with 4% PFA for 1 hour. A series of background fluorescence images were taken, and an optimised antibody panel containing fluorescent antibodies against Vα7.2, CD161, CD2, CD4 and CD8 was added — followed by a second round of imaging. (A) Background-subtracted fluorescent labelling of a single (left) MAIT cell and (right) $CD4^+$ T cell. (B) Automated cell identification followed by gating of $CD161^{++}$ T cells (yellow circle). (C) Chip cytometry plot of CD3, CD4, CD8α, CD161 and Vα7.2 expressing cells in the PBMCs of a LNTB patient.

of AF488 labelling (e.g CD3, CD14, CD19 etc.). Therefore, the lineage specific T cell marker (CD3) was chosen for the AF488 channel, to maximise the utility of the MAIT cell panel for other investigators in the future.

For the remaining markers, different clones and fluorophores were tested to give optimal staining (data not shown) — resulting in a five colour MAIT cell panel. To test the panel on clinically relevant samples following a period of extended storage, PBMCs from patients with LNTB were immobilised onto a 'Zellsafe' chip, fixed with 4% PFA for 1 hour (4°C) and stored at 4°C for three months. The MAIT cell antibody panel was then added to the chips, and after imaging across the five channels, individual MAIT and non-MAIT (e.g. $CD4^+$ T) cells could be identified (Fig. 6.8 A). Automated cell identification and calculation of *per cell* fluorescence intensities enabled gating and automatic detection of cell sub-populations (Fig. 6.8 B), which were analysed subsequently by conventional dot-plots (Fig. 6.8 C).

Following on from the antibody screen for PFA-fixation compatible epitopes, a mixture of $CD8^+$ T cells stimulated with TCR beads + IL-12/-18 overnight, and rested $CD8^+$ T cells from one healthy donor, were pooled and immobilised on a Zellsafe chip. The chip was stained and imaged in multiple rounds for activation markers highlighted in the antibody screen (Fig. 6.9). Automated cell identification was performed and $CD161^{++}$/MAIT cells were assessed qualitatively for expression of activation markers in the context of other $CD8^+$ T cells present.

Antibodies were found capable of identifying $CD161^{++}$/MAIT cell expression of CD25, CD69, CD71, CD97 and CD137 — however, very few cells were observed to express CD38, CD131 and CD279. A representative image of four $CD161^{++}$/MAIT cells (yellow circles) is shown in Fig. 6.9 A — with only the cell in the lower left hand corner staining positive for CD69, CD71, CD97 and weakly positive for CD25 and CD137.

In order to assess whether MAIT cells expressing any of these activation markers could be identified by chip-cytometry, PBMCs and ITLN samples from patients with LNTB were stained sequentially for CD71, CD38, CD25, CD69 and CD97, with representative images shown in Fig. 6.10.

Within the PBMC samples, T cell expression of CD25, CD38, CD69 and CD71 could be detected — with non-T cell expression of CD25, CD38, CD69, CD71 and CD97 also observed. PBMC MAIT cells however appeared to express very little of each of these markers (Fig. 6.10 A, B). Nonetheless, this demonstrates the ability, in particular, of CD25, CD38, CD71 and CD97 antibodies to identify expressing cells by chip-cytometry. Within the ITLN samples, very few MAIT cells were identified — although they were clearly detectable using the five colour

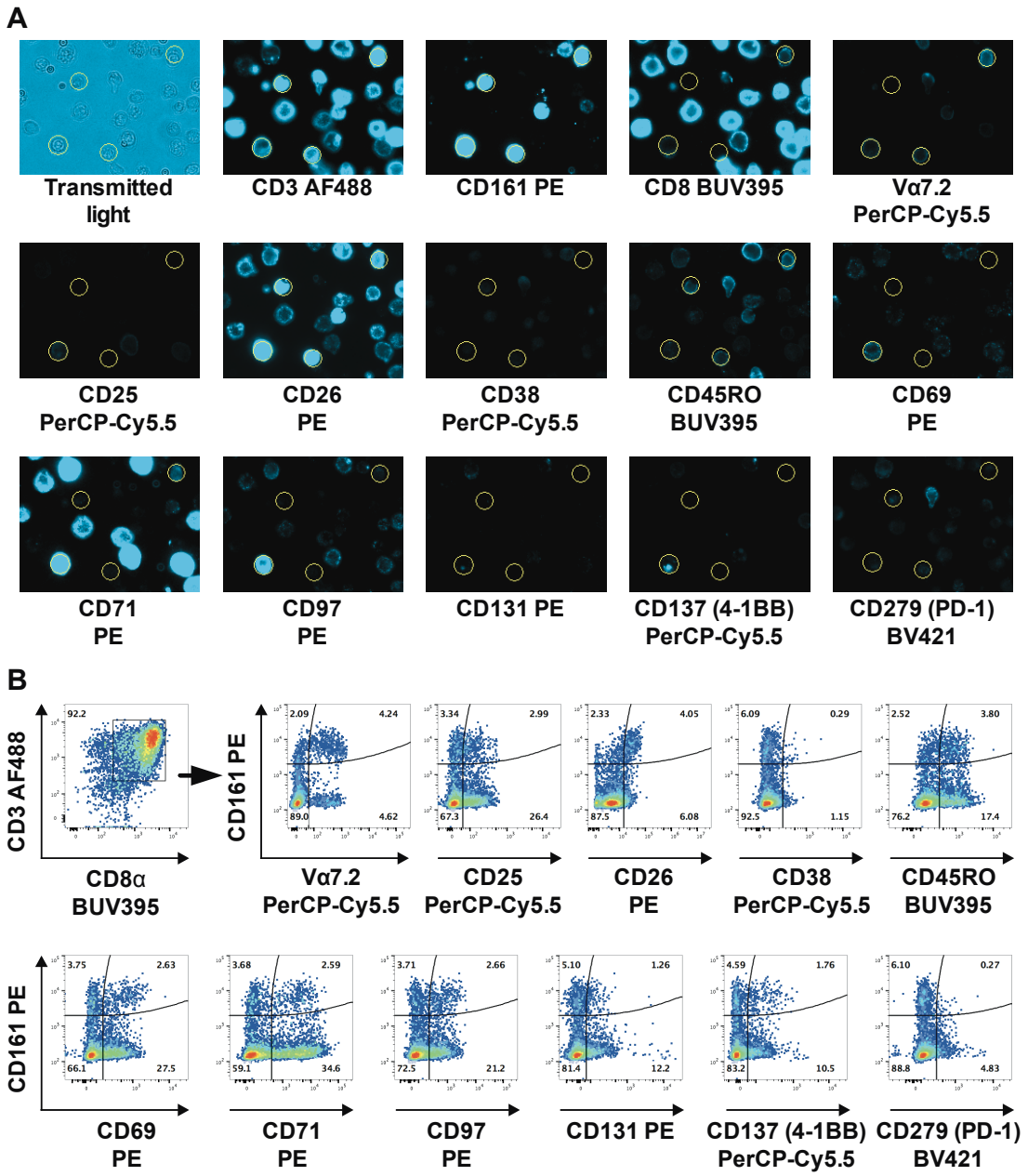


Figure 6.9: Identification of CD8$^+$ T cell activation markers by chip cytometry. Magnetically enriched CD8$^+$ T cells from a healthy donor were stimulated with αCD2/CD3/CD28 beads for 18 hours, or left unstimulated; pooled, then immobilised on a Zellsafe chip and fixed with 4% PFA. Multiple rounds of: bleach, image, stain, image were performed to identify activation markers expressed and identified by antibody clones tested. (A) Automated cell identification followed by gating of CD161^{++} T cells (yellow circle) overlaid on background subtracted images. (B) Chip cytometry plots of different cell markers against CD161. Cells gated on CD3$^+$ CD8$^+$.

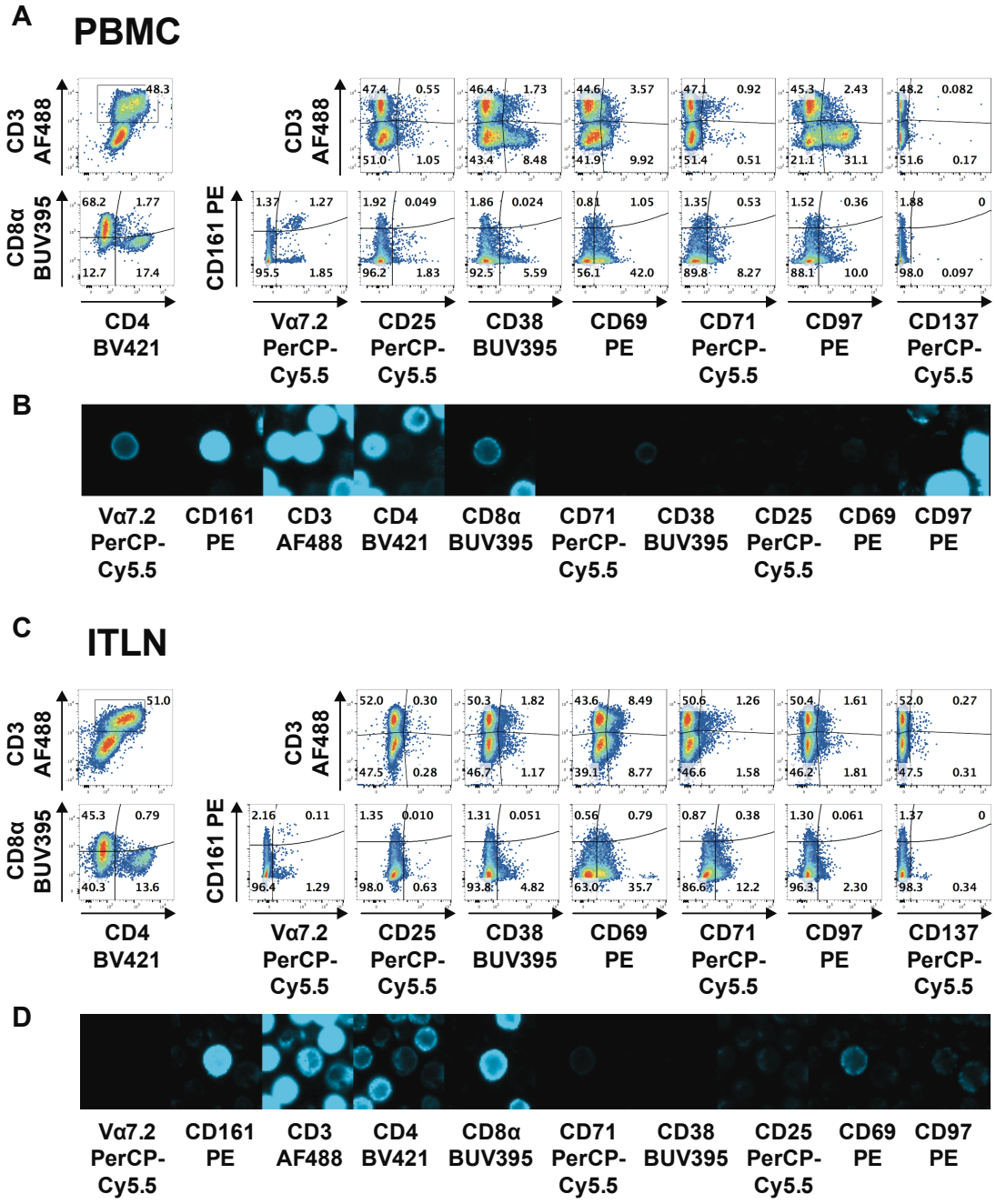


Figure 6.10: Assessment by chip cytometry of MAIT cell activation in blood and the ITLNs of LNTB patients. PBMC and EBUS-TBNA samples from LNTB patients were immobilised on Zellsafe chips and fixed with 4% PFA. Chips were stained for MAIT cells, and subsequently for activation markers as shown. (A, C) Chip cytometry plots of (A) PBMC, and (C) ITLN samples from one patient. Top row shows expression of markers on PBMC against CD3 expression, bottom row shows expression of markers on CD3$^+$ T cells against CD161. (B, D) Fluorescent images of single CD161^{++} T cells from (A) PBMC and (B) ITLN samples, after repeat staining cycles. Blank images illustrate absence of staining.

MAIT cell antibody panel, demonstrating utility in analysis of site of disease samples by chip-cytometry. Expression levels of markers assessed were qualitatively similar to those in PBMC, although with fewer CD38 and CD97 positive $CD3^{-}$ cells. Very little $CD161^{++}$/MAIT cell expression of these markers was identified; although assessment of more patient samples — in particular, those with higher MAIT cell frequencies — will be necessary to gain adequate evidence to draw biologically meaningful conclusions.

To summarise; a flow cytometry screen using 324 PE-conjugated antibodies was performed on activated and resting, fixed and unfixed PBMCs, to identify candidate antibodies for use in chip-cytometry. Several of these markers were subsequently assessed for their ability to identify MAIT cells activated in response to IL-12/-18 ± TCR, or mycobacterial stimulation — identifying CD71 as a marker of MAIT cells activated in response to live bacteria, which has not previously been reported. Candidate antibodies were then tested on PBMC and ITLN samples from LNTB patients — immobilised on a 'Zellsafe' chip and stored for 3 months — with very little expression of activation markers detected on $CD161^{++}$/MAIT cells. $CD161^{++}$/MAIT cells, however, were few in number — and some expression was detectable on other cell-types present. Together with the five-colour MAIT cell panel, the data from the antibody screen will be useful for future investigations of MAIT — and other — cells by chip-cytometry. Overall, these data show proof of principle for a novel technology enabling long term storage and analysis of clinically important ITLN samples from LNTB patients.

6.5 Discussion

6.5.1 MAIT cells in lymphatic tuberculosis and sarcoidosis

Mtb is thought to latently infect approximately one third of the world's population [254]. Whilst active pulmonary disease is the major route of transmission, extra-pulmonary manifestations are common — with TB of the lymph node being the most frequent [422]. *Mtb* bacilli are transported to the lymph node in order to prime the adaptive immune system, although it has been suggested that this process might be part of the bacterial strategy for accessing distinct anatomical sites — with lymph nodes representing a gateway [265]. In comparison with tuberculosis, sarcoidosis is a granulomatous disease of unknown aetiology; however it shares a range of immunological and histopathological features in common with tuberculosis — including the formation of granulomas within the intrathoracic lymph nodes.

MAIT cells are an innate-like cell subset, with an emerging role in the immunology of various infectious diseases, including tuberculosis, and inflammatory disorders. Despite the relative lack of abundance of MAIT cells at lymphatic sites, MAIT cells express several chemokine receptors implicated in T cell recruitment in tuberculosis [134, 156, 291]. With access to clinical EBUS-TBNA samples from patients with tuberculosis and sarcoidosis, it was hypothesised that MAIT cells are recruited to the lymphatic site of disease in patients with TB, but not in sarcoidosis patients — who share similar histopathological features, but lack detectable *Mtb*.

6.5.1.1 MAIT cells are present in the blood and lymph nodes in LNTB

Assessment of the peripheral blood of LNTB and sarcoidosis patients revealed that, in fact, MAIT cells were relatively depleted in sarcoidosis patients — but not those with LNTB. Several studies have indicated that MAIT cells are depleted in the blood of patients with active, but not latent tuberculosis — suggesting their ability to home to sites of infection. However, Jiang *et al.* found that MAIT cells were depleted in the peripheral blood of both *Mtb* sputum positive and negative TB patients; and not those defined in their study as latently infected (LTBI). These individuals exhibited relatively normal peripheral MAIT cell frequencies relative to healthy control subjects [220], indicating a threshold of pathology required to induce a substantive MAIT cell depletion, which was not met in LTBI. In this study of LNTB patients, MAIT cells were not depleted from the periphery, consistent with a relatively low gross burden of pathology. Interestingly, this suggests overlap between patients typically defined as latently infected, those with sub-clinical TB, and those with LNTB. In comparison with tonsillar lymphoid tissue; MAIT cells were also increased in frequency in the intrathoracic lymph nodes of LNTB patients — but not those with sarcoidosis, supporting the hypothesis that MAIT cells are recruited to the ITLN in patients with LNTB.

There are several potential caveats worth noting. One is that tonsillar tissue may differ in MAIT cell composition relative to healthy ITLN — MAIT cells may be present at higher numbers within the ITLN of healthy subjects than in tonsillar tissue. Secondly, it is plausible that matched blood and lymph node samples from a healthy control group could show more distinct differences than between LNTB and sarcoidosis patients, as both of these groups exhibited lymphadenopathy. Thirdly, through assessing paired lymph node and blood MAIT cell frequencies within the same individuals, it was evident that in some patients there were few ITLN MAIT cells; whilst in others they were comparable with the peripheral blood. This was observed to some degree in both patient groups. The explanation for this is not

clear, however heterogeneity between patient phenotypes may account for some of the difference. Alternatively, MAIT cells may preferentially accumulate within specific regions of the lymph node. In this case the specific region of the lymph node sampled may affect the frequency of MAIT cells detected. Of note, the CD161 ligand LLT1 was recently found to be expressed by B cells localised to the germinal centre in tonsillar tissue [423]. Whether ITLN MAIT cells can preferentially accumulate within discrete regions richer in LLT1, such as the germinal centre, is not known.

6.5.1.2 MAIT cell frequencies in the ITLN reflect those in the blood

Given this, data from both patient groups were pooled and assessed together in order to ascertain whether there were any shared features that coincided with high frequencies of MAIT cells within the lymph nodes. Interestingly, there was little to suggest that histopathological features were responsible. By contrast, patients with higher frequencies of lymph node MAIT cells had higher frequencies of circulating MAIT cells, and were on average 15 years younger. It has been observed elsewhere that circulating MAIT cell frequencies decline with age [139, 424, 425]. Despite their presence in the ITLN of certain patients, it is possible that this reflects their relative abundance in the peripheral circulation — as opposed to specific homing in response to inflammatory signals.

In a recent study performed by Eberhard *et al.*, the frequency of MAIT cells in the blood and lymph nodes of HIV patients were assessed, with the finding that both were depleted of MAIT cells and that, furthermore, this correlated with higher levels of MAIT cell activation [175]. The absence of paired samples in that study precluded assessment of the relationship between MAIT cell frequency in the peripheral circulation, and in the lymph nodes within the same individuals. A strength of this study was the assessment of paired EBUS-TBNA and PBMC samples, indicating that irrespective of *Mtb*-infection — high frequencies of MAIT cells within the intrathoracic lymph nodes can be predicted through assessment of the frequencies in the peripheral blood (Fig. 6.5 B). The frequencies of MAIT cells in the peripheral blood vary between individuals in health, and typically diminish in disease. An implication of this data therefore, is that MAIT cell presence in the lymph nodes varies alongside that of the blood, and diminishes in in old age and disease.

6.5.1.3 Systemic and local MAIT cell expression of CD69 in LNTB

In both sarcoidosis and LNTB patients, a substantial proportion (> 60%) of lymph node MAIT cells were $CD69^+$, demonstrating that MAIT cells present in the ITLN in both patient groups exhibited signs of activation. Similarly, peripheral blood MAIT cells from both patient groups also exhibited an increase in frequency of CD69-expression, in comparison to healthy control subjects. Bulk T cells from both patient groups also exhibited signs of activation (approx. 40% $CD69^+$) within the lymph nodes — whilst within PBMCs there were very few bulk T cells expressing CD69. Therefore, in both tuberculous and sarcoid lymphadenopathy, bulk T cells — including MAIT cells — present at the site of disease exhibit signs of activation; whilst, MAIT cell — and not bulk T cell — activation is evident in the peripheral blood.

The explanation for this is not clear. One possibility is that CD69-expressing T cells in the lymph node are retained there whilst MAIT cells, by contrast, may preferentially relocate back to the circulation. This would enable their detection as an increase in $CD69^+$ MAIT cells in PBMC. Alternatively, peripheral blood MAIT cells may express CD69 in response to soluble mediators in the serum; and so MAIT cells in the ITLN and in PBMCs may represent distinct groups. Of note, a recent study investigating soluble mediators within the peripheral blood of tubercular lymphadenopathy patients identified raised serum levels of a number of cytokines — including IL-12 and IL-18 [426]. These cytokines are able to induce CD69 on MAIT cells in a dose-dependent manner, independent of TCR stimulation (see Chapter 3.4.1).

6.5.1.4 MAIT cell CD4-expression is increased in sarcoidosis

In sarcoidosis patients with lymphadenopathy, there were two observations of note. Firstly, there appeared to be a depletion of peripheral blood MAIT cells. This has been reported in a large variety of conditions including those due to infection, chronic inflammation and cancer (see Table 1.2, p. 27). In most cases, MAIT cell depletion has been most commonly attributed to MAIT cells homing to pathological sites and/or their activation induced cell death. In this study, no enrichment was seen in the ITLNs in sarcoidosis relative to peripheral blood of the same patients, or compared to tonsillar tissue from anonymous donors. However this does not rule out migration of MAIT cells to additional sites of pulmonary pathology. To assess this, additional investigations in sarcoidosis such as those of the lung mucosal surfaces via assessment of bronchoalveolar lavage may be insightful.

The second observation was that there was a significant increase in the relative frequency of $CD4^+$ MAIT cells in the circulation in sarcoidosis. An important caveat to note regarding this observation is that $CD4^+$ MAIT cells were gated by virtue of expression of Vα7.2 TCR, CD3, CD4 and high levels of CD161, as has been reported elsewhere [425]. However, it is not possible to categorically confirm the identity of these cells as MAIT cells in the absence of an MR1 tetramer reagent. Nonetheless in a small number of patients the increase in CD4 co-receptor usage by MAIT cells was substantial. Overall, this may reflect the reported altered $CD4^+$:$CD8^+$ ratio of T cells in sarcoidosis [414] although $CD4^+$ MAIT cells have been reported to increase as a frequency of the total circulating MAIT cell population with age [425]. This possibility must be considered, as sarcoidosis patients in this study were on average older than the other patient groups. Whether the influence of age is sufficient to explain the effect size seen, is not clear. Interestingly, $CD4^+$ MAIT cells have also been observed to increase in liver diseases [392] although the functional relevance of co-receptor usage for MAIT cells in disease is not clear, and will require additional investigation.

6.5.1.5 The role of MAIT cells in LNTB and sarcoidosis

In the present study, MAIT cells were found to express CD69 in LNTB and sarcoidosis, and to be depleted in the blood of sarcoidosis patients. An important consideration to these findings are whether such changes in frequency and surface phenotype in MAIT cells are driven primarily by their role in the disease, or arise in response to other disease processes — whether the changes observed are likely to be cause or effect of the underlying immunopathology. Whilst the aetiology of sarcoidosis is not well understood, suggested triggers range from the environmental [427–429] to microbiological, including antigens derived from mycobacteria [430, 431]. Indeed, it has been argued that sarcoidosis and tuberculosis may coexist on opposite ends along a spectrum of disease [413]. Given the possible importance of microbial PAMPs in sarcoidosis, mechanisms of innate signalling have been investigated finding potential roles for PRRs, including TLR2 [432, 433] and TLRs 10, 1 and 6 [434].

Similar to the tuberculosis granulomatous response, sarcoid granuloma formation relies on the accumulation of T cells and macrophages, orchestrated through the presence of proinflammatory cytokines [435, 436]. Cytokines consistent with a type-1 response have been implicated — including IL-12 and IL-18 [437, 438], which can stimulate enhanced IFNγ expression from sarcoidosis patient BAL cells, relative to normal controls [439]. In blood, MAIT cells are the major T cell subset able to express IFNγ in response to IL-12 and IL-18 alone [93], which as shown in

Chapter 3 occurs on exposure to sufficiently high cytokine concentrations. Thus, in response to raised levels of IL-12/-18, the potential exists for MAIT cells to exacerbate the pro-inflammatory environment — the increased expression of CD69 on peripheral blood MAIT cells in sarcoidosis and LNTB patients is consistent with such a role. It is important to note, however, that data presented in Chapter 4.3.2 (p. 113) demonstrated the ability of MAIT cells to respond to soluble mediators in a cell-contact independent manner through expressing CD69, in the absence of expression of IFNγ or TNFα. Therefore, MAIT cell CD69 expression — in both LNTB and sarcoidosis, may alternatively demonstrate MAIT cell detection of soluble mediators related to the disease process, without in fact contributing further to the inflammatory milieu.

The role of CD69 following its expression has also not yet been fully defined, although an immunoregulatory function has been suggested [440]. In order to better understand the functional state of MAIT cells in *ex vivo* site of disease samples, alternative markers of activation with better characterised functions may be required. Granzyme B expression is one such marker of MAIT cell activation, which was recently demonstrated to be upregulated following exposure to bacteria in an MR1-dependent manner [168]; and by dengue virus, hepatitis C virus and influenza virus in a TCR-independent, cytokine dependent manner [206]. In addition to CD69 expression levels, assessing MAIT cell granzyme B expression levels may provide a further indication of the functional status of MAIT cells in LNTB and sarcoidosis.

In sarcoidosis patients, but not those with LNTB or healthy control subjects, a numerical deficiency of MAIT cells was observed. MAIT cells are particularly susceptible to activation induced cell death (AICD) following exposure to bacterial infection, and such AICD has been proposed as a mechanism for MAIT cell depletion in HIV infection [219]. In HIV, depletion of MAIT cells may indicate a role for MAIT cells in supporting the integrity of the gut mucosa, attempting to compensate for the loss of $CD4^+$ T cells [441]. Similar rationales have been employed broadly by investigators attempting to assess the role of MAIT cells in numerous other infectious and non-infectious chronic inflammatory states, with numerous investigators noting depletion of MAIT cells in diverse inflammatory processes (see Table 1.2, p. 27 for detailed summary). However, whilst commonly attributed as a sign of MAIT cell involvement in the disease process, resulting from either AICD of MAIT cells or homing to the affected tissues, the large number of such studies may well be indicative of a common effect secondary to primary immunopathology, for which MAIT cells are particularly sensitive. However, iNKT cells are an innate-like lymphocyte subset that exhibit similar numerical deficiencies in sarcoidosis, an

observation from which a protective immunoregulatory role has been suggested [442]. Whilst rare in humans relative to MAIT cells, murine iNKT cells are similarly capable of being activated through TCR and cytokine dependent mechanisms [443]. In addition to their numerical deficiency, iNKT cells in sarcoidosis demonstrate increased expression of CD69 and PD-1, and were less capable of expressing IFNγ alone or in combination with TNFα [444]. By analogy, given their absence in sarcoidosis, the loss of MAIT cell immunoregulatory function may be a contributing factor to the immunopathogenesis of sarcoidosis, although this does not necessarily follow from the present study and will need to be tested in future experiments.

Ultimately, the numerical deficiency of MAIT cells in sarcoidosis, and their expression of CD69 in both LNTB and sarcoidosis, indicates the active response of MAIT cells to signals present in both disease processes — but there are limitations with regards to interpreting what the nature of such active responses may be. $CD8^+$ T cells and iNKT cells have been shown to demonstrate anti-mycobacterial effector functions *in vitro* [341], with a protective role in TB indicated in particular for $CD8^+$ T cells through abrogation by anti-TNFα therapy [342] and depletion in the macaque model [334] resulting in enhanced risk of disease. MAIT cells may therefore participate in protective immune response in *Mtb* infection. Conversely, TNFα is considered to also be a key factor promoting granuloma formation in sarcoidosis [445], and MAIT cells could therefore contribute to sarcoidosis immunopathogenesis. Alternatively, their relative absence and CD69 expression may signify the loss of protective functions, as has been suggested with iNKT cells [442]. The exact nature of MAIT cell IFNγ and TNFα, and cytotoxic effector mechanisms, with regards to protection and pathogenesis in both TB and sarcoidosis will therefore need to be closely examined in future experiments. One important approach will be to abrogate or inhibit MAIT cells in animal models, for which protocols and reagents will need to be developed. In that regard, progress is being made — recently Greene *et al.* have published a study of MAIT cells in mycobacterial infection in nonhuman primates [393]. Future work in such models will be extremely valuable in delineating the role of MAIT cells, and understanding their contribution to both protective and pathogenic responses in LNTB and sarcoidosis — as well as many other of the disease states for which human MAIT cells have been found depleted from the peripheral blood compartment.

6.5.1.6 Summary

MAIT cells did not appear to be depleted from the peripheral circulation of LNTB patients, indicating that the burden of pathology required to induce a reduction in frequency of PBMC MAIT cells was not met — in line with a recent study of patients with LTBI [220]. Relatively high frequencies of MAIT cells were observed in some patients with LNTB — but also in some patients with sarcoidosis, with no obvious histopathological features to account for this. Indeed, the frequency of ITLN MAIT cells seems most strongly linked to the frequency of MAIT cells in the peripheral circulation. Nonetheless, MAIT cells present within the ITLN of LNTB patients exhibited signs of activation, suggesting their ability to participate in anti-*Mtb* responses at this site of disease. Similarly, MAIT cells present within the ITLN of sarcoidosis patients exhibited signs of activation, suggesting likewise a role in the inflammatory processes in sarcoid lymphadenopathy. Depletion of MAIT cells from the blood — whether due to age, HIV co-infection, or other causes — may further diminish the presence of MAIT cells from this anatomical niche, potentially leading to increased risk of dissemination and re-activation of disease. Animal studies could shed further light on the relative distribution of MAIT cells within the blood, lymph nodes and lung parenchyma, their functional abilities *in vivo*, and the pathological consequences of presence and absence from the lymph node. Potentially, *ex vivo* expansion of MAIT cells could represent a possible immunotherapeutic approach to eliminating mycobacterial infection of the lymph nodes, however further work will be required to confirm the ability of MAIT cells within the ITLN to mount protective, rather than pathogenic responses.

6.5.2 Chip cytometry for the assessment of EBUS-TBNA

Chip cytometry is a novel imaging based technique that could help in the investigation of small populations of cells from clinical patient samples. In order to assess the suitability of chip cytometry for the investigation of MAIT cells in LNTB, an antibody screen was initially performed in order to identify MAIT cell activation markers detectable following fixation with 4% PFA. The screen identified several markers of interest. CD69, CD71 (transferrin receptor) and CD25 (IL-2Rα) were induced by IL-12/-18 and/or TCR stimulation — and in response to BCG infected antigen presenting cells. CD71 induction is notable, as this has not yet been shown as an activation marker of MAIT cells — though consistent with observations made regarding general T cell activation [446].

Each of these markers — together with CD38, CD137 (4-1BB) and CD97 were then assessed for detection on $CD8^+$ T cells activated by TCR beads + IL-12/-18; and a MAIT cell detection panel for chip cytometry was developed and tested on PBMCs from patients with LNTB. Finally, MAIT cells were identified within the ITLN of LNTB patients, and the expression of these markers were assessed. Despite limited MAIT cell expression of these markers in the samples tested, some expression was detected for each marker on other cell subsets therefore demonstrating the potential for the technique in this setting.

6.5.2.1 Strengths and weaknesses of chip cytometry

One strength of the technology observed included the ability to store samples long-term, prior to antibody staining and imaging. Indeed, MAIT cells were identified within the PBMC and ITLN of LNTB patients approximately three months after the samples were taken. The ability to store chips long-term, bleach fluorophores, and re-stain is also extremely useful in permitting a 'stain-think-stain' approach. However, it became apparent that some markers were more sensitive to the extended fixation required to assess BSL3 samples than others. In particular, CD69 is expressed by a proportion of MAIT cells under basal conditions; was identified by the antibody screen as being detectable following PFA fixation; and successfully stained $CD8^+$ T cells by chip cytometry following *in vitro* stimulation. However, staining for CD69 failed to convincingly identify activated cells within ITLN samples — despite the large proportion of T cells expressing CD69 within the ITLN (Fig. 6.3, p. 191), therefore indicating sensitivity to extended PFA fixation.

Furthermore, the technique is extremely slow. Whilst 100,000 events can be collected by flow cytometry within minutes — the same number of events take approximately two hours to image by chip cytometry, which is therefore more suited to analysis of small numbers of samples. In the future, it will be possible to modify the experimental approach to make the most of the technology. Bar-coding should be possible, by labelling cells from different samples with different fluorophores prior to immobilisation on the microfluidic chip — and this will increase the efficiency of the imaging. Reducing the fixation time will also enable the use of antibodies detected by the antibody screen — and wider use will identify further reagents amenable to the technique, which were not known during this assessment.

Overall, the technique shows great potential for the analysis of small numbers of samples from important clinical samples, and should be a valuable tool for complementing the use of flow cytometry, conventional microscopy and gene expression studies in the future. Establishing a library of antibodies amenable to detecting PFA-fixed epitopes should be helpful for future users of the technology (see Appendix A).

6.5.3 Conclusions

This chapter hypothesised that MAIT cells would be depleted from the blood, and enriched in the lymph nodes of LNTB, but not sarcoidosis patients. In fact, MAIT cells were present in the blood at normal numbers in LNTB patients, whilst depleted in the sarcoidosis patients — and in both patient groups, some individuals were observed with high frequencies of ITLN MAIT cells; approximately in line with the frequency of MAIT cells in the peripheral blood. Assessment of CD69-expression of MAIT cells indicated activation in both patient groups within the ITLN; and in the peripheral blood relative to healthy controls. Together these data argue against specific MAIT cell homing to the ITLN during lymphadenopathy. MAIT cells are capable of exhibiting many of the T cell effector mechanisms that could result in *Mtb* sterilisation, and in this light the lymph nodes may represent a niche that MAIT cells find difficult to infiltrate. Nonetheless, in donors with high frequencies of peripheral MAIT cells, MAIT cells were observed within the ITLN; where they exhibit an activated phenotype, suggesting that, where present, they may play an active role.

MAIT cells have been show to be depleted early on from the peripheral blood of HIV patients [183, 219], and a recent study indicated their loss also from the lymph nodes [175]. Data in in this study indicate these two are strongly linked within individuals. Furthermore, *Mtb*-infection of the ITLN did not appear to attract large numbers of MAIT cells, where they were few in the periphery. Therefore loss of MAIT cells from blood and lymph nodes in HIV infection, is likely to remove MAIT cells non-reversibly from this niche. This may be an important contributing factor to the early increase in risk of reactivation of tuberculosis seen in HIV patients. Future studies will be required to better understand the functional role of MAIT cells in lymphatic tuberculosis, and as MAIT cells presence within the ITLN appears to reflect frequencies in the blood, enhancing MAIT cell frequencies in the blood could represent a potential future immunotherapeutic strategy.

6.5.3.1 Summary of findings

- MAIT cells are present in the blood of LNTB patients at normal frequencies, but exhibit an activated phenotype.
- MAIT cells are depleted in the blood of sarcoidosis patients, where they exhibit an increase in the use of the CD4-co-receptor.
- The $CD4^+$ MAIT cells present in sarcoidosis patients do not exhibit an activated phenotype.

- MAIT cells are present in the ITLN in both LNTB and sarcoidosis patients — in numbers that reflect circulating MAIT cell frequencies.
- MAIT cells within the ITLN express CD69; indicating that they may play an active role in the immunopathophysiology of tuberculosis and sarcoidosis.
- Chip cytometry is a novel technique with applicability in the assessment of the presence of cell subsets and their activation status in site of disease clinical samples.

7 Discussion

Contents

7.1 Activation of MAIT cells 224
7.1.1 MAIT activation signals vary by effector function 225
7.1.2 MAIT cells exhibit several levels of activation 226
7.1.3 MAIT cell 'bystander' activation? 229
7.2 The role of MAIT cells in tuberculosis 232
7.2.1 MAIT cells in TB may require IL-12/-18 and MR1 . . . 233
7.2.2 MAIT cells in tuberculous and sarcoid lymphadenitis . 235
7.2.3 Caveats 238
7.2.4 Future perspectives 241
7.3 Summary 247

7.1 Activation of MAIT cells

MAIT cells are a population of innate-like lymphocytes, typically abundant in the circulation and tissues. They possess the capacity to be activated by two distinct mechanisms; TCR stimulation, via MR1 presentation of antigen — and independently of TCR involvement, by IL-12 + IL-18. The pre-existence of large numbers of MAIT cells, and their ability to respond to cytokines expressed following PRR ligation suggests an important role for MAIT cells in the innate phase of the immune response to bacteria, viruses and fungi. Distinguishing conceptually between TCR and cytokine mediated stimulation enables convenient assessment of activation, function and role. However, it is unlikely that these signals arise in isolation. Riboflavin synthesising bacteria are likely to trigger innate PRRs during infection, resulting in the presence of numerous cytokines as well as MR1-Ag complexes. Similarly, commensal sources of vitamin B_2 derivatives may be sufficient for MAIT cell activation during chronic inflammation and infection by non-riboflavin synthesising microbes or viruses. Therefore, the context of activation — including the cytokines present, timing of exposure and proximity to sources of both cytokine and MR1 are each likely to prominently influence the immunopathological role of MAIT cells *in vivo*. From the results within this thesis, there are several themes regarding the activation of MAIT cells and their role in infection, inflammation and immunity — in particular:

- Different TCR and cytokine requirements for different effector functions.
- Exquisite sensitivity to low concentrations of cytokine following TCR ligation.
- Different modes of activation for intermediate and high levels of cytokine expression.
- MAIT cell anergy in response to sustained TCR signalling.
- The relevance of proximity and cell contact for TCR independent MAIT cell activation.

7.1.1 MAIT activation signals vary by effector function

Through expression of their semi-invariant Vα7.2$^+$ TCR, MAIT cells possess the ability to recognise conserved antigens resembling molecular patterns via MR1 [32]. This canonical TCR therefore affords MAIT cells the opportunity to respond to activation by a diverse array of microbes in a highly specific, targeted manner,

under the regulation of the MR1 antigen presentation pathway. However, in apparent conflict between the ability of MAIT cells to respond to bacteria via MR1, MAIT cells have been reported as relatively resistant to TCR stimulation for IFNγ expression [138, 140, 356, 357].

In this thesis, $CD161^{++}$/MAIT cells indeed appeared anergic with respect to IFNγ expression in response to TCR stimulation with αCD2/3/28 coated beads alone, indicating that TCR crosslinking and CD28 co-stimulation are not sufficient for MAIT cell IFNγ expression. However, MAIT cells placed onto an artificial bilayer with mono-biotinylated ICAM-1 and αCD3 Fab fragments freely, and rapidly (within minutes), formed immunological synapses with distinct distal, peripheral and central SMACs visible — demonstrating the functional machinery immediately downstream of TCR ligation. Additionally, αCD2/3/28 mediated stimulation resulted in near uniform expression of CD69 by MAIT cells within 24 hours — with a proportion of MAIT cells capable of a rapid, transient burst of TNFα-expression within 5 hours, and upregulation of CD25 and CD71 within 24 hours. From this, we can conclude that MAIT cells are not refractory to TCR ligation, but highly responsive — depending on the functional readout.

Additionally, MR1 signalling was necessary for TNFα induction by BCG infected APCs, further corroborating the importance of the MAIT cell TCR in response to bacterial infection. This is in line with previous studies, which have reported MR1 dependent activation of MAIT cells in response to bacterial challenge [138, 178], and the importance of MR1 in Granzyme B upregulation and degranulation [168]. Recently a separate study similarly found TNFα-expression to occur transiently within 6 hours of αCD3/28 stimulation of sorted MAIT cells from three donors. Interestingly, a limited and transient IFNγ-response in response to αCD3/28 stimulation was also observed, consistent with the early response to bacteria reported in this thesis, but not evident in the response to αCD2/3/28 beads. The reasons for this discrepancy are not clear, but may be accounted for by experimental variations including the strength of stimulus provided by different TCR bead formulations, using sorted vs. enriched cells, and/or differences in electronic gating strategies. Overall, TCR ligation in the absence of cytokines is sufficient to induce immediate MAIT cell immunological synapse formation, and rapid, but transient effector function within 5 hours.

7.1.2 MAIT cells exhibit several levels of activation

With regards to the role of MAIT cells in infection, the quality of effector function is also important. The use of flow cytometry for assessment of T cell cytokine expression enables single cell resolution, as opposed to a pooled average determined through supernatant analysis by ELISA. Cytokine expression by flow cytometry, however, is often assessed as binary; above or below a threshold. In this study, the proportion of responding cells, and the magnitude of their response were both assessed, using the GMFI of IFNγ and TNFα staining as a proxy for cytokine expression intensity on a *per cell* basis. Interestingly, three levels of activation were resolved for both IFNγ and TNFα expression — off (IFNγ/TNFα^{-}), intermediate (IFNγ/TNFα^{int}) and high (IFNγ/TNFα^{hi}).

Notably, sustained exposure to high concentrations of IL-12/-18 was sufficient for IFNγ^{hi}, and CD69 expression, but not TNFα expression or Vα7.2 downregulation. TCR ligation licensed additional CD161^{++}/MAIT cells to express IFNγ, but with minimal enhancement to IFNγ expression at high concentrations of IL-12/-18, where responding cells were already capable of expressing high levels. In the absence of TCR ligation, CD161^{++}/MAIT cells were unable to respond to low levels of IL-12/-18 — however, by contrast, in combination with TCR crosslinking, cells were able to respond to to low levels of IL-12/-18 by expressing intermediate levels of IFNγ (Fig. 7.1).

TNFα-expression required TCR ligation and was induced rapidly — however, high expression of TNFα occurred only for CD161^{++}/MAIT cells pre-stimulated with IL-12/-18. In the absence of prior IL-12/-18, a burst of TNFα secretion still occurred within 5 hours — but transiently, and at intermediate levels only. CD161^{++}/MAIT cells therefore appear sensitive to IL-12/-18 stimulation for excitement to a higher energy state — whilst a key role of TCR ligation appears to be the release of cytokine expression at a level determined by this energy state.

iNKT cell anergy has been reported in response to robust TCR and costimulatory signalling [447]. Following exposure to plate bound αCD3/28 in this study, CD161^{++}/MAIT cells became anergic to TNFα expression in response to further TCR signalling + IL-12/-18. IFNγ and CD69 expression, by contrast, were unaffected. TCR downregulation occurred in response to both sustained TCR and cytokine signalling, and may represent functional exhaustion. Through reducing TCR surface expression levels, this may also represent a mechanism for the self-limitation of the MAIT cell TNFα and cytotoxic response.

In summary, these findings show that cytokine signals are important for tuning the MAIT cell response in the context of MR1 presentation of antigen. In the

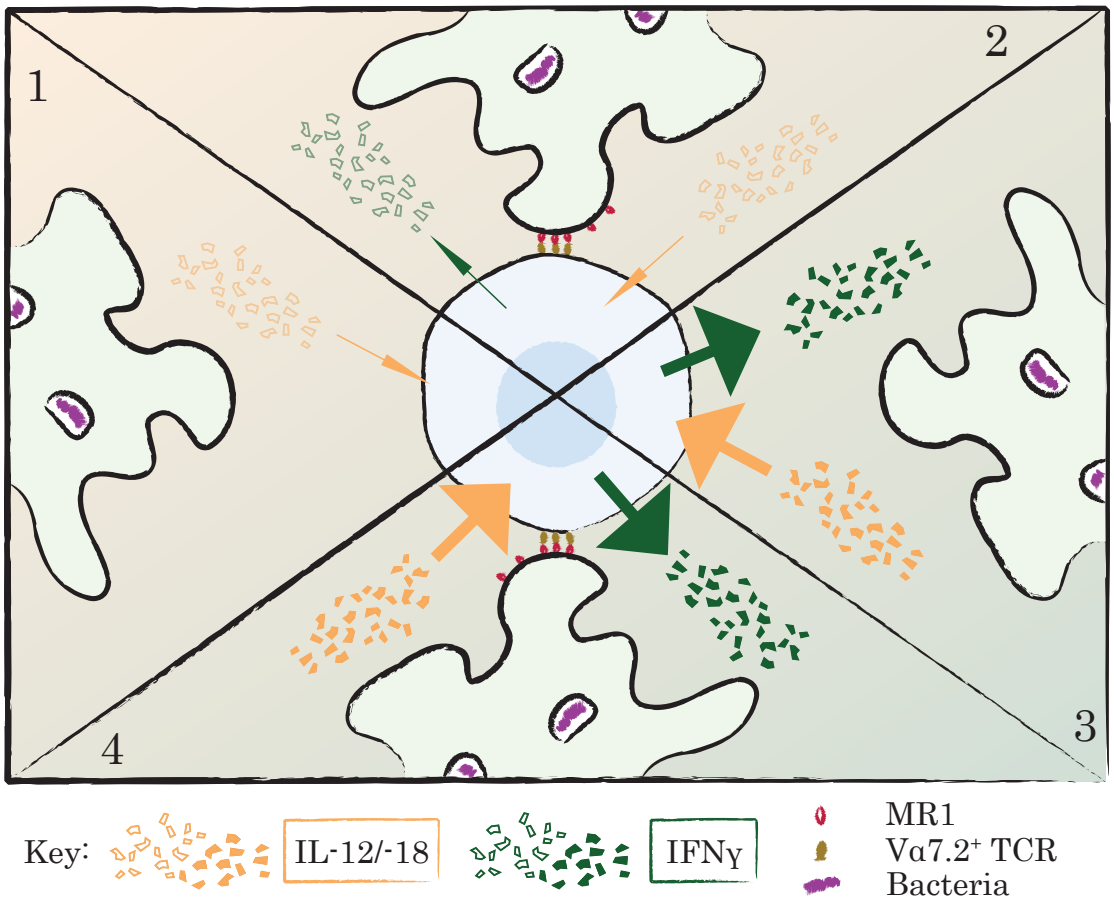


Figure 7.1: Modes of IL-12/-18 dependent IFNγ-expression by MAIT cells. Depending on the presence/absence of TCR signal, and the concentration of cytokines, MAIT cells can undergo several modes of activation for IFNγ-expression. (1) In the absence of TCR ligation, MAIT cells are unable to express IFNγ in response to low concentrations of IL-12/-18. (2) In the presence of TCR ligation, MAIT cells can detect low concentrations of IL-12/-18, and can respond by expressing IFNγ^{int}. (3) In the absence of TCR ligation, MAIT cells can detect high concentrations of IL-12/-18, and can respond by expressing IFNγ^{hi}. (4) In the presence of TCR ligation, MAIT cells can detect high concentrations of IL-12/-18, but respond similarly by expressing IFNγ^{hi}.

absence of TCR ligation, a proportion of MAIT cells are able to express IFNγ in response to high concentrations of, and sustained exposure to IL-12/-18 alone. However, despite the ability to express CD69 and high levels of IFNγ under these conditions, TCR ligation is necessary for the expression of TNFα at high levels. In addition, TCR ligation is sufficient for the detection of extremely low levels of IL-12/-18 by MAIT cells, which they can respond to through the expression of low/intermediate levels of IFNγ. Only in response to TCR ligation, and high concentrations of IL-12/-18 did MAIT cells robustly downregulate their TCR. Therefore, TCR stimulation and IL-12/-18 stimulation each contribute to the

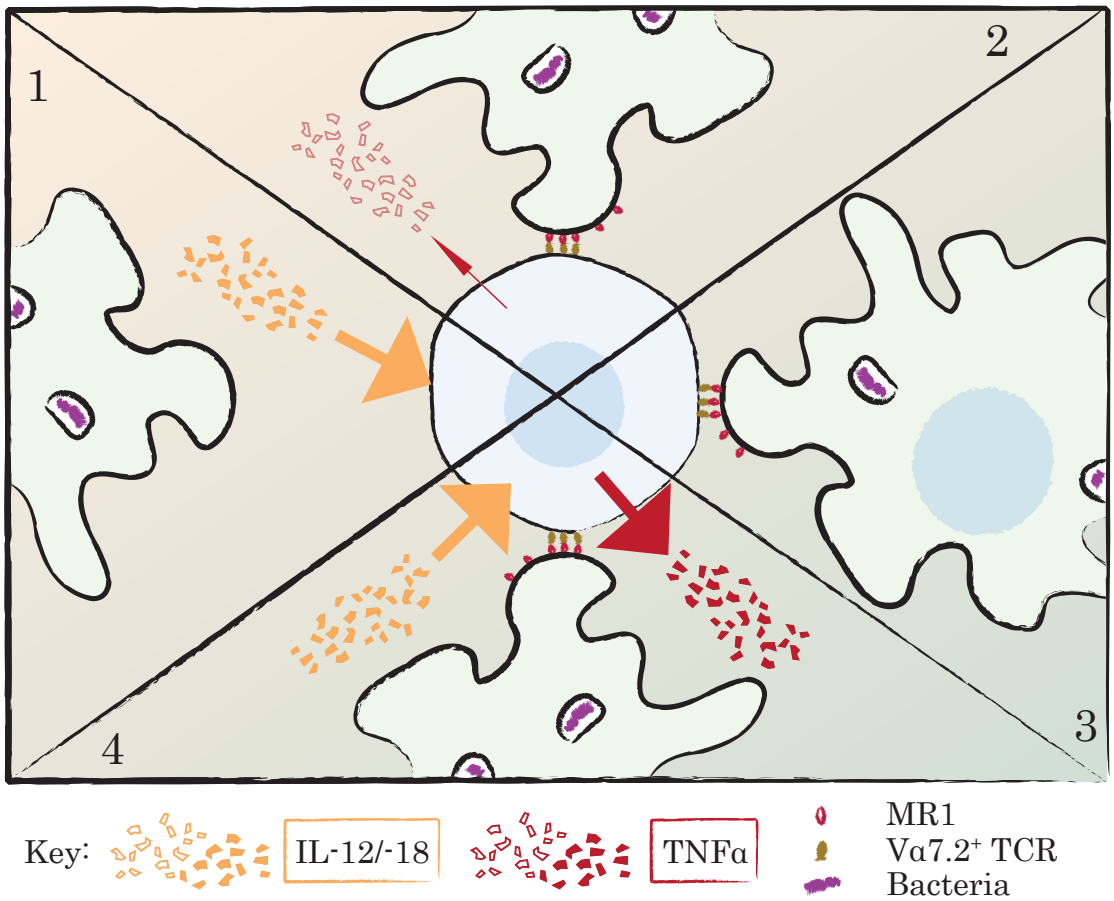


Figure 7.2: Modes of TCR and IL-12/-18 dependent TNFα-expression by MAIT cells. Depending on the nature of TCR stimulus, and the presence of cytokines, MAIT cells can undergo several modes of activation for TNFα-expression. (1) In the absence of TCR ligation, MAIT cells are unable to express TNFα in response to even higher concentrations of IL-12/-18. (2) Following TCR ligation in the absence of cytokines, MAIT cells rapidly respond to TCR ligation to express TNFα^{int}. (3) Following an initial TCR ligation event, MAIT cells become anergic to TCR stimulation for further expression of TNFα. (4) Following sustained exposure to high concentrations of IL-12/-18, MAIT cells respond rapidly to TCR ligation to express TNFα^{hi}.

quality of the MAIT cell response, which may have implications for MAIT cell involvement in both protective and pathogenic immune responses.

7.1.3 MAIT cell 'bystander' activation?

An additional theme assessed within this thesis was the proximity to sources of cytokine, and the potential significance of the immunological synapse for targeted delivery of cytokine. Interestingly, despite a lack of IFNγ-expression in response to TCR stimulation alone, the presence of extremely low concentrations (picograms per ml) of IL-12 were sufficient to induce IFNγ^{int}-expression from αCD2/3/28

stimulated CD161^{++}/MAIT cells. It was hypothesised that a mechanism by which extremely low levels of cytokine may have an enhanced effect on MAIT cell activation would be though enrichment of cytokine receptors — specifically IL-18Rα — at the immunological synapse (IS) during the process of TCR ligation. Indeed the presence of IL-18Rα at the IS was confirmed with TIRF microscopy, with IL-18Rα visible in the cSMAC, pSMAC and dSMAC regions. In the absence of TCR signalling, however, IL-18Rα was also observed to be distributed throughout the interfacial region between bilayer and MAIT cell. Confocal microscopy additionally confirmed the presence of IL-18Rα across the entirety of the MAIT cell surface, irrespective of TCR ligation. The preferential accumulation of downstream signalling molecules, such as MyD88, at the immunological synapse following TCR ligation remain to be assessed.

TCR-independent, and bystander activation are terms often used interchangeably. One consequence of the finding that high cytokine concentrations are required for TCR independent activation, is to emphasise the distinction between the two. During chronic inflammation tissue cytokine concentrations may reach levels sufficient to induce TCR-independent activation of MAIT cells, leading to bystander involvement of MAIT cells. Alternatively, active recruitment of MAIT cells may lead to their physical association with pathogen infected cells. MAIT cell association with artificial bilayers occurred in the presence of LFA-1–ICAM-1 interactions, and MAIT cells may similarly associate with APCs infected with non-riboflavin synthesising bacteria, and viruses. Indeed, almost all MAIT cells in the liver express LFA-1 [392]. The presence of IL-18Rα at the interfacial region between MAIT cells and cytokine secreting APC is consistent with an ability to detect cytokines at a high local concentration during cell–cell contact, reducing the APC IL-12/-18 expression levels required for TCR-independent MAIT cell activation.

MAIT cells have been shown recently to exert antiviral effector functions in response to IL-12/-18 stimulation [206]. The restriction of this mode of activation to high IL-12/-18 concentrations, and the presence of IL-18Rα at the cell-bilayer interface, are consistent with the ability to specifically target virally infected cells with IFNγ in such a TCR-independent, non bystander manner. In that respect, it is notable that despite provision of αCD2/3/28 beads, MAIT cells separated from bacteria-fed APCs by a transwell were not activated to the same extent as during cell–cell contact, emphasising the role of proximity in MAIT cell activation. However, TCR ligation may also increase the available pool of MAIT cells capable of responding in this way, as shown by licensing MAIT cells for subsequent TCR-independent activation by pre-stimulation with αCD3/28 coated plates. Therefore, MR1-dependent interactions with commensal organism-derived

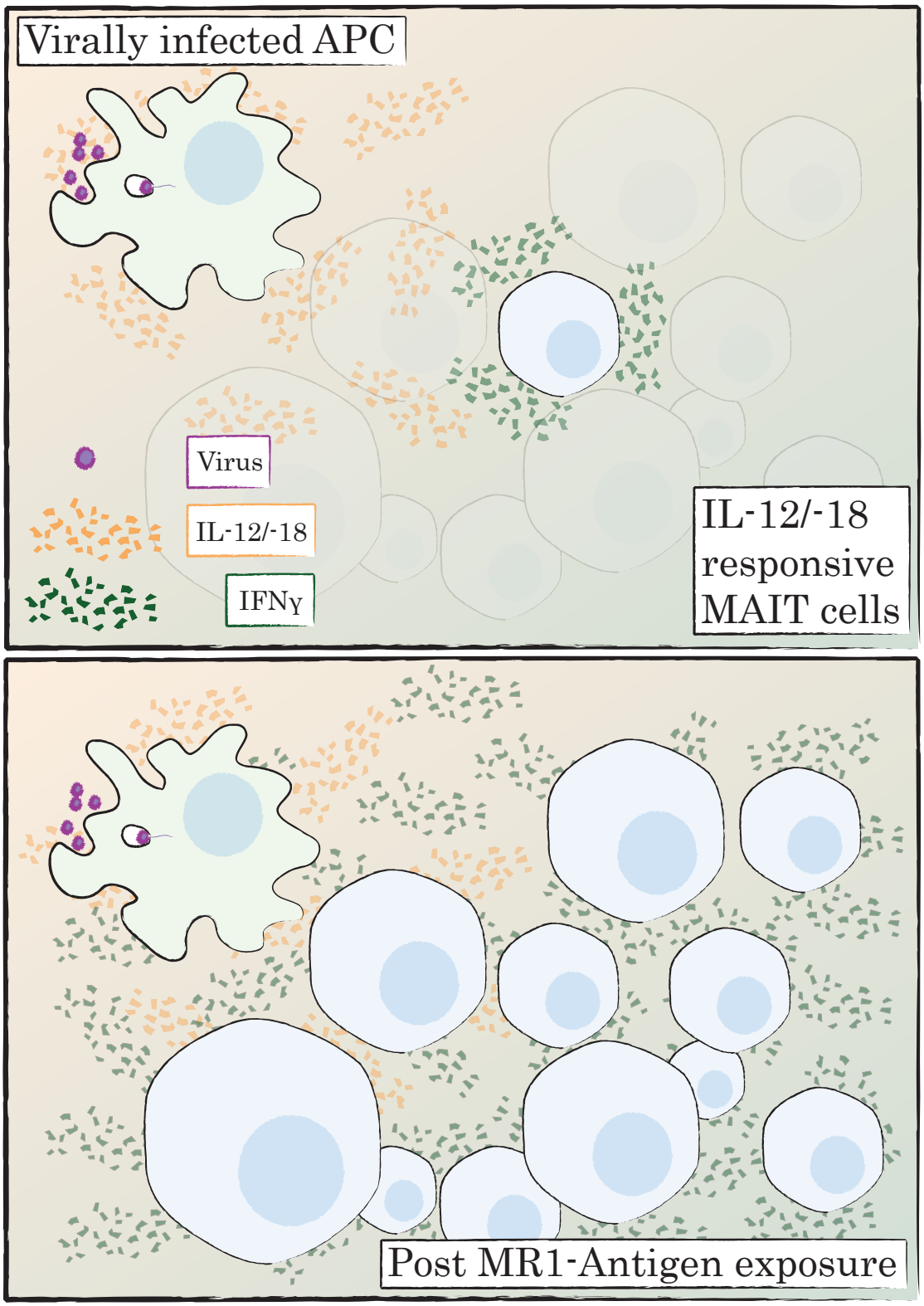


Figure 7.3: TCR ligation may license MAIT cells for cytokine-only activation by viruses. At steady state, a smaller proportion of circulating MAIT cells are responsive to IL-12/-18 stimulation (top). MR1 presentation of ligand derived from commensal sources, or bacterial/fungal co-infection may increase the pool of MAIT cells with capacity to respond to cytokines only (bottom). This may enhance local immunity, or cross over into driving pathogenesis in chronic inflammation.

antigen in the liver and lung may be sufficient to maintain a large pool of MAIT cells capable of associating with virally infected cells, and responding to viruses in a TCR-independent manner (Fig. 7.3). This supports a role for MAIT cells in the immune response to viruses [93, 203, 206].

7.2 The role of MAIT cells in tuberculosis

In this thesis, the MR1 and IL-12/-18 dependence of MAIT cell activation by BCG and *Mtb* were assessed, together with the ability of primary human MAIT cells to inhibit *Mtb* in an *in vitro* intracellular infection model. MAIT cells were found to respond robustly to cells infected with BCG or *Mtb*, and both MR1 and IL-12/-18 played non-redundant roles, according to the time-point and effector mechanisms investigated. In the intracellular infection model, fewer *Mtb* were recovered on lysis of intracellularly infected cells, indicating MAIT cell suppression of *Mtb*. Additionally, the presence and activation status of MAIT cells within the lymph nodes of patients with tuberculous lymphadenitis were investigated, finding that MAIT cell presence in the intrathoracic lymph nodes (ITLN) varied according to their abundance as detected in the blood. Together, these findings are consistent with a protective role for MAIT cells in tuberculosis, and suggest the ability of MAIT cells to play a role in the lymph nodes in some tuberculosis patients with lymph node involvement, which has not previously been suggested.

7.2.1 MAIT cells in TB may require IL-12/-18 and MR1

Despite the fact that MR1-dependent activation by mycobacteria has been well-reported in humans [138, 178], IL-12 — not MR1 — was crucial for MAIT cell activation in a murine model of BCG infection [247]. Therefore, it was not clear whether this was a feature of the response to BCG, the use of a murine model, or whether human MAIT cells may exhibit a dependency on cytokines in response to *Mtb* that had not previously been appreciated.

In Chapter 5 infection of THP1 cells with mycobacteria induced a robust response from MAIT cells, irrespective of whether exposure was to attenuated *M. bovis* BCG, or virulent *Mtb* H37Rv. Furthermore, in both cases, MAIT cells demonstrated similar dependencies on MR1 and IL-12/-18 activating signals at the time points assessed. Blocking MR1 completely abrogated IFNγ-expression, TNFα-expression and degranulation of $CD161^{++}$/MAIT cells within 5 hours, demonstrating the necessity of TCR signalling for rapid MAIT cell effector function. Conversely, blocking IL-12/-18 had little effect on cells rapidly expressing IFNγ, TNFα, CD69 or

degranulating within 5 hours of exposure to BCG/*Mtb* demonstrating the IL-12/-18 independent nature of the induction of immediate MAIT cell effector functions (Fig. 7.4, p. 242). Although the proportion of responding cells was diminished, MAIT cell TNFα-expression following 20–24 hours exposure to *Mtb* or BCG remained wholly dependent on MR1, with similar effects seen for degranulation.

In the murine model of BCG infection by Chua *et al.*, blocking the IL-12p40 signal inhibited MAIT cell expression of IFNγ, whilst MR1 blockade did not [247]. Those findings are consistent with the ones presented in this thesis. MAIT cell expression of IFNγ in response to *Mtb* and BCG here was entirely dependent on MR1 only within the first 5 hours. Importantly, at this time point, IFNγ expression *per cell*, and the frequency of MAIT cells capable of responding are relatively low. Over time, both increase — and activation of MAIT cells beyond 5 hours becomes dependent on the IL-12/-18 cytokine signal. In the study by Chua *et al.*, the MAIT cell *in vitro* control of mycobacterial growth was dependent on IL-12p40 in experiments lasting 72h [247].

In this thesis, the ability of human MAIT cells to suppress intracellular virulent *Mtb* over 24h was investigated. THP1 cells were infected with the virulent strain H37Rv, and MAIT cells were added at various E:T ratios. A linear trend was evident, with MAIT cells found to be capable of limiting the recovery of viable *Mtb* CFUs in a dose-dependent manner. From this experiment it is not possible to say with certainty which mechanisms were responsible — however the 24 hour time point assessed may have allowed insufficient time for the activation of infected THP1 cells via IL-12/-18 and IFNγ dependent mechanisms. In light of the kinetics of MAIT cell activation assessed in other experiments, MAIT cell cytotoxicity via degranulation and TNFα expression may have been involved. However, it seems reasonable to expect that with long-culture times, human MAIT cells may similarly rely on IL-12/-18 rather than MR1 for the suppression of *Mtb in vitro* through their ability to express IFNγ robustly in response to *Mtb*-infected cells.

Beyond the ability to directly suppress *Mtb*, a hallmark of human TB are well formed granulomas that can constrain bacilli; or, become necrotic and breakdown, leading to their release [260]. Therefore, in addition to the ability of MAIT cells to suppress mycobacteria via IL-12-dependent IFNγ-mediated mechanisms, additional MAIT cell functions — in particular those supporting granuloma integrity — may play an important role in controlling *Mtb* infection in humans. TNFα in particular is understood to play a key role in the initiation and maintenance of the TB granuloma [329], and so this function of MAIT cells may be important in the earliest stages of granuloma formation, before the influx of adaptive T cells. MAIT

cell TNFα-expression was strongly dependent on MR1 function in all of the *in vitro* experiments in this thesis, suggesting that the MR1 signal may be crucial for any role MAIT cells play at the tuberculosis granuloma. Intriguingly, the rapid induction of MAIT cell TNFα expression appears to result in subsequent anergy with respect to further TNFα expression, and conversely this may ultimately limit the influence of MAIT cell provision of TNFα during chronic *Mtb* infection. Thus, the patient-specific abundance of MAIT cells, and the ability of circulating MAIT cells to traffic to sites of infection, to replace anergic MAIT cells, may be an important factor in the importance of MR1 signal.

The role of cytokines in the activation of MAIT cells by mycobacteria, therefore, is not a feature only of non-virulent mycobacteria; or specific to the use of a murine model — but is a previously unappreciated mechanism for activation of human MAIT cells by *Mtb*. Furthermore, data presented in this thesis has highlighted the dual role of MR1 and IL-12/-18 signals for a full range of MAIT cell IFNγ, TNFα and degranulation responses to *Mtb*. The MR1 signal is important for the rapid activation of MAIT cells, and is key, in particular for TNFα and degranulation. The IL-12/-18 signal, by contrast, is important for robust IFNγ expression after 20–24 hours — but also for the strongest MAIT cell TNFα-expression, for which pre-exposure to cytokines play an important role. Therefore, both cytokine and MR1 signals may play important roles in the induction of MAIT cell function for effective anti-*Mtb* immunity, and the control of *Mtb* during early infection.

7.2.2 MAIT cells in tuberculous and sarcoid lymphadenitis

Lymphatic TB is a common manifestation of extrapulmonary TB, representing approximately 40% of cases [422]. However, MAIT cells do not typically express lymph node homing markers [134, 156], and are not normally found in the lymph nodes in large numbers [13, 134, 173, 175]. In this thesis, the presence and activation status of MAIT cells were assessed during lymphatic TB by flow cytometry with the following observations:

Enrichment MAIT cells are present in the intrathoracic lymph nodes (ITLN) of TB patients at similar levels to those within the blood — enriched relative to tonsillar tissue, but not compared to the ITLN of sarcoidosis patients.

Depletion Within the blood, MAIT cells were not depleted during LNTB, relative to healthy controls. By contrast, MAIT cells were depleted in the blood of sarcoidosis patients.

Activation MAIT cells in the ITLN of either LNTB or sarcoidosis patients expressed CD69, although the frequency of $CD69^+$ MAIT cells was not significantly increased over those of bulk T cells. Within the blood, MAIT cell expression of CD69 was increased in both LNTB and sarcoidosis patients over those of healthy controls.

Co-receptor usage In sarcoidosis, there was more prevalent use of the CD4 co-receptor by MAIT cells, over that seen in LNTB or healthy patients.

Together, these results indicate that MAIT cells can enter the ITLN where they may be able to participate in the local immune response to *Mtb*. Their lack of depletion in the blood, however, and lack of enrichment relative to blood, suggest that MAIT cells are not recruited in large numbers to the ITLN. One implication of the link between levels of MAIT cells within the blood and within ITLN, is that depletion of MAIT cells in the periphery due to infection and inflammation is likely to result in depletion within the ITLN. Indeed, this has been shown for HIV-infection, where MAIT cells are depleted in both the blood and lymph nodes [175]. The risk of developing extrapulmonary TB is increased in HIV/AIDS [448], which can be attributed to low $CD4^+$ T cell counts [449]. However, following the trafficking of *Mtb* bacilli to the lymph nodes early in infection, it is not clear what impact MAIT cell depletion from the blood and lymph nodes may have. In light of their ability to express IFNγ and TNFα, and to suppress *Mtb in vitro*, it is possible that fewer MAIT cells would result in a further delay to *Mtb* control, and therefore increased bacterial burdens within the infected lymph node. Alternatively, other innate and innate-like cell types such as NK cells, γδ T cells and/or iNKT cells exhibit anti-*Mtb* effector functions [388, 450–454] and may play redundant or non-redundant roles with MAIT cells in the ITLN in LNTB.

In LNTB patients, MAIT cell expression of CD69 in the blood was elevated, although their frequencies in the blood were comparable with the healthy control group. However, in pulmonary active TB, MAIT cells have been reported as exhibiting signs of functional exhaustion, through reduced ability to express IFNγ and increased expression of PD-1 and CD69 [171, 207]. Following depletion of MAIT cells in other infectious diseases, residual MAIT cells are also reported to exhibit signs of reduced responsiveness to MR1; expressing diminished IFNγ, TNFα, GrzB upregulation and degranulation [212, 216]. MAIT cells are capable of an early burst of cytokine production in an TCR dependent manner, however the ability to respond subsequently depends on the cytokine assessed, as TNFα is not expressed by MAIT cells after a primary TCR stimulation event. Macaques undergoing

TNFα neutralisation are at greater risk of reactivation of TB — with reactivation frequently occurring first in the ITLNs [321]. Despite their variable presence, MAIT cells may provide TNFα in the ITLN following initial TCR ligation events, and therefore their functional exhaustion, and reduced expression of TNFα over time could be associated with increased reactivation of disease during latency.

In addition to tuberculosis, sarcoidosis is a major cause of granulomatous lymphadenitis, and both share many similarities in their respective gene expression profiles in blood and at the site of disease [415, 416, 455, 456]. In comparison to tuberculosis, however, no role for MAIT cells in sarcoidosis has yet been described. Interestingly, in this study, MAIT cells were depleted in blood and found to disproportionately express the CD4 co-receptor. Expression of various transcription factors have been compared between $CD8^+$, DN and $CD4^+$ MAIT cells with no difference seen between $CD8^+$ and DN MAIT cells, but with both expressing higher levels of PLZF, RORγt, Eomes and Helios (but not T-bet) compared to $CD4^+$ MAIT cells [163]. Therefore, there may be a functional consequence of this skewing of co-receptor usage. Notably, MAIT cell frequencies were diminished in sarcoidosis — it is possible that $CD8^+$ and DN MAIT cells were preferentially lost, enriching the remaining MAIT cells for $CD4^+$ MAIT cells.

In addition to the potential influence of age (discussed in Chapter 6.5.1, p. 210), a further caveat is that in the absence of MR1-tetramer staining, it is not possible to definitively prove the identity of $CD4^+$ $CD161^{++}$ $V\alpha7.2^+$ T cells as MAIT cells. Indeed, germline-encoded mycolyl-reactive (GEM) T cells are a recently characterised CD1b-restricted unconventional T cell subset which use the CD4 co-receptor and share expression of $V\alpha7.2^+$ TCR with MAIT cells [457]. Further work will be required to confirm the identity of these cells as $CD4^+$ MAIT cells, and to better understand the importance of their increased presence with regards to cause and effect in sarcoidosis, as well as any further functional consequences.

7.2.3 Caveats

There are several caveats to data presented within this thesis worth discussing. In order to assess the mechanisms of activation of $CD161^{++}$/MAIT cells by bacteria and ability of MAIT cells to demonstrate an anti-mycobacterial effect, THP1 cells were used. THP1 cells are derived from the blood of a child with acute monocytic leukaemia [458], and the same biological changes which enable their growth in lab culture conditions may alter their function in responding to infection and activating MAIT cells. Future experiments using primary macrophages may be of interest to assess the induction of primary monocyte-derived macrophage activation and

suppression of *Mtb* by MAIT cells. Nonetheless, the use of long-lived cell lines widely employed by other research groups are extremely useful for providing consistency and a bench-mark between experiments.

Assays assessing the viability of mycobacteria remain a gold standard for the investigation of new anti-*Mtb* drugs, or the anti-*Mtb* functional capabilities of immune effector cells [459]. In order to assess the anti-*Mtb* effector functions of primary human MAIT cells, an intracellular infection model followed by colony counting on solid 7H10 media was developed. Several technical challenges were observed during the optimisation process regarding the balance between enabling sufficient effect sizes to be observed — for which larger experiments, greater E:T ratios, and higher bacterial loads are desired — whilst on the other needing to maximise viability of infected APCs for the duration of the experiment. The ability to adjust these experimental conditions is hampered by the slow growing nature of *Mtb*, which can take up to 4 weeks.

A benefit of using solid media to grow *Mtb* is that single *Mtb* bacilli can be detected, however other techniques such as liquid culture using the Mycobacterial Growth Indicator Tube (MGIT), PCR such as Xpert MTB/RIF, tritiated uracil incorporation or luminescence reporting may be appropriate alternatives with more rapid turnaround times for future experiments, enabling better optimisation of experimental conditions [460]. Future MAIT cell anti-*Mtb* assays could also use IL-15 to expand MAIT cells *in vitro* — access to greater numbers of MAIT cells should allow experiments with larger numbers of infected APCs, whilst permitting a reduction in the MOI used. Reducing the MOI in turn may allow longer culture times, enabling further assessment of the impact of MAIT cells on the intracellular growth of *Mtb*, and the mechanisms involved — in particular the importance of IL-12/-18 in the induction of later, more sustained MAIT cell anti-*Mtb* function.

Through removing the supernatant (for cytokine analysis), and assessing viable bacteria present only in the adherent macrophages, a broad anti-mycobacterial effect was tested. It is possible that some viable *Mtb* bacilli were released by dead and dying macrophages following interaction with MAIT cells, in which case the manner of their release from the macrophages may be important for the outcome of infection *in vivo* and will also be important to assess. Virulent strains of *Mtb*, including H37Rv, are capable of inducing necrotic cell death [461], whilst MAIT cells upregulate Granzyme B and express TNFα, and as such are capable of inducing apoptotic target cell death of bacterially infected cells [163]. Apoptotic rather than necrotic cell death of *Mtb* infected macrophages is more likely to lead to control of infection [462], including through the subsequent engulfment of apoptotic

cells by uninfected macrophages in a process termed efferocytosis [403]. Further experiments may be required to reveal whether MAIT cells are capable of inducing either apoptotic or necrotic cell death of *Mtb* infected macrophages.

A caveat of the EBUS data regards the clinical diagnostic criteria available for use, in particular arising from diagnostic challenges from patients with lymphadenopathy and suspected tuberculosis. Patients undergoing diagnostic EBUS procedures for suspected tuberculous lymphadenitis may present with few symptoms, which may occur in other conditions. Sarcoidosis, cancer and infection by alternative pathogens are examples of differential diagnoses. LNTB may also represent a disease subtype overlapping with both LTBI and subclinical 'percolating' TB [268], in which *Mtb* are in a more contained state, yet nonetheless replicating and inducing local immune responses [463]. Following assessment of EBUS-TBNA by cytology, the presence of epitheloid cell granulomas, giant cells and necrotic material are used to inform a diagnosis of TB. The gold standard remains the culture of viable mycobacteria, although this is not always possible [448].

On review of the 15 LNTB patients in the study in this thesis, one was re-classified as latent TB (LTBI), whilst four additional patients failed to provide positive TB cultures and so were diagnosed with TB based on further clinical signs and epidemiological information. In view of the heterogeneity of patient phenotype, and ambiguities regarding classification, the inclusion criteria used in Chapter 6.2 were kept broad. Re-analyses of the data with stricter inclusion criteria were also performed, excluding the LTBI patient (see Appendix B.1, p. 282) and the four additional *Mtb*-culture negative LNTB patients (see Appendix B.2, p. 283). Removing these patients reduced the cohort size and affected the power of the statistical tests, although the interpretation and conclusions remain the same.

More broadly, patient heterogeneity incorporates many distinct elements, including age, gender, ethnicity, distinct pathological features, co-morbidities, past morbidities and intercurrent or previous treatment — all of which might influence the data obtained. Additional future studies will help to confirm these findings, considering these complexities. Nevertheless, this is the first assessment of MAIT cells within the intrathoracic lymph node of patients with TB — and the first examination of MAIT cells in sarcoidosis.

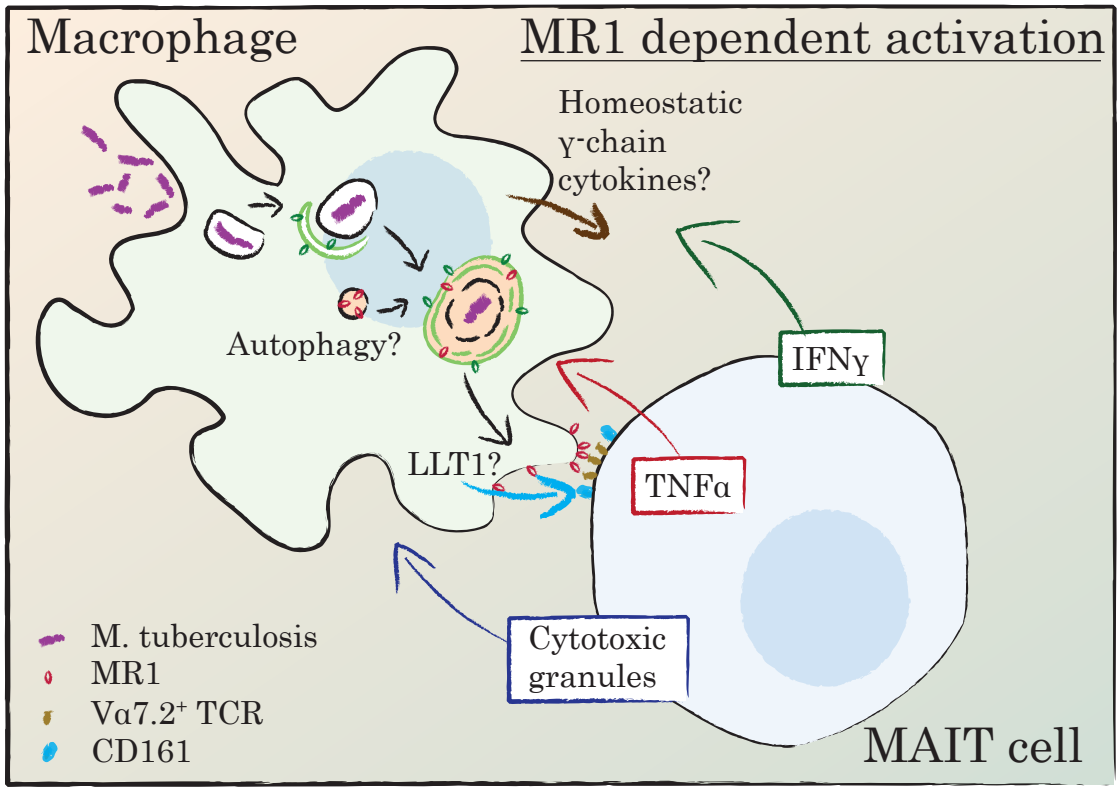


Figure 7.4: Future perspectives relating to MAIT cell activation by *Mtb*. MAIT cells are activated rapidly via TCR–MR1 interactions to express TNFα, IFNγ and to degranulate. It is not yet known whether MR1 antigen processing intersects with autophagy for access of *Mtb* ligands. CD161 also relocalises to the distal SMAC on formation of the MAIT cell immunological synapse, however it is not clear whether there is a functional role for LLT1 in MAIT cell activation by *Mtb*. Lastly, activation by BCG or *Mtb* — whilst inducing robust expression, did not lead to down-regulation of the MAIT cell TCR. Whether this is under the influence of homeostatic γ-chain cytokines is not known.

7.2.4 Future perspectives

Work in this study has shown that during TCR stimulation, MAIT cells are sensitive to extremely low levels of IL-12/-18, and are able to express increased IFNγ as exposure to IL-12/-18 rises. Importantly, IL-18 availability is limited not just by inflammasome activation and extent of release from activated cells, but also through the mediation of IL-18 binding-protein (IL-18BP), which functions to neutralise IL-18 following its release from activated cells [464]. The abundance of IL-18BP during TB is therefore of relevance with regards to the IL-12/-18 dependent activation of MAIT cells. As it may form an important balance for the extent of MAIT cell IFNγ expression during *Mtb*-infection, the role of IL-18BP in modulating MAIT cell function in TB should be assessed in future studies.

Interestingly, in response to mycobacteria, Vα7.2 TCR downregulation was not observed, despite robust Vα7.2 TCR downregulation in response to PFA-fixed *E. coli*. The reason for this is not clear, but could be due to sub-optimal stimulation of MAIT cells by live mycobacteria relative to the fixed *E. coli*. Alternatively, it may hint at the ability of MAIT cells to respond to additional signals induced by live bacteria/mycobacteria for the maintenance of surface TCR expression. Of relevance, MAIT cell TCR upregulation has been demonstrated through exogenous exposure to the homeostatic cytokine IL-7 [170]. Similarly, despite the inability of IL-12/-18 to induce MAIT cell activation with 5 hours, additional signals could be necessary — if not sufficient — for the immediate/early activation of MAIT cells in response to *Mtb*. In particular, IL-15 has been reported to enhance earlier TCR driven expression of IFNγ [172], and can also synergise with IL-12 and/or IL-12/-18 for IFNγ induction of MAIT cells [174, 206], whilst interestingly the common γ-chain receptor used by IL-15 is reduced in TB patients, but not healthy controls [171] .

TIRF microscopy revealed the localisation of CD161 to the dSMAC zone following TCR ligation of MAIT cells. It is possible, therefore, that CD161 plays a role in the TCR driven, rapid, response of MAIT cells to *Mtb*. The ligand for CD161 — LLT1 — can be expressed by macrophages [465] and the respiratory epithelium [466]; and is induced following TLR2/6 stimulation and IFNγ exposure during infection [466, 467] — all of which play important roles during *Mtb*-infection. The functional effect of CD161 ligation on MAIT cells is still controversial, however, and has been reported to enhance [136, 142] and diminish [147, 149] cytokine production. Future studies should provide some clarity on the role of CD161 and LLT1 during MAIT cell activation in TB (Fig. 7.4).

7.2.4.1 MR1 antigen processing and presentation in *Mtb* infection

The kinetics of MAIT cell TCR driven cytokine expression suggest an important rate-limiting role for MR1 antigen processing and presentation. It will therefore be important to better understand the impact of host–pathogen interactions on MR1 ligand acquisition during *Mtb*-infection. Differences in the kinetics of MR1 surface expression have been shown for MR1 antigens derived exogenously vs. those derived from invasive bacteria — as well as for stimulatory vs. non-stimulatory antigens [33, 119]. Whether intracellular *Mtb* produces distinct variations of MR1 antigen, with unique properties will need to be assessed. As well as the rate of cell surface transit, variations in MR1 antigens derived from *Mtb* versus other sources may lead to differential contacts with MAIT cell TCRs [359] potentially influencing the pool of responsive MAIT cells, and their effector functions.

Mtb employs numerous immune evasion strategies, including many targeting MHC class I, class II, and CD1 antigen processing and presentation pathways [384]. As yet unidentified *Mtb* immune evasion strategies targeting MR1 may also exist. Autophagy is a key process induced during *Mtb* infection, through which *Mtb* delivery to the lysosome is enhanced [24, 281]. Both MHC class I and II antigen presentation by macrophages is diminished in the absence of autophagy [468], which may similarly be important for presentation of antigen by MR1 during *Mtb*. Of note, loss of autophagy can also increase expression of IL-18 and other inflammatory cytokines [468, 469], and therefore autophagy may serve a dual purpose in the regulation of MAIT cell activation through both TCR-dependent, and independent mechanisms. Further investigations will be important to understand the importance of autophagy for MAIT cell activation in TB (Fig. 7.4).

7.2.4.2 Research priorities arising from the present study

In the early part of this thesis, the characteristic ability of MAIT cells to respond to IL-12 + IL-18 stimulation was investigated, in particular focussing on the effect of IL-12/-18 signal strength and the importance of the timing and order of cytokine and TCR signals for effector function induction. The TCR signal was found necessary for rapid function, and important for expression of TNFα, whilst the cytokine signal was found necessary for robust activation and prolonged IFNγ expression. An important effect was also seen in terms of enhanced sensitivity of MAIT cells to IL-12/-18 detection, with picograms/ml of cytokine sufficient following TCR ligation.

The surface expression of MR1 by APCs following bacterial exposure has been shown to be tightly regulated and dependent on TLR signalling [121], whilst a recent gene association study has identified an MR1 single-nucleotide polymorphism (rs1052632) with a link to MR1 gene expression associated with susceptibility to TB in a Vietnamese cohort [470]. In the context of these recent findings, an important consequence of the data presented in this thesis is that altered surface expression of MR1–ligand complexes, or affinity of ligand bound MR1 for the MAIT cell TCR, whilst likely to affect the pool of functionally responsive MAIT cells — will nonetheless remain highly dependent on the bioavailability of inflammatory cytokine signals for the induction of high intensity IFNγ and TNFα responses.

Manipulation of the MR1–TCR interaction, however, may represent a practicable option for either sensitising or de-sensitising MAIT cells to such inflammatory signals. Despite the highly conserved nature of MR1 [471], the full range of possible MR1 ligands remains to be fully defined [112]. Nonetheless, the capacity of MR1 to bind small molecules — and indeed the high sequence and structural conservation of MR1

— raises the possibility that therapeutic manipulation of MAIT cell function can be achieved via synthetic agonist binding. Indeed, through the use of *in silico* discovery approaches, a number of drugs and related small molecules have recently been identified with the ability to bind MR1 and stimulate MAIT cells — interestingly including metabolites of diclofenac, a non-steroidal anti-inflammatory drug [472].

Given the integration of MAIT cell TCR and cytokine signals identified in the present study, assessing the influence of small molecule agonists and antagonists on MAIT cell cytokine-dependent function should be a research priority. Pharmacological manipulation of MAIT cell cytokine sensitivity, and the effects of delivering synthetic MR1 ligands in the context of inflammatory signals within animal models will be one important avenue of investigation. Similarly, it will be important to understand the effect of widely used small-molecule drugs with predicted or demonstrated MR1 binding ability, such as diclofenac, on the TCR-dependent and cytokine-dependent activation of MAIT cells — both for potential future therapeutic use, and also to understand off-target consequences in relation to MAIT cell function. Further down the line, the delivery of synthetic MR1 ligands and TLR agonists to manipulate MAIT cell numbers/function could be assessed in the context of novel vaccines and immunotherapies, potentially within the context of a broad range of human inflammatory and infectious disease.

In the second half of the thesis, the mechanisms of activation of MAIT cells in the context more specifically of bacterial infection was investigated, as well as their presence at the site of disease in tuberculous and sarcoid lymphadenitis. MAIT cells were identified in the lung draining lymph nodes in certain — but not all individuals with LNTB and sarcoidosis. These data were generated from samples taken by ultrasound-guided trans-bronchial fine-needle aspiration, and the exact region of the node sampled could be a factor in the variation of MAIT cell frequencies observed. An important step therefore, will be to determine the precise location of MAIT cells *ex vivo* in healthy lymph nodes, and those exhibiting granulomatous inflammation. In particular, this will help clarify their presence as being related to immunopathology, or due to a biological role within lymph nodes that is yet to be described. The presence of MAIT cells within some affected lymph nodes and their expression of CD69, however, indicates a potential role for MAIT cells in granulomatous inflammatory responses.

In order to demonstrate this, future work should focus on assessing the presence function of MAIT cells in and around the granuloma. Unlike conventional effector-memory T cells which expand following exposure to cognate antigen in a primary infection, MAIT cells have the potential to participate in the earliest stages of

many disease processes by virtue of their already large numbers, due to expansion following exposure to commensal microorganisms during infancy [124]. They are therefore unsually placed amongst T cells in being able to participate in the earliest stages of inflammatory disease processes, such as those marked by granuloma formation. *In vitro* granuloma formation assays may help to identify the role of MAIT cells in granuloma formation, whilst IL-12/-18 and MR1 blockade would clarify dependency on TCR-dependent or independent mechanisms. Imaging of MAIT cells within granulomas *ex vivo* would provide evidence for affinity towards granulomatous inflammation in disease, and would place MAIT cells at a location where cytokine levels may be most likely to exceed the threshold required for high-intensity IFNγ and TNFα expression.

MAIT cells were able to diminish the recovery of viable *Mtb* from adherent THP1 cells in an intracellular infection model; but understanding the viability of bacilli released from THP1 cells following MAIT cell exposure is important for assessing the contribution of this MAIT cell effector function to protection versus pathogenesis. To the same end, *in vivo* animal — and, in particular macaque — infection models will be key. Abrogation of MAIT cells within macaques prior to *Mtb* exposure will shed light on their role in the earliest stages of infection, whilst their abrogation during latent infection should help to elucidate their functional role during *Mtb* latent infection. In addition to gross immunopathology and survival, bacillary loads — in particular of *Mtb* granulomas — will similarly provide important evidence on the effect of MAIT cell function with respect to events at the site of disease.

7.3 Summary

In this thesis, the requirement and sufficiency of pro-inflammatory cytokines IL-12 and IL-18, and TCR–MR1 signals for MAIT cell activation were assessed, together with the contact dependency of activation and events at the immunological synapse. The timing and signals involved in the MAIT cell response to *Mtb*, their ability to exert anti-mycobacterial effector functions and role in lymphatic tuberculosis were also investigated. MAIT cells were found to rapidly form a structured immunological synapse and to transiently express TNFα following TCR ligation. By contrast, in response to higher concentrations of IL-12/-18, they were able to express IFNγ independently of TCR signalling. In addition, these signals combined to enable increased TNFα-expression, and for MAIT cells to respond to pg/ml concentrations of IL-12/-18. MR1 signals were found to drive early activation of MAIT cells in response to BCG and *Mtb*, with IL-12/-18 required for sustained and robust

expression of IFNγ, and MAIT cells were found able to reduce the number of viable *Mtb* recovered from adherent THP1 cells in a 24h intracellular model of infection. In LNTB patients, MAIT cells were not depleted from the peripheral blood, whilst their presence in the intra-thoracic lymph nodes and expression of CD69 may indicate the capacity to contribute to localised immune responses. Lastly, MAIT cells were found to be depleted in the blood of sarcoidosis patients, with an increased use of the CD4 co-receptor observed.

Overall, this study describes the role of inflammatory IL-12/-18 signals in the induction of MAIT cell activation through TCR dependent, and independent mechanisms. IL-12 and IL-18 have the capacity to overcome an absence of MR1 signal for the activation of MAIT cells, as well as the ability to fine-tune MAIT cell effector function following TCR ligation. The contribution of MAIT cells to protection versus pathogenesis may therefore depend on the extent of exposure and proximity of MAIT cells to inflammatory signals *in vivo*. The increased expression of CD69 by MAIT cells in LNTB and sarcoidosis, and the depletion of MAIT cells in sarcoidosis are findings consistent with a specific role for MAIT cells in the primary immunopathology of these diseases, but which may nonetheless represent non-specific and/or systemic effects, secondary to the underlying disease. Therefore, the extent of the contribution of MAIT cells to either protective and/or pathogenic responses in tuberculosis, and the cause of the numerical deficiency of MAIT cells in sarcoidosis should be research priorities in future studies.

Appendices

A

BioLegend catalogue screen for PFA-stable epitopes

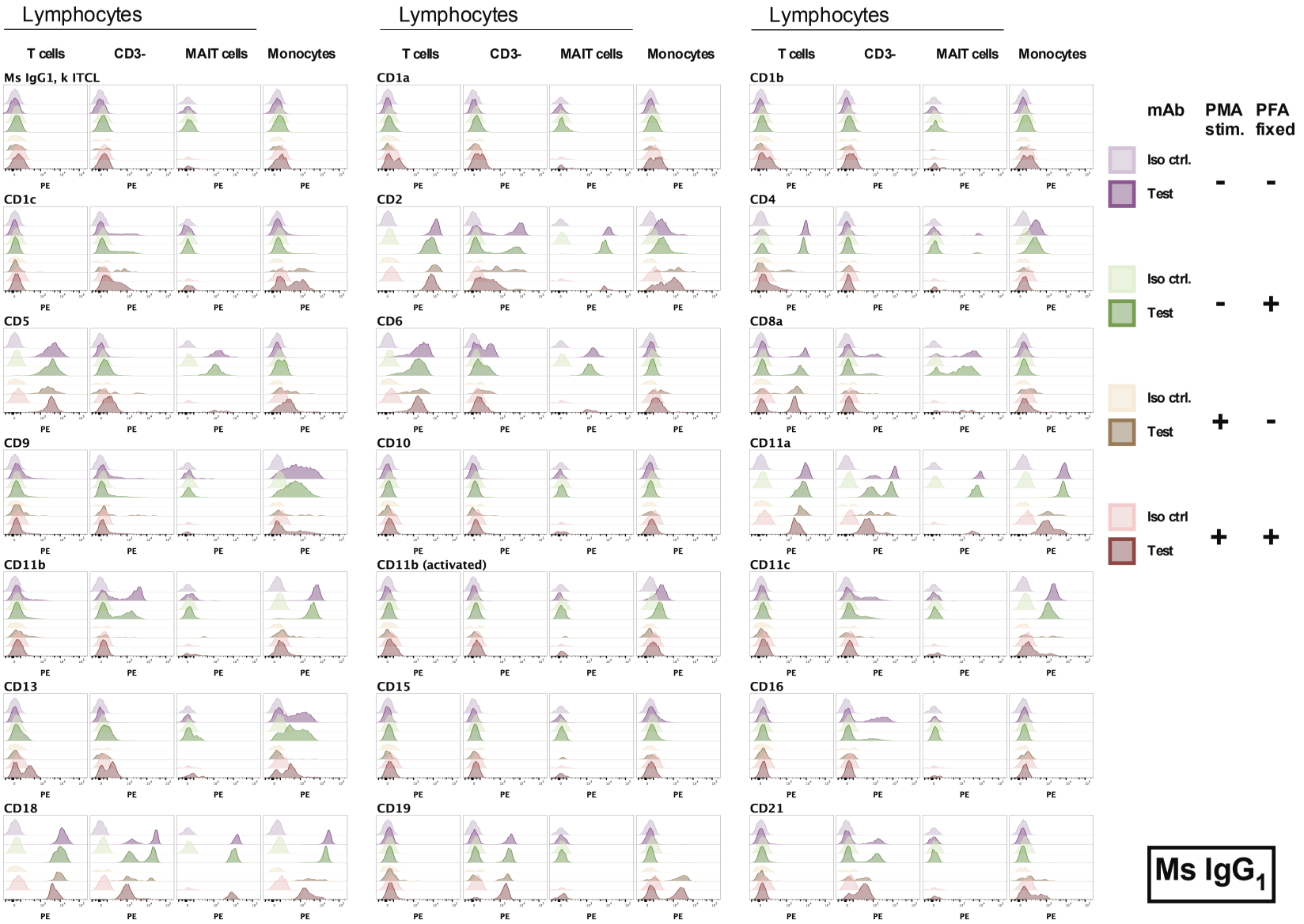
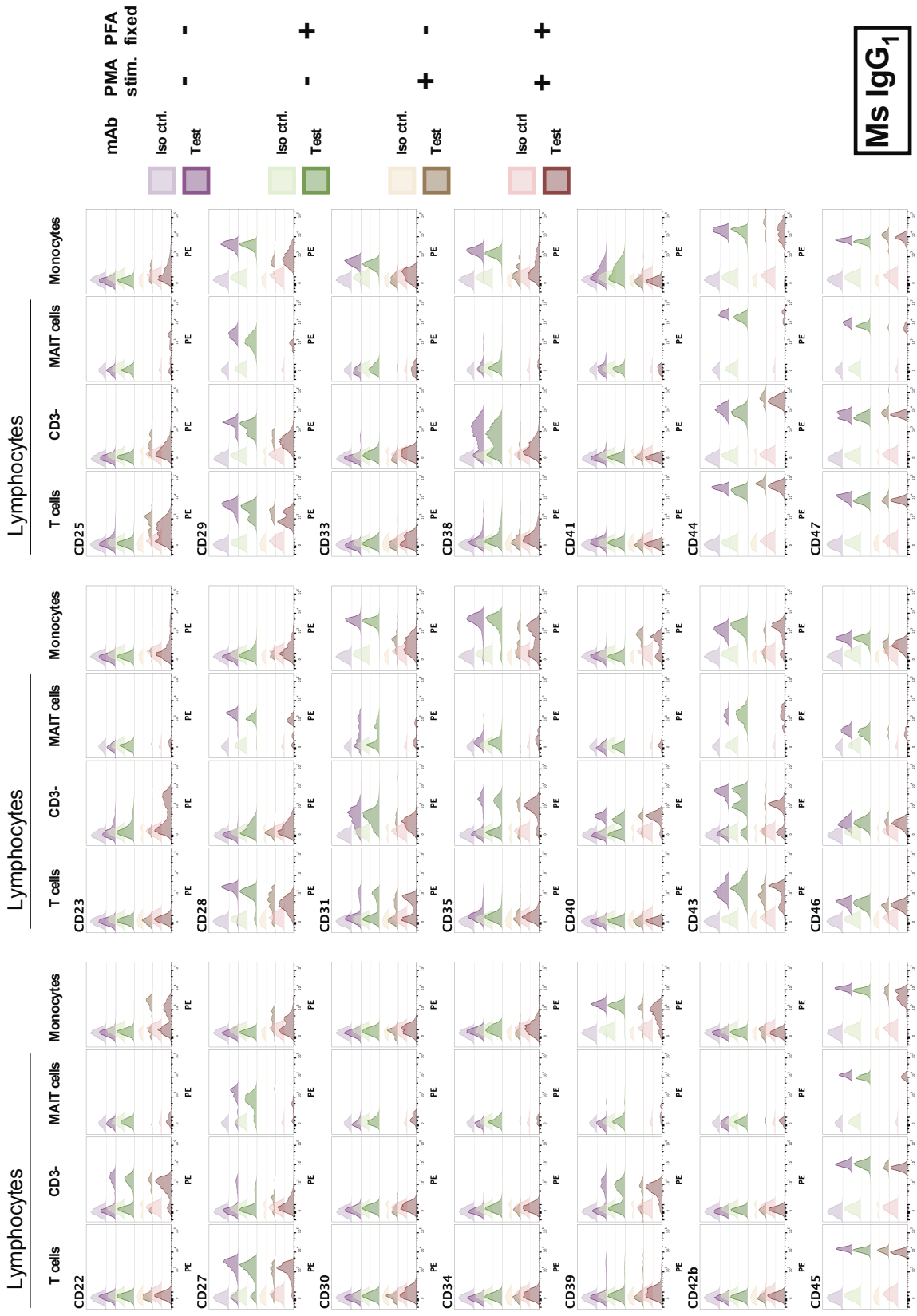
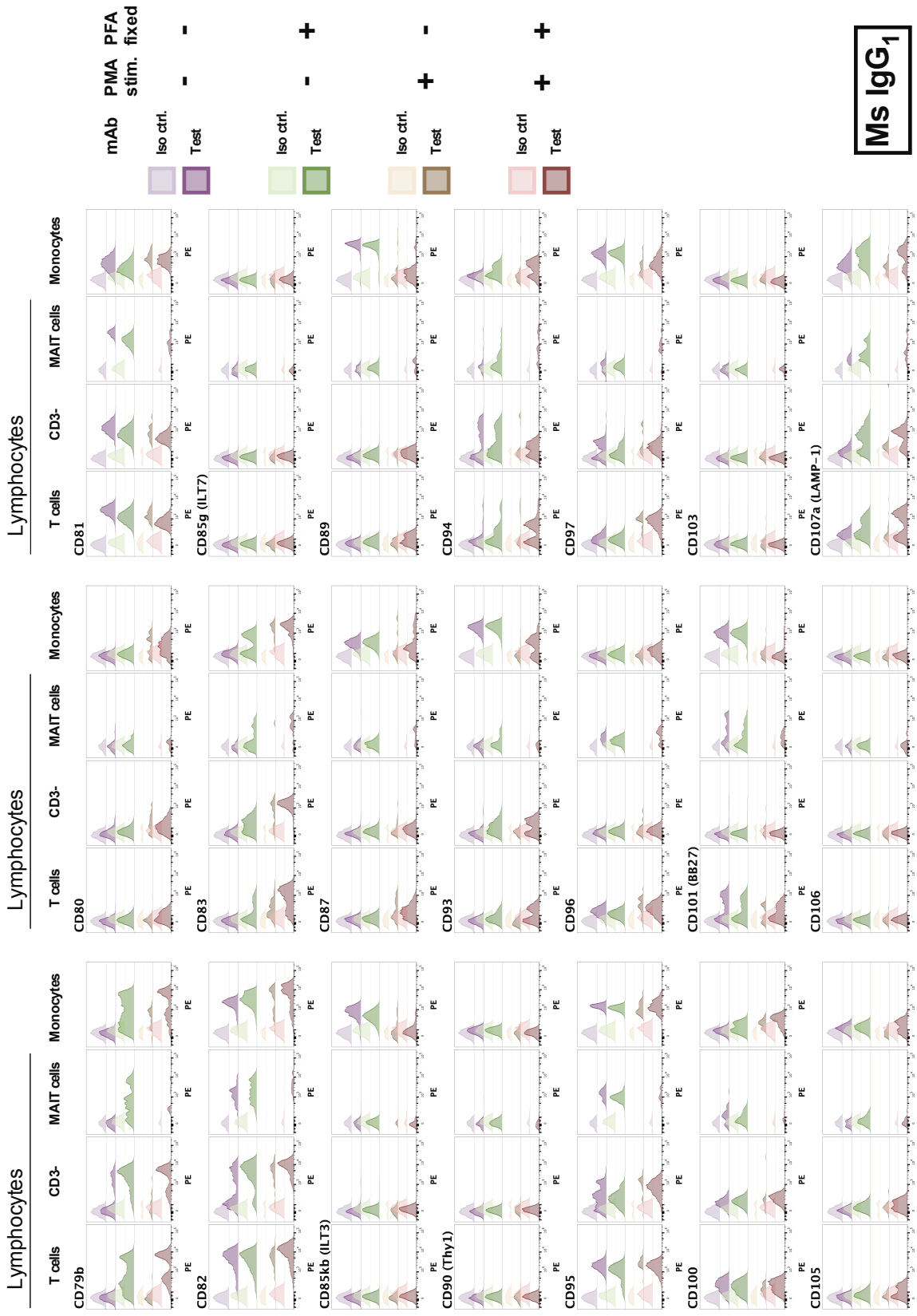


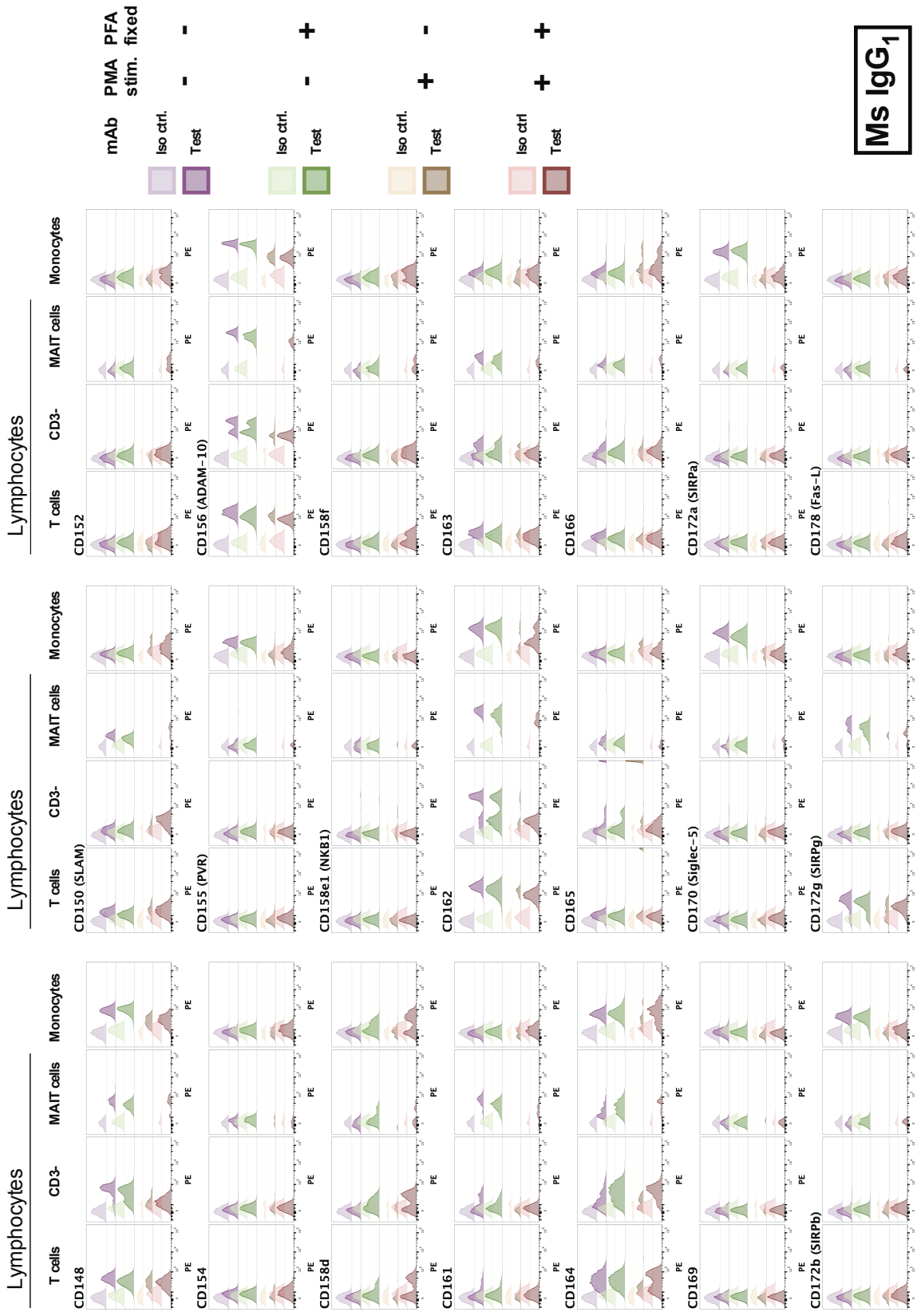
Figure A.1: MAIT cell IL-18Rα expression at the bilayer interface does not require TCR ligation.


Lymphocytes
T cells
CD3-
MAIT cells
Monocytes
CD22
CD23
CD25
CD27
CD28
CD29
CD30
CD31
CD33
CD34
CD35
CD38
CD39
CD40
CD41
CD42b
CD43
CD44
CD45
CD46
CD47
PE
mAb
PMA stim.
PFA fixed
Iso ctrl.
Test
Ms IgG1

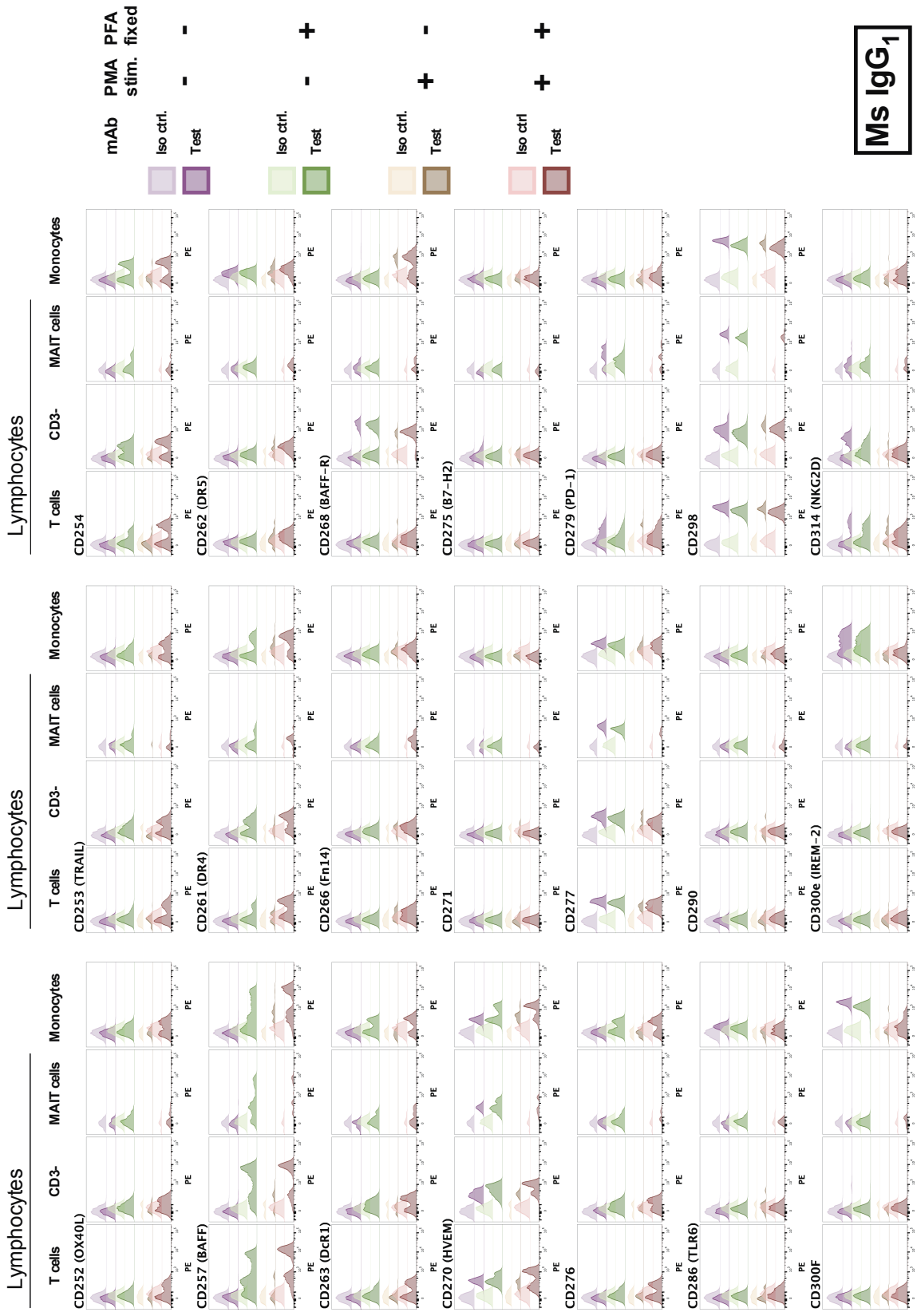
Lymphocytes
T cells
CD3-
MAIT cells
Monocytes
CD48
CD49a
CD49c
CD49d
CD50 (ICAM-3)
CD51_61
CD53
CD54
CD55
CD56 (NCAM)
CD58
CD61
CD62E
CD62L
CD62P (P-Selectin)
CD63
CD64
CD69
CD70
CD73
CD74
PE
mAb
PMA stim.
PFA fixed
Iso ctrl.
Test
Ms IgG1


Lymphocytes
T cells
CD3-
MAIT cells
Monocytes
CD79b
CD80
CD81
CD82
CD83
CD85g (ILT7)
CD85kb (ILT3)
CD87
CD89
CD90 (Thy1)
CD93
CD94
CD95
CD96
CD97
CD100
CD101 (BB27)
CD103
CD105
CD106
CD107a (LAMP-1)
PE
mAb
PMA stim.
PFA fixed
Iso ctrl.
Test
Iso ctrl
Ms IgG1

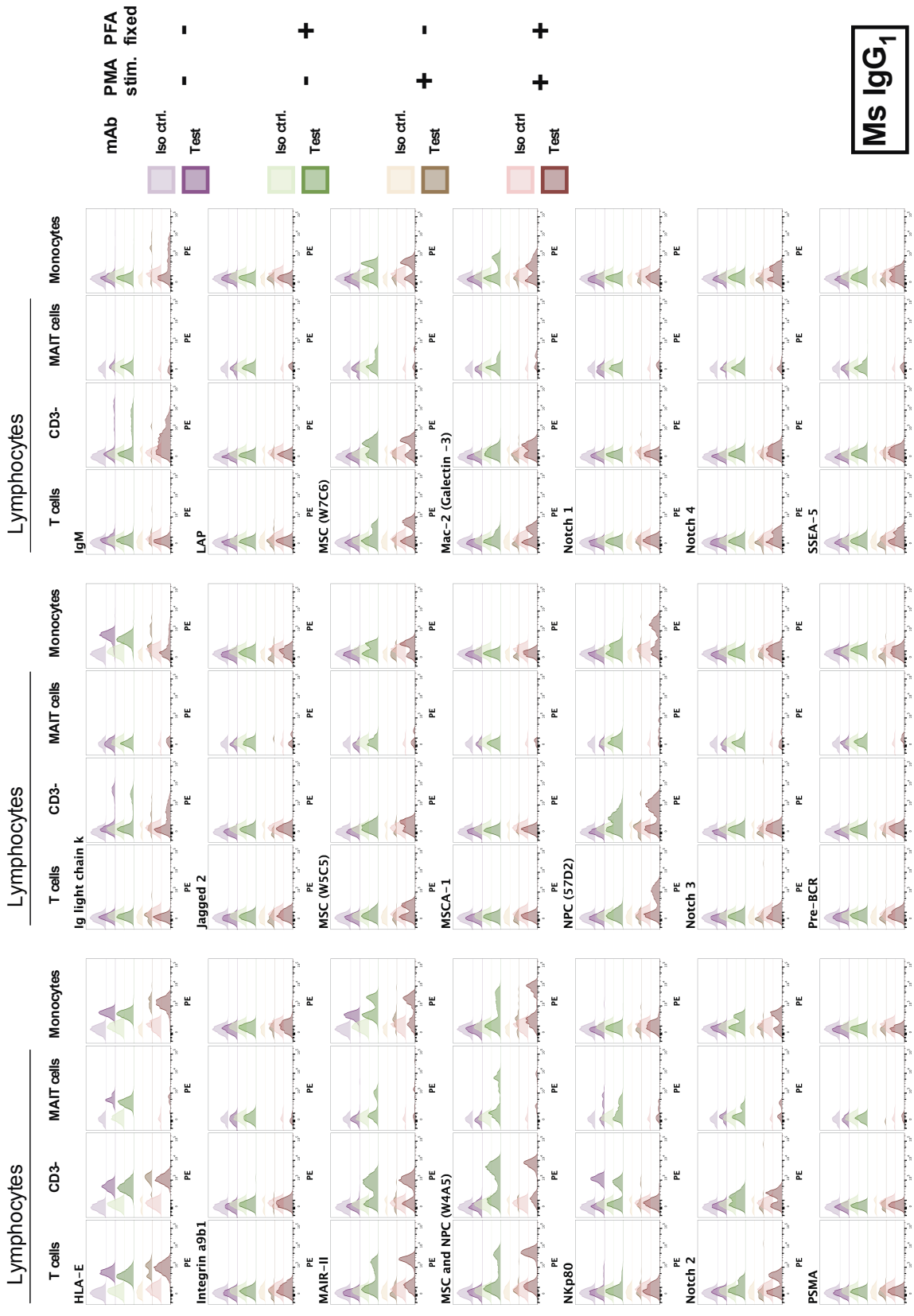
Lymphocytes
T cells
CD3-
MAIT cells
Monocytes
CD109
CD114
CD119 (IFNg R a chain)
CD126 (IL-6Ra)
CD134
CD137L (4-1BB L)
CD140b
CD111
CD116
CD122
CD127 (IL-7Ra)
CD135
CD138
CD141
CD112 (Nectin-2)
CD117 (c-kit)
CD123
CD131
CD137 (4-1BB)
CD140a
CD143
PE
mAb
PMA stim.
PFA fixed
Iso ctrl.
Test
Ms IgG1

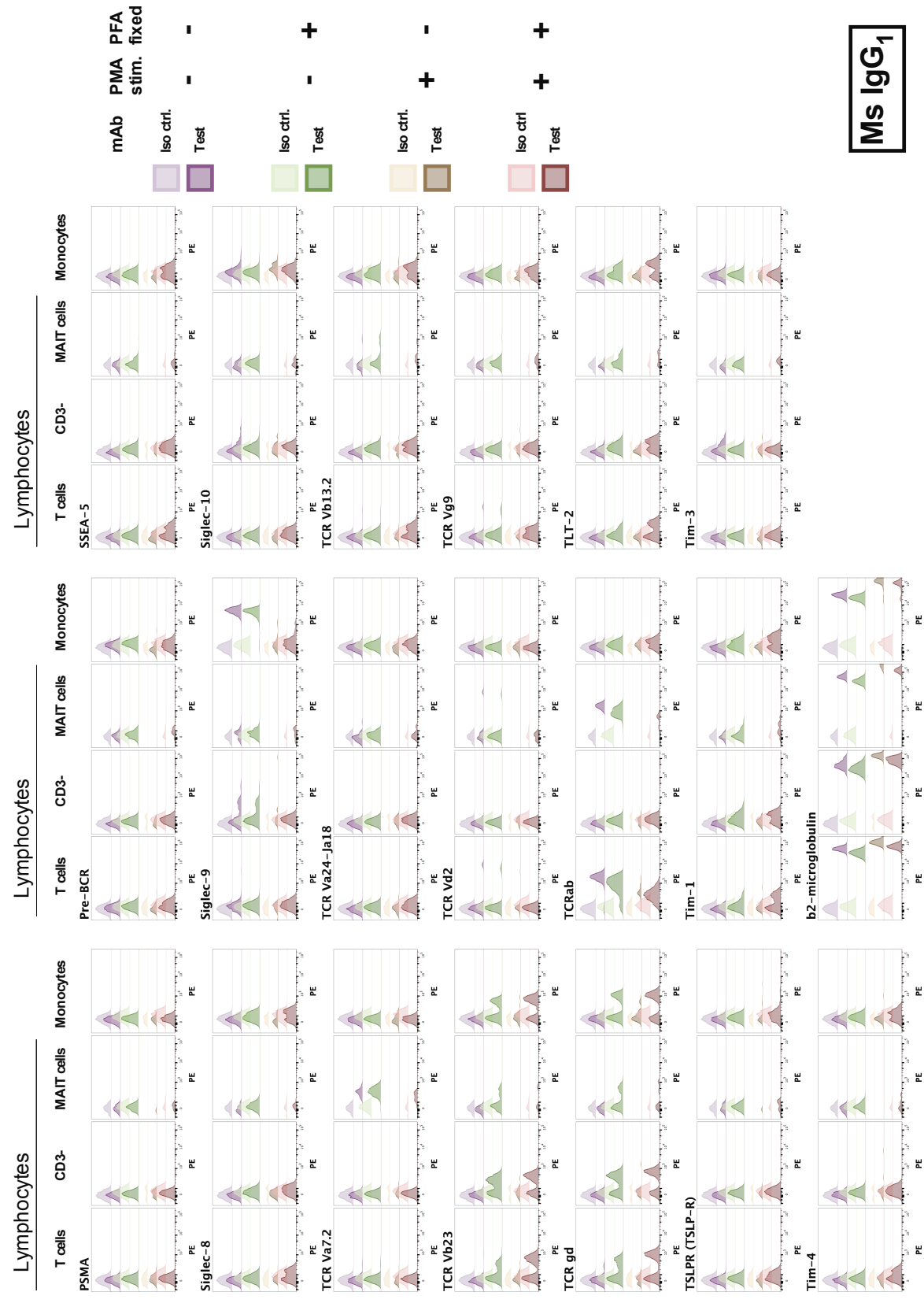

Lymphocytes
T cells
CD3-
MAIT cells
Monocytes
CD148
CD150 (SLAM)
CD152
CD154
CD155 (PVR)
CD156 (ADAM-10)
CD158d
CD158e1 (NKB1)
CD158f
CD161
CD162
CD163
CD164
CD165
CD166
CD169
CD170 (Siglec-5)
CD172a (SIRPa)
CD172b (SIRPb)
CD172g (SIRPg)
CD178 (Fas-L)
PE
mAb
PMA stim.
PFA fixed
Iso ctrl.
Test
Iso ctrl
Ms IgG1

Lymphocytes
T cells
CD3-
MAIT cells
Monocytes
CD179a
CD182 (CXCR2)
CD200 (OX2)
CD203c (E-NPP3)
CD207 (Langerin)
CD221 (IGF-1R)
CD231 (TALLA)
CD179b
CD183
CD200 R
CD205 (DEC-205)
CD213a2
CD226 (DNAM-1)
CD244 (2B4)
CD180 (RP105)
CD195 (CCR5)
CD202 (Tie2_Tek)
CD206 (MMR)
CD218a (IL-18Ra)
CD229 (Ly-9)
CD245 (p220_240)
PE
mAb
PMA stim.
PFA fixed
Iso ctrl.
Test
Ms IgG1


Lymphocytes
T cells
CD3-
MAIT cells
Monocytes
CD252 (OX40L)
CD253 (TRAIL)
CD254
CD257 (BAFF)
CD261 (DR4)
CD262 (DR5)
CD263 (DcR1)
CD266 (Fn14)
CD268 (BAFF-R)
CD270 (HVEM)
CD271
CD275 (B7-H2)
CD276
CD277
CD279 (PD-1)
CD286 (TLR6)
CD290
CD298
CD300F
CD300e (IREM-2)
CD314 (NKG2D)
PE
mAb
PMA stim.
PFA fixed
Iso ctrl.
Test
Iso ctrl
Ms IgG1

Lymphocytes
T cells
CD3-
MAIT cells
Monocytes
CD317
CD328 (Siglec-7)
CD336 (NKp44)
CD344 (Frizzled -4)
CD354 (TREM-1)
DLL1
EGFR
CD324 (E-Cadherin)
CD334 (FGFR4)
CD337 (NKp30)
CD351
CD357 (GITR)
DLL4
Galectin-9
CD325
CD335 (NKp46)
CD340 (erbB2)
CD352 (NTB-A)
CD360 (IL-21R)
DR3 (TRAMP)
HLA-DQ
PE
mAb
PMA stim.
PFA fixed
Iso ctrl.
Test
Ms IgG1

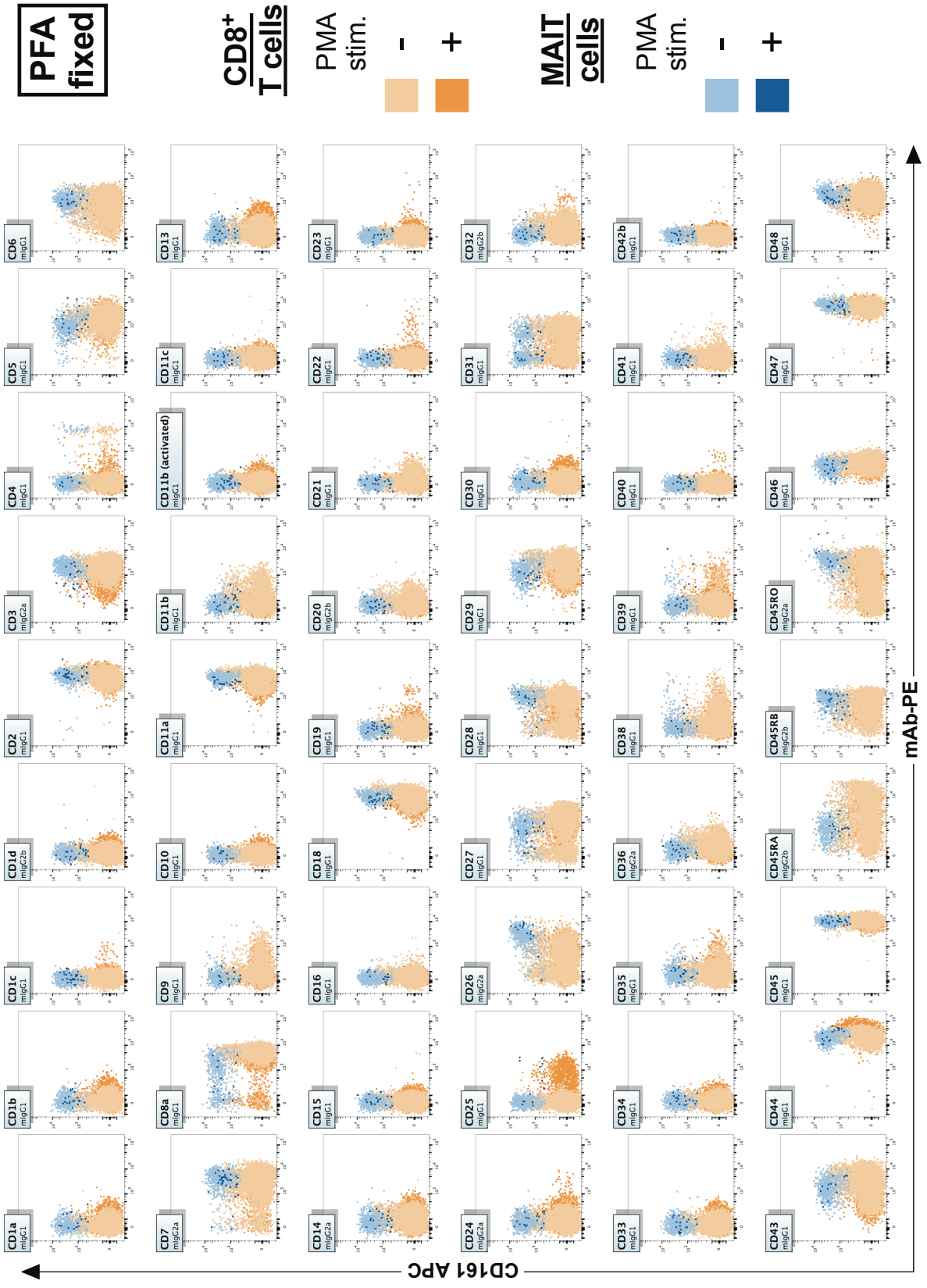

Lymphocytes
T cells
CD3-
MAIT cells
Monocytes
HLA-E
Integrin a9b1
MAIR-II
MSC and NPC (W4A5)
NKp80
Notch 2
PSMA
Ig light chain k
Jagged 2
MSC (W5C5)
MSCA-1
NPC (57D2)
Notch 3
Pre-BCR
IgM
LAP
MSC (W7C6)
Mac-2 (Galectin -3)
Notch 1
Notch 4
SSEA-5
mAb
PMA stim.
PFA fixed
Iso ctrl.
Test
Iso ctrl
Ms IgG1
PE

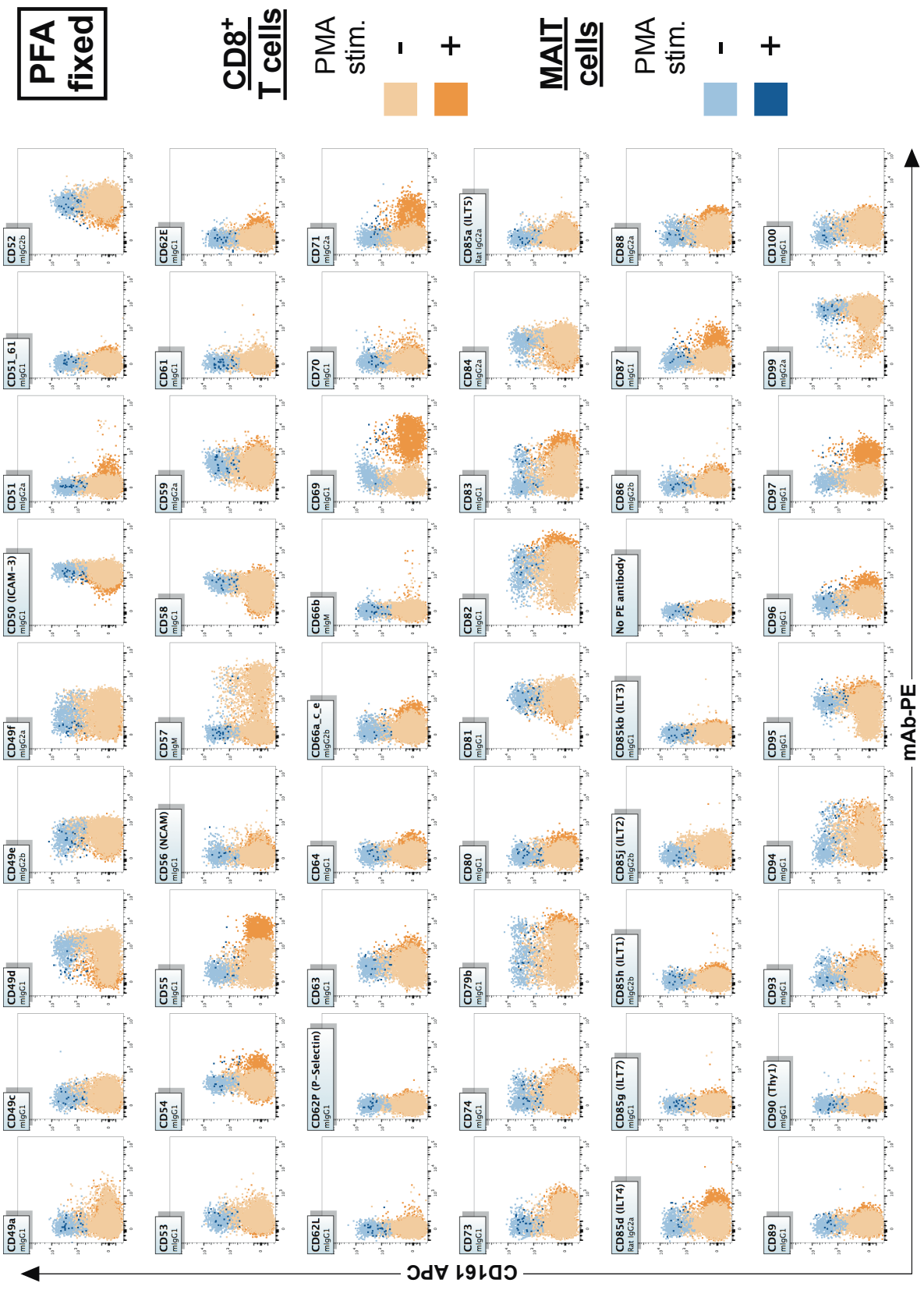

Lymphocytes
T cells
CD3-
MAIT cells
Monocytes
PSMA
Siglec-8
TCR Va7.2
TCR Vb23
TCR gd
TSLPR (TSLP-R)
Tim-4
Pre-BCR
Siglec-9
TCR Va24-Ja18
TCR Vd2
TCRab
Tim-1
b2-microglobulin
SSEA-5
Siglec-10
TCR Vb13.2
TCR Vg9
TLT-2
Tim-3
mAb
PMA stim.
PFA fixed
Iso ctrl.
Test
Ms IgG1
PE

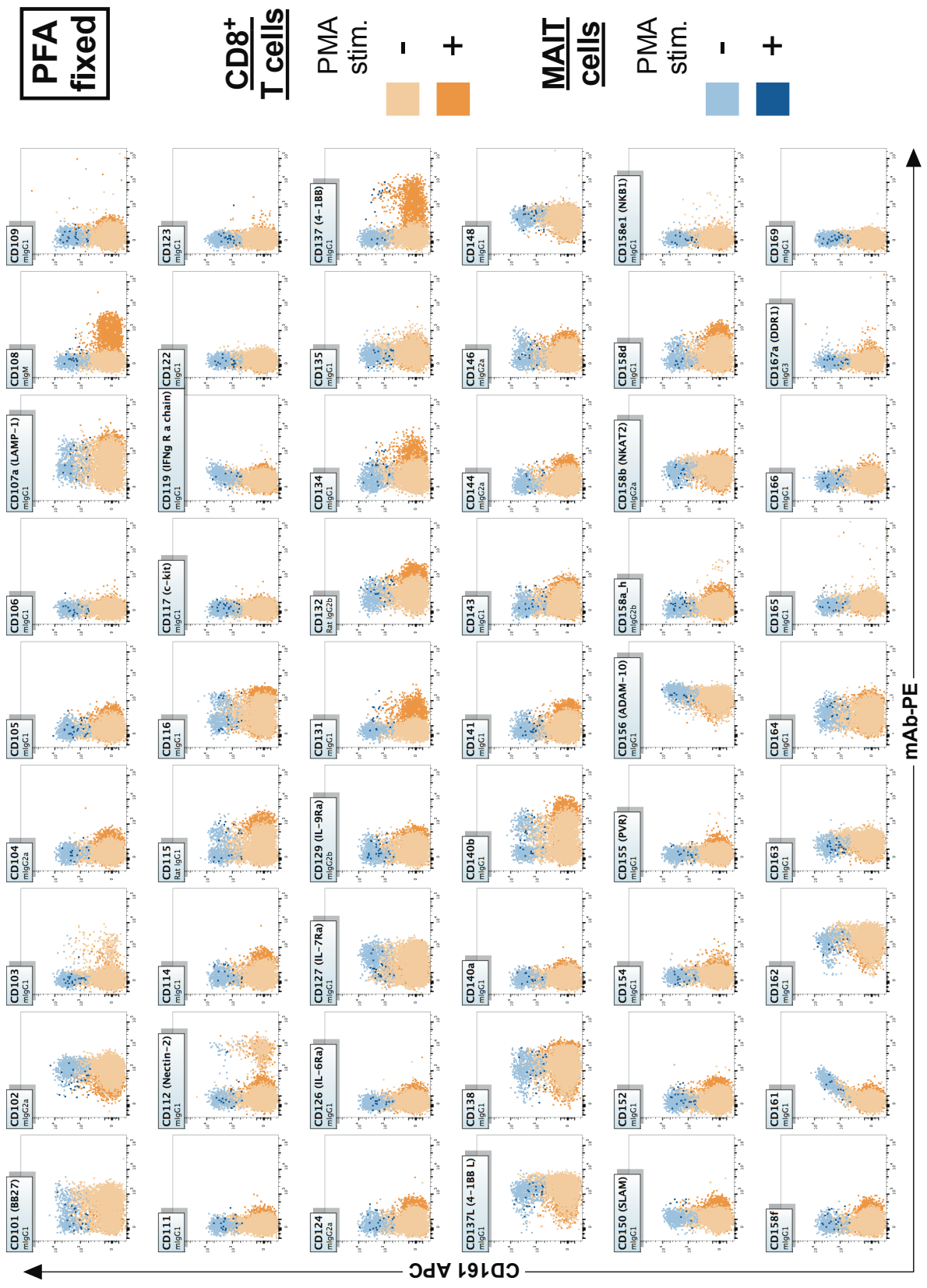

Lymphocytes
T cells
CD3-
MAIT cells
Monocytes
BTLA
CD14
CD36
CD51
CD84
CD102
CD144
CD3
CD24
CD45RO
CD59
CD88
CD104
CD146
CD7
CD26
CD49f
CD71
CD99
CD124
CD158b (NKAT2)
PE
mAb
PMA stim.
PFA fixed
Iso ctrl.
Test
Ms IgG2A

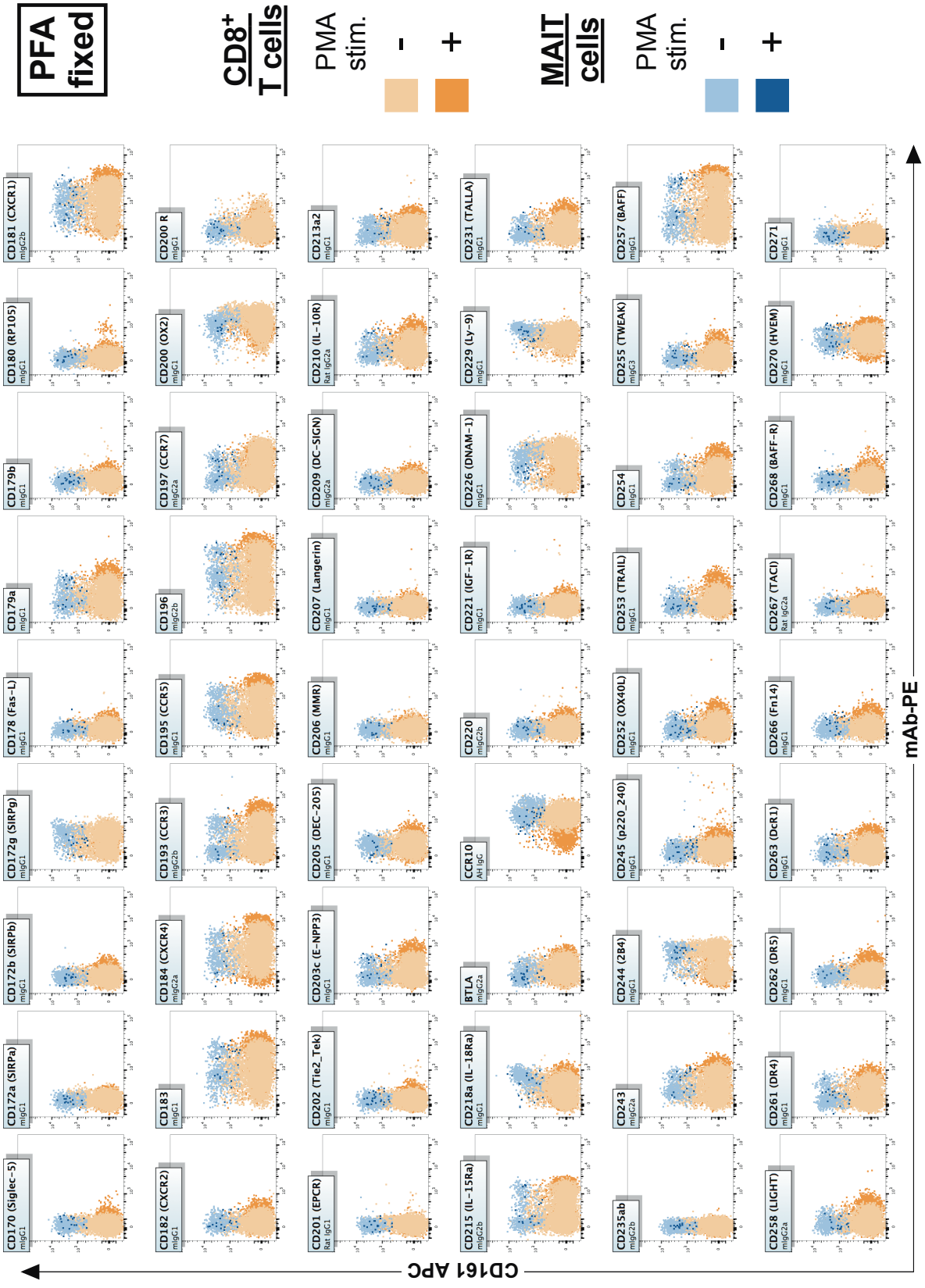
Lymphocytes
T cells
CD3-
MAIT cells
Monocytes
CD184 (CXCR4)
CD243
CD282 (TLR2)
CD303
CD355 (CRTAM)
C5L2
HLA-G
CD197 (CCR7)
CD258 (LIGHT)
CD284 (TLR4)
CD304
CLEC-9A
HLA-A,B,C
IL-28RA
CD209 (DC-SIGN)
CD273 (B7-DC)
CD301
CD307
CLEC12A
HLA-DR
Ig light chain lambda
PE
mAb
PMA stim.
PFA fixed
Iso ctrl.
Test
Ms IgG2A

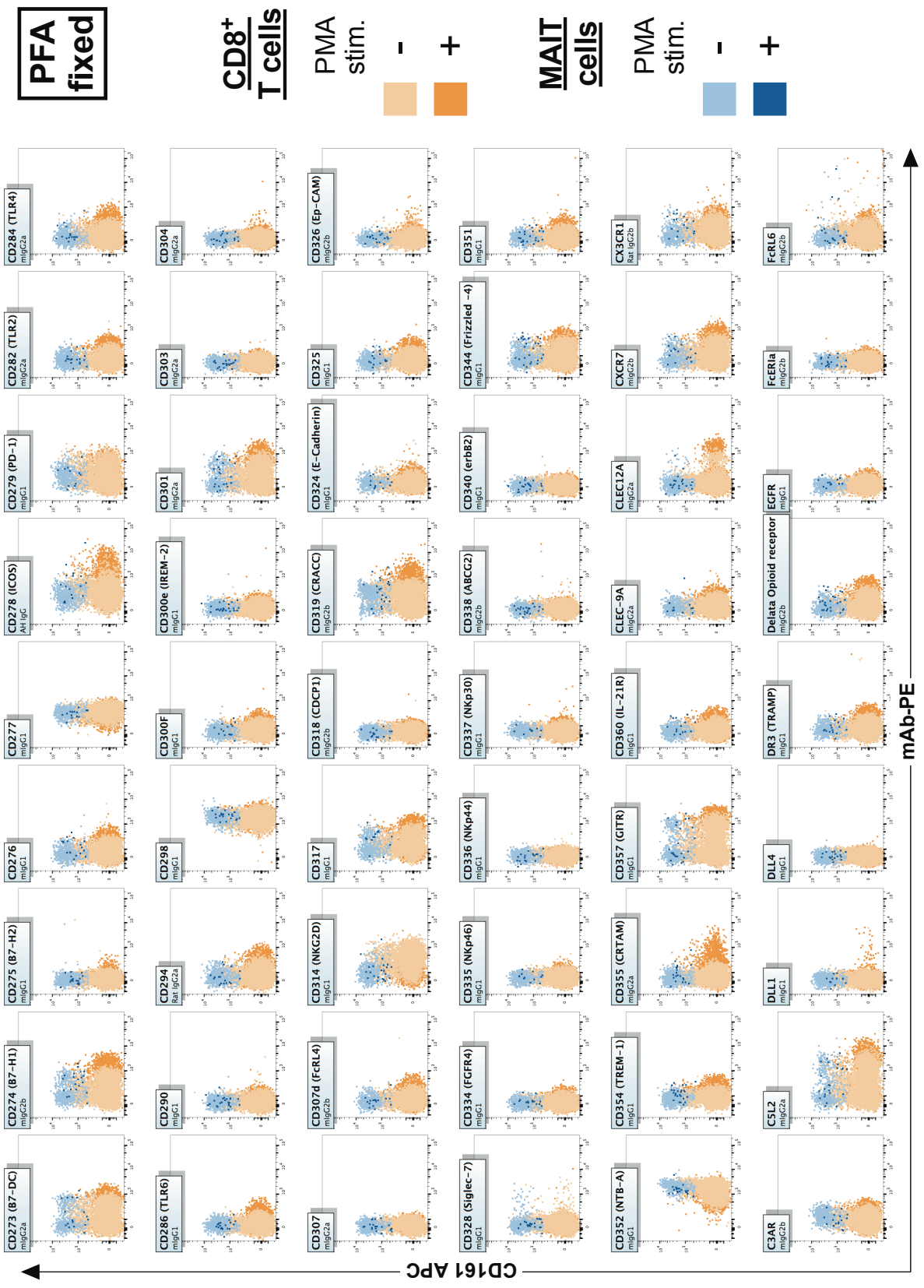
Lymphocytes
T cells
CD3-
MAIT cells
Monocytes
IgD
MSC (W3D5)
Integrin b5
Ms IgG2a, k ITCL
MICA_MICB
erbB3_HER-3
PE
mAb
PMA stim.
PFA fixed
Iso ctrl.
Test
Iso ctrl
Ms IgG2A

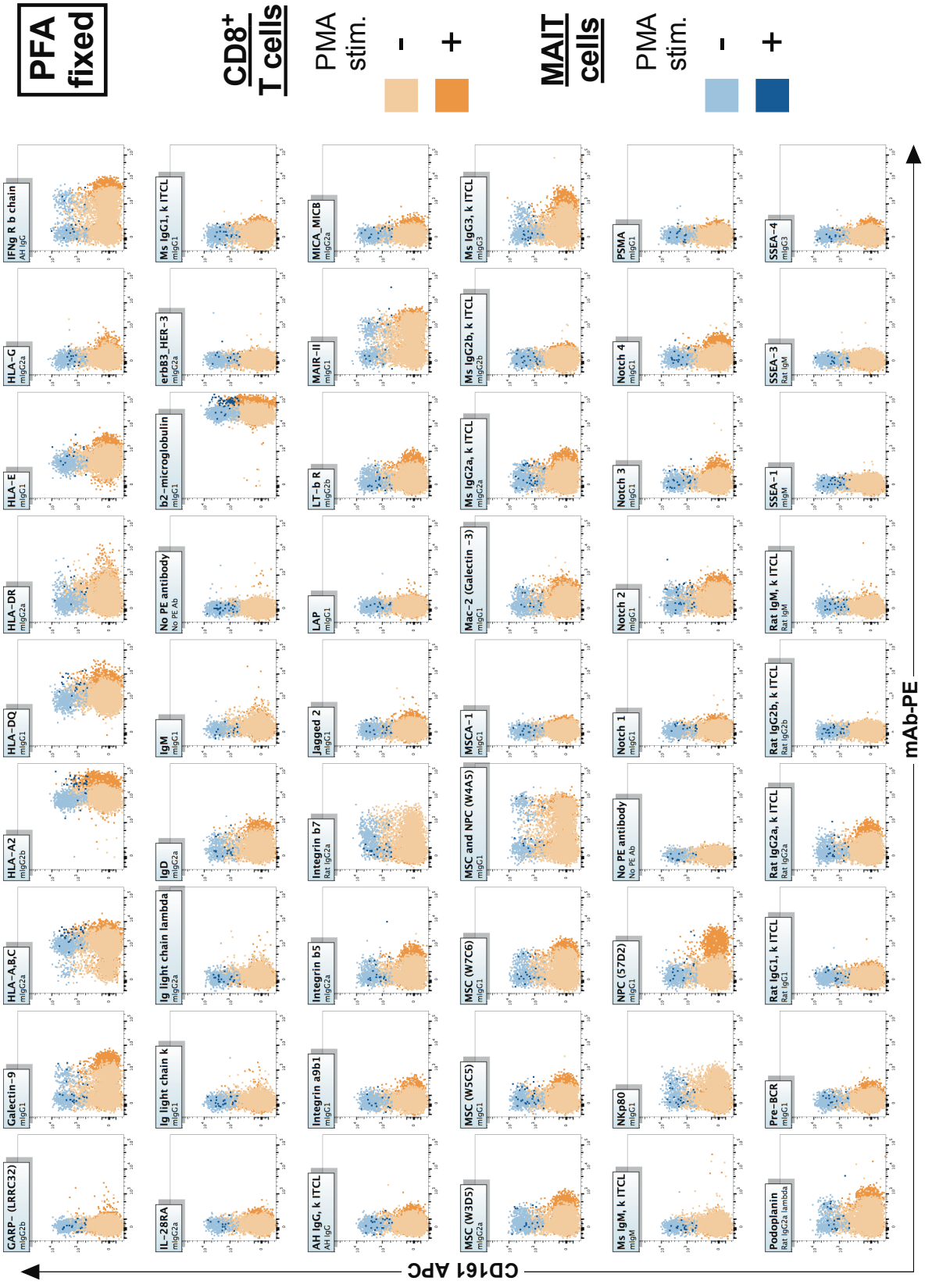

PFA fixed
CD8+ T cells
PMA stim.
-
+
MAIT cells
PMA stim.
-
+
CD161 APC
mAb-PE
CD1a mIgG1
CD1b mIgG1
CD1c mIgG1
CD1d mIgG2b
CD2 mIgG1
CD3 mIgG2a
CD4 mIgG1
CD5 mIgG1
CD6 mIgG1
CD7 mIgG2a
CD8a mIgG1
CD9 mIgG1
CD10 mIgG1
CD11a mIgG1
CD11b mIgG1
CD11b (activated) mIgG1
CD11c mIgG1
CD13 mIgG1
CD14 mIgG2a
CD15 mIgG1
CD16 mIgG1
CD18 mIgG1
CD19 mIgG1
CD20 mIgG2b
CD21 mIgG1
CD22 mIgG1
CD23 mIgG1
CD24 mIgG2a
CD25 mIgG1
CD26 mIgG2a
CD27 mIgG1
CD28 mIgG1
CD29 mIgG1
CD30 mIgG1
CD31 mIgG1
CD32 mIgG2b
CD33 mIgG1
CD34 mIgG1
CD35 mIgG1
CD36 mIgG2a
CD38 mIgG1
CD39 mIgG1
CD40 mIgG1
CD41 mIgG1
CD42b mIgG1
CD43 mIgG1
CD44 mIgG1
CD45 mIgG1
CD45RA mIgG2b
CD45RB mIgG2b
CD45RO mIgG2a
CD46 mIgG1
CD47 mIgG1
CD48 mIgG1

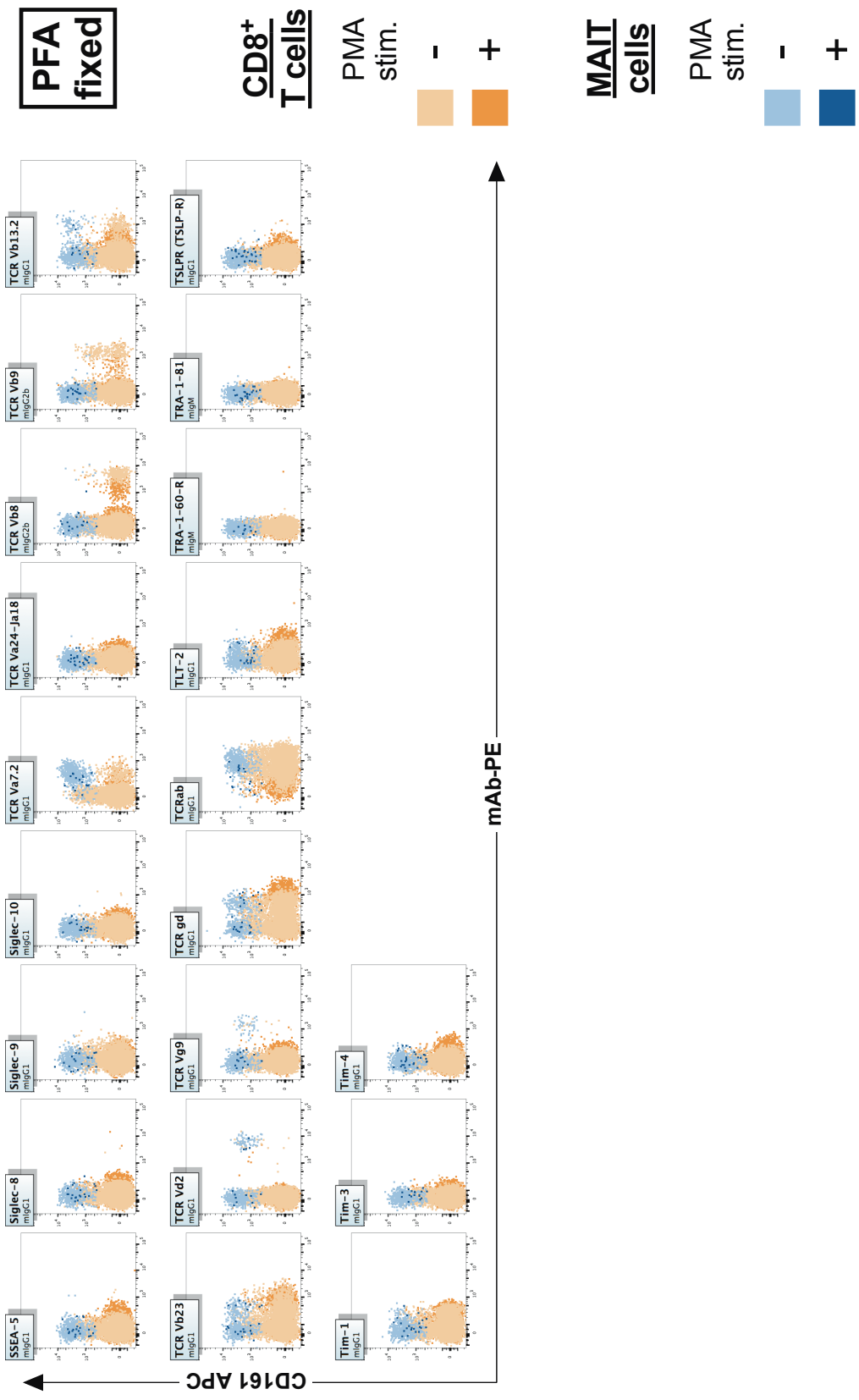

PFA fixed
CD8+ T cells
PMA stim.
-
+
MAIT cells
PMA stim.
-
+
CD161 APC
mAb-PE
CD49a mIgG1
CD49c mIgG1
CD49d mIgG1
CD49e mIgG2b
CD49f mIgG2a
CD50 (ICAM-3) mIgG1
CD51 mIgG2a
CD51_61 mIgG1
CD52 mIgG2b
CD53 mIgG1
CD54 mIgG1
CD55 mIgG1
CD56 (NCAM) mIgG1
CD57 mIgM
CD58 mIgG1
CD59 mIgG2a
CD61 mIgG1
CD62E mIgG1
CD62L mIgG1
CD62P (P-Selectin) mIgG1
CD63 mIgG1
CD64 mIgG1
CD66a_c_e mIgG2b
CD66b mIgM
CD69 mIgG1
CD70 mIgG1
CD71 mIgG2a
CD73 mIgG1
CD74 mIgG1
CD79b mIgG1
CD80 mIgG1
CD81 mIgG1
CD82 mIgG1
CD83 mIgG1
CD84 mIgG2a
CD85a (ILT5) Rat IgG2a
CD85d (ILT4) Rat IgG2a
CD85g (ILT7) mIgG1
CD85h (ILT1) mIgG2b
CD85j (ILT2) mIgG2b
CD85kb (ILT3) mIgG1
No PE antibody
CD86 mIgG2b
CD87 mIgG1
CD88 mIgG2a
CD89 mIgG1
CD90 (Thy1) mIgG1
CD93 mIgG1
CD94 mIgG1
CD95 mIgG1
CD96 mIgG1
CD97 mIgG1
CD99 mIgG2a
CD100 mIgG1


PFA fixed
CD8+ T cells
PMA stim.
-
+
MAIT cells
PMA stim.
-
+
CD161 APC
mAb-PE
CD101 (BB27) mIgG1
CD102 mIgG2a
CD103 mIgG1
CD104 mIgG2a
CD105 mIgG1
CD106 mIgG1
CD107a (LAMP-1) mIgG1
CD108 mIgM
CD109 mIgG1
CD111 mIgG1
CD112 (Nectin-2) mIgG1
CD114 mIgG1
CD115 Rat IgG1
CD116 mIgG1
CD117 (c-kit) mIgG1
CD119 (IFNg R a chain) mIgG1
CD122 mIgG1
CD123 mIgG1
CD124 mIgG2a
CD126 (IL-6Ra) mIgG1
CD127 (IL-7Ra) mIgG1
CD129 (IL-9Ra) mIgG2b
CD131 mIgG1
CD132 Rat IgG2b
CD134 mIgG1
CD135 mIgG1
CD137 (4-1BB) mIgG1
CD137L (4-1BB L) mIgG1
CD138 mIgG1
CD140a mIgG1
CD140b mIgG1
CD141 mIgG1
CD143 mIgG1
CD144 mIgG2a
CD146 mIgG2a
CD148 mIgG1
CD150 (SLAM) mIgG1
CD152 mIgG1
CD154 mIgG1
CD155 (PVR) mIgG1
CD156 (ADAM-10) mIgG1
CD158a_h mIgG2b
CD158b (NKAT2) mIgG2a
CD158d mIgG1
CD158e1 (NKB1) mIgG1
CD158f mIgG1
CD161 mIgG1
CD162 mIgG1
CD163 mIgG1
CD164 mIgG1
CD165 mIgG1
CD166 mIgG1
CD167a (DDR1) mIgG3
CD169 mIgG1


PFA fixed
CD8+ T cells
PMA stim.
-
+
MAIT cells
PMA stim.
-
+
CD161 APC
mAb-PE
CD170 (Siglec-5)
CD172a (SIRPa)
CD172b (SIRPb)
CD172g (SIRPg)
CD178 (Fas-L)
CD179a
CD179b
CD180 (RP105)
CD181 (CXCR1)
CD182 (CXCR2)
CD183
CD184 (CXCR4)
CD193 (CCR3)
CD195 (CCR5)
CD196
CD197 (CCR7)
CD200 (OX2)
CD200 R
CD201 (EPCR)
CD202 (Tie2_Tek)
CD203c (E-NPP3)
CD205 (DEC-205)
CD206 (MMR)
CD207 (Langerin)
CD209 (DC-SIGN)
CD210 (IL-10R)
CD213a2
CD215 (IL-15Ra)
CD218a (IL-18Ra)
BTLA
CCR10
CD220
CD221 (IGF-1R)
CD226 (DNAM-1)
CD229 (Ly-9)
CD231 (TALLA)
CD235ab
CD243
CD244 (2B4)
CD245 (p220_240)
CD252 (OX40L)
CD253 (TRAIL)
CD254
CD255 (TWEAK)
CD257 (BAFF)
CD258 (LIGHT)
CD261 (DR4)
CD262 (DR5)
CD263 (DcR1)
CD266 (Fn14)
CD267 (TACI)
CD268 (BAFF-R)
CD270 (HVEM)
CD271


PFA fixed
CD8+ T cells
PMA stim.
-
+
MAIT cells
PMA stim.
-
+
CD161 APC
mAb-PE
CD273 (B7-DC)
CD274 (B7-H1)
CD275 (B7-H2)
CD276
CD277
CD278 (ICOS)
CD279 (PD-1)
CD282 (TLR2)
CD284 (TLR4)
CD286 (TLR6)
CD290
CD294
CD298
CD300F
CD300e (IREM-2)
CD301
CD303
CD304
CD307
CD307d (FcRL4)
CD314 (NKG2D)
CD317
CD318 (CDCP1)
CD319 (CRACC)
CD324 (E-Cadherin)
CD325
CD326 (Ep-CAM)
CD328 (Siglec-7)
CD334 (FGFR4)
CD335 (NKp46)
CD336 (NKp44)
CD337 (NKp30)
CD338 (ABCG2)
CD340 (erbB2)
CD344 (Frizzled -4)
CD351
CD352 (NTB-A)
CD354 (TREM-1)
CD355 (CRTAM)
CD357 (GITR)
CD360 (IL-21R)
CLEC-9A
CLEC12A
CXCR7
CX3CR1
C3AR
CSL2
DLL1
DLL4
DR3 (TRAMP)
Delata Opioid receptor
EGFR
FcERIa
FcRL6


PFA fixed
CD8+ T cells
PMA stim.
-
+
MAIT cells
PMA stim.
-
+
CD161 APC
mAb-PE
GARP- (LRRC32)
Galectin-9
HLA-A,B,C
HLA-A2
HLA-DQ
HLA-DR
HLA-E
HLA-G
IFNg R b chain
IL-28RA
Ig light chain k
Ig light chain lambda
IgD
IgM
Integrin a9b1
Integrin b5
Integrin b7
Jagged 2
LAP
LT-b R
MAIR-II
MICA_MICB
b2-microglobulin
erbB3_HER-3
Ms IgG1, k ITCL
AH IgG, k ITCL
MSC (W3D5)
MSC (W5C5)
MSC (W7C6)
MSC and NPC (W4A5)
MSCA-1
Mac-2 (Galectin -3)
Ms IgG2a, k ITCL
Ms IgG2b, k ITCL
Ms IgG3, k ITCL
Ms IgM, k ITCL
NKp80
NPC (57D2)
No PE antibody
Notch 1
Notch 2
Notch 3
Notch 4
PSMA
Podoplanin
Pre-BCR
Rat IgG1, k ITCL
Rat IgG2a, k ITCL
Rat IgG2b, k ITCL
Rat IgM, k ITCL
SSEA-1
SSEA-3
SSEA-4


PFA fixed
CD8+ T cells
PMA stim.
-
+
MAIT cells
PMA stim.
-
+
CD161 APC
mAb-PE
SSEA-5 mIgG1
Siglec-8 mIgG1
Siglec-9 mIgG1
Siglec-10 mIgG1
TCR Va7.2 mIgG1
TCR Va24-Ja18 mIgG1
TCR Vb8 mIgG2b
TCR Vb9 mIgG2b
TCR Vb13.2 mIgG1
TCR Vb23 mIgG1
TCR Vd2 mIgG1
TCR Vg9 mIgG1
TCR gd mIgG1
TCRab mIgG1
TLT-2 mIgG1
TRA-1-60-R mIgM
TRA-1-81 mIgM
TSLPR (TSLP-R) mIgG1
Tim-1 mIgG1
Tim-3 mIgG1
Tim-4 mIgG1

Human LEGENDScreen™

Antibody Information Tables

Plate 1

Well ID	Specificity	Clone	Isotype	BioLegend Cat. No.
A1	Blank			
A2	CD1a	HI149	Mouse IgG1, κ	300106
A3	CD1b	SN13 (K5-1B8)	Mouse IgG1, κ	329108
A4	CD1c	L161	Mouse IgG1, κ	331506
A5	CD1d	51.1	Mouse IgG2b, κ	350306
A6	CD2	RPA-2.10	Mouse IgG1, κ	300208
A7	CD3	HIT3a	Mouse IgG2a, κ	300308
A8	CD4	RPA-T4	Mouse IgG1, κ	300508
A9	CD5	UCHT2	Mouse IgG1, κ	300608
A10	CD6	BL-CD6	Mouse IgG1, κ	313906
A11	CD7	CD7-6B7	Mouse IgG2a, κ	343106
A12	CD8a	HIT8a	Mouse IgG1, κ	300908
B1	CD9	HI9a	Mouse IgG1, κ	312106
B2	CD10	HI10a	Mouse IgG1, κ	312204
B3	CD11a	HI111	Mouse IgG1, κ	301208
B4	CD11b	ICRF44	Mouse IgG1, κ	301306
B5	CD11b (activated)	CBRM1/5	Mouse IgG1, κ	301406
B6	CD11c	3.9	Mouse IgG1, κ	301606
B7	CD13	WM15	Mouse IgG1, κ	301704
B8	CD14	M5E2	Mouse IgG2a, κ	301806
B9	CD15 (SSEA-1)	W6D3	Mouse IgG1, κ	323006
B10	CD16	3G8	Mouse IgG1, κ	302008
B11	CD18	TS1/18	Mouse IgG1, κ	302108
B12	CD19	HIB19	Mouse IgG1, κ	302208
C1	CD20	2H7	Mouse IgG2b, κ	302306
C2	CD21	Bu32	Mouse IgG1, κ	354904
C3	CD22	HIB22	Mouse IgG1, κ	302506

Plate 1

Well ID	Specificity	Clone	Isotype	BioLegend Cat. No.
C4	CD23	EBVCS-5	Mouse IgG1, κ	338508
C5	CD24	ML5	Mouse IgG2a, κ	311106
C6	CD25	BC96	Mouse IgG1, κ	302606
C7	CD26	BA5b	Mouse IgG2a, κ	302706
C8	CD27	O323	Mouse IgG1, κ	302808
C9	CD28	CD28.2	Mouse IgG1, κ	302908
C10	CD29	TS2/16	Mouse IgG1, κ	303004
C11	CD30	BY88	Mouse IgG1, κ	333906
C12	CD31	WM59	Mouse IgG1, κ	303106
D1	CD32	FUN-2	Mouse IgG2b, κ	303206
D2	CD33	WM53	Mouse IgG1, κ	303404
D3	CD34	581	Mouse IgG1, κ	343506
D4	CD35	E11	Mouse IgG1, κ	333406
D5	CD36	5-271	Mouse IgG2a, κ	336206
D6	CD38	HIT2	Mouse IgG1, κ	303506
D7	CD39	A1	Mouse IgG1, κ	328208
D8	CD40	HB14	Mouse IgG1, κ	313006
D9	CD41	HIP8	Mouse IgG1, κ	303706
D10	CD42b	HIP1	Mouse IgG1, κ	303906
D11	CD43	CD43-10G7	Mouse IgG1, κ	343204
D12	CD44	BJ18	Mouse IgG1, κ	338808
E1	CD45	HI30	Mouse IgG1, κ	304008
E2	CD45RA	HI100	Mouse IgG2b, κ	304108
E3	CD45RB	MEM-55	Mouse IgG2b, κ	310204
E4	CD45RO	UCHL1	Mouse IgG2a, κ	304206
E5	CD46	TRA-2-10	Mouse IgG1	352402
E6	CD47	CC2C6	Mouse IgG1, κ	323108

Plate 1

Well ID	Specificity	Clone	Isotype	BioLegend Cat. No.
E7	CD48	BJ40	Mouse IgG1, κ	336708
E8	CD49a	TS2/7	Mouse IgG1, κ	328304
E9	CD49c	ASC-1	Mouse IgG1, κ	343804
E10	CD49d	9F10	Mouse IgG1, κ	304304
E11	CD49e	NKI-SAM-1	Mouse IgG2b, κ	328010
E12	CD49f	GoH3	Rat IgG2a, κ	313612
F1	CD50 (ICAM-3)	CBR-IC3/1	Mouse IgG1, κ	330005
F2	CD51	NKI-M9	Mouse IgG2a, κ	327910
F3	CD51/61	23C6	Mouse IgG1, κ	304406
F4	CD52	HI186	Mouse IgG2b, κ	316006
F5	CD53	HI29	Mouse IgG1, κ	325406
F6	CD54	HA58	Mouse IgG1, κ	353106
F7	CD55	JS11	Mouse IgG1, κ	311308
F8	CD56 (NCAM)	HCD56	Mouse IgG1, κ	318306
F9	CD57	HCD57	Mouse IgM, κ	322312
F10	CD58	TS2/9	Mouse IgG1, κ	330905
F11	CD59	p282 (H19)	Mouse IgG2a, κ	304708
F12	CD61	VI-PL2	Mouse IgG1, κ	336406
G1	CD62E	HAE-1f	Mouse IgG1, κ	336008
G2	CD62L	DREG-56	Mouse IgG1, κ	304806
G3	CD62P (P-Selectin)	AK4	Mouse IgG1, κ	304906
G4	CD63	H5C6	Mouse IgG1, κ	353004
G5	CD64	10.1	Mouse IgG1, κ	305008
G6	CD66a/c/e	ASL-32	Mouse IgG2b, κ	342304
G7	CD66b	G10F5	Mouse IgM, κ	305106
G8	CD69	FN50	Mouse IgG1, κ	310906
G9	CD70	113-16	Mouse IgG1, κ	355104
G10	CD71	CY1G4	Mouse IgG2a, κ	334106

Plate 1

Well ID	Specificity	Clone	Isotype	BioLegend Cat. No.
G11	CD73	AD2	Mouse IgG1, κ	344004
G12	CD74	LN2	Mouse IgG1, κ	326808
H1	CD79b	CB3-1	Mouse IgG1, κ	341404
H2	CD80	2D10	Mouse IgG1, κ	305208
H3	CD81	5A6	Mouse IgG1, κ	349506
H4	CD82	ASL-24	Mouse IgG1, κ	342104
H5	CD83	HB15e	Mouse IgG1, κ	305308
H6	CD84	CD84.1.21	Mouse IgG2a, κ	326008
H7	CD85a (ILT5)	MKT5.1	Rat IgG2a, κ	337704
H8	CD85d (ILT4)	42D1	Rat IgG2a, κ	338706
H9	CD85g (ILT7)	17G10.2	Mouse IgG1, κ	326408
H10	CD85h (ILT1)	24	Mouse IgG2b, κ	337904
H11	CD85j (ILT2)	GHI/75	Mouse IgG2b, κ	333708
H12	CD85k (ILT3)	ZM4.1	Mouse IgG1, κ	333008

Plate 2

Well ID	Specificity	Clone	Isotype	BioLegend Cat. No.
A1	Blank			
A2	CD86	IT2.2	Mouse IgG2b, κ	305406
A3	CD87	VIM5	Mouse IgG1, κ	336906
A4	CD88	S5/1	Mouse IgG2a, κ	344304
A5	CD89	A59	Mouse IgG1, κ	354104
A6	CD90 (Thy1)	5E10	Mouse IgG1, κ	328110
A7	CD93	VIMD2	Mouse IgG1, κ	336108
A8	CD94	DX22	Mouse IgG1, κ	305506
A9	CD95	DX2	Mouse IgG1, κ	305608
A10	CD96	NK92.39	Mouse IgG1, κ	338406
A11	CD97	VIM3b	Mouse IgG1, κ	336308
A12	CD99	HCD99	Mouse IgG2a, κ	318008
B1	CD100	A8	Mouse IgG1, κ	328408
B2	CD101 (BB27)	BB27	Mouse IgG1, κ	331006
B3	CD102	CBR-IC2/2	Mouse IgG2a, κ	328506
B4	CD103	Ber-ACT8	Mouse IgG1, κ	350206
B5	CD104	58XB4	Mouse IgG2a, κ	327808
B6	CD105	43A3	Mouse IgG1, κ	323206
B7	CD106	STA	Mouse IgG1, κ	305806
B8	CD107a (LAMP-1)	H4A3	Mouse IgG1, κ	328608
B9	CD108	MEM-150	Mouse IgM, κ	315704
B10	CD109	W7C5	Mouse IgG1, κ	323306
B11	CD111	R1.302	Mouse IgG1, κ	340404
B12	CD112 (Nectin-2)	TX31	Mouse IgG1, κ	337410
C1	CD114	LMM741	Mouse IgG1, κ	346106
C2	CD115	9-4D2-1E4	Rat IgG1, κ	347304
C3	CD116	4H1	Mouse IgG1, κ	305908
C4	CD117 (c-kit)	104D2	Mouse IgG1, κ	313204

Plate 2

Well ID	Specificity	Clone	Isotype	BioLegend Cat. No.
C5	CD119 (IFN-g R α chain)	GIR-208	Mouse IgG1, κ	308606
C6	CD122	TU27	Mouse IgG1, κ	339006
C7	CD123	6H6	Mouse IgG1, κ	306006
C8	CD124	G077F6	Mouse IgG2a, κ	355004
C9	CD126 (IL-6Rα)	UV4	Mouse IgG1, κ	352804
C10	CD127 (IL-7Rα)	A019D5	Mouse IgG1, κ	351304
C11	CD129 (IL-9 R)	AH9R7	Mouse IgG2b, κ	310404
C12	CD131	1C1	Mouse IgG1, κ	306104
D1	CD132	TUGh4	Rat IgG2b, κ	338606
D2	CD134	Ber-ACT35 (ACT35)	Mouse IgG1, κ	350004
D3	CD135	BV10A4H2	Mouse IgG1, κ	313306
D4	CD137 (4-1BB)	4B4-1	Mouse IgG1, κ	309804
D5	CD137L (4-1BB Ligand)	5F4	Mouse IgG1, κ	311504
D6	CD138	DL-101	Mouse IgG1, κ	352306
D7	CD140a	16A1	Mouse IgG1, κ	323506
D8	CD140b	18A2	Mouse IgG1, κ	323606
D9	CD141	M80	Mouse IgG1, κ	344104
D10	CD143	5-369	Mouse IgG1, κ	344204
D11	CD144	BV9	Mouse IgG2a, κ	348506
D12	CD146	SHM-57	Mouse IgG2a, κ	342004
E1	CD148	A3	Mouse IgG1, κ	328708
E2	CD150 (SLAM)	A12 (7D4)	Mouse IgG1, κ	306308
E3	CD152	L3D10	Mouse IgG1, κ	349906
E4	CD154	24-31	Mouse IgG1, κ	310806
E5	CD155 (PVR)	SKII.4	Mouse IgG1, κ	337610
E6	CD156c (ADAM10)	SHM14	Mouse IgG1, κ	352704
E7	CD158a/h	HP-MA4	Mouse IgG2b, κ	339506

Plate 2

Well ID	Specificity	Clone	Isotype	BioLegend Cat. No.
E8	CD158b (KIR2DL2/L3, NKAT2)	DX27	Mouse IgG2a, κ	312606
E9	CD158d	mAb 33 (33)	Mouse IgG1, κ	347006
E10	CD158e1 (KIR3DL1, NKB1)	DX9	Mouse IgG1, κ	312708
E11	CD158f	UP-R1	Mouse IgG1, κ	341304
E12	CD161	HP-3G10	Mouse IgG1, κ	339904
F1	CD162	KPL-1	Mouse IgG1, κ	328806
F2	CD163	GHI/61	Mouse IgG1, κ	333606
F3	CD164	67D2	Mouse IgG1, κ	324808
F4	CD165	SN2 (N6-D11)	Mouse IgG1, κ	329010
F5	CD166	3A6	Mouse IgG1, κ	343904
F6	CD167a (DDR1)	51D6	Mouse IgG3, κ	334006
F7	CD169	7-239	Mouse IgG1, κ	346004
F8	CD170 (Siglec-5)	1A5	Mouse IgG1, κ	352004
F9	CD172a (SIRPa)	SE5A5	Mouse IgG1, κ	323806
F10	CD172b (SIRPb)	B4B6	Mouse IgG1, κ	323906
F11	CD172g (SIRPg)	LSB2.20	Mouse IgG1, κ	336606
F12	CD178 (Fas-L)	NOK-1	Mouse IgG1, κ	306407
G1	CD179a	HSL96	Mouse IgG1, κ	347404
G2	CD179b	HSL11	Mouse IgG1, κ	349804
G3	CD180 (RP105)	MHR73-11	Mouse IgG1, κ	312906
G4	CD181 (CXCR1)	8F1/CXCR1	Mouse IgG2b, κ	320608
G5	CD182 (CXCR2)	5E8/CXCR2	Mouse IgG1, κ	320706
G6	CD183	G025H7	Mouse IgG1, κ	353706
G7	CD184 (CXCR4)	12G5	Mouse IgG2a, κ	306506
G8	CD193 (CCR3)	5E8	Mouse IgG2b, κ	310706
G9	CD195 (CCR5)	T21/8	Mouse IgG1, κ	321406
G10	CD196	G034E3	Mouse IgG2b, κ	353410

Plate 2

Well ID	Specificity	Clone	Isotype	BioLegend Cat. No.
G11	CD197 (CCR7)	G043H7	Mouse IgG2a, κ	353204
G12	CD200 (OX2)	OX-104	Mouse IgG1, κ	329206
H1	CD200 R	OX-108	Mouse IgG1, κ	329306
H2	CD201 (EPCR)	RCR-401	Rat IgG1, κ	351904
H3	CD202b (Tie2/Tek)	33.1 (Ab33)	Mouse IgG1, κ	334206
H4	CD203c (E-NPP3)	NP4D6	Mouse IgG1, κ	324606
H5	CD205 (DEC-205)	HD30	Mouse IgG1, κ	342204
H6	CD206 (MMR)	15-2	Mouse IgG1, κ	321106
H7	CD207 (Langerin)	10E2	Mouse IgG1, κ	352204
H8	CD209 (DC-SIGN)	9E9A8	Mouse IgG2a, κ	330106
H9	CD210 (IL-10 R)	3F9	Rat IgG2a, κ	308804
H10	CD213a2	SHM38	Mouse IgG1, κ	354404
H11	CD215 (IL-15Rα)	JM7A4	Mouse IgG2b, κ	330208
H12	CD218a (IL-18Rα)	H44	Mouse IgG1, κ	313808

Plate 3

Well ID	Specificity	Clone	Isotype	BioLegend Cat. No.
A1	Blank			
A2	CD220	B6.220	Mouse IgG2b, κ	352604
A3	CD221 (IGF-1R)	1H7/CD221	Mouse IgG1, κ	351806
A4	CD226 (DNAM-1)	11A8	Mouse IgG1, κ	338306
A5	CD229 (Ly-9)	HLy-9.1.25	Mouse IgG1, κ	326108
A6	CD231 (TALLA)	SN1a (M3-3D9)	Mouse IgG1, κ	329406
A7	CD235ab	HIR2	Mouse IgG2b, κ	306604
A8	CD243	UIC2	Mouse IgG2a, κ	348606
A9	CD244 (2B4)	C1.7	Mouse IgG1, κ	329508
A10	CD245 (p220/240)	DY12	Mouse IgG1, κ	Inquire
A11	CD252 (OX40L)	11C3.1	Mouse IgG1, κ	326308
A12	CD253 (Trail)	RIK-2	Mouse IgG1, κ	308206
B1	CD254	MIH24	Mouse IgG1, κ	347504
B2	CD255 (TWEAK)	CARL-1	Mouse IgG3, κ	308305
B3	CD257 (BAFF, BLYS)	T7-241	Mouse IgG1, κ	318606
B4	CD258 (LIGHT)	T5-39	Mouse IgG2a, κ	318706
B5	CD261 (DR4, TRAIL-R1)	DJR1	Mouse IgG1, κ	307206
B6	CD262 (DR5, TRAIL-R2)	DJR2-4 (7-8)	Mouse IgG1, κ	307406
B7	CD263 (DcR1, TRAIL-R3)	DJR3	Mouse IgG1, κ	307006
B8	CD266 (Fn14, TWEAK Receptor)	ITEM-1	Mouse IgG1, κ	314004
B9	CD267 (TACI)	1A1	Rat IgG2a, κ	311906
B10	CD268 (BAFF-R, BAFFR)	11C1	Mouse IgG1, κ	316906
B11	CD270 (HVEM)	122	Mouse IgG1, κ	318806
B12	CD271	ME20.4	Mouse IgG1, κ	345106
C1	CD273 (B7-DC, PD-L2)	24F.10C12	Mouse IgG2a, κ	329606
C2	CD274 (B7-H1, PD-L1)	29E.2A3	Mouse IgG2b, κ	329706

Plate 3

Well ID	Specificity	Clone	Isotype	BioLegend Cat. No.
C3	CD275 (B7-H2, B7-RP1, ICOSL)	9F.8A4	Mouse IgG1, κ	329806
C4	CD276	MIH42	Mouse IgG1, κ	351004
C5	CD277	BT3.1	Mouse IgG1, κ	342704
C6	CD278 (ICOS)	C398.4A	Arm. Hamster IgG	313508
C7	CD279 (PD-1)	EH12.2H7	Mouse IgG1, κ	329906
C8	CD282 (TLR2)	TL2.1	Mouse IgG2a, κ	309708
C9	CD284 (TLR4)	HTA125	Mouse IgG2a, κ	312806
C10	CD286 (TLR6)	TLR6.127	Mouse IgG1, κ	334708
C11	CD290	3C10C5	Mouse IgG1, κ	354604
C12	CD294	BM16	Rat IgG2a, κ	350106
D1	CD298	LNH-94	Mouse IgG1, κ	341704
D2	CD300e (IREM-2)	UP-H2	Mouse IgG1, κ	339704
D3	CD300F	UP-D2	Mouse IgG1, κ	340604
D4	CD301	H037G3	Mouse IgG2a, κ	354704
D5	CD303	201A	Mouse IgG2a, κ	354204
D6	CD304	12C2	Mouse IgG2a, κ	354504
D7	CD307	509f6	Mouse IgG2a, κ	340304
D8	CD307d (FcRL4)	413D12	Mouse IgG2b, κ	340204
D9	CD314 (NKG2D)	1D11	Mouse IgG1, κ	320806
D10	CD317	RS38E	Mouse IgG1, κ	348406
D11	CD318 (CDCP1)	CUB1	Mouse IgG2b, κ	324006
D12	CD319 (CRACC)	162.1	Mouse IgG2b, κ	331806
E1	CD324 (E-Cadherin)	67A4	Mouse IgG1, κ	324106
E2	CD325	8C11	Mouse IgG1, κ	350805
E3	CD326 (Ep-CAM)	9C4	Mouse IgG2b, κ	324206
E4	CD328 (Siglec-7)	6-434	Mouse IgG1, κ	339204
E5	CD334 (FGFR4)	4FR6D3	Mouse IgG1, κ	324306

Plate 3

Well ID	Specificity	Clone	Isotype	BioLegend Cat. No.
E6	CD335 (NKp46)	9E2	Mouse IgG1, κ	331908
E7	CD336 (NKp44)	P44-8	Mouse IgG1, κ	325108
E8	CD337 (NKp30)	P30-15	Mouse IgG1, κ	325208
E9	CD338 (ABCG2)	5D3	Mouse IgG2b, κ	332008
E10	CD340 (erbB2/ HER-2)	24D2	Mouse IgG1, κ	324406
E11	CD344 (Frizzled-4)	CH3A4A7	Mouse IgG1, κ	326606
E12	CD351	TX61	Mouse IgG1, κ	137306
F1	CD352 (NTB-A)	NT-7	Mouse IgG1, κ	317208
F2	CD354 (TREM-1)	TREM-26	Mouse IgG1, κ	314906
F3	CD355 (CRTAM)	Cr24.1	Mouse IgG2a, κ	339106
F4	CD357 (GITR)	621	Mouse IgG1, κ	311604
F5	CD360 (IL-21R)	2G1-K12	Mouse IgG1, κ	347806
F6	β2-micro-globulin	2M2	Mouse IgG1, κ	316306
F7	BTLA	MIH26	Mouse IgG2a, κ	344506
F8	C3AR	hC3aRZ8	Mouse IgG2b	345804
F9	C5L2	1D9-M12	Mouse IgG2a, κ	342404
F10	CCR10	6588-5	Arm. hamster IgG	341504
F11	CLEC12A	50C1	Mouse IgG2a, κ	353604
F12	CLEC9A	8F9	Mouse IgG2a, κ	353804
G1	CX3CR1	2A9-1	Rat IgG2b, κ	341604
G2	CXCR7	8F11-M16	Mouse IgG2b, κ	331104
G3	δ-Opioid Receptor	DOR7D2A4	Mouse IgG2b, κ	327206
G4	DLL1	MHD1-314	Mouse IgG1, κ	346404
G5	DLL4	MHD4-46	Mouse IgG1, κ	346506
G6	DR3 (TRAMP)	JD3	Mouse IgG1, κ	307106
G7	EGFR	AY13	Mouse IgG1, κ	352904
G8	erbB3/HER-3	1B4C3	Mouse IgG2a, κ	324706

Plate 3

Well ID	Specificity	Clone	Isotype	BioLegend Cat. No.
G9	FcεRIα	AER-37 (CRA-1)	Mouse IgG2b, κ	334610
G10	FcRL6	2H3	Mouse IgG2b, κ	Inquire
G11	Galectin-9	9M1-3	Mouse IgG1, κ	348906
G12	GARP (LRRC32)	7B11	Mouse IgG2b, κ	352504
H1	HLA-A,B,C	W6/32	Mouse IgG2a, κ	311406
H2	HLA-A2	BB7.2	Mouse IgG2b, κ	343306
H3	HLA-DQ	HLADQ1	Mouse IgG1, κ	318106
H4	HLA-DR	L243	Mouse IgG2a, κ	307606
H5	HLA-E	3D12	Mouse IgG1, κ	342604
H6	HLA-G	87G	Mouse IgG2a, κ	335906
H7	IFN-g R b chain	2HUB-159	Hamster IgG	308504
H8	Ig light chain k	MHK-49	Mouse IgG1, κ	316508
H9	Ig light chain λ	MHL-38	Mouse IgG2a, κ	316608
H10	IgD	IA6-2	Mouse IgG2a, κ	348204
H11	IgM	MHM-88	Mouse IgG1, κ	314508
H12	IL-28RA	MHLICR2a	Mouse IgG2a, κ	337804

Plate 4

Well ID	Specificity	Clone	Isotype	BioLegend Cat. No.
A1	Blank			
A2	Integrin α9β1	Y9A2	Mouse IgG1, κ	351606
A3	integrin β5	AST-3T	Mouse IgG2a, κ	345204
A4	integrin β7	FIB504	Rat IgG2a, κ	321204
A5	Jagged 2	MHJ2-523	Mouse IgG1, κ	346904
A6	LAP	TW4-6H10	Mouse IgG1, κ	349704
A7	Lymphotoxin b Receptor (LT-bR)	31G4D8	Mouse IgG2b, κ	322008
A8	Mac-2 (Galectin-3)	Gal397	Mouse IgG1, κ	126705
A9	MAIR-II	TX45	Mouse IgG1, κ	334804
A10	MICA/MICB	6D4	Mouse IgG2a, κ	320906
A11	MSC (W3D5)	W3D5	Mouse IgG2a, κ	327506
A12	MSC (W5C5)	W5C5	Mouse IgG1, κ	327406
B1	MSC (W7C6)	W7C6	Mouse IgG1, κ	327606
B2	MSC and NPC (W4A5)	W4A5	Mouse IgG1, κ	330806
B3	MSCA-1 (MSC, W8B2)	W8B2	Mouse IgG1, κ	327306
B4	NKp80	5D12	Mouse IgG1, κ	346706
B5	Notch 1	MHN1-519	Mouse IgG1, κ	352106
B6	Notch 2	MHN2-25	Mouse IgG2a, κ	348304
B7	Notch 3	MHN3-21	Mouse IgG1, κ	345406
B8	Notch 4	MHN4-2	Mouse IgG1, κ	349004
B9	NPC (57D2)	57D2	Mouse IgG1, κ	327706
B10	Podoplanin	NC-08	Rat IgG2a, λ	337004
B11	Pre-BCR	HSL2	Mouse IgG1, κ	347904
B12	PSMA	LNI-17	Mouse IgG1, κ	342504
C1	Siglec-10	5G6	Mouse IgG1, κ	347604
C2	Siglec-8	7C9	Mouse IgG1, κ	347104
C3	Siglec-9	K8	Mouse IgG1, κ	351504

Plate 4

Well ID	Specificity	Clone	Isotype	BioLegend Cat. No.
C4	SSEA-1	MC-480	Mouse IgM, κ	125606
C5	SSEA-3	MC-631	Rat IgM, κ	330312
C6	SSEA-4	MC-813-70	Mouse IgG3, κ	330406
C7	SSEA-5	8E11	Mouse IgG1, κ	355204
C8	TCR g/d	B1	Mouse IgG1, κ	331210
C9	TCR Vβ13.2	H132	Mouse IgG1, κ	333108
C10	TCR Vβ23	αHUT7	Mouse IgG1, κ	349406
C11	TCR Vβ8	JR2 (JR.2)	Mouse IgG2b, κ	348104
C12	TCR Vβ9	MKB1	Mouse IgG2b, κ	349204
D1	TCR Vδ2	B6	Mouse IgG1, κ	331408
D2	TCR Vg9	B3	Mouse IgG1, κ	331308
D3	TCR Vα24-Jα18	6B11	Mouse IgG1, κ	342904
D4	TCR Vα7.2	3C10	Mouse IgG1, κ	351706
D5	TCR α/β	IP26	Mouse IgG1, κ	306708
D6	Tim-1	1D12	Mouse IgG1, κ	353904
D7	Tim-3	F38-2E2	Mouse IgG1, κ	345006
D8	Tim-4	9F4	Mouse IgG1, κ	354004
D9	TLT-2	MIH61	Mouse IgG1, κ	351104
D10	TRA-1-60-R	TRA-1-60-R	Mouse IgM, κ	330610
D11	TRA-1-81	TRA-1-81	Mouse IgM, κ	330708
D12	TSLPR (TSLP-R)	1B4	Mouse IgG1, κ	322806
E1	Ms IgG1, κ ITCL	MOPC-21	Mouse IgG1, κ	400112
E2	Ms IgG2a, κ ITCL	MOPC-173	Mouse IgG2a, κ	400212
E3	Ms IgG2b, κ ITCL	MPC-11	Mouse IgG2b, κ	400314
E4	Ms IgG3, κ ITCL	MG3-35	Mouse IgG3, κ	401320
E5	Ms IgM, κ ITCL	MM-30	Mouse IgM, κ	401609
E6	Rat IgG1, κ ITCL	RTK2071	Rat IgG1, κ	400408

Plate 4

Well ID	Specificity	Clone	Isotype	BioLegend Cat. No.
E7	Rat IgG2a, κ ITCL	RTK2758	Rat IgG2a, κ	400508
E8	Rat IgG2b, κ ITCL	RTK4530	Rat IgG2b, κ	400636
E9	Rat IgM, κ ITCL	RTK2118	Rat IgM, κ	400808
E10	AH IgG, ITCL	HTK888	Arm. Hamster IgG	400907
E11	Blank			
E12	Blank			
F1	Blank			
F2	Blank			
F3	Blank			
F4	Blank			
F5	Blank			
F6	Blank			
F7	Blank			
F8	Blank			
F9	Blank			
F10	Blank			
F11	Blank			
F12	Blank			
G1	Blank			
G2	Blank			
G3	Blank			
G4	Blank			
G5	Blank			
G6	Blank			
G7	Blank			
G8	Blank			
G9	Blank			
G10	Blank			
G11	Blank			
G12	Blank			
H1	Blank			
H2	Blank			
H3	Blank			
H4	Blank			
H5	Blank			
H6	Blank			
H7	Blank			
H8	Blank			
H9	Blank			

Plate 4

Well ID	Specificity	Clone	Isotype	BioLegend Cat. No.
H10	Blank			
H11	Blank			
H12	Blank			

B

Re-analysis of EBUS data with strict inclusion criteria

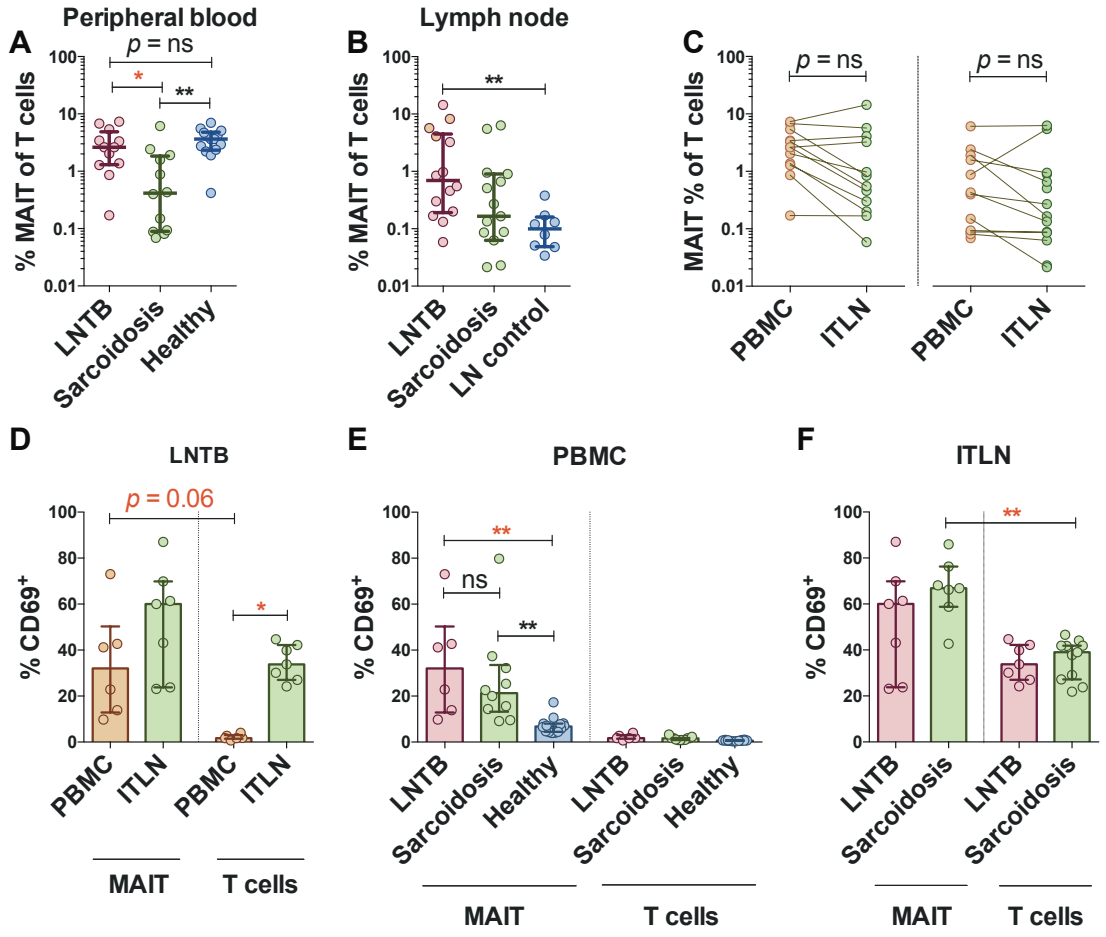


Figure B.1: MAIT cell EBUS data reanalysed without one LTBI individual in the LNTB group. PBMCs and EBUS-TBNA, or tonsillar tissue were assessed for MAIT cell frequencies, as a proportion of total T cells, and CD69-expression. One patient with lymphadenitis was diagnosed with latent TB infection, and is removed from this analysis. The remaining patients in the LNTB group were diagnosed with active TB. (A) MAIT cell frequency in PBMCs from lymph node TB (LNTB) and sarcoidosis patient groups, or healthy controls. (B) MAIT cell frequency in EBUS-TBNA samples from LNTB or sarcoidosis patient groups, or in tonsillar tissue homogenates from tonsillectomy patients. (C) Paired PBMC and intrathoracic lymph node (ITLN) MAIT cell frequencies in LNTB and sarcoidosis patients. (D) CD69-expression in LNTB patients, in PBMC and ITLN. (E) CD69-expression in LNTB, sarcoidosis and healthy controls, in PBMC. (F) CD69-expression in LNTB and sarcoidosis patients, in ITLN. Data shown as median ± IQR; analysed by (A, B, D–F) Kruskal-Wallis test with Dunn's multiple comparison post-test, and (C) Wilcoxon matched-pairs signed rank test. ***$p < 0.001$, **$p < 0.01$, *$p < 0.05$, ns = non-significant. Changes in statistical significance from the original analyses are indicated by red text. For original graphs inclusive of all LNTB patients according to initial criteria, see Fig. 6.2, p. 189, and Fig. 6.3, p. 191.

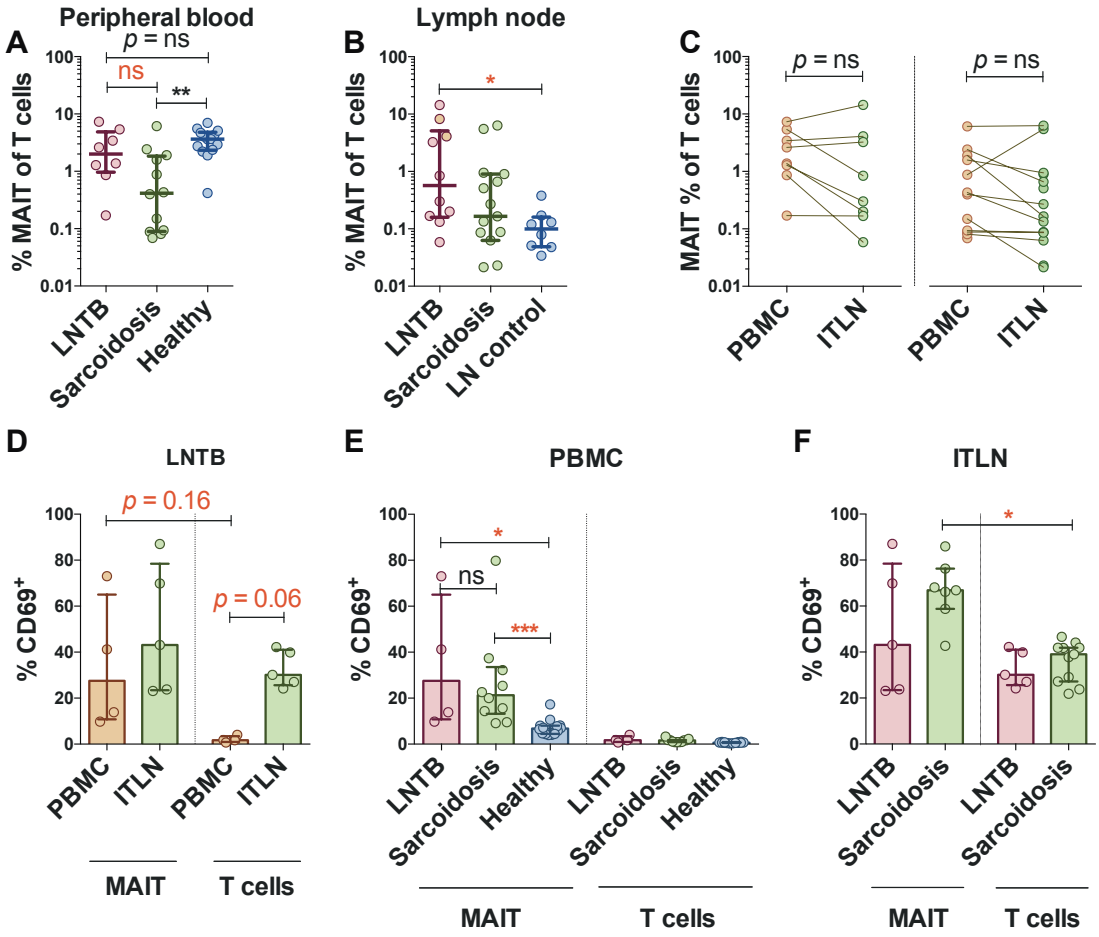


Figure B.2: MAIT cell EBUS data reanalysed without 5 *Mtb*-culture negative individuals in the LNTB group. PBMCs and EBUS-TBNA, or tonsillar tissue were assessed for MAIT cell frequencies, as a proportion of total T cells, and CD69-expression. Only *Mtb* culture positive individuals were included in the LNTB group. (A) MAIT cell frequency in PBMCs from lymph node TB (LNTB) and sarcoidosis patient groups, or healthy controls. (B) MAIT cell frequency in EBUS-TBNA samples from LNTB or sarcoidosis patient groups, or in tonsillar tissue homogenates from tonsillectomy patients. (C) Paired PBMC and intrathoracic lymph node (ITLN) MAIT cell frequencies in LNTB and sarcoidosis patients. (D) CD69-expression in LNTB patients, in PBMC and ITLN. (E) CD69-expression in LNTB, sarcoidosis and healthy controls, in PBMC. (F) CD69-expression in LNTB and sarcoidosis patients, in ITLN. Data shown as median ± IQR; analysed by (A, B, D–F) Kruskal-Wallis test with Dunn's multiple comparison post-test, and (C) Wilcoxon matched-pairs signed rank test. ***$p < 0.001$, **$p < 0.01$, *$p < 0.05$, ns = non-significant. Changes in statistical significance from the original analyses are indicated by red text. For original graphs inclusive of all LNTB patients according to initial criteria, see Fig. 6.2, p. 189, and Fig. 6.3, p. 191.

C

Representative FACS gating and purity test

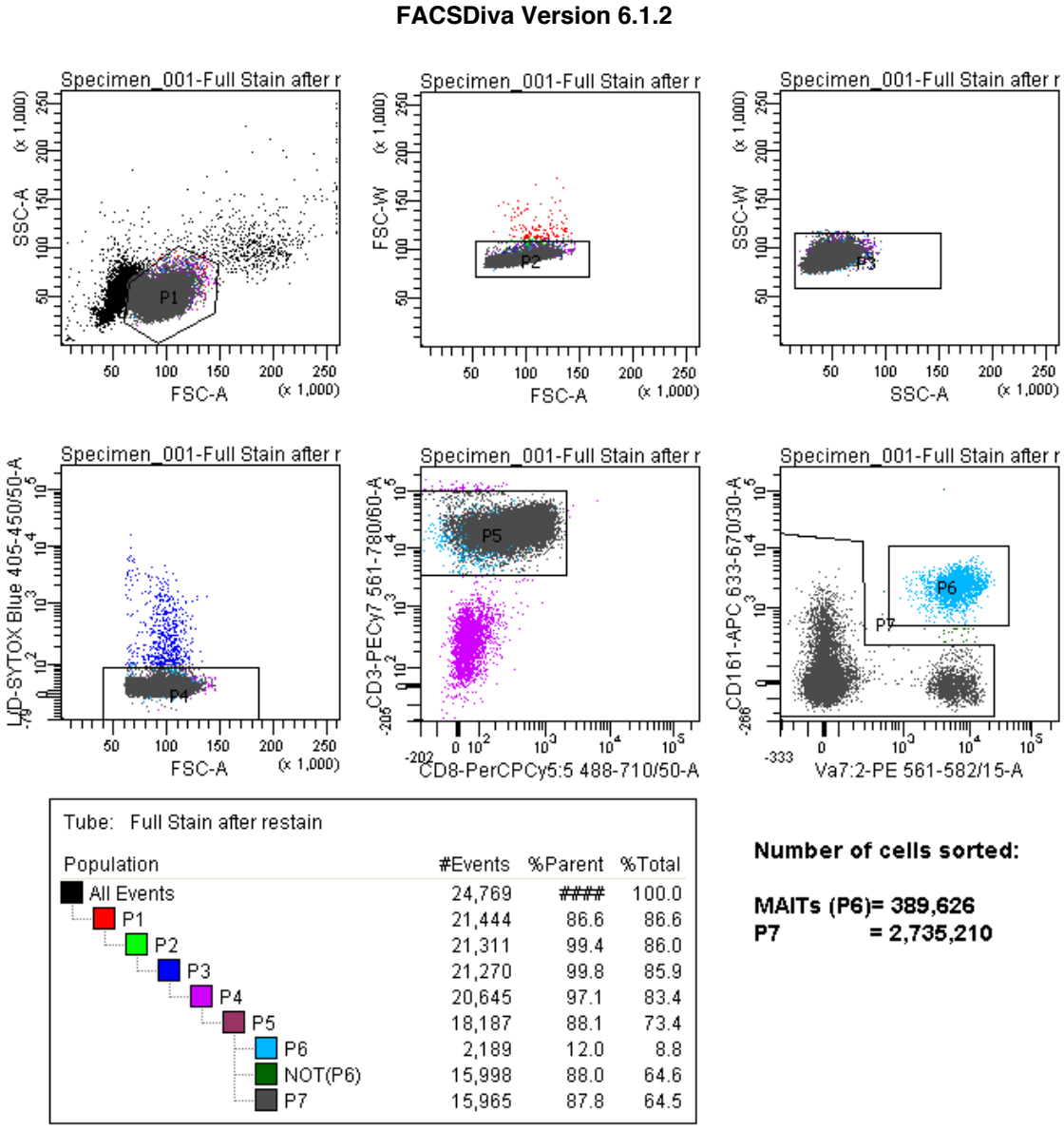


Figure C.1: Representative gating strategy for sort purification of MAIT cells. CD8α^+ T cells were magnetically enriched prior to staining with αCD3, CD8, CD161 and Vα7.2 antibodies. MAIT cells were gated according the figure. SYTOX Blue was included as a nucleic acid binding dye for the exclusion of dead cells. See Chapter 2.2.3, p. 44.

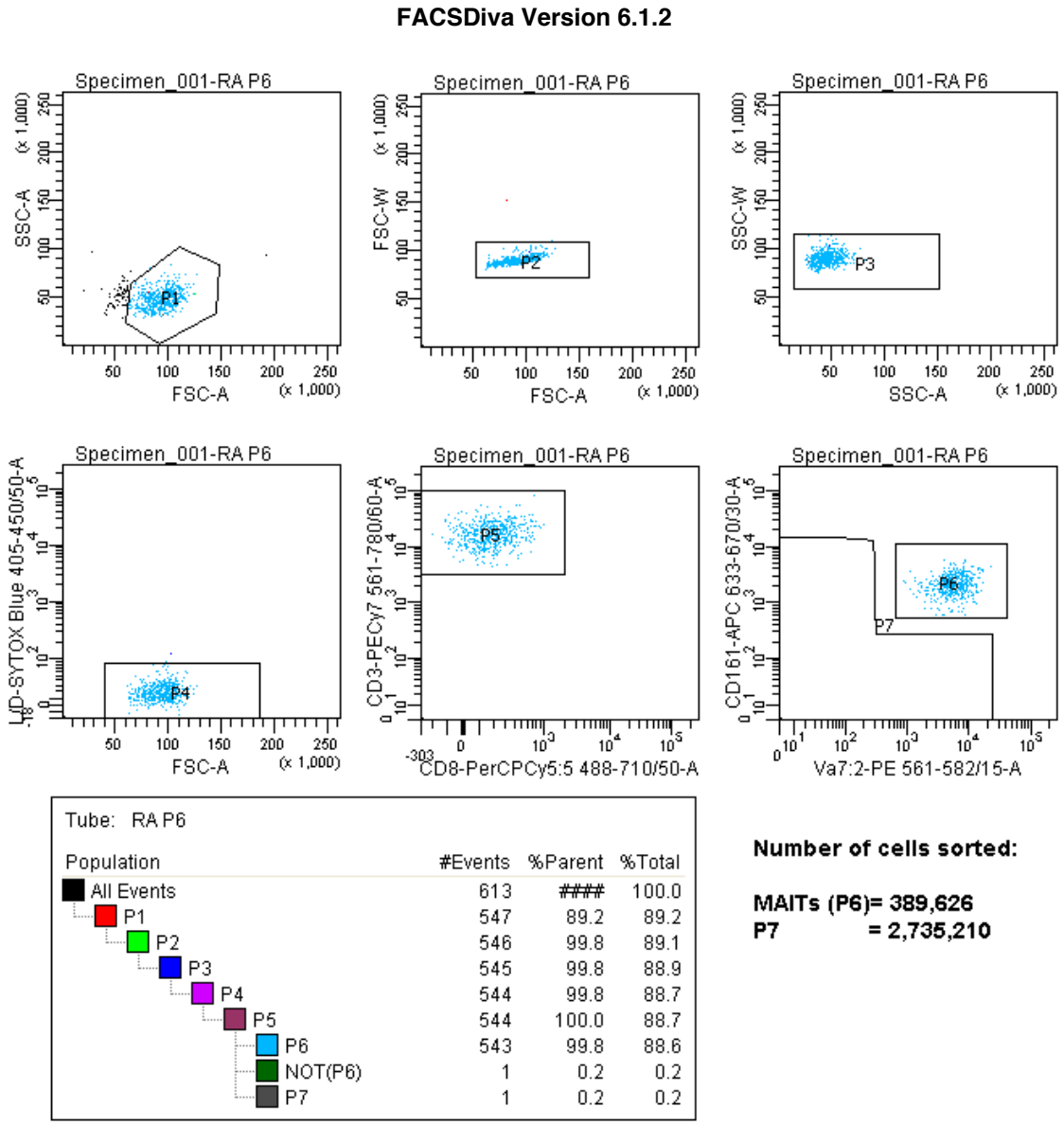


Figure C.2: Representative purity assessment following MAIT cell sort. Following each MAIT cell sort, a purity test was run. Purity was consistently > 95%, and typically >99%. See Chapter 2.2.3, p. 44.

D

Publications, presentations and awards

First author publications

- Ussher JE*, **Bilton M***, Attwod E, Shadwell J, Richardson R, de Lara C, Mettke E, Kurioka A, Hansen TH, Klenerman P, et al.: CD161++ CD8+ T cells, including the MAIT cell subset, are specifically activated by IL-12+IL-18 in a TCR-independent manner. Eur. J. Immunol. 2014, 44:195–203.

Conference presentations

- **Bilton M**, Nazneen A Siddiqi, David W Connell, Samuel Bremang, Heather Lambie, Onn-Min Kon, James E Ussher, Chris B Willberg, Ajit Lalvani, Paul Klenerman: TCR-dependent and independent activation of human MAIT cells by *M. tuberculosis* and their presence in lymph node disease. *Oral presentation.* CD1-MR1 conference. Mantra Lorne, Australia. 15–19 November, 2015.

- **Bilton M**, Nazneen Siddiqui, David W. Connell, James E. Ussher, Christan B. Willberg, Paul Klenerman, Ajit Lalvani: *In vitro* control of intracellular M. tuberculosis by primary human MAIT cells. *Poster presentation.* Host response in Tuberculosis conference. Santa Fe, New Mexico, USA. 22–27 January, 2015.

- James E. Ussher*, **Bilton M***, Emma Attwod, Jonathan Shadwell, Rachel Richardson, Catherine de Lara, Elisabeth Mettke, Ayako Kurioka, Ted H. Hansen, Paul Klenerman*, Christian B. Willberg*: $CD161^{++}CD8^{+}$ T cells, including the MAIT cell subset, are specifically activated by IL-12+IL-18 in a TCR-independent manner. *Poster presentation.* CD1-NKT symposium. Tours, France. 13–17 September 2013.

Awards

- Travel grant, CD1-MR1 conference. Mantra Lorne, Australia. 15–19 November, 2015.

European Journal of Immunology

CD161^{++}CD8^{+} T cells, including the MAIT cell subset, are specifically activated by IL-12+IL-18 in a TCR-independent manner

James E. Ussher[*1], Matthew Bilton*[*1], Emma Attwod[1], Jonathan Shadwell[1], Rachel Richardson[1], Catherine de Lara[1], Elisabeth Mettke[1], Ayako Kurioka[1], Ted H. Hansen[2], Paul Klenerman*[1,3] and Christian B. Willberg*[1,3]*

[1] Peter Medawar Building for Pathogen Research, University of Oxford, Oxford, UK
[2] Department of Pathology and Immunology, Washington University School of Medicine, St Louis, MO, USA
[3] Oxford NIHR Biomedical Research Centre, The John Radcliffe Hospital, Oxford, UK

CD161^{++}CD8^{+} T cells represent a novel subset that is dominated in adult peripheral blood by mucosal-associated invariant T (MAIT) cells, as defined by the expression of a variable-α chain 7.2 (Vα7.2)-Jα33 TCR, and IL-18Rα. Stimulation with IL-18+IL-12 is known to induce IFN-γ by both NK cells and, to a more limited extent, T cells. Here, we show the CD161^{++} CD8^{+} T-cell population is the primary T-cell population triggered by this mechanism. Both CD161^{++}Vα7.2^{+} and CD161^{++}Vα7.2^{-} T-cell subsets responded to IL-12+IL-18 stimulation, demonstrating this response was not restricted to the MAIT cells, but to the CD161^{++} phenotype. Bacteria and TLR agonists also indirectly triggered IFN-γ expression via IL-12 and IL-18. These data show that CD161^{++} T cells are the predominant T-cell population that responds directly to IL-12+IL-18 stimulation. Furthermore, our findings broaden the potential role of MAIT cells beyond bacterial responsiveness to potentially include viral infections and other inflammatory stimuli.

Keywords: CD161^{++} T cells · IL-12 · IL-18 · MAIT cells · T cells

Additional supporting information may be found in the online version of this article at the publisher's web-site

Introduction

High expression of CD161 by CD8^{+} T cells defines the overlapping Tc17 and mucosal-associated invariant T (MAIT) cell populations. Both subsets are thought to develop from a pool of precommitted CD161 high expressing T cells [1]. Human MAIT cells comprise up to ~5% of the total T-cell population, compared with ~0.1% invariant natural killer T (NKT) cells (Vα24-Jα18^{+}), and dominate the CD161^{++}CD8^{+}T cell population within adult peripheral blood, representing up to 95% of this population [1, 2]. Thus, these cells represent a major innate-like T lymphocyte population within the human body.

MAIT cells express a semi-invariant TCR, composed of the invariant variable-α chain 7.2 (Vα7.2)-Jα33 [1, 3, 4]. They are

Correspondence: Dr. Christian B. Willberg
e-mail: Chris.Willberg@ndm.ox.ac.uk

*These authors contributed equally to this work.

© 2013 The Authors. *European Journal of Immunology* published by Wiley-VCH Verlag GmbH & Co. KGaA Weinheim.
This is an open access article under the terms of the Creative Commons Attribution License, which permits use, distribution and reproduction in any medium, provided the original work is properly cited.

restricted to the evolutionarily conserved, nonpolymorphic MHC-related protein (MR) 1 [3–5]. Evidence from a number of groups has suggested that the source of the MR1 ligand is bacterial [6–9]. Recently, Kjer-Nielsen et al. demonstrated that the riboflavin metabolite, rRL-6-CH_2OH, was able to stabilize MR1 and activate MAIT cells, suggesting that MAIT cells are specific for riboflavin-producing microorganisms [10].

$CD161^{++}CD8^+$ T cells, and the MAIT cell subset, are found at potential sites of pathogen entry within epithelia, in particular lamina propria, as well as in high numbers in the liver [4, 11, 12]. The MAIT cell subset has been associated with protection from bacterial infections in a number of mouse models: *Klebsiella pneumoniae* [13], *Escherichia coli* [8], *Mycobacterium abscessus* [8], and BCG [14]. Furthermore, in humans, MAIT cells have also been observed within the lungs of tuberculosis patients [15].

$CD161^{++}CD8^+$ T cells have also been implicated in a number of inflammatory settings independent of bacterial infection. They are enriched within the livers of patients with chronic hepatitis C (HCV) infection, autoimmune hepatitis, primary biliary cirrhosis, alcoholic liver disease, and nonalcoholic steatohepatitis [12, 16]. $CD161^{++}CD8^+$ T cells have been found in the brains of patients with multiple sclerosis and have been suggested to have a pathogenic role [17]. Moreover, Tc17 cells are thought to play an important role orchestrating skin inflammation in murine models of psoriasis [18].

Overall, there is strong evidence that $CD161^{++}CD8^+$ T cells, including the MAIT cell subset, have an important role in inflammation, even in the absence of bacterial infection. However, the mechanism(s) driving the activation of these cells is not clear.

Given the high expression of the IL-18 receptor observed on the $CD161^{++}CD8^+$ T-cell population [12], we hypothesized that $CD161^{++}CD8^+$ T cells, including the MAIT cell subset, could be activated by cytokine stimulation with IL-12 and IL-18, as has been reported with NK cells [19]. Here, we demonstrate that not only could this population express IFN-γ in response to cytokine stimulation, but it was also the primary T-cell population to do so. Furthermore, we demonstrate that bacteria, including nonriboflavin metabolizing species, and Toll-like receptor (TLR) agonists could indirectly activate $CD161^{++}CD8^+$ T cells via this mechanism.

Results

IL-12+IL-18 stimulation specifically activates $CD161^{++}CD8^+$ T cells

Initially, we confirmed the previous findings that $CD161^{++}CD8^+$ T cells expressed a significantly higher level of IL-18Rα compared with other $CD8^+$T cell subsets [12]. Indeed, $CD161^{++}CD8^+$ T cells expressed significantly higher IL-18Rα levels compared with either $CD161^+$ ($p \leq 0.001$) or $CD161^-$ subpopulations ($p \leq 0.001$, Fig. 1A and B). Interestingly, the level of expression was also almost threefold higher than on NK cells ($p \leq 0.001$).

It is well established that the combination of IL-12 and IL-18 induces IFN-γ expression by murine NK cells and T cells [20, 21]. Therefore, we asked if $CD161^{++}CD8^+$ T cells were more sensitive to IL-12+IL-18 stimulation compared with the other T-cell subsets. Surprisingly, only the $CD161^{++}CD8^+$ T-cell population responded robustly to stimulation (mean approximately 50%) (Fig. 1C and D). While both $CD161^+CD8^+$ T-cell and $CD161^+CD4^+$ T-cell populations made limited responses (mean response $\leq$ 10%), $CD161^-CD8^+$ T-cell and $CD161^-CD4^+$ T-cell populations did not respond. Stimulation with either IL-12 or IL-18 alone did not induce IFN-γ expression from any T-cell subset (Fig. 1E).

IL-12+IL-18-induced IFN-γ expression is TCR independent

In adults, MAIT cells dominate the $CD161^{++}CD8^+$ T-cell population, representing approximately 87% of the total population (Fig. 3A) [1]. They express a semi-invariant TCR and are restricted to MR1. However, little is known about the expression and regulation of MR1. Therefore, we investigated whether the stimulation of $CD161^{++}CD8^+$ T cells by IL-12+IL-18 was MR1 dependent.

First, PBMCs were stimulated with either IL-12+IL-18 or *E. coli* in the presence or absence of the MR1 blocking-antibody, clone 26.5 (Fig. 2A) [5]. Anti-MR1 did not affect the ability of the cells to respond IL-12+IL-18, but reduced IFN-γ expression induced by *E. coli* ($p = 0.0135$).

Next, to confirm that IL-12+IL-18 stimulation was truly TCR independent, PBMCs were stimulated with either IL-12+IL-18 or anti-CD2/CD3/CD28 beads in the presence or absence of inhibitors cyclosporin A, an inhibitor of TCR signaling, and SB203580, a p38-MAPK inhibitor (Fig. 2B). Cyclosporin A did not inhibit IFN-γ expression induced by IL-12+IL-18, but did significantly inhibit IFN-γ expression by anti-CD2/CD3/CD28 beads (p = ns and $p = 0.001$ respectively). In contrast, the p38-MAPK inhibitor (SB203580), which inhibits IL-12+IL-18 signaling [22], inhibited IL-12+IL-18-induced IFN-γ expression ($p = 0.001$), but not anti-CD2/CD3/CD28 stimulation. Thus, IL-12+IL-18-induced IFN-γ production was independent of TCR signaling.

IL-12+IL-18-induced IFN-γ expression is not restricted to the $CD161^{++}CD8^+$ T cells MAIT cell subset

As IL-12+IL-18-induced IFN-γ production was independent of MR1 and TCR signaling, we questioned whether IL-12+IL-18 responsiveness was a characteristic specific to the MAIT cells, or to the $CD161^{++}CD8^+$ T-cell population as a whole. T cells possessing the Vα7.2 TCR dominate the $CD161^{++}CD8^+$ T-cell population in adult peripheral blood, ranging from approximately 70–95% in healthy individuals (Fig. 3A).

We assessed IL-18Rα expression and found significantly higher levels of expression on $V\alpha7.2^+CD161^{++}CD8^+$ T cells compared with the smaller $V\alpha7.2^-CD161^{++}CD8^+$ T-cell subset ($p = 0.0091$, Fig. 3B). However, this difference did not result in increased sensitivity to IL-12+IL-18 stimulation as both subsets responded

© 2013 The Authors. *European Journal of Immunology* published by Wiley-VCH Verlag GmbH & Co. KGaA Weinheim.

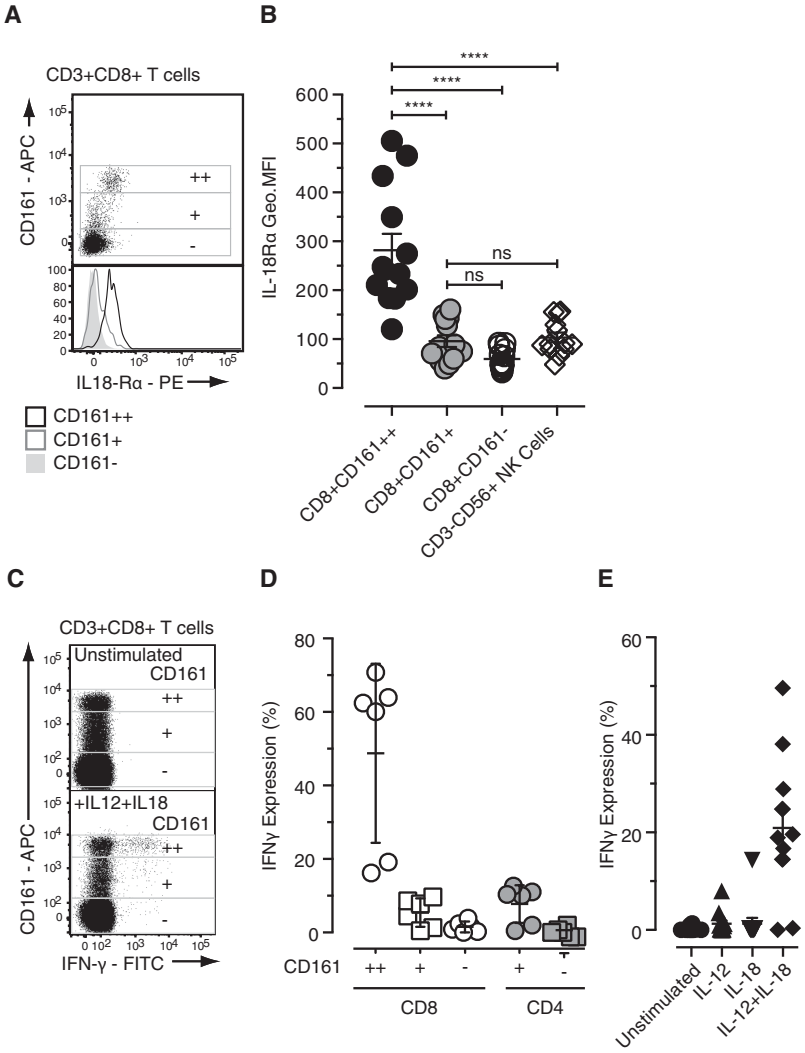


Figure 1. Intra- and extracellular IL-18Rα expression on $CD8^+$ T-cell subsets. (A) Representative flow cytometry plots of IL-18Rα expression are shown. (B) The geometric MFI of IL-18Rα expression for each subset is shown ($n = 13$). (C, D) IL-12+IL-18 specifically triggers $CD161^{++}CD8^+$ T cells to express IFN-γ. (C) Raw flow cytometry data, as well as (D) IFN-γ expression by the different T-cell subsets after stimulation with IL-12+IL-18 are shown ($n = 6$). (E) Neither IL-12 nor IL-18 alone induces IFN-γ expression by the $CD161^{++}$ $CD8^+$ T-cell population ($n = 10$). Each symbol represents an individual sample and bars represent means and SEM. Data shown are pooled from three experiments performed. $^{****}p < 0.0001$, one-way repeated measures ANOVA with Bonferroni's multiple comparison test.

equally to IL-12+IL-18 stimulation (Fig. 3C). Furthermore, titration of IL-18 did not reveal the MAIT cell subgroup to be more sensitive to lower IL-18 concentrations compared with either the $V\alpha7.2^-CD161^{++}CD8^+$ T-cell or NK-cell populations (Fig. 3D). This was true both in terms of the percentage of cells responding and the levels of IFN-γ expressed by each cell (as determined by the geometric MFI).

Therefore, the ability to respond to IL-12+IL-18 is TCR independent. Furthermore, this is a characteristic of all $CD161^{++}CD8^+$ T cells, and is not restricted to just the $V\alpha7.2^+CD161^{++}CD8^+$ T-cell (MAIT cell) subpopulation.

Bacterial stimulation indirectly activates $CD161^{++}CD8^+$ T cells via IL-12 and IL-18

The key characteristic of MAIT cells is their ability to respond to bacterial infection via MR1. However, exposure of antigen presenting cells (APCs), such as monocytes, macrophages, and dendritic cells (DCs), to bacteria results in the expression of a wide range of proinflammatory cytokines, including IL-12 and IL-18 [23, 24]. Thus, the total $CD161^{++}CD8^+$ T-cell population has the potential to respond indirectly to a wide range of microbial infections.

Using the THP-1 cell line as APCs, we first explored the contribution of MR1 and IL-12+IL-18 to the activation of $CD161^{++}CD8^+$ T cells by bacteria. When THP-1 cells were cultured overnight with paraformaldehyde-fixed *E. coli* and then cocultured with $CD8^+$ T cells for 5 h, activation was specific to $CD161^{++}CD8^+$ T cells and was predominantly MR1 mediated (Fig. 4A and C). Blocking with anti-MR1 inhibited all IFN-γ expression, while anti-IL-12 plus anti-IL-18 blocking antibodies had no effect. However, when $CD8^+$ T cells were cocultured with THP-1 cells and *E. coli* for 20 h, both MR1 and IL-12+IL-18 signaling contributed to IFN-γ expression, as blockade of either pathway reduced IFN-γ expression by ~50%. Moreover, when THP-1 cells were exposed to paraformaldehyde-fixed *Enterococcus faecalis*, a species unable to synthesize riboflavin, only anti-IL-12+IL-18 blocked IFN-γ expression at either time point and again this was specific to the $CD8^+CD161^{++}$ T cells (Fig. 4B and D), although the size of the response was much lower.

© 2013 The Authors. *European Journal of Immunology* published by Wiley-VCH Verlag GmbH & Co. KGaA Weinheim.

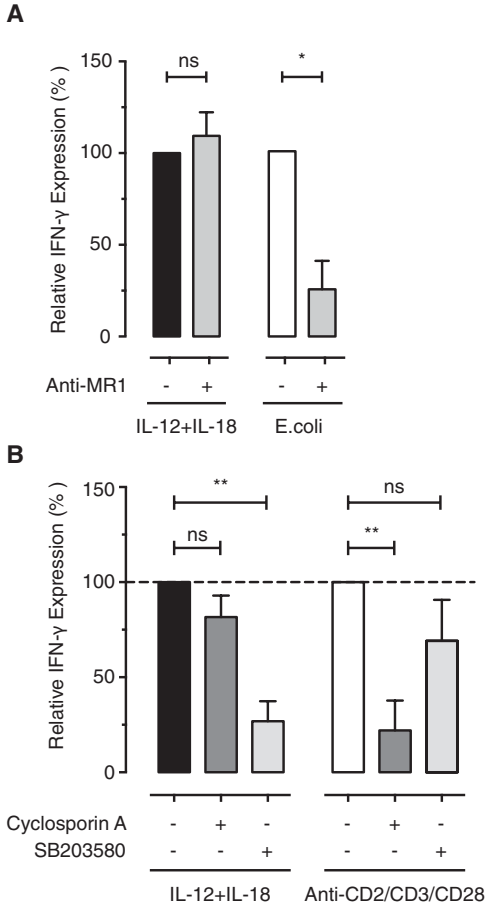


Figure 2. IFN-γ expression was not dependent on TCR signaling. (A) PBMCs were stimulated either with IL-12+IL-18 or with *E. coli* ± anti-MR1 (5 μg/mL) ($n = 7$). (B) PBMCs were stimulated with either IL-12+IL-18 or anti-CD2/CD3/CD28 ± inhibitors cyclosporin A or SB203580 ($n = 7$). Relative IFN-γ expression was determined by FACS. Data are shown as mean ± SEM of the indicated number of samples and are pooled from two experiments performed. $^{*}p < 0.05$, $^{**}p < 0.01$, one-way repeated measures ANOVA with Bonferroni's multiple comparison test.

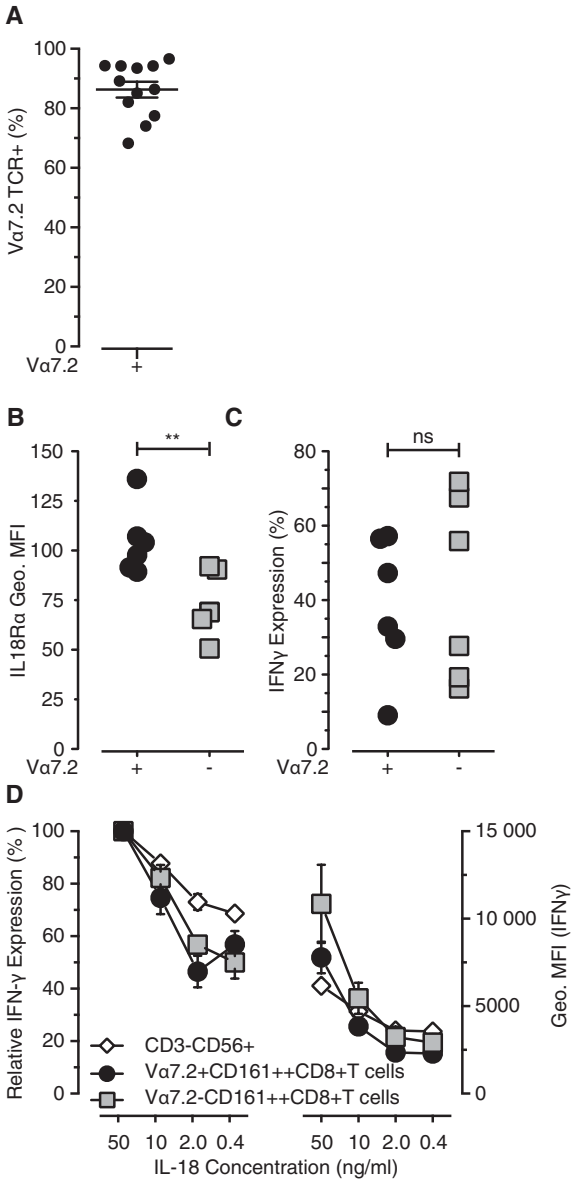


Figure 3. IFN-γ expression was not restricted to the MAIT cell subset of $CD161^{++}CD8^{+}$ T cells. (A) The percentage of $CD161^{++}CD8^{+}$ T cells that possess the Vα7.2 TCR. (B) The level of extracellular IL-18Rα expression was compared on the two $CD161^{++}CD8^{+}$ T cell subsets: $V\alpha7.2^{+}$ and $V\alpha7.2^{-}$ ($n = 6$). (C) The level of IFN-γ after IL-12+IL-18 stimulation was also measured for the two Vα7.2 subsets ($n = 6$). (D) IL-18 was titrated into PBMC cultures in the presence of IL-12. The percentage of maximum IFN-γ expression, induced by IL-18 at 50 ng/mL, was used to compare sensitivity to lower IL-18 concentrations ($n = 6$). The levels of IFN-γ expression were determined by the geometric MFI of the $IFN\text{-}\gamma^{+}$ population for each cell subset ($n = 6$). (A–C) Each symbol represents an individual population. (D) Data are shown as mean ± SEM of the indicated number of samples and are from one experiment representative of at least two performed. $^{**}p < 0.01$, paired *t*-test.

The differing ability of *E. coli* and *E. faecalis* treated THP1 cells to induce IFN-γ production from the $CD161^{++}CD8^{+}$ T cells was reflected in the amount of IL-12 and IL-18 secreted.

Treatment with *E. coli* resulted in considerably greater production of IL-12 compared to treatment with *E. faecalis*.

After a 20 h culture, the addition of 2×10^6 and 2×10^7 *E. coli* per 10^5 THP-1 cells resulted in a mean IL-12 concentration of 2170 and 1872 pg/mL respectively. However, *E. faecalis*, at equal MOIs, only induced a mean IL-12 concentration of 81 and 253 pg/mL, respectively (Supporting Information Fig. 2A). However, no difference was observed in their ability to induce IL-18 (Supporting Information Fig. 2B).

$CD161^{++}CD8^{+}$ T cells respond indirectly to TLR agonists

Bacteria are large complex microorganisms that can trigger a number of different pathogen recognition receptors, such as TLRs. TLRs are potent activators of the immune system and induce a number of proinflammatory cytokines, including IL-12 and IL-18 [25–28]. To test the importance of each TLR individually, we stimulated THP-1 cells with agonists to TLR 1–9 for 24 h, washed the cells extensively, and cocultured them with $CD8^{+}$

© 2013 The Authors. *European Journal of Immunology* published by Wiley-VCH Verlag GmbH & Co. KGaA Weinheim.

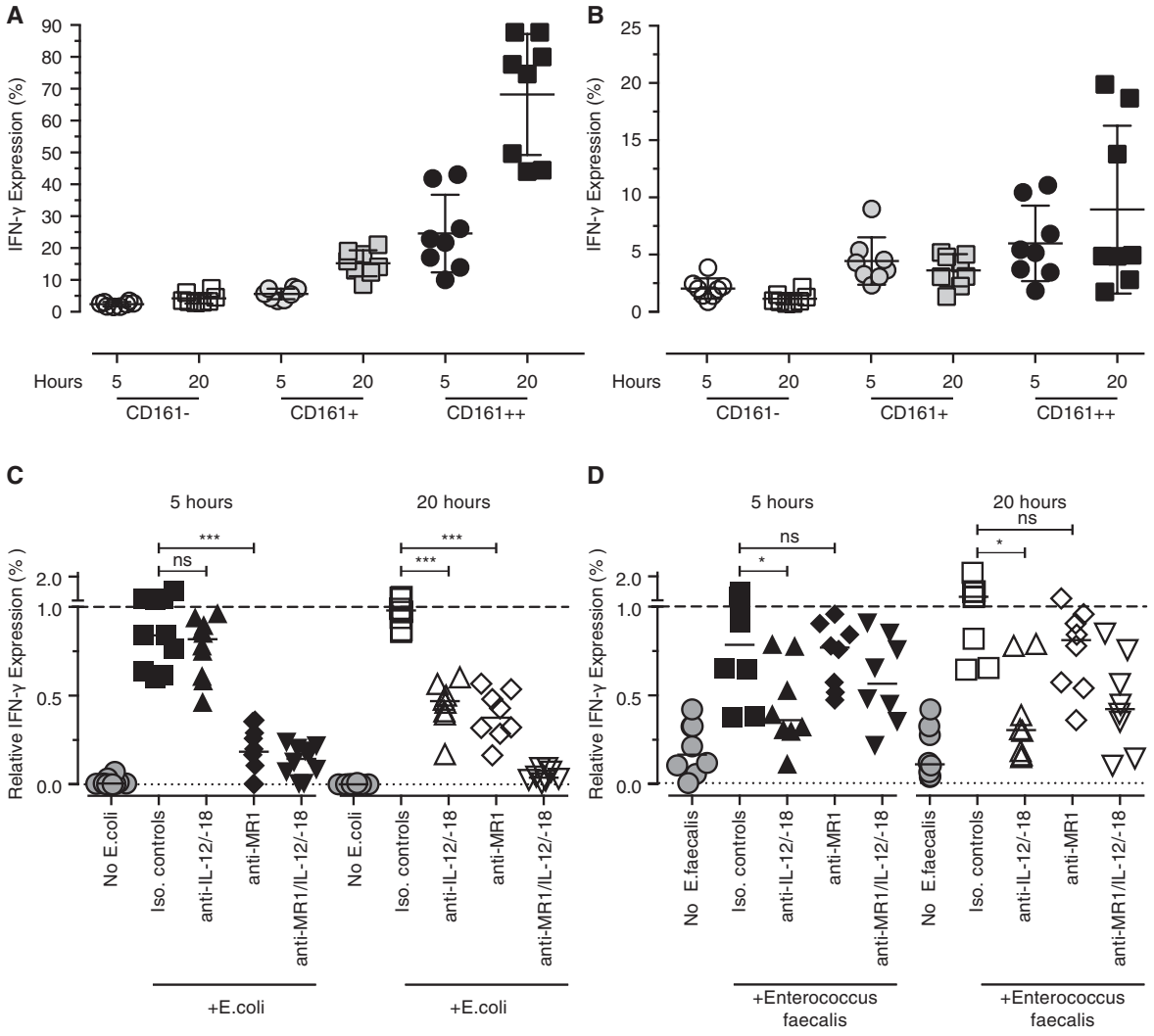


Figure 4. Bacterial or TLR agonist stimulation leads to IL-12+IL-18-mediated activation of CD161^{++}/MAIT cells. Percentage of IFN-γ expression by CD161^{++}, CD161^{+}, and CD161^{-} CD8^{+} T cells cocultured with THP-1 cells exposed to (A) *Escherichia coli* or (B) *Enterococcus faecalis*, for 5 or 20 h ($n = 8$). IFN-γ expression was compared between cocultures of CD8^{+} T cells and THP-1 cells, cultured with (C) *E. coli* or (D) *E. faecalis*, in the presence or absence of blocking antibodies against IL-12, IL-18, MR1 (10 μg/mL), or isotype controls, for either 5 or 20 h. Data are presented as relative IFN-γ expression compared with that of cocultures in the absence of any antibodies. Each symbol represents an individual sample and bars represent means. $^{*}p < 0.05$, $^{**}p < 0.01$, $^{***}p < 0.001$, one-way repeated measures ANOVA with Bonferroni's multiple comparison test.

T cells for 16 h. Only coculture with lipopolysaccharide (LPS) (TLR4 agonist) treated THP-1 cells stimulated IFN-γ production by CD161^{++}CD8^{+} T cells (Fig. 5A). This could be blocked by anti-IL-12 plus anti-IL-18 blocking-antibodies, but not by anti-MR1 (Fig. 5B).

The inability of the THP-1 cells, stimulated with the other TLR agonists, to activate CD161^{++}CD8^{+} T cells could reflect the TLRs expressed by this cell line. Therefore, we tested PBMCs with the different TLR agonists and assessed IFN-γ production by the CD161^{++}CD8^{+}T cell population. Unexpectedly, only the presence of the TLR8 agonist, ssRNA$_{40}$, induced IFN-γ expression by the CD161^{++}CD8^{+} T cells. This was not blocked by anti-MR1 ($p \leq 0.01$, Fig. 5C). However, again both IL-12 and IL-18 were required for activation (Fig. 5D).

IFN-γ expression, induced by both TLR4 and TLR8 agonists, was restricted to the CD161^{++}CD8^{+} T cell subset (Supporting Information Fig. 3A and B). This is consistent with the previous IL-12+IL-18 stimulation data (Fig. 1D).

To demonstrate that the response was TLR8 dependent, PBMCs were cultured with the TLR8 agonist plus the vacuolar-type H^{+} ATPase inhibitor, bafilomycin A1. Bafilomycin A1 significantly inhibited expression of IFN-γ by the CD161^{++}CD8^{+} T cells ($p \leq 0.01$, Fig. 5E).

Furthermore, the expression of the active form of IL-18 requires caspase-1 and the inflammasome [29]. To confirm the involvement of caspase-1, PBMCs were cultured with the TLR8 agonist and the caspase inhibitor Z-WEHD. This resulted in a significant reduction of IFN-γ production by the CD161^{++}CD8^{+} T cells ($p \leq 0.05$, Fig. 5E).

© 2013 The Authors. *European Journal of Immunology* published by Wiley-VCH Verlag GmbH & Co. KGaA Weinheim.

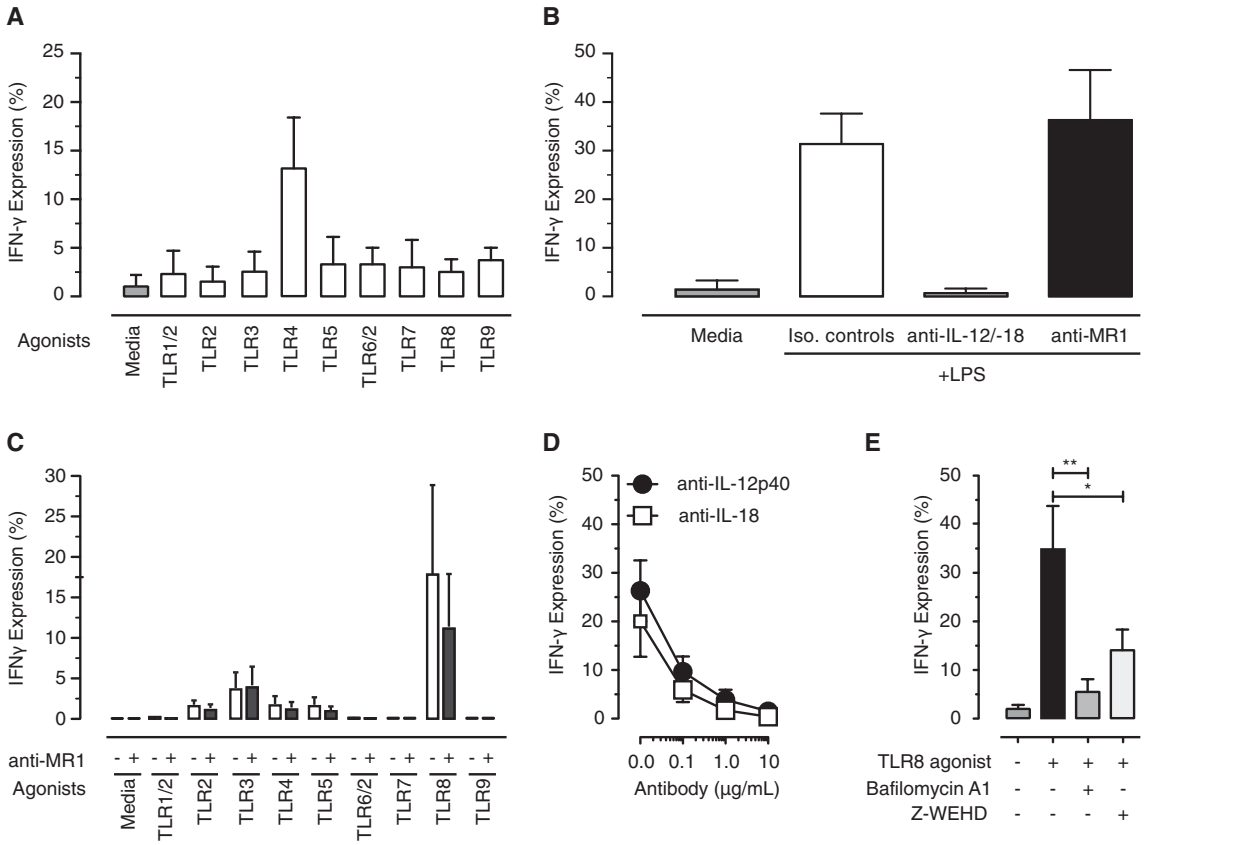


Figure 5. Toll-like receptor activation leads to IFN-γ expression by CD161^{++}CD8^{+} T cells indirectly by IL-12+IL-18 expression. (A) THP-1 cells were stimulated overnight with TLR agonists (1–9), prior to coculture with CD8^{+} T cells. IFN-γ expression by CD161^{++}CD8^{+} T cells was subsequently measured after a further 20 h incubation ($n = 4$). (B) LPS-stimulated THP-1 cells were cocultured with CD8^{+} T cells ± anti-IL-12, -IL-18, and -MR1 blocking antibodies (5 μg/mL) ($n = 2$). (C) PBMCs were stimulated for 24 h in the presence of TLR agonists (1–9) ± anti-MR1 and IFN-γ expression by CD161^{++}CD8^{+} T cells measured ($n = 8$). (D) TLR8 agonist-induced IFN-γ expression following titration of blocking antibodies against IL-12p40 or IL-18 ($n = 4$). (E) TLR8 agonist signaling is dependent on TLR8 and the inflammasome. PBMCs were stimulated with the TLR8 agonist ± bafilomycin A or Z-WEHD ($n = 7$). Data are shown as mean ± SEM of the indicated number of samples and are pooled from two experiments performed. $^{*}p < 0.05$, $^{**}p < 0.01$, one-way repeated measures ANOVA with Bonferroni's multiple comparison test.

Discussion

A number of studies have suggested that CD161^{++}CD8^{+} T cells, and the MAIT cell subset, are associated with viral and autoimmune inflammatory conditions [12, 16–18]. This has raised the question of whether these cells actively contribute to inflammation and if so by what mechanism. In this study, we have demonstrated that CD161^{++}CD8^{+} T cells, including both Vα7.2^{+} MAIT cells and Vα7.2^{-} cells, are able to produce IFN-γ in an MR1-independent fashion in response to IL-12 plus IL-18. This provides a mechanism by which these cells may contribute to the pathogenesis of inflammatory disease.

IL-18 was first identified as IFN-γ inducing factor by Okamura et al. in 1995 [30]. When combined with IL-12, IL-18 has been shown to be potent inducer of IFN-γ in human NK cells and, to a more limited extent, in human T cells [31]. In this study, we have shown that the CD161^{++}CD8^{+} T-cell population is the major T-cell population that produced IFN-γ in response to IL-12+IL-18 stimulation. Furthermore, the response to IL-12+IL-18 was TCR independent and was not restricted to the Vα7.2^{+} MAIT cell subpopulation, but was a characteristic of the entire CD161^{++}CD8^{+} T-cell population (both Vα7.2^{+} and Vα7.2^{-}). Although the MAIT cell subset expressed higher level of IL-18Rα compared to the CD161^{++}CD8^{+} Vα7.2^{-} T-cell population, they did not show a greater sensitivity to IL-18 stimulation. The higher levels of IL-18Rα could be a reflection of a more activated state of the MAIT cells, as they also express higher levels of CD69 (data not shown). However, the IL-18 receptor is a heterodimer comprising IL-18Rα and IL-18β chains. Thus, the lack of an associated increase in sensitivity may be due to the levels of expression of the IL-18β chain, which has been shown to be essential for signaling [32].

IL-12 and IL-18 are proinflammatory cytokines expressed by monocytes, macrophages, and DCs in response to a range of pathogenic stimuli [25, 28]. Using THP-1 cells as APCs, we demonstrated that both *E. coli* and *E. faecalis* induce sufficient IL-12 and IL-18 to activate CD161^{++}CD8^{+} T cells. In the case of *E. coli*, which contains the riboflavin synthetic pathway and is able to activate MAIT cells via MR1 [8, 10, 33], early activation (5 h) was solely MR1 dependent, while with longer coincubation (20 h) both TCR stimulation and IL-12+IL-18 contributed to

© 2013 The Authors. *European Journal of Immunology* published by Wiley-VCH Verlag GmbH & Co. KGaA Weinheim.

activation. In contrast, activation by *E. faecalis*, which lacks the riboflavin synthetic pathway and does not activate MAIT cells via MR1 [8, 10], was solely dependent on IL-12+IL-18. The weaker stimulation seen with *E. faecalis*, compared to *E. coli*, may reflect the differing abilities of the bacteria to induce cytokine production, in particular IL-12. Of note, a recent study in mice demonstrated that MAIT cells were able to control intracellular growth of BCG in an IL-12-dependent, MR1-independent manner, suggesting that TCR-independent activation may play the dominant role in MAIT cell effector function in vivo [14]. In contrast to mice, we found that human MAIT cells require both IL-12 and IL-18 stimulation for TCR-independent activation.

TLR stimulation has also been reported to induce production of IL-12 and IL-18 [28, 34, 35]. Using the THP-1 model, we demonstrated that LPS, a TLR4 agonist, but not other TLR agonists, was able to stimulate IFN-γ production by the $CD161^{++}CD8^{+}$ T-cell population in an IL-12+IL-18-dependent, MR1-independent manner. This is consistent with the stronger response observed to *E. coli* than to *E. faecalis*, which lacks LPS. Alternatively, TCR stimulation may allow the $CD161^{++}CD8^{+}$ T cells to respond more vigorously to IL-12+IL-18, as suggested by the partial blockade in response at 20 h with the MR-1 blocking antibody. Furthermore, that $CD161^{++}CD8^{+}$ T cells responded to *E. faecalis* in an IL-12+IL-18-dependent manner suggests that THP1s can produce IL-12+IL-18 to stimuli other than TLR4 agonists, such as combinations of pathogen-associated molecular patterns (PAMPs). Indeed, when a TLR agonist panel was tested on PBMCs, the TLR8 agonist was the most potent indirect activator of $CD161^{++}CD8^{+}$ T cells. Again, activation was dependent upon IL-12+IL-18 production. These data differ from those presented by Le Bourhis et al., who showed that murine bone marrow (BM) derived DCs, stimulated with LPS, were unable to activate MAIT cells in an overnight coculture, although a reduction in response to *E. coli* was seen at lower multiples of infection with *MyD88*$^{-/-}$ BMDCs [8]. This contrasts with Chua et al., who showed that BCG-mediated MAIT cell activation was dependent upon IL-12 production by infected macrophages [14]. These results are most likely due to differences in cytokines induced by different TLR agonists, or a difference in the response by the APCs involved. For example, Humann et al. demonstrated that murine BMDCs were unable to express IL-18 in response to LPS stimulation, although they were able to with *L. monocytogenes* stimulation [36]. Furthermore, it has not been reported whether murine MAIT cells express IL-18R. Therefore, differences between the data presented here and previous reports may reflect the different APCs used, as well as the ability of murine MAIT cells to respond to IL-12+IL-18. Overall, this suggests that in vivo, TCR-independent mechanisms of $CD161^{++}CD8^{+}$ T-cell activation will be dependent upon the interactions of local APCs and PAMPs.

Interestingly, in our model, IL-12+IL-18-induced IFN-γ expression by the $CD161^{++}CD8^{+}$ T cells was only seen at the 20 to 24 h time point, and not after 5 h. The lack of early IL-12+IL-18-induced IFN-γ is consistent with previous findings in NK cells and has been suggested to be due to the upregulation of transcription factors, such as IκBξ [37–39]. Furthermore, this highlights the 5 h THP1 model as a useful tool for probing the MR1-dependent activation of MAIT cells.

TCR-independent activation of $CD161^{++}CD8^{+}$ T cells provides a mechanism by which this population can respond to a wide range of pathogens, including those that do not provide a ligand for MR1. This is of particular interest for the MAIT cell populations, as the ability to respond to TLR8 agonist-induced IL-12 and IL-18 suggests that, in addition to the antibacterial role, they may play an important role in antiviral responses, as has been suggested for invariant NKT cells in in vivo infection models [40]. Interestingly, both HBV and HCV infections have been associated with IL-12 and IL-18 expression [41, 42]. We have previously shown $CD161^{++}CD8^{+}$ T cells are depleted in blood of patients with chronic hepatitis C, while Tc17 cells were enriched in the liver [12]. Future studies to investigate the role of $CD161^{++}CD8^{+}$ T-cell activation by IL-12 and IL-18 in context of viral infections, such as with hepatitis C virus, would be of particular interest.

Overall, this study demonstrates that $CD161^{++}CD8^{+}$ T cells, including the MAIT cell population it encompasses, are able to respond directly to the proinflammatory cytokines IL-12 and IL-18. This implicates this cell population in a range of infectious and noninfectious inflammatory diseases. Furthermore, their ability to specifically respond to TLR8 agonist-induced cytokines, IL-12 and IL-18, suggests that in addition to their antibacterial role, they could play an important role in antiviral responses. Detailed studies on the role and activation of $CD161^{++}CD8^{+}$ T cells in both autoimmune diseases, such as multiple sclerosis [43], and infectious disease may reveal potential novel therapeutic targets.

Material and methods

Cell and materials

PBMCs were prepared from whole blood leukocyte cones, obtained locally from the NHS Blood and Transplant UK, by layering onto Lymphoprep (Axis Shield) gradients.

$CD8^{+}$T cells were isolated from PBMCs by positive selection with anti-CD8 magnetic beads (Miltenyi Biotech) using an AutoMacsPro or MS columns (both Miltenyi Biotech). Purities achieved were ≥85%.

PBMCs, or isolated $CD8^{+}$ T cells, were stimulated for 24 h with IL-12 (Miltenyi Biotech) and/or IL-18 (R&D Systems Europe) at 50 ng/mL unless otherwise stated, or anti-CD2/CD3/CD28 beads (Miltenyi Biotech). Inhibitors used are as follows: 100 ng/mL cyclosporin A (Sigma-Aldrich), 5 μM SB203580 (Sigma-Aldrich), 10 nM bafilomycin A1 (Sigma Aldrich), or 10 μM Z-WEHD (R&D Systems). TLR agonists (Source Bioscience, UK) Pam3CSK4, HKLM, Poly(I:C), LPS *E. coli* K12, Flagellin *S. typhimurium*, FSL-1, Imiquimod, ssRNA40/Lyovec, and ODN2006 were used at 1 μg/mL.

THP-1 cells (ECACC, UK) were incubated with paraformaldehyde-fixed *E. coli* (DH5α, Invitrogen) or *E. faecalis* (clinical isolate, John Radcliffe Hospital, Oxford—species identity

© 2013 The Authors. *European Journal of Immunology* published by Wiley-VCH Verlag GmbH & Co. KGaA Weinheim.

confirmed by MALDI-ToF) at 25 bacteria per cell. Isolated $CD8^+$ T cells were either added at the beginning (20 h coculture) or following overnight incubation (5 h coculture).

Blocking antibodies against IL-12p70 (R&D Systems Europe), IL-12p40/70 (eBioscience), and IL-18 (MBL International, USA) were used at 5 μg/mL, and against MR1 at 10μg/mL unless otherwise stated (clone 26.5, described [9]).

Flow cytometry

Antibodies/dyes used were as follows: viability dye Live/Dead fixable-Near-IR (Invitrogen), CD3-eFluor450 (eBioscience), CD3-PECy7 (eBioscience), CD4-VioGreen (clone BW135/80, Miltenyi Biotech), CD8 V450 (BD), IL-18Rα-PE (Biolegend), CD161-APC (Miltenyi Biotech), IFN-γ-FITC (Miltenyi Biotech), Vα7.2-PE or -FITC (Biolegend). Gating strategy is shown in Supporting Information Fig. 1. All data were acquired on a MACSQuant (Miltenyi Biotech) and analyzed on FlowJo (Tree Star Inc.).

Cytokine analysis

Cell culture supernatants, from THP-1 cells cultured for 20 h in the presence of either *E. coli* or *E. faecalis* at the indicated MOIs, were analyzed for total IL-12 (IL-12+p40 human ELISA kit, Invitrogen) and IL-18 (Invitrogen) ELISA detection kits, following the manufactures instructions.

Statistical analysis

All graphs and statistical analysis were completed using Prism software version 6 (Graph Pad, San Diego, CA, USA). Statistical significance was assessed using a one-way repeated measures ANOVA with Bonferroni's multiple comparison test or a paired *t*-test.

Acknowledgements: The authors would like to thank Joannah Fergusson, Ruth Simmons, Alba Llibre, and Kira Smith for their comments and critical reading of this manuscript. This research was supported by the NIHR Biomedical Research Program (Oxford), the Wellcome Trust (WT091663MA), the James Martin School for the 21st Century (Oxford), the NIAID U19 Bio-defense Program (NIH NIAID 1U19AI082630-01), and the Oxford Dominions Trust.

Conflict of interest: The authors declare no financial or commercial conflict of interest.

References

1 **Walker, L. J., Kang, Y.-H., Smith, M. O., Tharmalingham, H., Ramamurthy, N., Fleming, V., Sahgal, N. et al.**, Human MAIT and CD8αα cells develop from a pool of type-17 pre-committed CD8+ T cells. *Blood* 2011. **119**: 422–433.

2 **Treiner, E. and Lantz, O.**, CD1d- and MR1-restricted invariant T cells: of mice and men. *Curr. Opin. Immunol.* 2006. **18**: 519–526.

3 **Tilloy, F., Treiner, E., Park, S. H., Garcia, C., Lemonnier, F., la Salle de, H., Bendelac, A. et al.**, An invariant T cell receptor alpha chain defines a novel TAP-independent major histocompatibility complex class Ib-restricted alpha/beta T cell subpopulation in mammals. *J. Exp. Med.* 1999. **189**: 1907–1921.

4 **Treiner, E., Duban, L., Bahram, S., Radosavljevic, M., Wanner, V., Tilloy, F., Affaticati, P. et al.**, Selection of evolutionarily conserved mucosal-associated invariant T cells by MR1. *Nature* 2003. **422**: 164–169.

5 **Huang, S., Gilfillan, S., Cella, M., Miley, M. J., Lantz, O., Lybarger, L., Fremont, D. H. et al.**, Evidence for MR1 antigen presentation to mucosal-associated invariant T cells. *J. Biol. Chem.* 2005. **280**: 21183–21193.

6 **Chua, W.-J., Kim, S., Myers, N., Huang, S., Yu, L., Fremont, D. H., Diamond, M. S. et al.**, Endogenous MHC-related protein 1 is transiently expressed on the plasma membrane in a conformation that activates mucosal-associated invariant T cells. *J. Immunol.* 2011. **186**: 4744–4750.

7 **Reantragoon, R., Kjer-Nielsen, L., Patel, O., Chen, Z., Illing, P. T., Bhati, M., Kostenko, L. et al.**, Structural insight into MR1-mediated recognition of the mucosal associated invariant T cell receptor. *J. Exp. Med.* 2012. **209**: 761–774.

8 **Le Bourhis, L., Martin, E., Péguillet, I., Guihot, A., Froux, N., Coré, M., Lévy, E. et al.**, Antimicrobial activity of mucosal-associated invariant T cells. *Nat. Immunol.* 2010. **11**: 701–708.

9 **Miley, M. J., Truscott, S. M., Yu, Y. Y. L., Gilfillan, S., Fremont, D. H., Hansen, T. H. and Lybarger, L.**, Biochemical features of the MHC-related protein 1 consistent with an immunological function. *J. Immunol.* 2003. **170**: 6090–6098.

10 **Kjer-Nielsen, L., Patel, O., Corbett, A. J., Le Nours, J., Meehan, B., Liu, L., Bhati, M. et al.**, MR1 presents microbial vitamin B metabolites to MAIT cells. *Nature* 2012. **491**: 1–9.

11 **Tang, X.-Z., Jo, J., Tan, A. T., Sandalova, E., Chia, A., Tan, K. C., Lee, K. H. et al.**, IL-7 licenses activation of human liver intrasinusoidal mucosal-associated invariant T cells. *J. Immunol.* 2013. **190**: 3142–3152.

12 **Billerbeck, E., Kang, Y.-H., Walker, L., Lockstone, H., Grafmueller, S., Fleming, V., Flint, J. et al.**, Analysis of CD161 expression on human CD8+ T cells defines a distinct functional subset with tissue-homing properties. *Proc. Natl. Acad. Sci.* 2010. **107**: 3006–3011.

13 **Georgel, P., Radosavljevic, M., Macquin, C. and Bahram, S.**, The non-conventional MHC class I MR1 molecule controls infection by *Klebsiella pneumoniae* in mice. *Mol. Immunol.* 2011. **48**: 769–775.

14 **Chua, W. J., Truscott, S. M., Eickhoff, C. S., Blazevic, A., Hoft, D. F. and Hansen, T. H.**, Polyclonal MAIT cells have unique innate functions in bacterial infection. *Infect. Immun.* 2012. **80**: 3256–3267.

15 **Gold, M. C., Cerri, S., Smyk-Pearson, S., Cansler, M. E., Vogt, T. M., Delepine, J., Winata, E. et al.**, Human mucosal associated invariant T cells detect bacterially infected cells. *PLoS Biol.* 2010. **8**: e1000407.

16 **Oo, Y. H., Banz, V., Kavanagh, D., Liaskou, E., Withers, D. R., Humphreys, E., Reynolds, G. M. et al.**, CXCR3-dependent recruitment and CCR6-mediated positioning of Th-17 cells in the inflamed liver. *J. Hepatol.* 2012. **57**: 1044–1051.

© 2013 The Authors. *European Journal of Immunology* published by Wiley-VCH Verlag GmbH & Co. KGaA Weinheim.

17 **Annibali, V., Ristori, G., Angelini, D. F., Serafini, B., Mechelli, R., Cannoni, S., Romano, S. et al.**, CD161highCD8+T cells bear pathogenetic potential in multiple sclerosis. *Brain* 2011. **134**: 542–554.

18 **Gunderson, A. J., Mohammed, J., Horvath, F. J., Podolsky, M. A., Anderson, C. R. and Glick, A. B.**, CD8(+) T cells mediate RAS-induced psoriasis-like skin inflammation through IFN-γ. *J. Invest. Dermatol.* 2013. **133**: 955–963.

19 **Gorski, K. S., Waller, E. L., Bjornton-Severson, J., Hanten, J. A., Riter, C. L., Kieper, W. C., Gorden, K. B. et al.**, Distinct indirect pathways govern human NK-cell activation by TLR-7 and TLR-8 agonists. *Int. Immunol.* 2006. **18**: 1115–1126.

20 **Micallef, M. J., Ohtsuki, T., Kohno, K., Tanabe, F., Ushio, S., Namba, M., Tanimoto, T. et al.**, Interferon-gamma-inducing factor enhances T helper 1 cytokine production by stimulated human T cells: synergism with interleukin-12 for interferon-gamma production. *Eur. J. Immunol.* 1996. **26**: 1647–1651.

21 **Kohno, K., Kataoka, J., Ohtsuki, T., Suemoto, Y., Okamoto, I., Usui, M., Ikeda, M. et al.**, IFN-gamma-inducing factor (IGIF) is a costimulatory factor on the activation of Th1 but not Th2 cells and exerts its effect independently of IL-12. *J. Immunol.* 1997. **158**: 1541–1550.

22 **Ariel, A., Novick, D., Rubinstein, M., Dinarello, C. A., Lider, O. and Hershkoviz, R.**, IL-12 and IL-18 induce MAP kinase-dependent adhesion of T cells to extracellular matrix components. *J. Leukocyte Biol.* 2002. **72**: 192–198.

23 **Fagundes, C. T., Costa, V. V., Cisalpino, D., Amaral, F. A., Souza, P. R. S., Souza, R. S., Ryffel, B. et al.**, IFN-γ production depends on IL-12 and IL-18 combined action and mediates host resistance to dengue virus infection in a nitric oxide-dependent manner. *PLoS Negl. Trop. Dis.* 2011. **5**: e1449.

24 **Pirhonen, J., Matikainen, S. and Julkunen, I.**, Regulation of virus-induced IL-12 and IL-23 expression in human macrophages. *J. Immunol.* 2002. **169**: 5673–5678.

25 **Rintahaka, J., Wiik, D., Kovanen, P. E., Alenius, H. and Matikainen, S.**, Cytosolic antiviral RNA recognition pathway activates caspases 1 and 3. *J. Immunol.* 2008. **180**: 1749–1757.

26 **Lee, M. S. and Kim, Y.-J.**, Signaling pathways downstream of pattern-recognition receptors and their cross talk. *Annu. Rev. Biochem.* 2007. **76**: 447–480.

27 **Takeda, K., Kaisho, T. and Akira, S.**, Toll-like receptors. *Annu. Rev. Immunol.* 2003. **21**: 335–376.

28 **Bachmann, M., Horn, K., Poleganov, M. A., Paulukat, J., Nold, M., Pfeilschifter, J. and Mühl, H.**, Interleukin-18 secretion and Th1-like cytokine responses in human peripheral blood mononuclear cells under the influence of the toll-like receptor-5 ligand flagellin. *Cell. Microbiol.* 2006. **8**: 289–300.

29 **Ghayur, T., Banerjee, S., Hugunin, M., Butler, D., Herzog, L., Carter, A., Quintal, L. et al.**, Caspase-1 processes IFN-gamma-inducing factor and regulates LPS-induced IFN-gamma production. *Nature* 1997. **386**: 619–623.

30 **Okamura, H., Tsutsi, H., Komatsu, T., Yutsudo, M., Hakura, A., Tanimoto, T., Torigoe, K. et al.**, Cloning of a new cytokine that induces IFN-gamma production by T cells. *Nature* 1995. **378**: 88–91.

31 **Otani, T., Nakamura, S., Toki, M., Motoda, R., Kurimoto, M. and Orita, K.**, Identification of IFN-gamma-producing cells in IL-12/IL-18-treated mice. *Cell Immunol.* 1999. **198**: 111–119.

32 **Cheung, H., Chen, N.-J., Cao, Z., Ono, N., Ohashi, P. S. and Yeh, W.-C.**, Accessory protein-like is essential for IL-18-mediated signaling. *J. Immunol.* 2005. **174**: 5351–5357.

33 **Cosgrove, C., Ussher, J. E., Rauch, A., Gärtner, K., Kurioka, A., Hühn, M. H., Adelmann, K. et al.**, Early and nonreversible decrease of CD161++/MAIT cells in HIV infection. *Blood* 2013. **121**: 951–961.

34 **Tada, H., Aiba, S., Shibata, K.-I., Ohteki, T. and Takada, H.**, Synergistic effect of Nod1 and Nod2 agonists with toll-like receptor agonists on human dendritic cells to generate interleukin-12 and T helper type 1 cells. *Infect. Immun.* 2005. **73**: 7967–7976.

35 **Seki, E., Tsutsui, H., Nakano, H., Tsuji, N., Hoshino, K., Adachi, O., Adachi, K. et al.**, Lipopolysaccharide-induced IL-18 secretion from murine Kupffer cells independently of myeloid differentiation factor 88 that is critically involved in induction of production of IL-12 and IL-1beta. *J. Immunol.* 2001. **166**: 2651–2657.

36 **Humann, J. and Lenz, L. L.**, Activation of naive NK cells in response to *Listeria monocytogenes* requires IL-18 and contact with infected dendritic cells. *J. Immunol.* 2010. **184**: 5172–5178.

37 **Kannan, Y., Yu, J., Raices, R. M., Seshadri, S., Wei, M., Caligiuri, M. A. and Wewers, M. D.**, IκBζ augments IL-12- and IL-18-mediated IFN-γ production in human NK cells. *Blood* 2011. **117**: 2855–2863.

38 **Nakahira, M., Tomura, M., Iwasaki, M., Ahn, H. J., Bian, Y., Hamaoka, T., Ohta, T. et al.**, An absolute requirement for STAT4 and a role for IFN-gamma as an amplifying factor in IL-12 induction of the functional IL-18 receptor complex. *J. Immunol.* 2001. **167**: 1306–1312.

39 **Barbulescu, K., Becker, C., Schlaak, J. F., Schmitt, E., Meyer zum Büschenfelde, K. H. and Neurath, M. F.**, IL-12 and IL-18 differentially regulate the transcriptional activity of the human IFN-gamma promoter in primary CD4+ T lymphocytes. *J. Immunol.* 1998. **160**: 3642–3647.

40 **Tyznik, A. J., Tupin, E., Nagarajan, N. A., Her, M. J., Benedict, C. A. and Kronenberg, M.**, Cutting edge: the mechanism of invariant NKT cell responses to viral danger signals. *J. Immunol.* 2008. **181**: 4452–4456.

41 **Szkaradkiewicz, A., Jopek, A. and Wysocki, J.**, Effects of IL-12 and IL-18 on HBcAg-specific cytokine production by CD4 T lymphocytes of children with chronic hepatitis B infection. *Antiviral Res.* 2005. **66**: 23–27.

42 **Schvoerer, E., Navas, M. C., Thumann, C., Fuchs, A., Meyer, N., Habersetzer, F. and Stoll-Keller, F.**, Production of interleukin-18 and interleukin-12 in patients suffering from chronic hepatitis C virus infection before antiviral therapy. *J. Med. Virol.* 2003. **70**: 588–593.

43 **Miyazaki, Y., Miyake, S., Chiba, A., Lantz, O. and Yamamura, T.**, Mucosal-associated invariant T cells regulate Th1 response in multiple sclerosis. *Int. Immunol.* 2011. **23**: 529–535.

Abbreviations: **MAIT cell**: mucosal-associated invariant T cell · **Vα7.2**: variable-α chain 7.2

Full correspondence: Dr. Christian Willberg, Peter Medawar Building for Pathogen Research, University of Oxford, South Parks Road, Oxford, OX1 3SY, UK
Fax: +44-(0)1865-281890
e-mail: Chris.Willberg@ndm.ox.ac.uk

Received: 8/3/2013
Revised: 10/7/2013
Accepted: 6/9/2013
Accepted article online: 10/9/2013

© 2013 The Authors. *European Journal of Immunology* published by Wiley-VCH Verlag GmbH & Co. KGaA Weinheim.

References

1. Lanier, L. L. & Sun, J. C. Do the terms innate and adaptive immunity create conceptual barriers? *Nat. Rev. Immunol.* **9,** 302–303 (May 2009).
2. Lanier, L. L. Shades of grey–the blurring view of innate and adaptive immunity. *Nat. Rev. Immunol.* **13,** 73–4 (Feb. 2013).
3. Janeway, C. A. & Medzhitov, R. Innate immune recognition. *Annu. Rev. Immunol.* **20,** 197–216 (2002).
4. Bianchi, M. E. DAMPs, PAMPs and alarmins: all we need to know about danger. *J. Leukoc. Biol.* **81,** 1–5 (Jan. 2007).
5. Beachboard, D. C. & Horner, S. M. Innate immune evasion strategies of DNA and RNA viruses. *Curr. Opin. Microbiol.* **32,** 113–9 (Aug. 2016).
6. Baxt, L. a., Garza-Mayers, A. C. & Goldberg, M. B. Bacterial subversion of host innate immune pathways. *Science* **340,** 697–701 (May 2013).
7. Chu, H. & Mazmanian, S. K. Innate immune recognition of the microbiota promotes host-microbial symbiosis. *Nat. Immunol.* **14,** 668–75 (July 2013).
8. Davies, D. R. & Cohen, G. H. Interactions of protein antigens with antibodies. *Proc. Natl. Acad. Sci.* **93,** 7–12 (Jan. 1996).
9. Tanner, J. J., Komissarov, A. A. & Deutscher, S. L. Crystal structure of an antigen-binding fragment bound to single-stranded DNA. *J. Mol. Biol.* **314,** 807–22 (Dec. 2001).
10. Garcia, K. C. & Adams, E. J. How the T cell receptor sees antigen–a structural view. *Cell* **122,** 333–6 (Aug. 2005).
11. Arstila, T. P. *et al.* A direct estimate of the human alphabeta T cell receptor diversity. *Science* **286,** 958–61 (Oct. 1999).
12. Gapin, L. Development of invariant natural killer T cells. *Curr. Opin. Immunol.* **39,** 68–74 (Apr. 2016).
13. Lepore, M. *et al.* Parallel T-cell cloning and deep sequencing of human MAIT cells reveal stable oligoclonal TCRβ repertoire. *Nat. Commun.* **5,** 3866 (May 2014).
14. Klein, L., Kyewski, B., Allen, P. M. & Hogquist, K. a. Positive and negative selection of the T cell repertoire: what thymocytes see (and don't see). *Nat. Rev. Immunol.* **14,** 377–391 (May 2014).
15. Bendelac, A. Positive selection of mouse NK1+ T cells by CD1-expressing cortical thymocytes. *J. Exp. Med.* **182,** 2091–6 (Dec. 1995).
16. Seach, N. *et al.* Double positive thymocytes select mucosal-associated invariant T cells. *J. Immunol.* **191,** 6002–9 (Dec. 2013).
17. Von Boehmer, H. *et al.* Crucial function of the pre-T-cell receptor (TCR) in TCR beta selection, TCR beta allelic exclusion and alpha beta versus gamma delta lineage commitment. *Immunol. Rev.* **165,** 111–9 (Oct. 1998).
18. Narayan, K. & Kang, J. Molecular events that regulate alphabeta versus gammadelta T cell lineage commitment: old suspects, new players and different game plans. *Curr. Opin. Immunol.* **19,** 169–75 (Apr. 2007).

19. Godfrey, D. I., Uldrich, A. P., McCluskey, J., Rossjohn, J. & Moody, D. B. The burgeoning family of unconventional T cells. *Nat. Immunol.* **16,** 1114–23 (Nov. 2015).

20. Gaur, L. K. & Nepom, G. T. Ancestral major histocompatibility complex DRB genes beget conserved patterns of localized polymorphisms. *Proc. Natl. Acad. Sci. U. S. A.* **93,** 5380–3 (May 1996).

21. Marsh, S. G. E. *et al.* Nomenclature for factors of the HLA system, 2010. *Tissue Antigens* **75,** 291–455 (Apr. 2010).

22. Jones, E. Y. MHC class I and class II structures. *Curr. Opin. Immunol.* **9,** 75–9 (Feb. 1997).

23. Blum, J. S., Wearsch, P. A. & Cresswell, P. Pathways of antigen processing. *Annu. Rev. Immunol.* **31,** 443–73 (2013).

24. Puleston, D. J. & Simon, A. K. Autophagy in the immune system. *Immunology* **141,** 1–8 (Jan. 2014).

25. Rodgers, J. R. & Cook, R. G. MHC class Ib molecules bridge innate and acquired immunity. *Nat. Rev. Immunol.* **5,** 459–71 (June 2005).

26. Braud, V., Jones, E. Y. & McMichael, A. The human major histocompatibility complex class Ib molecule HLA-E binds signal sequence-derived peptides with primary anchor residues at positions 2 and 9. *Eur. J. Immunol.* **27,** 1164–9 (May 1997).

27. Diehl, M. *et al.* Nonclassical HLA-G molecules are classical peptide presenters. *Curr. Biol.* **6,** 305–14 (Mar. 1996).

28. Rohrlich, P. S. *et al.* Direct recognition by alphabeta cytolytic T cells of Hfe, a MHC class Ib molecule without antigen-presenting function. *Proc. Natl. Acad. Sci. U. S. A.* **102,** 12855–60 (Sept. 2005).

29. Ly, D. & Moody, D. B. The CD1 size problem: lipid antigens, ligands, and scaffolds. *Cell. Mol. Life Sci.* **71,** 3069–79 (Aug. 2014).

30. Van Rhijn, I., Godfrey, D. I., Rossjohn, J. & Moody, D. B. Lipid and small-molecule display by CD1 and MR1. *Nat. Rev. Immunol.* **15,** 643–654 (Sept. 2015).

31. Vartabedian, V. F., Savage, P. B. & Teyton, L. The processing and presentation of lipids and glycolipids to the immune system. *Immunol. Rev.* **272,** 109–19 (July 2016).

32. Kjer-Nielsen, L. *et al.* MR1 presents microbial vitamin B metabolites to MAIT cells. *Nature* **491,** 717–23 (Nov. 2012).

33. McWilliam, H. E. G. *et al.* The intracellular pathway for the presentation of vitamin B–related antigens by the antigen-presenting molecule MR1. *Nat. Immunol.* 1–9 (2016).

34. Huang, S. *et al.* MR1 uses an endocytic pathway to activate mucosal-associated invariant T cells. *J. Exp. Med.* **205,** 1201–11 (May 2008).

35. Itano, A. A. & Jenkins, M. K. Antigen presentation to naive CD4 T cells in the lymph node. *Nat. Immunol.* **4,** 733–9 (Aug. 2003).

36. Curtsinger, J. M., Lins, D. C. & Mescher, M. F. CD8+ memory T cells (CD44high, Ly-6C+) are more sensitive than naive cells to (CD44low, Ly-6C-) to TCR/CD8 signaling in response to antigen. *J. Immunol.* **160,** 3236–43 (Apr. 1998).

37. Curtsinger, J. M. *et al.* Inflammatory cytokines provide a third signal for activation of naive CD4+ and CD8+ T cells. *J. Immunol.* **162,** 3256–62 (Mar. 1999).

38. Curtsinger, J. M., Valenzuela, J. O., Agarwal, P., Lins, D. & Mescher, M. F. Type I IFNs provide a third signal to CD8 T cells to stimulate clonal expansion and differentiation. *J. Immunol.* **174,** 4465–9 (Apr. 2005).

39. Mitchell, T. C. *et al.* Immunological adjuvants promote activated T cell survival via induction of Bcl-3. *Nat. Immunol.* **2,** 397–402 (May 2001).

40. Valenzuela, J. O., Hammerbeck, C. D. & Mescher, M. F. Cutting edge: Bcl-3 up-regulation by signal 3 cytokine (IL-12) prolongs survival of antigen-activated CD8 T cells. *J. Immunol.* **174,** 600–4 (Jan. 2005).

41. Valenzuela, J., Schmidt, C. & Mescher, M. The roles of IL-12 in providing a third signal for clonal expansion of naive CD8 T cells. *J. Immunol.* **169,** 6842–9 (Dec. 2002).

42. Mescher, M. F. *et al.* Signals required for programming effector and memory development by CD8+ T cells. *Immunol. Rev.* **211,** 81–92 (June 2006).

43. Curtsinger, J. M. & Mescher, M. F. Inflammatory cytokines as a third signal for T cell activation. *Curr. Opin. Immunol.* **22,** 333–40 (June 2010).

44. Starbeck-Miller, G. R., Xue, H.-H. & Harty, J. T. IL-12 and type I interferon prolong the division of activated CD8 T cells by maintaining high-affinity IL-2 signaling in vivo. *J. Exp. Med.* **211,** 105–20 (Jan. 2014).

45. Kim, M. T. & Harty, J. T. Impact of Inflammatory Cytokines on Effector and Memory CD8+ T Cells. *Front. Immunol.* **5,** 295 (2014).

46. Curtsinger, J. M., Lins, D. C. & Mescher, M. F. Signal 3 determines tolerance versus full activation of naive CD8 T cells: dissociating proliferation and development of effector function. *J. Exp. Med.* **197,** 1141–51 (May 2003).

47. Xiao, Z., Casey, K. A., Jameson, S. C., Curtsinger, J. M. & Mescher, M. F. Programming for CD8 T cell memory development requires IL-12 or type I IFN. *J. Immunol.* **182,** 2786–94 (Mar. 2009).

48. Agarwal, P. *et al.* Gene regulation and chromatin remodeling by IL-12 and type I IFN in programming for CD8 T cell effector function and memory. *J. Immunol.* **183,** 1695–704 (Aug. 2009).

49. Takemoto, N., Intlekofer, A. M., Northrup, J. T., Wherry, E. J. & Reiner, S. L. Cutting Edge: IL-12 inversely regulates T-bet and eomesodermin expression during pathogen-induced CD8+ T cell differentiation. *J. Immunol.* **177,** 7515–9 (Dec. 2006).

50. Joshi, N. S. *et al.* Inflammation directs memory precursor and short-lived effector CD8(+) T cell fates via the graded expression of T-bet transcription factor. *Immunity* **27,** 281–95 (Aug. 2007).

51. Joshi, N. S. & Kaech, S. M. Effector CD8 T cell development: a balancing act between memory cell potential and terminal differentiation. *J. Immunol.* **180,** 1309–15 (Feb. 2008).

52. Hammarlund, E. *et al.* Duration of antiviral immunity after smallpox vaccination. *Nat. Med.* **9,** 1131–7 (Sept. 2003).

53. Barber, D. L., Wherry, E. J. & Ahmed, R. Cutting edge: rapid in vivo killing by memory CD8 T cells. *J. Immunol.* **171,** 27–31 (July 2003).

54. Byers, A. M., Kemball, C. C., Moser, J. M. & Lukacher, A. E. Cutting edge: rapid in vivo CTL activity by polyoma virus-specific effector and memory CD8+ T cells. *J. Immunol.* **171,** 17–21 (July 2003).

55. Lalvani, A. *et al.* Rapid effector function in CD8+ memory T cells. *J. Exp. Med.* **186,** 859–65 (Sept. 1997).

56. Bachmann, M. F., Barner, M., Viola, A. & Kopf, M. Distinct kinetics of cytokine production and cytolysis in effector and memory T cells after viral infection. *Eur. J. Immunol.* **29,** 291–9 (Jan. 1999).

57. Sathaliyawala, T. *et al.* Distribution and compartmentalization of human circulating and tissue-resident memory T cell subsets. *Immunity* **38,** 187–97 (Jan. 2013).

58. Setoguchi, R., Matsui, Y. & Mouri, K. mTOR signaling promotes a robust and continuous production of IFN-γ by human memory CD8+ T cells and their proliferation. *Eur. J. Immunol.* **45,** 893–902 (Mar. 2015).

59. Zundler, S. & Neurath, M. F. Interleukin-12: Functional activities and implications for disease. *Cytokine Growth Factor Rev.* **26,** 559–68 (Oct. 2015).

60. Kobayashi, M. *et al.* Identification and purification of natural killer cell stimulatory factor (NKSF), a cytokine with multiple biologic effects on human lymphocytes. *J. Exp. Med.* **170,** 827–45 (Sept. 1989).

61. El Mezayen, R. & Matsumoto, T. In vitro responsiveness to IL-18 in combination with IL-12 or IL-2 by PBMC from patients with bronchial asthma and atopic dermatitis. *Clin. Immunol.* **111,** 61–68 (Apr. 2004).

62. Trzeciak, M. *et al.* Interleukin 18 – a pleiotropic cytokine involved in the Th1 and Th2 immunological response. *Post Dermatol Alergol* **XXVIII,** 309–312 (2011).

63. Gracie, J. A., Robertson, S. E. & McInnes, I. B. Interleukin-18. *J. Leukoc. Biol.* **73,** 213–24 (Feb. 2003).

64. Nakahira, M. *et al.* Synergy of IL-12 and IL-18 for IFN-gamma gene expression: IL-12-induced STAT4 contributes to IFN-gamma promoter activation by up-regulating the binding activity of IL-18-induced activator protein 1. *J. Immunol.* **168,** 1146–53 (Feb. 2002).

65. Barbulescu, K. *et al.* IL-12 and IL-18 differentially regulate the transcriptional activity of the human IFN-gamma promoter in primary CD4+ T lymphocytes. *J. Immunol.* **160,** 3642–7 (Apr. 1998).

66. Okamura, H. *et al.* Cloning of a new cytokine that induces IFN-gamma production by T cells. *Nature* **378,** 88–91 (Nov. 1995).

67. Micallef, M. J. *et al.* Interferon-gamma-inducing factor enhances T helper 1 cytokine production by stimulated human T cells: synergism with interleukin-12 for interferon-gamma production. *Eur. J. Immunol.* **26,** 1647–51 (July 1996).

68. Chang, J. T., Segal, B. M., Nakanishi, K., Okamura, H. & Shevach, E. M. The costimulatory effect of IL-18 on the induction of antigen-specific IFN-gamma production by resting T cells is IL-12 dependent and is mediated by up-regulation of the IL-12 receptor beta2 subunit. *Eur. J. Immunol.* **30,** 1113–9 (Apr. 2000).

69. Ahn, H. J. *et al.* A mechanism underlying synergy between IL-12 and IFN-gamma-inducing factor in enhanced production of IFN-gamma. *J. Immunol.* **159,** 2125–31 (Sept. 1997).

70. Yoshimoto, T. *et al.* IL-12 up-regulates IL-18 receptor expression on T cells, Th1 cells, and B cells: synergism with IL-18 for IFN-gamma production. *J. Immunol.* **161,** 3400–7 (Oct. 1998).

71. Tomura, M. *et al.* Differential capacities of CD4+, CD8+, and CD4-CD8- T cell subsets to express IL-18 receptor and produce IFN-gamma in response to IL-18. *J. Immunol.* **160,** 3759–65 (Apr. 1998).

72. Lawless, V. A. *et al.* Stat4 regulates multiple components of IFN-gamma-inducing signaling pathways. *J. Immunol.* **165,** 6803–8 (Dec. 2000).

73. Sareneva, T., Julkunen, I. & Matikainen, S. IFN-alpha and IL-12 induce IL-18 receptor gene expression in human NK and T cells. *J. Immunol.* **165,** 1933–8 (Aug. 2000).

74. Kim, S. H. *et al.* Functional reconstitution and regulation of IL-18 activity by the IL-18R beta chain. *J. Immunol.* **166,** 148–54 (Jan. 2001).

75. Nakahira, M. *et al.* An absolute requirement for STAT4 and a role for IFN-gamma as an amplifying factor in IL-12 induction of the functional IL-18 receptor complex. *J. Immunol.* **167,** 1306–12 (Aug. 2001).

76. Raué, H.-P., Brien, J. D., Hammarlund, E. & Slifka, M. K. Activation of virus-specific CD8+ T cells by lipopolysaccharide-induced IL-12 and IL-18. *J. Immunol.* **173,** 6873–81 (Dec. 2004).

77. Fehniger, T. A. *et al.* Differential cytokine and chemokine gene expression by human NK cells following activation with IL-18 or IL-15 in combination with IL-12: implications for the innate immune response. *J. Immunol.* **162,** 4511–20 (Apr. 1999).

78. Trotta, R. *et al.* miR-155 regulates IFN-γ production in natural killer cells. *Blood* **119,** 3478–85 (Apr. 2012).

79. Guo, L., Junttila, I. S. & Paul, W. E. Cytokine-induced cytokine production by conventional and innate lymphoid cells. *Trends Immunol.* **33,** 598–606 (Dec. 2012).

80. Lertmemongkolchai, G., Cai, G., Hunter, C. a. & Bancroft, G. J. Bystander activation of CD8+ T cells contributes to the rapid production of IFN-gamma in response to bacterial pathogens. *J. Immunol.* **166,** 1097–1105 (Jan. 2001).

81. Soudja, S. M., Ruiz, A. L., Marie, J. C. & Lauvau, G. Inflammatory monocytes activate memory CD8(+) T and innate NK lymphocytes independent of cognate antigen during microbial pathogen invasion. *Immunity* **37,** 549–62 (Sept. 2012).

82. Berg, R. E., Crossley, E., Murray, S. & Forman, J. Memory CD8+ T cells provide innate immune protection against Listeria monocytogenes in the absence of cognate antigen. *J. Exp. Med.* **198,** 1583–93 (Nov. 2003).

83. Robinson, D. *et al.* IGIF does not drive Th1 development but synergizes with IL-12 for interferon-gamma production and activates IRAK and NFkappaB. *Immunity* **7,** 571–81 (Oct. 1997).

84. Berg, R. E., Cordes, C. J. & Forman, J. Contribution of CD8+ T cells to innate immunity: IFN-gamma secretion induced by IL-12 and IL-18. *Eur. J. Immunol.* **32,** 2807–16 (Oct. 2002).

85. Munk, R. B. *et al.* Antigen-independent IFN-γ production by human naïve CD4 T cells activated by IL-12 plus IL-18. *PLoS One* **6,** e18553 (Jan. 2011).

86. Papadakis, K. a. *et al.* TL1A synergizes with IL-12 and IL-18 to enhance IFN-gamma production in human T cells and NK cells. *J. Immunol.* **172,** 7002–7 (June 2004).

87. Szkaradkiewicz, A., Jopek, A. & Wysocki, J. Effects of IL-12 and IL-18 on HBcAg-specific cytokine production by CD4 T lymphocytes of children with chronic hepatitis B infection. *Antiviral Res.* **66,** 23–7 (Apr. 2005).

88. Sattler, A. *et al.* Cytokine-induced human IFN-gamma-secreting effector-memory Th cells in chronic autoimmune inflammation. *Blood* **113,** 1948–56 (Feb. 2009).

89. Netea, M. G., Kullberg, B. J. & van der Meer, J. W. M. Severely impaired IL-12/IL-18/IFNgamma axis in patients with hyper IgE syndrome. *Eur. J. Clin. Invest.* **35,** 718–21 (Nov. 2005).

90. Suwannasaen, D., Romphruk, A., Leelayuwat, C. & Lertmemongkolchai, G. Bystander T cells in human immune responses to dengue antigens. *BMC Immunol.* **11,** 47 (2010).

91. Bou Ghanem, E. N. & D'Orazio, S. E. F. Human CD8+ T cells display a differential ability to undergo cytokine-driven bystander activation. *Cell. Immunol.* **272,** 79–86 (Sept. 2011).

92. Austin, L. M., Ozawa, M., Kikuchi, T., Walters, I. B. & Krueger, J. G. The majority of epidermal T cells in Psoriasis vulgaris lesions can produce type 1 cytokines, interferon-gamma, interleukin-2, and tumor necrosis factor-alpha, defining TC1 (cytotoxic T lymphocyte) and TH1 effector populations: a type 1 differentiation bi. *J. Invest. Dermatol.* **113,** 752–9 (Nov. 1999).

93. Ussher, J. E. *et al.* CD161++ CD8+ T cells, including the MAIT cell subset, are specifically activated by IL-12+IL-18 in a TCR-independent manner. *Eur. J. Immunol.* **44,** 195–203 (Jan. 2014).

94. Hashimoto, K., Hirai, M. & Kurosawa, Y. A Gene Outside the Human MHC Related to Classical HLA Class I Genes. *Science (80-.).* **269,** 693–695 (1995).

95. Hashimoto, K. MR1 discovery. *Immunogenetics* **68,** 491–498 (Aug. 2016).

96. Tsukamoto, K., Deakin, J. E., Graves, J. a. M. & Hashimoto, K. Exceptionally high conservation of the MHC class I-related gene, MR1, among mammals. *Immunogenetics* **65,** 115–124 (Feb. 2013).

97. Yamaguchi, H., Hirai, M., Kurosawa, Y. & Hashimoto, K. A highly conserved major histocompatibility complex class I-related gene in mammals. *Biochem. Biophys. Res. Commun.* **238,** 697–702 (Sept. 1997).

98. Riegert, P., Wanner, V. & Bahram, S. Genomics, Isoforms, Expression, and Phylogeny of the MHC Class I-Related MR1 Gene. *J. Immunol.* **161,** 4066–4077 (Oct. 1998).

99. Parra-Cuadrado, J. F., del Moral, M. G., García-Pavía, P., Setién, F. & Martínez-Naves, E. Characterization of the MHC class I-related MR1 locus in nonhuman primates. *Immunogenetics* **53,** 643–8 (Oct. 2001).

100. Goldfinch, N. *et al.* Conservation of mucosal associated invariant T (MAIT) cells and the MR1 restriction element in ruminants, and abundance of MAIT cells in spleen. *Vet. Res.* **41,** 62 (Sept. 2010).

101. Parra-Cuadrado, J. F. *et al.* A study on the polymorphism of human MHC class I-related MR1 gene and identification of an MR1-like pseudogene. *Tissue Antigens* **56,** 170–2 (Aug. 2000).

102. Treiner, E. *et al.* Selection of evolutionarily conserved mucosal-associated invariant T cells by MR1. *Nature* **422,** 164–9 (Mar. 2003).

103. Walter, L. & Gunther, E. Isolation and molecular characterization of the rat MR1 homologue, a non-MHC-linked class I-related gene. *Immunogenetics* **47,** 477–82 (May 1998).

104. Yamaguchi, H. & Hashimoto, K. Association of MR1 protein, an MHC class I-related molecule, with beta(2)-microglobulin. *Biochem. Biophys. Res. Commun.* **290,** 722–9 (Jan. 2002).

105. Miley, M. J. *et al.* Biochemical features of the MHC-related protein 1 consistent with an immunological function. *J. Immunol.* **170,** 6090–8 (June 2003).

106. Huang, S. *et al.* Evidence for MR1 antigen presentation to mucosal-associated invariant T cells. *J. Biol. Chem.* **280,** 21183–21193 (June 2005).

107. Tilloy, F. *et al.* An invariant T cell receptor alpha chain defines a novel TAP-independent major histocompatibility complex class Ib-restricted alpha/beta T cell subpopulation in mammals. *J. Exp. Med.* **189,** 1907–21 (June 1999).

108. Abós, B. *et al.* Human MR1 expression on the cell surface is acid sensitive, proteasome independent and increases after culturing at 26 ° C. *Biochem. Biophys. Res. Commun.* **411,** 632–6 (Aug. 2011).

109. Kawano, T. *et al.* CD1d-restricted and TCR-mediated activation of valpha14 NKT cells by glycosylceramides. *Science* **278,** 1626–9 (Nov. 1997).

110. Okamoto, N. *et al.* Synthetic alpha-mannosyl ceramide as a potent stimulant for an NKT cell repertoire bearing the invariant Valpha19-Jalpha26 TCR alpha chain. *Chem. Biol.* **12,** 677–83 (June 2005).

111. Shimamura, M. *et al.* Modulation of Valpha19 NKT cell immune responses by alpha-mannosyl ceramide derivatives consisting of a series of modified sphingosines. *Eur. J. Immunol.* **37,** 1836–44 (July 2007).

112. McWilliam, H. E., Birkinshaw, R. W., Villadangos, J. A., McCluskey, J. & Rossjohn, J. MR1 presentation of vitamin B-based metabolite ligands. *Curr. Opin. Immunol.* **34C,** 28–34 (2015).

113. Eckle, S. B. G. *et al.* A molecular basis underpinning the T cell receptor heterogeneity of mucosal-associated invariant T cells. *J. Exp. Med.* **211,** 1585–600 (July 2014).

114. Corbett, A. J. *et al.* T-cell activation by transitory neo-antigens derived from distinct microbial pathways. *Nature* **509,** 361–5 (Apr. 2014).

115. Patel, O. *et al.* Recognition of vitamin B metabolites by mucosal-associated invariant T cells. *Nat. Commun.* **4,** 2142 (July 2013).

116. Aldemir, H. Novel MHC class I-related molecule MR1 affects MHC class I expression in 293T cells. *Biochem. Biophys. Res. Commun.* **366,** 328–34 (Feb. 2008).

117. Chua, W.-J. *et al.* Endogenous MHC-related protein 1 is transiently expressed on the plasma membrane in a conformation that activates mucosal-associated invariant T cells. *J. Immunol.* **186,** 4744–50 (May 2011).

118. Ljunggren, H. G. *et al.* Empty MHC class I molecules come out in the cold. *Nature* **346,** 476–80 (Aug. 1990).

119. Harriff, M. J. *et al.* Endosomal MR1 Trafficking Plays a Key Role in Presentation of Mycobacterium tuberculosis Ligands to MAIT Cells. *PLOS Pathog.* **12** (ed Salgame, P.) e1005524 (Mar. 2016).

120. Harriff, M. J. *et al.* Human Lung Epithelial Cells Contain Mycobacterium tuberculosis in a Late Endosomal Vacuole and Are Efficiently Recognized by CD8+ T Cells. *PLoS One* **9,** e97515 (Jan. 2014).

121. Ussher, J. E. *et al.* TLR signalling in human antigen-presenting cells regulates MR1-dependent activation of MAIT cells. *Eur. J. Immunol.* 1–41 (Apr. 2016).

122. Porcelli, S., Yockey, C. E., Brenner, M. B. & Balk, S. P. Analysis of T cell antigen receptor (TCR) expression by human peripheral blood CD4-8- alpha/beta T cells demonstrates preferential use of several V beta genes and an invariant TCR alpha chain. *J. Exp. Med.* **178,** 1–16 (July 1993).

123. Moss, P. A. & Bell, J. I. Sequence analysis of the human alpha beta T-cell receptor CDR3 region. *Immunogenetics* **42,** 10–8 (1995).

124. Martin, E. *et al.* Stepwise development of MAIT cells in mouse and human. *PLoS Biol.* **7,** e54 (Mar. 2009).

125. Leeansyah, E., Loh, L., Nixon, D. F. & Sandberg, J. K. Acquisition of innate-like microbial reactivity in mucosal tissues during human fetal MAIT-cell development. *Nat. Commun.* **5,** 3143 (Jan. 2014).

126. Gold, M. C. *et al.* Human thymic MR1-restricted MAIT cells are innate pathogen-reactive effectors that adapt following thymic egress. *Mucosal Immunol.* **6,** 35–44 (Jan. 2013).

127. Pellicci, D. G. *et al.* A natural killer T (NKT) cell developmental pathway iInvolving a thymus-dependent NK1.1(-)CD4(+) CD1d-dependent precursor stage. *J. Exp. Med.* **195,** 835–44 (Apr. 2002).

128. Wilson, R. P. *et al.* STAT3 is a critical cell-intrinsic regulator of human unconventional T cell numbers and function. *J. Exp. Med.* **212,** 855–64 (June 2015).

129. Okada, S. *et al.* Impairment of immunity to Candida and Mycobacterium in humans with bi-allelic RORC mutations. *Science (80-.).* **349,** 606–613 (Aug. 2015).

130. Savage, A. K. *et al.* The transcription factor PLZF directs the effector program of the NKT cell lineage. *Immunity* **29,** 391–403 (Sept. 2008).

131. Beaulieu, A. M. & Sant'Angelo, D. B. The BTB-ZF family of transcription factors: key regulators of lineage commitment and effector function development in the immune system. *J. Immunol.* **187,** 2841–7 (Sept. 2011).

132. Griewank, K. *et al.* Homotypic interactions mediated by Slamf1 and Slamf6 receptors control NKT cell lineage development. *Immunity* **27,** 751–62 (Nov. 2007).

133. Chung, B., Aoukaty, A., Dutz, J., Terhorst, C. & Tan, R. Signaling lymphocytic activation molecule-associated protein controls NKT cell functions. *J. Immunol.* **174,** 3153–7 (Mar. 2005).

134. Dusseaux, M. *et al.* Human MAIT cells are xenobiotic-resistant, tissue-targeted, CD161hi IL-17-secreting T cells. *Blood* **117,** 1250–9 (Jan. 2011).

135. Walker, L. J. *et al.* Human MAIT and CD8$\alpha\alpha$ cells develop from a pool of type-17 precommitted CD8+ T cells. *Blood* **119,** 422–33 (Jan. 2012).

136. Fergusson, J. R. *et al.* CD161 defines a transcriptional and functional phenotype across distinct human T cell lineages. *Cell Rep.* **9,** 1075–88 (Nov. 2014).

137. Gozalbo-López, B. *et al.* The MHC-related protein 1 (MR1) is expressed by a subpopulation of CD38+, IgA+ cells in the human intestinal mucosa. *Histol. Histopathol.* **24,** 1439–49 (Nov. 2009).

138. Le Bourhis, L. *et al.* Antimicrobial activity of mucosal-associated invariant T cells. *Nat. Immunol.* **11,** 701–8 (Aug. 2010).

139. Walker, L. J., Tharmalingam, H. & Klenerman, P. The rise and fall of MAIT cells with age. *Scand. J. Immunol.* **80,** 462–3 (Dec. 2014).

140. Reantragoon, R. *et al.* Antigen-loaded MR1 tetramers define T cell receptor heterogeneity in mucosal-associated invariant T cells. *J Exp Med* **210,** 2305–2320 (Oct. 2013).

141. Lanier, L. L., Chang, C. & Phillips, J. H. Human NKR-P1A. A disulfide-linked homodimer of the C-type lectin superfamily expressed by a subset of NK and T lymphocytes. *J. Immunol.* **153,** 2417–28 (Sept. 1994).

142. Aldemir, H. *et al.* Cutting edge: lectin-like transcript 1 is a ligand for the CD161 receptor. *J. Immunol.* **175,** 7791–5 (Dec. 2005).

143. Rosen, D. B. *et al.* Cutting edge: lectin-like transcript-1 is a ligand for the inhibitory human NKR-P1A receptor. *J. Immunol.* **175,** 7796–9 (Dec. 2005).

144. Boles, K. S., Barten, R., Kumaresan, P. R., Trowsdale, J. & Mathew, P. a. Cloning of a new lectin-like receptor expressed on human NK cells. *Immunogenetics* **50,** 1–7 (Oct. 1999).

145. Vogler, I. & Steinle, A. Vis-à-vis in the NKC: genetically linked natural killer cell receptor/ligand pairs in the natural killer gene complex (NKC). *J. Innate Immun.* **3,** 227–35 (2011).

146. Roth, P. *et al.* Malignant glioma cells counteract antitumor immune responses through expression of lectin-like transcript-1. *Cancer Res.* **67,** 3540–3544 (2007).

147. Rosen, D. B. *et al.* Functional consequences of interactions between human NKR-P1A and its ligand LLT1 expressed on activated dendritic cells and B cells. *J. Immunol.* **180,** 6508–17 (May 2008).

148. Poggi, A. *et al.* IL-12-mediated NKRP1A up-regulation and consequent enhancement of endothelial transmigration of V delta 2+ TCR gamma delta+ T lymphocytes from healthy donors and multiple sclerosis patients. *J. Immunol.* **162,** 4349–54 (Apr. 1999).

149. Le Bourhis, L. *et al.* MAIT Cells Detect and Efficiently Lyse Bacterially-Infected Epithelial Cells. *PLoS Pathog.* **9** (ed DeLeo, F. R.) e1003681 (Oct. 2013).

150. Ussher, J. E., Klenerman, P. & Willberg, C. B. Mucosal-associated invariant T-cells: new players in anti-bacterial immunity. *Front. Immunol.* **5,** 450 (Oct. 2014).

151. Battistini, L. *et al.* Phenotypic and cytokine analysis of human peripheral blood gamma delta T cells expressing NK cell receptors. *J. Immunol.* **159,** 3723–30 (Oct. 1997).

152. Cosmi, L. *et al.* Human interleukin 17-producing cells originate from a CD161+CD4+ T cell precursor. *J. Exp. Med.* **205,** 1903–16 (Aug. 2008).

153. Maggi, L. *et al.* CD161 is a marker of all human IL-17-producing T-cell subsets and is induced by RORC. *Eur. J. Immunol.* **40,** 2174–81 (Aug. 2010).

154. Pesenacker, A. M. *et al.* CD161 defines the subset of FoxP3+ T cells capable of producing proinflammatory cytokines. *Blood* **121,** 2647–58 (Apr. 2013).

155. Takahashi, T., Dejbakhsh-Jones, S. & Strober, S. Expression of CD161 (NKR-P1A) defines subsets of human CD4 and CD8 T cells with different functional activities. *J. Immunol.* **176,** 211–6 (Jan. 2006).

156. Billerbeck, E. *et al.* Analysis of CD161 expression on human CD8+ T cells defines a distinct functional subset with tissue-homing properties. *Proc. Natl. Acad. Sci. U. S. A.* **107,** 3006–11 (Feb. 2010).

157. Meermeier, E. W. *et al.* Human TRAV1-2-negative MR1-restricted T cells detect S. pyogenes and alternatives to MAIT riboflavin-based antigens. *Nat. Commun.* **7,** 12506 (2016).

158. Turtle, C. J., Swanson, H. M., Fujii, N., Estey, E. H. & Riddell, S. R. A distinct subset of self-renewing human memory CD8+ T cells survives cytotoxic chemotherapy. *Immunity* **31,** 834–44 (Nov. 2009).

159. Franciszkiewicz, K. *et al.* MHC class I-related molecule, MR1, and mucosal-associated invariant T cells. *Immunol. Rev.* **272,** 120–38 (July 2016).

160. Kreslavsky, T. *et al.* TCR-inducible PLZF transcription factor required for innate phenotype of a subset of gammadelta T cells with restricted TCR diversity. *Proc. Natl. Acad. Sci. U. S. A.* **106,** 12453–8 (July 2009).

161. Kovalovsky, D. *et al.* PLZF induces the spontaneous acquisition of memory/effector functions in T cells independently of NKT cell-related signals. *J. Immunol.* **184,** 6746–55 (June 2010).

162. Rahimpour, A. *et al.* Identification of phenotypically and functionally heterogeneous mouse mucosal-associated invariant T cells using MR1 tetramers. *J. Exp. Med.* **212,** 1095–108 (June 2015).

163. Leeansyah, E. *et al.* Arming of MAIT Cell Cytolytic Antimicrobial Activity Is Induced by IL-7 and Defective in HIV-1 Infection. *PLoS Pathog.* **11,** e1005072 (Aug. 2015).

164. Szabo, S. J. *et al.* A novel transcription factor, T-bet, directs Th1 lineage commitment. *Cell* **100,** 655–69 (Mar. 2000).

165. Pearce, E. L. *et al.* Control of effector CD8+ T cell function by the transcription factor Eomesodermin. *Science* **302,** 1041–3 (Nov. 2003).

166. Akimova, T., Beier, U. H., Wang, L., Levine, M. H. & Hancock, W. W. Helios expression is a marker of T cell activation and proliferation. *PLoS One* **6,** e24226 (2011).

167. Turtle, C. J. *et al.* Innate signals overcome acquired TCR signaling pathway regulation and govern the fate of human CD161(hi) CD8alpha(+) semi-invariant T cells. *Blood* **118,** 2752–62 (Sept. 2011).

168. Kurioka, A. *et al.* MAIT cells are licensed through granzyme exchange to kill bacterially sensitized targets. *Mucosal Immunol.* **8,** 429–40 (Mar. 2015).

169. Kallies, A., Xin, A., Belz, G. T. & Nutt, S. L. Blimp-1 transcription factor is required for the differentiation of effector CD8(+) T cells and memory responses. *Immunity* **31,** 283–95 (Aug. 2009).

170. Tang, X.-Z. *et al.* IL-7 licenses activation of human liver intrasinusoidal mucosal-associated invariant T cells. *J. Immunol.* **190,** 3142–52 (Apr. 2013).

171. Jiang, J. *et al.* Mucosal-associated invariant T cells from patients with tuberculosis exhibit impaired immune response. *J. Infect.* **72,** 338–52 (Mar. 2016).

172. Sattler, A., Dang-Heine, C., Reinke, P. & Babel, N. IL-15 dependent induction of IL-18 secretion as a feedback mechanism controlling human MAIT-cell effector functions. *Eur. J. Immunol.* **45,** 2286–98 (Aug. 2015).

173. Havenith, S. H. C. *et al.* Analysis of stem-cell-like properties of human CD161++IL-18Rα+ memory CD8+ T cells. *Int. Immunol.* **24,** 625–36 (Oct. 2012).

174. Slichter, C. K. *et al.* Distinct activation thresholds of human conventional and innate-like memory T cells. *JCI Insight* **1,** 1–16 (June 2016).

175. Eberhard, J. M. *et al.* CD161+ MAIT Cells Are Severely Reduced in Peripheral Blood and Lymph Nodes of HIV-Infected Individuals Independently of Disease Progression. *PLoS One* **9,** e111323 (Jan. 2014).

176. Brozova, J., Karlova, I. & Novak, J. Analysis of the Phenotype and Function of the Subpopulations of Mucosal-Associated Invariant T Cells. *Scand. J. Immunol.* **84,** 245–51 (Oct. 2016).

177. Salou, M. *et al.* Neuropathologic, phenotypic and functional analyses of Mucosal Associated Invariant T cells in Multiple Sclerosis. *Clin. Immunol.* **166-167,** 1–11 (Apr. 2016).

178. Gold, M. C. *et al.* Human mucosal associated invariant T cells detect bacterially infected cells. *PLoS Biol.* **8,** e1000407 (Jan. 2010).

179. Griffith, J. W., Sokol, C. L. & Luster, A. D. Chemokines and chemokine receptors: positioning cells for host defense and immunity. *Annu. Rev. Immunol.* **32,** 659–702 (2014).

180. Haga, K. *et al.* MAIT cells are activated and accumulated in the inflamed mucosa of ulcerative colitis. *J. Gastroenterol. Hepatol.* **31,** 965–72 (May 2016).

181. Greathead, L. *et al.* CD8+/CD161++ mucosal-associated invariant T-cell levels in the colon are restored on long-term antiretroviral therapy and correlate with CD8+ T-cell immune activation. *AIDS* **28,** 1690–2 (July 2014).

182. Sundström, P. *et al.* Human Mucosa-Associated Invariant T Cells Accumulate in Colon Adenocarcinomas but Produce Reduced Amounts of IFN-γ. *J. Immunol.* **195,** 3472–81 (Oct. 2015).

183. Leeansyah, E. *et al.* Activation, exhaustion and persistent decline of the anti-microbial MR1-restricted MAIT cell population in chronic HIV-1 infection. *Blood* **121,** 1124–35 (Dec. 2013).

184. Carolan, E. *et al.* Altered distribution and increased IL-17 production by mucosal-associated invariant T cells in adult and childhood obesity. *J. Immunol.* **194,** 5775–80 (June 2015).

185. Teunissen, M. B. M. *et al.* The IL-17A-producing CD8+ T-cell population in psoriatic lesional skin comprises mucosa-associated invariant T cells and conventional T cells. *J. Invest. Dermatol.* **134,** 2898–907 (Dec. 2014).

186. Hinks, T. S. C. *et al.* Steroid-induced Deficiency of Mucosal-associated Invariant T Cells in the COPD Lung: Implications for NTHi Infection. *Am. J. Respir. Crit. Care Med.* 1–63 (Apr. 2016).

187. Gibbs, A. *et al.* MAIT cells reside in the female genital mucosa and are biased towards IL-17 and IL-22 production in response to bacterial stimulation. *Mucosal Immunol.* 1–11 (Apr. 2016).

188. Taniguchi, T. & Minami, Y. The IL-2/IL-2 receptor system: a current overview. *Cell* **73,** 5–8 (Apr. 1993).

189. Reddy, M., Eirikis, E., Davis, C., Davis, H. M. & Prabhakar, U. Comparative analysis of lymphocyte activation marker expression and cytokine secretion profile in stimulated human peripheral blood mononuclear cell cultures: an in vitro model to monitor cellular immune function. *J. Immunol. Methods* **293,** 127–42 (Oct. 2004).

190. Shiow, L. R. *et al.* CD69 acts downstream of interferon-alpha/beta to inhibit S1P1 and lymphocyte egress from lymphoid organs. *Nature* **440,** 540–4 (Mar. 2006).

191. Sancho, D. *et al.* CD69 downregulates autoimmune reactivity through active transforming growth factor-beta production in collagen-induced arthritis. *J. Clin. Invest.* **112,** 872–82 (Sept. 2003).

192. Sancho, D., Gómez, M. & Sánchez-Madrid, F. CD69 is an immunoregulatory molecule induced following activation. *Trends Immunol.* **26,** 136–40 (Mar. 2005).

193. Radulovic, K. & Niess, J. H. CD69 is the crucial regulator of intestinal inflammation: a new target molecule for IBD treatment? *J. Immunol. Res.* **2015,** 497056 (2015).

194. Martin, P. & Sanchez-Madrid, F. CD69: an unexpected regulator of TH17 cell-driven inflammatory responses. *Sci. Signal.* **4,** pe14 (2011).

195. De la Fuente, H. *et al.* The leukocyte activation receptor CD69 controls T cell differentiation through its interaction with galectin-1. *Mol. Cell. Biol.* **34,** 2479–87 (July 2014).

196. Schroder, K., Hertzog, P. J., Ravasi, T. & Hume, D. A. Interferon-gamma: an overview of signals, mechanisms and functions. *J. Leukoc. Biol.* **75,** 163–89 (Feb. 2004).

197. Billiau, A. & Matthys, P. Interferon-gamma: a historical perspective. *Cytokine Growth Factor Rev.* **20,** 97–113 (Apr. 2009).

198. Sedger, L. M. & McDermott, M. F. TNF and TNF-receptors: From mediators of cell death and inflammation to therapeutic giants - past, present and future. *Cytokine Growth Factor Rev.* **25,** 453–72 (Aug. 2014).

199. Gaffen, S. L. An overview of IL-17 function and signaling. *Cytokine* **43,** 402–7 (Sept. 2008).

200. Chowdhury, D. & Lieberman, J. Death by a thousand cuts: granzyme pathways of programmed cell death. *Annu. Rev. Immunol.* **26,** 389–420 (2008).

201. Harari, A., Bellutti Enders, F., Cellerai, C., Bart, P.-A. & Pantaleo, G. Distinct profiles of cytotoxic granules in memory CD8 T cells correlate with function, differentiation stage, and antigen exposure. *J. Virol.* **83,** 2862–71 (Apr. 2009).

202. Wensink, A. C., Hack, C. E. & Bovenschen, N. Granzymes regulate proinflammatory cytokine responses. *J. Immunol.* **194,** 491–7 (Jan. 2015).

203. Jo, J. *et al.* Toll-like receptor 8 agonist and bacteria trigger potent activation of innate immune cells in human liver. *PLoS Pathog.* **10** (ed Walker, C. M.) e1004210 (June 2014).

204. Gold, M. C. *et al.* MR1-restricted MAIT cells display ligand discrimination and pathogen selectivity through distinct T cell receptor usage. *J. Exp. Med.* **211,** 1601–10 (July 2014).

205. Eckle, S. B. G. *et al.* Recognition of Vitamin B Precursors and Byproducts by Mucosal Associated Invariant T Cells. *J. Biol. Chem.* **290,** 30204–11 (Dec. 2015).

206. Van Wilgenburg, B. *et al.* MAIT cells are activated during human viral infections. *Nat. Commun.* **7,** 11653 (2016).

207. Kwon, Y. S. *et al.* Mucosal-associated invariant T cells are numerically and functionally deficient in patients with mycobacterial infection and reflect disease activity. *Tuberculosis* **95,** 267–274 (May 2015).

208. Ussher, J. E. *et al.* Molecular Analyses Define Vα7.2-Jα33+ MAIT Cell Depletion in HIV Infection: A Case-Control Study. *Medicine (Baltimore).* **94,** e1134 (July 2015).

209. Saeidi, A. *et al.* Attrition of TCR Valpha7.2+ CD161++ MAIT cells in HIV-tuberculosis co-infection is associated with elevated levels of PD-1 expression. *PLoS One* **10** (ed Sandberg, J. K.) e0124659 (Apr. 2015).

210. Spaan, M. *et al.* Frequencies of Circulating MAIT Cells Are Diminished in Chronic HCV, HIV and HCV/HIV Co-Infection and Do Not Recover during Therapy. *PLoS One* **11,** e0159243 (2016).

211. Barathan, M. *et al.* Peripheral loss of CD8(+) CD161(++) TCRValpha7.2(+) mucosal-associated invariant T cells in chronic hepatitis C virus-infected patients. *Eur. J. Clin. Invest.* **46,** 170–80 (Feb. 2016).

212. Hengst, J. *et al.* Nonreversible MAIT cell-dysfunction in chronic hepatitis C virus infection despite successful interferon-free therapy. *Eur. J. Immunol.* 1–7 (June 2016).

213. Loh, L. *et al.* Human mucosal-associated invariant T cells contribute to antiviral influenza immunity via IL-18-dependent activation. *Proc. Natl. Acad. Sci. U. S. A.* **113,** 10133–8 (Sept. 2016).

214. Grimaldi, D. *et al.* Bacterial sepsis induces a profound depletion in circulating mucosal-associated invariant T (MAIT) lymphocytes. *Intensive Care Med.* **37,** S257 (2011).

215. Smith, D. J., Hill, G. R., Bell, S. C. & Reid, D. W. Reduced mucosal associated invariant T-cells are associated with increased disease severity and Pseudomonas aeruginosa infection in cystic fibrosis. *PLoS One* **9,** e109891 (2014).

216. Kang, S.-J. *et al.* Activation, Impaired Tumor Necrosis Factor-Alpha Production, and Deficiency of Circulating Mucosal-Associated Invariant T Cells in Patients with Scrub Typhus. *PLoS Negl. Trop. Dis.* **10,** e0004832 (July 2016).

217. Booth, J. S. *et al.* Mucosal-Associated Invariant T Cells in the Human Gastric Mucosa and Blood: Role in Helicobacter pylori Infection. *Front. Immunol.* **6,** 466 (2015).

218. Leung, D. T. *et al.* Circulating mucosal associated invariant T cells are activated in Vibrio cholerae O1 infection and associated with lipopolysaccharide antibody responses. *PLoS Negl. Trop. Dis.* **8,** e3076 (Aug. 2014).

219. Cosgrove, C. *et al.* Early and nonreversible decrease of CD161++ /MAIT cells in HIV infection. *Blood* **121,** 951–61 (Feb. 2013).

220. Jiang, J. *et al.* Mucosal-associated invariant T-cell function is modulated by programmed death-1 signaling in patients with active tuberculosis. *Am. J. Respir. Crit. Care Med.* **190,** 329–39 (Aug. 2014).

221. Illes, Z., Shimamura, M., Newcombe, J., Oka, N. & Yamamura, T. Accumulation of Valpha7.2-Jalpha33 invariant T cells in human autoimmune inflammatory lesions in the nervous system. *Int. Immunol.* **16,** 223–30 (Feb. 2004).

222. Miyazaki, Y., Miyake, S., Chiba, A., Lantz, O. & Yamamura, T. Mucosal-associated invariant T cells regulate Th1 response in multiple sclerosis. *Int. Immunol.* **23,** 529–35 (Sept. 2011).

223. Abrahamsson, S. V. *et al.* Non-myeloablative autologous haematopoietic stem cell transplantation expands regulatory cells and depletes IL-17 producing mucosal-associated invariant T cells in multiple sclerosis. *Brain* **136,** 2888–903 (Sept. 2013).

224. Willing, A. *et al.* CD8+ MAIT cells infiltrate into the CNS and alterations in their blood frequencies correlate with IL-18 serum levels in multiple sclerosis. *Eur. J. Immunol.* **44,** 3119–28 (Oct. 2014).

225. Negrotto, L. *et al.* Peripheral blood non-MAIT CD8+CD161hi cells are decreased in relapsing-remitting multiple sclerosis patients treated with interferon beta. *J. Neuroimmunol.* **288,** 98–101 (Nov. 2015).

226. Cho, Y.-N. *et al.* Mucosal-associated invariant T cell deficiency in systemic lupus erythematosus. *J. Immunol.* **193,** 3891–901 (Oct. 2014).

227. Sugimoto, C. *et al.* Mucosal-associated invariant T cell is a potential marker to distinguish fibromyalgia syndrome from arthritis. *PLoS One* **10,** e0121124 (2015).

228. Serriari, N.-E. *et al.* Innate mucosal-associated invariant T (MAIT) cells are activated in inflammatory bowel diseases. *Clin. Exp. Immunol.* **176,** 266–74 (May 2014).

229. Hiejima, E. *et al.* Reduced Numbers and Proapoptotic Features of Mucosal-associated Invariant T Cells as a Characteristic Finding in Patients with Inflammatory Bowel Disease. *Inflamm. Bowel Dis.* **21,** 1529–40 (July 2015).

230. Dunne, M. R. *et al.* Persistent changes in circulating and intestinal $\gamma\delta$ T cell subsets, invariant natural killer T cells and mucosal-associated invariant T cells in children and adults with coeliac disease. *PLoS One* **8,** e76008 (2013).

231. Braudeau, C. *et al.* Persistent deficiency of circulating mucosal-associated invariant T (MAIT) cells in ANCA-associated vasculitis. *J. Autoimmun.* **70,** 73–9 (June 2016).

232. Wang, J. J., Macardle, C., Weedon, H., Beroukas, D. & Banovic, T. Mucosal-associated invariant T cells are reduced and functionally immature in the peripheral blood of primary Sjogren's syndrome patients. *Eur. J. Immunol.* **58,** 7250–7 (July 2016).

233. Li, J. *et al.* The frequency of mucosal-associated invariant T cells is selectively increased in dermatitis herpetiformis. *Australas. J. Dermatol.* **In print.** (Mar. 2016).

234. Kim, J.-C. *et al.* Deficiencies of Circulating Mucosal-associated Invariant T Cells and Natural Killer T Cells in Patients with Acute Cholecystitis. *J. Korean Med. Sci.* **30,** 606–11 (May 2015).

235. Hayashi, E. *et al.* Involvement of Mucosal-associated Invariant T cells in Ankylosing Spondylitis. *J. Rheumatol.* **43,** 1695–703 (Sept. 2016).

236. Gracey, E. *et al.* IL-7 primes IL-17 in mucosal-associated invariant T (MAIT) cells, which contribute to the Th17-axis in ankylosing spondylitis. *Ann. Rheum. Dis.* annrheumdis–2015–208902 (May 2016).

237. Kwon, Y. S. *et al.* Mucosal-Associated Invariant T Cell Deficiency in Chronic Obstructive Pulmonary Disease. *COPD* **13,** 196–202 (Apr. 2016).

238. Peterfalvi, A. *et al.* Invariant Valpha7.2-Jalpha33 TCR is expressed in human kidney and brain tumors indicating infiltration by mucosal-associated invariant T (MAIT) cells. *Int. Immunol.* **20,** 1517–25 (Dec. 2008).

239. Won, E. J. *et al.* Clinical relevance of circulating mucosal-associated invariant T cell levels and their anti-cancer activity in patients with mucosal-associated cancer. *Oncotarget* **In print.** (Aug. 2016).

240. Zabijak, L. *et al.* Increased tumor infiltration by mucosal-associated invariant T cells correlates with poor survival in colorectal cancer patients. *Cancer Immunol. Immunother.* **64,** 1601–8 (Dec. 2015).

241. Ling, L. *et al.* Circulating and tumor-infiltrating mucosal associated invariant T (MAIT) cells in colorectal cancer patients. *Sci. Rep.* **6,** 20358 (2016).

242. Sugimoto, C., Fujita, H. & Wakao, H. Mucosal-associated invariant T cells from induced pluripotent stem cells: A novel approach for modeling human diseases. *World J. Stem Cells* **8,** 158–69 (Apr. 2016).

243. Baron, M. *et al.* Innate-like and conventional T cell populations from hemodialyzed and kidney transplanted patients are equally compromised. *PLoS One* **9,** e105422 (2014).

244. Wong, E. B. *et al. MAIT Cells Are Highly Enriched in the Bronchoalveolar Lavage Fluid of Patients With TB* in *Conf. retroviruses opportunistic Infect.* (Boston, Massachusetts, 2014).

245. Georgel, P., Radosavljevic, M., Macquin, C. & Bahram, S. The non-conventional MHC class I MR1 molecule controls infection by Klebsiella pneumoniae in mice. *Mol. Immunol.* **48,** 769–75 (Feb. 2011).

246. Meierovics, A., Yankelevich, W.-J. C. & Cowley, S. C. MAIT cells are critical for optimal mucosal immune responses during in vivo pulmonary bacterial infection. *Proc. Natl. Acad. Sci.* **110,** E3119–28 (Aug. 2013).

247. Chua, W.-J. *et al.* Polyclonal MAIT Cells Have Unique Innate Functions in Bacterial Infection. *Infect. Immun.* **80,** 3256–3267 (July 2012).

248. Sakala, I. G. *et al.* Functional Heterogeneity and Antimycobacterial Effects of Mouse Mucosal-Associated Invariant T Cells Specific for Riboflavin Metabolites. *J. Immunol.* **195,** 587–601 (2015).

249. Koch, R. Classics in infectious diseases. The etiology of tuberculosis: Robert Koch. Berlin, Germany 1882. *Rev. Infect. Dis.* **4,** 1270–4 (Feb. 1959).

250. Comas, I. *et al.* Out-of-Africa migration and Neolithic coexpansion of Mycobacterium tuberculosis with modern humans. *Nat. Genet.* **45,** 1176–1182 (2013).

251. Wilson, L. G. Commentary: Medicine, population, and tuberculosis. *Int. J. Epidemiol.* **34,** 521–4 (June 2005).

252. Daniel, T. M. The history of tuberculosis. *Respir. Med.* **100,** 1862–70 (Nov. 2006).

253. Tiemersma, E. W., van der Werf, M. J., Borgdorff, M. W., Williams, B. G. & Nagelkerke, N. J. D. Natural history of tuberculosis: duration and fatality of untreated pulmonary tuberculosis in HIV negative patients: a systematic review. *PLoS One* **6,** e17601 (2011).

254. World Health Organisation. *Global tuberculosis report 2015* 20th ed., 192 (World Health Organization, Dec. 2015).

255. Dye, C., Scheele, S., Dolin, P., Pathania, V. & Raviglione, M. C. Consensus statement. Global burden of tuberculosis: estimated incidence, prevalence, and mortality by country. WHO Global Surveillance and Monitoring Project. *JAMA* **282,** 677–86 (Aug. 1999).

256. Lim, W. S. From latent to active TB: are IGRAs of any use? *Thorax* **71,** 585–6 (July 2016).

257. Fennelly, K. P. *et al.* Variability of infectious aerosols produced during coughing by patients with pulmonary tuberculosis. *Am. J. Respir. Crit. Care Med.* **186,** 450–7 (Sept. 2012).

258. O'Garra, A. *et al.* The immune response in tuberculosis. *Annu. Rev. Immunol.* **31,** 475–527 (Mar. 2013).

259. Kleinnijenhuis, J., Oosting, M., Joosten, L. a. B., Netea, M. G. & Van Crevel, R. Innate immune recognition of Mycobacterium tuberculosis. *Clin. Dev. Immunol.* **2011,** 405310 (Jan. 2011).

260. Ramakrishnan, L. Revisiting the role of the granuloma in tuberculosis. *Nat. Rev. Immunol.* **12,** 352–366 (Apr. 2012).

261. Andreu, J., Cáceres, J., Pallisa, E. & Martinez-Rodriguez, M. Radiological manifestations of pulmonary tuberculosis. *Eur. J. Radiol.* **51,** 139–49 (Aug. 2004).

262. Van Pinxteren, L. a., Cassidy, J. P., Smedegaard, B. H., Agger, E. M. & Andersen, P. Control of latent Mycobacterium tuberculosis infection is dependent on CD8 T cells. *Eur. J. Immunol.* **30,** 3689–98 (Dec. 2000).

263. Botha, T. & Ryffel, B. Reactivation of latent tuberculosis infection in TNF-deficient mice. *J. Immunol.* **171,** 3110–8 (Sept. 2003).

264. Chackerian, A. a., Alt, J. M., Perera, T. V., Dascher, C. C. & Behar, S. M. Dissemination of Mycobacterium tuberculosis is influenced by host factors and precedes the initiation of T-cell immunity. *Infect. Immun.* **70,** 4501–9 (Aug. 2002).

265. Behr, M. A. & Waters, W. R. Is tuberculosis a lymphatic disease with a pulmonary portal? *Lancet Infect. Dis.* **3099,** 1–6 (Nov. 2013).

266. Cooper, A. M. Cell-mediated immune responses in tuberculosis. *Annu. Rev. Immunol.* **27,** 393–422 (Jan. 2009).

267. Gengenbacher, M. & Kaufmann, S. H. E. Mycobacterium tuberculosis: success through dormancy. *FEMS Microbiol. Rev.* 1–19 (Feb. 2012).

268. Lin, P. L. *et al.* Quantitative comparison of active and latent tuberculosis in the cynomolgus macaque model. *Infect. Immun.* **77,** 4631–42 (Oct. 2009).

269. Frieden, T. R., Sterling, T. R., Munsiff, S. S., Watt, C. J. & Dye, C. Tuberculosis. *Lancet* **362,** 887–899 (Sept. 2003).

270. Rohde, K., Yates, R. M., Purdy, G. E. & Russell, D. G. Mycobacterium tuberculosis and the environment within the phagosome. *Immunol. Rev.* **219,** 37–54 (Oct. 2007).

271. Armstrong, J. A. & Hart, P. D. Response of cultured macrophages to Mycobacterium tuberculosis, with observations on fusion of lysosomes with phagosomes. *J. Exp. Med.* **134,** 713–40 (Sept. 1971).

272. Claus, V. *et al.* Lysosomal enzyme trafficking between phagosomes, endosomes, and lysosomes in J774 macrophages. Enrichment of cathepsin H in early endosomes. *J. Biol. Chem.* **273,** 9842–51 (Apr. 1998).

273. Yates, R. M., Hermetter, A., Taylor, G. A. & Russell, D. G. Macrophage activation downregulates the degradative capacity of the phagosome. *Traffic* **8,** 241–50 (Mar. 2007).

274. Van der Wel, N. *et al.* M. tuberculosis and M. leprae translocate from the phagolysosome to the cytosol in myeloid cells. *Cell* **129,** 1287–98 (June 2007).

275. Levitte, S. *et al.* Mycobacterial Acid Tolerance Enables Phagolysosomal Survival and Establishment of Tuberculous Infection In Vivo. *Cell Host Microbe* **20,** 250–8 (Aug. 2016).

276. Hamasaki, M. *et al.* Autophagosomes form at ER-mitochondria contact sites. *Nature* **495,** 389–93 (Mar. 2013).

277. Maiuri, M. C., Zalckvar, E., Kimchi, A. & Kroemer, G. Self-eating and self-killing: crosstalk between autophagy and apoptosis. *Nat. Rev. Mol. Cell Biol.* **8,** 741–752 (Sept. 2007).

278. Gutierrez, M. G. *et al.* Autophagy is a defense mechanism inhibiting BCG and Mycobacterium tuberculosis survival in infected macrophages. *Cell* **119,** 753–66 (Dec. 2004).

279. Watson, R. O., Manzanillo, P. S. & Cox, J. S. Extracellular M. tuberculosis DNA targets bacteria for autophagy by activating the host DNA-sensing pathway. *Cell* **150,** 803–15 (Aug. 2012).

280. Yuk, J.-M. *et al.* Vitamin D3 induces autophagy in human monocytes/macrophages via cathelicidin. *Cell Host Microbe* **6,** 231–43 (Sept. 2009).

281. Bradfute, S. B. *et al.* Autophagy as an immune effector against tuberculosis. *Curr. Opin. Microbiol.* 1–11 (June 2013).

282. Jones, B. W., Heldwein, K. a., Means, T. K., Saukkonen, J. J. & Fenton, M. J. Differential roles of Toll-like receptors in the elicitation of proinflammatory responses by macrophages. *Ann. Rheum. Dis.* **60 Suppl 3,** iii6–12 (Nov. 2001).

283. Pompei, L. *et al.* Disparity in IL-12 release in dendritic cells and macrophages in response to Mycobacterium tuberculosis is due to use of distinct TLRs. *J. Immunol.* **178,** 5192–9 (Apr. 2007).

284. Méndez-Samperio, P., Trejo, A. & Pérez, A. Mycobacterium bovis bacillus Calmette-Guerin induces CCL5 secretion via the Toll-like receptor 2-NF-kappaB and -Jun N-terminal kinase signaling pathways. *Clin. Vaccine Immunol.* **15,** 277–83 (Feb. 2008).

285. Brightbill, H. D. *et al.* Host defense mechanisms triggered by microbial lipoproteins through toll-like receptors. *Science* **285,** 732–6 (July 1999).

286. Quesniaux, V. J. *et al.* Toll-like receptor 2 (TLR2)-dependent-positive and TLR2-independent-negative regulation of proinflammatory cytokines by mycobacterial lipomannans. *J. Immunol.* **172,** 4425–34 (Apr. 2004).

287. Hossain, M. M. & Norazmi, M.-N. Pattern recognition receptors and cytokines in Mycobacterium tuberculosis infection–the double-edged sword? *Biomed Res. Int.* **2013,** 179174 (2013).

288. Saraav, I., Singh, S. & Sharma, S. Outcome of Mycobacterium tuberculosis and Toll-like receptor interaction: immune response or immune evasion? *Immunol. Cell Biol.* **92,** 741–6 (Oct. 2014).

289. Hemmi, H. *et al.* A Toll-like receptor recognizes bacterial DNA. *Nature* **408,** 740–5 (Dec. 2000).

290. Russell, D. G. Who puts the tubercle in tuberculosis? *Nat. Rev. Microbiol.* **5,** 39–47 (Jan. 2007).

291. Monin, L. & Khader, S. A. Chemokines in tuberculosis: the good, the bad and the ugly. *Semin. Immunol.* **26,** 552–8 (Dec. 2014).

292. Esin, S. & Batoni, G. Natural killer cells: A coherent model for their functional role in Mycobacterium tuberculosis infection. *J. Innate Immun.* **7,** 11–24 (2015).

293. Khader, S. a. *et al.* Interleukin 12p40 is required for dendritic cell migration and T cell priming after Mycobacterium tuberculosis infection. *J. Exp. Med.* **203,** 1805–15 (July 2006).

294. Wolf, A. J. *et al.* Mycobacterium tuberculosis infects dendritic cells with high frequency and impairs their function in vivo. *J. Immunol.* **179,** 2509–19 (Aug. 2007).

295. Wolf, A. J. *et al.* Initiation of the adaptive immune response to Mycobacterium tuberculosis depends on antigen production in the local lymph node, not the lungs. *J. Exp. Med.* **205,** 105–15 (Jan. 2008).

296. Gallegos, A. M., Pamer, E. G. & Glickman, M. S. Delayed protection by ESAT-6-specific effector CD4+ T cells after airborne M. tuberculosis infection. *J. Exp. Med.* **205,** 2359–68 (Sept. 2008).

297. Walton, S. M. *et al.* The dynamics of mouse cytomegalovirus-specific CD4 T cell responses during acute and latent infection. *J. Immunol.* **181,** 1128–34 (July 2008).

298. Rentenaar, R. J. *et al.* Development of virus-specific CD4(+) T cells during primary cytomegalovirus infection. *J. Clin. Invest.* **105,** 541–8 (Feb. 2000).

299. Lin, P. L. *et al.* Early events in Mycobacterium tuberculosis infection in cynomolgus macaques. *Infect. Immun.* **74,** 3790–3803 (2006).

300. Lee, S. W. *et al.* Time interval to conversion of interferon-gamma release assay after exposure to tuberculosis. *Eur. Respir. J.* **37,** 1447–52 (June 2011).

301. Flynn, J. L., Gideon, H. P., Mattila, J. T. & Lin, P. L. Immunology studies in non-human primate models of tuberculosis. *Immunol. Rev.* **264,** 60–73 (Mar. 2015).

302. Behar, S. M., Carpenter, S. M., Booty, M. G., Barber, D. L. & Jayaraman, P. Orchestration of pulmonary T cell immunity during Mycobacterium tuberculosis infection: immunity interruptus. *Semin. Immunol.* **26,** 559–77 (Dec. 2014).

303. Mogues, T., Goodrich, M. E., Ryan, L., LaCourse, R. & North, R. J. The relative importance of T cell subsets in immunity and immunopathology of airborne Mycobacterium tuberculosis infection in mice. *J. Exp. Med.* **193,** 271–80 (Feb. 2001).

304. Getahun, H., Gunneberg, C., Granich, R. & Nunn, P. HIV infection-associated tuberculosis: the epidemiology and the response. *Clin. Infect. Dis.* **50 Suppl 3,** S201–7 (May 2010).

305. Pawlowski, A., Jansson, M., Sköld, M., Rottenberg, M. E. & Källenius, G. Tuberculosis and HIV co-infection. *PLoS Pathog.* **8,** e1002464 (Feb. 2012).

306. Flesch, I. E. & Kaufmann, S. H. Mechanisms involved in mycobacterial growth inhibition by gamma interferon-activated bone marrow macrophages: role of reactive nitrogen intermediates. *Infect. Immun.* **59,** 3213–8 (Sept. 1991).

307. Chan, J., Xing, Y., Magliozzo, R. S. & Bloom, B. R. Killing of virulent Mycobacterium tuberculosis by reactive nitrogen intermediates produced by activated murine macrophages. *J. Exp. Med.* **175,** 1111–22 (Apr. 1992).

308. Bonecini-Almeida, M. G. *et al.* Induction of in vitro human macrophage anti-Mycobacterium tuberculosis activity: requirement for IFN-gamma and primed lymphocytes. *J. Immunol.* **160,** 4490–9 (May 1998).

309. Pieters, J. Mycobacterium tuberculosis and the macrophage: maintaining a balance. *Cell Host Microbe* **3,** 399–407 (June 2008).

310. Herbst, S., Schaible, U. E. & Schneider, B. E. Interferon gamma activated macrophages kill mycobacteria by nitric oxide induced apoptosis. *PLoS One* **6,** e19105 (2011).

311. Flynn, J. L. *et al.* An essential role for interferon gamma in resistance to Mycobacterium tuberculosis infection. *J. Exp. Med.* **178,** 2249–54 (Dec. 1993).

312. Cooper, A. M. *et al.* Disseminated Tuberculosis in Interferon-gamma Gene-disrupted Mice. *J. ...* **178,** 2243–7 (Dec. 1993).

313. Green, A. M., Difazio, R. & Flynn, J. L. IFN-γ from CD4 T cells is essential for host survival and enhances CD8 T cell function during Mycobacterium tuberculosis infection. *J. Immunol.* **190,** 270–7 (Jan. 2013).

314. Bustamante, J., Boisson-Dupuis, S., Abel, L. & Casanova, J.-L. Mendelian susceptibility to mycobacterial disease: genetic, immunological, and clinical features of inborn errors of IFN-γ immunity. *Semin. Immunol.* **26,** 454–70 (Dec. 2014).

315. Singhal, A., Jaiswal, A., Arora, V. K. & Prasad, H. K. Modulation of gamma interferon receptor 1 by Mycobacterium tuberculosis: a potential immune response evasive mechanism. *Infect. Immun.* **75,** 2500–10 (May 2007).

316. Sakai, S. *et al.* CD4 T Cell-Derived IFN-γ Plays a Minimal Role in Control of Pulmonary Mycobacterium tuberculosis Infection and Must Be Actively Repressed by PD-1 to Prevent Lethal Disease. *PLoS Pathog.* **12** (ed Fortune, S. M.) e1005667 (May 2016).

317. Robinson, C. M., Jung, J.-Y. & Nau, G. J. Interferon-γ, tumor necrosis factor, and interleukin-18 cooperate to control growth of Mycobacterium tuberculosis in human macrophages. *Cytokine* **60,** 233–41 (Oct. 2012).

318. Keane, J. *et al.* Tuberculosis associated with infliximab, a tumor necrosis factor alpha-neutralizing agent. *N. Engl. J. Med.* **345,** 1098–104 (Oct. 2001).

319. Iliopoulos, A., Psathakis, K., Aslanidis, S., Skagias, L. & Sfikakis, P. P. Tuberculosis and granuloma formation in patients receiving anti-TNF therapy. *Int. J. Tuberc. Lung Dis.* **10,** 588–90 (May 2006).

320. Delogu, G. & Goletti, D. The spectrum of tuberculosis infection: new perspectives in the era of biologics. *J. Rheumatol. Suppl.* **91,** 11–6 (May 2014).

321. Lin, P. L. *et al.* Tumor necrosis factor neutralization results in disseminated disease in acute and latent Mycobacterium tuberculosis infection with normal granuloma structure in a cynomolgus macaque model. *Arthritis Rheum.* **62,** 340–50 (Feb. 2010).

322. Roach, D. R. *et al.* TNF regulates chemokine induction essential for cell recruitment, granuloma formation, and clearance of mycobacterial infection. *J. Immunol.* **168,** 4620–7 (May 2002).

323. Flynn, J. L. *et al.* Tumor necrosis factor-alpha is required in the protective immune response against Mycobacterium tuberculosis in mice. *Immunity* **2,** 561–72 (June 1995).

324. Bean, A. G. *et al.* Structural deficiencies in granuloma formation in TNF gene-targeted mice underlie the heightened susceptibility to aerosol Mycobacterium tuberculosis infection, which is not compensated for by lymphotoxin. *J. Immunol.* **162,** 3504–11 (Mar. 1999).

325. Flórido, M. & Appelberg, R. Characterization of the deregulated immune activation occurring at late stages of mycobacterial infection in TNF-deficient mice. *J. Immunol.* **179,** 7702–8 (Dec. 2007).

326. Chakravarty, S. D. *et al.* Tumor necrosis factor blockade in chronic murine tuberculosis enhances granulomatous inflammation and disorganizes granulomas in the lungs. *Infect. Immun.* **76,** 916–26 (Mar. 2008).

327. Clay, H., Volkman, H. E. & Ramakrishnan, L. Tumor necrosis factor signaling mediates resistance to mycobacteria by inhibiting bacterial growth and macrophage death. *Immunity* **29,** 283–94 (Aug. 2008).

328. De Noronha, A. L. L., Bafica, A., Nogueira, L., Barral, A. & Barral-Netto, M. Lung granulomas from Mycobacterium tuberculosis/HIV-1 co-infected patients display decreased in situ TNF production. *Pathol. Res. Pract.* **204,** 155–61 (Jan. 2008).

329. Allie, N. *et al.* Prominent role for T cell-derived tumour necrosis factor for sustained control of Mycobacterium tuberculosis infection. *Sci. Rep.* **3,** 1809 (2013).

330. Lin, P. L. & Flynn, J. L. CD8 T cells and Mycobacterium tuberculosis infection. *Semin. Immunopathol.* **37,** 239–49 (May 2015).

331. Flynn, J. L., Goldstein, M. M., Triebold, K. J., Koller, B. & Bloom, B. R. Major histocompatibility complex class I-restricted T cells are required for resistance to Mycobacterium tuberculosis infection. *Proc. Natl. Acad. Sci. U. S. A.* **89,** 12013–7 (Dec. 1992).

332. Behar, S. M., Dascher, C. C., Grusby, M. J., Wang, C. R. & Brenner, M. B. Susceptibility of mice deficient in CD1D or TAP1 to infection with Mycobacterium tuberculosis. *J. Exp. Med.* **189,** 1973–80 (June 1999).

333. Capuano, S. V. *et al.* Experimental Mycobacterium tuberculosis infection of cynomolgus macaques closely resembles the various manifestations of human M. tuberculosis infection. *Infect. Immun.* **71,** 5831–44 (Oct. 2003).

334. Chen, C. Y. *et al.* A critical role for CD8 T cells in a nonhuman primate model of tuberculosis. *PLoS Pathog.* **5,** e1000392 (Apr. 2009).

335. Gideon, H. P. *et al.* Variability in tuberculosis granuloma T cell responses exists, but a balance of pro- and anti-inflammatory cytokines is associated with sterilization. *PLoS Pathog.* **11** (ed Lewinsohn, D. M.) e1004603 (Jan. 2015).

336. Randhawa, P. S. Lymphocyte subsets in granulomas of human tuberculosis: an in situ immunofluorescence study using monoclonal antibodies. *Pathology* **22,** 153–5 (July 1990).

337. Lewinsohn, D. M. *et al.* Characterization of Human CD8+ T Cells Reactive with Mycobacterium tuberculosis–infected Antigen-presenting Cells. *J. Exp. Med.* **187,** 1633–1640 (1998).

338. Cho, S. *et al.* Antimicrobial activity of MHC class I-restricted CD8+ T cells in human tuberculosis. *Proc. Natl. Acad. Sci. U. S. A.* **97,** 12210–5 (Oct. 2000).

339. Stenger, S. *et al.* An antimicrobial activity of cytolytic T cells mediated by granulysin. *Science* **282,** 121–5 (Oct. 1998).

340. Silver, R. F., Li, Q., Boom, W. H. & Ellner, J. J. Lymphocyte-dependent inhibition of growth of virulent Mycobacterium tuberculosis H37Rv within human monocytes: requirement for CD4+ T cells in purified protein derivative-positive, but not in purified protein derivative-negative subjects. *J. Immunol.* **160,** 2408–17 (Mar. 1998).

341. Carranza, C. *et al.* Mycobacterium tuberculosis growth control by lung macrophages and CD8 cells from patient contacts. *Am. J. Respir. Crit. Care Med.* **173,** 238–45 (Jan. 2006).

342. Bruns, H. *et al.* Anti-TNF immunotherapy reduces CD8+ T cell–mediated antimicrobial activity against Mycobacterium tuberculosis in humans. *J. Clin. Invest.* **119,** 1167–1177 (May 2009).

343. Harris, J. & Keane, J. How tumour necrosis factor blockers interfere with tuberculosis immunity. *Clin. Exp. Immunol.* **161,** 1–9 (July 2010).

344. Lewinsohn, D. M., Briden, a. L., Reed, S. G., Grabstein, K. H. & Alderson, M. R. Mycobacterium tuberculosis-reactive CD8+ T lymphocytes: the relative contribution of classical versus nonclassical HLA restriction. *J. Immunol.* **165,** 925–30 (July 2000).

345. Morrison, J., Pai, M. & Hopewell, P. C. Tuberculosis and latent tuberculosis infection in close contacts of people with pulmonary tuberculosis in low-income and middle-income countries: a systematic review and meta-analysis. *Lancet. Infect. Dis.* **8,** 359–68 (June 2008).

346. Riley, R. L. *et al.* Aerial dissemination of pulmonary tuberculosis. *Am. Rev. Tuberc.* **76,** 931–41 (Dec. 1957).

347. Williams, B. G. & Dye, C. Antiretroviral drugs for tuberculosis control in the era of HIV/AIDS. *Science* **301,** 1535–7 (Sept. 2003).

348. Sonnenberg, P. *et al.* How soon after infection with HIV does the risk of tuberculosis start to increase? A retrospective cohort study in South African gold miners. *J. Infect. Dis.* **191,** 150–8 (Jan. 2005).

349. Lawn, S. D., Bekker, L.-G. & Wood, R. How effectively does HAART restore immune responses to Mycobacterium tuberculosis? Implications for tuberculosis control. *AIDS* **19,** 1113–24 (July 2005).

350. Sadek, M. I., Sada, E., Toossi, Z., Schwander, S. K. & Rich, E. A. Chemokines induced by infection of mononuclear phagocytes with mycobacteria and present in lung alveoli during active pulmonary tuberculosis. *Am. J. Respir. Cell Mol. Biol.* **19,** 513–21 (Sept. 1998).

351. Saukkonen, J. J. *et al.* Beta-chemokines are induced by Mycobacterium tuberculosis and inhibit its growth. *Infect. Immun.* **70,** 1684–93 (Apr. 2002).

352. Napier, R. J., Lewinsohn, D. M. & Gold, M. C. MR1-restricted mucosal associated invariant T (MAIT) cells in the immune response to Mycobacterium tuberculosis. *Immunol. Rev.* **264,** 154–166 (2015).

353. Vankayalapati, R. *et al.* Production of interleukin-18 in human tuberculosis. *J. Infect. Dis.* **182,** 234–9 (July 2000).

354. Schneider, B. E. *et al.* A role for IL-18 in protective immunity against Mycobacterium tuberculosis. *Eur. J. Immunol.* **40,** 396–405 (Feb. 2010).

355. Trickett, A. & Kwan, Y. L. T cell stimulation and expansion using anti-CD3/CD28 beads. *J. Immunol. Methods* **275,** 251–5 (Apr. 2003).

356. Annibali, V. *et al.* CD161(high)CD8+T cells bear pathogenetic potential in multiple sclerosis. *Brain* **134,** 542–54 (Feb. 2011).

357. Cui, Y. *et al.* Mucosal-associated invariant T cell-rich congenic mouse strain allows functional evaluation. *J. Clin. Invest.* **125,** 4171–85 (Nov. 2015).

358. Chen, Z. *et al.* Mucosal-associated invariant T-cell activation and accumulation after in vivo infection depends on microbial riboflavin synthesis and co-stimulatory signals. *Mucosal Immunol.* **In print.** (May 2016).

359. Gherardin, N. A. *et al.* Diversity of T Cells Restricted by the MHC Class I-Related Molecule MR1 Facilitates Differential Antigen Recognition. *Immunity* **44,** 32–45 (Jan. 2016).

360. Valitutti, S., Müller, S., Cella, M., Padovan, E. & Lanzavecchia, A. Serial triggering of many T-cell receptors by a few peptide-MHC complexes. *Nature* **375,** 148–51 (May 1995).

361. Fergusson, J. R. *et al.* CD161(int)CD8+ T cells: a novel population of highly functional, memory CD8+ T cells enriched within the gut. *Mucosal Immunol.* **9,** 401–13 (Mar. 2016).

362. Simms, P. E. & Ellis, T. M. Utility of flow cytometric detection of CD69 expression as a rapid method for determining poly- and oligoclonal lymphocyte activation. *Clin. Diagn. Lab. Immunol.* **3,** 301–4 (May 1996).

363. Maino, V. C., Suni, M. A. & Ruitenberg, J. J. Rapid flow cytometric method for measuring lymphocyte subset activation. *Cytometry* **20,** 127–33 (June 1995).

364. Biselli, R., Matricardi, P. M., D'Amelio, R. & Fattorossi, A. Multiparametric flow cytometric analysis of the kinetics of surface molecule expression after polyclonal activation of human peripheral blood T lymphocytes. *Scand. J. Immunol.* **35,** 439–47 (Apr. 1992).

365. Salerno-Goncalves, R., Rezwan, T. & Sztein, M. B. B cells modulate mucosal associated invariant T cell immune responses. *Front. Immunol.* **4,** 511 (Jan. 2014).

366. Monks, C. R., Freiberg, B. A., Kupfer, H., Sciaky, N. & Kupfer, A. Three-dimensional segregation of supramolecular activation clusters in T cells. *Nature* **395,** 82–6 (Sept. 1998).

367. Dustin, M. L. The immunological synapse. *Cancer Immunol. Res.* **2,** 1023–33 (Nov. 2014).

368. Alarcón, B., Mestre, D. & Martínez-Martín, N. The immunological synapse: a cause or consequence of T-cell receptor triggering? *Immunology* **133,** 420–5 (Aug. 2011).

369. Altin, J. G. & Sloan, E. K. The role of CD45 and CD45-associated molecules in T cell activation. *Immunol. Cell Biol.* **75,** 430–45 (Oct. 1997).

370. Thauland, T. J., Koguchi, Y., Wetzel, S. A., Dustin, M. L. & Parker, D. C. Th1 and Th2 cells form morphologically distinct immunological synapses. *J. Immunol.* **181,** 393–9 (July 2008).

371. Stinchcombe, J. C., Bossi, G., Booth, S. & Griffiths, G. M. The immunological synapse of CTL contains a secretory domain and membrane bridges. *Immunity* **15,** 751–61 (Nov. 2001).

372. Davis, D. M. & Dustin, M. L. What is the importance of the immunological synapse? *Trends Immunol.* **25,** 323–327 (2004).

373. Choudhuri, K. *et al.* Polarized release of T-cell-receptor-enriched microvesicles at the immunological synapse. *Nature* **507,** 118–23 (2014).

374. Beal, A. M. *et al.* Protein kinase C theta regulates stability of the peripheral adhesion ring junction and contributes to the sensitivity of target cell lysis by CTL. *J. Immunol.* **181,** 4815–24 (Oct. 2008).

375. Liu, D. *et al.* Integrin-dependent organization and bidirectional vesicular traffic at cytotoxic immune synapses. *Immunity* **31,** 99–109 (July 2009).

376. Huse, M., Lillemeier, B. F., Kuhns, M. S., Chen, D. S. & Davis, M. M. T cells use two directionally distinct pathways for cytokine secretion. *Nat. Immunol.* **7,** 247–55 (Mar. 2006).

377. Tommaso, A. D. I. *et al.* Formaldehyde Treatment of Proteins Can Constrain Presentation to T Cells by Limiting Antigen Processing. *Infect. Immun.* **62,** 1830–1834 (1994).

378. Martin, M. D. & Badovinac, V. P. Antigen-dependent and –independent contributions to primary memory CD8 T cell activation and protection following infection. *Sci. Rep.* **5,** 18022 (Dec. 2015).

379. Beadling, C. & Slifka, M. K. Differential regulation of virus-specific T-cell effector functions following activation by peptide or innate cytokines. *Blood* **105,** 1179–86 (Feb. 2005).

380. Raue, H.-P., Beadling, C., Haun, J. & Slifka, M. K. Cytokine-mediated programmed proliferation of virus-specific CD8(+) memory T cells. *Immunity* **38,** 131–9 (Jan. 2013).

381. Ma, A., Koka, R. & Burkett, P. Diverse functions of IL-2, IL-15, and IL-7 in lymphoid homeostasis. *Annu. Rev. Immunol.* **24,** 657–79 (2006).

382. Intlekofer, A. M. *et al.* Effector and memory CD8+ T cell fate coupled by T-bet and eomesodermin. *Nat. Immunol.* **6,** 1236–44 (Dec. 2005).

383. Thurley, K., Gerecht, D., Friedmann, E. & Höfer, T. Three-Dimensional Gradients of Cytokine Signaling between T Cells. *PLoS Comput. Biol.* **11,** e1004206 (Apr. 2015).

384. Baena, A. & Porcelli, S. Evasion and subversion of antigen presentation by Mycobacterium tuberculosis. *Tissue Antigens* **74,** 189–204 (Sept. 2009).

385. Nunes-Alves, C. *et al.* In search of a new paradigm for protective immunity to TB. *Nat. Rev. Microbiol.* **12,** 289–99 (Apr. 2014).

386. Fox, G. J., Barry, S. E., Britton, W. J. & Marks, G. B. Contact investigation for tuberculosis: a systematic review and meta-analysis. *Eur. Respir. J.* **41,** 140–56 (Jan. 2013).

387. Brookes, R. H. *et al.* CD8+ T cell-mediated suppression of intracellular Mycobacterium tuberculosis growth in activated human macrophages. *Eur. J. Immunol.* **33,** 3293–302 (Dec. 2003).

388. Rothchild, A. C., Jayaraman, P., Nunes-Alves, C. & Behar, S. M. iNKT Cell Production of GM-CSF Controls Mycobacterium tuberculosis. *PLoS Pathog.* **10** (ed Lewinsohn, D. M.) e1003805 (Jan. 2014).

389. Lewis, K. N. *et al.* Deletion of RD1 from Mycobacterium tuberculosis mimics bacille Calmette-Guerin attenuation. *J. Infect. Dis.* **187,** 117–23 (2003).

390. Sharma, P. K. *et al.* High expression of CD26 accurately identifies human bacteria-reactive MR1-restricted MAIT cells. *Immunology* **145,** 443–53 (July 2015).

391. Lopez-Sagaseta, J. *et al.* MAIT recognition of a stimulatory bacterial antigen bound to MR1. *J. Immunol.* **191,** 5268–77 (Nov. 2013).

392. Jeffery, H. C. *et al.* Biliary epithelium and liver B cells exposed to bacteria activate intrahepatic MAIT cells through MR1. *J. Hepatol.* **64,** 1118–27 (May 2016).

393. Greene, J. M. *et al.* MR1-restricted mucosal-associated invariant T (MAIT) cells respond to mycobacterial vaccination and infection in nonhuman primates. *Mucosal Immunol.* (Oct. 2016).

394. Dias, J., Sobkowiak, M. J., Sandberg, J. K. & Leeansyah, E. Human MAIT-cell responses to Escherichia coli: activation, cytokine production, proliferation, and cytotoxicity. *J. Leukoc. Biol.* **100,** 1–8 (2016).

395. Theus, S. A., Cave, M. D. & Eisenach, K. D. Activated THP-1 cells: an attractive model for the assessment of intracellular growth rates of Mycobacterium tuberculosis isolates. *Infect. Immun.* **72,** 1169–73 (Feb. 2004).

396. Kohro, T. *et al.* A comparison of differences in the gene expression profiles of phorbol 12-myristate 13-acetate differentiated THP-1 cells and human monocyte-derived macrophage. *J. Atheroscler. Thromb.* **11,** 88–97 (Jan. 2004).

397. Loeuillet, C. *et al.* Mycobacterium tuberculosis subverts innate immunity to evade specific effectors. *J. Immunol.* **177,** 6245–55 (Nov. 2006).

398. Park, E. K. *et al.* Optimized THP-1 differentiation is required for the detection of responses to weak stimuli. *Inflamm. Res.* **56,** 45–50 (Jan. 2007).

399. Daigneault, M., Preston, J. a., Marriott, H. M., Whyte, M. K. B. & Dockrell, D. H. The identification of markers of macrophage differentiation in PMA-stimulated THP-1 cells and monocyte-derived macrophages. *PLoS One* **5,** e8668 (Jan. 2010).

400. Cho, J.-E., Kim, Y. S., Park, S., Cho, S.-N. & Lee, H. Mycobacterium tuberculosis-induced expression of Leukotactin-1 is mediated by the PI3-K/PDK1/Akt signaling pathway. *Mol. Cells* **29,** 35–9 (Jan. 2010).

401. Macdonald, S. H.-F. *et al.* Networked T cell death following macrophage infection by Mycobacterium tuberculosis. *PLoS One* **7,** e38488 (Jan. 2012).

402. Cho, J.-E., Park, S., Lee, H., Cho, S.-N. & Kim, Y. S. Mycobacterium tuberculosis-induced expression of granulocyte-macrophage colony stimulating factor is mediated by PI3-K/MEK1/p38 MAPK signaling pathway. *BMB Rep.* **46,** 213–8 (Apr. 2013).

403. Martin, C. J. *et al.* Efferocytosis is an innate antibacterial mechanism. *Cell Host Microbe* **12,** 289–300 (Sept. 2012).

404. Mahamed, D. *et al.* Intracellular growth of Mycobacterium tuberculosis after macrophage cell death leads to serial killing of host cells. *Elife* **6** (Jan. 2017).

405. Guo, H., Callaway, J. B. & Ting, J. P.-Y. Inflammasomes: mechanism of action, role in disease, and therapeutics. *Nat. Med.* **21,** 677–87 (July 2015).

406. Saiga, H. *et al.* Critical role of AIM2 in Mycobacterium tuberculosis infection. *Int. Immunol.* **24,** 637–44 (Oct. 2012).

407. Mishra, B. B. *et al.* Mycobacterium tuberculosis protein ESAT-6 is a potent activator of the NLRP3/ASC inflammasome. *Cell. Microbiol.* **12,** 1046–63 (Aug. 2010).

408. Tan, H. Y. *et al.* Aberrant Inflammasome Activation Characterizes Tuberculosis-Associated Immune Reconstitution Inflammatory Syndrome. *J. Immunol.* **196,** 4052–63 (May 2016).

409. Barrios-Payán, J. *et al.* Extrapulmonary locations of mycobacterium tuberculosis DNA during latent infection. *J. Infect. Dis.* **206,** 1194–205 (Oct. 2012).

410. Rahman, S. *et al.* Compartmentalization of immune responses in human tuberculosis: few CD8+ effector T cells but elevated levels of FoxP3+ regulatory t cells in the granulomatous lesions. *Am. J. Pathol.* **174,** 2211–24 (June 2009).

411. Iannuzzi, M. C., Rybicki, B. A. & Teirstein, A. S. Sarcoidosis. *N. Engl. J. Med.* **357,** 2153–65 (Nov. 2007).

412. Heinle, R. & Chang, C. Diagnostic criteria for sarcoidosis. *Autoimmun. Rev.* **13,** 383–7 (2014).

413. Agrawal, R. *et al.* Tuberculosis or sarcoidosis: Opposite ends of the same disease spectrum? *Tuberculosis* **98,** 21–26 (May 2016).

414. Costabel, U., Bonella, F., Ohshimo, S. & Guzman, J. Diagnostic modalities in sarcoidosis: BAL, EBUS, and PET. *Semin. Respir. Crit. Care Med.* **31,** 404–8 (Aug. 2010).

415. Tomlinson, G. S. *et al.* Transcriptional Profiling of Endobronchial Ultrasound-Guided Lymph Node Samples Aids Diagnosis of Mediastinal Lymphadenopathy. *Chest* **149,** 535–44 (Feb. 2016).

416. Maertzdorf, J. *et al.* Common patterns and disease-related signatures in tuberculosis and sarcoidosis. *Proc. Natl. Acad. Sci. U. S. A.* **109,** 7853–8 (May 2012).

417. Navani, N. *et al.* Utility of endobronchial ultrasound-guided transbronchial needle aspiration in patients with tuberculous intrathoracic lymphadenopathy: a multicentre study. **66,** 889–893 (2011).

418. Sun, J. *et al.* Endobronchial ultrasound-guided transbronchial needle aspiration in diagnosing intrathoracic tuberculosis. *Ann. Thorac. Surg.* **96,** 2021–7 (Dec. 2013).

419. Low, S. Y., Koh, M. S., Ong, T. H., Phua, G. C. & Anantham, D. Use of endobronchial ultrasound-guided transbronchial needle aspiration (EBUS-TBNA) in the diagnosis of granulomatous mediastinal lymphadenopathy. *Ann. Acad. Med. Singapore* **43,** 250–4 (May 2014).

420. Geake, J. *et al.* Utility of EBUS-TBNA for diagnosis of mediastinal tuberculous lymphadenitis: a multicentre Australian experience. *J. Thorac. Dis.* **7,** 439–48 (Mar. 2015).

421. Hennig, C., Adams, N. & Hansen, G. A versatile platform for comprehensive chip-based explorative cytometry. *Cytometry. A* **75,** 362–70 (Apr. 2009).

422. Peto, H. M., Pratt, R. H., Harrington, T. a., LoBue, P. a. & Armstrong, L. R. Epidemiology of extrapulmonary tuberculosis in the United States, 1993-2006. *Clin. Infect. Dis.* **49,** 1350–7 (Nov. 2009).

423. Llibre, A. *et al.* LLT1 and CD161 Expression in Human Germinal Centers Promotes B Cell Activation and CXCR4 Downregulation. *J. Immunol.* **196,** 2085–94 (Mar. 2016).

424. Novak, J., Dobrovolny, J., Novakova, L. & Kozak, T. The decrease in number and change in phenotype of mucosal-associated invariant T cells in the elderly and differences in men and women of reproductive age. *Scand. J. Immunol.* **80,** 271–5 (Oct. 2014).

425. Lee, O.-J. *et al.* Circulating mucosal-associated invariant T cell levels and their cytokine levels in healthy adults. *Exp. Gerontol.* **49C,** 47–54 (Jan. 2014).

426. Abhimanyu *et al.* Establishment of Elevated Serum Levels of IL-10, IL-8 and TNF-β as Potential Peripheral Blood Biomarkers in Tubercular Lymphadenitis: A Prospective Observational Cohort Study. *PLoS One* **11,** e0145576 (2016).

427. Prezant, D. J. *et al.* The incidence, prevalence, and severity of sarcoidosis in New York City firefighters. *Chest* **116,** 1183–1193 (1999).

428. Newman, L. S. *et al.* A case control etiologic study of sarcoidosis: Environmental and occupational risk factors. *Am. J. Respir. Crit. Care Med.* **170,** 1324–1330 (2004).

429. Deubelbeiss, U., Gemperli, A., Schindler, C., Baty, F. & Brutsche, M. H. Prevalence of sarcoidosis in Switzerland is associated with environmental factors. *Eur. Respir. J.* **35,** 1088–97 (May 2010).

430. Song, Z. *et al.* Mycobacterial catalase-peroxidase is a tissue antigen and target of the adaptive immune response in systemic sarcoidosis. *J Exp Med* **201,** 755–767 (2005).

431. Chen, E. S. *et al.* T cell responses to mycobacterial catalase-peroxidase profile a pathogenic antigen in systemic sarcoidosis. *J. Immunol.* **181,** 8784–8796 (2008).

432. Chen, E. S. *et al.* Serum amyloid a regulates granulomatous inflammation in sarcoidosis through toll-like receptor-2. *Am. J. Respir. Crit. Care Med.* **181,** 360–373 (2010).

433. Wiken, M., Grunewald, J., Eklund, A. & Wahlstrom, J. Higher monocyte expression of TLR2 and TLR4, and enhanced pro-inflammatory synergy of TLR2 with NOD2 stimulation in sarcoidosis. *J. Clin. Immunol.* **29,** 78–89 (Jan. 2009).

434. Veltkamp, M., van Moorsel, C. H. M., Rijkers, G. T., Ruven, H. J. T. & Grutters, J. C. Genetic variation in the Toll-like receptor gene cluster (TLR10-TLR1-TLR6) influences disease course in sarcoidosis. *Tissue Antigens* **79,** 25–32 (Jan. 2012).

435. Chen, E. S. & Moller, D. R. Sarcoidosis–scientific progress and clinical challenges. *Nat. Rev. Rheumatol.* **7,** 457–67 (July 2011).

436. Valeyre, D. *et al.* Sarcoidosis. *Lancet (London, England)* **383,** 1155–67 (Mar. 2014).

437. Moller, D. R. *et al.* Enhanced expression of IL-12 associated with Th1 cytokine profiles in active pulmonary sarcoidosis. *J. Immunol.* **156,** 4952–60 (1996).

438. Greene, C. M. *et al.* Role of IL-18 in CD4+ T lymphocyte activation in sarcoidosis. *J. Immunol.* **165,** 4718–24 (Oct. 2000).

439. Shigehara, K. *et al.* IL-12 and IL-18 are increased and stimulate IFN-gamma production in sarcoid lungs. *J. Immunol.* **166,** 642–9 (Jan. 2001).

440. Gonzalez-Amaro, R., Cortes, J. R., Sanchez-Madrid, F. & Martin, P. Is CD69 an effective brake to control inflammatory diseases? *Trends Mol. Med.* **19,** 625–32 (Oct. 2013).

441. Saeidi, A. *et al.* Functional role of mucosal-associated invariant T cells in HIV infection. *J. Leukoc. Biol.* **100,** 305–14 (Aug. 2016).

442. Ho, L. P., Urban, B. C., Thickett, D. R., Davies, R. J. O. & McMichael, A. J. Deficiency of a subset of T cells with immunoregulatory properties in sarcoidosis. *Lancet* **365,** 1062–1072 (2005).

443. Reilly, E. C., Wands, J. R. & Brossay, L. Cytokine dependent and independent iNKT cell activation. *Cytokine* **51,** 227–231 (2010).

444. Snyder-Cappione, J. E. *et al.* Invariant natural killer T (iNKT) cell exhaustion in sarcoidosis. *Eur. J. Immunol.* **43,** 2194–205 (Aug. 2013).

445. Zissel, G. Cellular activation in the immune response of sarcoidosis. *Semin. Respir. Crit. Care Med.* **35,** 307–15 (June 2014).

446. Shipkova, M. & Wieland, E. Surface markers of lymphocyte activation and markers of cell proliferation. *Clin. Chim. Acta.* **413,** 1338–49 (Sept. 2012).

447. Iyoda, T. *et al.* Invariant NKT cell anergy is induced by a strong TCR-mediated signal plus co-stimulation. *Int. Immunol.* **22,** 905–13 (Nov. 2010).

448. Handa, U., Mundi, I. & Mohan, S. Nodal tuberculosis revisited: A review. *J. Infect. Dev. Ctries.* **6,** 6–12 (2012).

449. Leeds, I. L. *et al.* Site of extrapulmonary tuberculosis is associated with HIV infection. *Clin. Infect. Dis.* **55,** 75–81 (July 2012).

450. Feng, C. G. *et al.* NK cell-derived IFN-gamma differentially regulates innate resistance and neutrophil response in T cell-deficient hosts infected with Mycobacterium tuberculosis. *J. Immunol.* **177,** 7086–93 (Nov. 2006).

451. Brill, K. J. *et al.* Human Natural Killer Cells Mediate Killing of Intracellular Mycobacterium tuberculosis H37Rv via Granule-Independent Mechanisms. *Infect. Immun.* **69,** 1755–1765 (2001).

452. Korbel, D. S., Schneider, B. E. & Schaible, U. E. Innate immunity in tuberculosis: myths and truth. *Microbes Infect.* **10,** 995–1004 (July 2008).

453. Abebe, F. The Role of T cells In Mucosal Immunity against Mycobacterium tuberculosis (Mtb) Infection: A Review of Current Understanding. *J. Clin. Cell. Immunol.* **5** (2014).

454. Meraviglia, S., El Daker, S., Dieli, F., Martini, F. & Martino, A. $\gamma\delta$ T cells cross-link innate and adaptive immunity in Mycobacterium tuberculosis infection. *Clin. Dev. Immunol.* **2011,** 587315 (2011).

455. Koth, L. L. *et al.* Sarcoidosis blood transcriptome reflects lung inflammation and overlaps with tuberculosis. *Am. J. Respir. Crit. Care Med.* **184,** 1153–63 (Nov. 2011).

456. Bloom, C. I. *et al.* Transcriptional blood signatures distinguish pulmonary tuberculosis, pulmonary sarcoidosis, pneumonias and lung cancers. *PLoS One* **8,** e70630 (2013).

457. Liuzzi, A. R., McLaren, J. E., Price, D. A. & Eberl, M. Early innate responses to pathogens: pattern recognition by unconventional human T-cells. *Curr. Opin. Immunol.* **36,** 31–7 (Oct. 2015).

458. Tsuchiya, S. *et al.* Establishment and characterization of a human acute monocytic leukemia cell line (THP-1). *Int. J. cancer* **26,** 171–6 (Aug. 1980).

459. Tanner, R., O'Shea, M. K., Fletcher, H. A. & McShane, H. In vitro mycobacterial growth inhibition assays: A tool for the assessment of protective immunity and evaluation of tuberculosis vaccine efficacy. *Vaccine* **34,** 4656–65 (Sept. 2016).

460. Van Zyl-Smit, R. N. *et al.* Comparison of quantitative techniques including Xpert MTB/RIF to evaluate mycobacterial burden. *PLoS One* **6,** e28815 (2011).

461. Chen, M., Gan, H. & Remold, H. G. A Mechanism of Virulence: Virulent Mycobacterium tuberculosis Strain H37Rv, but Not Attenuated H37Ra, Causes Significant Mitochondrial Inner Membrane Disruption in Macrophages Leading to Necrosis. *J. Immunol.* **176,** 3707–3716 (2006).

462. Pan, H. *et al.* Ipr1 gene mediates innate immunity to tuberculosis. *Nature* **434,** 767–72 (Apr. 2005).

463. Tully, G. *et al.* Highly focused T cell responses in latent human pulmonary Mycobacterium tuberculosis infection. eng. *J. Immunol.* **174,** 2174–84 (Feb. 2005).

464. Dinarello, C. a., Novick, D., Kim, S. & Kaplanski, G. Interleukin-18 and IL-18 Binding Protein. *Front. Immunol.* **4,** 289 (Jan. 2013).

465. Chalan, P. *et al.* Expression of Lectin-Like Transcript 1, the Ligand for CD161, in Rheumatoid Arthritis. *PLoS One* **10** (ed Graca, L.) e0132436 (July 2015).

466. Satkunanathan, S., Kumar, N., Bajorek, M., Purbhoo, M. a. & Culley, F. J. Respiratory syncytial virus infection, TLR3 ligands, and proinflammatory cytokines induce CD161 ligand LLT1 expression on the respiratory epithelium. *J. Virol.* **88,** 2366–73 (Mar. 2014).

467. Germain, C. *et al.* Induction of lectin-like transcript 1 (LLT1) protein cell surface expression by pathogens and interferon-γ contributes to modulate immune responses. *J. Biol. Chem.* **286,** 37964–75 (Nov. 2011).

468. Stranks, A. J. *et al.* Autophagy Controls Acquisition of Aging Features in Macrophages. *J. Innate Immun.* **7,** 375–91 (2015).

469. Saitoh, T. *et al.* Loss of the autophagy protein Atg16L1 enhances endotoxin-induced IL-1beta production. *Nature* **456,** 264–8 (Nov. 2008).

470. Seshadri, C. *et al.* A polymorphism in human MR1 is associated with mRNA expression and susceptibility to tuberculosis. *Genes Immun.* **18,** 8–14 (Jan. 2017).

471. Krovi, S. H. & Gapin, L. Structure and function of the non-classical major histocompatibility complex molecule MR1. *Immunogenetics* **68,** 549–559 (Aug. 2016).

472. Keller, A. N. *et al.* Drugs and drug-like molecules can modulate the function of mucosal-associated invariant T cells. *Nat. Immunol.* (Feb. 2017).